frontiers | Research Topics

Edible and medicinal plants: From ethnopharmacological practices to interdisciplinary approaches and regulations

Edited by
X. Y. Zhang, Alberto Carlos Pires Dias and Norberto Peporine Lopes

Published in
Frontiers in Pharmacology
Frontiers in Plant Science

ISSN 1664-8714
ISBN 978-2-83251-526-6
DOI 10.3389/978-2-83251-526-6

About Frontiers

Frontiers is more than just an open access publisher of scholarly articles: it is a pioneering approach to the world of academia, radically improving the way scholarly research is managed. The grand vision of Frontiers is a world where all people have an equal opportunity to seek, share and generate knowledge. Frontiers provides immediate and permanent online open access to all its publications, but this alone is not enough to realize our grand goals.

Frontiers journal series

The Frontiers journal series is a multi-tier and interdisciplinary set of open-access, online journals, promising a paradigm shift from the current review, selection and dissemination processes in academic publishing. All Frontiers journals are driven by researchers for researchers; therefore, they constitute a service to the scholarly community. At the same time, the *Frontiers journal series* operates on a revolutionary invention, the tiered publishing system, initially addressing specific communities of scholars, and gradually climbing up to broader public understanding, thus serving the interests of the lay society, too.

Dedication to quality

Each Frontiers article is a landmark of the highest quality, thanks to genuinely collaborative interactions between authors and review editors, who include some of the world's best academicians. Research must be certified by peers before entering a stream of knowledge that may eventually reach the public - and shape society; therefore, Frontiers only applies the most rigorous and unbiased reviews. Frontiers revolutionizes research publishing by freely delivering the most outstanding research, evaluated with no bias from both the academic and social point of view. By applying the most advanced information technologies, Frontiers is catapulting scholarly publishing into a new generation.

What are Frontiers Research Topics?

Frontiers Research Topics are very popular trademarks of the *Frontiers journals series*: they are collections of at least ten articles, all centered on a particular subject. With their unique mix of varied contributions from Original Research to Review Articles, Frontiers Research Topics unify the most influential researchers, the latest key findings and historical advances in a hot research area.

Find out more on how to host your own Frontiers Research Topic or contribute to one as an author by contacting the Frontiers editorial office: frontiersin.org/about/contact

Edible and medicinal plants: From ethnopharmacological practices to interdisciplinary approaches and regulations

Topic editors

X. Y. Zhang — University of Guelph, Canada

Alberto Carlos Pires Dias — University of Minho, Portugal

Norberto Peporine Lopes — University of São Paulo, Bauru, Brazil

Citation

Zhang, X. Y., Dias, A. C. P., Lopes, N. P., eds. (2023). *Edible and medicinal plants: From ethnopharmacological practices to interdisciplinary approaches and regulations*. Lausanne: Frontiers Media SA. doi: 10.3389/978-2-83251-526-6

Table of contents

frontiers | Frontiers in Pharmacology

TYPE Editorial
PUBLISHED 16 December 2022
DOI 10.3389/fphar.2022.1074511

OPEN ACCESS

EDITED BY
Javier Echeverria,
University of Santiago, Chile

REVIEWED BY
Dâmaris Silveira,
University of Brasilia, Brazil

*CORRESPONDENCE
Xiaoying Zhang,
zhang@bio.uminho.pt

SPECIALTY SECTION
This article was submitted to Ethnopharmacology, a section of the journal Frontiers in Pharmacology

RECEIVED 19 October 2022
ACCEPTED 06 December 2022
PUBLISHED 16 December 2022

CITATION
Zhang X, Dias ACP and Lopes NP (2022), Editorial: Edible and medicinal plants: From ethnopharmacological practices to interdisciplinary approaches and regulations.
Front. Pharmacol. 13:1074511.
doi: 10.3389/fphar.2022.1074511

Editorial: Edible and medicinal plants: From ethnopharmacological practices to interdisciplinary approaches and regulations

Xiaoying Zhang[1,2,3]*, Alberto C. P. Dias[2] and Norberto Peporine Lopes[4]

[1]Qinba State Key Laboratory of Biological Resources and Ecological Environment, College of Biological Science and Engineering, Shaanxi University of Technology, Hanzhong, Shaanxi, China, [2]Department of Biology, Centre of Molecular and Environmental Biology (CBMA), University of Minho, Campus de Gualtar, Braga, Portugal, [3]Department of Biomedical Sciences, Ontario Veterinary College, University of Guelph, Guelph, ON, Canada, [4]Núcleo de Pesquisa em Produtos Naturais e Sintéticos (NPPNS), Department of Biomolecular Sciences, Faculty of Pharmaceutical Sciences of Ribeirão Preto, University of São Paulo, RibeirãoPreto, SãoPaulo, Brazil

KEYWORDS

edible plants, medicinal plants, pharmacological effect, health benefit, health product, regulation

Editorial on the Research Topic
Edible and medicinal plants: From ethnopharmacological practices to interdisciplinary approaches and regulations

The investigation on plants that are both medicinal and edible is rooted in different ethno-medicinal systems (Yao et al.) Emerging diseases and health issues, lifestyle and diet changes urge us in seeking novel bioactive substances and formulations from plant sources (Sofowora et al., 2013; Xia et al., 2021). Related study requires interdisciplinary approaches including pharmaceutical, food, medicinal, and plant sciences, and policy study on food and drug administration.

Along with the strong increase in the publication of medicine food homology study (Figure 1), research highlights can be observed from the recent publications, which cover the applications of medicine food homology to modern lifestyle related diseases and health concerns, active substances and groups, mushroom study, increasing strengthening on the concept of nutraceuticals, etc. However, there are still a lack of scientific understanding and investigations for active ingredients and their synergistic and networking effects, lack of clear boundary

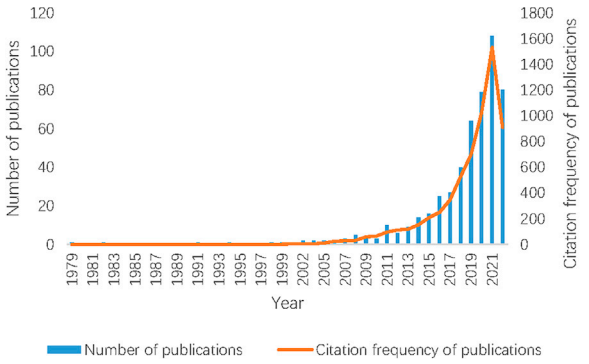

FIGURE 1
Number and citation frequency of medicine food homology related publications. Note: Data were collected from Web of Science Core Research Topic with the following search strategy: Topical Subject = ("Medicinal and Edible" OR "medicine food homology") OR Title = ("Medicinal and Edible" OR "medicine food homology") OR Abstract = ("Medicinal and Edible" OR "medicine food homology"), the language was English. A total of 508 papers were obtained, including 53 reviews and 455 articles. Figure only includes studies that met the inclusion criteria of the search strategy (Data as of Jul. 2022).

TABLE 1 Edible and medicinal plants and products investigated in the present Research Topic.

Name	Major finding(s)	References
Crocus sativus L. (Saffron), Crocetin and its Glycoside Crocin	The anti-angiogenic effects and underlying mechanisms confirmed on human umbilical vein endothelial cells and zebrafish Through VEGFR2/SRC/FAK and VEGFR2/MEK/ERK Signalling Pathways	Zhao etal.
Maianthemum atropurpureum, a wild vegetable	The local people's practice of consuming *Maianthemum atropurpureum* is reasonable due to its high levels of vitamins, minerals, essential amino-acids, and phytochemicals	Xu et al.
Pantao Pill (a traditional Chinese medicines formulation containing Aloes, wood incense, frankincense, myrrh areca, etc.)	Based on Network pharmacology investigations, Pantao Pill can significantly improve the learning and memory abilities of APP/PS1 mice, with mechanisms related to the increase of neurotransmitter acetylcholine and norepinephrine levels, the reduction of the excessive autophagic activation, and the suppression of oxidative stress and excessive apoptotic activity	Xin et al.

(Continued in next column)

TABLE 1 (*Continued*) Edible and medicinal plants and products investigated in the present Research Topic.

Name	Major finding(s)	References
Artemisia capillaris and 6,7-Dimethylesculetin	*Artemisia capillaris* and 6,7-dimethylesculetin induce Cyp2a5 expression at both mRNA and protein levels. Additionally, 6,7-dimethylesculetin significantly increases cytochrome P450 2a5 expression at the transcriptional level through transactivation by constitutive androstane receptor	Kim et al.
Morus alba L. Leaves	Low temperature may be a key trigger in flavonoid biosynthesis of mulberry leaves by increasing the expression of flavonoid biosynthesis-related genes. This study also provided a theoretical basis for the optimal harvest time of mulberry leaves	Xu et al.
Yeokwisan, a Standardized Herbal Formula	The study showed the clinical relevance of *Yeokwisan*, in treating functional dyspepsia, especially in promoting gastric emptying but not small intestinal transit. The main mechanisms corresponding to these effects may involve the modulation of the ghrelin pathway and activation of interstitial cells of Cajal in stomach tissue	Hwang et al.
Sophora davidi (Franch.) Skeels	*Sophora davidi* (Franch.) Skeels fruits extract demonstrated clear anti–aging effect on d–galactose–induced acute aging in mice, and its mechanism may be relevant to the activation of the SIRT1/p53 signal pathway	Lin et al.
Epimedii Folium	Both species and geographical location variations have impacts on the quality and composition of Epimedii Folium. *Epimedii sagittatum* from Sichuan showed the highest content of bioactive compounds	Li et al.
Edible Bird's Nest Extract	The extract effectively improved skin wrinkles, is beneficial for skin health and can be used as a skin nutritional supplement	Kim et al.
Phyllanthus emblica	Aqueous extract potentially ameliorates non-alcoholic fatty liver disease induced by a choline-deficient, L-amino acid-defined, high-fat diet through a mechanism associated with its modulatory effects on the gut microbiota and microbial metabolism	Luo et al.

TABLE 2 Plants or topics reviewed in the present Research Topic

Plant or topic reviewed	Major summary or debate	References
Systematic cross-cultural ethnobotanical knowledge assembly & Genus *Lycium*	A framework for a systematic understanding on any taxon's ethnobotanical knowledge is proposed. The assembly of the genus *Lycium* indicates the requirement for a documentation-based taxonomic revision to current updated international species checklists	Yao et al.
Coptis	Current research situation, knowledge base and research hotspots in *Coptis* research was analysed using Bibliometrics methods	Huang et al.
Emerging Applications of Metabolomics to Assess the Efficacy of Traditional Chinese Medicines for Treating Type 2 Diabetes Mellitus	Metabolomics can be used to systematically explore the pathophysiology of type 2 diabetes mellitus and elucidate overall molecular mechanism underlying the known positive effects of treatment with traditional Chinese medicine. Network pharmacology methods, in combination with experimental pharmacology, can be further used to identify the bioactive ingredients in traditional Chinese medicine and their targets, which could inform the development of new therapies for type 2 diabetes mellitus	Zhang et al.
Tongxinluo Capsule (a Chinese medicinal product composed of *Panax ginseng* C.A.Mey. *Hirudo nipponica* Whitman, *Scolopendra subspinipes mutilans* L. Koch, *Eupolyphaga sinensis* Walker, etc.)	Meta-analysis showed that Tongxinluo could reduce the rate of cardiovascular disease, all-cause mortality and the number and summation of segment depression, decreased serum hypersensitive C-reactive protein level, improve the electrocardiogram abnormalities and clinical efficacy in unstable angina pectoris, relieve the unstable angina pectoris symptoms, as well as increase plasma NO concentrations. Nevertheless, side effects such as gastrointestinal symptoms, bleeding gums, bradycardia, and hypotension still occurred at an inconvenient low frequency	Li et al.
Red Yeast Rice Preparations	Red Yeast Rice Preparations significantly reduce the occurrence of mortality and major adverse cardiovascular events in metabolic syndrome and improve blood glucose, lipid profiles, and blood pressure. Red Yeast Rice Preparations could improve clinical endpoints, and prevent metabolic diseases	Yuan et al.
Isodon rubescens (Hemls.) Hara	ethnomedicinal uses, phytochemical composition, pharmacological activity, quality control, and toxicology of *I. rubescens*; updated information for the further development and application as functional food and drug candidate	Chen et al.
Traditional Uses of Animals in the Himalayan Region of Azad Jammu and Kashmir	This study provides baseline data valuable for the conservation of vertebrate and invertebrate diversity in the region of Himalayan of Azad Jammu and Kashmir. It is possible that screening this fauna for medicinally active chemicals could contribute to the development of new animal-based drugs	Faiz et al.

definition in medicinal use and functional use, lack of clear inclusion criteria and regulation policies in the related studies and products. It could be of interest and needs for the scientific community to consider topics such as the development of proper pharmacological and physiological models, the development of novel and practical active substance delivery systems, holistic evaluation of the short term and long-term effects of the plants and the phytoconstituents. Articles merging these topics and ethnopharmacology may be helpful in reaching an international consensus among scientific and industrial communities.

In this Research Topic, we have provided a discussion forum for the community, and received 47 full length article submissions, with 17 papers published, which covers cultivation and pharmacognosy of medicinal and food plants, ethno-pharmacological practices and pharmacological investigation, food function and safety evaluation of selected plants; identification of novel pharmacological and biological effects of plants, strategy on the development of pharmaceutical, nutraceuticals and functional products, reviews as well as general methodology and research advancement (Tables 1, 2).

This Research Topic provides a platform and community space for sharing and enlightening the state-of-art discovery and scientific understanding in edible and medicinal plants (Table 1). Efforts are expected for further explorations of this Research Topic in a global perspective with stronger networking. Despite of long-standing application in some cultural systems, the understanding and regulation on edible and medicinal plant are still various and in different approaches among food and drug regulatory authorities of different countries. Consensus on

the definition and scope, research and evaluation methodology, and rational application and supervision of edible and medicinal plant are anticipated.

Author contributions

All authors listed have made a substantial, direct and intellectual contribution to the work, and approved it for publication.

Acknowledgments

We would like to thank all the authors, reviewers and frontiers editorial team for their valuable input and contributions.

Conflict of interest

The authors declare that the research was conducted in the absence of any commercial or financial relationships that could be construed as a potential conflict of interest.

Publisher's note

All claims expressed in this article are solely those of the authors and do not necessarily represent those of their affiliated organizations, or those of the publisher, the editors and the reviewers. Any product that may be evaluated in this article, or claim that may be made by its manufacturer, is not guaranteed or endorsed by the publisher.

References

Sofowora, A., Ogunbodede, E., and Onayade, A. (2013). The role and place of medicinal plants in the strategies for disease prevention. *Afr. J. Tradit. Complement. Altern. Med.* 10, 210–229. doi:10.4314/ajtcam.v10i5.2

Xia, L., Shi, Y., Su, J., Friedemann, T., Tao, Z., Lu, Y., et al. (2021). Shufeng Jiedu, a promising herbal therapy for moderate COVID-19:Antiviral and anti-inflammatory properties, pathways of bioactive compounds, and a clinical real-world pragmatic study. *Phytomedicine.* 85, 153390. doi:10.1016/j.phymed.2020.153390

Yao, R., Heinrich, M., Wei, J., and Xiao, P. (2021). Cross-cultural ethnobotanical assembly as a new tool for understanding medicinal and culinary values-the genus lycium as A case study. *Front. Pharmacol.* 12, 708518. doi:10.3389/fphar.2021.708518

frontiers in Pharmacology

ORIGINAL RESEARCH
published: 30 April 2021
doi: 10.3389/fphar.2021.675359

Crocetin and Its Glycoside Crocin, Two Bioactive Constituents From *Crocus sativus* L. (Saffron), Differentially Inhibit Angiogenesis by Inhibiting Endothelial Cytoskeleton Organization and Cell Migration Through VEGFR2/SRC/FAK and VEGFR2/MEK/ERK Signaling Pathways

Chen Zhao[1], *Hio-Tong Kam*[1], *Yan Chen*[1], *Guiyi Gong*[1], *Maggie Pui-Man Hoi*[1], *Krystyna Skalicka-Woźniak*[2], *Alberto Carlos Pires Dias*[3] *and Simon Ming-Yuen Lee*[1]*

[1]State Key Laboratory of Quality Research in Chinese Medicine and Institute of Chinese Medical Sciences, University of Macau, Macao, China, [2]Independent Laboratory of Natural Products Chemistry, Department of Pharmacognosy, Medical University of Lublin, Lublin, Poland, [3]Centre for the Research and Technology of Agro-Environment and Biological Sciences (CITAB-UM), AgroBioPlant Group, Department of Biology, University of Minho, Braga, Portugal

OPEN ACCESS

Edited by:
Gordon Kirby,
University of Guelph, Canada

Reviewed by:
Karl Tsim,
Hong Kong University of Science and Technology, Hong Kong
Ki-Tae Ha,
Pusan National University, South Korea

***Correspondence:**
Simon Ming-Yuen Lee
simonlee@um.edu.mo

Specialty section:
This article was submitted to Ethnopharmacology, a section of the journal Frontiers in Pharmacology

Received: 03 March 2021
Accepted: 21 April 2021
Published: 30 April 2021

Citation:
Zhao C, Kam H-T, Chen Y, Gong G, Hoi MP-M, Skalicka-Woźniak K, Dias ACP and Lee SM-Y (2021) Crocetin and Its Glycoside Crocin, Two Bioactive Constituents From Crocus sativus L. (Saffron), Differentially Inhibit Angiogenesis by Inhibiting Endothelial Cytoskeleton Organization and Cell Migration Through VEGFR2/SRC/FAK and VEGFR2/MEK/ERK Signaling Pathways. Front. Pharmacol. 12:675359. doi: 10.3389/fphar.2021.675359

Crocetin and crocin are two important carotenoids isolated from saffron (*Crocus sativus* L.), which have been used as natural biomedicines with beneficial effects for improving the suboptimal health status associated with abnormal angiogenesis. However, the anti-angiogenic effects and underlying mechanisms of the effects of crocetin and crocin have not been investigated and compared. The anti-angiogenic effects of crocetin and crocin were tested on human umbilical vein endothelial cells (HUVECs) *in vitro*, and in zebrafish *in vivo*. *In vivo*, crocetin (20 μM) and crocin (50 and 100 μM) significantly inhibited subintestinal vein vessels formation, and a conversion process between them existed in zebrafish, resulting in a difference in their effective concentrations. In the HUVEC model, crocetin (10, 20 and 40 μM) and crocin (100, 200 and 400 μM) inhibited cell migration and tube formation, and inhibited the phosphorylation of VEGFR2 and its downstream pathway molecules. *In silico* analysis further showed that crocetin had a higher ability to bind with VEGFR2 than crocin. These results suggested that crocetin was more effective than crocin in inhibiting angiogenesis through regulation of the VEGF/VEGFR2 signaling pathway. These compounds, especially crocetin, are potential candidate natural biomedicines for

Abbreviations: AMD, age-related macular degeneration; CNV, choroidal neovascularization; hpf, hours post fertilization; HPLC, high-performance liquid chromatography; HRMECs, human retinal microvascular endothelial cells; HUVECs, human umbilical vein endothelial cells; MTA, microtubule-targeting agents; RPE, retinal pigment epithelia; SIVs, subintestinal vein vessels; TBHP, tert-butyl hydrotert-butyl hydroperoxide; VEGF, vascular endothelial growth factor; VEGFR, VEGF receptor; VRI, VEGFR tyrosine kinase inhibitor II.

the management of diseases associated with abnormal blood vessel growth, such as age-related macular degeneration.

Keywords: crocetin, crocin, angiogenesis, VEGF, zebrafish, HUVEC

INTRODUCTION

Crocetin and crocin (also known as crocin-I or α-crocin) are two important carotenoids isolated from the dried stigma of the flowers of *Crocus sativus* L. (saffron). Carotenoids have been implicated as playing a versatile role in human health; however, animals (including humans) rarely produce them, and thus need to obtain them *via* the diet (Melendez-Martinez, 2019). One of the most popular applications of saffron in food is as a colorant, with the coloring effect attributed to crocetin and crocin (Bagur et al., 2018; Bian et al., 2020). Crocetin is a lipophilic carotenoid and crocin is the hydrophilic diester of crocetin with gentiobiose (**Figure 1**). Both compounds have been shown to exhibit a number of biological properties, such as anti-oxidative, anti-inflammatory, anti-lipidemic and anti-tumor activities, and have potential health benefits by modifying different disease processes, including in cardiovascular diseases, metabolic syndromes, ocular disorders and cancer (Alavizadeh and Hosseinzadeh, 2014; Bukhari et al., 2018; Hashemi and Hosseinzadeh, 2019).

In comparison to their anti-hypoxic and anti-tumor effects, only a few previous studies have investigated the effects of crocetin and crocin on angiogenesis. One study reported that crocetin inhibited VEGF-induced tube formation in a co-culture model of human umbilical vein endothelial cells (HUVECs) and fibroblasts, and in a similar fashion inhibited the proliferation and migration of human retinal microvascular endothelial cells (HRMECs) (Umigai et al., 2012). In another study, crocin inhibited HUVEC proliferation and decreased CD34 expression (a marker for endothelial cell differentiation) in tumor tissues in mice (Chen et al., 2019). A previous study also found that crocetin promoted angiogenesis by increasing the cell viability of HUVECs (Nasirzadeh et al., 2019). Although the angiogenic effects of crocetin and crocin in different experimental models have been investigated, their interaction *in vivo*, effective concentrations, and modes of action still need to be studied and compared systematically. In addition, crocetin and crocin have recently been shown to display microtubule-targeting properties that inhibit tubulin assembly and suppress the migration and proliferation of cancer cells (Hire et al., 2017; Sawant et al., 2019; Colapietro et al., 2020). Many microtubule-targeting agents (MTA) are also highly anti-angiogenic due to their abilities to disrupt microtubule dynamics, which play key roles in endothelial cell motility during angiogenic sprouting (Dumontet and Jordan, 2010). However, it is not clear whether crocetin and crocin can inhibit endothelial cell motility or sprouting angiogenesis, nor the difference between them in these respects.

Angiogenesis is a highly regulated process of new blood vessel growth from pre-existing ones. Normal angiogenesis has fundamental roles in physiological conditions, such as wound healing and tissue regeneration, but excessive angiogenesis promotes tumorigenesis and ocular disorders such as age-related macular degeneration (AMD) (Potente et al., 2011; Fallah et al., 2019). AMD is characterized by choroidal neovascularization (CNV), wherein abnormal proliferating blood vessels from the choroidal layer invade the overlaying retina. Vascular endothelial growth factor (VEGF) is secreted in response to oxidative stress and plays important roles in the development of CNV (Ambati and Fowler, 2012). VEGFs are key inducers of angiogenesis that bind with high affinity to receptor tyrosine kinases (VEGFRs), with VEGFA and VEGFR2 being the principal ligand and signaling receptor, respectively, in vascular endothelial cells. The signal transduction network initiated by the VEGFA-VEGFR2 ligand-receptor system leads to the activation of various downstream pathways that play a crucial role in regulating endothelial cell proliferation, survival and migration in the process of angiogenesis (Simons et al., 2016). Anti-VEGF agents are currently used for the treatment of CNV in AMD. Interestingly, a recent study showed that saffron extract ameliorated the retinal degenerative processes in AMD patients, possibly through neuroprotective activities (Di Marco et al., 2019), while another study showed that crocetin prevented retinal pigment epithelia (RPE) from incurring oxidative stress-

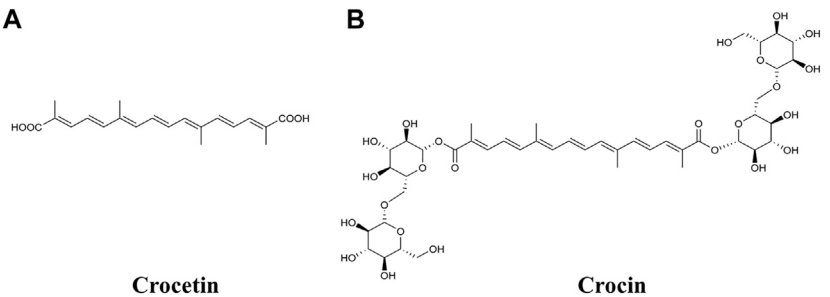

FIGURE 1 | Chemical structures of **(A)** crocetin and **(B)** crocin.

induced damage and might halt or delay AMD disease progression (Karimi et al., 2020). Additionally, lutein (another carotenoid) has been recommended as a health supplement for AMD patients by the NIH (Melendez-Martinez, 2019). A prospective follow-up study (conducted over two decades) found that the incidence of advanced AMD could be reduced by intake of catenoids (Wu et al., 2015). Compared to lutein, AMD patients could benefit from saffron supplementation to slow down AMD progression (Di Marco et al., 2019). Therefore, it is meaningful to investigate if crocetin and crocin can inhibit VEGF-induced angiogenesis; this will provide insight facilitating the discovery and development of new agents for the treatment of AMD.

In the present study, we determined the effective dose ranges of crocetin and crocin for inhibiting sprouting angiogenesis in *Tg(fli1:EGFP)* zebrafish. Since orally administered crocin was previously reported to be transformed into crocetin in rat (Zhang et al., 2017), we also examined the metabolism of crocetin and crocin in zebrafish by using high-performance liquid chromatography (HPLC). Furthermore, we investigated the underlying molecular mechanisms of the anti-angiogenic effects of crocetin and crocin in HUVECs *in vitro*.

MATERIALS AND METHODS

Ethics Statement

All animal experiments were conducted according to the ethical guidelines of ICMS, University of Macau and the protocol was approved by ICMS, University of Macau (UMARE-303-2017)

Chemicals, Regents, Cell Lines and Animals

Crocetin and crocin (purity by HPLC ≥98.0%) were purchased from Sichuan Weikeqi Biotech Co., Ltd (Sichuan, P.R. China). Crocetin and crocin were dissolved in dimethylsulfoxide (DMSO) as 10 mM and 100 mM stock solution, respectively. All of the stock solutions were stored at −20°C and diluted into different concentrations in appropriate assay media as required.

Kaighn's modification of Han's F12 medium (F-12 K), fetal bovine serum (FBS), penicillin-streptomycin (P/S), phosphate-buffered saline (PBS) and 0.25% (w/v) trypsin/1 mM EDTA were purchased from Invitrogen (Carlsbad, CA, United States). Endothelial cell growth supplement (ECGS), heparin, gelatin and dimethyl sulfoxide (DMSO) were purchased from Sigma-Aldrich Co. (St. Louis, MO, United States). Cell Proliferation Kit II (XTT) was obtained from Roche, Mannheim, Germany. VEGF was obtained from R&D Systems (Minneapolis, MN, United States). Growth factor reduced (GFR) Matrigel™ was supplied by BD Biosciences (Bedford, MA, United States). VEGF receptor (VEGFR) tyrosine kinase inhibitor II (VRI) was obtained from CalbioChem (Merck, Germany) and SU5416 was obtained from Sigma Aldrich Co. The following antibodies were used: ERK1/2 (Cell Signaling Technology, Danvers, MA, United States; Cat# 9102S), phospho-ERK1/2 (Thr202/Tyr204) (Cell Signaling Technology; Cat# 9101S), SRC (Cell Signaling Technology; Cat# 2109S), phospho-SRC (Tyr527) (Cell Signaling Technology; Cat# 2105S), MEK (Cell Signaling Technology; Cat# 9122L), phospho-MEK (Ser217/221) (Cell Signaling Technology; Cat# 9121S), FAK (Cell Signaling Technology; Cat# 3285S), phospho-FAK (Tyr576/577) (Cell Signaling Technology; Cat# 3281S), VEGFR2 (Cell Signaling Technology; Cat# 2472S), phospho-VEGFR2 (Tyr1175) (Cell Signaling Technology; Cat# 2478L) and GAPDH (Cell Signaling Technology; Cat# 2118L). The HPLC-grade methanol, formic acid and acetonitrile used in the HPLC analysis were provided by Merck (Darmstadt, Germany).

HUVECs were obtained from Invitrogen. Transgenic zebrafish *Tg(fli1:EGFP)* expressing enhanced green fluorescent protein (EGFP) under the control of fli1 promoter were provided by the Zebrafish Information Network (ZFIN, Eugene, OR, United States).

Maintenance of Zebrafish and Their Embryos

Transgenic zebrafish *Tg(fli1:EGFP)* and wild-type zebrafish were maintained as described in the Zebrafish Handbook. Adult zebrafish were kept in a controlled environment at 28.5°C, under a 14 h light/10 h dark cycle. They were fed general tropical fish food once daily and live brine shrimp twice daily. Zebrafish embryos were generated by natural pairwise mating and collected to be raised in embryo media at 28.5°C in an incubator. Dead and unfertilized embryos were picked out at 4 hours post fertilization (hpf), and embryos were distributed into a multi-plate with 8–12 embryos in each group depending on the assay at 24 hpf.

Zebrafish Embryo Morphological Observations

Normally developing *Tg(fli1:EGFP)* zebrafish embryos were digested with 1 mg/ml of protease at 24 hpf, and then distributed into a 24-well plate with 10 embryos per group. Each group was incubated with 1 ml embryo water containing different concentrations of compounds for an additional 48 h. Embryos receiving DMSO (0.1%) served as vehicle control, and those receiving 50 ng/ml of VRI served as a positive control. The subintestinal vessels (SIVs) of embryos were observed and imaged at 72 hpf under an Olympus Spinning Disk Confocal Microscope System (IX81 Motorized Inverted Microscope [w/ZDC], IX2 universal control box, X-cite series 120, DP71 CCD Camera; Olympus, Tokyo, Japan). Images were captured at 40× and 100× magnifications. The total area (A) of SIVs was quantified with ImageJ (NIH, Bethesda, MD, United States) and the SIV inhibition rate was calculated using the following formula:

$$\textbf{SIV Inhibition}\% = 1 - \frac{\mathbf{A\,(Drug\ treatment)}}{\mathbf{A\,(Vehicle)}} \times 100\%$$

Metabolic Analysis of Zebrafish Larvae by HPLC

Tg(fli1:EGFP) zebrafish embryos were digested with 1 mg/ml of protease, and then distributed into a 12-well plate with 30

embryos per group in 24 hpf. Zebrafish larvae were treated with incubation medium (vehicle control), crocetin (20 μM) and crocin (100 μM) for 48 h and then collected to determine the metabolism of crocin and crocetin. After washing three times with Milli-Q water, zebrafish larvae were homogenized with 100 μL methanol in a 1.5 ml centrifuge tube. All samples were centrifuged at 15,000 g for 15 min, and the supernatants were obtained and subsequently subjected to HPLC analysis with a XBridge™ C-18 column (5 μm, 4.6 × 250 mm). The column temperature was set at 30°C and the injection volume was 10 μL. By comparison with and optimization based on published studies, the detection wavelength was selected at 440 nm (Chryssanthi et al., 2011; Mary et al., 2016). The mobile phase consisted of 0.1% formic acid in water (A) and acetonitrile (B); the flow rate was set at 1 ml/min. A gradient elution program was set as follows: 0–9 min, 20-50% B; 9–11 min, 50–70% B; 11–20 min, 70–95% B; 20–24 min, 95% B; 24–30 min, 95-20% B at a flow rate of 1.0 ml/min.

Cell Culture

HUVECs were cultured in F-12K medium supplemented with 100 g/ml heparin, 30 g/ml ECGS, 10% FBS and 1% P/S at 37°C in a humidified atmosphere with 5% CO_2 (v/v). Early passages (3–7 passages) were used in all assays.

Cell Viability Assay

HUVECs (1×10^4 cells/ml) were seeded into 96-well plate in F-12K complete medium for 24 h for attachment. Then, the cells were treated with various concentrations of crocetin and crocin in low serum media (0.5% FBS) for 24 h. Cells receiving 0.1% DMSO served as vehicle control. Cell viability was assessed by using XTT assay, as described previously (Lam et al., 2012). Absorbance was measured using a Microplate Reader (Molecular Devices, San Jose, CA, United States) at wavelengths of 490 and 650 nm. For each compound, three independent experiments were conducted.

In Vitro Wound Healing Assay

HUVECs in growth medium were seeded into 24-well plates and grown to confluence. A wound area was created on the monolayer cells by scratching with 200 μL pipette tips. Non-adherent cells were removed by washing with PBS, and high serum (10% FBS) medium containing various concentrations of compounds, 0.1% DMSO (vehicle control) and SU5416 of 10 μM (positive control) was added to each well. After 20 h incubation, cells were washed with PBS. Images were taken at 0 and 20 h independently using an inverted light microscope (IX73 Motorized Inverted Microscope; Olympus). Images were analyzed by ImageJ, which is able to analyze the ability for cell migration by calculating the wound area. The distance migrated was calculated and analyzed by Image Pro-Plus 6.0. The values were observed from three randomly selected fields. The relative inhibition rate was expressed relative to the vehicle control group.

In Vitro Capillary-Like Tube Formation Assay

Capillary-like tube formation assay was performed using HUVECs as described previously (Li et al., 2020). GFR Matrigel was thawed at 4°C overnight. A pre-chilled 96-well plate was coated with 50 μL Matrigel (for each well) and incubated at 37°C for 30 min for solidification. HUVECs resuspended and diluted at a density of 1×10^4 per well, in low serum (0.5% FBS) F-12K medium containing the indicated concentrations of agents, were seeded onto the Matrigel-coated 96-well plate and incubated at 37°C. After 6 h, capillary-like tubes were formed in the vehicle control group; then, cells were stained with 1 mM Calcein AM (Life Technologies, Carlsbad, CA, United States) for 30 min at 37°C. Images were captured at 4× magnification under a fluorescent inverted microscope (IX73 Motorized Inverted Microscope; Olympus). Capillary-like tube formation was quantified by measuring tube length in three randomly selected fields by ImageJ.

Western Blot Assay

HUVECs were seeded in 6-well plates and incubated overnight for confluence. After starving in low serum (0.5% FBS) F-12K medium for 2 h, HUVECs were treated with various concentrations of compounds, 0.1% DMSO and SU5416 (10 μM) for 4 h before stimulating with 50 ng/ml VEGF for 15 min. Then, cells were rinsed with PBS and lyzed in RIPA buffer with the addition of cocktail and PMSF. The concentration of protein extracts was quantified with a BCA Protein Kit according to the protocol described by the manufacturer. Protein (30 μg) was denatured for 5 min at 95°C and subjected to 10% SDS-PAGE. After electrically transferring the proteins to PVDF membranes, they were blocked with 5% non-fat milk in TBS-0.1% Tween 20 (TBST) for 1 h at room temperature, and then incubated with primary antibodies of ERK1/2, phospho-ERK1/2, FAK, phospho-FAK, MEK, phospho-MEK, SRC, phospho-SRC, VEGFR2, phospho-VEGFR2, and GAPDH at 4°C overnight. After washing with TBST, membranes were incubated with horseradish peroxidase-conjugated goat anti-rabbit antibody (Beyotime, Shanghai, China) for 1 h at room temperature. After repeated washing with TBST, immunoreactive bands of proteins were visualized using an ECL advanced Western blotting detection kit. Images of the protein bands were taken using Image Lab (Bio-Rad, Hercules, CA, United States). The density of each band was measured by Bio-Rad Image 3.0, and the ratios of phosphorylated protein/total protein were calculated in corresponding bands from the same blot.

Molecular Docking Analysis

Molecular docking was employed to explore molecular interactions between VEGFR2 and crocetin or crocin. The X-ray crystallography structure of VEGFR2 (PDB ID: 5EW3) (Bold et al., 2016) was retrieved from the RCSB Protein Data Bank (http://www.rcsb.org/pdb). Co-crystallized ligand and crystal water molecules were removed from the protein structure, and the nonpolar hydrogen atoms were added. A gridbox was created to enclose VEGFR2, allowing us to find the most suitable binding site of crocetin or crocin. The best docking results were selected based on their estimated protein–ligand complex binding free energy and are presented in the present study. PyMOL 1.8 was

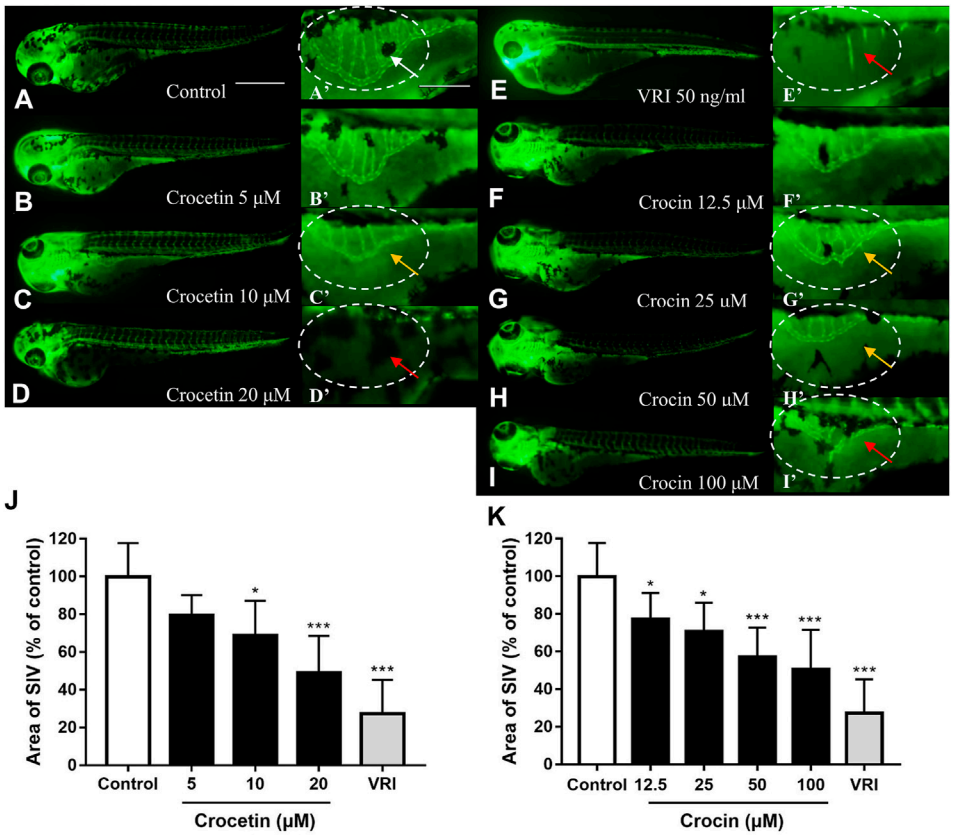

FIGURE 2 | Crocetin and crocin inhibited SIV formation in *Tg(fli1:EGFP)* zebrafish embryos. Zebrafish embryos at 24 hpf were treated by **(A,A')** 0.1% DMSO (Control) **(E,E')** 50 ng/ml VRI, **(B-D,B'-D')** crocetin, or **(F–I,F'–I')** crocin for 48 h. **(A'–I')** Magnified views (100× magnification) of the panels labelled A to I (40× magnification). Mature SIVs are indicated by white arrows. Moderately defective SIVs are indicated with yellow arrows and severely defective SIVs are indicated with red arrows (J and K) Quantification of the total area of SIVs reduced by crocetin and crocin. Data are percentages of the control, measured as means ± SD (10 zebrafish embryos per well from three time-independent experiments, n = 3). Scale bar = 200 μm. Statistical analysis was performed by one-way ANOVA followed by the Dunnett's test. *p<0.05 and ***p<0.001 versus control group.

used to analyze and visualize the molecular interactions between each compound and VEGFR2 (Salentin et al., 2015).

Data and Statistical Analysis

All values are presented as mean ± SD of three independent experiments. Data were analyzed by GraphPad Prism 7.0 (GraphPad Software Inc., La Jolla, CA, United States). The statistical significance of data was evaluated using one-way ANOVA followed by Dunnett's multiple comparison test. p values less than 0.05 were considered statistically significant.

RESULTS

Crocetin and Crocin Exhibited Anti-angiogenic Effects in *Tg(fli1:EGFP)* Zebrafish

Transgenic zebrafish *Tg(fli1:EGFP)* embryos showing green fluorescent protein expression in vascular endothelial cells under the control of promoter fli1 (Lawson and Weinstein, 2002) were used to investigate the effects of crocetin and crocin on angiogenesis *in vivo*. The process of SIV formation angiogenesis in zebrafish embryo is widely used as a visual guide when inspecting and evaluating of pro- and anti-angiogenic agents. Zebrafish embryos (24 hpf) were incubated with crocetin or crocin for 48 h, and the structure of SIVs was examined. As shown in **Figure 2A'**, at 72 hpf the vascular plexus of SIVs formed a smooth basket-like structure arranged in an orderly manner in the control group. The crocetin and crocin treatments significantly reduced the vasculature formation of SIVs (indicated by yellow arrows in **Figures 2C',G',H'**). At higher concentrations of crocetin (20 μM) and crocin (100 μM), the structure of the vascular plexus became defective or nearly absent (indicated by red arrows in **Figures 2D',I'**). Quantification of the total area of SIVs showed that both crocetin and crocin significantly reduced the formation of SIVs in a concentration-dependent manner, and the maximal effects were comparable to VRI, a strong VEGFR inhibitor that greatly inhibits SIVs angiogenesis (Li et al., 2014).

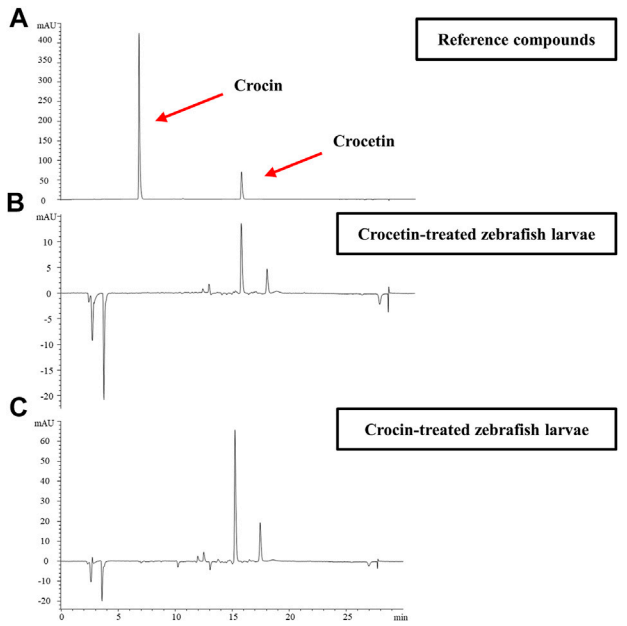

FIGURE 3 | Representative HPLC profiles for **(A)** reference compounds of crocetin and crocin **(B)** Compounds detected in zebrafish larvae homogenates collected within 72 hpf after crocin treatment (100 μM) **(C)** Compounds detected in zebrafish larvae homogenates collected within 72 hpf after crocetin treatment (20 μM).

Metabolism of Crocetin and Crocin in Zebrafish Larvae

We further investigated the metabolism of crocetin and crocin in zebrafish larvae by using HPLC. **Figure 3A** shows that the retention times of crocetin and crocin were 6.570 and 15.223°min, respectively with regard to the reference compound profiles. Interestingly, after the administration of crocin to zebrafish larvae, the peak for crocin could not be detected, although the peak for crocetin was detected (**Figure 3B**). In the case of crocetin administration, only crocetin was detected (**Figure 3C**). This result suggested that a conversion process between crocetin and crocin existed in the zebrafish larvae. Given that crocetin is recognized as the bio-active compound produced by converting crocin (Xi et al., 2007; Zhang et al., 2017), we speculated that crocetin was the active compound responsible for the anti-angiogenic effects in zebrafish.

Effects of Crocetin and Crocin on Endothelial Cell Viability

To evaluate the effects of crocetin and crocin on endothelial cell viability, HUVECs were treated with increasing concentrations of crocetin (0.2, 0.3, 0.5, and 1 mM) and crocin (1, 2, and 4 mM) for 24 h followed by assessment with XTT assay. Crocetin inhibited cell viability in a concentration-dependent manner with an IC_{50} of 372.6 μM (**Figure 4A**), whereas crocin showed no obvious inhibitory effect up to 4 mM (**Figure 4B**).

Crocetin and Crocin Inhibited Migration and Tube Formation in HUVECs

Angiogenesis is a complex process that involves endothelial cell migration and alignment to form tubular structures. We determined the effects of crocetin and crocin on endothelial cell migration and capillary-like formation using the wound healing assay and tube formation Matrigel model. **Figures 5A,B** showed that there was significant migration of HUVECs to the scraped area in the vehicle control group 20 h after wounding. Crocetin caused 18.8, 34.8, and 39.2% reductions in HUVEC migration at 10, 20, and 40 μM, respectively. Similarly, crocin caused 15.5%, 59.7%, and 72.3% reductions in HUVEC migration at 100, 200, and 400 μM, respectively. **Figures 5C,D** showed that when HUVECs were cultured on Matrigel in the vehicle control, they aligned and formed capillary-like tube structures after 6 h, and both crocetin and crocin inhibited the morphogenetic changes in tube formation in HUVECs. Crocetin caused 38.6, 48.8, and 70.1% reductions in tube length at 10, 20, and 40 μM, respectively. Similarly, crocin caused 39.3, 51.6, and 71.8% reductions in tube length at 100, 200, and 400 μM, respectively. Statistical analysis of the quantitative measurements showed that both crocetin and crocin induced significant reductions in HUVECs migration and tube formation in concentration-dependent manners. The effects of crocetin and crocin were comparable to SU5416 (a selective inhibitor of VEGFR2) (Litz et al., 2004).

Crocetin and Crocin Inhibited the Activation of Key Proteins Involved in Angiogenesis Signaling in HUVECs

To investigate the possible mechanisms underlying the anti-angiogenic effects of crocetin and crocin in HUVECs, protein expression levels were determined for several key proteins involved in the regulation of angiogenesis by Western blot. As shown in **Figure 6**, crocetin (10, 20, and 40 μM) and crocin (100, 200 and 400 μM) concentration-dependently inhibited the upregulation in protein expression levels of p-VEGFR2 induced by VEGF (50 ng/ml), as well as the downstream signaling kinases p-SRC, p-FAK, p-MEK, and p-ERK. Notably, the two pathways (VEGFR2/MEK/ERK and VEGFR2/MEK/ERK) showed different sensitivity to the inhibitory effects of crocetin and crocin. At 10 μM, crocetin had no effect on MEK phosphorylation; however, reduced the protein levels of p-SRC, p-FAK, and p-ERK. And crocetin reduced the protein levels of p-SRC and p-FAK more effectively than those of p-ERK at 40 μM. In the case of crocin, high concentrations significantly reduced p-SRC, p-FAK, and p-MEK, and to a lesser extent p-ERK. The VEGFR2/SRC/FAK pathway is mainly involved in focal adhesion turnover, cell shape and migration, and the VEGFR2/MEK/ERK pathway is mainly involved in endothelial gene transcription and proliferation (Simons et al., 2016; Fallah et al., 2019). Thus, these results suggested that crocetin and crocin might effectively inhibit angiogenesis by inhibiting endothelial cytoskeleton organization and cell migration *via* regulation of VEGFR2/SRC/FAK, and to a lesser extent, VEGFR2/MEK/ERK signaling.

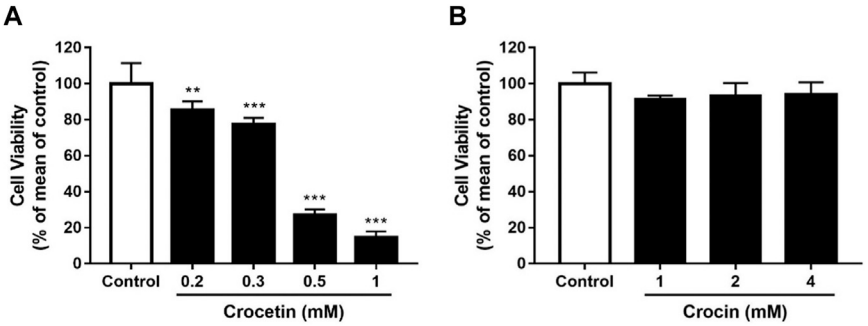

FIGURE 4 | Cytotoxicity of crocetin and crocin on HUVECs (A) HUVECs were treated with different concentrations of crocetin (0.2, 0.3, 0.5, and 1 mM) and **(B)** crocin (1, 2 and 4 mM) for 24 h and examined by XTT assay. The IC_{50} value of crocetin **(A)** is 372.6 μM. Data are means ± SD of three independent experiments ($n = 3$) as a percentage of control. Statistical analysis was performed by one-way ANOVA followed by Dunnett's test. **p<0.01; ***p<0.001 versus control group.

Molecular Docking Studies of Crocetin and Crocin With VEGFR2

Since crocetin and crocin down-regulated p-VEGFR2 and its downstream signaling kinases differently, molecular docking studies were carried out to investigate the binding sites between crocetin or crocin and VEGFR2. The binding site of VEGFR2 was defined by a co-crystallized compound (AAL993) (Bold et al., 2016). Crocetin was well docked with the binding site of VEGFR2 (**Figure 7A**) through hydrophobic interactions and a hydrogen bond, with an affinity of −8.6 kcal/mol. In addition, crocetin was trapped in a hydrophobic pocket, which was composed of Leu 840, Ala 866, Val 899, Val 916, Phe 918, Leu 1035 and Phe 1047. A hydrogen bond was also generated between crocetin and the key residue Asp 1046. In comparison, crocin bound to a different site than the co-crystallized compound (AAL993) *via* hydrophobic interactions and hydrogen bonds, with an affinity of −8.4 kcal/mol (**Figure 7B**). Although the computed Gibbs free energy values of crocetin and crocin were similar, their predicted binding sites to VEGFR2 were different. It appears that crocin did not have a stable interaction with VEGFR2. These results suggested that crocetin showed more ability to bind with VEGFR2 than crocin, which might explain their different anti-angiogenic effects.

DISCUSSION

Saffron is widely used as a natural spice against many diseases (Shahi et al., 2016). Since crocetin and crocin are two important carotenoids derived from saffron and have been used for centuries, it is useful to investigate and compare the difference in their therapeutic values and biological effects. The present study represented the first detailed investigation of the anti-angiogenic activities of crocetin and crocin, and used transgenic *Tg(fli1:EGFP)* zebrafish embryos *in vivo* and endothelial cell model HUVECs *in vitro*.

We evaluated the effects of crocetin and crocin by using a *Tg(fli1:EGFP)* zebrafish model *in vivo*, which allowed for direct observation of angiogenesis in real-time (Lawson and Weinstein, 2002; Gong et al., 2016). Our group has previously identified several natural compounds that exhibited anti-angiogenic effects by using the zebrafish model, such as indirubin (Alex et al., 2010), citrus flavonoids (Lam et al., 2012) and an andrographolide derivative (Li et al., 2020). In the present study, we observed that there was no obvious toxicity in zebrafish embryos treated with crocetin and crocin (**Supplementary Figure S1**). More importantly, crocetin and crocin inhibited SIV formation in a concentration-dependent manner (**Figure 2**). Moreover, the effective concentrations of crocetin (5, 10 and 20 μM) were lower than those of crocin (12.5, 25, 50 and 100 μM), which led us to investigate whether the different anti-angiogenic responses between crocetin and crocin might be caused by their metabolic characteristics. Therefore, we evaluated the metabolism of crocetin and crocin in zebrafish larvae after the drug administration using HPLC. It was interesting to note that there was a conversion between crocetin and crocin in zebrafish *in vivo* (**Figure 3**). This finding was in agreement with a previous study indicating that crocetin might be the active metabolite of crocin in rats (Zhang et al., 2017). Therefore, we postulated that crocetin was the active metabolite of crocin responsible for inducing the anti-angiogenic effect in zebrafish.

Given the differences in metabolism and anti-angiogenic activities of crocetin and crocin in zebrafish, their mechanisms for inhibiting angiogenesis were further investigated in HUVECs *in vitro*. Several recent studies suggested that saffron extract and/or crocetin might halt or delay disease progress in AMD. It has been shown that saffron extract was effective at ameliorating the retinal degenerative processes in AMD patients, possibly through neuroprotective activities (Di Marco et al., 2019), while crocetin prevented RPE from incurring oxidative stress-induced damage (Karimi et al., 2020). In addition, clinical studies showed that saffron supplementation could improve retinal function in AMD patients (Falsini et al., 2010; Piccardi et al., 2012). AMD is characterized by CNV, wherein VEGF is secreted in response to oxidative stress and induces abnormal angiogenesis from the choroidal layer to the overlaying retina (Ambati and Fowler, 2012). Currently, anti-VEGF therapies with bevacizumab (monoclonal anti-VEGF antibody) and pegaptanib (anti-VEGF aptamer) are FDA-approved for treating AMD (Solomon et al., 2014). Our result showed that crocetin (10, 20 and 40 μM) and crocin (100, 200 and 400 μM) were effective anti-angiogenic agents

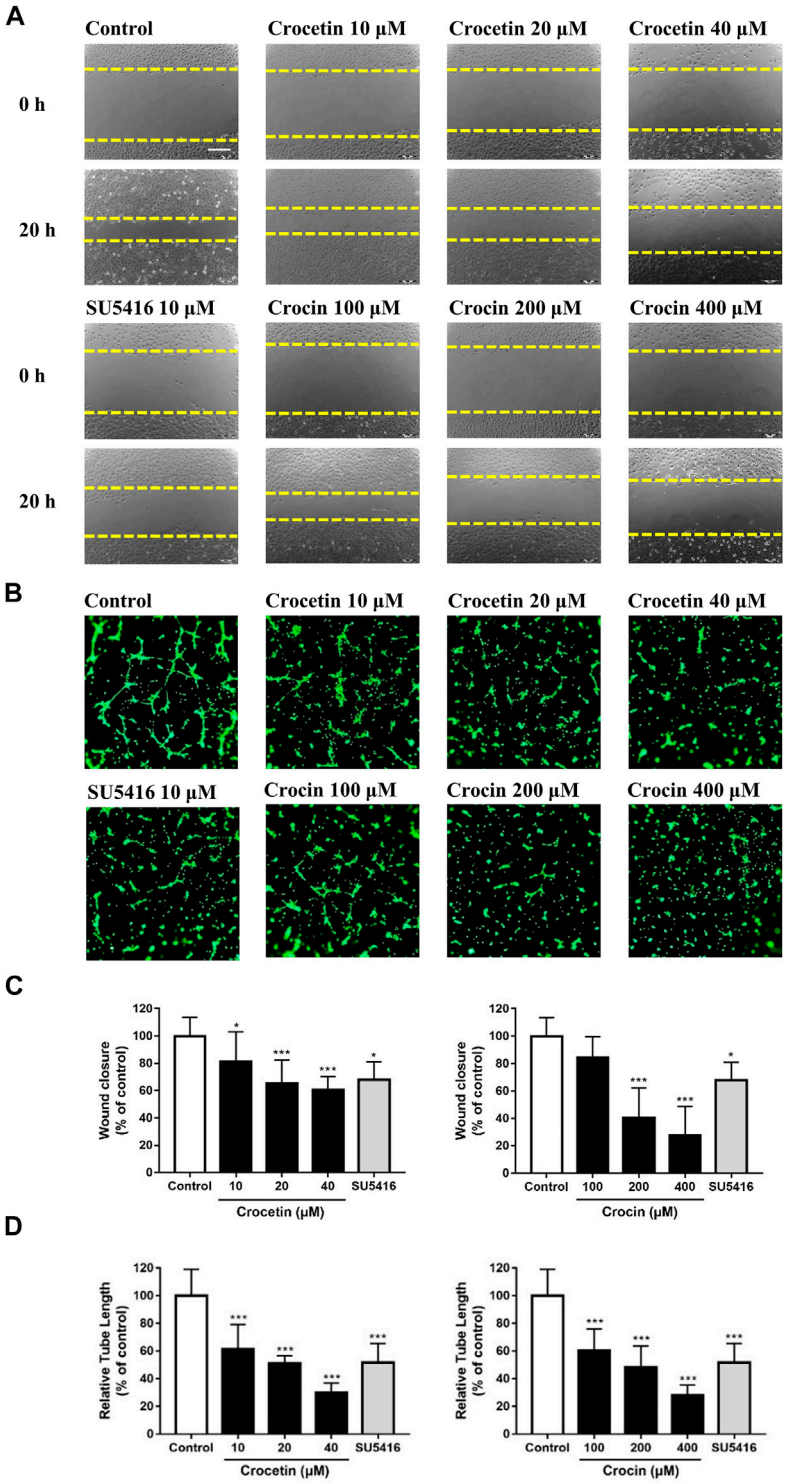

FIGURE 5 | Crocetin and crocin inhibited endothelial cell migration and capillary-like tube formation. **(A)** Wound healing assay for HUVEC migration after 20 h of incubation with vehicle control or drug treatments. **(B)** The migratory ability was evaluated by measuring the mean length of the scraped area of each well and comparing it to the control group. Yellow dashed lines indicated the wound edges. **(C)** Morphological features of the capillary-like tube formation of HUVECs in Matrigel after 6 h of incubation with vehicle control or drug treatments. **(D)** The tube formation ability was evaluated by measuring the total tube length of HUVECs and comparing it to the control group. Scale bar = 200 μm. Data are means ± SD of three independent experiments. Statistical analysis was performed by one-way ANOVA followed by Dunnett's test. *p<0.05 and ***p<0.001 versus control group.

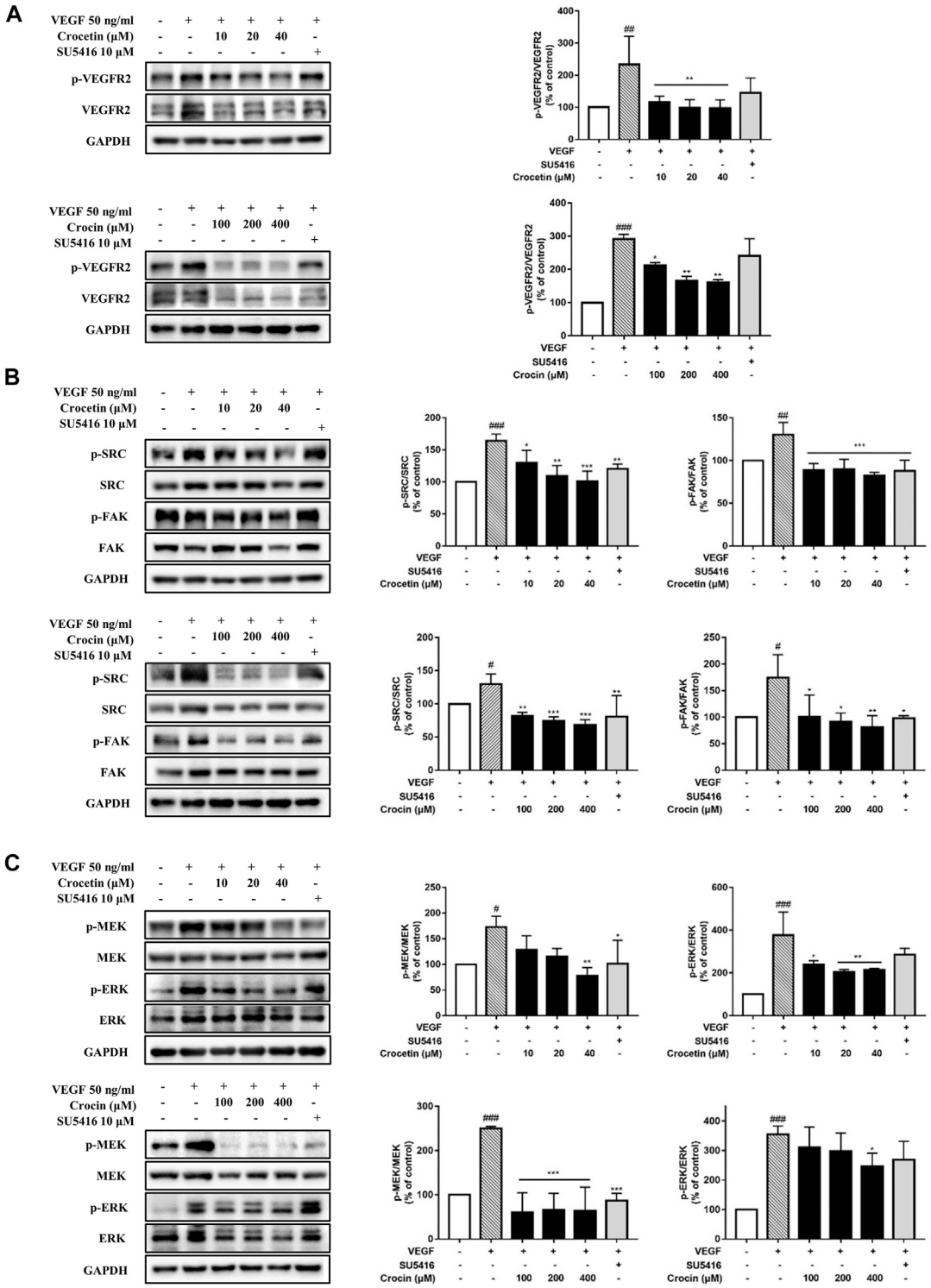

FIGURE 6 | Crocetin and crocin inhibited the activation of VEGFR2 and its downstream signaling pathways. HUVECs were starved for 2 h and then pretreated with crocetin (10, 20 and 40 μM) or crocin (100, 200 and 400 μM) for 4 h before being stimulated by VEGF (50 ng/ml) for 15 min. Western blot assay was used for investigating the expression levels of the major proteins involved in VEGF-mediated angiogenesis signaling in HUVECs. Crocetin and crocin down-regulated the expression levels of **(A)** p-VEGFR2 **(B)** p-SRC and p-FAK, and **(C)** p-MEK and p-ERK. Protein expression levels were quantified by densitometry. Results are percentages relative to control; means ± SD of three independent experiments (n = 3) are shown. Statistical analysis was performed by one-way ANOVA followed by Dunnett's test. *p<0.05; **p<0.01 and ***p<0.001 versus VEGF treatment group. #p<0.05; ##p<0.01 and ###p<0.001 versus control group.

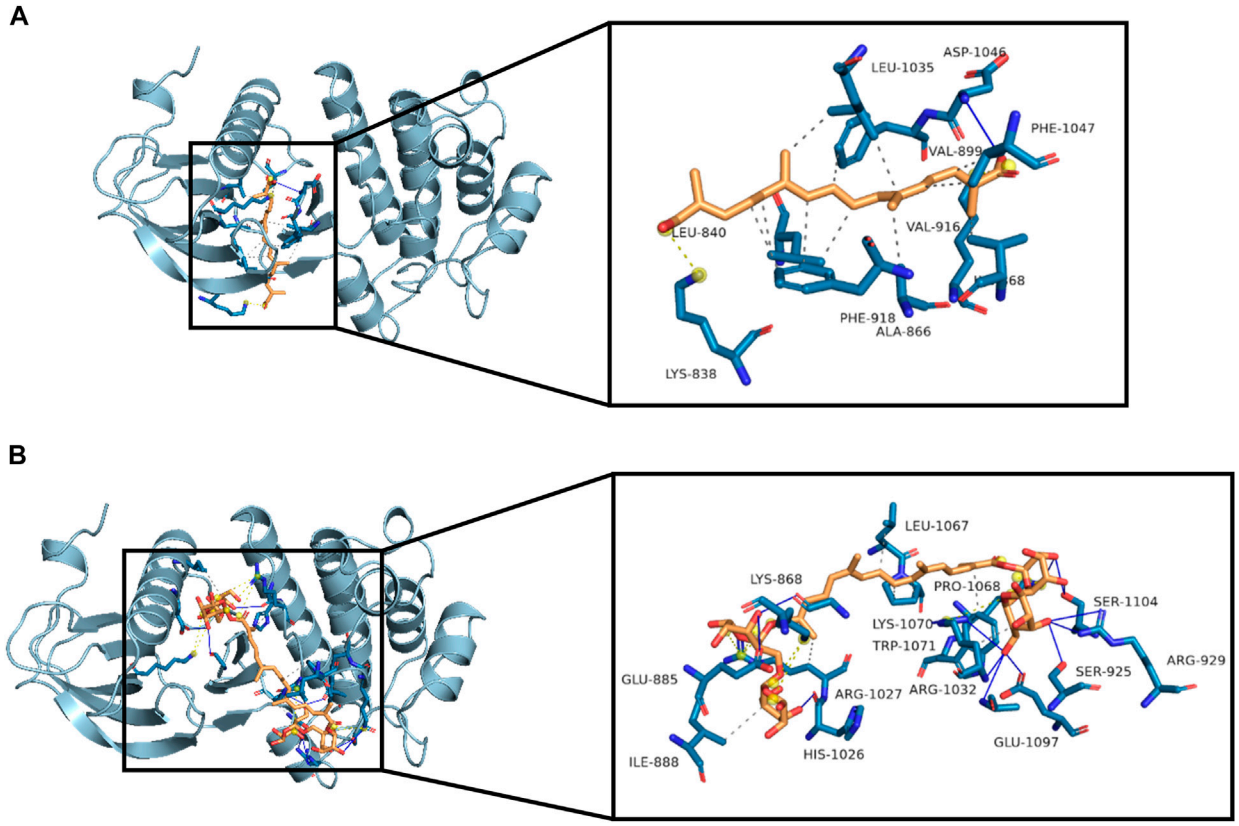

FIGURE 7 | Molecular interactions between crocetin or crocin with VEGFR2. Three-dimensional view of crocetin and crocin located in the binding site of VEGFR2 are shown in **(A)** and **(B)**, with affinities of −8.6 and −8.4 kcal/mol, respectively. Hydrophobic interactions (dashed lines), hydrogen bonds (blue lines) and important residues of the binding site are shown.

that significantly inhibited HUVEC migration in wound healing assay, as well as tube formation in a Matrigel model in a concentration-dependent manner (**Figure 5**). The cytotoxicity of crocetin (0.2 mM) was higher than that of crocin (>4 mM) in HUVECs (**Figure 4**). In line with our results, a previous study (Umigai et al., 2012) reported that crocetin inhibited proliferation and tube formation in a HUVEC and fibroblast co-culture. They also showed that crocetin inhibited VEGF-induced proliferation and migration of HRMECs *via* the inhibition of p38 activation (Umigai et al., 2012). Here, we demonstrated that crocetin and crocin inhibited VEGFR2 signaling and suppressed downstream p-SRC, p-FAK, p-MEK, and p-ERK activation in HUVECs (**Figure 8**), but we did not observe suppression of p38 (data not shown). In endothelial VEGF signaling networks, SRC and FAK are tyrosine kinases that play crucial roles in cytoskeletal reorganization, cell motility and migration, while MEK/ERK signaling is a well-studied pathway that mainly regulates endothelial proliferation among other important processes in angiogenesis, including survival, differentiation and migration (Simons et al., 2016; Fallah et al., 2019). Moreover, crosstalk between MEK/ERK and SRC/FAK is also observed in the regulation of VEGF-mediated angiogenesis (Hood et al., 2003). Activation of the ERK pathway by crocetin seems to be important for improving AMD; in a recent study (Karimi et al., 2020), crocetin prevented tert-butyl hydroperoxide (TBHP)-induced oxidative stress in RPE cells by activating the ERK pathway to preserve energy production pathways. It is not known if the SRC/FAK and MEK/ERK pathways are also modulated in HRMECs, and further studies with relevant cellular models are needed. More evidence from molecular docking studies indicated that crocetin had a more stable molecular interaction with VEGFR2 than crocin (**Figure 7**). Crocetin docked well with the binding site of VEGFR2 by forming an essential hydrogen bone with the residue Asp1046 (Guan et al., 2015), and generating a key hydrophobic interaction with the "gate keeper" residue (Val 916) of VEGFR2 (Bold et al., 2016).

An additional important result obtained in the present study on the anti-angiogenic effects of crocetin and crocin was that crocetin was more effective than crocin, because the effective concentrations of crocetin were lower than those of crocin. Moreover, crocetin showed more stable binding patterns than crocin. To understand the different effects of crocetin and crocin, their membrane permeability, caused by carboxyl or glycosyl groups at the ends of the backbone, should be considered (Bian et al., 2020). Crocetin showed better permeative ability by

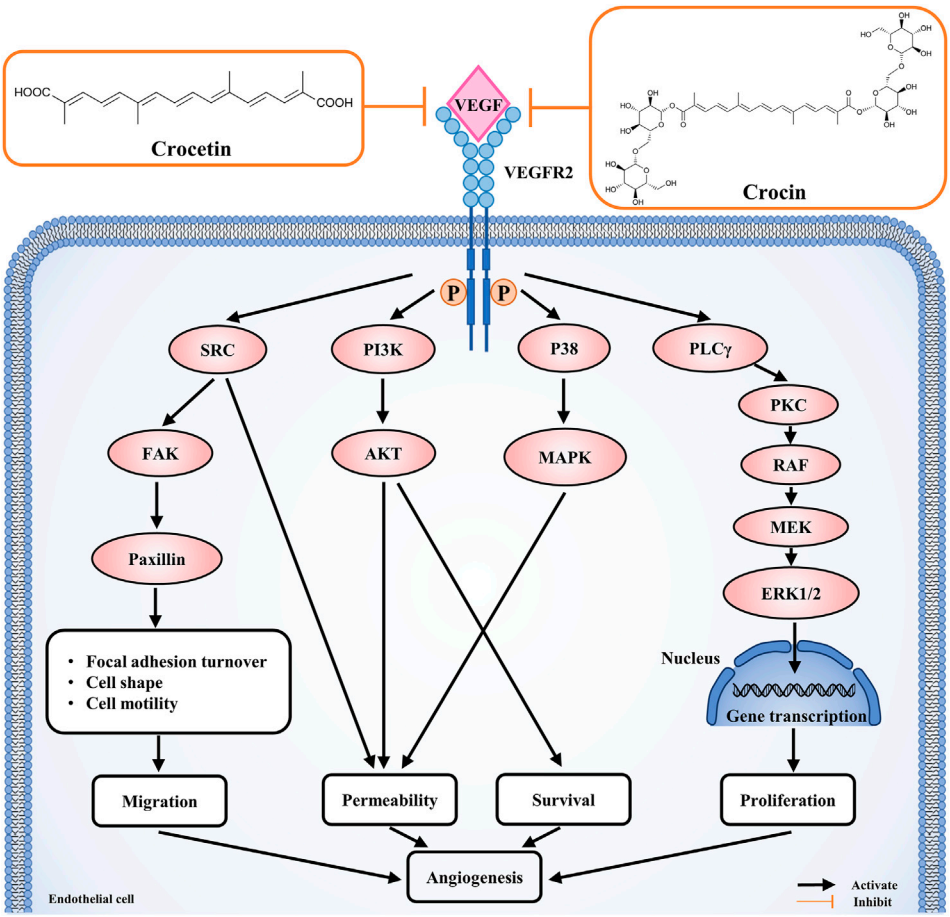

FIGURE 8 | Crocetin and crocin inhibited angiogenesis *via* the inhibition of VEGFR2 signaling and downstream SRC, FAK, MEK, ERK kinase activation.

penetrating intestinal mucosa, whereas crocin could not penetrate an intestinal model even at a concentration of 1000 mM (Lautenschlager et al., 2015). Accordingly, a pharmacokinetic study showed that crocin was hydrolyzed to crocetin through the gastro-intestinal tract, and then absorbed and detected in plasma (Xi et al., 2007). In addition, the structure-activity relationship of carotenoids (including crocetin and crocin) suggested that diverse terminal structures, such as electron-rich aromatic methyl substituent and the polyene chain structures, were responsible for the antioxidant activity of carotenoids (Kim et al., 2019). These findings, together with the fact that crocetin is more effective than crocin, suggesting that crocetin may act as an active compound with a stronger anti-angiogenic effect. However, further studies such as pharmacokinetic ones and studies of the structure-activity relationship, are needed to support this hypothesis.

Collectively, our findings provided strong evidence supporting the anti-angiogenic activities of crocetin and crocin, and indicated that crocetin had more anti-angiogenic and anti-VEGF therapeutic value for AMD.

DATA AVAILABILITY STATEMENT

The original contributions presented in the study are included in the article/**Supplementary Material**, further inquiries can be directed to the corresponding author.

ETHICS STATEMENT

Animal welfare and experimental procedures were conducted according to the ethical guidelines of ICMS, University of Macau and the protocol was approved by ICMS, University of Macau. (UMARE-303-2017).

AUTHOR CONTRIBUTIONS

CZ: Conceptualization, Methodology, Formal analysis, Writing-original Draft. H-TK: Methodology, Data curation, Investigation. YC: Investigation, Validation. GG: Investigation, Validation. MH: Writing-Review and Editing.

KS-W: Writing-Review and Editing. AD: Writing-Review and Editing. SL: Writing-Review and Editing, Supervision.

FUNDING

This work was supported by The Science and Technology Development Fund, Macau SAR (File no. 0058/2019/A1 and 0016/2019/AKP), and University of Macau (MYRG2019-00105-ICMS).

SUPPLEMENTARY MATERIAL

The Supplementary Material for this article can be found online at: https://www.frontiersin.org/articles/10.3389/fphar.2021.675359/full#supplementary-material

REFERENCES

Alavizadeh, S. H., and Hosseinzadeh, H. (2014). Bioactivity Assessment and Toxicity of Crocin: a Comprehensive Review. *Food Chem Toxicol.* 64, 65–80. doi:10.1016/j.fct.2013.11.016

Alex, D., Lam, I. K., Lin, Z., and Lee, S. M. Y. (2010). Indirubin Shows Anti-angiogenic Activity in an In Vivo Zebrafish Model and an In Vitro HUVEC Model. *J. Ethnopharmacology*. 131 (2), 242–247. doi:10.1016/j.jep.2010.05.016

Ambati, J., and Fowler, B. J. (2012). Mechanisms of Age-Related Macular Degeneration. *Neuron*. 75 (1), 26–39. doi:10.1016/j.neuron.2012.06.018

Bagur, M. J., Salinas, G. L. A., Jimenez-Monreal, A. M., Chaouqi, S., Llorens, S., Martinez-Tome, M., et al. (2018). Saffron: An Old Medicinal Plant and a Potential Novel Functional Food. *Molecules*. 23 (1), 30. doi:10.3390/molecules23010030

Bian, Y., Zhao, C., and Lee, S. M.-Y. (2020). Neuroprotective Potency of Saffron Against Neuropsychiatric Diseases, Neurodegenerative Diseases, and Other Brain Disorders: From Bench to Bedside. *Front. Pharmacol.* 11, 579052. doi:10.3389/fphar.2020.579052

Bold, G., Schnell, C., Furet, P., McSheehy, P., Brüggen, J., Mestan, J., et al. (2016). A Novel Potent Oral Series of VEGFR2 Inhibitors Abrogate Tumor Growth by Inhibiting Angiogenesis. *J. Med. Chem.* 59 (1), 132–146. doi:10.1021/acs.jmedchem.5b01582

Bukhari, S. I., Manzoor, M., and Dhar, M. K. (2018). A Comprehensive Review of the Pharmacological Potential of Crocus Sativus and its Bioactive Apocarotenoids. *Biomed. Pharmacother.* 98, 733–745. doi:10.1016/j.biopha.2017.12.090

Chen, S.-S., Gu, Y., Lu, F., Qian, D.-P., Dong, T.-T., Ding, Z.-H., et al. (2019). Antiangiogenic Effect of Crocin on Breast Cancer Cell MDA-MB-231. *J. Thorac. Dis.* 11 (11), 4464–4473. doi:10.21037/jtd.2019.11.18

Chryssanthi, D. G., Lamari, F. N., Georgakopoulos, C. D., and Cordopatis, P. (2011). A New Validated SPE-HPLC Method for Monitoring Crocetin in Human Plasma-Application after Saffron Tea Consumption. *J. Pharm. Biomed. Anal.* 55 (3), 563–568. doi:10.1016/j.jpba.2011.02.018

Colapietro, A., Mancini, A., Vitale, F., Martellucci, S., Angelucci, A., Llorens, S., et al. (2020). Crocetin Extracted from Saffron Shows Antitumor Effects in Models of Human Glioblastoma. *Int J Mol Sci.* 21 (2), 423. doi:10.3390/ijms21020423

Di Marco, S., Carnicelli, V., Franceschini, N., Di Paolo, M., Piccardi, M., Bisti, S., et al. (2019). Saffron: A Multitask Neuroprotective Agent for Retinal Degenerative Diseases. *Antioxidants*. 8 (7), 224. doi:10.3390/antiox8070224

Dumontet, C., and Jordan, M. A. (2010). Microtubule-binding Agents: a Dynamic Field of Cancer Therapeutics. *Nat. Rev. Drug Discov.* 9 (10), 790–803. doi:10.1038/nrd3253

Fallah, A., Sadeghinia, A., Kahroba, H., Samadi, A., Heidari, H. R., Bradaran, B., et al. (2019). Therapeutic Targeting of Angiogenesis Molecular Pathways in Angiogenesis-dependent Diseases. *Biomed. Pharmacother.* 110, 775–785. doi:10.1016/j.biopha.2018.12.022

Falsini, B., Piccardi, M., Minnella, A., Savastano, C., Capoluongo, E., Fadda, A., et al. (2010). Influence of Saffron Supplementation on Retinal Flicker Sensitivity in Early Age-Related Macular Degeneration. *Invest. Ophthalmol. Vis. Sci.* 51 (12), 6118–6124. doi:10.1167/iovs.09-4995

Gong, G., Lin, Q., Xu, J., Ye, F., Jiang, L., Liu, W., et al. (2016). *In vivo* SAR and STR Analyses of Alkaloids from Picrasma Quassioides Identify 1-Hydroxymethyl-8-Hydroxy-β-Carboline as a Novel Natural Angiogenesis Inhibitor. *RSC Adv.* 6 (12), 9484–9494. doi:10.1039/c5ra22391a

Guan, Y.-Y., Liu, H.-J., Luan, X., Xu, J.-R., Lu, Q., Liu, Y.-R., et al. (2015). Raddeanin A, a Triterpenoid Saponin Isolated from Anemone Raddeana, Suppresses the Angiogenesis and Growth of Human Colorectal Tumor by Inhibiting VEGFR2 Signaling. *Phytomedicine*. 22 (1), 103–110. doi:10.1016/j.phymed.2014.11.008

Hashemi, M., and Hosseinzadeh, H. (2019). A Comprehensive Review on Biological Activities and Toxicology of Crocetin. *Food Chem Toxicol* 130, 44–60. doi:10.1016/j.fct.2019.05.017

Hire, R. R., Srivastava, S., Davis, M. B., Kumar Konreddy, A., and Panda, D. (2017). Antiproliferative Activity of Crocin Involves Targeting of Microtubules in Breast *Cancer* Cells. *Sci. Rep.* 7, 44984. doi:10.1038/srep44984

Hood, J. D., Frausto, R., Kiosses, W. B., Schwartz, M. A., and Cheresh, D. A. (2003). Differential αv Integrin-Mediated Ras-ERK Signaling during Two Pathways of Angiogenesis. *J. Cel Biol.* 162 (5), 933–943. doi:10.1083/jcb.200304105

Karimi, P., Gheisari, A., Gasparini, S. J., Baharvand, H., Shekari, F., Satarian, L., et al. (2020). Crocetin Prevents RPE Cells from Oxidative Stress through Protection of Cellular Metabolic Function and Activation of ERK1/2. *Int J Mol Sci.* 21 (8), 2949. doi:10.3390/ijms21082949

Kim, D., Shi, G., Kim, Y., and Koo, S. (2019). Fast Assembly and High-Throughput Screening of Structure and Antioxidant Relationship of Carotenoids. *Org. Lett.* 21 (3), 714–718. doi:10.1021/acs.orglett.8b03915

Lam, I. K., Alex, D., Wang, Y.-H., Liu, P., Liu, A.-L., Du, G.-H., et al. (2012). *In vitro* and In Vivo Structure and Activity Relationship Analysis of Polymethoxylated Flavonoids: Identifying Sinensetin as a Novel Antiangiogenesis Agent. *Mol. Nutr. Food Res.* 56 (6), 945–956. doi:10.1002/mnfr.201100680

Lautenschläger, M., Sendker, J., Hüwel, S., Galla, H. J., Brandt, S., Düfer, M., et al. (2015). Intestinal Formation of Trans-crocetin from Saffron Extract (Crocus Sativus L.) and In Vitro Permeation through Intestinal and Blood Brain Barrier. *Phytomedicine*. 22 (1), 36–44. doi:10.1016/j.phymed.2014.10.009

Lawson, N. D., and Weinstein, B. M. (2002). *In vivo* imaging of Embryonic Vascular Development Using Transgenic Zebrafish. *Dev. Biol.* 248 (2), 307–318. doi:10.1006/dbio.2002.0711

Li, J., Li, F., Tang, F., Zhang, J., Li, R., Sheng, D., et al. (2020). AGS-30, an Andrographolide Derivative, Suppresses Tumor Angiogenesis and Growth In Vitro and In Vivo. *Biochem Pharmacol* 171, 113694. doi:10.1016/j.bcp.2019.113694

Li, S., Dang, Y. Y., Oi Lam Che, G., Kwan, Y. W., Chan, S. W., Leung, G. P. H., et al. (2014). VEGFR Tyrosine Kinase Inhibitor II (VRI) Induced Vascular Insufficiency in Zebrafish as a Model for Studying Vascular Toxicity and Vascular Preservation. *Toxicol Appl. Pharmacol.* 280 (3), 408–420. doi:10.1016/j.taap.2014.09.005

Litz, J., Warshamana-Greene, G. S., Sulanke, G., Lipson, K. E., and Krystal, G. W. (2004). The Multi-Targeted Kinase Inhibitor SU5416 Inhibits Small Cell Lung Cancer Growth and Angiogenesis, in Part by Blocking Kit-Mediated VEGF Expression. *Lung Cancer*. 46 (3), 283–291. doi:10.1016/j.lungcan.2004.05.005

Mary, T. A., Shanthi, K., Vimala, K., and Soundarapandian, K. (2016). PEG Functionalized Selenium Nanoparticles as a Carrier of Crocin to Achieve Anticancer Synergism. *RSC Adv.* 6 (27), 22936–22949. doi:10.1039/c5ra25109e

Melendez-Martinez, A. J. (2019). An Overview of Carotenoids, Apocarotenoids, and Vitamin A in Agro-Food, Nutrition, Health, and Disease. *Mol. Nutr. Food Res.* 63 (15), e1801045. doi:10.1002/mnfr.201801045

Nasirzadeh, M., Rasmi, Y., Rahbarghazi, R., Kheradmand, F., Karimipour, M., Aramwit, P., et al. (2019). CROCETIN PROMOTES ANGIOGENESIS IN

HUMAN ENDOTHELIAL CELLS THROUGH PI3K-AKT-ENOS SIGNALING PATHWAY. *Excli J.* 18, 936–949. doi:10.17179/excli2O19-1175

Piccardi, M., Marangoni, D., Minnella, A. M., Savastano, M. C., Valentini, P., Ambrosio, L., et al. (2012). A Longitudinal Follow-Up Study of Saffron Supplementation in Early Age-Related Macular Degeneration: Sustained Benefits to Central Retinal Function. *Evidence-Based Complement. Altern. Med.* 2012, 429124. doi:10.1155/2012/429124

Potente, M., Gerhardt, H., and Carmeliet, P. (2011). Basic and Therapeutic Aspects of Angiogenesis. *Cell.* 146 (6), 873–887. doi:10.1016/j.cell.2011.08.039

Salentin, S., Schreiber, S., Haupt, V. J., Adasme, M. F., and Schroeder, M. (2015). PLIP: Fully Automated Protein-Ligand Interaction Profiler. *Nucleic Acids Res.* 43 (W1), W443–W447. doi:10.1093/nar/gkv315

Sawant, A. V., Srivastava, S., Prassanawar, S. S., Bhattacharyya, B., and Panda, D. (2019). Crocin, a Carotenoid, Suppresses Spindle Microtubule Dynamics and Activates the Mitotic Checkpoint by Binding to Tubulin. *Biochem Pharmacol.* 163, 32–45. doi:10.1016/j.bcp.2019.01.023

Shahi, T., Assadpour, E., and Jafari, S. M. (2016). Main Chemical Compounds and Pharmacological Activities of Stigmas and Tepals of "red Gold"; Saffron. *Trends Food Sci. Technol.* 58, 69–78. doi:10.1016/j.tifs.2016.10.010

Simons, M., Gordon, E., and Claesson-Welsh, L. (2016). Mechanisms and Regulation of Endothelial VEGF Receptor Signalling. *Nat. Rev. Mol. Cel Biol.* 17 (10), 611–625. doi:10.1038/nrm.2016.87

Solomon, S. D., Lindsley, K., Vedula, S. S., Krzystolik, M. G., and Hawkins, B. S. (2014). Anti-vascular Endothelial Growth Factor for Neovascular Age-Related Macular Degeneration. *Cochrane Database Syst. Rev.* 8 (8), CD005139. doi:10.1002/14651858.CD005139.pub3

Umigai, N., Tanaka, J., Tsuruma, K., Shimazawa, M., and Hara, H. (2012). Crocetin, a Carotenoid Derivative, Inhibits VEGF-Induced Angiogenesis via Suppression of P38 Phosphorylation. *Curr Neurovasc Res.* 9 (2), 102–109. doi:10.2174/156720212800410830

Wu, J., Cho, E., Willett, W. C., Sastry, S. M., and Schaumberg, D. A. (2015). Intakes of Lutein, Zeaxanthin, and Other Carotenoids and Age-Related Macular Degeneration During 2 Decades of Prospective Follow-Up. *Jama Ophthalmol.* 133 (12), 1415–1424. doi:10.1001/jamaophthalmol.2015.3590

Xi, L., Qian, Z., Du, P., and Fu, J. (2007). Pharmacokinetic Properties of Crocin (Crocetin Digentiobiose Ester) Following Oral Administration in Rats. *Phytomedicine.* 14 (9), 633–636. doi:10.1016/j.phymed.2006.11.028

Zhang, Y., Fei, F., Zhen, L., Zhu, X., Wang, J., Li, S., et al. (2017). Sensitive Analysis and Simultaneous Assessment of Pharmacokinetic Properties of Crocin and Crocetin after Oral Administration in Rats. *J Chromatogr. B.* 1044-1045, 1–7. doi:10.1016/j.jchromb.2016.12.003

Conflict of Interest: The authors declare that the research was conducted in the absence of any commercial or financial relationships that could be construed as a potential conflict of interest.

frontiers in Pharmacology

ORIGINAL RESEARCH
published: 16 July 2021
doi: 10.3389/fphar.2021.708518

Cross-Cultural Ethnobotanical Assembly as a New Tool for Understanding Medicinal and Culinary Values–The Genus *Lycium* as A Case Study

Ruyu Yao[1], *Michael Heinrich*[2], *Jianhe Wei*[1] *and Peigen Xiao*[1]*

[1]Institute of Medicinal Plant Development, Chinese Academy of Medical Sciences and Peking Union Medical College, Beijing, China, [2]Research Group "Pharmacognosy and Phytotherapy", UCL School of Pharmacy, Univ. London, London, United Kingdom

Ethnobotanical knowledge is indispensable for the conservation of global biological integrity, and could provide irreplaceable clues for bioprospecting aiming at new food crops and medicines. This biocultural diversity requires a comprehensive documentation of such intellectual knowledge at local levels. However, without systematically capturing the data, those regional records are fragmented and can hardly be used. In this study, we develop a framework to assemble the cross-cultural ethnobotanical knowledge at a genus level, including capturing the species' diversity and their cultural importance, integrating their traditional uses, and revealing the intercultural relationship of ethnobotanical data quantitatively. Using such a cross-cultural ethnobotanical assembly, the medicinal and culinary values of the genus *Lycium* are evaluated. Simultaneously, the analysis highlights the problems and options for a systematic cross-cultural ethnobotanical knowledge assembly. The framework used here could generate baseline data relevant for conservation and sustainable use of plant diversity as well as for bioprospecting within targeting taxa.

Keywords: ethnobotany, ethnopharmacology, Lycium, medicine and food homology, traditional use

OPEN ACCESS

Edited by:
XY Zhang,
University of Minho, Portugal

Reviewed by:
Chunlin Long,
Minzu University of China, China
Wong Kah Hui,
University of Malaya, Malaysia

***Correspondence:**
Peigen Xiao
pgxiao@implad.ac.cn

Specialty section:
This article was submitted to Ethnopharmacology, a section of the journal Frontiers in Pharmacology

Received: *12 May 2021*
Accepted: *07 July 2021*
Published: *16 July 2021*

Citation:
Yao R, Heinrich M, Wei J and Xiao P (2021) Cross-Cultural Ethnobotanical Assembly as a New Tool for Understanding Medicinal and Culinary Values–The Genus Lycium *as A Case Study. Front. Pharmacol. 12:708518. doi: 10.3389/fphar.2021.708518*

INTRODUCTION

Ethnobotanical research records how indigenous peoples use plants and manage the ecosystem, is indispensable for the conservation of global biological integrity, and could provide essential information on bioprospecting aiming at new food crops and medicines (Hoban et al., 2020; Pei et al., 2020; Ulian et al., 2020; Atanasov et al., 2021). The diversity of regional plants and peoples making their traditional knowledge enormously diverse. Therefore, to achieve a comprehensive documentation of such intellectual knowledge should rely on studies at local level (Gaoue et al., 2017; Teixidor-Toneu et al., 2018). Since both the plant species and their associated traditional knowledge are at risk of being lost, their conservation and sustainable use have become a topic of global concern. At the same time, in recent decades, regional studies have recorded tremendous ethnobotanical knowledge (Borrell et al., 2020; Pei et al., 2020). However, there is a need for capturing that information systematically, since otherwise those regional records are fragmented and can hardly be used.

In genomics, scientists use the strategy of "assembly" to fuse fragmented sequences (reads), which are obtained from sequencing technologies, into longer sequences or even into the level of chromosome or genome, thus the genetic information of an organism can be studied further (Nagarajan and Pop, 2013; Dominguez Del Angel et al., 2018). Borrowing the concept from genomics, we propose to assemble the scattered local ethnobotanical knowledge globally. Considering that the chemical constitutions and usages of plants are often phylogenetically conserved (Gaoue et al., 2017; Garnatje et al., 2017), it is advisable to assemble the ethnobotanical knowledge using a group of closely related taxa (e.g., a genus) as a basic unit. Accordingly, we propose a framework for a systematic understanding on any taxon's ethnobotanical knowledge cross-culturally, including 1) a documentation-based taxonomical revision, 2) evaluating the traditional uses, 3) evaluating the use values of species, and 4) comparing the ethnobotanical knowledge among cultures. Such an assemblage offers a pragmatic solution to understanding (ethno-) botanical diversity.

The genus *Lycium* is used widely as food and medicine (Yao et al., 2018a), and its global distribution and diverse uses make it an ideal example for such an assembly study. For example, in recent years *L. barbarum* L., the most commonly used species of this genus, has become a globally used commodity China produces 250,000–300,000 tons of dried fruits annually, while the amounts produced in other countries are not well known. Many other *Lycium* spp. are also used regionally as food and medicine (Yao et al., 2018a; Yao et al., 2018b). Therefore, as a case study, the present study applies the proposed framework to this genus of global importance.

MATERIALS AND METHODS

Documentation-Based Taxonomic Revision

Accepted species were extracted from the global important plant databases including Catalogue of Life (COL) (Roskov et al., 2020), Plants of the World Online (POWO) (POWO, 2019), World Flora Online (WFO) (WFO, 2021), and the Plant List (TPL) (The Plant List, 2013). GBIF (gbif.org) is among the global important plant databases, since it is a secondary database, its constitute datasets have heavy overlaps with the above (e.g., COL), the current research does not include it. A comparison table was created using the above species lists (see **Supplementary Material**), which was used to generate a revised species list as follows:

(1) Species were classed as taxonomically valid (i.e., "accepted"), if they were accepted in all the three databases;
(2) Varieties and hybrids were removed;
(3) Species names accepted only in one or two of the databases were cross-checked using primary taxonomic sources and regional floras, as well as virtual specimens of the disputed species;
(4) debatable names were accepted based on the International Code of Botanical Nomenclature, with consideration of the information collected in step (3);
(5) The status of synonyms was ascertained based on the above evidences, and confirmed synonyms were removed.

Thus, the accept species together formed a revised species list. An UpSet graph was then produced.

Evaluating the Traditional Uses

The traditional uses of *Lycium* spp. as food, medicine and in rituals were extracted from journal articles, ethnobotanical monographs, online ethnobotanical databases. The medical usages were categorized following International Classification of Diseases 11th Revision (ICD-11) (World Health Organization, 2020), and the traditional medical indications were categorized according to chapter two6 of ICD-11, with extra classifications when necessary. The culture backgrounds were extracted from the source literatures, and, if this was not stated in the reference, their languages and language families were searched with WALS (The World Atlas of Language Structures) (Dryer and Haspelmath, 2013) and international standards of ISO 639-2 (Library of Congress, 2017) and ISO 639-5 (Library of Congress, 2013). A 3-letter code of the language family is used as an identity of the cultural background. Languages of jpn and kor, belonging to the family of tut, were treated as independent cultures considering they have succeeded the Chinese (which is belonging to sit) knowledge of using *Lycium* directly. Note that if an abbreviation was not included the above references, a 3-letter code was then created, such as languages in Chile and Argentina, Austro-Asiatic (Vietnamese), Matacoan-Chorote, Aboriginal (Australian), Keresan-Acoma, Guaicuruan, Muskogean, and Kiowa-Tanoan [for a complete check list of language (families) and their codes see **Supplementary Material**]. Accordingly, a matrix including all species and their corresponding usages and cultural backgrounds was built and presented as a heatmap using TBtools (Chen et al., 2020).

The sequence of the granule-bound starch synthase gene (GBSSI) was used as a DNA barcode to show the phylogenetic relationship amongst the selected *Lycium* spp. 72 *Lycium* spp. were selected, which included 34 of the 36 traditional used species, with *Nolana werdermannii* as the outgroup, and their accession numbers of NCBI were listed in **Supplementary Material**. The phylogenetic tree was constructed using the statistical method of Maximum Likelihood, and tested by bootstrap method with 500 replications. The phylogenetic tree was then fitted to the above heatmap.

In order to evaluate the potential of *Lycium* for any traditional uses, we used a modified Fidelity Level (FL) Index (Friedman et al., 1986), since we use it for the evaluation of a genus instead of a species. FL was calculated as follows:

$$FL_u = \frac{R_u}{N}$$

Where: Fl_u is the FL of a specific use, while R_u is the number of reports for a specific use, and N is the number of cultures with a recorded use.

The FL_u values were then appended to the above heatmap.

Evaluating the Use Values of Species

Cultural Importance Index (CII) (Tardío and Pardo-de-Santayana, 2008), Relative Frequency of Citation (RFC) (Tardío and Pardo-de-Santayana, 2008), and Use Value (UV)

(Rossato et al., 1999) were used to evaluate the importance of every species, with adaptions. The above indices were calculated as follows.

$$CII_s = \frac{R_{uc.s}}{N}$$

Where: CII_s is the CII of a specific species S; $R_{uc.\ s}$ is the number of reports for a use category (here the categories of medicinal use, food use, and ritual use are calculated respectively) of the species; N is the number of informants (here it refers to number of all the cultures).

$$RFC_s = \frac{N_s}{N}$$

Where: RFC_s is the RFC of a specific species S; N_s is the number of informants who report the use of species S; N is the number of informants (here it refers to number of all the cultures).

$$UV_{c.s} = \frac{R_{c.s}}{N_s}$$

Where: $UV_{c.s}$ is the UV of a specific species S for the use category C; Rs is the number of use reports of species S; N_s is the number of informants who report the use of species S. Considering there was no subgroup for food or ritual uses, only the UVs of medicinal use were calculated.

Comparing the Ethnobotanical Knowledge Among Cultures

Jaccard Index (JI), an index widely used in many fields of science was used to study the ethnobotanical knowledge based on cultural backgrounds (Wang and Wang, 2017). In this case, JI was employed to compare the species used by peoples of different language families, with adaptions. The data on uses was categorized by the language families of people, and then, pairwise comparisons were calculated according to the following formula.

$$JI_{AB} = \frac{N_{A\cap B}}{N_{A\cup B}} \times 100$$

Where: JI_{AB} is the JI between the two cultural backgrounds of A and B; $N_{A\cup B}$ is the number of union species used in A and B; $N_{A\cap B}$ is the number of intersection species used in A and B.

The results were then complied into a correction matrix, which was further presented as a correction heatmap.

RESULTS AND DISCUSSION

Documentation-Based Species List Revision

Similar to a defined sequence of a gene or group of genes, the valid botanical name is the identifier of a plant, without which even the entity of the traditional knowledge is ambiguous (Bennett and Balick, 2014; Rivera et al., 2014; Yao et al., 2021). Considering its importance to the biodiversity conservation, "an online flora of all known plants" was set as the primary target of the Global Strategy for Plant Conservation (GSPC) (Jackson and Miller, 2015). Currently, Catalogue of Life (COL), Plants of the World Online (POWO), World Flora Online (WFO) have been widely recognized as the important global nomenclatural standards for species names (POWO, 2019; Roskov et al., 2020; WFO, 2021). Moreover, the Plant List (TPL not updated since 2013) was used as the starting point for the Taxonomic Backbone of the WFO (The Plant List, 2013). Tropicos provides an index of plant names and references (Missouri Botanical Garden, 2021). Clearly, regional floras provide important baseline data for the species description and identification. Using on-line herbaria and libraries, the type specimens and the original published literature of controversial names were traced, based on which a corrected list of the genus *Lycium* was constructed. A comparison of *Lycium* species lists of COL, POWO, WFO, TPL, and the revised list is provided in the **Supplementary Material**. It is found that the lists of *Lycium* species are markedly different among those global databases (**Figure 1**). The numbers of accepted scientific names included in those databases range from 88 to 103, with only 65 in common to all five sources. Eleven names are only indexed in TPL while 13 spp. are included in the other four, showing the progress of revision work since 2013. The revised species list we developed has corrected several misused names in the present international databases.

Assembly of Traditional Uses

The species used and their usages were extracted from journal articles, ethnobotanical monographs, and online ethnobotanical databases. The medical usages were categorized following International Classification of Diseases 11th Revision (ICD-11) with extra classifications when necessary. All species with their corresponding usages and cultural backgrounds (**Figure 2**,) include the cultural backgrounds represented by the language families (see **Supplementary Material**). 36 *Lycium* species are recorded to be used as food or medicine by peoples of diverse cultural backgrounds. Of these, 28 species are used for culinary purposes, with a Fidelity Level (FL) of as high as 1.84 (**Figure 2**, bottom). As for medicinal uses, *Lycium* spp. are frequently applied to treatments for diseases of the spleen, brain, skin, eye, musculoskeletal (MSK), kidney, heart, lung, dental, among others, with FL ranging from 0.72 to 0.40, indicating their high potential medicinal values for related drugs. Besides, solitary medical uses, such as urribaqla, eghindi, Mizaj, etc., are found in local records only, many of which are panacea-like with special conceptual indications and with very low FL. Moreover, *Lycium* spp. are also reported as cosmetics (FL = 0.24) and for ritual uses (FL = 0.28). While there are a variety of useful properties, six species are reported to be toxic in specific conditions. This ethnobotanical knowledge assemblage provides useful clues for finding new food sources and new drugs from the genus. Bioprospecting aiming at new drugs from plants requires specific verifications at different stages, when the chemical composition of a plant is clear, its traditional uses could be verified preliminarily with network pharmacology (Lu et al., 2020).

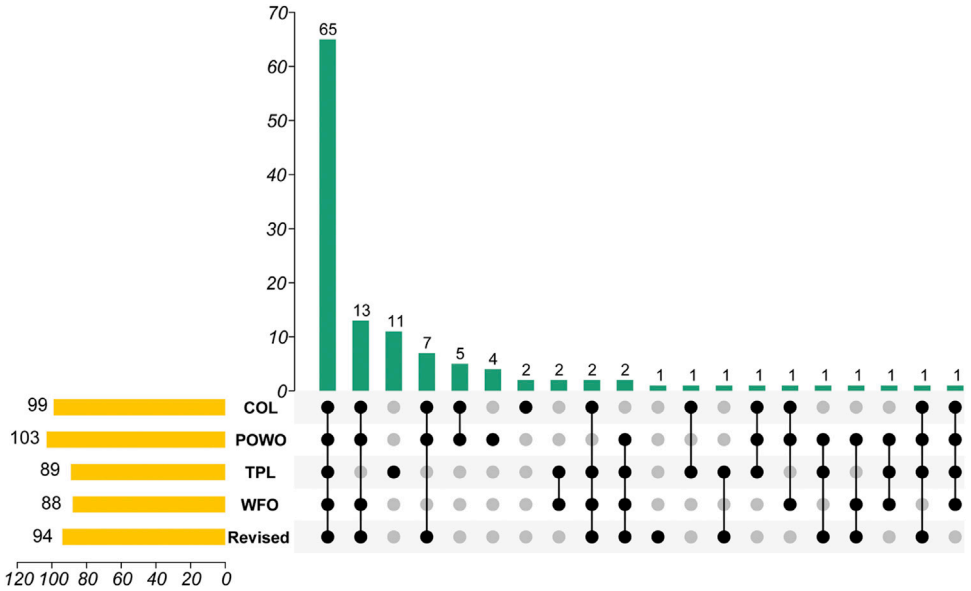

FIGURE 1 | An UpSet graph of *Lycium* spp. among databases covering species. Data source: Catalogue of Life (COL), Plants of the World Online (POWO), World Flora Online (WFO), and the Plant List (TPL). The bottom part indicates the coverage of individual species in the respective databases. For example, the second vertical bar indicates that there are 13 species listed in four (COL, POWO, WFO, and Revised) of the five databases, excluding TPL, while the third vertical bar indicates eleven are only found in TPL.

Using the sequence of the granule-bound starch synthase gene (GBSSI) as a DNA barcode, the phylogenetic relationship of the selected *Lycium* spp. is presented with a biogeographic pattern: The New World species are separated from those of the Old World, while those eastern Asian species form a sub-cluster within the cluster of Old World species (**Figure 2**, left side). Apparently, the usages of the Old World species are more diverse than those of the New World. Hot clades of culinary or medicinal used species are found in the clusters of eastern Asian species, western Asian and Mediterranean species, and a cluster compromises of several South and North American species.

Quantitative Evaluation of Medicinal and Culinary Values

The cultural importance of individual species can be indicated by their Cultural Importance Index (CII), Relative Frequency of Citation (RFC), and Useful Value (UV), as are shown in **Figure 3**. Five species of the Old World, *viz. L. chinense, L. barbarum, L. shawii, L. europaeum,* and *L. afrum*, have considerable importance in medical uses, with CII ranging from 1.52 to 0.76, and their significant medical values are also supported by the high RFC and UV. In contrast, the species of New World are more commonly used as food, especially *L. pallidum* and *L. andersonii* with CIIs of 0.28 and 0.12, respectively. Moreover, using diverse processing methods, fruits, shoots, and leaves of *Lycium* spp. are prepared into the forms of syrup, beverage, delicacy, mixed paste, porridge, and so on, and consuming the fresh fruits is also common. Furthermore, four species are found to be used for ritual purposes, which emphases the important role of *Lycium* in indigenous peoples' daily lives.

The "medicine and food homology" is commonly seen in the traditional uses of plants (Jennings et al., 2015; Liu, 2018), which indicates the commonality of plants' medicinal and culinary values. The above analyses give a quantitative overview on the medicinal and food uses of targeting species at a global level, thus to make the ethnobotanical knowledge available for further research.

Cross-Cultural Comparison of the Traditional Uses

Since the traditional use of plants is impacted by the cultural background, which can be represented by the language family of people, here we use language families of people as indicators of their cultural backgrounds. Jaccard Index (JI), an index commonly used in ecologic studies, is applied to compare the use similarity among cultures. As is shown in **Figure 4**, the use in four cultures of South America (Agt, Chl, Gua, and Mat), two cultures of North America (Mus and xnd), one culture of Africa (map), and one culture of Australia (Aus) are isolated. The discrete distribution of the species and the lack of communication among cultures may lead to the isolated knowledge on uses (Quave and Pieroni, 2015). High JI regions are found among seven cultures of North America, as well as 10 cultures of Africa and Eurasia. North American cultures are geographically contiguous, providing the opportunities for sharing plant resources and knowledge. The southern African cultures are less similar compared to others but with significant similarity with their close neighbours. The culture of ine (Indo-European) and afa (Afro-Asiatic) have broad link with many other cultures, including those of long geographic distances.

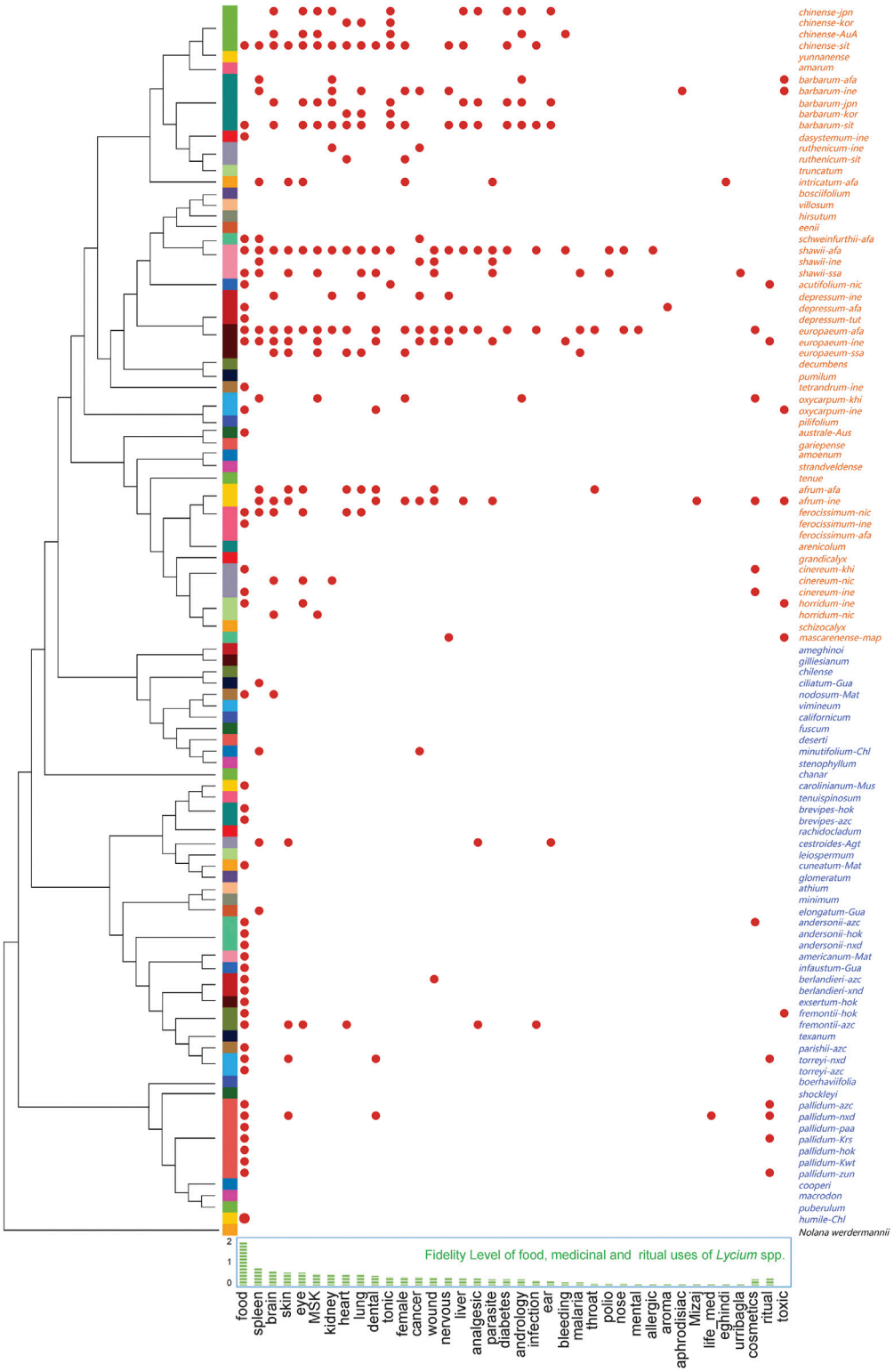

FIGURE 2 | The food, medicine, and ritual use of *Lycium* spp., with phylogenetic relationship reconstructed by sequences of the granule-bound starch synthase gene (GBSSI), and the Fidelity Level of the uses. Note that items are named as "epitheton-language family" (the Old World species are in orange and the New World species are in blue), and language families are obtained by WALS (The World Atlas of Language Structures) and international standards of ISO 639-2 and ISO 639-5; GBSSI sequences were retrieved from NCBI. Lists of language families, IDs of selected sequences, and references of the plant uses are presented in the **Supplementary Material**.

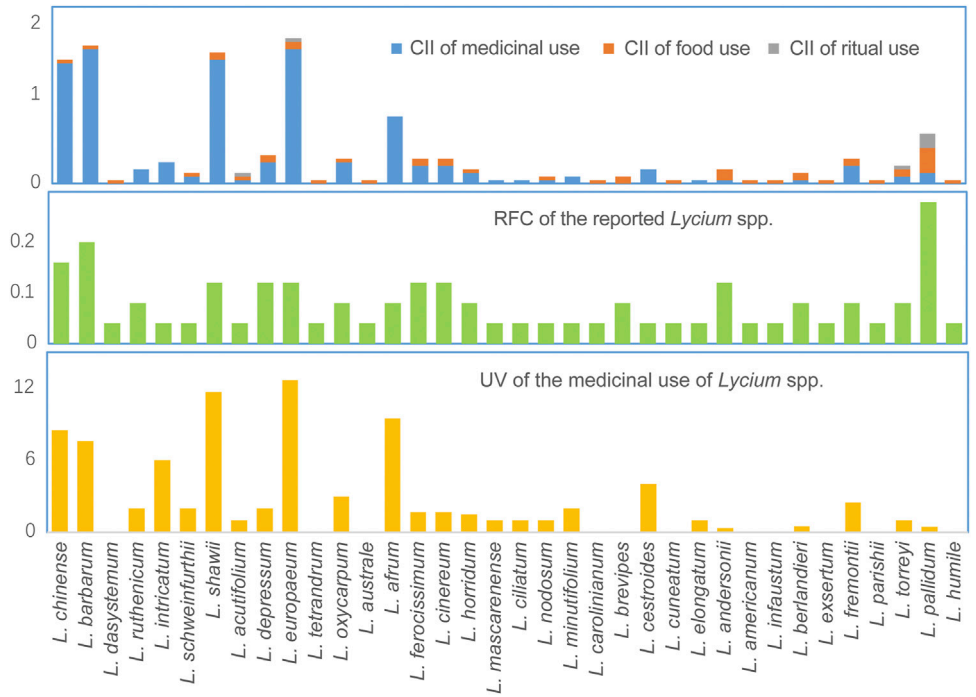

FIGURE 3 | Cultural Importance Index (CII) and Relative Frequency of Citation (RFC) of *Lycium* spp., and Useful Value (UV) of their medicinal uses.

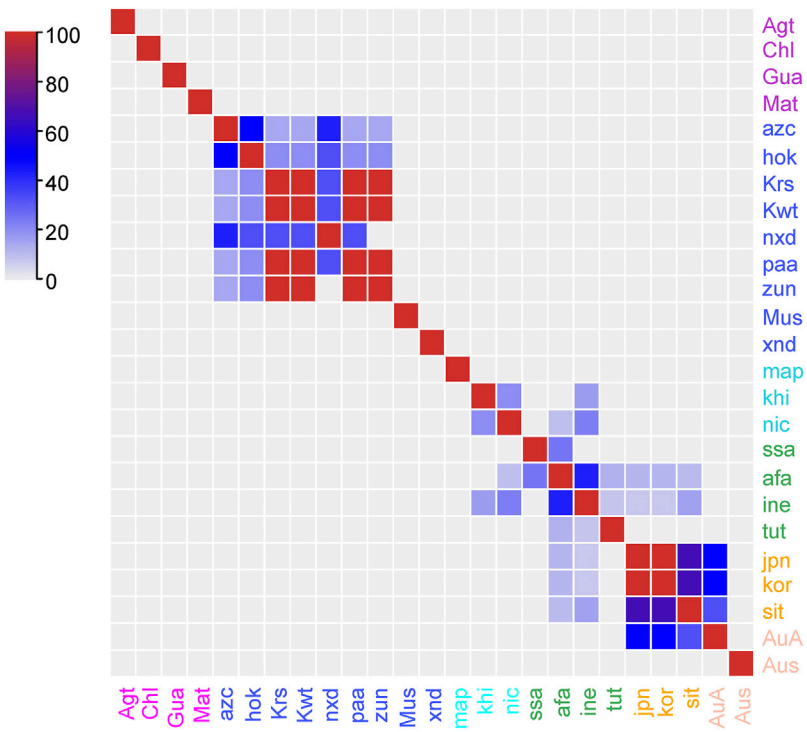

FIGURE 4 | Pairwise comparison of the Jaccard Index (JI) between ethnobotanical knowledge on *Lycium* spp. of different cultures as represented by language families.

These two language families cover large geographic region and the splendid ancient civilizations of the world. In the early times, people of ine and afa were the frequent travellers especially for business across the continents, and played important roles in cross-cultural communications.

A verifiable source of evidence is an ancient Islamic-oriented herbal, *Huihui Yaofang*, which was written in Chinese in the era of Genghis Khan, and it is still being used by people of western China (Kong and Chen, 1996). Moreover, cultures of sit (Sino-Tibetan), kor (Korean), jpn (Japan), and AuA (Austro-Asiatic) show considerable similarity. Except for their geographic linkage, the cross-cultural communication among them has contributed to knowledge sharing, which are supported by the historical herbals and traditional phytotherapies communicated for over one millennium, such as the Chinese-derived Dongui Bogam and Kampo. Consequently, as one would expect (Heinrich et al., 2005), the similarity of ethnobotanical knowledge reflects the cross-cultural communication, which could be understood using a JI analysis.

The conservation and sustainable use of plant resources and their associated traditional knowledge have given rise to global concerns. Considering their importance in biodiversity conservation, "an online flora of all known plants" was set as the primary target of the GSPC. Simultaneously, indigenous and local knowledge of plant species is also been stressed in the Aichi Biodiversity Targets (Convention on Biological Diversity, 2012a; Convention on Biological Diversity, 2012b; Jackson and Miller, 2015). The framework presented here allows for the plant name revision and ethnobotanical knowledge organization of any taxon, which is a pragmatic tool for the implementation of GSPC and the Aichi Targets. While emphasizing the culinary and medicinal assessment, it could provide irreplaceable clues for bioprospecting aiming at new foods and medicines.

CONCLUSION

Ethnobotanical knowledge is critical for the conservation and utilization of local plants. Although plant resources and their popular and traditional usages in different geographic regions and by people with different cultural backgrounds are recorded increasingly, such fragmented catalogues have limited scientific value without systematic system to capture and compare data. This problem is especially urgent since the plant species and their associated traditional knowledge are at risk of being lost. Therefore, borrowing the concept of assemblage from genomics, we propose a framework for a systematic understanding on any taxon's ethnobotanical knowledge. The assembly of the genus *Lycium* indicates the requirement for a documentation-based taxonomic revision to current updated international species checklists. Additionally, the quantitative evaluations highlight the medicinal and culinary value of *Lycium* spp., while the corresponding species are also clarified, which contributes a deeper understanding into the cultural importance of this genus. It can be applied to groups of related taxa like genera or groups of related genera. Next a larger picture at a family level and beyond can be built up. Moreover, the comparisons among cultures support that the cross-cultural communications lead to the sharing of ethnobotanical knowledge. This paper offers a perspective and a framework for achieving this and the concept will need to be refined further using other case studies The extending application of this framework will facilitate a better appreciation of plant biodiversity, and will be helpful for the conservation and sustainable utilization of local ethnobotanical knowledge.

DATA AVAILABILITY STATEMENT

The datasets presented in this study can be found in online repositories. The names of the repository/repositories and accession number(s) can be found in the article/ **Supplementary Material**.

AUTHOR CONTRIBUTIONS

RY, PX, and MH developed the idea. RY conducted the literature research and data analysis, and drafted the manuscript. PX and MH contributed conceptual and methodological input. JW provided input into the design. All authors revised the manuscript.

FUNDING

The earlier part of this work was supported by Chinese Government Scholarship (No. 201306910001) and the Claraz Schenkung, with critical supervision provided by PD Dr. Caroline Weckerle. The primary work is financially supported by the Strategic Consulting Project of Chinese Academy of Engineering (2021-X2-10), the International Postdoctoral Exchange Fellowship Program and China Postdoctoral Science Foundation (2019M660552).

ACKNOWLEDGMENTS

The first author would like to greatly thank the above-mentioned people and funders.

SUPPLEMENTARY MATERIAL

The Supplementary Material for this article can be found online at: https://www.frontiersin.org/articles/10.3389/fphar.2021.708518/full#supplementary-material

REFERENCES

Atanasov, A. G., Zotchev, S. B., Zotchev, S. B., Dirsch, V. M., and Supuran, C. T. (2021). Natural Products in Drug Discovery: Advances and Opportunities. *Nat. Rev. Drug Discov.* 20, 200–216. doi:10.1038/s41573-020-00114-z

Bennett, B. C., and Balick, M. J. (2014). Does the Name Really Matter? the Importance of Botanical Nomenclature and Plant Taxonomy in Biomedical Research. *J. Ethnopharmacology* 152, 387–392. doi:10.1016/j.jep.2013.11.042

Borrell, J. S., Dodsworth, S., Forest, F., Pérez-Escobar, O. A., Lee, M. A., Mattana, E., et al. (2020). The Climatic challenge: Which Plants Will People Use in the Next century? *Environ. Exp. Bot.* 170, 103872. doi:10.1016/j.envexpbot.2019.103872

Chen, C., Chen, H., Zhang, Y., Thomas, H. R., Frank, M. H., He, Y., et al. (2020). TBtools: An Integrative Toolkit Developed for Interactive Analyses of Big Biological Data. *Mol. Plant* 13, 1194–1202. doi:10.1016/j.molp.2020.06.009

Convention on Biological Diversity (2012b). *Strategic Plan for Biodiversity 2011–2020 and the Aichi Targets*.

Convention on Biological Diversity (2012a). *The Global Strategy for Plant Conservation: 2011-2020*. Richmond, UK: Botanic Gardens Conservation International for the Convention on Biological Diversity.

Dominguez Del Angel, V., Hjerde, E., Sterck, L., Capella-Gutierrez, S., Notredame, C., Vinnere Pettersson, O., et al. (2018). Ten Steps to Get Started in Genome Assembly and Annotation. *F1000Res* 7, 148. doi:10.12688/f1000research.13598.1

Dryer, M. S., and Haspelmath, M. (2013). *The World Atlas of Language Structures Online*. Leipzig: Max Planck Institute for Evolutionary Anthropology (Accessed on 12 26, 2020).

Friedman, J., Yaniv, Z., Dafni, A., and Palewitch, D. (1986). A Preliminary Classification of the Healing Potential of Medicinal Plants, Based on a Rational Analysis of an Ethnopharmacological Field Survey Among Bedouins in the Negev Desert, Israel. *J. Ethnopharmacology* 16, 275–287. doi:10.1016/0378-8741(86)90094-2

Gaoue, O. G., Coe, M. A., Bond, M., Hart, G., Seyler, B. C., and Mcmillen, H. (2017). Theories and Major Hypotheses in Ethnobotany. *Econ. Bot.* 71, 269–287. doi:10.1007/s12231-017-9389-8

Garnatje, T., Peñuelas, J., and Vallès, J. (2017). Ethnobotany, Phylogeny, and 'Omics' for Human Health and Food Security. *Trends Plant Sci.* 22, 187–191. doi:10.1016/j.tplants.2017.01.001

Heinrich, M., Pieroni, A., and Bremner, P. (2005). "Medicinal Plants and Phytomedicines," in *The Cultural History of Plants*. Editors G. Prance and M. Nesbitt (New York: Routledge), 205–238.

Hoban, S., Bruford, M., D'urban Jackson, J., Lopes-Fernandes, M., Heuertz, M., Hohenlohe, P. A., et al. (2020). Genetic Diversity Targets and Indicators in the CBD post-2020 Global Biodiversity Framework Must Be Improved. *Biol. Conservation* 248, 108654. doi:10.1016/j.biocon.2020.108654

Jackson, P. W., and Miller, J. S. (2015). Developing a World Flora Online - a 2020 challenge to the World's Botanists from the International Community. *Rodriguésia* 66, 939–946. doi:10.1590/2175-7860201566402

Jennings, H. M., Merrell, J., Thompson, J. L., and Heinrich, M. (2015). Food or Medicine? the Food-Medicine Interface in Households in Sylhet. *J. Ethnopharmacology* 167, 97–104. doi:10.1016/j.jep.2014.09.011

Kong, Y. C., and Chen, D. S. (1996). Elucidation of Islamic Drugs in Hui Hui Yao Fang: a Linguistic and Pharmaceutical Approach. *J. Ethnopharmacology* 54, 85–102. doi:10.1016/s0378-8741(96)01452-3

Library of Congress (2017). *ISO 639-2 Codes for the Representation of Names of Languages– Part 2: Alpha-3 Code*.

Library of Congress (2013). *ISO 639-5 Codes for the Representation of Names of Languages– Part 5: Alpha-3 Code for Language Families and Groups*.

Liu, C. (2018). Understanding ``medicine and Food Homology'', Developing Utilization in Medicine Functions. *Chin. Herbal Medicines* 10, 337–338. doi:10.1016/j.chmed.2018.10.006

Lu, Y., Sun, J., Hu, M., Kong, X., Zhong, W., and Li, C. (2020). Network Pharmacology Analysis to Uncover the Potential Mechanisms of *Lycium Barbarum* on Colorectal Cancer. *Interdiscip. Sci. Comput. Life Sci.* 12, 515–525. doi:10.1007/s12539-020-00397-1

Missouri Botanical Garden (2021). Tropicos.org. Available at: http://www.tropicos.org (access on Jan 16, 2021).

Nagarajan, N., and Pop, M. (2013). Sequence Assembly Demystified. *Nat. Rev. Genet.* 14, 157–167. doi:10.1038/nrg3367

Pei, S., Alan, H., and Wang, Y. (2020). Vital Roles for Ethnobotany in Conservation and Sustainable Development. *Plant Divers.* 42, 399–400. doi:10.1016/j.pld.2020.12.001

POWO (2019). Plants of the World Online. Facilitated by the Royal Botanic Gardens, Kew. Available at: http://www.plantsoftheworldonline.org/ (Retrieved on Jan 03, 2021).

Quave, C. L., and Pieroni, A. (2015). A Reservoir of Ethnobotanical Knowledge Informs Resilient Food Security and Health Strategies in the Balkans. *Nat. Plants* 1, 14021. doi:10.1038/NPLANTS.2014.21

Rivera, D., Allkin, R., Obón, C., Alcaraz, F., Verpoorte, R., and Heinrich, M. (2014). What Is in a Name? the Need for Accurate Scientific Nomenclature for Plants. *J. Ethnopharmacology* 152, 393–402. doi:10.1016/j.jep.2013.12.022

Roskov, Y., Ower, G., Orrell, T., Nicolson, D., Bailly, N., Kirk, P. M., et al. (2020). *Catalogue of Life, 2020-12-01. Digital Resource at*. Leiden: Naturalis. , Available at: www.catalogueoflife.org.

Rossato, S. C., De LeitâO-Filho, H. F., and Begossi, A. (1999). Ethnobotany of Caiçaras of the Atlantic Forest Coast (Brazil). *Econ. Bot.* 53, 387–395. doi:10.1007/bf02866716

Tardío, J., and Pardo-De-Santayana, M. (2008). Cultural Importance Indices: A Comparative Analysis Based on the Useful Wild Plants of Southern Cantabria (Northern Spain)1. *Econ. Bot.* 62, 24–39. doi:10.1007/s12231-007-9004-5

Teixidor-Toneu, I., Jordan, F. M., and Hawkins, J. A. (2018). Comparative Phylogenetic Methods and the Cultural Evolution of Medicinal Plant Use. *Nat. Plants* 4, 754–761. doi:10.1038/s41477-018-0226-6

The Plant List (2013). The Plant List: A Workingmlist of All Plant Species. Available at: http://www.theplantlist.org/> (Accessed on Jan 03, 2021).

Ulian, T., Diazgranados, M., Pironon, S., Padulosi, S., Liu, U., Davies, L., et al. (2020). Unlocking Plant Resources to Support Food Security and Promote Sustainable Agriculture. *Plants People Planet.* 2, 421–445. doi:10.1002/ppp3.10145

Wang, Y., and Wang, C. (2017). *General Research Methods for Ethnobotany*. China: Zhejiang Education Publishing House. doi:10.2991/iceemr-17.2017.21

WFO (2021). World Flora Online. Available at: http://www.worldfloraonline.org (Accessed on Jan 03, 2021).

World Health Organization (2020). International Classification of Diseases 11th Revision (ICD-11). Available at: https://icd.who.int/browse11/l-m/en.

Yao, R., Heinrich, M., Wang, Z., and Weckerle, C. S. (2018b). Quality Control of Goji (Fruits of *Lycium Barbarum* L. And *L. Chinense* Mill.): A Value Chain Analysis Perspective. *J. Ethnopharmacology* 224, 349–358. doi:10.1016/j.jep.2018.06.010

Yao, R., Heinrich, M., and Weckerle, C. S. (2018a). The Genus *Lycium* as Food and Medicine: A Botanical, Ethnobotanical and Historical Review. *J. Ethnopharmacology* 212, 50–66. doi:10.1016/j.jep.2017.10.010

Yao, R., Heinrich, M., Zhao, X., Wang, Q., Wei, J., and Xiao, P. (2021). What's the Choice for Goji: Lycium Barbarum L. Or L. Chinense Mill.?. *J. Ethnopharmacology* 276, 114185. doi:10.1016/j.jep.2021.114185

Conflict of Interest: The authors declare that the research was conducted in the absence of any commercial or financial relationships that could be construed as a potential conflict of interest.

frontiers in Pharmacology

ORIGINAL RESEARCH
published: 30 July 2021
doi: 10.3389/fphar.2021.710487

Nutraceutical Study on *Maianthemum atropurpureum*, a Wild Medicinal Food Plant in Northwest Yunnan, China

Li Xu[1,2†], *Yizhou Wang*[1,2†], *Yuanyuan Ji*[1,2,3,4†], *Ping Li*[1,2], *Wujisiguleng Cao*[1,2,3], *Shibiao Wu*[4], *Edward Kennelly*[4,5] *and Chunlin Long*[1,2,3*]

[1]Key Laboratory of Ecology and Environment in Minority Areas, National Ethnic Affairs Commission, Minzu University of China, Beijing, China, [2]College of Life and Environmental Sciences, Minzu University of China, Beijing, China, [3]Key Laboratory of Ethnomedicine, Ministry of Education, Minzu University of China, Beijing, China, [4]Department of Biological Sciences, Lehman College City University of New York, New York, NY, United States, [5]Ph.D. Programs in Biochemistry, Biology, and Chemistry, The Graduate Center, City University of New York, New York, NY, United States

OPEN ACCESS

Edited by:
X. Y. Zhang,
University of Minho, Portugal

Reviewed by:
Simon Ming Yuen Lee,
University of Macau, China
Umakanta Sarker,
Bangabandhu Sheikh Mujibur Rahman Agricultural University, Bangladesh

***Correspondence:**
Chunlin Long
long.chunlin@muc.edu.cn

[†]These authors have contributed equally to this work

Specialty section:
This article was submitted to Ethnopharmacology, a section of the journal Frontiers in Pharmacology

Received: 16 May 2021
Accepted: 20 July 2021
Published: 30 July 2021

Citation:
Xu L, Wang Y, Ji Y, Li P, Cao W, Wu S, Kennelly E and Long C (2021) Nutraceutical Study on Maianthemum atropurpureum, a Wild Medicinal Food Plant in Northwest Yunnan, China. Front. Pharmacol. 12:710487. doi: 10.3389/fphar.2021.710487

Maianthemum atropurpureum (Franch) LaFrankie (Asparagaceae), called *nibai* in Tibetan or *dongka* in Drung or *zhu-ye-cai* in local Chinese, is a wild vegetable consumed by the Tibetan people and other ethnic groups in Northwest Yunnan, China. It is also a traditional medicinal plant used by different linguistic groups for antimicrobial purposes. However the nutritional and phytochemical compositions of this important medicinal food plant have not been well studied previously. In this study, the nutrient content for *nibai* was determined by the China National Standards (GB) methods, and the phytochemical analysis involved multiple chromatographic and spectral methods including LC-TOF-MS analysis. Dried *nibai* is a rich source of protein (ca. 24.6%), with 18 of the 21 common amino acids. The amino acid content of *nibai* can reach up to 17.9/100 g, with the essential amino acids as major contributors, corresponding to 42.3% of the total amino acids. *Nibai* contains rich mineral elements, dietary fiber, vitamins, β-carotene, carbohydrates, and lipids. The phytochemical content of *nibai* was examined by conventional isolation strategies, as well as HR-ESI-TOF-MS to detect and identify 16 compounds including nine steroid saponins and seven flavonoids. Among these compounds, uridine, adenosine, guanosine, and β-methyl-6-methyl-d-glucopyranoside were found from the genus *Maianthemum* for the first time. These results help to demonstrate that the local people's practice of consuming *Maianthemum atropurpureum* is reasonable due to its high levels of vitamins, minerals, essential amino-acids, and phytochemicals. *Nibai* may be further developed in Tibet and surrounding regions, and beyond as a health food, nutraceutical, and/or dietary supplement product.

Keywords: ***Maianthemum atropurpureum*, ethnic people, east Himalayas, nutraceutical profile, steroid saponins**

Abbreviations: GB, national standard method of the people's republic of China (initial of Guo Biao); MS/MS, mass spectrometry/mass spectrometry; NMR, nuclear magnetic resonance; PDA, photo-diode array; HR-ESI-TOF-MS, high resolution electrospray ionization time-of-flight mass spectrometry; TIC, total ion currency chromatograms; ESI-MS, electrospray ionization mass spectrometry; LC-TOF-MS, liquid chromatography time-of-flight mass spectrometry; MFCs, minimum fungicidal concentrations.

INTRODUCTION

Wild edible plants play an important role in furthering food security and improving the nutrition in the diets of people around the world, especially in poor rural communities (Lulekal et al., 2011). The utilization of wild edible plants is receiving more and more attention, not only due to their health benefits but also the opportunities they may present to rural economies (Multari et al., 2016). In daily life, wild vegetables may be a significant source of nutrients, including minerals, vitamins, fiber, and essential amino acids which are critical for good health, but often their nutrient and phytochemical content are not well studied (Turan et al., 2003). Many edible plants are also considered medicinal herbs (Liu et al., 2018; Luo et al., 2019; Sarker and Oba, 2019a, Sarker and Oba, 2020a; Sarker and Oba, 2020b). Some wild vegetables are gaining more widespread popularity due to their unique flavors, colors, and potential health properties (Costa et al., 2013; Sarker and Oba, 2019b).

The ethnic groups including Nu, Dulong (Drung), Lisu, Yi, Pumi, Bai, Naxi and Tibetan as well in northwest Yunnan (including Nujiang, Diqing, Dali and Lijiang provinces) of China, reside at high elevation areas with mountains and deep valleys. To better survive in these extreme conditions, local ethnic people often turn to wild (uncultivated) plants to supplement their diet and therebey enrich their food diversity. Ahmad and Pieroni found that certain wild edible plants have been embraced by a particular local culture because of their traditionally acquired knowledge-based principles, feelings, and manners (Ahmad and Pieroni, 2016). Moreover, wild foods contribute to overcoming periods of famine, and dishes made of wild plants can be very healthy by providing local people with various essential nutritious elements, such as vitamins and minerals.

The local people in northwest Yunnan collect the young shoots (tender aerial parts) of a group of seven species in *Maianthemum* Web. for food, including *M. atropurpureum* (Franch.) LaFrankie, *M. purpurea* (Wall.) LaFrankie, *M. oleracea* (Baker) LaFrankie, *M. tatsienense* (Franch.) LaFrankie, *M. forrestii* (W.W. Sm.) LaFrankie, *M. fuscum* (Wall.) LaFrankie, and *M. henryi* (Baker) LaFrankie (Ju et al., 2012), belonging to the family Asparagaceae. Among them, *M. atropurpureum* is the most well-known, and considered to taste the best. *Maianthemum atropurpureum* (Franch.) LaFrankie, called *nibai* in Tibetan, *dongka* in Drung, *zhu-ye-cai* in local language, or *gao-da-lu-yao* in Mandarin, a flavorful seasonal wild vegetable with unique flavors. It grows at high attitude on mountains, and can be collected in May when the snow has just melted (**Figure 1**). It was one of the major vegetables consumed by local herdsmen in the Tea Horse Road trade route. The previous studies reported that everyday about 2 tons (2000 kg) of would be sold in a single market of a town in northwest Yunnan, while more *Maianthemum atropurpureum* (*nibai*) were collected and directly consumed by the local people (Gui et al., 2000a; Gui et al., 2000b). Now it is considered by Tibetan, Nu, Drung, Lisu, Bai, Yi, Pumi, and Naxi people as a delicacy used to celebrate festivals and entertain guests. There are many ways to prepare *M. atropurpureum*: the fresh shoots can be used in soups, stir-fried with pork, or eaten raw as salad, and the dried shoots can be served in wintertime hot pot dishes.

Maianthemum atropurpureum is also considered to be an excellent medicine for annealing, heat-clearing, detoxicating, and lowering blood pressure in traditional Chinese medicine practice. The rhizome, as a folk medicine, has been used to treat lung ailment, rheumatism, menstrual disturbance, mammitis, cuts, bruises, kidney diseases, and also to activate blood circulation and to alleviate pain (Jiang, 1977; State Administration of Traditional Chinese Medicine, 1999). The minerals, vitamins, essential amino-acids, carbohydrates and lipids in leaves of

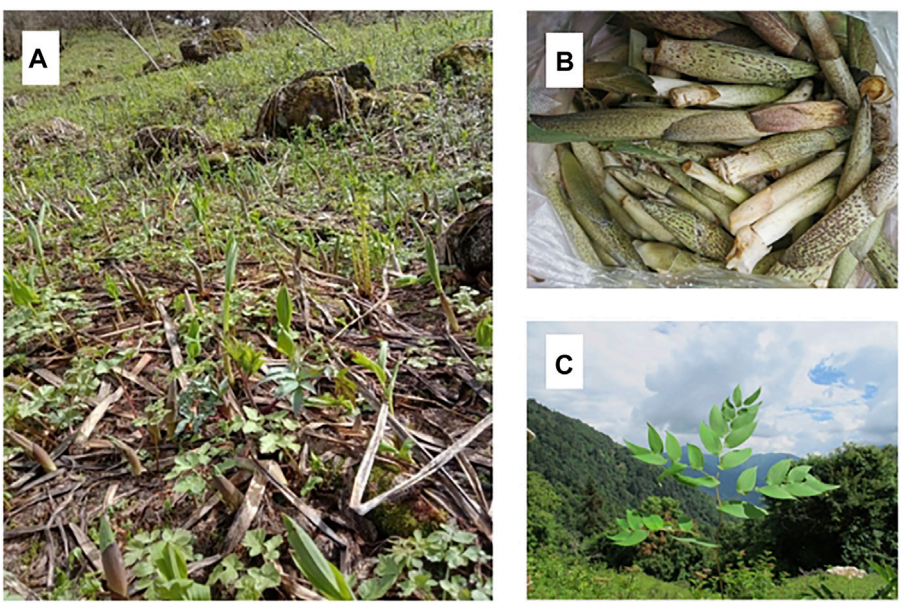

FIGURE 1 | The plant of *Maianthemum atropurpureum*. **(A)** Wild habitat; **(B)** Shoots sold on market; **(C)** Mature leaves (photographed by the authors).

Maianthemum atropurpureum (*nibai*) have been preliminarily investigated (Gui et al., 2000a). In addition, steroid saponins, nucleosides and flavonoids, were isolated from *nibai* (Yang, 2003; Zhang et al., 2006; Yang et al., 2009).

Seven new steroidal saponins, atropurosides A–G, with new polyhydroxylated aglycones, were identified from the rhizomes of *Maianthemum atropurpureum*, together with a known saponin and dioscin. Among them, atropurosides B and F showed moderate inhibitory activity against *Candida albicans*, *Candida glabrata*, *Cryptococcus neoformans*, and *Aspergillus fumigatus*, while dioscin was more active against *C. albicans* and *C. glabrata* (Zhang et al., 2006). These three compounds are moderately cytotoxic. It appears that the antifungal activity of these steroidal saponins correlates with their cytotoxicity against mammalian cells (Zhang et al., 2006).

Thesecondary metabolites from young edible shoots of *Maianthemum atropurpureum* have not been reported. Further work on *Maianthemum atropurpureum*, therefore, is necessary since its bioactive constituents are not fully understood. Its nutritional composition also need to be re-examined based on modern standard techniques. This study investigated the nutritional content and chemical constituents of this typical medicinal and food plant valued by the Tibetan, Nu, Drung and other linguistic groups, and discuss its potential to be developed as new functional food or nutraceutical.

MATERIALS AND METHODS

Samples and Sample Preparation

The aerial parts of *Maianthemum atropurpureum* (Franch.) LaFrankie were collected in Gongshan County, Nujiang Prefecture, NW Yunnan, China, in May 2013 and identified by Prof. Chun-Lin Long (Minzu University of China). The voucher specimen (No. 20130584) was deposited at the Herbarium of Minzu University of China. Some of the sample (300 g) was boiled with salt water and dried for the determination of nutrient content. The remaining sample (8.5 kg) was dried in the Sun directly for phytochemical studies.

Solvents, Reagents and Standards

The general laboratory solvents, including methanol (MeOH), ethanol (EtOH), petroleum ether (Pet), ethyl acetate (EtOAc), n-butyl alcohol (n-BuOH), acetone, chloroform ($CHCl_3$), and dichloromethane (DCM) were of analytical grade and were purchased from Beijing Chemical Works (Beijing, China). Chromatography and extraction solvents (acetonitrile, methanol, formic acid) were of HPLC grade obtained from VWR Inc (Bridgeport, PA, United States). UPLC grade water was prepared by using the Millipore Milli-RO 12 system (Millipore, Bedford, United States). All pure isolated compounds were characterized by HR-ESI-MS, ^{1}H NMR, and ^{13}C NMR spectroscopic methods for identification purposes.

Determination of Proximate Composition

Percentages of moisture was determined by vacuum oven under 105°C for 2 h to constant weight per the China national standards (GB) method (GB 5009.3-2010) (Zhang et al., 2009). Ash was determined by direct analysis according to the China standards method (GB 5009.4-2010), the sample was fully carbonized with a low flame until no smoke was produced, and weighed. The dry sample was then placed in a muffle furnace to burn under 550 ± 25°C for 4 h, removed, and placed into a desiccator for 30 min after cooling down to 200°C. The whole process was repeated until to a constant weight (Nie et al., 2014). Total lipid content was determined by Soxhlet extraction using the China standards method (GB/T 5009.6-2003) (Wang et al., 2005; Liu et al., 2015). Protein content was determined by Kjeldahl nitrogen using the China standards method (GB/T5009.5-2010) (Zhang, 2008), and the percentage of crude protein was estimated as the total nitrogen content multiplied by the conversion factor 6.25. Total carbohydrates were calculated by subtracting the total percentage of other components (saccharides, starch and dietary fiber) from 100.

Determination of Dietary Fiber

Total fiber, soluble fiber, and insoluble fiber contents were determined by Dietary Fiber Determination System (VELP GDE + CSF6, Italian) using the GB/T 5009.88-2008 method (Zhou, 2014).

Determination of Minerals, Vitamins and β-carotene

Minerals, vitamins, and β-carotene were analyzed according to corresponding China standard methods GB/T (Wang et al., 2005), among which K, Na, Fe, Mn, Mg, Ca, Cu and Zn were determined using inductively coupled plasma-mass spectrometery (ICP-MS) (Wang et al., 2005); P and vitamin C were determined by ultra-violet and visible spectrophotometery (UVPC) (Wang et al., 2005); Cr was determined using an atomic absorption spectrometer (AAS) (Wang et al., 2005); vitamin A was determined using ultra performance liquid chromatography (UPLC) (Wang et al., 2005); vitamin B_2 was determined using molecular fluorescence photometer (Wang et al., 2005). The determination of β-carotene was carried out by high-performance liquid chromatography (HPLC) as previously reported (Sun et al., 2009).

Determination of Amino Acids

Amino acids were measured according to the method GB/T 5009.124-2003 by Amino acid Analyzer (Hitachi L-8900, Japan) (Wang et al., 2005; Xing et al., 2012). Data were expressed as milligrams of amino acid per 100 g of *nibai*.

Isolation and Identification of Chemical Compounds

Dried and powdered samples of *Maianthemum atropurpureum* (*nibai*) (8.5 kg) were extracted five times with 70% EtOH under reflux to give an ethanol extract. After evaporation under reduced pressure, the extracted residue was suspended in water and partitioned successively with petroleum ether, ethyl acetate, and n-BuOH. The n-BuOH extract (109 g) was subjected to

silica gel (200–300 mesh) column chromatography eluting with EtOAc-acetone gradient (1:0→0:1) and pooled based on TLC profiles to yield seven fractions (Fr.1-Fr.7). Fr.2 (3.24 g) was dissolved with MeOH, and the insoluble part was recrystallized with MeOH and gave compound 1. The soluble part was subjected to silica gel (200–300 mesh) column chromatography eluting with CH_2Cl_2-MeOH gradient (25:1→2:1) to yield Fr.2.3 and Fr.2.5. Fr.2.3 was purified by Sephadex LH-20 chromatography using MeOH as the eluent to yield compound 3. In addition, Fr.2.5 was repeated chromatographed by silica gel column under different gradient conditions with CH_2Cl_2-MeOH to give compounds 4, 5, and 7. The insoluble part in Fr.3 (3.01 g) was also recrystallized with MeOH and gave compound 2, and the soluble part was further purified by successive silica gel column chromatography with CH_2Cl_2-MeOH (20:1, 15:1, 10:1) followed by CH_2Cl_2-MeOH (15:1, 10:1), yielding 8 mg of compound 6. Fr.5 (4.47 g) was subjected to Si gel column chromatography with CH_2Cl_2-MeOH (18:1, 15:1, 10:1) and pooled based on TLC profiles to yield five fractions (Fr.5.1-Fr.5.5). Fr.5.3 was purified by silica gel column chromatography (15:1, 12:1) to yield compound 10. Fr.5.4 was repeated silica gel medium pressure liquid chromatography gradient eluted with a MeOH-H_2O solvent system (5, 10, 20, 40, 60, and 100%), followed by preparative HPLC with 50% MeOH (MeOH-H_2O) and further purified by silica gel column to yield compounds 8 and 9.

Liquid Chromatography Time-of-Flight Mass Spectrometry Analysis

LC-TOF-MS analysis of the n-BuOH extract was performed using a Waters (Milford, MA, United States) Alliance 2695 system equipped with 2695 separation module units and 2998 PDA detectors using a 100 mm × 2.0 mm, 2.5 μm Phenomenex Synergi Hydro-RP 100 A column with 3 mm × 4.0 mm Phenomenex Security Guard column (Torrance, CA United States). The mobile phase consisted of solvents (A) 0.1% aqueous formic acid solution and (B) acetonitrile using a stepwise gradient elution of 3% B for 5 min, 3%–15% B at 5–15 min, 15% B for 5 min, 15%–45% B at 21–35 min, 45%–90% B at 35–40 min, and this proportion of solvent kept for 10 min. The UV-Vis spectra were recorded from 190 to 700 nm. The flow rate and the injection volume were 0.2 ml/min and 10 μL, respectively. Both column and sample temperatures were 25°C. LC/MS-grade methanol was used to redissolve the freeze-dried sample, and then brought up to 2 mg/ml and filtered using 25 mm syringe filter (0.45 μm PTFE membrane) prior to injection.

High-resolution electrospray ionization time of flight mass spectrometry (HR-ESI-TOF-MS) was performed using an LCT Premier XE TOF mass spectrometer (Waters, Milford, MA) equipped with an ESI interface and controlled by Mass Lynx V4.1 software. Mass spectra were acquired in both positive and negative modes over range m/z 100–1500. The capillary voltages were set at 3000 V (positive mode) and 2700 V (negative mode), respectively, and the cone voltage was 30 V. Nitrogen gas was used for both the nebulizer and desolvation. The desolvation and cone gas flow rates were 600 and 20 L/h, respectively. The desolvation temperature was 400°C, and the source temperature was 120°C.

TABLE 1 | Compositional and nutritional characteristics of *zhu-ye-cai* compared with other well-known edible greens. (Values per 100 g of *zhu-ye-cai* dried after boiling with salted water)

Parameters	Unit	*zhu-ye-cai*	fiddlehead[a]	spinach[a]
Approximate composition				
Moisture	G	7.22	nd	Nd
Ash	G	13.5	nd	Nd
Crude lipid	G	4.9	0.9	0.6
Crude protein	G	24.6	6.6	6.4
Total carbohydrate	G	23.8	54.2	63
Dietary fiber				
Total dietary fiber	G	26.1	25.5	12.7
Soluble dietary fiber (SDF)	G	0.07	nd	Nd
Insoluble dietary fiber (IDF)	G	26.0	nd	Nd
Minerals				
K	Mg	1800	59	919
Na	Mg	2490	20.4	242
Ca	Mg	252	851	411
Mg	Mg	231	82	183
Fe	Mg	20.3	23.7	25.9
Mn	Mg	5.98	2.31	1.61
Zn	Mg	4	18.11	3.91
Cu	Mg	6.62	2.79	2.08
Cr	Mg	0.84	nd	Nd
P	Mg	313	253	222
Vitamins and β- carotene				
β-carotene	Mg	7.95	nd	Nd
Vitamin A	Mg	9.8	0	598
Vitamin B_2	Mg	0.2	nd	Nd
Vitamin C	Mg	2	3	82

[a]*From* Chinese Food Composition Table.[35].

All of these vegetables are dehydrated, and zhu-ye-cai *is dried after boiling with salt water so the Sodium content is extremely high; nd means not detected (below the detection level).*

RESULTS AND DISCUSSIONS

Nutrient Composition and Dietary Fiber

The nutrient composition and dietary fiber content of *Maianthemum atropurpureum* (Franch.) LaFrankie (*nibai*) are listed in **Table 1**. Insoluble dietary fiber was the predominant component (26.0/100 g), followed by protein (24.6/100 g), while carbohydrate and lipid contents were much lower. The dietary fiber content is comparable with that of fiddlehead fern (*Pteridium aquilinum* var. *latiusculum*) with 25.5/100 g, one of the most important wild food plants in China (Liu et al., 2012), and higher than that of spinach (*Spinacia oleracea*) with 12.7/100 g. The protein and carbohydrate content among three species are very different; *nibai* has the highest protein content (24.6/100 g), and the lowest carbohydrate content (23.8/100 g). The protein and carbohydrate content of *nibai* is much higher than different vegetable amaranth species, such as *Amaranthus blitum* (Sarker and Oba, 2020c), stem amaranth (Sarker et al., 2020a), green morph amaranth (Sarker et al., 2020b) and red morph amaranth (Sarker and Oba, 2019c).

TABLE 2 | Amino acids of *zhu-ye-cai* (Values per 100 g of *zhu-ye-cai* dried after boiling with salted water).

Amino acids	unit	*zhu-ye-cai*
Aspartic acid (Asp)	g	1.73
Threonine (Thr)*	g	0.73
Serine (Ser)	g	0.74
Glutamate (Glu)	g	2.98
Proline (Pro)	g	0.64
Glycine (Gly)	g	0.9
Alanine (Ala)	g	1.29
Cystine (Crs)	g	0.26
Valine (Val)*	g	1.24
Methionine (Met)*	g	0.11
Isoleucine (Ile)*	g	1.09
Leucine (Leu)*	g	1.71
Tyrosine (Tyr)	g	0.41
Phenylalanine (Phe)*	g	1.16
Lysine (Lys)*	g	1.36
Histidine (His)	g	0.34
Tryptophan (Try)*	g	0.17
Arginine (Arg)	g	0.92
Essential amino acids(E)	g	7.57
Total amino acids(T)	g	17.9
E/T	%	42.29
Lys/T	%	7.59

Note ** indicates essential amino acids.*

Dietary fiber is indispensable to a healthy diet, and its health benefits have been known for decades (Le et al., 2016). In the gastrointestinal tract, dietary fibers can promote intestinal peristalsis to accelerate the removal of carcinogenic substances and toxic matter, and reduce bacterial growth. Dietary fiber can also help to reduce cholesterol levels, prevent obesity and chronic diseases (Patil et al., 2009). Dietary fiber significantly contributed to the cure of constipation, digestibility, and palatability (Sarker et al., 2020c; Sarker and Oba, 2020d; Sarker and Oba, 2020e). *Nibai* has a high content of protein, along with a low carbohydrate content, making it a potentially healthy food plant for people looking to reduce carbohydrate intake. With the growing obesity epidemic in developed nations, foods with high protein and diet fiber content, and low carbohydrate and lipid content has been advocated by certain nutritionists. Thus, *nibai* could potentially be considered a functional food which can meet the modern healthy diet requirement.

Minerals, Vitamins and β-Carotene

Ten minerals have been detected in *nibai*, and five of them are essential microelements of human body, including Fe, Zn, Cu, Cr, and Mg (**Table 1**). The content of Fe (20.3 mg/100 g) is comparable with that of spinach (25.9 mg/100 g) and fiddlehead (23.7 mg/100 g) which are commonly considered Fe-rich vegetables. However, it is much higher than commonly considered Fe rich *Amaranthus hypochondriacus* (Sarker and Oba, 2020d). The Mg, Cu and P levels in *nibai* are the highest, when compared to spinach and fiddlehead fern. Mg, Cu and P were much higher than vegetable amaranth (Sarker and Oba, 2020e). Zn levels in *nibai* are similar to spinach, but both are significantly lower than fiddlehead. However, Zn content was much lower than vegetable amaranth (Sarker et al., 2020c). It has been estimated that half the world's population is iron deficient (Karakoy et al., 2012). Therefore, *nibai* could be a very useful dietary source for Fe and other nutrients to help maintain good health for people with certain nutrient deficiencies. Vitamins serve many physiological functions and are of the essence to maintain health. Compared with spinach and vegetable amaranth, the contents of vitamins A, B_2, and C in *nibai* are lower, but it is still an important source of vitamins for Tibetans and other linguistic groups through the famine and the food shortages caused by the extreme environment. Consuming *nibai* contribute to prevent vitamins and trace elements deficiencies and maintain the normal bodily functions.

Amino Acids

The 18 amino acids identified and quantified in *nibai* are presented in **Table 2**, in which eight are essential to humans. Tryptophan was detected in *nibai* for the first time (Gui et al., 2000a; Gui et al., 2000b). The total amino acid content is up to 17.9 g/100 g, and the percentage of essential amino acids in total amino acids (E/T) reach up to 42.29%, which is higher than that of soybean (33%). According to the ideal model proposed by WHO/FAO, the ratio of E/T of good quality protein is about 40%, and the ratio of E/N (the percentage of essential amino acids to nonessential amino acid) is above 60% (Zhang et al., 2013). The composition of amino acid of *nibai* meets this ideal model. Additionally, the content of glutamic acid is the highest (2.98 g/100 g), followed by aspartic acid (1.73 g/100 g), leucine (1.71 g/100 g), lysine (1.32 g/100 g), and alanine (1.29 g/100 g), respectively.

Glutamate and arginine play important roles in regulating gene expression, cell signaling, antioxidative responses, and immunity (Wu, 2010). Our work showed that *nibai* is a good source of amino acids, which can provide indigenous people with nearly all the amino acids that humans require. Four amino acids in *nibai*, aspartic acid and glutamate contribute to its umami taste, while glycine and alanine contribute to its sweet taste (Bu et al., 2013). The total content of these four amino acids in *nibai* was 6.9 g/100 g, accounting for 38.6% of the total amino acids, these four amino acid contribute a characteristic taste to the flavor of *nibai*.

Phytochemical Constituents

Sixteen compounds were detected and tentatively identified using a method based on HPLC coupled with both PDA and HR-ESI-TOF-MS. The TIC chromatography of the n-BuOH extract of *M. atropurpureum* is displayed in the supplementary material (**DataSheet 1**). Their retention times, UV spectra, and exact mass spectral fragmental ions in positive and negative modes are shown in **Table 3**, and compared with literature values. Furthermore, the molecular formula was calculated based upon fragment ion peak data along with previous reports in SciFinder and other databases. The structures of part selected compounds are shown in **Figure 2**.

Seven known compounds (**Figures 2A–G**) have been isolated using conventional column chromatography and elucidated on the basis of detailed spectroscopic analyses from *nibai*, including thymidine 1) (Yang and Liu, 2003), uridine 2) (Gong and Ding,

TABLE 3 | LC-MS-TOF data of the compounds identified from the n-butonal extract of *Maianthemum atropurpureum*.

No	R.T. (min)	UV	[M + H]$^+$ or [M-H]$^-$ (M.F., ppm)	Adduct and fragmental ion exact masses [M-X]$^+$ or [M-X]$^-$ (M.F., ppm)	Identification	References
8	8.3	230, 256	611.1619 [M + H]$^+$ ($C_{27}H_{31}O_{16}$, 1.1) 609.1428 [M-H]$^-$ ($C_{27}H_{29}O_{16}$, -4.6)	633.1429 [M + Na]$^+$ ($C_{27}H_{30}O_{16}$ Na,-0.5); 465.1053 [M + H-146(Rha)]$^+$ ($C_{21}H_{21}O_{12}$, 4.3) 655.1569 [M-H + HCOOH]$^-$ ($C_{28}H_{31}O_{18}$, 9.0)	Rutin	Kaneta et al. (1980)
9	10.5	230, 256	465.1055 [M + H]$^+$($C_{21}H_{21}O_{12}$, 4.7) 463.0916 [M-H]$^-$ ($C_{21}H_{19}O_{12}$, 8.4)	303.0497 [M + H- Glc]$^+$ ($C_{15}H_{11}O_7$,–2.6); 487.0862 [M + Na]$^+$ ($C_{21}H_{20}O_{12}$Na, 2.1) —	Quercetin 3-O-galactoside	Kaneta et al. (1980)
10	13.1	230, 256	611.1620 [M + H]$^+$($C_{27}H_{31}O_{16}$, 1.3) 609.1505 [M-H]$^-$ ($C_{27}H_{29}O_{16}$, 8.0)	633.1478 [M + Na]$^+$($C_{27}H_{30}O_{16}$ Na,7.3); 465.1027 [M + H-146(Rha)]$^+$ ($C_{21}H_{21}O_{12}$, -1.3); 303.0521 [M + H-Rha-Glc]$^+$($C_{15}H_{11}O_7$, -1.3) 655.1569 [M-H + HCOOH]$^-$ ($C_{28}H_{31}O_{18}$, 9.0)	Quercetin 3-O-glucoside 7-O-rhamnoside	Kaneta et al. (1980)
11	13.6	230, 256	625.1740 [M + H]$^+$($C_{28}H_{33}O_{16}$,-4.6) 623.1763 [M-H]$^-$ ($C_{28}H_{31}O_{16}$,- 0.3)	479.1211 [M-Rha + H]$^+$ ($C_{22}H_{23}O_{12}$,4.4); 317.0660 [M-Rha-Glc + H]$^+$ ($C_{16}H_{13}O_7$,-0.3); 647.1553 [M + Na]$^+$($C_{28}H_{32}O_{16}$Na, -5.4) 669.1641 [M-H + HCOOH]$^-$ ($C_{29}H_{33}O_{18}$,-3.9)	Isorhamnetin-3-Rutinoside	El-Alfy et al. (1975)
12	14.6	—	755.4235 [M + H]$^+$($C_{39}H_{63}O_{14}$,2.3)	593.3706 [M-Glc + H]$^+$ ($C_{33}H_{53}O_9$,2.7);	27-epi-Trikamsteroside A	Yokosuka et al. (2008)
13	15.0	—	— 887.4696 [M-H]$^-$ ($C_{44}H_{71}O_{18}$, 6.3)	871.4673 [M-H_2O + H]$^+$($C_{44}H_{71}O_{17}$, –2.1); 793.4024 [M-Xyl+2H_2O + H]$^+$ ($C_{39}H_{69}O_{16}$,1.3); 725.4124 [M-Rha-H_2O + H]$^+$ ($C_{38}H_{61}O_{13}$,1.7); 593.3668 [M- Xyl-Rha- H_2O + H]$^+$ ($C_{35}H_{53}O_9$, –3.7); 413.3078 [M- Xyl-Rha-Gal- 2H_2O + H]$^+$($C_{27}H_{41}O_3$,5.3); 911.4673 [M + Na]$^+$ ($C_{44}H_{72}O_{18}$Na, 6.3) 933.4628 [M-H + HCOOH]$^-$($C_{45}H_{73}O_{20}$,-7.2)	(3β,5α,6β,25R)-spirostane-3,5,6-triol-3-O-β-D-apiofuranosyl-(1→ 3)-[α-L-rhamnopyranosyl-(1→2)]- β-D-glucopyranoside	Wu et al. (2012)
14	15.9	—	901.4814 [M + H]$^+$($C_{45}H_{73}O_{18}$,1.9)	923.4615 [M + Na]$^+$ ($C_{45}H_{72}O_{18}$ Na, –0.1); 739.4250 [M -Glc + H]$^+$($C_{39}H_{63}O_{13}$, –2.6); 577.3737 [M-2Glc- + H]$^-$($C_{33}H_{53}O_8$, –0.5)	Funkioside D	Yang et al. (2009)
	—		899.4673 [M-H]$^-$ ($C_{45}H_{71}O_{18}$,3.7)	945.4709 [M-H + HCOOH]$^-$ ($C_{46}H_{75}O_{20}$,1.5)	—	—
15	16.8	—	—	885.4833 [M + H-H_2O]$^+$($C_{45}H_{73}O_{17}$, –1.7); 739.4282 [M -Rha-H_2O + H]$^+$($C_{39}H_{63}O_{13}$, 1.8); 577.3737 [M-Gal-Rha- H_2O + H]$^+$($C_{33}H_{53}O_8$, –0.5); 415.3230 [M-Gal-Glc-Rha-H_2O + H]$^+$ ($C_{27}H_{43}O_3$, 4.3); 925.4753 [M + Na]$^+$ ($C_{45}H_{74}O_{18}$Na, –2.2)	Slimacinoside C	Yang et al. (2009)
	—		901.4769 [M-H]$^-$ ($C_{45}H_{73}O_{18}$, –3.1)	947.4926 [M-H + HCOOH]$^-$ ($C_{46}H_{75}O_{20}$, 7.8)	—	—
16	17.7	230, 256	303.0494 [M + H]$^+$($C_{15}H_{11}O_7$, -3.6)	—	Quercetin	Zhao et al. (2009)
	—		301.0342 [M-H]$^-$ ($C_{15}H_9O_7$, -2.0)	—	—	—
17	17.9	230, 256	287.0549 [M + H]$^+$($C_{15}H_{11}O_6$, -2.4)	—	Luteolin	Zhao et al. (2009)
	—		285.0405 [M-H]$^-$ ($C_{15}H_9O_6$, 2.1)	—	—	—
18	18.1	—	—	739.4282 [M-Rha-H_2O + H]$^+$($C_{39}H_{63}O_{13}$, 0.0); 577.3745 [M-Gal-Rha-H_2O + H]$^+$ ($C_{33}H_{53}O_8$,0.9); 415.3211 [M-Gal-Glc-Rha-H_2O + H]$^+$ ($C_{27}H_{43}O_3$, –0.2); 397.3138 [M-Gal-Glc-Rha-H_2O + H]$^+$ ($C_{27}H_{43}O_3$, –0.2); 925.4819 [M + Na]$^+$ ($C_{45}H_{74}O_{18}$Na, 5.0)	(3β,22α)-26-(β-D-glucopyranosyloxy)-22-hydroxyfurost-5-en-3-yl2-O-(6-deoxy-α-L-mannopyranosyl) -β-D-glucopyranoside	
	—		901.4828 [M-H]$^-$ ($C_{45}H_{73}O_{18}$, 3.4)	947.4926 [M-H + HCOOH]$^-$ ($C_{46}H_{75}O_{20}$, 7.8)	—	—
19	18.7	230, 256	—	353.4832 [M + Na]$^+$ ($C_{22}H_{35}$ O_2 Na, 3.9)	1-Phenanthren-emethanol	Kitajima et al. (1982)
	—		329.4812M-H]$^-$ ($C_{22}H_{33}O_2$, –2.1)	—	—	—
20	18.9	230, 256	885.4838 [M + H]$^+$($C_{45}H_{73}O_{17}$,-1.1)	907.4659 [M + Na]$^+$ ($C_{45}H_{72}O_{17}$Na, –0.9); 739.4293 [M-Rha + H]$^+$($C_{39}H_{63}O_{13}$, 3.2); 577.3766 [M-Glc-Rha + H]$^+$($C_{33}H_{53}O_8$, 4.5); 415.3199 [M-2Glc-Rha + H]$^+$ ($C_{27}H_{43}O_3$, –3.1)	Gracillin	Inoue et al., 1995; Zhao et al., 2011
	—		883.4691 [M-H]$^-$ ($C_{45}H_{71}O_{17}$, -4.0)	929.4808 [M-H + HCOOH]$^-$ ($C_{46}H_{73}O_{19}$, 6.7)	—	—
21	19.7	—	—	355 [M + Na]$^+$ ($C_{22}H_{37}$ O_2 Na, –3.4)	Ent-kaur-15-en-17-ol	Kitajima et al. (1982)
	—		331 [M-H]$^-$ ($C_{22}H_{35}O_2$,1.9)		—	—
22	19.9	230, 256	301.0717 [M + H]$^+$ ($C_{16}H_{13}O_6$, 1.7)	—	5,7,4′-trihydroxy-3′-methoxyflavone	Zhao et al. (2009)
	—		299.0573 [M-H]$^-$ ($C_{16}H_{11}O_6$, 5.7)	345.0599 [M-H + HCOOH]$^-$ ($C_{17}H_{13}O_8$, –3.2)	—	—
23	20.9	—	—	577.3740 [M-H_2O + H]$^+$($C_{33}H_{63}O_8$, 6.8); 617.3685 [M + Na]$^+$ ($C_{33}H_{54}O_9$Na,3.1)	26-O-β-D-glucopyranosyl-(25R)-furost-5-ene-3β, 22ξ, 26-triol	Wu et al., 2012
	—		593.3697 [M-H]$^-$ ($C_{33}H_{53}O_9$, 1.2)	639.3683 [M-H + HCOOH]$^-$ ($C_{34}H_{55}O_{11}$, –9.5)	—	—

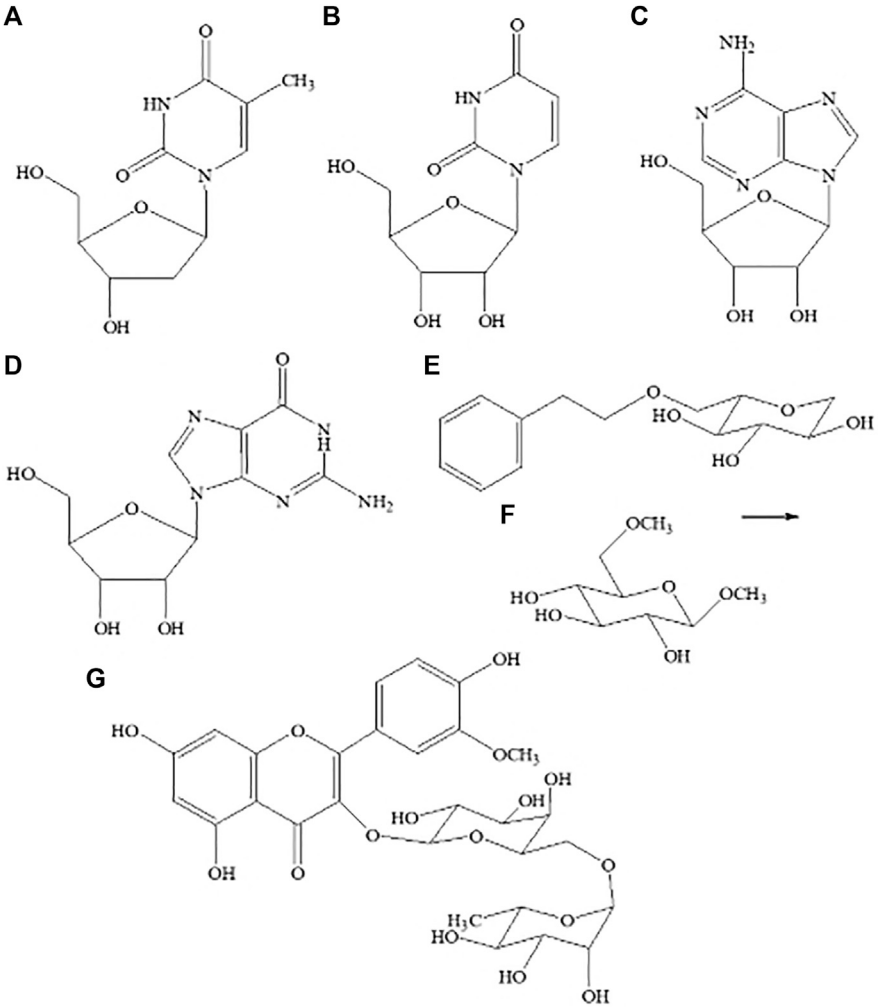

FIGURE 2 | Structures of seven compounds isolated from *Maianthemum atropurpureum*. Thymidine **(A)**, uridine **(B)**, adenosine **(C)**, guanosine **(D)**, 2-Phenylethyl-*β*-D-glucopyranoside **(E)**, *β*-methyl-6-methyl-D-glucopyranoside **(F)**, isorhamnetin-3-*O*-robinobioside **(G)**.

2005), adenosine 3) (Yang and Liu, 2003), guanosine 4) (Gong and Ding, 2005), 2-phenylethyl- *β*-D-glucopyranoside 5) (Kim et al., 2008), *β*-methyl-6-methyl-D-glucopyranoside 6) (Gong and Ding, 2005), and isorhamnetin-3-*O*-robinobioside 7) (Wang et al., 2010). Among them, compounds 2, 3, 4, 6 were found from the genus *Maianthemum* for the first time.

More compounds had been identified from *Maianthemum atropurpureum* comparing with current literatures (Yang and Liu, 2003; Gong and Ding, 2005; Kim et al., 2008). In particular, four compounds including uridine, adenosine, guanosine, and β-methyl-6-methyl-d-glucopyranoside had not been reported from *Maianthemum* in any previous references. Our methods adopted for isolating chemical compounds may be more appropriate.

Thymidine 1) was isolated as colorless acicular crystal. All NMR data are in agreement with literature data (Yang and Liu, 2003). The molecular formula was obtained *via* ESI-MS and deduced as $C_{10}H_{14}N_2O_5$ (observed m/z at 243 $[M + H]^+$ (calcd for $C_{10}H_{14}N_2O_5$, 243). The identification of uridine 2) which was isolated as colorless acicular crystal was confirmed by comparing the ^{13}C NMR data with literature and database values (Gong and Ding, 2005). ESI-MS m/z 245 $[M + H]^+$, $C_9H_{12}N_2O_6$. Compared with that of 1, upfield shifts in the C-5 and C-2′ indicated that there was no methyl substitute group, but with ribose connected. Based on these data, compound 2 was identified as uridine. Adenosine 3) was white powder; ^1H NMR and ^{13}C NMR were in agreement with literature values. ESI-MS m/z 267 $[M + H]^+$ (calcd for $C_{10}H_{13}N_5O_4$, 267) corresponded with those reported in the literature (Yang and Liu, 2003). Guanosine 4) was identified as white powder; ^1H NMR and ^{13}C NMR were in agreement with the literature (Gong and Ding, 2005); ESI-MS m/z 283 $[M + H]^+$ (calcd for $C_{10}H_{13}N_5O_5$, 283) and was identical to literature data (Gong and Ding, 2005). 2-Phenylethyl-*β*-D-glucopyranoside 5) was gummy, colorless, solid; ^1H NMR^{13}C-NMR are in agreement with published values. ESI-MS m/z 285 $[M + H]^+$ (calcd for $C_{14}H_{20}O_6$, 285) was identical to literature data (Kim et al., 2008). *β*-methyl-6-methyl-D-glucopyranoside 6) was white powder; ^{13}C NMR (75 MHz, MeOD): δ 103.5 (C-1), 78.2 (C-3), 74.1 (C-5), 73.7 (C-2), 72.5 (C-6), 71.9 (C-4), 66.5 (C6-O$\underline{CH_3}$), 64.5(C1-

$O\underline{CH_3}$); ESI-MS m/z 208 [M] (calcd for $C_8H_{16}O_6$). Comparing with NMR database, the ^{13}C NMR data showed 75% similarity to that of ethyl-β-D-fructopyranoside, from which the hydroxyl substituent fructose was confirmed. The ^1H NMR spectrum of 6 showed the presence of six hydrogens at δ1.74 and 2 carbons at δ 66.5 and 64.5, pointing to the existence of two methoxy groups. Comparing all the carbon chemical shift data of *β*-methyl-D-glucopyranoside with 6-*O*-methyl-*β*-D-glucopyranoside, the data were in agreement with those obtained from the literature data (Gong and Ding, 2005). Therefore, 6 was identified as *β*-methyl-6-methyl-D-glucopyranoside. Isorhamnetin-3-*O*-robinobioside (7): pale yellow crystal; ^1H NMR and ^{13}C NMR are in agreement with published data (Kaneta et al., 1980), ESI-MS m/z 467 $[M + Na]^+$ (calcd for $C_{28}H_{32}O_{16}$, 467) (Wang et al., 2010).

Biological Activities

The biological activities of *nibai* are attributed to its diverse bioactive components, especially the main constituents. According to this study and previous literature, the primary chemical components of *M. atropurpureum* are steroid saponins, nucleosides, and flavonoids, especially the large polarity constituents, some of which have considerable biological activities. For instance, the smilacinoside A, aspidistrin, and funkioside D isolated from the aerial parts of *M. atropurpureum* exhibited prominent activity *in vitro* cytotoxicity against K562 tumor cell line with IC_{50} values of 1.09, 0.47, and 2.93 μg/ml, respectively (Yang et al., 2009). Nucleosides also exerted a variety of biological activities, such as antitumor (Ogawa et al., 1998), antivirus (Ruth and Cheng, 1981) and gene therapy effects (Parker et al., 1997). Thymidine, for instance, is the nucleus of stavudine and zidovudine which are both anti-AIDS drugs (Ross et al., 2001). Moreover, adenosine has a range of significant pharmacological effects, including making blood vessels diastolic, lowering blood pressure, slowing heart rate, inhibiting platelet gathering, relaxing vascular smooth muscle, improving cardio-cerebral blood circulation, preventing arrhythmia, inhibiting the release of neurotransmitters, and adjusting the activities of adenosine activation enzyme (Layland et al., 2014). Flavonoids, such as rutin, quercetin, luteolin, and their glycosides are the most common and widely distributed group of plant phenolics (Sarker and Oba, 2018a; Sarker and Oba, 2018b). Many studies have demonstrated their antioxidant, scavenging free radical, anti-inflammatory, antibacterial, antiviral, and immunomodulatory effects (Sarker and Oba, 2020f; Sarker and Oba, 2020g; Sarker and Oba, 2021). All of these bioactive constituents as well as vitamin C, β-carotene and several minerals (Fe, Zn, and Mn), along with amino acids have contributed to *nibai*'s medicinal effects and thus demonstrate the current utilization of this wild plant to treat diseases and enhance immunity in humans.

Many studies have correlated diet and certain chronic diseases such as cancer, cardiovascular disease, diabetes, and osteoporosis. Bioactive compounds from edible plants have the potential to prevent certain chronic conditions (Patil et al., 2009; Sarker and Oba, 2018c; Sarker and Oba, 2018d; Sarker and Oba, 2018e). *Nibai*, *dongka* or *zhu-ye-cai* (*M. atropurpureum*), an endemic species to the Hengduan Mountains, is a less common wild vegetable rich in nutrient and phytochemical content. It plays an important role not only in providing local Tibetans and other linguistic groups with various essential nutrition elements, but may also contribute to maintaining health, promoting immunity, and preventing several kinds of diseases. Consequently, *nibai* can be considered a promising new functional health food and/or nutraceutical.

DATA AVAILABILITY STATEMENT

The datasets presented in this article are not readily available because, All datasets had been included in the paper. Requests to access the datasets should be directed to long@mail.kib.ac.cn or long.chunlin@muc.edu.cn.

ETHICS STATEMENT

Prior Informed Consent was obtained before collecting information related to traditional knowledge of *Maianthemum* from local people in northwest Yunnan.

AUTHOR CONTRIBUTIONS

LX, YW, and YJ equally contributed to the article. LX: Investigation, Writing-original Draft. YW and YJ: Methodology, Data curation, Investigation, Formal analysis, Writing-Editing. PL, WC, SW, and EK: Validation, Writing-Review and Editing. CL: Conceived the study, Writing-Review and Editing, Supervision.

FUNDING

This work was supported by the Minzu University of China (No. 2020MDJC03), the Biodiversity Survey and Assessment Project of the Ministry of Ecology and Environment of China (No. 2019HJ2096001006), the National Natural Science Foundation of China (Nos. 31761143001 and 31870316) and the Ministry of Education of China (No. B08044).

ACKNOWLEDGMENTS

We are very grateful to the staff of the PONY Testing Company (Beijing) for testing nutritional ingredients. Special thanks go to all informants of NW Yunnan, especially the collectors, retailers and restaurateurs in Diqing Tibetan Autonomous Prefecture and Nujiang Lisu Autonomous Prefecture for their unreserved information and patience, and Ms. Yan Ju from College of Life and Environmental Sciences, Minzu University of China.

SUPPLEMENTARY MATERIAL

The Supplementary Material for this article can be found online at: https://www.frontiersin.org/articles/10.3389/fphar.2021.710487/full#supplementary-material

REFERENCES

Ahmad, K., and Pieroni, A. (2016). Folk Knowledge of Wild Food Plants Among the Tribal Communities of Thakht-E-Sulaiman Hills, North-West Pakistan. *J. Ethnobiol. Ethnomedicine* 12, 17–32. doi:10.1186/s13002-016-0090-2

Bu, J. Z., Dai, Z. Y., Li, Y., Wang, H. H., Zhao, Q. L., and Jiang, Q. Q. (2013). Analysis of Nutritional and Flavor Compounds in Crab Boiled Liquid. *J. Chin. Inst. Food Sci. Tech.* 9, 207–216. doi:10.13386/j.issn1002-0306.2017.03.003

Costa, A. G. V., Garcia-Diaz, D. F., Jimenez, P., and Silva, P. I. (2013). Bioactive Compounds and Health Benefits of Exotic Tropical Red-Black Berries. *J. Funct. Foods* 5, 539–549. doi:10.1016/j.jff.2013.01.029

El-Alfy, T. S., and Paris, R. R. (1975). On the Flavonoids of *Ruscus Hypoglossum* L. (Liliaceae). *Pl. Med. Phytother.* 9, 308–314.

Gong, Y. H., and Ding, L. S. (2005). *Analysis of Natural Products*. Kunming: Yunnan Science and Technology Press, 856–947.

Gui, M. Y., Chen, B., ShenJ.and Tian, Y. S. (2000a). The Nutritional Value of *Maianthemum Atropurpurea* and its Exploitation. *Guihaia* 20, 71–74.

Gui, M. Y., Li, Z. J., Chen, B., Shen, J., and Tian, Y. S. (2000b). The Compare of the Sample of Different Treatment Procedures to the Nutrition Contents of *Similacina Atropurpurea*. *J. Jishou Univ.* 21 (2), 55–57.

Inoue, K., Kobayashi, S., Noguchi, H., Sakawa, U., and Ebizuka, Y. (1995). Spirostanol and Furostanol Glycosides of *Costus Speciosus* (Koenig.). *SM. Nat. Med.* 49, 336–339.

Jiang, S. X. (1977). *Traditional Chinese Medicine*. Shanghai: Shanghai People's Publishing House, 754.

Ju, Y., Zhuo, J., Liu, B., and Long, C. (2013). Eating from the Wild: Diversity of Wild Edible Plants Used by Tibetans in Shangri-La Region, Yunnan, China. *J. Ethnobiol. Ethnomedicine* 9, 28–176. doi:10.1186/1746-4269-9-28

Kaneta, M., Hikichi, H., Endo, S., and Sugiyama, N. (1980). Identification of Flavones in Thirteen Liliaceae Species. *Agric. Biol. Chem.* 44, 1405–1406. doi:10.1080/00021369.1980.1086413810.1271/bbb1961.44.1405

Karaköy, T., Erdem, H., Baloch, F. S., Toklu, F., Eker, S., Kilian, B., et al. (2012). Diversity of Macro- and Micronutrients in the Seeds of Lentil Landraces. *Scientific World J.* 2012, 1–9. doi:10.1100/2012/710412

Kim, K. H., Lee, K. H., Choi, S. U., Kim, Y. H., and Lee, K. R. (2008). Terpene and Phenolic Constituents of *Lactuca Indica* L. *Arch. Pharm. Res.* 31, 983–988. doi:10.1007/s12272-001-1256-8

Kitajima, J., Komori, T., and Kawasaki, T. (1982). Studies on the Constituents of the Crude Drug "Fritillariae bulbus." III. On the Diterpenoid Constituents of Fresh Bulbs of Fritillaria Thunbergii Miq. *Chem. Pharm. Bull.* 30, 3912–3921. doi:10.1248/cpb.30.3912

Layland, J., Carrick, D., Lee, M., Oldroyd, K., and Berry, C. (2014). Adenosine. *JACC: Cardiovasc. Interventions* 7, 581–591. doi:10.1016/j.jcin.2014.02.009

Le Gall, S., Even, S., and Lahaye, M. (2016). Fast Estimation of Dietary Fiber Content in Apple. *J. Agric. Food Chem.* 64, 1401–1405. doi:10.1021/acs.jafc.5b05301

Liu, Y. L., Hu, W. Z., Jiang, A. L., Liu, C. H., and Bai, L. L. (2015). Determination of Fat and Fatty Acid in Chili and Chili Processing Food. *Sci. Tech. Food Ind.* 36, 285–291. doi:10.13386/j.issn1002-0306.2015.01.051

Liu, Y., Liu, Q., Li, P., Xing, D., Hu, H., Li, L., et al. (2018). Plants Traditionally Used to Make Cantonese Slow-Cooked Soup in China. *J. Ethnobiol. Ethnomedicine* 14, 4. doi:10.1186/s13002-018-0206-y

Liu, Y. N., Liang, Y., and Wang, G. J. (2014). Pharmacokinetics Research on Ophiopogonins Components in *Ophiopogon Japonicus* Extract. *Chin. J. Experim. Tradit. Med. Formul.* 20, 137–142. doi:10.13422/j.cnki.syfjx.2014090137

Liu, Y., Wujisguleng, W., and Long, C. (2012). Food Uses of Ferns in China: a Review. *Acta Soc. Bot. Pol.* 81, 263–270. doi:10.5586/asbp.2012.046

Lulekal, E., Asfaw, Z., Kelbessa, E., and Van Damme, P. (2011). Wild Edible Plants in Ethiopia: a Review on Their Potential to Combat Food Insecurity. *Af* 24, 71–121. doi:10.21825/af.v24i2.4998

Luo, B., Li, F., Ahmed, S., and Long, C. (2019). Diversity and Use of Medicinal Plants for Soup Making in Traditional Diets of the Hakka in West Fujian, China. *J. Ethnobiol. Ethnomedicine* 15, 60. doi:10.1186/s13002-019-0335-y

Multari, S., Neacsu, M., Scobbie, L., Cantlay, L., Duncan, G., Vaughan, N., et al. (2016). Nutritional and Phytochemical Content of High-Protein Crops. *J. Agric. Food Chem.* 64, 7800–7811. doi:10.1021/acs.jafc.6b00926

Nie, X. L., Sun, W., and Xu, C. X. (2014). The Applicability of Two Methods for Ash Determination in Food. *J. Food Saf. Qual.* 5, 925–928. doi:10.19812/j.cnki.jfsq11-5956/ts.2014.03.051

Ogawa, A., Tanaka, M., Sasaki, T., and Matsuda, A. (1998). Nucleosides and Nucleotides. 180. Synthesis and Antitumor Activity of Nucleosides that Have a Hydroxylamino Group Instead of a Hydroxyl Group at the 2'- or 3'-Position of the Sugar Moiety1. *J. Med. Chem.* 41, 5094–5107. doi:10.1002/chin.19991724310.1021/jm980466g

Parker, W. B., King, S. A., Allan, P. W., Bennett, L. L., Secrist, J. A., Montgomery, J. A., et al. (1997). In VivoGene Therapy of Cancer withE. coliPurine Nucleoside Phosphorylase. *Hum. Gene Ther.* 8, 1637–1644. doi:10.1089/hum.1997.8.14-1637

Patil, B. S., Jayaprakasha, G. K., Chidambara Murthy, K. N., and Vikram, A. (2009). Bioactive Compounds: Historical Perspectives, Opportunities, and Challenges. *J. Agric. Food Chem.* 57, 8142–8160. doi:10.1021/jf9000132

Ross, L., Scarsella, A., Raffanti, S., Henry, K., Becker, S., Fisher, R., et al. (2001). Thymidine Analog and Multinucleoside Resistance Mutations Are Associated with Decreased Phenotypic Susceptibility to Stavudine in HIV Type 1 Isolated from Zidovudine-Naive Patients Experiencing Viremia on Stavudine-Containing Regimens. *AIDS Res. Hum. Retroviruses* 17, 1107–1115. doi:10.1089/088922201316912718

Ruth, J. L., and Cheng, Y. C. (1981). Nucleoside Analogues with Clinical Potential in Antivirus Chemotherapy. The Effect of Several Thymidine and 2'-deoxycytidine Analogue 5'-triphosphates on Purified Human (Alpha, Beta) and Herpes Simplex Virus (Types 1, 2) DNA Polymerases. *Mol. Pharmacol.* 20, 415–422. doi:10.0000/PMID6272095

Sarker, U., Hossain, M. M., and Oba, S. (2020b). Nutritional and Antioxidant Components and Antioxidant Capacity in green Morph *Amaranthus* Leafy Vegetable. *Sci. Rep.* 10, 1336. doi:10.1038/s41598-020-57687-3

Sarker, U., Hossain, M. N., Iqbal, M. A., and Oba, S. (2020c). Bioactive Components and Radical Scavenging Activity in Selected advance Lines of Salt-Tolerant Vegetable Amaranth. *Front. Nutr.* 7, 587257. doi:10.3389/fnut.2020.587257

Sarker, U., Islam, M. T., and Oba, S. (2018e). Salinity Stress Accelerates Nutrients, Dietary Fiber, Minerals, Phytochemicals and Antioxidant Activity in *Amaranthus Tricolor* Leaves. *PLoS ONE* 13, e0206388. doi:10.1371/journal.pone.0206388

Sarker, U., and Oba, S. (2019a). Antioxidant Constituents of Three Selected Red and green Color *Amaranthus* Leafy Vegetable. *Sci. Rep.* 9, 18233. doi:10.1038/s41598-019-52033-8

Sarker, U., and Oba, S. (2018b). Augmentation of Leaf Color Parameters, Pigments, Vitamins, Phenolic Acids, Flavonoids and Antioxidant Activity in Selected Amaranthus Tricolor under Salinity Stress. *Sci. Rep.* 8, 12349. doi:10.1038/s41598-018-30897-6

Sarker, U., and Oba, S. (2021). Color Attributes, Betacyanin, and Carotenoid Profiles, Bioactive Components, and Radical Quenching Capacity in Selected *Amaranthus Gangeticus* Leafy Vegetables. *Sci. Rep.* 11, 11559. doi:10.1038/s41598-021-91157-8

Sarker, U., Oba, S., and Daramy, M. A. (2020a). Nutrients, Minerals, Antioxidant Pigments and Phytochemicals, and Antioxidant Capacity of the Leaves of Stem Amaranth. *Sci. Rep.* 10, 3892. doi:10.1038/s41598-020-60252-7

Sarker, U., and Oba, S. (2018a). Drought Stress Enhances Nutritional and Bioactive Compounds, Phenolic Acids and Antioxidant Capacity of *Amaranthus* Leafy Vegetable. *BMC Plant Biol.* 18, 258. doi:10.1186/s12870-018-1484-1

Sarker, U., and Oba, S. (2020f). Leaf Pigmentation, its Profiles and Radical Scavenging Activity in Selected *Amaranthus Tricolor* Leafy Vegetables. *Sci. Rep.* 10, 18617. doi:10.1038/s41598-020-66376-0

Sarker, U., and Oba, S. (2019b). Nutraceuticals, Antioxidant Pigments, and Phytochemicals in the Leaves of *Amaranthus Spinosus* and *Amaranthus Viridis* Weedy Species. *Sci. Rep.* 9, 20413. doi:10.1038/s41598-019-50977-5

Sarker, U., and Oba, S. (2020e). Nutraceuticals, Phytochemicals, and Radical Quenching Ability of Selected Drought-Tolerant advance Lines of Vegetable Amaranth. *BMC Plant Biol.* 20, 564. doi:10.1186/s12870-020-02780-y

Sarker, U., and Oba, S. (2020c). Nutrients, Minerals, Pigments, Phytochemicals, and Radical Scavenging Activity in *Amaranthus Blitum* Leafy Vegetables. *Sci. Rep.* 10, 3868. doi:10.1038/s41598-020-59848-w

Sarker, U., and Oba, S. (2020d). Nutritional and Bioactive Constituents and Scavenging Capacity of Radicals in Amaranthus Hypochondriacus. *Sci. Rep.* 10, 19962. doi:10.1038/s41598-020-71714-3

Sarker, U., and Oba, S. (2020a). Phenolic Profiles and Antioxidant Activities in Selected Drought-Tolerant Leafy Vegetable Amaranth. *Sci. Rep.* 10, 18287. doi:10.1038/s41598-020-71727-y

Sarker, U., and Oba, S. (2020b). Polyphenol and Flavonoid Profiles and Radical Scavenging Activity in Leafy Vegetable *Amaranthus Gangeticus*. *BMC Plant Biol.* 20, 499. doi:10.1186/s12870-020-02700-0

Sarker, U., and Oba, S. (2019c). Protein, Dietary Fiber, Minerals, Antioxidant Pigments and Phytochemicals, and Antioxidant Activity in Selected Red Morph *Amaranthus* Leafy Vegetable. *PLoS ONE* 14, e0222517. doi:10.1371/journal.pone.0222517

Sarker, U., and Oba, S. (2018c). Response of Nutrients, Minerals, Antioxidant Leaf Pigments, Vitamins, Polyphenol, Flavonoid and Antioxidant Activity in Selected Vegetable Amaranth under Four Soil Water Content. *Food Chem.* 252, 72–83. doi:10.1016/j.foodchem.2018.01.097

Sarker, U., and Oba, S. (2018d). Salinity Stress Enhances Color Parameters, Bioactive Leaf Pigments, Vitamins, Polyphenols, Flavonoids and Antioxidant Activity in Selected *Amaranthus* Leafy Vegetables. *J. Sci. Food Agric.* 99, 2275–2284. doi:10.1002/jsfa.9423

Sarker, U., and Oba, S. (2020). The Response of Salinity Stress-Induced *A. Tricolor* to Growth, Anatomy, Physiology, Non-enzymatic and Enzymatic Antioxidants. *Front. Plant Sci.* 11, 559876. doi:10.3389/fpls.2020.559876

State Administration of Traditional Chinese Medicine. *Zhong Hua Ben Cao* (Shanghai: Shanghai Science and Technology Press), 8, 156–157.

Sun, J., Peng, H. X., Dong, X. H., Zhu, E. J., and Ren, J. Y. HPLC Analysis Method on β-carotene in Sweet Potato. *Food Sci. Techn* 1, 236–238.

Turan, M., Kordali, S., Zengin, H., Dursun, A., and Sezen, Y. (2003). Macro and Micro mineral Content of Some Wild Edible Leaves Consumed in Eastern Anatolia. *Acta Agriculturae Scand. Section B - Soil Plant Sci.* 53, 129–137. doi:10.1080/090647103100095

Wang, G. Y. (2009). *Chinese Food Composition Table*. 2nd Edition. Beijing: Peking University Medical Press. Available at: http://yingyang.911cha.com/M2F3.html.

Wang, Z. B., Gao, H. Y., and Wu, L. J. (2010). Isolation and Identification of Chemical Constituents of Flavones from the Leaves of *Acanthopanax Senticosus* Harms. *J. Shenyang Pharm. Univ.* 27, 533–538. doi:10.14066/j.cnki.cn21-1349/r.2010.07.002

Wang, Z. T., Lan, Z., Lu, J., and Jiang, D. G. (2005). Introduction of GB/T 5009-2003 Methods of Food Hygienic Analysis-Physical and Chemical Section. *Chin. J. Food Hyg.* 17, 193–211. doi:10.13590/j.cjfh.2005.03.001

Wu, G. (2010). Functional Amino Acids in Growth, Reproduction, and Health. *Adv. Nutr.* 1, 31–37. doi:10.3945/an.110.1008

Wu, X., Wang, L., Wang, H., Dai, Y., Ye, W.-C., and Li, Y.-L. (2012). Steroidal Saponins from *Paris Polyphylla* Var. *Yunnanensis*. *Phytochemistry* 81, 133–143. doi:10.1016/j.phytochem.2012.05.034

Xing, J., Li, Q. L., Geng, T. H., Yi, H., and Song, S. Y. (2012). Research Development for Amino Acid Analysis and Determination. *China Food Add* 5, 187–191.

Yang, S.-L., Liu, X.-K., Wu, H., Wang, H.-B., and Qing, C. (2009). Steroidal Saponins and Cytoxicity of the Wild Edible Vegetable-Smilacina Atropurpurea. *Steroids* 74, 7–12. doi:10.1016/j.steroids.2008.08.008

Yang, S. L. (2003). Nucleosides from *Smilacina Atropurpurea*. *Chin. J. Nat. Med.* 4, 196–198.

Yokosuka, A., and Mimaki, Y. (2008). Steroidal Glycosides from the Underground Parts of *Trillium Erectum* and Their Cytotoxic Activity. *Phytochemistry* 69, 2724–2730. doi:10.1016/j.phytochem.2008.08.004

Zhang, A. W. (2008). Advance of Research on Determination of Protein in Food. *J. Farm Prod. Process.* 1, 80–82.

Zhang, H. P., Zhang, J., Liu, A. J., Zhang, P., and Sun, R. G. (2013). Analysis of Nutritional Components and Bioactive Substances of *Pleurotus Eryngii*. *Acta Nutr. Sin.* 3, 307–309. doi:10.13325/j.cnki.acta.nutr.sin.2013.03.002

Zhang, M. L., Guo, M. H., and Chen, D. H. (2009). Discussion on the Methods of Moisture Determination in Different Food. *Mod. Agr. Sci. Tech* 21, 291–293.

Zhang, Y., Li, H.-Z., Zhang, Y.-J., Jacob, M. R., Khan, S. I., Li, X.-C., et al. (2006). Atropurosides A-G, New Steroidal Saponins from Smilacina Atropurpurea. *Steroids* 71, 712–719. doi:10.1016/j.steroids.2006.04.005

Zhao, S. J., Han, M., Han, Z. M., Li, Y. L., and Yang, L. M. (2009). Separation and Identification of Flavonoids from *Smilacina Japonica* by High Speed Counter-current Chromatography. *Chin. J. Anal. Chem.* 37, 1354–1358. doi:10.1159/000210413

Zhao, X. L., Jing, W. G., Han, S. Y., Sun, G. L., Liu, Y. M., Zhang, Q. W., et al. (2011). Two New Steroidal Saponins from *Dioscorea Panthaica*. *Phytochemistry Lett.* 4, 267–270. doi:10.1016/j.phytol.2011.04.011

Zhou, Z. (2014). Application of Phase Coded Pulse Compression Method to Air-Coupled Ultrasonic Testing Signal Processing. *Jme* 50, 48–50. doi:10.16465/j.gste.2014.03.00410.3901/jme.2014.02.048

Conflict of Interest: The authors declare that the research was conducted in the absence of any commercial or financial relationships that could be construed as a potential conflict of interest.

Publisher's Note: All claims expressed in this article are solely those of the authors and do not necessarily represent those of their affiliated organizations, or those of the publisher, the editors and the reviewers. Any product that may be evaluated in this article, or claim that may be made by its manufacturer, is not guaranteed or endorsed by the publisher.

frontiers in Pharmacology

ORIGINAL RESEARCH
published: 12 August 2021
doi: 10.3389/fphar.2021.725162

Scientometric Analysis of Medicinal and Edible Plant *Coptis*

Zhibang Huang[1], Zhengkun Hou[2], Fengbin Liu[2,3], Mei Zhang[4], Wen Hu[5] and Shaofen Xu[1]*

[1]Postgraduate College, Guangzhou University of Chinese Medicine, Guangzhou, China, [2]Department of Gastroenterology, First Affiliated Hospital, Guangzhou University of Chinese Medicine, Guangzhou, China, [3]Baiyun Hospital of the First Affiliated Hospital, Guangzhou University of Chinese Medicine, Guangzhou, China, [4]Department of Integrative Medicine, Changsha Central Hospital, University of South China, Changsha, China, [5]Intensive Care Unit, Huanggang Hospital of Traditional Chinese Medicine, Huanggang, China

Objective: A scientometric analysis to obtain knowledge mapping of *Coptis* revealed the current research situation, knowledge base and research hotspots in *Coptis* research.

Methods: *Coptis*-related documents published from 1987 to 2020 were selected through the Web of Science Core Collection. CiteSpace, VOSviewer and Microsoft Excel were used to construct knowledge maps of the *Coptis* research field.

Results: A total of 367 documents and their references were analyzed. These papers were primarily published in mainland China (214), followed by Japan (57) and South Korea (52), and they each formed respective cooperation networks. The document co-citation analysis suggested that the identification of *Coptis* Salisb. species, the production of alkaloids, and the mechanisms of action of these alkaloids formed the knowledge bases in this field. A keyword analysis further revealed that the research hotspots were primarily concentrated in three fields of research involving berberine, *Coptis chinensis* Franch, and *Coptis japonica* (Thunb) Makino. Oxidative stress, rat plasma (for the determination of plasma alkaloid contents), and Alzheimer's disease are recent research hotspots associated with *Coptis*.

Conclusion: *Coptis* research was mainly distributed in three countries: China, Japan, and South Korea. Researchers were concerned with the identification of *Coptis* species, the production of *Coptis* alkaloids, and the efficacy and pharmacological mechanism of the constituent alkaloids. In addition, the anti-oxidative stress, pharmacokinetics, and Alzheimer's disease treatment of *Coptis* are new hotspots in this field. This study provides a reference for *Coptis* researchers.

Keywords: *Coptis*, berberine, scientometric, CiteSpace, VOSviewer

OPEN ACCESS

Edited by:
XY. Zhang,
University of Minho, Portugal

Reviewed by:
B. Elango,
IFET College of Engineering, India
Andrej Kastrin,
University of Ljubljana, Slovenia

****Correspondence:***
Zhengkun Hou
fenghou5128@126.com

Specialty section:
This article was submitted to Ethnopharmacology, a section of the journal Frontiers in Pharmacology

Received: *15 June 2021*
Accepted: *04 August 2021*
Published: *12 August 2021*

Citation:
Huang Z, Hou Z, Liu F, Zhang M, Hu W and Xu S (2021) Scientometric Analysis of Medicinal and Edible Plant Coptis. *Front. Pharmacol. 12:725162. doi: 10.3389/fphar.2021.725162*

INTRODUCTION

Coptis Salisb. is a genus of Ranunculaceae Juss., with six species found in China. Of these, the dried rhizome of *Coptis chinensis* Franch is a famous traditional Chinese medicine (TCM) and is widely used to treat diseases (Meng et al., 2018; Yang et al., 2021). It is primarily produced in Sichuan and Chongqing. *Coptis deltoidea* C. Y. Cheng et Hsiao and *Coptis teeta* Wall. are also used in TCM (Chen, Fan, and He, 2017).

From the perspective of TCM, the medicinal properties of *C. chinensis* are closely related to its efficacy. *C. chinensis* has a bitter taste and cold nature, and belongs to the heart, spleen, stomach, liver, gallbladder, and large intestine meridian. Its effects include clearing heat and dampness,

purging fire and detoxification. It is often used in combination with other TCMs as a component of prescriptions with different therapeutic effects. For example, Gegen Qinlian decoction consists of four medicines: *C. chinensis*, *Scutellaria baicalensis* Georgi, *Pueraria montana* var. lobata (Willd.), and *Glycyrrhiza uralensis* Fisch. ex DC., which are used to treat patients experiencing diarrhea, dysentery and fever (Xu et al., 2015; Li et al., 2016; Lv et al., 2019). Another common prescription is the Huanglian Jiedu decoction, which is composed of *C. chinensis*, *S. baicalensis*, *Phellodendron chinense* C.K.Schneid. and *Gardenia jasminoides* J. Ellis. This prescription is used to treat symptoms such as high fever and disturbances of consciousness (Chen et al., 2017).

From a pharmacological standpoint, the rhizome of *C. chinensis* contains a variety of alkaloids (Chen et al., 2008), including berberine, coptisine, palmatine, epiberberine, jatrorrhizine, worenine, and magnoflorine, which are the main components responsible for its biological activity. Berberine is the alkaloid present in the highest concentrations in the rhizomes of *C. chinensis*. It has antipathogen (Yan et al., 2008; Mangiaterra et al., 2021), antibacterial toxin, anti-inflammatory (Cuellar et al., 2001), hypoglycemic (Lee et al., 2006), anti-gastric ulcer, antitumor, and positive muscle strength effects and exerts a negative frequency on the myocardium. With further research, an increasing number of pharmacological effects induced by berberine have been discovered, and the corresponding mechanisms of action have also been explained.

To date, many *Coptis* studies have been conducted, and some of the research results are highly influential (Shitan et al., 2003). Although many papers associated with *Coptis* have been published in journals, these studies did not examine the relationship of *Coptis* research members, the main authors, institutions or literature in the field; summarize the current research focus; or predict the future trends in the field. Therefore, considerable time is needed for beginners to systematically understand the research on *Coptis*. In addition, it is important for researchers to guide future research and improve its productivity. Thus, it is very important and necessary to overcome a series of research obstacles. Scientometric analysis is a method used to analyze the frontiers and development trends of a specific field or discipline (Hood and Wilson, 2001; Lu et al., 2020). The goal is to gain insights into the development of scientific research on a specific subject, a broader field of inquiry, and even the entire scientific knowledge system (Chen et al., 2012). This objective is achieved by mining data from scientific literature or other media on specific topics. These data are usually extracted from citation databases that generally concentrate on journal articles, conference proceedings, papers, and other types of media (Waltman, 2016). Although many papers related to *Coptis* have been published in journals, to date, there has been no research using scientometrics to analyze the knowledge base and emerging trends in *Coptis* research. Therefore, the purpose of this study is to use scientometric analysis to draw a knowledge map of *Coptis* research to outline the current background knowledge and developmental trends in this field.

MATERIALS AND METHODS

Data Source and Search Strategy

The Web of Science (WoS) database is the most commonly used database in scientometric research (Lu et al., 2020). The "Core Collection" of the WoS database was searched as the data source on April 18, 2021, with index dates ranging from 1985 to 2020. The search strategy was "TI = (coptis OR goldthread OR goldthreads) OR AK = (coptis OR goldthread OR goldthreads)". When we searched the WoS database, TI (title) indicated the title of a document, and AK (Author Keywords) were the keywords provided by the authors. All the records were downloaded from the WoS and imported into software for analysis. Although the value of including certain types of literature in the analysis is not high, this approach more comprehensively presents the data type distribution of the sample.

Statistical Analysis

In this study, Microsoft Office Excel (v.2016) was used to create a figure on annual research output, and the bibliometric software VOSviewer1.6.15 and CiteSpace5.8. R1 were used to perform scientometric visualization analysis. VOSviewer was developed by van Eck and Waltman (van Eck and Waltman, 2017). This software is one of the most widely used tools in the bibliometric mapping field (Li et al., 2020). It provides visualization through similarity mapping technology and creates network visualization, in which the distance between nodes shows the relationship between them (van Eck and Waltman, 2010). In this study, the VOSviewer was used to identify the co-authors countries, author co-citations, and document co-citations. CiteSpace is a scientometric software that was developed by Professor Chaomei Chen. It was designed based on scientific revolution theory, structural hole theory, and optimal information foraging theory (Chen, 2006; Liang et al., 2017). Researchers have used CiteSpace to construct a co-authorship network and to cluster visualization of a co-occurring keyword analysis. We also created a dual-map overlay of the journals and detected the citation burst strength of the keywords. The parameters of CiteSpace are as follows: Links strength (cosine), scope (within slices). The selection criteria parameters were: g-index (k = 25), Top N (N = 50), Top N% (N = 10), link retaining factor (LRF = 3.0), look back years (LBY = 8), e for top N (e = 2.0), time span (1987–2020), and years per slice (1).

RESULTS

Distribution of Publications

The distribution of publications is a key indicator that provides insights into research activities on a given topic (Zhu and Hua, 2017). This study used a descriptive analysis method to analyze *Coptis*-related publication types, annual publication trends, and published journals.

We retrieved 367 documents related to *Coptis* from the WoS Core Collection. The types of publications retrieved included

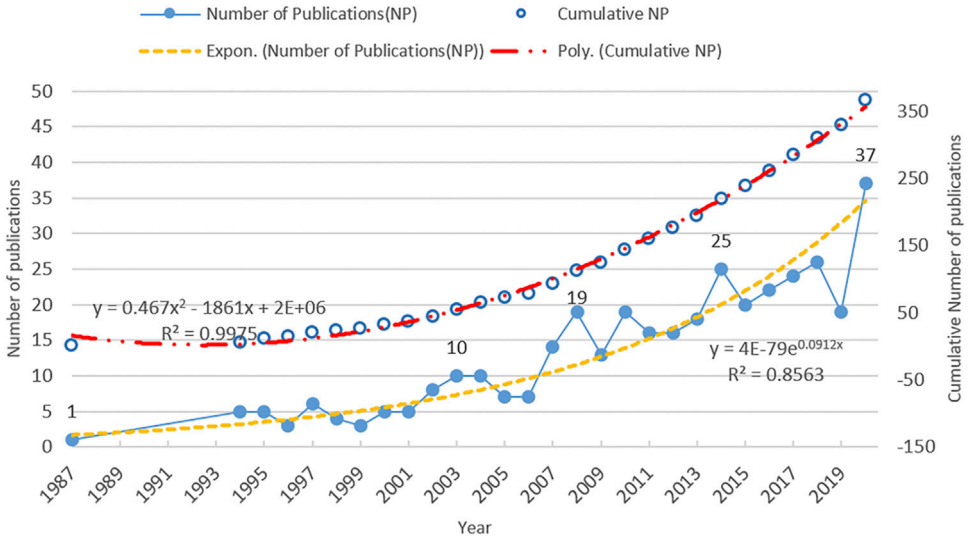

FIGURE 1 | Annual distribution of *Coptis* research output.

TABLE 1 | Journals that appeared at least 5 times in coupling analysis.

Source	Documents	Citations	Total Link Strength
Planta Medica	16	385	196
Evidence-Based Complementary and Alternative Medicine	12	54	203
Plant and Cell Physiology	12	297	279
Journal of Ethnopharmacology	11	221	193
Journal of Pharmaceutical and Biomedical Analysis	11	343	194
American Journal of Chinese Medicine	9	225	53
Fitoterapia	7	283	235
Archives of Pharmacal Research	6	251	109
Bioscience Biotechnology and Biochemistry	6	90	139
Phytochemistry	6	106	211
Journal of Biological Chemistry	5	523	272
Journal of Separation Science	5	54	172
Molecules	5	61	137
Phytotherapy Research	5	98	67

articles (319), meeting abstracts (31), reviews (10), news items (3), editorial material (2), corrections (1), letters (1) and proceedings papers (1). All the documents were published in 177 journals, of which 115 journals (65%) are members of the Committee on Publication Ethics (COPE). COPE is committed to educating and supporting editors, publishers and those involved in publication ethics to promote the culture of publishing towards one where ethical practice becomes a normal part of the publishing culture. In addition, other journals not included in COPE, also support a manuscript review process that also includes peer review. The annual distribution of *Coptis* research output is shown in **Figure 1**. The time interval of the publications was from 1987 to 2020, spanning 33 years. There was a total of 367 documents published during this period, with an average of 11 documents published per year, which also meant that more than one core paper was published every month. A trend line was used to fit the growth trend in the annual publication volumes. Its formula was $y = 4E\text{-}79e^{0.0912x}$. R^2 (0.8824), suggesting that the trend line adequately fitted the annual growth trend in publication volume. Although the annual volume of publications fluctuated, the trend line in the number of publications was growing exponentially. The figure also shows that the cumulative number of publications also had an exponential growth trend. Three significant peaks could be observed in the publication curve: 19 documents in 2008, 25 documents in 2014, and 37 documents in 2020. The number of publications began to rise sharply in 2006, each peak marked a high-yield period, and the number of records continued to increase exponentially during the later period.

Distribution of Publication Source Journals

Coptis-related research papers were distributed in 177 different source journals. **Supplementary Figure S1** shows the result of journal coupling analysis related to Coptis research. The distribution of journals with ≥5 publications is shown in

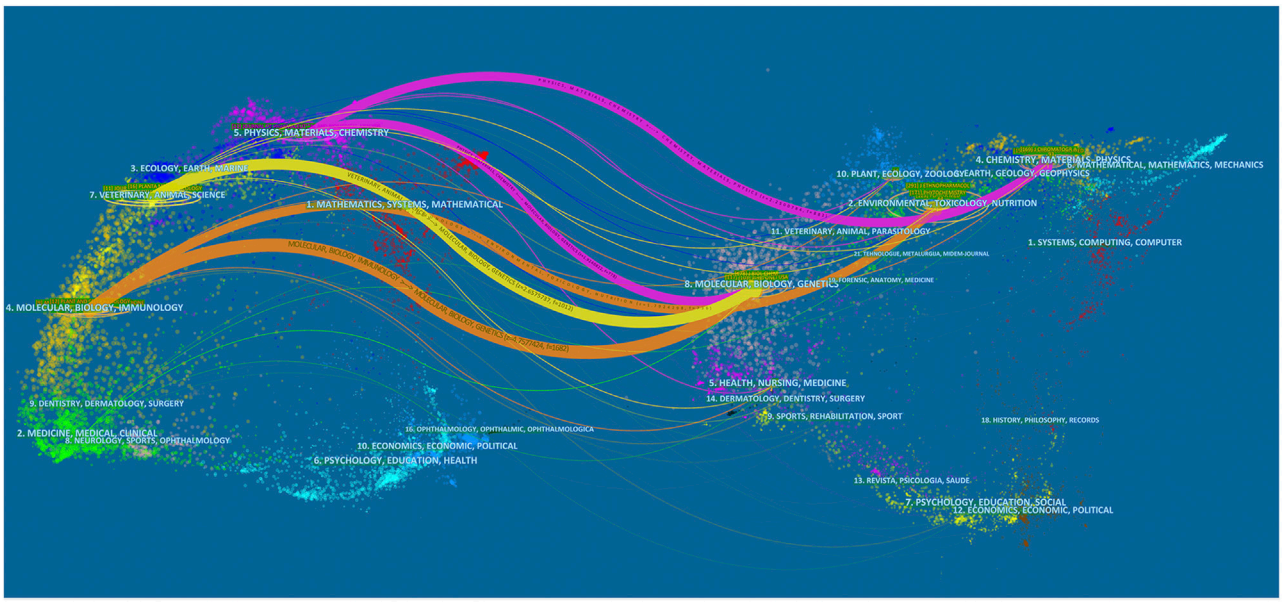

FIGURE 2 | The dual-map overlay of journals.

Table 1. The top five journals, based on the number of publications, were *Planta Medica* (16), *Evidence Based Complementary and Alternative Medicine* (12), *Plant and Cell Physiology* (12), *Journal of Ethnopharmacology* (11), and *Journal of Pharmaceutical and Biomedical Analysis* (11). The output distribution of the paper sources was unbalanced, with the top five journals accounting for 16.89% of all papers. Among them, *Planta Medica*, the number one publication, accounted for 4.36% of all papers, with 385 citations and a link strength of 196.

A dual-map overlay analysis was performed on the journals. The base map is the presentation of data on different topics in the journal, and the overlay is the co-citation map of the *Coptis* research field. The dual-map overlay shows the cooperative relationship between citing publications and cited references in different fields (Hou et al., 2018) (**Figure 2**). Citing papers primarily centered on three fields: molecular biology and immunology, veterinary animal science, and physics and materials chemistry. Among these fields, the circles representing the fields of molecular biology and immunology and animal science were larger, indicating that the numbers of co-authors and the numbers of published publications were relatively large. The line in the figure represents the link between citing publications and cited references. Each cited field has publications citing it. Molecular biogenetics were cited by publications in other fields, suggesting that this field had an important position in the cited references of *Coptis* research.

Network of Collaboration

National Collaborative Network

This section used the information at the levels of countries/regions where the research was performed to analyze the geographical distribution of documents published from 1987 to 2020. The nodes and lines in the collaborative network use different colors to represent different periods. As shown in **Figure 3**, the size of nodes and labels are related to the cooperative frequency of a country/region, and the thickness of the connection represents the strength of cooperation (Liao et al., 2018). The figure shows the average publication year (APY) of each country/region. Japanese and Korean publications were published relatively early, in the 2008–2012 period; American publications appeared in approximately 2013; China, Pakistan, and Russia appeared later, and they are currently countries/regions where research in the *Coptis* field is relatively active.

Table 2 lists 10 countries/regions with the highest output of *Coptis* research, corresponding to the network in the figure. Mainland China was the most prolific country in the field of *Coptis* research, with 214 papers, accounting for 58.31% of the total. China was followed by Japan (57 documents, 15.53%), and South Korea (52 documents, 14.17%). In terms of the number of citations, **Table 2** shows that mainland China had the most citations (3471), followed by Japan (1710), and South Korea (1011). However, the average number of citations per document in mainland China was lower than that of Japan, South Korea, and European and American countries. This finding might be related to the publication date.

Institutional Collaborative Network

Table 3 lists the top 10 institutions that had published literature on *Coptis*. The institutional collaboration network is shown in **Supplementary Figure S2**. Kyoto University had published 37 papers, accounting for 10.08% of the global total, and it ranked first in *Coptis* research. It was followed by Chengdu University of Traditional Chinese Medicine (22, 5.99%) and the Chinese Academy

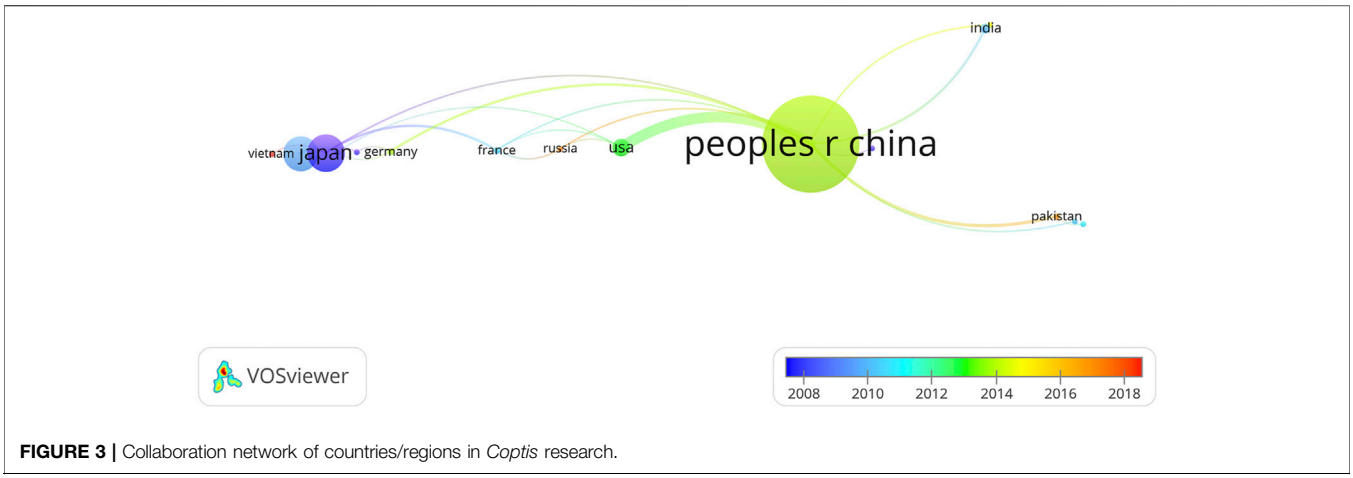

FIGURE 3 | Collaboration network of countries/regions in *Coptis* research.

TABLE 2 | The top 10 countries/regions in *Coptis* research.

No.	Country/Region	Continent	Documents	Citations	Total Link Strength
1	Peoples R China	Asia	214	3471	37
2	Japan	Asia	57	1710	13
3	South Korea	Asia	52	1011	6
4	United States	N. America	20	386	19
5	Taiwan	Asia	14	411	0
6	India	Asia	9	91	5
7	England	Europe	5	181	5
8	France	Europe	5	235	8
9	Germany	Europe	5	106	5
10	Pakistan	Asia	5	156	6

of Sciences (17, 4.63%). In terms of citations, Kyoto University and Chengdu University of Traditional Chinese Medicine had the highest number of citations. **Table 3** and **Figure 3** show that Chinese universities were producing increasingly more output in *Coptis* research, and seven universities in mainland China had entered the top 10.

Figure 4 shows the cooperation network of different countries/regions and institutions over the same period, from which we could obtain the primary research institutions of each country/region and their evolution. The results showed that *Coptis* research was largely concentrated in three countries: mainland China, Japan, and South Korea. The primary research institutions in mainland China were Chengdu University of Traditional Chinese Medicine (Wu et al., 2016), Chinese Academy of Sciences, China Academy of Chinese Medical Sciences, Southwest University, and other institutions; most papers were published within the 2010–2017 period. Japanese research was primarily performed at Kyoto University (Shitan et al., 2003; Kato et al., 2007), and the publication dates were mainly during the period of 2005–2010. South Korea's primary institutions were Kyung Hee University (Bae et al., 1998) and Kyungpook National University, and the publication dates of the literature were primarily concentrated in the year 2013.

Author Collaborative Network

Collaborative authors form research communities, in which the collaboration between authors within a research community is stronger than the collaboration with authors outside this community (Chen, Song, et al., 2008). As shown in **Figure 5**, the author cooperation network in the *Coptis* research field mainly consists of three clusters, which are composed of researchers from China, Japan, and South Korea. Chinese scholars had the largest cooperation network and the largest number of scholars. The author's APY can also be calculated to show the time dynamics of the cooperation (Hong et al., 2020). The lines between the nodes in the figure show different colors: yellow represents a recently published date, and purple represents earlier published date. In examining the figure, it was clear that Japanese and Korean scholars published studies earlier, while Chinese scholars published studies during a later time period.

There were a total of 1550 co-authors citing publications on *Coptis*-related research. Among them, 24 authors had published ≥5 papers. The author with the most published papers was Sato F with 32 papers, followed by Yazaki K (17 papers), and Shitan N (12 papers). These were all researchers engaged in *Coptis* research at Kyoto University and were primarily concentrated in the school's Research Institute for Sustainable Humanosphere and Graduate School of Biostudies. The fourth- and fifth-ranked authors were He Y and Fan G, respectively, who were from the College of Medical Technology and State Key Lab of Characteristic Chinese Medicine Resources at Chengdu University of Traditional Chinese Medicine.

Author co-citation occurs when two authors are cited by other publications (Ke et al., 2020). By analyzing authors co-cited relationship, an author co-citation network can be obtained, which reveals the highly cited authors and academic communities within references in this research field (Huang et al., 2019). We extracted authors whose cited frequency was ≥15 to construct an author co-citation density view, as shown in **Figure 6**. In the density map, the larger the author's label, the higher the frequency of the author's papers being cited. The higher the frequency of author's papers being cited, the higher density of the view, and the closer the view is to red. The figure

TABLE 3 | The top 10 institutions in *Coptis* research.

No.	Organization	Country	Documents	%/367	Citations	Total Link Strength
1	Kyoto Univ	Japan	37	10.08	1411	21
2	Chengdu Univ Tradit Chinese Med	Peoples R China	22	5.99	284	22
3	Chinese Acad Sci	Peoples R China	17	4.63	158	36
4	China Acad Chinese Med Sci	Peoples R China	13	3.54	270	26
5	Kyung Hee Univ	South Korea	8	2.18	219	19
6	Southwest Univ	Peoples R China	8	2.18	133	6
7	Beijing Univ Chinese Med	Peoples R China	7	1.91	43	12
8	Kyungpook Natl Univ	South Korea	7	1.91	81	10
9	Wuhan Univ	Peoples R China	7	1.91	110	1
10	Zhejiang Univ	Peoples R China	7	1.91	102	9

FIGURE 4 | Collaboration network of countries/regions and institutions in *Coptis* research.

shows that papers published by Japanese scholar Sato F at Kyoto University as the first unit had been cited 90 times in total, ranking him first among all authors. He and Morishige T (30), Ikezawa N (22), Yamada Y (20), and other major authors formed the largest network of cited references. The second largest was the subnetwork formed by the Chinese scholars Kong WJ (42) and Chen JH (37) and the Korean scholar Jung HA (41).

Topics and Keywords

At the macro level, *Coptis* research topics can be characterized by the professional journals in which the papers are published. At the micro level, natural language processing can be used to extract terms that characterize the paper topic from the titles, abstracts, and keywords of these journal articles to analyze and research the main topic investigated (Chen and Wu, 2017); although, the author selects the appropriate keywords that offer a higher-level of generalization of the theme of the study, so an analysis of the keywords provided by the author can also characterize the core topic of the publication (Niazi and Hussain, 2011). The topic mining results of natural language processing can more clearly characterize the structure of the field, while the results analyzed by using keywords allow a more intuitive understanding of the research content of the field.

Using the keyword processing method, 615 different words were identified from the keywords of 367 *Coptis*-related research documents, and high-frequency words were filtered and are presented in **Figure 7**. **Table 4** lists the keywords with frequency ≥10 appearances. The colors of the nodes and links in the figure represent different dates, while the sizes of the nodes and labels are

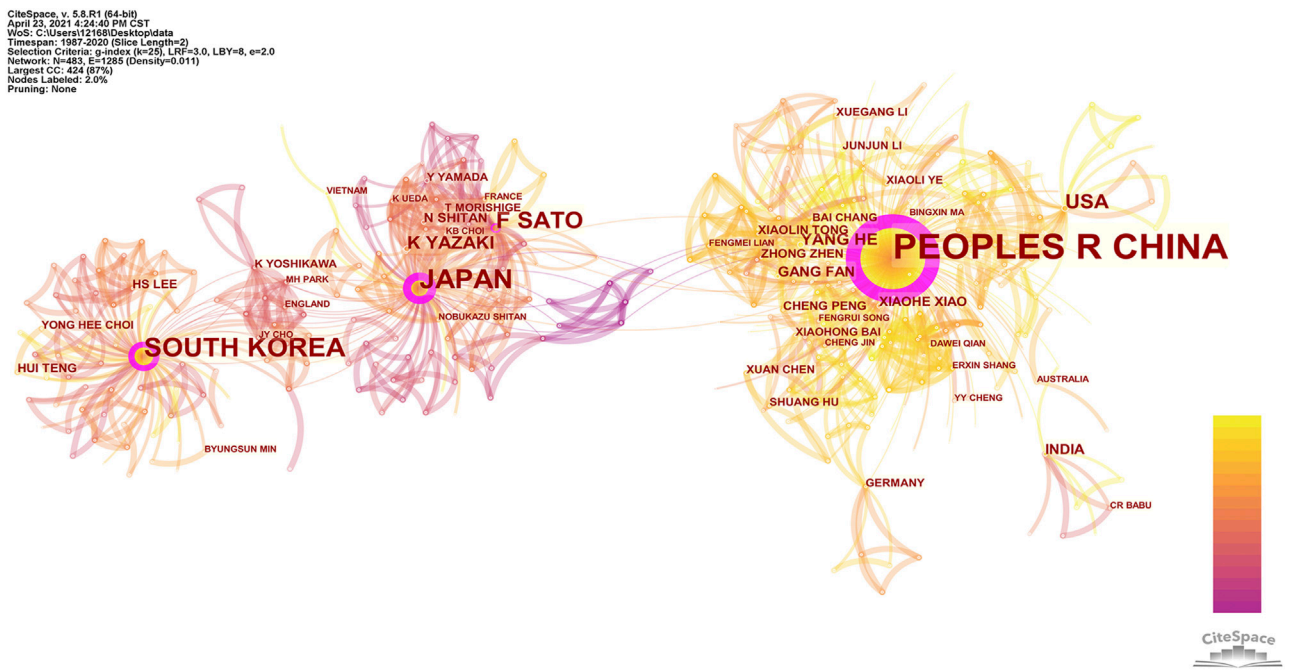

FIGURE 5 | Countries/regions and authors collaboration network of *Coptis* research.

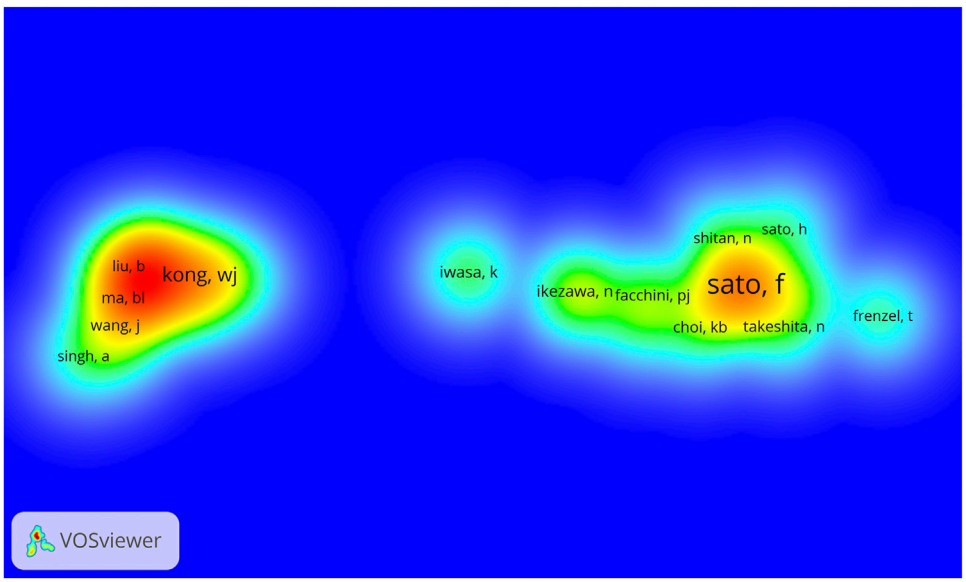

FIGURE 6 | Cluster density view of the author co-citation analysis of *Coptis* research.

proportional to the word frequency. The word frequency represents the number of papers in which the keyword appears. The nodes in purple circles show high betweenness centrality, with a value of ≥0.1, which also is an indication of the importance of these nodes (Qian, 2014), which are often connected to different subnetworks and are the intermediary or bridge between nodes. On combining the graphs, we can see that berberine was the keyword with the highest frequency. It first appeared in 1994 in the keywords of the collected publications, and its betweenness centrality was 0.61, which was the highest in the keyword co-occurrence network, indicating that it played an important connecting role. The second most frequent keyword was *C. chinensis*. Its frequency was 125, and the betweenness centrality was 0.39, which suggested that *C. chinensis* received widespread attention from researchers.

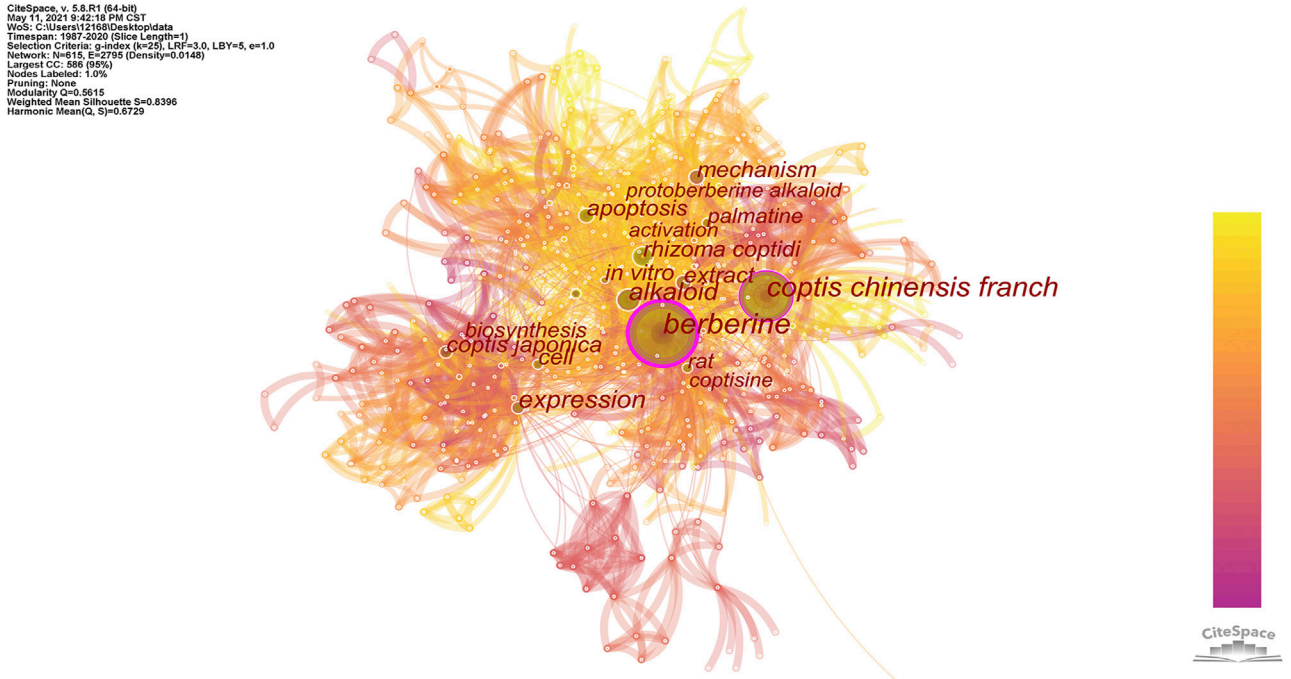

FIGURE 7 | Map of keyword co-occurrence related to *Coptis* research.

The distance between keywords in the cluster map is an index of the similarity between them. Two keywords with similar semantics are relatively closer in the cluster graph, so the keywords are spatially clustered into categories of different sizes. In this study, the log-likelihood rate (LLR) was used to divide the obtained keyword co-occurrence network into clusters; the relevant parameters were adjusted to clarify the obtained clusters and made them more representative. After clustering, the nodes are assigned to different clusters, which are represented by different colors; the cluster map and information obtained are shown in **Figure 8** and **Supplementary Table S1**. According to the

TABLE 4 | Keywords that appeared at least 10 times in *Coptis* research.

No.	Keyword	Freq	Degree	Centrality	Year	Cluster ID
1	berberine	129	197	0.61	1994	1
2	Coptis chinensis Franch	125	162	0.39	1995	2
3	alkaloid	57	96	0.14	1994	1
4	rhizoma coptidi	40	65	0.06	2005	1
5	Coptis japonica	32	57	0.09	1994	0
6	expression	31	91	0.17	1994	0
7	extract	24	70	0.1	2007	4
8	apoptosis	23	62	0.08	2005	8
9	mechanism	23	64	0.11	1996	3
10	Cell	21	67	0.09	1994	0
11	*in vitro*	19	65	0.09	1999	6
12	ranunculaceae	16	39	0.03	1994	3
13	Rat	15	43	0.07	2007	6
14	palmatine	14	43	0.04	1996	3
15	plant	13	13	0.01	1994	1
16	constituent	11	38	0.04	1995	1
17	activation	11	41	0.03	2006	4
18	identification	10	25	0.03	1997	2
19	biosynthesis	10	49	0.06	1994	0
20	protoberberine alkaloid	10	40	0.03	2006	3
21	coptisine	10	41	0.04	2000	10
22	adenosyl l methionine	10	35	0.01	1994	0

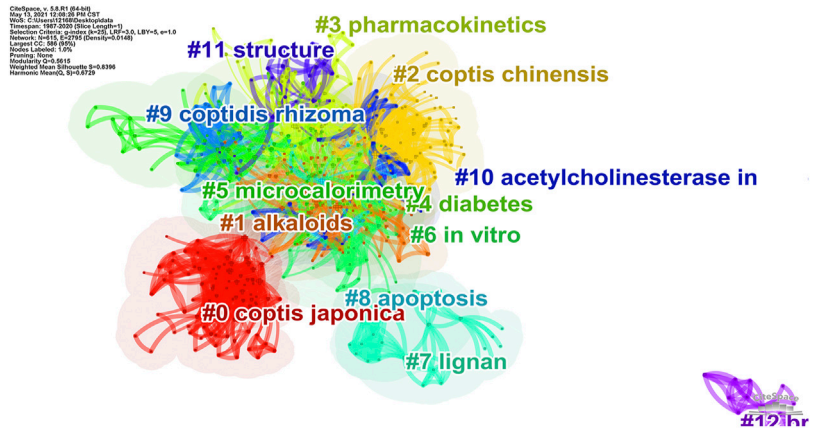

FIGURE 8 | Cluster map of keyword co-occurrence in *Coptis* research.

Top 15 Keywords with the Strongest Citation Bursts

Keywords	Year	Strength	Begin	End	1987 - 2020
coptis japonica	1987	7.84	1994	2008	
adenosyl l methionine	1987	2.91	1994	2003	
biosynthesis	1987	2.47	1994	2005	
alkaloid biosynthesis	1987	2.65	2001	2008	
protoberberine alkaloid	1987	2.38	2006	2010	
ranunculaceae	1987	3	2008	2011	
extract	1987	3.94	2012	2018	
palmatine	1987	3.27	2012	2015	
rhizoma coptidi	1987	5.41	2014	2018	
rat plasma	1987	2.37	2014	2020	
oxidative stress	1987	3.24	2015	2020	
performance liquid chromatography	1987	2.36	2015	2017	
toxicity	1987	3.96	2016	2018	
model	1987	2.64	2016	2020	
alzheimers disease	1987	2.36	2018	2020	

FIGURE 9 | Top 15 keywords with the strongest citation bursts.

results of the analysis, this research can be divided into 13 main research areas. The cluster with the largest size was Cluster 0 (*Coptis japonica*), followed by Cluster 1 (alkaloid), and Cluster 2 (*Coptis chinensis*). This showed that *Coptis japonica* (Thunb.) Makino occupied an important position in this field and was a hot research topic that should be explored. Alkaloids are effective components of *Coptis*. The node with the highest centrality in this cluster, berberine, is an alkaloid. *C. chinensis* is a commonly used Chinese medicine, and its primary research involved scholars from China.

Burst keywords can show how the frequency of keyword appearance has changed in the short term. The more burst nodes a cluster contains, the more active or emerging the trends there are in this field. The top 15 keywords with the strongest citation burst results in the *Coptis* research are shown in **Figure 9**. From the view of burst strength, *C. japonica* was the keyword with the strongest burst strength and the longest burst period. It emerged during 1994–2008, indicating that *C. japonica* was a research hotspot in this field for over a decade. The results of class 0 were consistent. From the perspective of emergence of the keywords over time, oxidative stress, rat plasma and Alzheimer's disease were the keywords having the most recent burst time, and these topics are new hotspots in *Coptis* research (Cao et al., 2018; Li et al., 2019).

Document Co-citation Network

This study uses the document co-citation method to analyze the relationship among cited references. We extracted 8346 documents from the references, limited the number of citations to ≥10, and obtained a co-cited network of 32 references and 233 links, as shown in **Figure 10**. Each node in the graph corresponds to a reference. The size of the node and the font indicates the frequency with which the reference is cited. The color of the node indicates the cluster to which the reference belongs, and the line between the nodes indicates the co-cited relationship between the references. **Table 5** summarizes information relative to the top ten cited references.

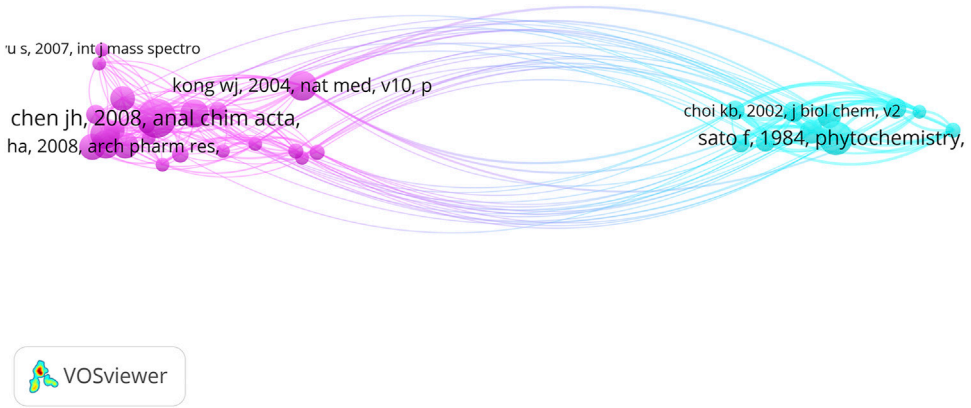

FIGURE 10 | Network map of references co-citation of *Coptis* research.

The references in the table are listed in descending order based on the number of citations. The most frequently cited reference was published by Chinese scholar Chen JH in 2008, "Analysis of alkaloids in *Coptis chinensis* Franch by accelerated solvent extraction combined with ultra-performance liquid chromatographic analysis with photodiode array and tandem mass spectrometry detections". The second most frequent citations involved the research result of Japanese scholar Sato F published in *Phytochemistry* in 1984. This result was followed by a paper published by Chinese scholar Kong WJ in *Nature Medicine* in 2004.

DISCUSSION

General Information

Coptis is used in the form of decoctions for complementary foods, dietary cures, and disease treatment in traditional medicine, which is homologs of medicine and food. Among the 367 documents we have obtained, six documents showed that *Coptis* can be used as an edible plant. The topic of these six studies involves the *Coptis chinensis* inflorescence, which is composed of peduncle, rachis and flowers. It is a by-product of *C. chinensis*. In the habitat of Tujia National Minority in China, the *C. chinensis* inflorescences are prepared as teas and are sold together with other functional foods in the local market (Ma et al., 2016). In addition, these studies mainly focused on the antioxidative, anti-phototoxicity, hypoglycemic, and hypocholesterolemic effects of *C. chinensis* inflorescence as an edible plant. Of course, *Coptis* is also a medicinal plant, which is the focus of most studies. *Coptis* has many functions, and exerts antipathogen, antibacterial toxin, anti-inflammatory, hypoglycemic, anti-gastric ulcer, and antitumor activity. The medicinal efficacy and pharmacological mechanism of *Coptis* are also the focus of research in this field.

The output of papers is one of the basic indicators for measuring the development of *Coptis* research, reflecting the degree of activity in the *Coptis* field. The trend line in annual publications shows that the number of papers had increased exponentially, with the largest number in 2020, reaching 37. This information showed that *Coptis* research has received attention from researchers, and an increasing number of resources (funds, scholars) will be invested in this field. *Coptis* research will become more active.

Journals Distribution

The citing documents in this study were from 177 journals. Upon combining the number of documents and the number of

TABLE 5 | Frequently cited references in *Coptis* research.

No.	Cited Reference	Citations	Total Link Strength
1	Chen Jh, 2008, Anal Chim Acta, v613, p184, doi 10.1016/j.aca. 2008.02.060	28	25
2	Sato F, 1984, Phytochemistry, v23, p281, doi 10.1016/s0031-9422(0080318–0)	24	42
3	Kong Wj, 2004, Nat Med, v10, p1344, doi 10.1038/nm1135	21	30
4	Yuan Lj, 2006, Plant Food Hum Nutr, v61, p139, doi 10.1007/s11130-006-0023–7	21	18
5	Jung Ha, 2009, Biol Pharm Bull, v32, p1433, doi 10.1248/bpb.32.1433	20	22
6	Tang J, 2009, J Ethnopharmacol, v126, p5, doi 10.1016/j.jep. 2009.08.009	20	16
7	Jung Ha, 2008, Arch Pharm Res, v31, p1405, doi 10.1007/s12272-001-2124-z	19	20
8	Yan D, 2008, J Biochem Bioph Meth, v70, p845, doi 10.1016/j.jbbm. 2007.07.009	19	16
9	Kuo Cl, 2004, Cancer Lett, v203, p127, doi 10.1016/j.canlet. 2003.09.002	18	21
10	Morishige T, 2000, J Biol Chem, v275, p23398, doi 10.1074/jbc.m002439200	17	50

citations, we found that *Planta Medica* was the journal with the most publications, and it contributes the most to *Coptis* research. The *Journal of Biological Chemistry* (JBC) was the most cited journal, and it contributed the greatest number of citations to this research. *Planta Medica* is one of the leading international journals in the fields of medicinal plants and natural product research. The journal covers the following research fields: biological and pharmacological activities, natural product chemistry and analysis research, pharmacokinetic research, natural product formulation and delivery systems. JBC mainly publishes the latest substantive scientific discoveries in various fields of biochemistry and molecular biology and clarifies the molecular and cellular basis of biological processes.

The dual-map overlay of journals indicates that the number of citing publications and coauthors in the fields of molecular biology and animal science was relatively large, indicating that *Coptis* research-related publications were mainly published in core journals in the fields of molecular biology and animal science. In cited references, articles in the molecular biology field had been cited by other areas, suggesting that this field had an important position in the cited references on *Coptis* research. This finding provided an important reference for new researchers in the *Coptis* field to perform experiments and write papers.

Cooperation Network

Coptis research publications were primarily concentrated in China, Japan, and South Korea. Judging from the date of publication, studies from Japan and South Korea were published earlier, and those from China were published later. China is currently a relatively active country in *Coptis* research. In terms of the number of publications, China was the most prolific country, followed by Japan and South Korea. We believe that the reasons are as follows. First, Asia is a region where traditional medicines are used and studied more frequently. Among them, China, Japan, and South Korea are the most obvious centers for this work. Second, China is the country with the highest production and application of *Coptis chinensis*. Finally, there are more Chinese medicine researchers in China than other countries.

In the author cooperation network, the author with the most documents, Sato F, is a researcher from Kyoto University, Japan. He formed a cooperative team with many Japanese researchers, including Yazaki K and Shitan N (Shitan et al., 2013). The second was the cooperative team formed by Chinese researchers He Y and Fan G (Li et al., 2020), who were engaged in the study of different *Coptis* species in China. Their research was of great significance to the distribution and identification of *Coptis* species. In the author co-citation analysis, the document published by Japanese scholar Sato F had the highest number of citations overall. Sato F along with Morishige T, Ikezawa N, Yamada Y and other major authors formed the largest network of cited references. The second-largest co-cited network was formed by the Chinese researchers Kong WJ and Chen JH, and the Korean researcher Jung HA. Their research results are discussed below in the knowledge base section.

Sato F is an important researcher in *Coptis* researchwith him as the central author, a group of Japanese researchers has been formed (Minami et al., 2007; Ikezawa et al., 2008). Articles be Sato F have been cited numerous times, and served as the knowledge base in the *Coptis* research field. Further, Sato F is an expert in plant cell molecular biology and is among the first group of researchers worldwide to use microorganisms to successfully produce isoquinoline alkaloids (Sato et al., 2007), which are typical secondary metabolites from plants. Sato F has established cultured cells (Sato et al., 1994) that can efficiently produce isoquinoline alkaloids from plants, such as the medicinal plant *C. japonica*. He discovered a variety of enzymes that control the biosynthesis of isoquinoline alkaloids and isolated associated genes (Inui et al., 2012). Sato F's research has made important contributions to the *Coptis* field, and his research results have been cited by many investigators in this field.

Knowledge Base

In bibliometrics, references constitute the knowledge base of the field. We can determine the knowledge base of the *Coptis* research field by analyzing the co-cited network of references (Li et al., 2018). By combining the number of citations of a reference and the strength of the connection, three references were found that have important knowledge-based functions. The following are their main findings.

Due to the variety of *Coptis* species and because it is difficult to distinguish among them, Chen JH established a method for the identification and quantification of the main alkaloids in *C. chinensis* extracts based on ASE and UPLC. The results show that the UPLC fingerprint based on the distribution of eight major alkaloids can be used as a fast and reliable method for the identification and quality evaluation of traditional Chinese medicine (Chen et al., 2008).

Sato F used a screening method to establish a *C. japonica* cell culture capable of producing a large amount of berberine and obtained a stable and high-yield *C. japonica* cell line through repeated cloning, enabling the stable and efficient production of berberine.

Chinese researcher Kong WJ identified berberine as a new cholesterol-lowering drug (Kong et al., 2004). Clinical experiments show that berberine can reduce serum cholesterol, triglycerides, and low-density lipoprotein (LDL) cholesterol in patients with hypercholesterolemia. Animal experiments show that berberine can reduce the serum cholesterol and LDL cholesterol of hyperlipidemic hamsters and increase liver low-density lipoprotein receptor (LDLR) mRNA and LDLR protein. Using human liver cancer cells, they found that berberine upregulate the expression of LDLR depending on the activation of extracellular signal-regulated kinase (ERK). Berberine increase the expression of LDLR by stabilizing the post-transcriptional mechanism of mRNA. Using luciferase as a heterologous system for reporter genes, scholars have further identified five proximal regions of the untranslated region of LDLR mRNA 3', which are responsible for the regulation of berberine. These findings indicate that berberine is a new lipid-lowering drug, and its mechanism of action is different from that of statins.

Research Hotspots

A hotspot refers to a scientific issue or topic keyword that is internally related to a specific period, which is discussed in a specific set of publications, and allows the generalization of the topic in the publications. The analysis of high-frequency keywords can identify hot spots in the *Coptis* research field (Wu et al., 2019).

In this study, berberine was the keyword with the highest frequency and betweenness centrality, indicating that berberine has received widespread attention from scholars studying *Coptis*. The second-largest cluster tag in the keyword clustering, "alkaloid", could also explain its importance. The rhizome of *Coptis* contains a variety of alkaloids, of which berberine has the highest content and is also the most widely studied. Berberine has a variety of pharmacological effects (Lee et al., 2006; Tang et al., 2009; Kabary et al., 2018) such as inhibiting pathogens, lowering hyperglycemia, inhibiting gastric ulcers, and inhibiting tumors. Its pharmacological effects of inhibiting pathogens and lowering hyperglycemia have attracted the attention of many researchers. The inhibitory activity of berberine has been evaluated against sortase, a bacterial surface protein anchoring transpeptidase, from *Staphylococcus aureus* ATCC 6538p. Berberine is a potent inhibitor of sortase, with an IC50 value of 8.7 mug/ml and has antibacterial activity against Gram-positive bacteria with a minimum inhibitory concentration (MIC) in the range of 50,400 mug/ml. These results indicate that berberine may be developed as a bacterial sortase inhibitor (Kim et al., 2004). Berberine has been prescribed for the treatment of diabetes. Glucose and lipid metabolism can be regulated by berberine via varied pathways, such as the AMP-activated protein kinase-(AMPK-) p38 MAPK-GLUT4, PI3K-Akt pathway, JNK pathway, PPARα pathway, etc. Activation of these pathways results in the up-regulation of the insulin receptor gene, thereby restoring insulin sensitivity (Yang et al., 2014). Thus, we believe that berberine has the effect of treating diabetes.

The frequency and centrality of *C. chinensis* among the keywords were second only to berberine, which was the third largest cluster in the keyword clustering. *C. chinensis* is a commonly used TCM (Wang et al., 2019). It was the most important species of *Coptis* in this field and was the main research focus of Chinese researchers, who were the largest research group in this study. The research content of *C. chinensis* mainly involved pharmacological effects and quality evaluation. Pharmacological effects of *C. chinensis* are similar to those of berberine and will not be repeated here. Quality control is a key factor in the development of the traditional medicine industry. However, a more effective quality control practice for *C. chinensis* should include the analysis of a group of major alkaloids, rather than a single species. Hence, many of the studies we included did not only involve the analysis of berberine. The UPLC-PDA method combined with ASE extraction was established to quantitatively determine the three main alkaloids berberine, palmatine and jatrorrhizine in the crude extract of *C. chinensis*. In addition, using the distribution pattern of the eight main alkaloids in the samples, the researchers established a UPLC-based fingerprinting method for the quality evaluation of *C. chinensis* (Chen et al., 2008). UPLC-based fingerprinting method provides a powerful tool for the quality evaluation of natural medicines.

In addition, this study clustered the study keywords and generated 13 clusters, of which the largest cluster was *C. japonica*. *C. japonica* was also the keyword with the strongest burst strength and the longest burst duration, which indicated that *C. japonica* occupied an important position in this field and was an active research hotspot during the evaluated period. Research evaluating *C. japonica* should be further explored. A research group focusing on *C. japonica* was formed with Japanese scholar Sato F as the central member. Their research hotspot was the use of microorganisms to produce isoquinoline alkaloids (Ikezawa et al., 2003; Yamada et al., 2011), which are metabolites of *C. japonica*. A variety of enzymes have been discovered that control the biosynthesis of isoquinoline alkaloids and related genes have been isolated, providing theoretical support for the large-scale production of berberine.

Keyword bursts can reflect that the frequency of keyword appearance has greatly changed in the short term. From the perspective of burst time, oxidative stress (OS), rat plasma and Alzheimer's disease were the keywords with the most recent burst date, and they represent recent hotspots in *Coptis* research. OS refers to a state in which the body's oxidation and antioxidant effects are out of balance. The state tends to be oxidized, contributing to the inflammatory infiltration of neutrophils, increased secretion of proteases, and the production of a large number of free radicals. Oxidative stress is believed to be an important factor leading to aging and disease (Friedemann et al., 2014). The most common diseases induced by elevated oxidative stress levels are heart disease, cancer, osteoarthritis, rheumatoid arthritis, diabetes, and neurodegenerative problems such as Alzheimer's disease and Parkinson's disease. Research related to OS suggests that Coptidis alkaloids inhibit oxidative stress, thereby improving the pathology of the above diseases (Friedemann et al., 2015). Studies involving the rat plasma concern the pharmacokinetics of *Coptis* alkaloids, which primarily measure the plasma contents of alkaloids after oral administration in rats (Liu et al., 2016). The burst of studies on Alzheimer's disease began in 2018. The primary research indicates that Coptidis alkaloids can protect nerves and can be used in treating Alzheimer's disease. *Coptis chinensis* Franch polysaccharide (CCP) appears to have a protective effect against amyloid-beta (Aβ)-induced toxicity in the *Caenorhabditis elegans* AD model partly by increasing lifespan, reducing Aβ accumulation, and up-regulating heat shock proteins. This study provides a new theoretical foundation regarding CCP for AD treatment (Li et al., 2018). The above subjects are recent research hotspots in the *Coptis* field, and researchers can conduct studies based on these hotspots.

STRENGTHS AND LIMITATIONS

This study has several strengths. First, this is the first systematic analysis of *Coptis* research using scientometric methods to provide a reference source for researchers. Second, we employed two widely used scientometric software programs to

simultaneously obtain our findings, both of which have been widely used in the field of scientometrics (Ke et al., 2020). However, similar to other scientometric research, our research also has some limitations. First, we only searched the WoS database, and none of the other large medical databases such as Scopus or Embase. It is worth noting that WoS is the most commonly used database in scientometric research (Lu et al., 2020). Due to the limited number of retrievable documents from the WoS, our study likely did not contain an exhaustive number of records regarding *Coptis* research, including the earliest documents. Nevertheless, the earliest document record may not be representative of the earliest *Coptis* research. In addition, the currently available bibliometric software exhibit great difficulty in analyzing data from multiple databases simultaneously. Second, all the data were extracted using software, unlike systematic reviews or data overviews that are manually extracted by two or more reviewers. Therefore, the data used to support our results may be biased. With the development of machine learning and data science, these problems may be solved in the future (Kehl et al., 2019). Third, we did not include papers related to *Coptis* in 2021 because these data were not complete when we searched the database.

CONCLUSION

This study used scientometric tools to identify the knowledge base and research hotspots for *Coptis*. The documents in this field were mainly concentrated in China, Japan and South Korea. The research results of Sato F and Chen JH are widely recognized in *Coptis* field. In a study published by Sato F, he investigated both metabolic regulation and the selection of cell lines for the production of large amounts of berberine in cultured *Coptis* cells, which led to berberine being produced stably and efficiently. The Chinese scholar Chen JH pointed out that UPLC fingerprints based on the distribution of eight major alkaloids can quickly and reliably be used to perform identification verification and quality evaluation of TCM. Through document co-citation analysis, three areas were presented in the knowledge base on *Coptis* research: the identification of *Coptis* species, the production of alkaloids, and the elucidation of the efficacy of alkaloids and their mechanism of action. *Coptis* research hotspots were primarily concentrated in the three fields of berberine, *C. chinensis*, and *C. japonica*. Regarding berberine, the effects of inhibiting pathogens and lowering hyperglycemia have attracted the attention of many researchers. The research content of *C. chinensis* mainly involved pharmacological effects and quality evaluation. Using microorganisms to successfully produce isoquinoline alkaloids was the research focus of *C. japonica*. Finally, oxidative stress, rat plasma as an indicator of alkaloids content and Alzheimer's disease emerged as the strongest burst keywords and recent hotspots related to *Coptis*. Researchers can conduct research based on the hotspots in this field.

DATA AVAILABILITY STATEMENT

The original contributions presented in the study are included in the article/**Supplementary Material**, further inquiries can be directed to the corresponding author.

AUTHOR CONTRIBUTIONS

ZhiH, and ZheH designed this study. ZhiH contributed toward manuscript writing. ZhiH, and FL performed the search. MZ, and WH collected and rechecked the data. ZhiH, ZheH, and SX performed the analysis. All the authors reviewed and revised the manuscript.

FUNDING

This work was supported by the National Natural Science Foundation of China (No. 81774450), the Key Field Project of Ordinary Colleges and Universities in Guangdong Province (No. 2020ZDZX3011), the Pearl River S&T Nova Program of Guangzhou, China (No. 201710010077), and the "Double top-class" and High-Level University Discipline Collaborative Innovation Team Project of Guangzhou University of Chinese Medicine (No. 2021XK18).

SUPPLEMENTARY MATERIAL

The Supplementary Material for this article can be found online at: https://www.frontiersin.org/articles/10.3389/fphar.2021.725162/full#supplementary-material

REFERENCES

Bae, E.-A., Han, M. J., Kim, N.-J., and Kim, D.-H. (1998). Anti-Helicobacter pylori Activity of Herbal Medicines. *Biol. Pharm. Bull.* 21 (9), 990–992. doi:10.1248/bpb.21.990

Cao, T. Q., Ngo, Q.-M. T., Seong, S. H., Youn, U. J., Kim, J. A., Kim, J., et al. (2018). Cholinesterase Inhibitory Alkaloids from the Rhizomes of Coptis Chinensis. *Bioorg. Chem.* 77, 625–632. doi:10.1016/j.bioorg.2018.01.038

Chen, C. (2006). CiteSpace II: Detecting and Visualizing Emerging Trends and Transient Patterns in Scientific Literature. *J. Am. Soc. Inf. Sci.* 57 (3), 359–377. doi:10.1002/asi.20317

Chen, C., Hu, Z., Liu, S., and Tseng, H. (2012). Emerging Trends in Regenerative Medicine: a Scientometric Analysis inCiteSpace. *Expert Opin. Biol. Ther.* 12 (5), 593–608. doi:10.1517/14712598.2012.674507

Chen, C., Song, I.-Y., Yuan, X., and Zhang, J. (2008). The Thematic and Citation Landscape of Data and Knowledge Engineering (1985-2007). *Data Knowledge Eng.* 67 (2), 234–259. doi:10.1016/j.datak.2008.05.004

Chen, G., Xu, Y., Jing, J., Mackie, B., Zheng, X., Zhang, X., et al. (2017). The Anti-sepsis Activity of the Components of Huanglian Jiedu Decoction with High Lipid A-Binding Affinity. *Int. Immunopharmacology* 46, 87–96. doi:10.1016/j.intimp.2017.02.025

Chen, H., Fan, G., and He, Y. (2017). Species Evolution and Quality Evaluation of Four Coptis Herbal Medicinal Materials in Southwest China. *3 Biotech.* 7, 8. doi:10.1007/s13205-017-0679-8

Chen, J., Wang, F., Liu, J., Lee, F. S.-C., Wang, X., and Yang, H. (2008). Analysis of Alkaloids in Coptis Chinensis Franch by Accelerated Solvent Extraction Combined with Ultra Performance Liquid Chromatographic Analysis with Photodiode Array and Tandem Mass Spectrometry Detections. *Analytica Chim. Acta* 613 (2), 184–195. doi:10.1016/j.aca.2008.02.060

Chen, Y., and Wu, C. (2017). The Hot Spot Transformation in the Research Evolution of Maker. *Scientometrics* 113 (3), 1307–1324. doi:10.1007/s11192-017-2542-4

Cuéllar, M. J., Giner, R. M., Recio, M. C., Máñez, S., and Ŕıos, J. L. (2001). Topical Anti-inflammatory Activity of Some Asian Medicinal Plants Used in Dermatological Disorders. *Fitoterapia* 72 (3), 221–229. doi:10.1016/s0367-326x(00)00305-1

Friedemann, T., Otto, B., Klätschke, K., Schumacher, U., Tao, Y., Leung, A. K.-M., et al. (2014). Coptis Chinensis Franch. Exhibits Neuroprotective Properties against Oxidative Stress in Human Neuroblastoma Cells. *J. Ethnopharmacology* 155 (1), 607–615. doi:10.1016/j.jep.2014.06.004

Friedemann, T., Schumacher, U., Tao, Y., Kai-Man Leung, Alexander., Leung, A. K.-M., and Schröder, S. (2015). Neuroprotective Activity of Coptisine fromCoptis chinensis(Franch). *Evidence-Based Complement. Altern. Med.* 2015, 1–9. doi:10.1155/2015/827308

Hong, R., Liu, H., Xiang, C., Song, Y., and Lv, C. (2020). Visualization and Analysis of Mapping Knowledge Domain of Oxidation Studies of Sulfide Ores. *Environ. Sci. Pollut. Res.* 27 (6), 5809–5824. doi:10.1007/s11356-019-07226-z

Hood, W. W., and Wilson, C. S. (2001). The Literature of Bibliometrics, Scientometrics, and Informetrics. *Scientometrics* 52 (2), 291–314. doi:10.1023/a:1017919924342

Hou, J., Yang, X., and Chen, C. (2018). Emerging Trends and New Developments in Information Science: a Document Co-citation Analysis (2009-2016). *Scientometrics* 115 (2), 869–892. doi:10.1007/s11192-018-2695-9

Huang, X., Fan, X., Ying, J., and Chen, S. (2019). Emerging Trends and Research Foci in Gastrointestinal Microbiome. *J. Transl Med.* 17, 11. doi:10.1186/s12967-019-1810-x

Ikezawa, N., Iwasa, K., and Sato, F. (2008). Molecular Cloning and Characterization of CYP80G2, a Cytochrome P450 that Catalyzes an Intramolecular C-C Phenol Coupling of (S)-Reticuline in Magnoflorine Biosynthesis, from Cultured Coptis Japonica Cells. *J. Biol. Chem.* 283 (14), 8810–8821. doi:10.1074/jbc.M705082200

Ikezawa, N., Tanaka, M., Nagayoshi, M., Shinkyo, R., Sakaki, T., Inouye, K., et al. (2003). Molecular Cloning and Characterization of CYP719, a Methylenedioxy Bridge-Forming Enzyme that Belongs to a Novel P450 Family, from Cultured Coptis Japonica Cells. *J. Biol. Chem.* 278 (40), 38557–38565. doi:10.1074/jbc.M302470200

Inui, T., Kawano, N., Shitan, N., Yazaki, K., Kiuchi, F., Kawahara, N., et al. (2012). Improvement of Benzylisoquinoline Alkaloid Productivity by Overexpression of 3′-Hydroxy-N-Methylcoclaurine 4′-O-Methyltransferase in Transgenic Coptis Japonica Plants. *Biol. Pharm. Bull.* 35 (5), 650–659. doi:10.1248/bpb.35.650

Kabary, D. M., Helmy, M. W., Elkhodairy, K. A., Fang, J.-Y., and Elzoghby, A. O. (2018). Hyaluronate/lactoferrin Layer-By-Layer-Coated Lipid Nanocarriers for Targeted Co-delivery of Rapamycin and Berberine to Lung Carcinoma. *Colloids Surf. B: Biointerfaces* 169, 183–194. doi:10.1016/j.colsurfb.2018.05.008

Kato, N., Dubouzet, E., Kokabu, Y., Yoshida, S., Taniguchi, Y., Dubouzet, J. G., et al. (2007). Identification of a WRKY Protein as a Transcriptional Regulator of Benzylisoquinoline Alkaloid Biosynthesis in Coptis Japonica. *Plant Cel Physiol.* 48 (1), 8–18. doi:10.1093/pcp/pcl041

Ke, L., Lu, C., Shen, R., Lu, T., Ma, B., and Hua, Y. (2020). Knowledge Mapping of Drug-Induced Liver Injury: A Scientometric Investigation (2010-2019). *Front. Pharmacol.* 11, 842. doi:10.3389/fphar.2020.00842

Kehl, K. L., Elmarakeby, H., Nishino, M., Van AllenVan Allen, E. M., Lepisto, E. M., Hassett, M. J., et al. (2019). Assessment of Deep Natural Language Processing in Ascertaining Oncologic Outcomes from Radiology Reports. *JAMA Oncol.* 5 (10), 1421–1429. doi:10.1001/jamaoncol.2019.1800

Kim, S.-H., Shin, D.-S., Oh, M.-N., Chung, S.-C., Lee, J.-S., and Oh, K.-B. (2004). Inhibition of the Bacterial Surface Protein Anchoring Transpeptidase Sortase by Isoquinoline Alkaloids. *Biosci. Biotechnol. Biochem.* 68 (2), 421–424. doi:10.1271/bbb.68.421

Kong, W., Wei, J., Abidi, P., Lin, M., Inaba, S., Li, C., et al. (2004). Berberine Is a Novel Cholesterol-Lowering Drug Working through a Unique Mechanism Distinct from Statins. *Nat. Med.* 10 (12), 1344–1351. doi:10.1038/nm1135

Lee, Y. S., Kim, W. S., Kim, K. H., Yoon, M. J., Cho, H. J., Shen, Y., et al. (2006). Berberine, a Natural Plant Product, Activates AMP-Activated Protein Kinase with Beneficial Metabolic Effects in Diabetic and Insulin-Resistant States. *Diabetes* 55 (8), 2256–2264. doi:10.2337/db06-0006

Li, J., Fan, G., and He, Y. (2020). Predicting the Current and Future Distribution of Three Coptis Herbs in China under Climate Change Conditions, Using the MaxEnt Model and Chemical Analysis. *Sci. Total Environ.* 698, 134141. doi:10.1016/j.scitotenv.2019.134141

Li, J., Goerlandt, F., Reniers, G., and Zhang, B. (2020). Sam Mannan and His Scientific Publications: A Life in Process Safety Research. *J. Loss Prev. Process Industries* 66, 104140. doi:10.1016/j.jlp.2020.104140

Li, R., Chen, Y., Shi, M., Xu, X., Zhao, Y., Wu, X., et al. (2016). Gegen Qinlian Decoction Alleviates Experimental Colitis via Suppressing TLR4/NF-Kb Signaling and Enhancing Antioxidant Effect. *Phytomedicine* 23 (10), 1012–1020. doi:10.1016/j.phymed.2016.06.010

Li, X., Du, J., and Long, H. (2018). A Comparative Study of Chinese and Foreign Green Development from the Perspective of Mapping Knowledge Domains. *Sustainability* 10 (12), 4357. doi:10.3390/su10124357

Li, Y., Guan, S., Liu, C., Chen, X., Zhu, Y., Xie, Y., et al. (2018). Neuroprotective Effects of Coptis Chinensis Franch Polysaccharide on Amyloid-Beta (Aβ)-Induced Toxicity in a Transgenic *Caenorhabditis elegans* Model of Alzheimer's Disease (AD). *Int. J. Biol. Macromolecules* 113, 991–995. doi:10.1016/j.ijbiomac.2018.03.035

Li, Y., Wang, B., Liu, C., Zhu, X., Zhang, P., Yu, H., et al. (2019). Inhibiting C-Jun N-Terminal Kinase (JNK)-mediated Apoptotic Signaling Pathway in PC12 Cells by a Polysaccharide (CCP) from Coptis Chinensis against Amyloid-β (Aβ)-Induced Neurotoxicity. *Int. J. Biol. Macromolecules* 134, 565–574. doi:10.1016/j.ijbiomac.2019.05.041

Liang, Y.-D., Li, Y., Zhao, J., Wang, X.-Y., Zhu, H.-Z., and Chen, X.-H. (2017). Study of Acupuncture for Low Back Pain in Recent 20 years: a Bibliometric Analysis via CiteSpace. *Jpr* Vol. 10, 951–964. doi:10.2147/jpr.S132808

Liao, H., Tang, M., Luo, L., Li, C., Chiclana, F., and Zeng, X.-J. (2018). A Bibliometric Analysis and Visualization of Medical Big Data Research. *Sustainability* 10 (1), 166. doi:10.3390/su10010166

Liu, L., Wang, Z.-B., Song, Y., Yang, J., Wu, L.-J., Yang, B.-Y., et al. (2016). Simultaneous Determination of Eight Alkaloids in Rat Plasma by UHPLC-MS/Simultaneous Determination of Eight Alkaloids in Rat Plasma by UHPLC-MS/MS after Oral Administration of Coptis deltoidea C. Y. Cheng et Hsiao and Coptis chinensis Franch. *Molecules* 21 (7), 913. doi:10.3390/molecules21070913

Lu, C., Liu, M., Shang, W., Yuan, Y., Li, M., Deng, X., et al. (2020). Knowledge Mapping of Angelica Sinensis (Oliv.) Diels (Danggui) Research: A Scientometric Study. *Front. Pharmacol.* 11, 294. doi:10.3389/fphar.2020.00294

Lv, J., Jia, Y., Li, J., Kuai, W., Li, Y., Guo, F., et al. (2019). Gegen Qinlian Decoction Enhances the Effect of PD-1 Blockade in Colorectal Cancer with Microsatellite Stability by Remodelling the Gut Microbiota and the Tumour Microenvironment. *Cell Death Dis* 10. doi:10.1038/s41419-019-1638-6

Ma, B., Tong, J., Zhou, G., Mo, Q., He, J., and Wang, Y. (2016). Coptis Chinensis Inflorescence Ameliorates Hyperglycaemia in 3T3-L1 Preadipocyte and Streptozotocin-Induced Diabetic Mice. *J. Funct. Foods* 21, 455–462. doi:10.1016/j.jff.2015.12.021

Mangiaterra, G., Cedraro, N., Laudadio, E., Minnelli, C., Citterio, B., Andreoni, F., et al. (2021). The Natural Alkaloid Berberine Can Reduce the Number of Pseudomonas aeruginosa Tolerant Cells. *J. Nat. Prod.* 84 (4), 993–1001. doi:10.1021/acs.jnatprod.0c01151

Meng, F.-C., Wu, Z.-F., Yin, Z.-Q., Lin, L.-G., Wang, R., and Zhang, Q.-W. (2018). Coptidis Rhizoma and its Main Bioactive Components: Recent Advances in Chemical Investigation, Quality Evaluation and Pharmacological Activity. *Chin. Med.* 13, 18. doi:10.1186/s13020-018-0171-3

Minami, H., Dubouzet, E., Iwasa, K., and Sato, F. (2007). Functional Analysis of Norcoclaurine Synthase in Coptis Japonica. *J. Biol. Chem.* 282 (9), 6274–6282. doi:10.1074/jbc.M608933200

Niazi, M., and Hussain, A. (2011). Agent-based Computing from Multi-Agent Systems to Agent-Based Models: a Visual Survey. *Scientometrics* 89 (2), 479–499. doi:10.1007/s11192-011-0468-9

Qian, G. (2014). Scientometric Sorting by Importance for Literatures on Life Cycle Assessments and Some Related Methodological Discussions. *Int. J. Life Cycle Assess.* 19 (7), 1462–1467. doi:10.1007/s11367-014-0747-9

Sato, F., Inui, T., and Takemura, T. (2007). Metabolic Engineering in Isoquinoline Alkaloid Biosynthesis. *Curr. Pharm. Biotechnol.* 8 (4), 211–218. doi:10.2174/138920107781387438

Sato, F., Tsujita, T., Katagiri, Y., Yoshida, S., and Yamada, Y. (1994). Purification and Characterization of S-Adenosyl-L-Methionine:norcoclaurine 6-O-Methyltransferase from Cultured Coptis Japonica Cells. *Eur. J. Biochem.* 225 (1), 125–131. doi:10.1111/j.1432-1033.1994.00125.x

Shitan, N., Bazin, I., Dan, K., Obata, K., Kigawa, K., Ueda, K., et al. (2003). Involvement of CjMDR1, a Plant Multidrug-resistance-type ATP-Binding Cassette Protein, in Alkaloid Transport in Coptis Japonica. *Proc. Natl. Acad. Sci.* 100 (2), 751–756. doi:10.1073/pnas.0134257100

Shitan, N., Dalmas, F., Dan, K., Kato, N., Ueda, K., Sato, F., et al. (2013). Characterization of Coptis Japonica CjABCB2, an ATP-Binding Cassette Protein Involved in Alkaloid Transport. *Phytochemistry* 91, 109–116. doi:10.1016/j.phytochem.2012.02.012

Tang, J., Feng, Y., Tsao, S., Wang, N., Curtain, R., and Wang, Y. (2009). Berberine and Coptidis Rhizoma as Novel Antineoplastic Agents: A Review of Traditional Use and Biomedical Investigations. *J. Ethnopharmacology* 126 (1), 5–17. doi:10.1016/j.jep.2009.08.009

van Eck, N. J., and Waltman, L. (2017). Citation-based Clustering of Publications Using CitNetExplorer and VOSviewer. *Scientometrics* 111 (2), 1053–1070. doi:10.1007/s11192-017-2300-7

van Eck, N. J., Waltman, L., and Waltman, Ludo. (2010). Software Survey: VOSviewer, a Computer Program for Bibliometric Mapping. *Scientometrics* 84 (2), 523–538. doi:10.1007/s11192-009-0146-3

Waltman, L. (2016). A Review of the Literature on Citation Impact Indicators. *J. Informetrics* 10 (2), 365–391. doi:10.1016/j.joi.2016.02.007

Wang, J., Wang, L., Lou, G.-H., Zeng, H.-R., Hu, J., Huang, Q.-W., et al. (2019). Coptidis Rhizoma: a Comprehensive Review of its Traditional Uses, Botany, Phytochemistry, Pharmacology and Toxicology. *Pharm. Biol.* 57 (1), 193–225. doi:10.1080/13880209.2019.1577466

Wu, J., Zhang, H., Hu, B., Yang, L., Wang, P., Wang, F., et al. (2016). Coptisine from Coptis Chinensis Inhibits Production of Inflammatory Mediators in Lipopolysaccharide-Stimulated RAW 264.7 Murine Macrophage Cells. *Eur. J. Pharmacol.* 780, 106–114. doi:10.1016/j.ejphar.2016.03.037

Wu, P., Ata-Ul-KarimAta-Ul-Karim, S. T., Singh, B. P., Wang, H., Wu, T., Liu, C., et al. (2019). A Scientometric Review of Biochar Research in the Past 20 Years (1998-2018). *Biochar* 1 (1), 23–43. doi:10.1007/s42773-019-00002-9

Xu, J., Lian, F., Zhao, L., Zhao, Y., Chen, X., Zhang, X., et al. (2015). Structural Modulation of Gut Microbiota during Alleviation of Type 2 Diabetes with a Chinese Herbal Formula. *Isme J.* 9 (3), 552–562. doi:10.1038/ismej.2014.177

Yamada, Y., Kokabu, Y., Chaki, K., Yoshimoto, T., Ohgaki, M., Yoshida, S., et al. (2011). Isoquinoline Alkaloid Biosynthesis Is Regulated by a Unique bHLH-type Transcription Factor in Coptis Japonica. *Plant Cel Physiol.* 52 (7), 1131–1141. doi:10.1093/pcp/pcr062

Yan, D., Jin, C., Xiao, X.-H., and Dong, X.-P. (2008). Antimicrobial Properties of Berberines Alkaloids in Coptis Chinensis Franch by Microcalorimetry. *J. Biochem. Biophysical Methods* 70 (6), 845–849. doi:10.1016/j.jbbm.2007.07.009

Yang, T.-C., Chao, H.-F., Shi, L.-S., Chang, T.-C., Lin, H.-C., and Chang, W.-L. (2014). Alkaloids from Coptis Chinensis Root Promote Glucose Uptake in C2C12 Myotubes. *Fitoterapia* 93, 239–244. doi:10.1016/j.fitote.2014.01.008

Yang, Y., Vong, C. T., Zeng, S., Gao, C., Chen, Z., Fu, C., et al. (2021). Tracking Evidences of Coptis Chinensis for the Treatment of Inflammatory Bowel Disease from Pharmacological, Pharmacokinetic to Clinical Studies. *J. Ethnopharmacology* 268, 113573. doi:10.1016/j.jep.2020.113573

Zhu, J., and Hua, W. (2017). Visualizing the Knowledge Domain of Sustainable Development Research between 1987 and 2015: a Bibliometric Analysis. *Scientometrics* 110 (2), 893–914. doi:10.1007/s11192-016-2187-8

Conflict of Interest: The authors declare that the research was conducted in the absence of any commercial or financial relationships that could be construed as a potential conflict of interest.

Publisher's Note: All claims expressed in this article are solely those of the authors and do not necessarily represent those of their affiliated organizations, or those of the publisher, the editors and the reviewers. Any product that may be evaluated in this article, or claim that may be made by its manufacturer, is not guaranteed or endorsed by the publisher.

frontiers in Pharmacology

REVIEW
published: 17 September 2021
doi: 10.3389/fphar.2021.735410

Emerging Applications of Metabolomics to Assess the Efficacy of Traditional Chinese Medicines for Treating Type 2 Diabetes Mellitus

Yumeng Zhang[1†], *Yingbo Yang*[1,2†], *Lili Ding*[1], *Zhengtao Wang*[1], *Ying Xiao*[1]* *and Wei Xiao*[1,2]*

[1]*The Ministry of Education (MOE) Key Laboratory for Standardization of Chinese Medicines, Institute of Chinese Materia Medica, Shanghai University of Traditional Chinese Medicine, Shanghai, China,* [2]*Jiangsu Kanion Pharmaceutical Co., Ltd., Lianyungang, China*

OPEN ACCESS

Edited by:
XY Zhang,
University of Minho, Portugal

Reviewed by:
You YUN,
China Academy of Chinese Medical Sciences, China
Shao Li,
Tsinghua University, China

***Correspondence:**
Ying Xiao
xiaoyingtcm@shutcm.edu.cn
Wei Xiao
xw_kanion@163.com

[†]*These authors have contributed equally to this article*

Specialty section:
This article was submitted to Ethnopharmacology, a section of the journal Frontiers in Pharmacology

Received: *02 July 2021*
Accepted: *08 September 2021*
Published: *17 September 2021*

Citation:
Zhang Y, Yang Y, Ding L, Wang Z, Xiao Y and Xiao W (2021) Emerging Applications of Metabolomics to Assess the Efficacy of Traditional Chinese Medicines for Treating Type 2 Diabetes Mellitus. Front. Pharmacol. 12:735410. doi: 10.3389/fphar.2021.735410

Diabetes is a common and complex disease that can exacerbate the complications related to cardiovascular disease, and this is especially true for type 2 diabetes mellitus (T2DM). In addition to the standard pharmacological therapies, T2DM has also been treated with nonconventional regimens such as traditional Chinese medicine (TCM), e.g., herbal medicines and TCM prescriptions, although the mechanisms underlying the therapeutic benefits remain unclear. In this regard, many studies have used metabolomics technology to elucidate the basis for the efficacy of TCM for T2DM. Metabolomics has recently attracted much attention with regard to drug discovery and pharmacologically relevant natural products. In this review, we summarize the application of metabolomics to the assessment of TCM efficacy for treating T2DM. Increasing evidence suggests that the metabolic profile of an individual patient may reflect a specific type of T2DM syndrome, which may provide a new perspective for disease diagnosis. In addition, TCM has proved effective for countering the metabolic disorders related to T2DM, and this may constitute the basis for TCM efficacy. Therefore, further determining how TCM contributes to the reversal of metabolic disorders, such as using network pharmacology or by assessing the contribution of host–gut microbiota interactions, will also provide researchers with new potential targets for pharmacologic-based therapies.

Keywords: traditional Chinese medicine, metabolomics, type 2 diabetes, metabolic regulation, metabolome

Abbreviations: Akt, protein kinase B; AMPK, adenosine monophosphate-activated protein kinase; GC/MS, gas chromatography-mass spectrometry; GGJTW, Ge-Gen-Jiao-Tai-Wan; GGQLD, Ge-Gen-Qin-Lian Decoction; HLD, Huang Lian Decoction; HPLC, high-performance liquid chromatography; K-OPLS, gas chromatography-mass spectrometry; MS, mass spectrometry; NMR, nuclear magnetic resonance; SPA, subwindow permutation analysis; T2DM, type 2 diabetes mellitus; TCM, traditional Chinese medicine; TG, triglycerides.

INTRODUCTION

Diabetes is one of the most prevalent chronic diseases worldwide, affecting 463 million people in 2019. It is expected that this number will rise to 700 million by 2045 (Saeedi et al., 2019). Type 2 diabetes mellitus (T2DM) is the most common type of diabetes and is characterized by insulin resistance. Two troublesome effects of T2DM, cardiovascular disease and metabolic disorders, can cause high morbidity and mortality. T2DM is mainly a consequence of environmental and behavioral factors such as a sedentary lifestyle and/or poor dietary choices, which often cause obesity; however, several genetic susceptibilities contribute to disease onset or exacerbate its severity (Zimmet et al., 2001). These factors lead to persistent hyperglycemia and subsequently to decreased insulin sensitivity, which in turn can lead to a spectrum of metabolic abnormalities (Ferrannini et al., 2013). Moreover, persistent disorders of glucose and lipid metabolism may lead to various complications of the microvasculature and macrovasculature, such as stroke, ischemic heart disease, diabetic nephropathy, cognitive dysfunction, and retinopathy (Brownlee, 2001). These conditions have a severe impact on quality of life. Therefore, new and effective measures are needed to prevent the onset of T2DM and improve the management of patients.

Clinically proven medicines for treating T2DM include thiazolidinediones (Thangavel et al., 2017; Nanjan et al., 2018; Oikonomou et al., 2018) as well as sulfonylureas, which stimulate insulin secretion and increase insulin sensitivity to biguanides (Setter et al., 2003). These drugs activate the genes encoding hepatic adenosine monophosphate-activated protein kinase (AMPK) (Wang Q. et al., 2018; Glosse and Föller, 2018; Różańska and Regulska-Ilow, 2018), phosphatidylinositol 3-kinase, and protein kinase B (Akt) (John et al., 2018; Mabhida et al., 2018; Garcia-Galiano et al., 2019). Stimulation of fatty-acid oxidation in an AMPK- and peroxisome proliferator activated receptor-α-dependent manner inhibits interference with c-Jun amino-terminal kinases and insulin action activated by inflammatory cytokines and free fatty acids (Hirosumi et al., 2002; Ferguson et al., 2013). These approaches and candidate drug targets constitute potential means for reducing blood sugar and the incidence of obesity and diabetes symptoms.

Glucose transporter type 4 also plays an important role in maintaining blood glucose homeostasis, which prevents insulin resistance and facilitates the transfer of glucose from blood to the liver through the phosphatidylinositol 3-kinase and Akt signaling pathways. However, the vasculature can be damaged by dysfunction of several metabolic pathways, including the hexamine pathway, the protein kinase C pathway, the glycosylation end-product pathway, and the classic polyol pathway (Hunt and Wolff, 1991; Sheetz and King, 2002).

In addition to the aforementioned drug classes for treating diabetes (i.e., biguanides, thiazolidinediones, and sulfonylureas), alpha-glucosidase inhibitors are also commonly used (Choi and Kim, 2010; Zhou et al., 2013; Ishii et al., 2018). However, these inhibitors often have considerable negative effects, such as drug resistance, hypoglycemia, edema, and weight gain. Advances in the treatment of diabetes have changed the focus from hyperglycemia to controlling glucose metabolism, enhancing the sensitivity of insulin receptors, inhibiting insulin resistance, regulating the non-enzymatic glycosylation of proteins, and downregulating fatty-acid metabolism, among other treatment modalities (Weyer et al., 2001; de Dios et al., 2007). Although many strategies and drugs have been developed for the prevention and treatment of diabetes, current disease management options fall short of complete containment. Current therapies mainly rely on drugs; however, many recently approved diabetes drugs have serious complications, such as hypoglycemia, liver and kidney function damage, and diarrhea (Bekele, 2019). Conventional therapies treat the symptoms of diabetes but do not mitigate metabolic syndrome, which is the major complication of the disease. Traditional Chinese herbal medicines, however, contain a variety of bioactive ingredients that can provide therapeutic benefit for several conditions. For example, *Gynostemma pentaphyllum* (Thunb.) Makino (Jiao-Gu-Lan), *Coptis chinensis* Franch. (Huang-Lian), and *Salvia miltiorrhiza* Bunge (Dan-Shen) can simultaneously enhance insulin sensitivity, reduce visceral fat, and improve hyperlipidemia (Garcia-Galiano et al., 2019). Chinese herbal medicines can also help treat diabetes complications by reversing abnormalities related to blood viscosity, microcirculation, and oxidative stress. Therefore, there is great potential merit in developing new, safe, and effective natural anti-hyperglycemia agents as alternatives to conventional treatments for diabetes and its complications.

The American Dietary Guidelines and the American Diabetes Association (Evert et al., 2013) recommend that diabetes patients as well as healthy individuals eat less refined grains, red meat or processed meat, and sugary drinks to help prevent the onset of T2DM. In addition, in many countries, T2DM patients often take botanical medicines or alternative medicines to potentiate the therapeutic effects of conventional medicines; among these alternatives, traditional Chinese herbal medicines account for a relatively high proportion. Traditional Chinese medicines (TCMs) and their natural bioactive ingredients have a variety of anti-hyperglycemia effects. For example, by eliminating oxygen free-radicals, they help thwart blood hypercoagulability, inhibit the non-enzymatic glycosylation of proteins, inhibit aldose reductase, modulate the metabolism of fats and proteins, and effectively control or delay the onset of diabetes and its complications (Zhang and Jiang, 2012; Lao et al., 2014; Sun et al., 2016; Sharma et al., 2017; Feng et al., 2018). Although an increasing volume of evidence shows that TCMs have a substantial positive impact on treatment of diabetes, research on TCM efficacy remains incomplete.

For many years, researchers have attempted to understand T2DM to formulate interventions and treatment plans to improve patient health (Floegel et al., 2013; Roberts et al., 2014; Zheng et al., 2016). In this regard, high-throughput metabolomics technology has recently begun providing insight into the pathophysiological pathways underlying T2DM (Rhee et al., 2011; Würtz et al., 2012; Padberg et al., 2014).

Metabolomics is the systematic analysis of metabolites in biological samples (Guasch-Ferré et al., 2016), including low-molecular-weight compounds such as amino acids, organic acids,

lipids, nucleotides, and sugars. Metabolomics often utilizes approaches based on nuclear magnetic resonance (NMR) and/or various mass spectrometry (MS) techniques, as these technologies not only identify complex metabolic phenotypes but can also be integrated with other "omics" strategies (i.e., transcriptomics, genomics, and proteomics) and bioinformatics data to elucidate potential biological mechanisms and discover clinically relevant diagnostic and prognostic markers of disease risk.

Metabolomics approaches have also been used to study and understand T2DM. A review of recent research revealed that many studies found correlations between T2DM and metabolomics characteristics (Tai et al., 2010). Metabolomics studies can provide insight into disease mechanisms by monitoring differences in metabolite abundance and/or profiles in patients (Cha, 2008; Chan et al., 2009; Carr et al., 2011). Therefore, metabolomics can be used to describe metabolic abnormalities that occur during diabetes progression. Furthermore, metabolomics also has been used for the discovery of disease-related biomarkers (Madsen et al., 2010; Malik et al., 2010), which are commonly used to assess disease severity and the underlying metabolic pathways (Zhang A. H. et al., 2013). Hence, metabolomics can provide a greater understanding of disease pathology and contribute to the development of new treatments (Cruz et al., 2007; Coen et al., 2008). A comprehensive review of T2DM metabolomics is provided by Sas et al. (2015), Gonzalez-Franquesa et al. (2016), and Guasch-Ferré et al. (2016).

APPLICATION OF METABOLOMICS IN STUDYING THE TRADITIONAL CHINESE MEDICINE TREATMENT OF TYPE 2 DIABETES MELLITUS

For hundreds of years in China, traditional medicine practices have been used to assess disease through personalized diagnosis, whereas modern medical practice is mainly concerned with treating symptoms. In the classic Chinese publication *The Yellow Emperor's Inner Classic*, the symptoms of "drinking more," "eating more," "polyuria," and "weight loss" that are typical of diabetes are classified as xiao ke zheng, for which TCM has long been a treatment (Ning et al., 2009). According to TCM theory, a disease state reflects an imbalance in any or all of four fundamental aspects—Yin (things related to the physical form of an object), Yang (things related to energy quality), Qi (life-force, which animates the forms of the world), and Xue (dense form of body fluids that have been acted upon and excited by Qi) (Wang et al., 2012) – which are in an unbalanced state when people suffer from a disease. Similarly, patients with T2DM could be classified as having deficiency or excess syndromes, which refer to the organs' insufficiency or excess in Qi, Xue, Yin, and Yang. A disease or syndrome can be diagnosed via comprehensive consideration of symptoms and signs, including tongue appearance and pulse rate, which can also help determine the cause, location, and nature of the disease as well as the patient's physical condition, disease status, and prognosis. The diagnosis of any particular disease or syndrome is the most notable attribute of TCM, and all diagnosis and treatment methods are derived from this principle.

Metabolomics technology has been applied to help differentiate among T2DM-related syndromes diagnosed based on TCM practices, and thus metabolomics can assist the standardization of TCM clinical diagnoses, inform our understanding of TCM theory, and provide a basis for modernizing TCM practice. Xu et al. (2012) used high-performance liquid chromatography (HPLC) to analyze the profiles of fatty acids in plasma samples from healthy controls and T2DM patients. They measured levels of 12 fatty acids and assessed four lipid parameters: total cholesterol, triglycerides (TG), and high- and low-density lipoproteins. This analysis documented the levels and profiles of common fatty acids in samples from patients with the three TCM syndromes, noting certain significant differences for the group having Qi deficiency vs. the group having both Qi and Yin deficiencies, and found that the unsaturated fatty acids C18:3 and C20:2 in TG and low-density lipoprotein are potential biomarkers and that C20:5, TG, and high-density lipoprotein are candidate biomarkers for Qi deficiency and damp heat. For Qi and Yin deficiency and damp heat, C14:0, C16:0, C18:1, C18:2, and high-density lipoprotein provide the main classification information, each of which is of great relevance to the diagnosis and treatment of T2DM (Xu et al., 2012). Wu et al. used gas chromatography-mass spectrometry (GC/MS) to carry out metabolic profiling of carbohydrates in urine samples from T2DM patients and healthy control subjects (Wu et al., 2012). They also conducted a comparative analysis of 366 subjects using GC/MS combined with kernel-based orthogonal projections to latent structures (K-OPLS) or subwindow permutation analysis (SPA) to 1) compare urinary carbohydrate profiles between T2DM patients and healthy subjects, 2) determine the relationship between urine carbohydrate levels and TCM syndromes in subjects with T2DM, and 3) determine the characteristics and differences in the distribution of TCM syndromes between patients with mild or severe syndromes. They found that, compared with healthy controls, T2DM patients with deficiency or excess syndromes had substantial abnormalities in glucose metabolism. Patients with deficiency syndrome were older than those with excess syndrome, consistent with TCM theory that Qi, Xue, Yin, and Yang are less prevalent in the elderly than the young. Furthermore, two potential biomarkers, xylose and C4 sugar 2, were discovered in the two syndromes using K-OPLS/SPA and Student's t-test. The analysis revealed elevated levels of xylose and C4 sugar 2 in patients with excess syndrome compared with those with deficiency syndrome.

In summary, syndrome differentiation (Qi, Xue, Yin, and Yang) is the foundation and essence of TCM theory, and the diagnostics mainly depend on overall observation of human symptoms including seeing, listening, questioning, and feeling the pulse rather than "micro" level tests. The metabolic profile is a highly sensitive means of detecting the physiological and pathological changes characteristic of T2DM patients. In addition, a profile can clarify the concept of "syndrome" in

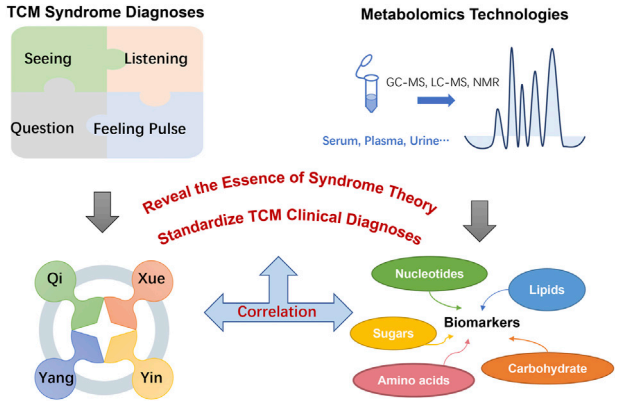

FIGURE 1 | Differentiating TCM syndromes among patients with T2DM.

the complex physiological system of TCM. Compared with using a single metabolite as a biomarker, using all metabolites to assess human health is more comprehensive and therefore more accurate (Goodacre, 2004; Lu et al., 2009). The research of Wu et al. (2012) demonstrated that the overall application of metabolic profiling in studies of the underlying mechanisms of TCM syndromes is reasonable. Discrimination of different syndromes and the discovery of syndrome-related biomarkers were meaningful for revealing the essence of syndromes. These potential biomarkers reflect dysregulation of metabolism in diabetes patients, which may be helpful for diagnosing diabetes and identifying TCM syndromes, and thus to standardize TCM clinical diagnoses (**Figure 1**).

METABOLOMICS REVEALS THE MECHANISMS UNDERLYING THE EFFICACY OF TRADITIONAL CHINESE MEDICINE FOR TREATING TYPE 2 DIABETES MELLITUS

TCM practice has documented success for treatment of T2DM. The guiding principle of TCM is that a variety of traditional Chinese herbal medicines should be used to treat xiao ke zheng, and many classic prescriptions have been passed on through generations of practitioners over thousands of years. The most common Chinese medicine formulations for treating T2DM are Huang-Lian Decoction (HLD) (Pan et al., 2020), Ge-Gen-Jiao-Tai-Wan (GGJTW) (Wang W. et al., 2018), and Qijian mixture (Gao et al., 2018). With continuous practice, experience, and refinement through treatment observations, TCM has formed its own advantages and characteristics relative to modern drugs in terms of regulating glucose and lipid metabolism and countering insulin resistance, having mild yet temporally stable therapeutic effects (Bailey and Day, 1989; Prabhakar and Doble, 2011; Tzeng et al., 2013). For example, Jin-Qi-Jiang-Tang tablets have been proven to improve sugar intake, lipid metabolism, insulin signal transduction, inflammation, and oxidative stress (Liu et al., 2017). Tang-Ning-Tong-Luo formula tablets can reduce liver degeneration, regulate glucose and lipid metabolism, and improve insulin resistance (Cheng et al., 2014). Contemporaneous with treatment, however, patients must adopt healthy dietary habits, emotional and physical exercise habits, and other lifestyle changes to effectively control both blood glucose and blood pressure. To explore the mechanisms underlying these multifaceted interventions, many studies have applied metabolomics methods and produced numerous interesting findings. **Table 1** summarizes the various experimental strategies and metabolomics results, including biomarkers and the relevant metabolic pathways.

Two main factors regulate insulin secretion: one is nutrients such as glucose, fatty acids, and amino acids; and the other includes neurotransmitters and hormones. Islet cells maintain a certain steady state of secretion in different physiological states through coordination and integration of these two types of factors. T2DM can cause an imbalance among metabolites, such as lipids, carbohydrates, and amino acids. These imbalances can be detected by metabolomics, toward the goal of identifying biomarkers of early-stage disease.

More than 70 years ago, elevated cellular levels of branched-chain amino acids were found to correlate with insulin resistance and diabetes (Luetscher, 1942; Felig et al., 1969; Felig et al., 1974). Metabolomics studies of 74 obese subjects and 67 lean subjects by Newgard et al. (2009) demonstrated that an overabundance of isoleucine, leucine, and valine correlated with the prevalence of coronary artery disease in a cardiac study cohort and also revealed a strong correlation between glutamate and insulin resistance (Newgard et al., 2009); a lower glutamine:glutamic acid ratio predicted an increased risk of developing diabetes (Cheng et al., 2012). Studies showed that an overabundance of free fatty acids (resulting from phospholipid catabolism) may be the main cause of insulin resistance (Taskinen, 2003; Krauss and Siri, 2004). Also, Liu et al. (2010) conducted metabolomics analyses of fatty acids in serum from healthy subjects, T2DM patients, and patients with postprandial hyperglycemia, revealing that elevated levels of palmitic, stearic, oleic, linolenic, and linolenic acids are key indicators of T2DM (Liu et al., 2010).

TCM has a long history of treating T2DM, but the underlying mechanism remains unknown. In agreement with the holistic concept of TCM, metabolomics has shown great potential in evaluating efficacy of TCM for treating T2DM. By analyzing endogenous metabolites of small molecules in samples from T2DM patients and examining the metabolic status of the organism, metabolomics can reveal the metabolic changes and the underlying mechanism involved in the pathogenesis of diabetic complications and the efficacy of TCM for treating the disease. Generally, TCM treatment may significantly change some metabolic disorders (e.g., glucose or lipid metabolism) associated with T2DM, promoting metabolic network reorganization through restoring of key metabolites and metabolic pathways, which may be the main mechanism providing the basis of TCM treatment of T2DM. In addition, the discovery of additional diabetes biomarkers would have breakthrough significance for the development of diabetes drugs (**Figure 2**). Below, we summarize several commonly

TABLE 1 | Information from metabolomics studies of TCM for lowering blood sugar in animal models.

Study ID	Treatment	Model	Control	Size	Sample	Platform	Potential biomarkers for T2DM	Key pathways
Wang W. et al. (2018)	Ge-Gen-Jiao-Tai-Wan	T2DM Sprague-Dawley rats	Control group, diabetes model group	180–200 g	Serum	UHPLC-QTOF/MS	CA, CDCA, TCA, GCA, TCDCA, and taurine↑ Hydroxyacetone, desmosterol, lathosterol, LysoPC(18:1(9Z)), and LysoPE(16:0/0:0) ↓	Bile acid biosynthesis
Gao et al. (2018)	Qijian mixture 0.942 g/kg/day for 8 weeks	Male KKay mice	QJM(H) vs. model	8–9 weeks	Liver	NMR	Leucine, isoleucine, valine, and alanine↑	Valine, leucine, and isoleucine biosynthesis
Cui et al. (2018)	*Scutellariae Radix* (SR), *Coptidis Rhizoma* (CR), and combined extracts 6.3 g/kg for 30 days	T2DM Sprague-Dawley rats	Normal group, model group, metformin group, SR group, CR group, and low dose of combined extracts group	200 ± 20 g	Plasma and urine	UHPLC-QTOF/MS	Cholic acid, deoxycholic acid, xanthosine and deoxyuridine↑ Glycocholic acid, LysoPE, LysoPC, and PC↓	Glycerophospholipid metabolism
Pan et al. (2020)	Huang-Lian Decoction (HLD) for 4 weeks	T2DM male Wistar rats	HLD group, model group, and control group	200 ± 20 g	Serum	HPLC-MS	Phenylalanine, L-carnitine, hippuric acid, betaine, and cytosine↑ Glucose, citrate, and phenylpyruvate↓	Glyoxylate and dicarboxylate metabolism, phenylalanine metabolism, and citrate cycle

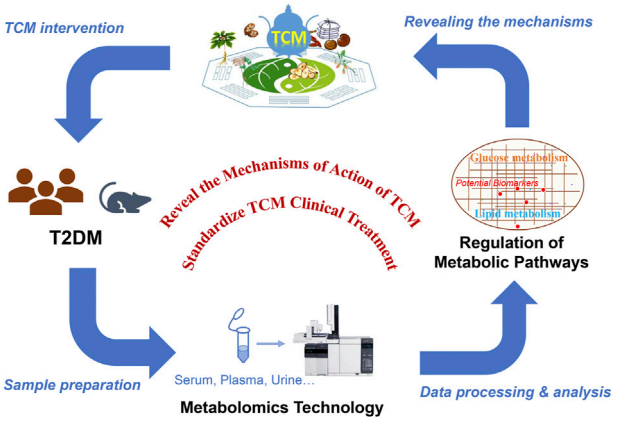

FIGURE 2 | Metabolomics reveals the mechanisms underlying the efficacy of TCM for treating T2DM.

used herbal medicines for diabetes treatment and the identification of potential T2DM biomarkers.

Georgi root, the dry root of *Scutellaria baicalensis* Georgi, has several biological activities such as anti-inflammation (Yang et al., 2018), anti-cancer (Cheng et al., 2018), and anti-oxidation (Zhang et al., 2011) and has been used to treat various diseases. The major bioactive components of Georgi root are flavonoids such as baicalin, wogonoside, baicalein, and wogonin. Accumulating research with T2DM patients has shown that baicalin can mitigate insulin resistance (Yang et al., 2012; Song et al., 2013) and suppress gluconeogenesis (Wang et al., 2017). *Coptidis Rhizoma*, the dried rhizome of *Coptis chinensis* Franch. (Huang-Lian), contains numerous alkaloids – the major ones being berberine, coptisine, and palmatine—and has been used to treat diarrhea for thousands of years in China. Modern studies have shown that berberine can also substantially lower blood glucose and promote insulin secretion (Zhang et al., 2014; Neag et al., 2018; Xie et al., 2018; Belwal et al., 2020), but the mechanism underlying its role in relieving T2DM symptoms remains unknown. However, potential biomarkers and related pathways have been identified via comparative analysis of plasma and urine metabolomics data for normal and T2DM rats (Cui et al., 2018). Several studies identified eight potential T2DM-related metabolites, including cholic, deoxycholic, and glycocholic acids, the latter of which may inhibit inflammation via TGR5 activation (Agarwal et al., 2018). Cholic and deoxycholic acids block glycocholic acid binding to TGR5. Three other compounds—phosphatidylcholines, lysophosphatidylcholines, and lysophosphatidylethanolamines—are mainly involved in the pathogenesis of inflammation and metabolic diseases such as diabetes. Another compound, xanthosine, promotes the production of uric acid, which is involved in several diabetes complications. The study demonstrated that extracts of Georgi root and *Coptidis Rhizoma* can have a substantial therapeutic effect for patients with T2DM by modulating the activities of both pro-inflammatory cytokines and enzymes related to glucose metabolism (Cui et al., 2018).

HLD was first described in the classic Chinese medicine volume *Treatise on Febrile Diseases* (Shang-Han-Lun), mainly

with regard to treatment of Yin and Qi deficiencies. Two other ancient books, *Physician's Record* (Ming-Yi-Bie-Lu) and *Explanation of Materia Medica* (Ben-Cao-Jing-Ji-Zhu), also promoted the use of prescriptions containing *Coptis chinensis* Franch. For more than 1,500 years, these prescriptions were found to benefit patients with T2DM and were first described in Ming-Yi-Bie-Lu during the Wei Jin Dynasty (An and Cui, 2008). HLD is composed of *Coptis chinensis* Franch. (Huang-Lian); *Rhizoma Zingiberis*, the fresh rhizome of *Zingiber officinale* Roscoe (Gan-Jiang); *Glycyrrhiza uralensis* Fisch. ex DC. (Gan-Cao); *Cinnamomum verum* J.Presl (Gui-Zhi); *Panax ginseng* C. A. Mey (Ren-Shen); *Pinellia ternata* (Thunb.) Makino (Ban-Xia); and *Ziziphus jujube* Mill. (Da-Zao). Pan et al. (2020) reported that HLD can effectively regulate the levels of numerous compounds in various metabolic pathways that are affected in patients with T2DM (Pan et al., 2020). Using HPLC-MS, they discovered that HLD regulates the production of several compounds – such as cytosine, phenylalanine, glucose, l-carnitine, phenylpyruvate, betaine, citrate, and hippuric acid—that are involved in dicarboxylate and glyoxylate metabolism, phenylalanine metabolism, and the tricarboxylic acid cycle. All these metabolites are related to glucose and lipid metabolism, which are affected by HLD.

GGJTW is composed of *Pueraria montana* var. *lobata* (Willd.) Maesen & S.M.Almeida ex Sanjappa & Predeep (Ge-Gen), *Coptis chinensis* Franch. (Huang-Lian), and *Cinnamomum verum* J.Presl (Rou-Gui). Jiao-tai-wan, which comprises solely the latter two herbs, was first mentioned as a treatment for insomnia in the classic medical work "Han-Shi-Yi-Tong" of the Ming Dynasty. Puerarin is one of the main bioactive ingredients in *Pueraria montana* var. *lobata* (Willd.) Maesen & S.M.Almeida ex Sanjappa & Predeep, and has been used therapeutically for diabetes and its complications (Wu et al., 2013). Puerarin can mitigate insulin resistance (Chen et al., 2018) and protect islet cells (Rojas et al., 2018). GGJTW is used to treat diabetes in China owing to its potent anti-hyperglycemia effect. However, little was known about the underlying metabolic mechanism until 37 potential biomarkers were detected using a metabolomics approach based on ultra-HPLC coupled with quantitative time-of-flight (QTOF) MS. The majority of these biomarkers participate in the biosynthesis of primary bile acids involving increased production of taurine and cholic, chenodeoxycholic, taurocholic, glycocholic, and taurochenodeoxycholic acids. The observed significant changes in the levels of these metabolites demonstrated the anti-hyperglycemia effect of GGJTW on diabetic rats and its potential metabolic mechanism (Wang W. et al., 2018).

The Qijian mixture contains four herbs, each of which is commonly used in TCM to treat diabetes: *Astragalus mongholicus* Bunge (Huang-Qi); *Pueraria montana* var. *lobata* (Willd.) Maesen & S.M.Almeida ex Sanjappa & Predeep (Ge-Gen); *Ramulus euonymi*, an extract of *Euonymus alatus* (Thunb.) Sieb. (Gui-Jian-Yu); and *Coptis chinensis* Franch. (Huang-Lian) (Gao et al., 2018). *Astragalus membranaceus* was formally described by Carl Linnaeus in his book *Plant Species* in 1753, and it has a long history in China with wide-ranging clinical applications. *Astragalus mongholicus* Bunge lowers blood lipids and blood sugar, eliminates edema and oxidative stress (Nozaki et al., 2017), and has a broad range of pharmacological effects on diabetes (Liao et al., 2017). For T2DM in particular, it has a potent therapeutic benefit (He et al., 2018). For example, Gao et al. (2018) used 1H-NMR to assess how the Qijian mixture affects the metabolomic profiles of various liver cell types in samples from T2DM patients and to explore the pharmacodynamics. The major metabolites affected by the Qijian mixture follow: isoleucine, choline, leucine, valine, sn-glycero-3-phosphocholine, citrate, myo-inositol, glycerol, anserine, trimethylamine n-oxide, glutarate, lactate, trimethylamine n-oxide, alanine, glucose, acetate, homoserine, inosine, 3-hydroxybutyrate, glutathione, taurine, niacinamide, xanthine, glycine, and adenine (**Table 1**). Four metabolites—valine, alanine, isoleucine, and leucine—potentially mediate the anti-hyperglycemia effect. The results demonstrated that the Qijian mixture can regulate amino-acid metabolism by decreasing the levels of these four amino acids. The catabolism of leucine, isoleucine, and valine is linked to insulin sensitivity, i.e., an increase in the levels of these three free-amino-acids in serum promotes insulin sensitivity. The biosynthetic pathways for alanine, aspartate, and glutamate contribute to the pathogenesis of metabolic syndrome in T2DM. Thus, four pathways—branched-chain fatty-acid metabolism and the alanine, aspartate, and glutamate biosynthesis pathways – are closely associated with T2DM, confirming the therapeutic potential of the Qijian mixture for T2DM.

FURTHER PERSPECTIVES IN METABOLOMICS STUDIES OF TRADITIONAL CHINESE MEDICINE FOR TREATING TYPE 2 DIABETES MELLITUS

Network Pharmacology for Discovery of New Drugs for Treating Type 2 Diabetes Mellitus With Traditional Chinese Medicine

Metabolomics can show the reversal of metabolic disorders caused by TCM treatment, whereas network pharmacology can help to determine how TCM contributes to these changes (Zhang G. B. et al., 2013; Mao et al., 2017). Network pharmacology employs "omics" technologies to detect different molecules (genes, enzymes, and metabolites) and annotate them by comparing with specific databases. Specifically, TCM network pharmacology is used to investigate TCM from a systems perspective and at the molecular level, updating the research paradigm from the current "one target, one drug" mode to a new "network target, multi-components" mode. This method is specialized to prioritize disease-associated genes, to predict the target profiles and pharmacological actions of herbal compounds, to reveal drug–gene–disease co-module associations, to screen synergistic multi-compounds from herbal medicines in a high-throughput manner, and to interpret the combinatorial rules and network regulation effects of herbal medicines (Li and Zhang,

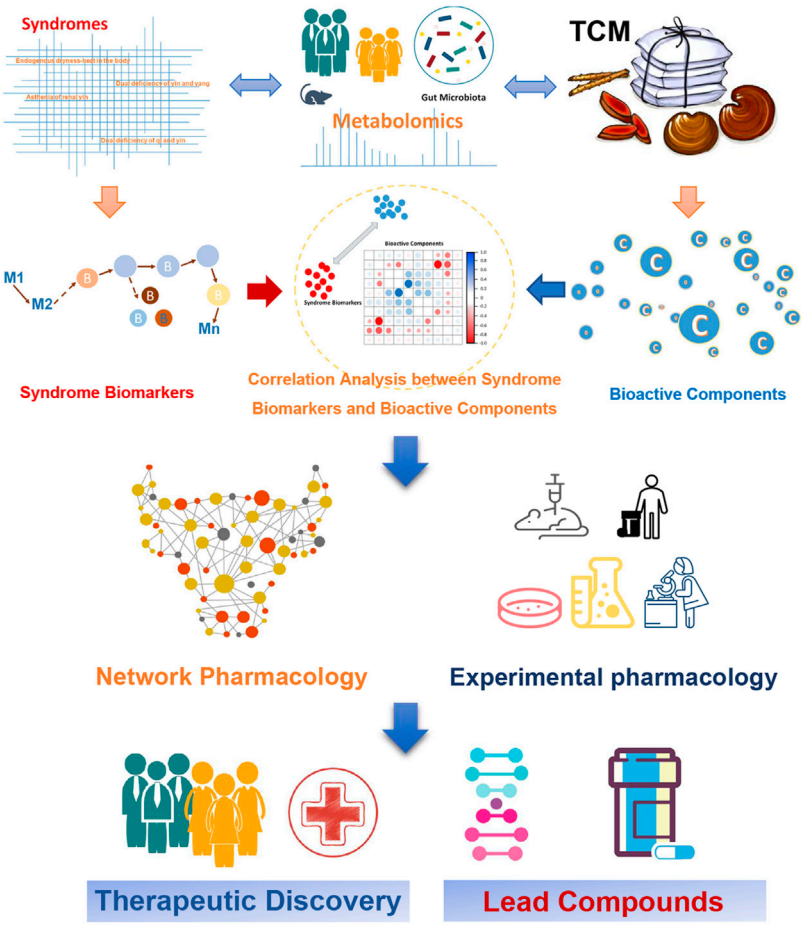

FIGURE 3 | Application of metabolomics to assess the efficacy of TCM for treating T2DM, for the purpose of developing new anti-diabetes therapeutics.

2013). The network-based method has been demonstrated effective to identify the key ingredients in TCM formulations and predict potential molecular targets in T2DM. Below, we summarize some typical examples.

The classic TCM formulation Ge-Gen-Qin-Lian Decoction (GGQLD) has good clinical effects on T2DM which consists of four herbs: *Pueraria montana* var. *lobata* (Willd.) Maesen & S.M.Almeida ex Sanjappa & Predeep (Ge-Gen), *Scutellaria baicalensis* Georgi (Huang-Qin), *Coptis chinensis* Franch. (Huang-Lian), and *Glycyrrhiza glabra* L. (Gan-Cao) (Tong et al., 2011; Zhang C. H. et al., 2013). A network pharmacology approach was employed to determine the potential antidiabetic ingredients from the GGQLD formula. Further *in vitro* antidiabetic trials demonstrated that a predicted antidiabetic ingredient from Ge-Gen, 4-hydroxymephenytoin, can increase the insulin secretion in RIN-5F cells and improve insulin resistance in 3T3-L1 adipocytes (Li et al., 2014), indicating that the network pharmacology strategy is a powerful means for identifying bioactive ingredients and mechanisms of action for TCM herbal formulae.

Compound Lian-Ge granules are composed of *Coptis chinensis* Franch. (Huang-Lian), *Pueraria montana* var. *lobata* (Willd.) Maesen & S.M.Almeida ex Sanjappa & Predeep (Ge-Gen), *Salvia miltiorrhiza* Bunge (Dan-Shen), and *Thlaspi arvense* L. (Hai-Zao), resveratrol, and taurine Xue et al. (2019) used network pharmacology methods to predict the 24 bioactive components of compound Lian-Ge granules for lowering blood sugar, including berberine, puerarin, danshinolic acid A, and sinigrin, for which nine targets and 111 metabolic pathways were implicated (Xue et al., 2019). Using network pharmacology methods and technologies, this study predicted the hypoglycemic targets of main active ingredients in Lian-Ge granules and revealed their action modes of in multiple pathways, providing a theoretical basis and a clue for exploration of the hypoglycemic mechanism of compound Lian-Ge granules.

As a traditional Chinese herbal medicine, *Astragalus mongholicus* Bunge is widely used clinically to treat diabetes. Li et al. (2019) discovered 13 key T2DM targets and found that *A. membranaceus* can treat T2DM by upregulating the activity of casein kinase, by ensuring the normal regulation of lipid metabolism, and by enhancing insulin resistance, thereby upregulating insulin signaling. Several key targets were randomly selected for quantitative real-time PCR validation, and the results indicated that the analysis of network

pharmacology was robust and targets identified via this process were worthy of validation (Li et al., 2019).

In summary, these studies confirmed the feasibility of combining metabolomics and network pharmacology to study the metabolic pathways involved in T2DM that are affected by TCM. In future studies, this combined approach may be a potentially powerful tool for discovery of bioactive components of TCM and elucidation of their action mechanisms for treating T2DM.

Role of Gut Microbiota in Treating Type 2 Diabetes Mellitus

In recent decades, the gut microbiome has emerged as an integral aspect of the efficacy of TCM, and increasing evidence supports a role for the microbiome in the treatment of T2DM. Subjects of T2DM can be distinguished based on a reduced number of gut Clostridiales bacteria (*Roseburia* species and *Faecalibacterium prausnitzii*), which produce the short-chain fatty acid butyrate (Qin et al., 2012; Karlsson et al., 2013). Short-chain fatty acids are one of the most important metabolites produced by the gut microbiota, because these metabolites can affect host glucose–insulin homeostasis by modulating the activities of G protein-coupled receptors, promoting the secretion of various hormones, and stimulating the vagus nerve. Finally, another important metabolite of lipopolysaccharide-producing, Gram-negative bacteria has been identified as a trigger of insulin resistance (Cani et al., 2007).

Gegen Qinlian Decoction has long been used to treat common metabolic diseases such as T2DM. Xu et al. found that treatment with both berberine and Gegen Qinlian Decoction significantly altered the overall profile of the gut microbiome and enriched many butyrate-producing bacteria, including *Faecalibacterium* and *Roseburia*, thereby reducing intestinal inflammation and lowering blood glucose level (Xu et al., 2020). *Sophora flavescens* Aiton (Ku-Shen) is a well-known Chinese herbal medicine that has been used to combat T2DM (Jung et al., 2008). It was recently reported that flavonoid compounds in the ethyl-acetate extract of *Sophora flavescens* Aiton can regulate the metabolism of lipids, carbohydrates, and especially amino acids in patients with T2DM by mediating the host–microbe metabolic axis (Shao et al., 2020). Therefore, it is feasible to identify potential gut microbiota-related targets in T2DM patients for patient-specific treatment with TCM.

CONCLUSION AND PERSPECTIVE

T2DM is a major global health problem, which is treated as "Xiaoke" in the TCM system, and the related herbal medicines have been used over thousands of years. However, due to its complexity, it is very difficult to decipher the scientific basis and systematic features of TCM for treating T2DM. In the systemic context, metabolomics has a convergence with TCM, therefore it could provide useful tools for uncovering the essence of TCM. Metabolomics can be used to systematically explore the pathophysiology of T2DM and elucidate the overall molecular mechanism underlying the known positive effects of treatment with TCM. Previous studies have shown that metabolomics can help distinguish the various T2DM syndromes. In addition, metabolic disorders in diabetes patients can be mitigated by treatment with TCM, reflecting TCM's anti-hyperglycemia effect. Research has shown that network pharmacology methods, in combination with experimental pharmacology, can be further used to identify the bioactive ingredients in TCM and their targets, which could inform the development of new therapies for T2DM (**Figure 3**). The emerging application of metabolomics to elucidate the pathways underlying the efficacy of TCM for T2DM will assist efforts to identify new T2DM biomarkers and develop novel anti-diabetes therapeutics. Moreover, the integration of metabolomics and TCM shows promise in bridging the gap between Chinese and Western medicine and helping to interpret the essence of TCM, and thus perhaps enabling a revolution for future health care.

It is noteworthy that although a considerable number of potential biomarkers for T2DM have been identified via integration of metabolomic approaches into TCM, there are still some limitations. Due to the lack of a universal analysis platform and a mature and consistent operation plan, most of them have not been analyzed in a standard fashion, and few have been clinically validated. Therefore, it is necessary to establish a comprehensive and complete operation method by expanding the research content of metabolic tissue, improving technical methods, and perfecting the database. Furthermore, it is required to strengthen the combined application of metabolomics technology with other multi-omics, such as genomics and proteomics, to make up for the shortcomings of metabolomics itself, so as to achieve comprehensive and efficient clinical application from research content, and accelerate the standardization and modernization of TCM for treating T2DM.

AUTHOR CONTRIBUTIONS

YZ, YY, and YX wrote the first draft. LD, ZW, YX, and WX provided critical revisions. All authors approved the final version of the manuscript for submission.

FUNDING

This work was supported by the National Natural Science Foundation of China Grants (81874335, 32170402, 81920108033, and 81703682), Shanghai Rising-Star Program (18QB1402700, China), and Special Funds for transformation and upgrading of industrial informatization of industry and information technology department of Jiangsu in 2020 (Research on Key technologies of multi-component traditional Chinese medicines).

REFERENCES

Agarwal, S., Sasane, S., Kumar, J., Deshmukh, P., Bhayani, H., Giri, P., et al. (2018). Evaluation of Novel TGR5 Agonist in Combination With Sitagliptin for Possible Treatment of Type 2 Diabetes. *Bioorg. Med. Chem. Lett.* 28, 1849–1852. doi:10.1016/j.bmcl.2018.04.011

An, X. P., and Cui, Q. R. (2008). The Reasrch Progress of Rhizoma Coptidis in Treating Diabetes. *Gansu. J. TCM.* 21, 57–58. doi:10.3969/j.issn.1004-6852.2008.01.039

Bailey, C. J., and Day, C. (1989). Traditional Plant Medicines as Treatments for Diabetes. *Diabetes Care* 12, 553–564. doi:10.2337/diacare.12.8.553

Bekele, B. B. (2019). The Prevalence of Macro and Microvascular Complications of DM Among Patients in Ethiopia 1990-2017: Systematic Review. *Diabetes Metab. Syndr.* 13, 672–677. doi:10.1016/j.dsx.2018.11.046

Belwal, T., Bisht, A., Devkota, H. P., Ullah, H., Khan, H., Pandey, A., et al. (2020). Phytopharmacology and Clinical Updates of *Berberis* Species Against Diabetes and Other Metabolic Diseases. *Front. Pharmacol.* 11, 41. doi:10.3389/fphar.2020.00041

Brownlee, M. (2001). Biochemistry and Molecular Cell Biology of Diabetic Complications. *Nature* 414, 813–820. doi:10.1038/414813a

Cani, P. D., Amar, J., Iglesias, M. A., Poggi, M., Knauf, C., Bastelica, D., et al. (2007). Metabolic Endotoxemia Initiates Obesity and Insulin Resistance. *Diabetes* 56, 1761–1772. doi:10.2337/db06-1491

Carr, P. W., Stoll, D. R., and Wang, X. (2011). Perspectives on Recent Advances in the Speed of High-Performance Liquid Chromatography. *Anal. Chem.* 83, 1890–1900. doi:10.1021/ac102570t

Cha, Y. S. (2008). Effects of L-Carnitine on Obesity, Diabetes, and as an Ergogenic Aid. *Asia Pac. J. Clin. Nutr.* 17 (Suppl. 1), 306–308. doi:10.6133/apjcn.2008.17.s1.75

Chan, J. C., Malik, V., Jia, W., Kadowaki, T., Yajnik, C. S., Yoon, K. H., et al. (2009). Diabetes in Asia: Epidemiology, Risk Factors, and Pathophysiology. *JAMA* 301, 2129–2140. doi:10.1001/jama.2009.726

Chen, X., Wang, L., Fan, S., Song, S., Min, H., Wu, Y., et al. (2018). Puerarin Acts on the Skeletal Muscle to Improve Insulin Sensitivity in Diabetic Rats Involving μ-opioid Receptor. *Eur. J. Pharmacol.* 818, 115–123. doi:10.1016/j.ejphar.2017.10.033

Cheng, S., Rhee, E. P., Larson, M. G., Lewis, G. D., McCabe, E. L., Shen, D., et al. (2012). Metabolite Profiling Identifies Pathways Associated with Metabolic Risk in Humans. *Circulation* 125, 2222–2231. doi:10.1161/CIRCULATIONAHA.111.067827

Cheng, L., Meng, X. B., Lu, S., Wang, T. T., Liu, Y., Sun, G. B., et al. (2014). Evaluation of Hypoglycemic Efficacy of Tangningtongluo Formula, a Traditional Chinese Miao Medicine, in Two Rodent Animal Models. *J. Diabetes Res.* 2014, 745419. doi:10.1155/2014/745419

Cheng, C. S., Chen, J., Tan, H. Y., Wang, N., Chen, Z., and Feng, Y. (2018). Scutellaria Baicalensis and Cancer Treatment: Recent Progress and Perspectives in Biomedical and Clinical Studies. *Am. J. Chin. Med.* 46, 25–54. doi:10.1142/S0192415X18500027

Choi, K., and Kim, Y. B. (2010). Molecular Mechanism of Insulin Resistance in Obesity and Type 2 Diabetes. *Korean J. Intern. Med.* 25, 119–129. doi:10.3904/kjim.2010.25.2.119

Coen, M., Holmes, E., Lindon, J. C., and Nicholson, J. K. (2008). NMR-based Metabolic Profiling and Metabonomic Approaches to Problems in Molecular Toxicology. *Chem. Res. Toxicol.* 21, 9–27. doi:10.1021/tx700335d

Cruz, C., Correa-Rotter, R., Sánchez-González, D. J., Hernández-Pando, R., Maldonado, P. D., Martínez-Martínez, C. M., et al. (2007). Renoprotective and Antihypertensive Effects of S-Allylcysteine in 5/6 Nephrectomized Rats. *Am. J. Physiol. Ren. Physiol.* 293, F1691–F1698. doi:10.1152/ajprenal.00235.2007

Cui, X., Qian, D. W., Jiang, S., Shang, E. X., Zhu, Z. H., and Duan, J. A. (2018). Scutellariae Radix and Coptidis Rhizoma Improve Glucose and Lipid Metabolism in T2DM Rats via Regulation of the Metabolic Profiling and MAPK/PI3K/Akt Signaling Pathway. *Int. J. Mol. Sci.* 19, 3634. doi:10.3390/ijms19113634

de Dios, S. T., Frontanilla, K. V., Nigro, J., Ballinger, M. L., Ivey, M. E., Cawson, E. A., et al. (2007). Regulation of the Atherogenic Properties of Vascular Smooth Muscle Proteoglycans by Oral Anti-hyperglycemic Agents. *J. Diabetes Complications* 21, 108–117. doi:10.1016/j.jdiacomp.2006.03.003

Evert, A. B., Boucher, J. L., Cypress, M., Dunbar, S. A., Franz, M. J., Mayer-Davis, E. J., et al. (2013). Nutrition Therapy Recommendations for the Management of Adults with Diabetes. *Diabetes Care* 36, 3821–3842. doi:10.2337/dc13-2042

Felig, P., Marliss, E., and Cahill, G. F. (1969). Plasma Amino Acid Levels and Insulin Secretion in Obesity. *N. Engl. J. Med.* 281, 811–816. doi:10.1056/NEJM196910092811503

Felig, P., Wahren, J., Hendler, R., and Brundin, T. (1974). Splanchnic Glucose and Amino Acid Metabolism in Obesity. *J. Clin. Invest.* 53, 582–590. doi:10.1172/JCI107593

Feng, Y., Fang, Y., Wang, Y., and Hao, Y. (2018). Acupoint Therapy on Diabetes Mellitus and its Common Chronic Complications: A Review of its Mechanisms. *Biomed. Res. Int.* 2018, 3128378. doi:10.1155/2018/3128378

Ferguson, R. D., Gallagher, E. J., Scheinman, E. J., Damouni, R., and LeRoith, D. (2013). The Epidemiology and Molecular Mechanisms Linking Obesity, Diabetes, and Cancer. *Vitam. Horm.* 93, 51–98. doi:10.1016/B978-0-12-416673-8.00010-1

Ferrannini, E., Natali, A., Camastra, S., Nannipieri, M., Mari, A., Adam, K. P., et al. (2013). Early Metabolic Markers of the Development of Dysglycemia and Type 2 Diabetes and Their Physiological Significance. *Diabetes* 62, 1730–1737. doi:10.2337/db12-0707

Floegel, A., Stefan, N., Yu, Z., Mühlenbruch, K., Drogan, D., Joost, H. G., et al. (2013). Identification of Serum Metabolites Associated with Risk of Type 2 Diabetes Using a Targeted Metabolomic Approach. *Diabetes* 62, 639–648. doi:10.2337/db12-0495

Gao, K., Yang, R., Zhang, J., Wang, Z., Jia, C., Zhang, F., et al. (2018). Effects of Qijian Mixture on Type 2 Diabetes Assessed by Metabonomics, Gut Microbiota and Network Pharmacology. *Pharmacol. Res.* 130, 93–109. doi:10.1016/j.phrs.2018.01.011

Garcia-Galiano, D., Borges, B. C., Allen, S. J., and Elias, C. F. (2019). PI3K Signalling in Leptin Receptor Cells: Role in Growth and Reproduction. *J. Neuroendocrinol.* 31, e12685. doi:10.1111/jne.12685

Glosse, P., and Föller, M. (2018). AMP-Activated Protein Kinase (AMPK)-Dependent Regulation of Renal Transport. *Int. J. Mol. Sci.* 19, 3481. doi:10.3390/ijms19113481

Gonzalez-Franquesa, A., Burkart, A. M., Isganaitis, E., and Patti, M. E. (2016). What Have Metabolomics Approaches Taught Us about Type 2 Diabetes? *Curr. Diab. Rep.* 16, 74. doi:10.1007/s11892-016-0763-1

Goodacre, R. (2004). Metabolic Profiling: Pathways in Discovery. *Drug Discov. Today* 9, 260–261. doi:10.1016/S1359-6446(04)03027-2

Guasch-Ferré, M., Hruby, A., Toledo, E., Clish, C. B., Martínez-González, M. A., Salas-Salvadó, J., et al. (2016). Metabolomics in Prediabetes and Diabetes: A Systematic Review and Meta-Analysis. *Diabetes Care* 39, 833–846. doi:10.2337/dc15-2251

He, K. Q., Li, W. Z., Chai, X. Q., Yin, Y. Y., Jiang, Y., and Li, W. P. (2018). Astragaloside IV Prevents Kidney Injury Caused by Iatrogenic Hyperinsulinemia in a Streptozotocin-induced D-iabetic R-at M-odel. *Int. J. Mol. Med.* 41, 1078–1088. doi:10.3892/ijmm.2017.3265

Hirosumi, J., Tuncman, G., Chang, L., Görgün, C. Z., Uysal, K. T., Maeda, K., et al. (2002). A central Role for JNK in Obesity and Insulin Resistance. *Nature* 420, 333–336. doi:10.1038/nature01137

Hunt, J. V., and Wolff, S. P. (1991). Oxidative Glycation and Free Radical Production: A Causal Mechanism of Diabetic Complications. *Free Radic. Res. Commun.* 12-13 Pt 1, 115–123. doi:10.3109/10715769109145775

Ishii, H., Hayashino, Y., Akai, Y., Yabuta, M., and Tsujii, S. (2018). Dipeptidyl Peptidase-4 Inhibitors as Preferable Oral Hypoglycemic Agents in Terms of Treatment Satisfaction: Results from a Multicenter, 12-week, Open Label, Randomized Controlled Study in Japan (PREFERENCE 4 Study). *J. Diabetes Investig.* 9, 137–145. doi:10.1111/jdi.12659

John, C. M., Mohamed Yusof, N. I. S., Abdul Aziz, S. H., and Mohd Fauzi, F. (2018). Maternal Cognitive Impairment Associated with Gestational Diabetes Mellitus-A Review of Potential Contributing Mechanisms. *Int. J. Mol. Sci.* 19, 3894. doi:10.3390/ijms19123894

Jung, H. A., Yoon, N. Y., Kang, S. S., Kim, Y. S., and Choi, J. S. (2008). Inhibitory Activities of Prenylated Flavonoids from Sophora Flavescens against Aldose Reductase and Generation of Advanced Glycation Endproducts. *J. Pharm. Pharmacol.* 60, 1227–1236. doi:10.1211/jpp.60.9.0016

Karlsson, F. H., Tremaroli, V., Nookaew, I., Bergström, G., Behre, C. J., Fagerberg, B., et al. (2013). Gut Metagenome in European Women with normal, Impaired and Diabetic Glucose Control. *Nature* 498, 99–103. doi:10.1038/nature12198

Krauss, R. M., and Siri, P. W. (2004). Dyslipidemia in Type 2 Diabetes. *Med. Clin. North. Am.* 88, 897–x. doi:10.1016/j.mcna.2004.04.004

Lao, Y., Wang, X., Xu, N., Zhang, H., and Xu, H. (2014). Application of Proteomics to Determine the Mechanism of Action of Traditional Chinese Medicine Remedies. *J. Ethnopharmacol.* 155, 1–8. doi:10.1016/j.jep.2014.05.022

Li, S., and Zhang, B. (2013). Traditional Chinese Medicine Network Pharmacology: Theory, Methodology and Application. *Chin. J. Nat. Med.* 11, 110–120. doi:10.1016/S1875-5364(13)60037-0

Li, H., Zhao, L., Zhang, B., Jiang, Y., Wang, X., Guo, Y., et al. (2014). A Network Pharmacology Approach to Determine Active Compounds and Action Mechanisms of Ge-Gen-Qin-Lian Decoction for Treatment of Type 2 Diabetes. *Evid. Based. Complement. Alternat. Med.* 2014, 495840. doi:10.1155/2014/495840

Li, J., Huang, Y., Zhao, S., Guo, Q., Zhou, J., Han, W., et al. (2019). Based on Network Pharmacology to Explore the Molecular Mechanisms of astragalus Membranaceus for Treating T2 Diabetes Mellitus. *Ann. Transl. Med.* 7, 633. doi:10.21037/atm.2019.10.118

Liao, H., Hu, L., Cheng, X., Wang, X., Li, J., Banbury, L., et al. (2017). Are the Therapeutic Effects of Huangqi (Astragalus Membranaceus) on Diabetic Nephropathy Correlated with its Regulation of Macrophage iNOS Activity? *J. Immunol. Res.* 2017, 3780572. doi:10.1155/2017/3780572

Liu, L., Li, Y., Guan, C., Li, K., Wang, C., Feng, R., et al. (2010). Free Fatty Acid Metabolic Profile and Biomarkers of Isolated post-challenge Diabetes and Type 2 Diabetes Mellitus Based on GC-MS and Multivariate Statistical Analysis. *J. Chromatogr. B Analyt Technol. Biomed. Life Sci.* 878, 2817–2825. doi:10.1016/j.jchromb.2010.08.035

Liu, Q., Liu, S., Gao, L., Sun, S., Huan, Y., Li, C., et al. (2017). Anti-diabetic Effects and Mechanisms of Action of a Chinese Herbal Medicine Preparation JQ-R *In Vitro* and in Diabetic KKAy Mice. *Acta Pharm. Sin. B* 7, 461–469. doi:10.1016/j.apsb.2017.04.010

Lu, D., Wo, X., Wo, L., Li, Y., Tang, L., and Yang, Z. (2009). Effects of Warm and Tonify Kidney-Yang Herbs on Liver Mitochondria Proteome of Kidney-Yang Deficiency Rats. *Zhongguo Zhong Yao Za Zhi* 34, 1251–1256. doi:10.3321/j.issn:1001-5302.2009.10.017

Luetscher, J. A. (1942). The Metabolism of Amino Acids in Diabetes Mellitus. *J. Clin. Invest.* 21, 275–279. doi:10.1172/JCI101300

Mabhida, S. E., Dludla, P. V., Johnson, R., Ndlovu, M., Louw, J., Opoku, A. R., et al. (2018). Protective Effect of Triterpenes against Diabetes-Induced β-cell Damage: An Overview of *In Vitro* and *In Vivo* Studies. *Pharmacol. Res.* 137, 179–192. doi:10.1016/j.phrs.2018.10.004

Madsen, R., Lundstedt, T., and Trygg, J. (2010). Chemometrics in Metabolomics-Aa Review in Human Disease Diagnosis. *Anal. Chim. Acta* 659, 23–33. doi:10.1016/j.aca.2009.11.042

Malik, V. S., Popkin, B. M., Bray, G. A., Després, J. P., and Hu, F. B. (2010). Sugar-sweetened Beverages, Obesity, Type 2 Diabetes Mellitus, and Cardiovascular Disease Risk. *Circulation* 121, 1356–1364. doi:10.1161/CIRCULATIONAHA.109.876185

Mao, Y., Hao, J., Jin, Z. Q., Niu, Y. Y., Yang, X., Liu, D., et al. (2017). Network Pharmacology-Based and Clinically Relevant Prediction of the Active Ingredients and Potential Targets of Chinese Herbs in Metastatic Breast Cancer Patients. *Oncotarget* 8, 27007–27021. doi:10.18632/oncotarget.15351

Nanjan, M. J., Mohammed, M., Prashantha Kumar, B. R., and Chandrasekar, M. J. N. (2018). Thiazolidinediones as Antidiabetic Agents: A Critical Review. *Bioorg. Chem.* 77, 548–567. doi:10.1016/j.bioorg.2018.02.009

Neag, M. A., Mocan, A., Echeverría, J., Pop, R. M., Bocsan, C. I., Crişan, G., et al. (2018). Berberine: Botanical Occurrence, Traditional Uses, Extraction Methods, and Relevance in Cardiovascular, Metabolic, Hepatic, and Renal Disorders. *Front. Pharmacol.* 9, 557. doi:10.3389/fphar.2018.00557

Newgard, C. B., An, J., Bain, J. R., Muehlbauer, M. J., Stevens, R. D., Lien, L. F., et al. (2009). A Branched-Chain Amino Acid-Related Metabolic Signature that Differentiates Obese and Lean Humans and Contributes to Insulin Resistance. *Cell Metab.* 9, 311–326. doi:10.1016/j.cmet.2009.02.002

Ning, G., Hong, J., Bi, Y., Gu, W., Zhang, Y., Zhang, Z., et al. (2009). Progress in Diabetes Research in China. *J. Diabetes* 1, 163–172. doi:10.1111/j.1753-0407.2009.00037.x

Nozaki, T., Minaguchi, J., Takehana, K., and Ueda, H. (2017). Anti-diabetic Activities of Traditional Chinese Herbal Medicine in Streptozotocin-Induced Diabetic Rats. *Okajimas Folia Anat. Jpn.* 93, 111–118. doi:10.2535/ofaj.93.111

Oikonomou, E., Mourouzis, K., Fountoulakis, P., Papamikroulis, G. A., Siasos, G., Antonopoulos, A., et al. (2018). Interrelationship Between Diabetes Mellitus and Heart Failure: the Role of Peroxisome Proliferator-Activated Receptors in Left Ventricle Performance. *Heart Fail. Rev.* 23, 389–408. doi:10.1007/s10741-018-9682-3

Padberg, I., Peter, E., González-Maldonado, S., Witt, H., Mueller, M., Weis, T., et al. (2014). A New Metabolomic Signature in Type-2 Diabetes Mellitus and its Pathophysiology. *PLoS One* 9, e85082. doi:10.1371/journal.pone.0085082

Pan, L., Li, Z., Wang, Y., Zhang, B., Liu, G., and Liu, J. (2020). Network Pharmacology and Metabolomics Study on the Intervention of Traditional Chinese Medicine Huanglian Decoction in Rats with Type 2 Diabetes Mellitus. *J. Ethnopharmacol.* 258, 112842. doi:10.1016/j.jep.2020.112842

Prabhakar, P. K., and Doble, M. (2011). Mechanism of Action of Natural Products Used in the Treatment of Diabetes Mellitus. *Chin. J. Integr. Med.* 17, 563–574. doi:10.1007/s11655-011-0810-3

Qin, J., Li, Y., Cai, Z., Li, S., Zhu, J., Zhang, F., et al. (2012). A Metagenome-Wide Association Study of Gut Microbiota in Type 2 Diabetes. *Nature* 490, 55–60. doi:10.1038/nature11450

Rhee, E. P., Cheng, S., Larson, M. G., Walford, G. A., Lewis, G. D., McCabe, E., et al. (2011). Lipid Profiling Identifies a Triacylglycerol Signature of Insulin Resistance and Improves Diabetes Prediction in Humans. *J. Clin. Invest.* 121, 1402–1411. doi:10.1172/JCI44442

Roberts, L. D., Koulman, A., and Griffin, J. L. (2014). Towards Metabolic Biomarkers of Insulin Resistance and Type 2 Diabetes: Progress from the Metabolome. *Lancet. Diabetes Endocrinol.* 2, 65–75. doi:10.1016/S2213-8587(13)70143-8

Rojas, J., Bermudez, V., Palmar, J., Martínez, M. S., Olivar, L. C., Nava, M., et al. (2018). Pancreatic Beta Cell Death: Novel Potential Mechanisms in Diabetes Therapy. *J. Diabetes Res.* 2018, 9601801. doi:10.1155/2018/9601801

Różańska, D., and Regulska-Ilow, B. (2018). The Significance of Anthocyanins in the Prevention and Treatment of Type 2 Diabetes. *Adv. Clin. Exp. Med.* 27, 135–142. doi:10.17219/acem/64983

Saeedi, P., Petersohn, I., Salpea, P., Malanda, B., Karuranga, S., Unwin, N., et al. (2019). Global and Regional Diabetes Prevalence Estimates for 2019 and Projections for 2030 and 2045: Results from the International Diabetes Federation Diabetes Atlas, 9th Edition. *Diabetes Res. Clin. Pract.* 157, 107843. doi:10.1016/j.diabres.2019.107843

Sas, K. M., Karnovsky, A., Michailidis, G., and Pennathur, S. (2015). Metabolomics and Diabetes: Analytical and Computational Approaches. *Diabetes* 64, 718–732. doi:10.2337/db14-0509

Setter, S. M., Iltz, J. L., Thams, J., and Campbell, R. K. (2003). Metformin Hydrochloride in the Treatment of Type 2 Diabetes Mellitus: A Clinical Review with a Focus on Dual Therapy. *Clin. Ther.* 25, 2991–3026. doi:10.1016/S0149-2918(03)90089-0

Shao, J., Liu, Y., Wang, H., Luo, Y., and Chen, L. (2020). An Integrated Fecal Microbiome and Metabolomics in T2DM Rats Reveal Antidiabetes Effects from Host-Microbial Metabolic Axis of EtOAc Extract from Sophora Flavescens. *Oxid. Med. Cel. Longev.* 2020, 1805418. doi:10.1155/2020/1805418

Sharma, B. R., Gautam, L. N., Adhikari, D., and Karki, R. (2017). A Comprehensive Review on Chemical Profiling of Nelumbo Nucifera: Potential for Drug Development. *Phytother. Res.* 31, 3–26. doi:10.1002/ptr.5732

Sheetz, M. J., and King, G. L. (2002). Molecular Understanding of Hyperglycemia's Adverse Effects for Diabetic Complications. *JAMA* 288, 2579–2588. doi:10.1001/jama.288.20.2579

Song, K. H., Lee, S. H., Kim, B. Y., Park, A. Y., and Kim, J. Y. (2013). Extracts of Scutellaria Baicalensis Reduced Body Weight and Blood Triglyceride in Db/db Mice. *Phytother. Res.* 27, 244–250. doi:10.1002/ptr.4691

Sun, G. D., Li, C. Y., Cui, W. P., Guo, Q. Y., Dong, C. Q., Zou, H. B., et al. (2016). Review of Herbal Traditional Chinese Medicine for the Treatment of Diabetic Nephropathy. *J. Diabetes Res.* 2016, 5749857. doi:10.1155/2016/5749857

Tai, E. S., Tan, M. L., Stevens, R. D., Low, Y. L., Muehlbauer, M. J., Goh, D. L., et al. (2010). Insulin Resistance Is Associated with a Metabolic Profile of Altered Protein Metabolism in Chinese and Asian-Indian Men. *Diabetologia* 53, 757–767. doi:10.1007/s00125-009-1637-8

Taskinen, M. R. (2003). Diabetic Dyslipidaemia: from Basic Research to Clinical Practice. *Diabetologia* 46, 733–749. doi:10.1007/s00125-003-1111-y

Thangavel, N., Al Bratty, M., Akhtar Javed, S., Ahsan, W., and Alhazmi, H. A. (2017). Targeting Peroxisome Proliferator-Activated Receptors Using Thiazolidinediones: Strategy for Design of Novel Antidiabetic Drugs. *Int. J. Med. Chem.* 2017, 1069718. doi:10.1155/2017/1069718

Tong, X.-L., Zhao, L.-H., Lian, F.-M., Zhou, Q., Xia, L., Zhang, J.-C., et al. (2011). Clinical Observations on the Dose-Effect Relationship of Gegen Qin Lian Decoction on 54 Out-Patients With Type 2 Diabetes. *J. Tradit. Chin. Med.* 31, 56–59. doi:10.1016/s0254-6272(11)60013-7

Tzeng, T. F., Liou, S. S., and Liu, I. M. (2013). The Selected Traditional Chinese Medicinal Formulas for Treating Diabetic Nephropathy: Perspective of Modern Science. *J. Tradit. Complement. Med.* 3, 152–158. doi:10.4103/2225-4110.114893

Wang, L. M., Zhao, X., Wu, X. L., Li, Y., Yi, D. H., Cui, H. T., et al. (2012). Diagnosis Analysis of 4 TCM Patterns in Suboptimal Health Status: A Structural Equation Modelling Approach. *Evid. Based. Complement. Alternat. Med.* 2012, 970985. doi:10.1155/2012/970985

Wang, T., Jiang, H., Cao, S., Chen, Q., Cui, M., Wang, Z., et al. (2017). Baicalin and its Metabolites Suppresses Gluconeogenesis through Activation of AMPK or AKT in Insulin Resistant HepG-2 Cells. *Eur. J. Med. Chem.* 141, 92–100. doi:10.1016/j.ejmech.2017.09.049

Wang, Q., Liu, S., Zhai, A., Zhang, B., and Tian, G. (2018). AMPK-Mediated Regulation of Lipid Metabolism by Phosphorylation. *Biol. Pharm. Bull.* 41, 985–993. doi:10.1248/bpb.b17-00724

Wang, W., Zhao, L., He, Z., Wu, N., Li, Q., Qiu, X., et al. (2018). Metabolomics-Based Evidence of the Hypoglycemic Effect of Ge-Gen-Jiao-Tai-Wan in Type 2 Diabetic Rats via UHPLC-QTOF/MS Analysis. *J. Ethnopharmacol.* 219, 299–318. doi:10.1016/j.jep.2018.03.026

Weyer, C., Funahashi, T., Tanaka, S., Hotta, K., Matsuzawa, Y., Pratley, R. E., et al. (2001). Hypoadiponectinemia in Obesity and Type 2 Diabetes: Close Association with Insulin Resistance and Hyperinsulinemia. *J. Clin. Endocrinol. Metab.* 86, 1930–1935. doi:10.1210/jcem.86.5.7463

Wu, T., Yang, M., Wei, H. F., He, S. H., Wang, S. C., and Ji, G. (2012). Application of Metabolomics in Traditional Chinese Medicine Differentiation of Deficiency and Excess Syndromes in Patients with Diabetes Mellitus. *Evid. Based. Complement. Alternat. Med.* 2012, 968083. doi:10.1155/2012/968083

Wu, K., Liang, T., Duan, X., Xu, L., Zhang, K., and Li, R. (2013). Anti-Diabetic Effects of Puerarin, Isolated from *Pueraria lobata* (Willd.), on Streptozotocin-Diabetogenic Mice through Promoting Insulin Expression and Ameliorating Metabolic Function. *Food Chem. Toxicol.* 60, 341–347. doi:10.1016/j.fct.2013.07.077

Würtz, P., Tiainen, M., Mäkinen, V. P., Kangas, A. J., Soininen, P., Saltevo, J., et al. (2012). Circulating Metabolite Predictors of Glycemia in Middle-Aged Men and Women. *Diabetes Care* 35, 1749–1756. doi:10.2337/dc11-1838

Xie, H., Wang, Q., Zhang, X., Wang, T., Hu, W., Manicum, T., et al. (2018). Possible Therapeutic Potential of Berberine in the Treatment of STZ Plus HFD-Induced Diabetic Osteoporosis. *Biomed. Pharmacother.* 108, 280–287. doi:10.1016/j.biopha.2018.08.131

Xu, W., Zhang, L., Huang, Y., Yang, Q., Xiao, H., and Zhang, D. (2012). Discrimination of Type 2 Diabetes Mellitus Corresponding to Different Traditional Chinese Medicine Syndromes Based on Plasma Fatty Acid Profiles and Chemometric Methods. *J. Ethnopharmacol.* 143, 463–468. doi:10.1016/j.jep.2012.06.045

Xu, X., Gao, Z., Yang, F., Yang, Y., Chen, L., Han, L., et al. (2020). Antidiabetic Effects of Gegen Qinlian Decoction via the Gut Microbiota are Attributable to its Key Ingredient Berberine. *Genom. Proteom. Bioinform.* 18, 721–736. doi:10.1016/j.gpb.2019.09.007

Xue, J., Shi, Y., Li, C., and Song, H. (2019). Network Pharmacology-Based Prediction of the Active Ingredients, Potential Targets, and Signaling Pathways in Compound Lian-Ge Granules for Treatment of Diabetes. *J. Cel. Biochem.* 120, 6431–6440. doi:10.1002/jcb.27933

Yang, M. D., Chiang, Y. M., Higashiyama, R., Asahina, K., Mann, D. A., Mann, J., et al. (2012). Rosmarinic Acid and Baicalin Epigenetically Derepress Peroxisomal Proliferator-Activated Receptor γ in Hepatic Stellate Cells for Their Antifibrotic Effect. *Hepatology* 55, 1271–1281. doi:10.1002/hep.24792

Yang, X., Zhang, Q., Gao, Z., Yu, C., and Zhang, L. (2018). Baicalin Alleviates IL-1β-induced Inflammatory Injury via Down-Regulating miR-126 in Chondrocytes. *Biomed. Pharmacother.* 99, 184–190. doi:10.1016/j.biopha.2018.01.041

Zhang, X. W., Li, W. F., Li, W. W., Ren, K. H., Fan, C. M., Chen, Y. Y., et al. (2011). Protective Effects of the Aqueous Extract of Scutellaria Baicalensis against Acrolein-Induced Oxidative Stress in Cultured Human Umbilical Vein Endothelial Cells. *Pharm. Biol.* 49, 256–261. doi:10.3109/13880209.2010.501803

Zhang, A. H., Sun, H., Qiu, S., and Wang, X. J. (2013). Recent Highlights of Metabolomics in Chinese Medicine Syndrome Research. *Evid. Based. Complement. Alternat. Med.* 2013, 402159. doi:10.1155/2013/402159

Zhang, C. H., Xu, G. L., Liu, Y. H., Rao, Y., Yu, R. Y., Zhang, Z. W., et al. (2013). Anti-Diabetic Activities of Gegen Qinlian Decoction in High-Fat Diet Combined with Streptozotocin-Induced Diabetic Rats and in 3T3-L1 Adipocytes. *Phytomedicine* 20, 221–229. doi:10.1016/j.phymed.2012.11.002

Zhang, G. B., Li, Q. Y., Chen, Q. L., and Su, S. B. (2013). Network Pharmacology: A New Approach for Chinese Herbal Medicine Research. *Evid. Based. Complement. Alternat. Med.* 2013, 621423. doi:10.1155/2013/621423

Zhang, T. T., and Jiang, J. G. (2012). Active Ingredients of Traditional Chinese Medicine in the Treatment of Diabetes and Diabetic Complications. *Expert Opin. Investig. Drugs* 21, 1625–1642. doi:10.1517/13543784.2012.713937

Zhang, Z., Zhang, H., Li, B., Meng, X., Wang, J., Zhang, Y., et al. (2014). Berberine Activates Thermogenesis in white and Brown Adipose Tissue. *Nat. Commun.* 5, 5493. doi:10.1038/ncomms6493

Zheng, Y., Ceglarek, U., Huang, T., Li, L., Rood, J., Ryan, D. H., et al. (2016). Weight-loss Diets and 2-y Changes in Circulating Amino Acids in 2 Randomized Intervention Trials. *Am. J. Clin. Nutr.* 103, 505–511. doi:10.3945/ajcn.115.117689

Zhou, J., Huang, K., and Lei, X. G. (2013). Selenium and Diabetes-Eevidence from Animal Studies. *Free Radic. Biol. Med.* 65, 1548–1556. doi:10.1016/j.freeradbiomed.2013.07.012

Zimmet, P., Alberti, K. G., and Shaw, J. (2001). Global and Societal Implications of the Diabetes Epidemic. *Nature* 414, 782–787. doi:10.1038/414782a

Conflict of Interest: Authors YY and WX were employed by the company Jiangsu Kanion Pharmaceutical Co., Ltd.

The remaining authors declare that the research was conducted in the absence of any commercial or financial relationships that could be construed as a potential conflict of interest.

Publisher's Note: All claims expressed in this article are solely those of the authors and do not necessarily represent those of their affiliated organizations, or those of the publisher, the editors and the reviewers. Any product that may be evaluated in this article, or claim that may be made by its manufacturer, is not guaranteed or endorsed by the publisher.

frontiers in Pharmacology

ORIGINAL RESEARCH
published: 22 September 2021
doi: 10.3389/fphar.2021.753153

Yeokwisan, a Standardized Herbal Formula, Enhances Gastric Emptying via Modulation of the Ghrelin Pathway in a Loperamide-induced Functional Dyspepsia Mouse Model

Seung-Ju Hwang[1], Jing-Hua Wang[1], Jin-Seok Lee[1], Hwa-Dong Lee[2], Tae-Joon Choi[3], Seo-Hyung Choi[4] and Chang-Gue Son[1]**

[1]Liver and Immunology Research Center, Daejeon Oriental Hospital of Daejeon University, Daejeon, South Korea, [2]National Institute for Korean Medicine, Daejeon, South Korea, [3]Wooje IM Inc., Daejeon, South Korea, [4]Department of Internal Medicine, Gangnam Weedahm Korean Medical Hospital, Daejeon, South Korea

OPEN ACCESS

Edited by:
XY Zhang,
University of Minho, Portugal

Reviewed by:
Ramanathan Muthiah,
PSG College of Pharmacy, India
Hsien-Hui Chung,
Kaohsiung Veterans General Hospital, Taiwan

***Correspondence:**
Seo-Hyung Choi
hana912@korea.com
orcid.org/0000-0002-6939-5085;
Chang-Gue Son
ckson@dju.ac.kr
orcid.org/0000-0002-6963-5229

Specialty section:
This article was submitted to Ethnopharmacology, a section of the journal Frontiers in Pharmacology

Received: 04 August 2021
Accepted: 09 September 2021
Published: 22 September 2021

Citation:
Hwang S-J, Wang J-H, Lee J-S, Lee H-D, Choi T-J, Choi S-H and Son C-G (2021) Yeokwisan, a Standardized Herbal Formula, Enhances Gastric Emptying via Modulation of the Ghrelin Pathway in a Loperamide-induced Functional Dyspepsia Mouse Model. Front. Pharmacol. 12:753153. doi: 10.3389/fphar.2021.753153

Background: Yeokwisan, a standardized herbal formula, has exhibited clinical benefit for patients suffering from refractory functional dyspepsia (FD) in Korea since 2016. However, data about the mechanism of action of this formula are yet not available.

Aim of the study: To evaluate and explore the effects of Yeokwisan on gastric emptying, a major symptom of functional dyspepsia, and its underlying mechanisms of action using a mouse model.

Materials and methods: BALB/C mice were pretreated with Yeokwisan (100, 200, and 400 mg/kg, po) or mosapride (3 mg/kg, po) for 5 days and then treated with loperamide (10 mg/kg, ip) after 20 h of fasting. A solution of 0.05% phenol red (500 μL) or diet of 5% charcoal (200 μL) was orally administered, followed by assessment of gastric emptying or intestinal transit. Plasma acyl-ghrelin (ELISA), C-kit (immunofluorescence and western blotting), nNOS (western blotting) and gastric contraction- and ghrelin-related gene/protein expression levels were examined in stomach and small intestine tissues.

Results: Loperamide injection substantially delayed gastric emptying, while Yeokwisan pretreatment (especially 200 and 400 mg/kg Yeokwisan) significantly attenuated this peristaltic dysfunction, as evidenced by the quantity of phenol red retained in the stomach ($p < 0.05$ or 0.01) and stomach weight ($p < 0.05$ or 0.01). The levels of plasma acyl-ghrelin and expression of gastric ghrelin-related genes, such as growth hormone secretagogue receptor (GHSR), ghrelin-O-acyltransferase (GOAT), adrenergic receptor β1 (ADRB1) and somatostatin receptor (SSTR), were significantly normalized ($p < 0.05$ or 0.01) by Yeokwisan (400 mg/kg). Yeokwisan (400 mg/kg) significantly tempered the loperamide-induced alterations in the c-kit and nNOS levels ($p < 0.01$) as well as the expression of contraction- and ghrelin-related genes, such as 5-HT4 receptor (5-HT4R), anoctamin-1 (ANO1), ryanodine receptor 3 (RYR3) and smooth muscle myosin light chain kinase (smMLCK), in the stomach, but not in the small intestine.

Conclusion: The present results showed the clinical relevance of Yeokwisan, in treating FD, especially in promoting gastric emptying but not small intestinal transit. The main mechanisms corresponding to these effects may involve the modulation of the ghrelin pathway and activation of interstitial cells of Cajal in stomach tissue.

Keywords: functional dyspepsia, ghrelin, gastric emptying, herbal formula, interstitial cells of cajal

INTRODUCTION

Approximately one-fifth of the general population complains of dyspeptic symptoms, such bloating, anorexia, early satiety, and epigastric discomfort (Ford et al., 2015). Eighty percent of them cannot be explained either structurally or organically, and these symptoms are referred to as functional dyspepsia (FD) (Ford et al., 2020). FD accounts for 11–29.2% of the global prevalence of these symptoms, with differences among countries (Mahadeva and Goh, 2006). The economic burden of FD is estimated to be over 18 billion dollars per year in the United States (Lacy et al., 2013).

FD is diagnosed by symptom-based criteria, and the Rome IV criteria were most recently revised in 2016 (Stanghellini et al., 2016). FD is generally divided into three subtypes depending on the main symptoms: postprandial fullness and early satiety (postprandial distress syndrome, PDS), epigastric pain/burning symptoms (epigastric pain syndrome, EPS), and a combination of these symptoms (Asano et al., 2016). In Asia, the PDS subtype is known to be more prevalent than the EPS or combination type, especially in Korea and Japan (Lee and Chua, 2012).

The main causes of FD generally include abnormal gastrointestinal (GI) motility, visceral hypersensitivity, oversecretion of gastric acid, and *Helicobacter pylori* infection (Enck et al., 2017). Based on these etiological factors, prokinetic drugs, such as ghrelin receptor agonists, serotonin (5-hydroxytryptamine, 5-HT) receptor agonists, muscarinic receptor antagonists, proton pump inhibitors (PPIs), and *H. pylori* eradicating drugs are used to treat patients with FD (Ford et al., 2020). However, these treatments have clinical limitations, such as a high recurrence rate after cessation-, for example, the recurrence rate after cessation of acotiamide, a prokinetic, therapy, is a half (Shinozaki et al., 2020), and unexpected adverse effects, such as an increased risk of myocardial infraction and risk of ventricular arrhythmias after long-term use of PPIs or cisapride (a 5-HT receptor agonist) (De Maeyer et al., 2008; Shah et al., 2015).

On the other hand, herbal medicine has been used as a treatment option for patients with GI disorders. One study reported that approximately one-third of surveyed patients with functional GI disorders used herbal medicines (Lahner et al., 2013). Many patients with FD have chosen herbal products from traditional Korean medicine (TKM) and traditional Chinese medicine (TCM). Many studies have shown the therapeutic effects of multiherbal decoctions in clinical trials (Kim et al., 2014; Kim et al., 2021) and animal experiments (Jeon et al., 2019; Tan et al., 2020). In particular, the pharmacological theories of TKM and TCM emphasize the synergistic actions of multiherbal combinations for the treatment of multifactorial disorders, such as FD (Liu et al., 2013; Kim et al., 2021).

Yeokwisan, a standardized Korean herbal formula, is composed by six herbs including *Poncirus trifoliata* Rafinesque (*P. trifoliata*), *Scutellaria baicalensis* Georgi (*S. baicalensis*), *Glycyrrhiza uralensis* Fischer (*G. uralensis*), Massa medicata Fermentata, *Phyllostachys bambusoides* Sieb. et Zucc (*P. bambusoides*), and *Ostrea gigas* Thunberg (*O. gigas*). It has been prescribed for patients suffering from refractory FD including gastroesophageal reflux disease (GERD) in clinic since 2016. However, data about the mechanism of action this formula are yet not available. Accordingly, we aimed to evaluate and explore the effects and underlying mechanisms of this formula *in vivo* using a loperamide-induced FD mouse model.

MATERIALS AND METHODS

Chemicals and Reagents

The following reagents and chemicals were obtained from Sigma-Aldrich (MO, United States): loperamide hydrochloride, mosapride citrate salt dihydrate, phenol red, sodium carboxymethyl cellulose (CMC-Na), sodium hydroxide, trichloroacetic acid (TCA), Tris base, sodium chloride, Triton X, 10% neutral formalin, calcium carbonate, calcium sulfate, catechin, chlorogenic acid, porcirin, naringin, rutin, benzaldehyde, aqueous mounting buffer, and 4′,6-diamidino-2-phenylindole dihydrochloride (DAPI).

Other reagents and chemicals were purchased from the following manufacturers: arabic gum (JUNSEI, Tokyo, Japan), activated charcoal power (YAKURI, Tokyo, Japan), Tween 20 (Glentham Life Science, Corsham, United Kingdom), skim milk (LPS solution, Daejeon, Korea), bovine serum albumin (GenDEPOT, TX, United States), hydrochloride (DUKSAN, Seoul, Korea), and hydroperoxide (SAMCHUN, Seoul, Korea).

Preparation and Fingerprinting Analyses of *Yeokwisan*

Poncirus trifoliata Rafinesque (*P. trifoliata*), *Scutellaria baicalensis* Georgi (*S. baicalensis*), *Glycyrrhiza uralensis* Fischer (*G. uralensis*), Massa medicata Fermentata, *Phyllostachys bambusoides* Sieb. et Zucc (*P. bambusoides*), and *Ostrea gigas* Thunberg (*O. gigas*) were obtained from Weedahm Korean Hospital (Seoul, Korea), and all the herbs were approved by the Ministry of Food and Drug Safety (MFDS) in Korea. *O. gigas* Thunberg and others were extracted with boiling water and 60% EtOH solution, respectively. Then, these herbal medicine extracts were prepared by mixing them in certain proportions. The mixed

TABLE 1 | The yield and mixing portion of herbal medicines comprising *Yeokwisan*.

Herb	Extraction solvent	Yield (%)	Mixture portion (%)
Poncirus trifoliata Rafinesque	60% EtOH	17.2	16.4
Scutellaria baicalensis Georgi	60% EtOH	50.4	47.8
Glycyrrhiza uralensis Fischer	60% EtOH	30.0	21.4
Massa medicata Fermentata	60% EtOH	11.3	11.1
Phyllostachys bambusoides Sieb. et Zucc	60% EtOH	2.2	1.9
Ostrea gigas Thunberg	Boiled water	0.4	1.4

formula was promptly stored at −70°C until use. Check **Table 1** shows the yield and formula ratio of each herbal medicine.

Fingerprinting analyses of *Yeokwisan* were conducted using high-performance liquid chromatography (HPLC). A total of 50 μg of *Yeokwisan* and 1 μg of each reference compound (naringin, baicalin, poncirin, baicalein, glycyrrhizic acid, and wogonin) were dissolved in 1 ml of 50% methanol, and the solution was filtered (0.2 μm). A 10 μL volume of each sample solution was injected into an Agilent 1,260 system, and separation was performed using a YMC-Triart C18 (5 μm, 4.6 × 250 mm, Agilent Technologies, CA, United States). The column was eluted at a flow rate of 1 ml/min and a wavelength of 230 nm using mobile phases A (0.05% phosphate in H_2O) and B (acetonitrile including phosphate).

Animals and Experimental Design

A total of one hundred-eight BALB/C male mice (6 weeks old; 19–21 g) were purchased from Daehanbio-link (Eumseong-gun, Chung-buk, Korea). These animals were maintained at room temperature (22 ± 2°C) and 60 ± 5% relative humidity under a 12-h light:12-h dark cycle. The mice were given free access to a commercial pellet diet (Daehanbio-link) and tap water.

After 7 days of acclimatization, the mice were randomly divided into three experimental sets: the first set was used to measure gastric emptying (n = 36), the second set was used to test intestinal motility (n = 36), and the third set was used to obtain tissues (stomach and small intestine) and blood samples (n = 36). Each set was divided into six groups (n = 6/group): the normal, control, three doses of *Yeokwisan* (100, 200, and 400 mg/kg), and mosapride groups. Commonly, the dose of *Yeokwisan* is 3 g per day in clinic for human adult, which is equivalent to 615 mg/kg of mouse according to animal equivalent dose calculation based on body surface (Food and Administration, 2005; Nair and Jacob, 2016). However, we have found that even though 400 mg/kg of *Yeokwisan* showed the significant prokinetic effect on stomach in our pilot experiment. Therefore, 400 mg/kg was set to the high dose in the present experiment.

Yeokwisan, mosapride and distilled water were orally treated separately in each corresponding group once a day for continuous 5 days. On the final day of the experiment, the mice were fasted for 20 h. Then, the mice were examined in accordance with the protocol for each experimental set, as follows: 1) gastric emptying test, 2) intestinal transit tests, and 3) biomolecular analysis. The corpus region in stomach and duodenum in small intestine (regions up to 5 cm from the pyloric sphincter) were used for biomolecule analysis.

The protocol was approved by the Institutional Animal Care and Use Committee of Daejeon University (Daejeon, Republic of Korea; Approval No. DJUARB 2021-013) and was conducted in accordance with the Guide for the Care and Use of Laboratory Animals, published by the National Institutes of Health (NIH, MD).

Determination of Gastric Emptying Using Phenol Red and Stomach Weight and Area

The mice were fasted for 20 h and given free access to tap water. Except for those in the normal group, the mice were intraperitoneally injected with loperamide hydrochloride (10 mg/kg, dissolved in normal saline). After 30 min, all the mice were orally administered phenol red solution (500 μL/mouse). Phenol red was dissolved in 1.5% sodium carboxymethyl cellulose sodium (dissolved in distilled water) at a concentration of 0.05%. Thirty minutes after phenol red treatment, the mice were euthanized in a CO_2 chamber (Jeungdo Bio and Plant, Seoul, Korea), and then, the stomachs were immediately removed and weighed. To measure the area of the stomach, all the stomachs were photographed, and then, the area of the stomach was calculated by ImageJ (NIH). In the experiments to determine gastric emptying, the choice of the phenol red solution volume and time point at which approximately 60% delayed gastric emptying was observed were established by our pilot experiment data (**Supplementary Figure S1**) and other protocols (Asano et al., 2016; Lee et al., 2016).

To measure the absorbance of the phenol red retained in the stomach, stomach samples were homogenized in 5 ml of 0.1 N sodium hydroxide solutions and 0.5 ml of 20% trichloroacetic acid. The homogenates were centrifuged at 3,000 rpm for 20 min, and then, 1 ml of supernatant was added to 4 ml of 0.5 N sodium hydroxide. Finally, the absorbance of these pink-colored solutions was determined at 560 nm by using a spectrophotometer.

The gastric emptying rates were calculated according to the following formula: gastric emptying (%) = (1-X/Y) * 100. X: Absorbance of stomach-retained phenol red, Y: Absorbance of naïve phenol red mixed with sodium hydroxide.

Determination of Intestinal Transit Rate Using Charcoal Diet

To evaluate the intestinal transit rate, the mice were intraperitoneally injected with loperamide hydrochloride

TABLE 2 | Summary for gene sequence.

Gene	Sense (5′→3′)	Anti-sense (5′→3′)
5-HT_4R	ATG GTC AAC AAG CCC TAT GC	AGG AAG GCA CGT CTG AAA GA
ANO1	GGT GTC GGG TTT GTG AAG AT	TGC ACG TTG TTC TCT TCA GG
RYR3	GGC CAA GAA CAT CAG AGT GAC TAA	TCA CTT CTG CCC TGT CAG TTT C
smMLCK	AGA AGT CAA GGA GGT AAA GAA TGA TGT	CGG GTC GCT TTT CAT TGC
Ghrelin	TCC AAG AAG CCA CCA GCT AA	AAC ATC GAA GGG AGC ATT GA
GHSR	CTA TCC AGC ATG GCC TTC TC	AAG ACG CTC GAC AC CCA TAC
GOAT	ATT TGT GAA GGG AAG GTG GAG-	CAG GAG AGC AGG GAA AAA GAG
ADRB1	GAA GGC GCT CAA GAC ACT GG	CCA GGT CGC GGT GGA A
SSTR	GGC GAA ATG CGT CCC AG	CGG AGT A GA TGA AAG AGA TCA GGA
GAPDH	CAT GGC CTT CCG TGT TCC T	CCT GCT TCA CCA CCT TCT TGA

5-HT_4 receptor, 5-HT_4R; anoctamin-1, ANO1; ryanodine receptor 3, RYR3; smooth muscle cell myosin light chain kinase, smMLCK; growth hormone secretagogue receptor, GHSR; ghrelin-O-acyltransferase, GOAT; adrenergic receptor β1, ADRB1; somatostatin receptor, SSTR.

(10 mg/kg), except for the mice in the normal group. After 30 min, all the mice were orally administered 5% charcoal dissolved in 10% arabic gum (200 μL/mouse), a black semisolid paste, as previously described (Nunes Marona and Bastos Lucchesi, 2004). The mice were sacrificed 30 min after the charcoal diet treatment, and the intestinal transit was determined by measuring the distance of charcoal transit from the pylorus to the cecum by using ImageJ (NIH). The time points examined in these experiments involving treatment with charcoal diet and loperamide were established by our pilot experiment data (**Supplementary Figure S2**) and other protocols (Mittelstadt et al., 2005).

Determination of Acylated Ghrelin Levels in Plasma by ELISA

Blood was immediately collected in K_2-ethylenediaminetetraacetic acid (EDTA) tubes. After shaking for 15 min, blood was centrifuged at 3,000 rpm for 15 min. Then, PMSF was added to isolated plasma to prevent the degradation of acyl-ghrelin. To evaluate systemic acyl-ghrelin levels, plasma was measured by using a commercial acylated ghrelin ELISA kit (A05117, Bertin Pharma, France) according to the manufacturer's protocol.

Stomach and Small Intestine Protein Expression Analysis by Western Blotting

To determine the expression of C-kit and neuronal nitric oxide synthase (nNOS) in the stomach and small intestine, the stomach and small intestine were prepared in RIPA lysis buffer. The proteins were separated by 7.5% polyacrylamide gel electrophoresis and transferred to polyvinylidene fluoride (PVDF) membranes. After blocking in 5% skim milk for 1 h at room temperature, the membranes were incubated with primary antibodies, such as C-kit (0.1 μg/ml, AF1356, R&D Systems), nNOS (1:1,000, ab76067, Abcam) or α-tubulin (1: 1,000, ab7291, Abcam) antibodies, overnight at 4°C. After washing with 0.1% TBS-T, the membranes were incubated with HRP-conjugated anti-goat (against C-kit, 1:2,500), anti-rabbit (against nNOS, 1:5,000), or anti-mouse (against α-tubulin, 1: 5,000) antibodies. These proteins were visualized using an enhanced chemiluminescence (ECL) advanced kit (Thermo Fisher Scientific, United States) and imaged using a FUSION Solo System (Vilber Lourmat, France). Protein expression was semiquantified using ImageJ (NIH).

Stomach and Small Intestine Gene Expression Analysis by Quantitative Real-Time PCR

Ghrelin-Related Genes

Expression of ghrelin-related genes was analyzed by quantitative real-time PCR. The ghrelin-related genes were as follows: ghrelin, ghrelin-O-acyltransferase (GOAT), growth hormone secretagogue receptor (GHSR), adrenergic receptor β1 (ADRB1) and somatostatin receptor (SSTR).

Smooth Muscle Contraction-Related Genes

Regarding smooth muscle cell contraction, quantitative real-time PCR analysis was conducted to evaluate the expression of the following four smooth muscle cell contraction-related gene: 5-HT_4 receptor (5-HT_4R), anoctamin-1 (ANO1), ryanodine receptor 3 (RYR3) and smooth muscle cell myosin light chain kinase (smMLCK).

Quantitative Real-Time PCR Performance

Total RNA was extracted from the stomach and small intestine tissues using QIAzol reagent (QIAGEN, Germany). cDNA was synthesized from total RNA (2 ug) using a High-Capacity cDNA Reverse Transcription Kit (4368814, Thermo Fisher Scientific, United States). Quantitative real-time PCR was performed using SYBR Green PCR Master Mix (Applied Biosystems, United States) and primers as described in **Table 2**. Gene expression data were analyzed using the IQ5 PCR Thermal Cycler (Bio-Rad, United States).

Stomach and Small Intestine Immunofluorescence Staining Analysis

Paraffin sections of stomach and small intestine tissues (4 μm) were dried at 60°C for 15 min. The sections were then subjected to

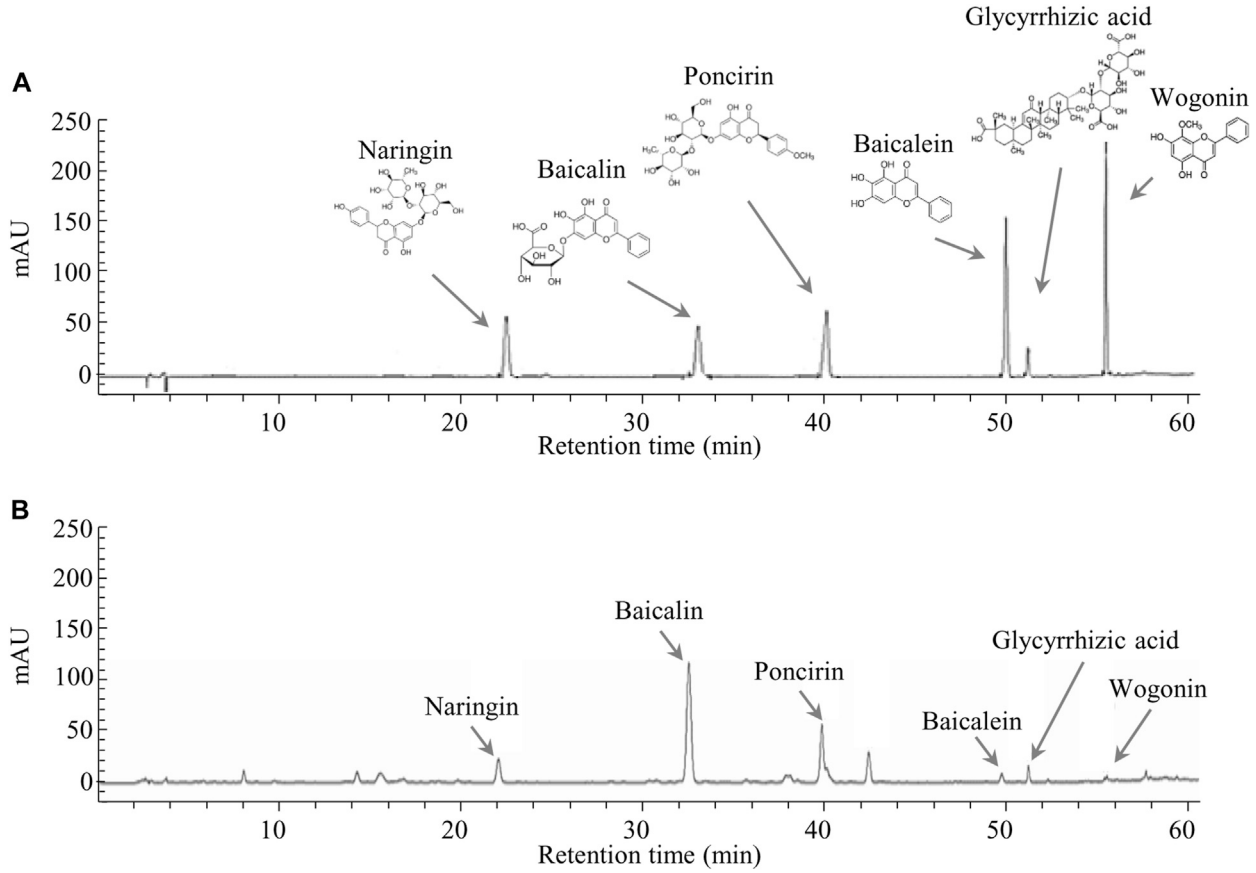

C

Compound	Retention time (min)	Molecular weight (g/mol)	Quantitative analysis of area (%)
Naringin	22.1	580.53	1.66
Baicalin	32.5	446.36	10.68
Poncirin	39.8	594.56	2.93
Baicalein	49.4	270.24	0.26
Glycyrrhizic acid	51.2	822.93	2.67
Wogonin	55.7	284.26	0.05

FIGURE 1 | Fingerprinting analysis of *Yeokwisan*. Chemical constitutions and quantitative analysis of *Yeokwisan* using high-performance liquid chromatography (HPLC). Six reference standards **(A)** and *Yeokwisan* **(B)** were subjected to UHPLC analysis. Quantitative analysis of *Yeokwisan* was conducted **(C)**.

deparaffinization with xylene and to rehydration with ethanol (with 100, 95, 85, 70, and 50% ethanol and tap water for 3 min each). Antigens were retrieved by incubating with 10 mM sodium citrate buffer for 10 min. After washing three times, nonspecific binding affinity was blocked for 1 h using normal goat serum, and then, the slides were incubated with the anti-c-kit antibody (1: 200) overnight at 4°C. After washing, the slides were incubated with a goat anti-rabbit Alexa Fluor-488 conjugated secondary antibody (1:200) for 1 h at RT. After washing three times for 10 min, the slides then were incubated with DAPI (1 μg/ml) for 2 min at RT in the dark. The c-kit signal was observed using an Axio-phot microscope (Carl Zeiss, Germany). The c-kit protein expression was semiquantified using ImageJ (NIH).

Statistical Analysis

The data are expressed as the mean ± standard deviation (SD) or fold changes in means. Statistical significance was determined by using one-way analysis of variance (ANOVA) followed by

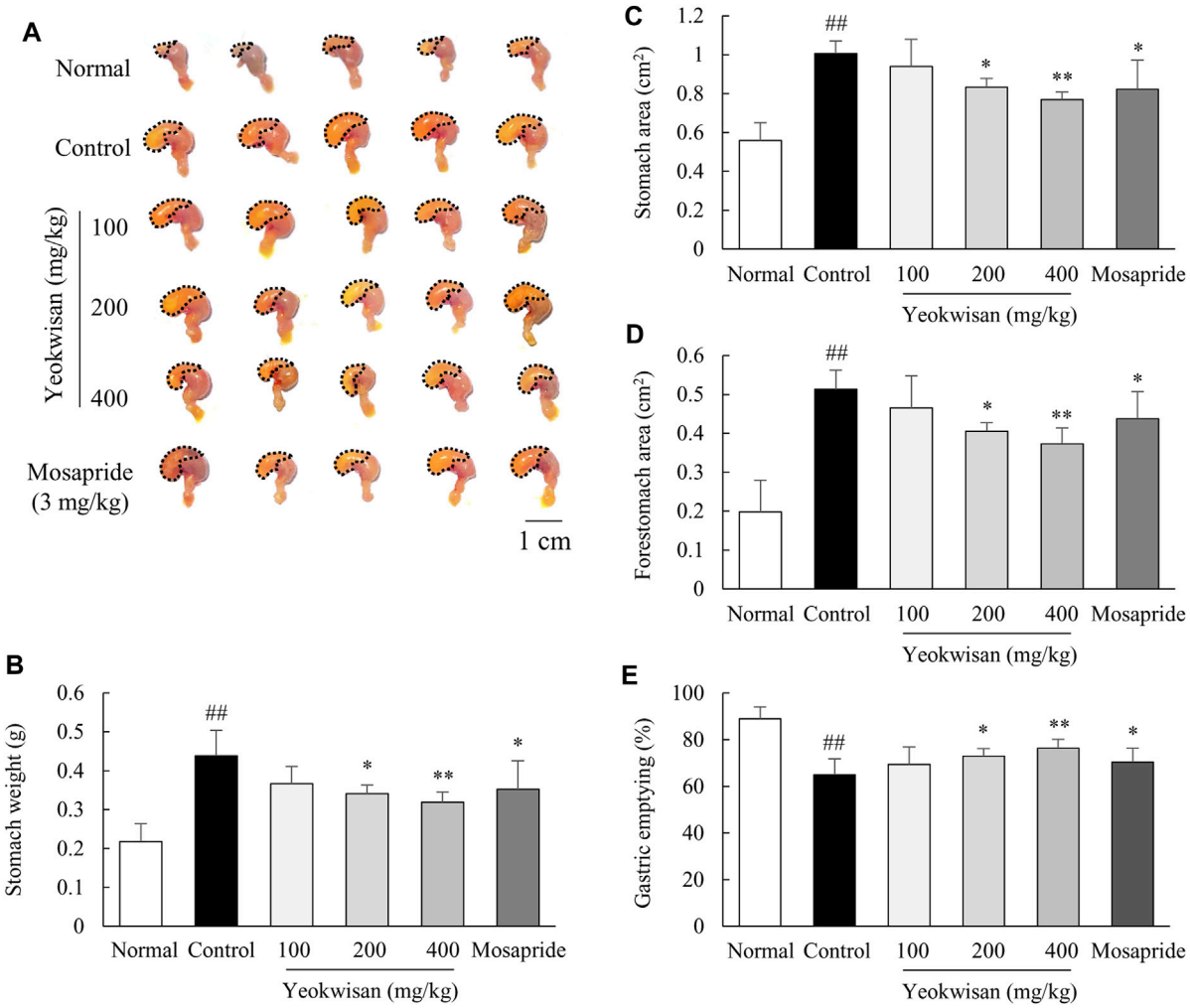

FIGURE 2 | Effects of *Yeokwisan* on gastric emptying. For 5 days, the mice (n = 6/group) were orally administered *Yeokwisan* (100, 200 and 400 mg/kg) or mosapride (3 mg/kg) and then intraperitoneally injected with loperamide (10 mg/kg). After the administration of phenol red, visual observation **(A)**, stomach weight **(B)**, stomach area **(C)**, forestomach area **(D)** and gastric emptying **(E)** were assessed. The data are presented as the mean ± SEM. ##$p < 0.01$ compared with the normal group; *$p < 0.05$, **$p < 0.01$ compared with the control group.

Dunnett's test. In all analyses, $p < 0.05$ was considered to indicate statistical significance.

RESULTS

Fingerprinting Analysis of *Yeokwisan*

The six compounds, namely naringin, baicalin, poncirin, baicalein, glycyrrhizic acid, and wogonin were detected at retention times of 22.1, 32.5, 39.8, 49.4, 51.2, and 55.7 min, respectively, in the tested samples. Semiquantitative analysis using the standard curves of the reference compounds showed *Yeokwisan* contained 1.66% naringin, 10.68% baicalin, 2.93% poncirin, 0.26% baicalein, 2.67% glycyrrhizic acid, and 0.05% wogonin (**Figure 1**).

Yeokwisan Reversed the Delayed Gastric Emptying Caused by Loperamide

As expected, loperamide injection inhibited the passage of phenol red, leading to fullness of the stomach, and this effect was significantly attenuated by pretreatment with *Yeokwisan* ($p < 0.05$ for 200 mg/kg and $p < 0.01$ for 400 mg/kg), as observed by the naked eye (**Figure 2A**), measurement of stomach weight (**Figure 2B**), calculation of whole and forestomach area (**Figures 2C,D**), and quantification of the amount of phenol red retained in the stomach (**Figure 2E**). The effect of mosapride was comparable to that of 200 mg/kg *Yeokwisan*.

Yeokwisan did Not Affect Intestinal Transit

Loperamide treatment also notably decreased intestinal transit, and mosapride significantly attenuated this effect. Unexpectedly,

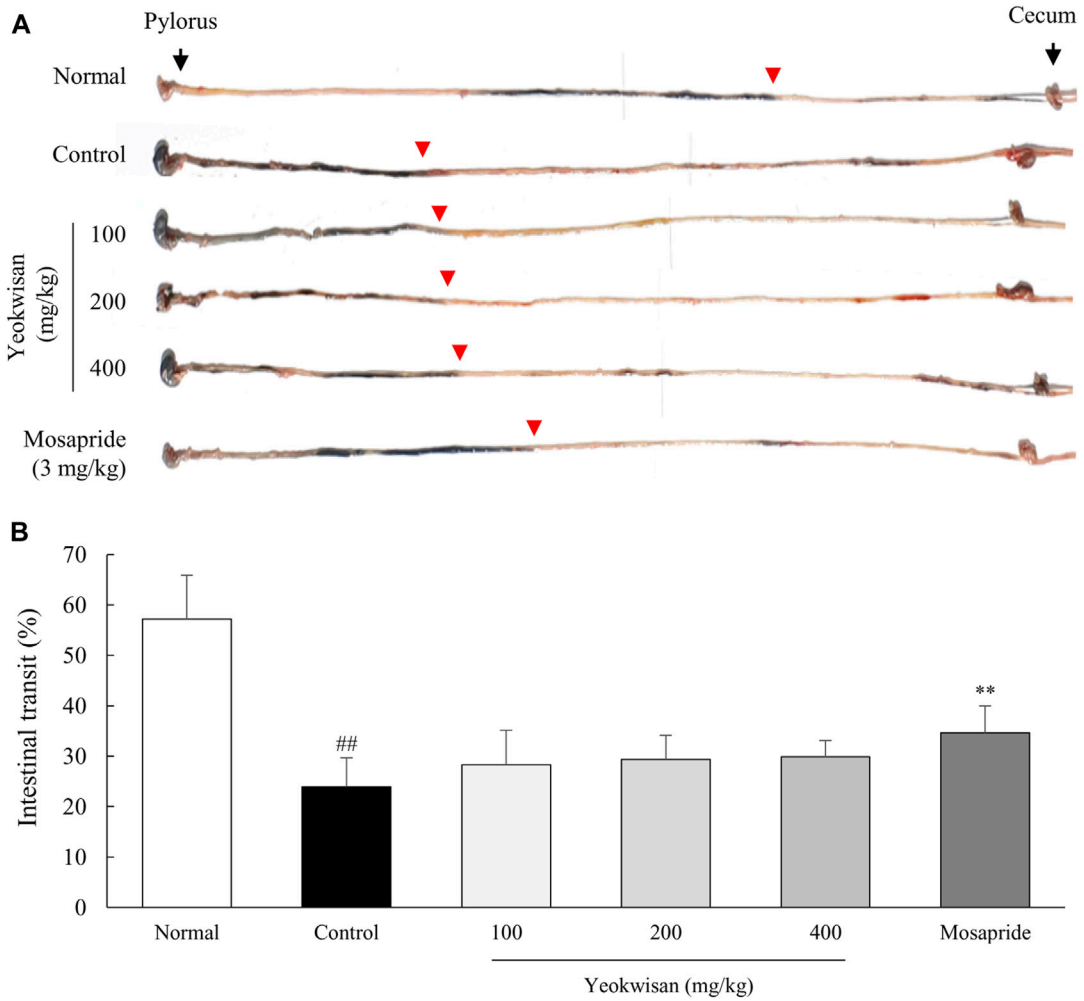

FIGURE 3 | Effects of *Yeokwisan* on small intestinal transit. For 5 days, the mice (n = 6/group) were orally administered *Yeokwisan* (100, 200 and 400 mg/kg) or mosapride (3 mg/kg) and then intraperitoneally injected with loperamide (10 mg/kg). Thirty minutes after the administration of charcoal diets, the transit distance of the diet was measured **(A)** and quantified **(B)**. Red arrowheads indicate how much charcoal diet moved into the cecum. The data are presented as the mean ± SEM. ##$p <$ 0.01 compared with the normal group; **$p <$ 0.01 compared with the control group.

Yeokwisan did not achieve a significant improvement of intestinal transit ($p > 0.05$ for all doses), even though it slightly accelerated the passage of the charcoal diet (**Figures 3A,B**).

Yeokwisan Upregulated the Expression of C-Kit in the Stomach

Loperamide radically suppressed C-kit expression in the stomach and small intestine, while *Yeokwisan* pretreatment significantly attenuated these alterations in the stomach tissue, as evidenced by immunohistochemistry ($p < 0.01$, **Figures 4A,B**) and protein assays ($p < 0.01$, **Figures 4C,D**). Interestingly, these effects of *Yeokwisan* were not observed in small intestinal tissues. Mosapride, however, showed positive effects both the stomach and small intestine ($p < 0.01$, **Figures 4E–H**).

Yeokwisan Upregulated the Expression of Proteins and Genes Associated With GI Motility

In the protein assay, *Yeokwisan* pretreatment significantly attenuated the notable loperamide-induced suppression of nNOS expression in the stomach ($p < 0.01$, **Figures 5A,B**), but not in the small intestine (**Figures 5D,E**). In addition, loperamide notably lowered the expression of smooth muscle contraction-related genes, such as 5-HT_4R, ANO1, RYR3, and smMLCK, in the stomach and small intestine. These alterations were significantly attenuated by *Yeokwisan* in the stomach ($p < 0.01$, **Figure 5C**) but not in the small intestine (**Figure 5F**). Mosapride treatment upregulated the expression of these protein and genes in both the stomach and small intestine ($p < 0.01$).

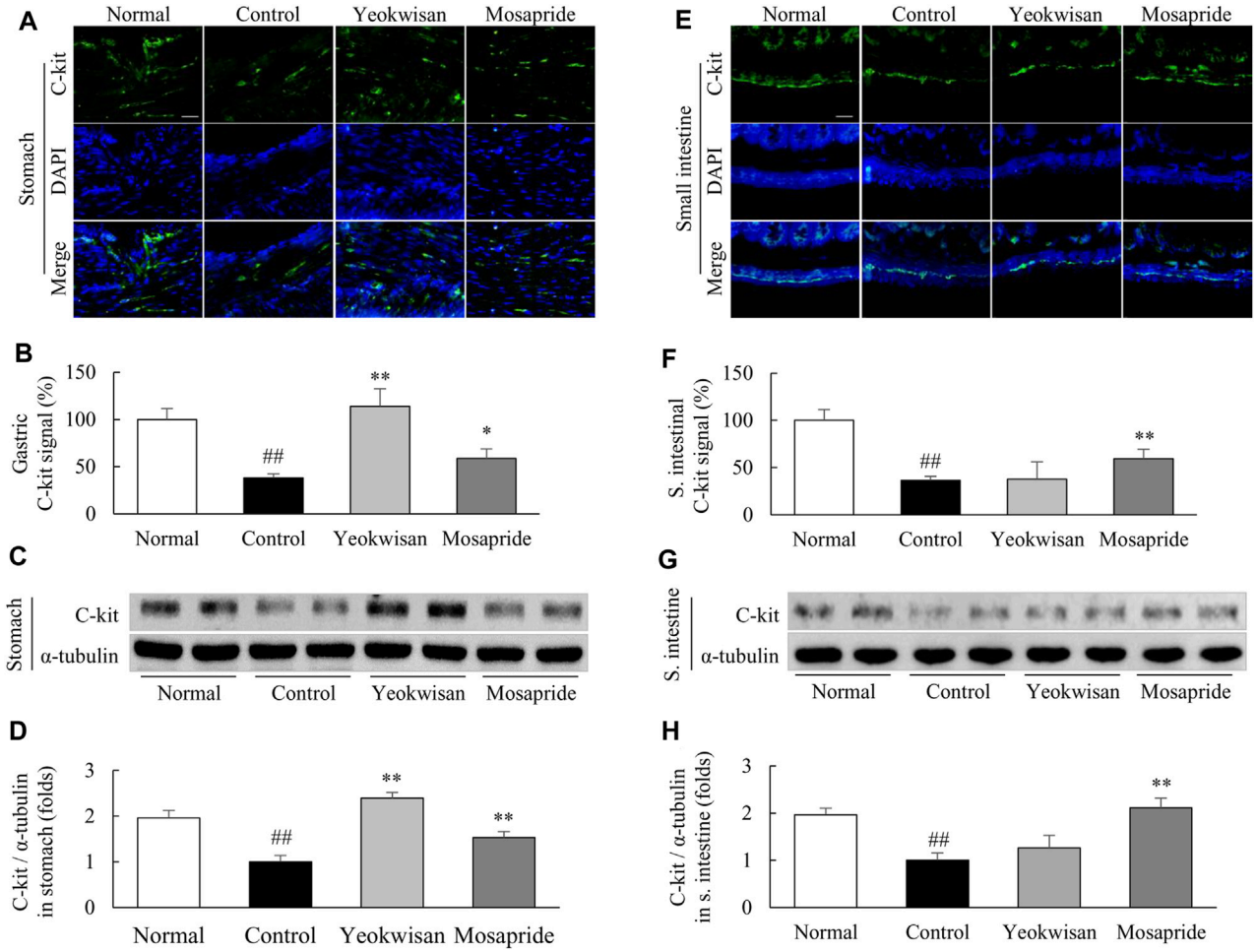

FIGURE 4 | Effects of *Yeokwisan* on C-kit protein expression in the stomach and small intestine tissues. C-kit protein expression was semiquantitatively measured using immunofluorescence in the stomach **(A,B)** and small intestine **(E,F)** and semiquantitatively measured using western blotting in the stomach **(C,D)** and small intestine **(G,H)**. Immunofluorescence was observed under an optical microscope (200× magnification), and the scale bar indicates 50 μm. The *Yeokwisan* group was treated with a dose of 400 mg/kg in these results. The data are presented as the mean ± SEM. ##$p < 0.01$ compared with the normal group; *$p < 0.05$, **$p < 0.01$ compared with the control group.

Yeokwisan Increased the Plasma Ghrelin Concentration and Affected Ghrelin-Related Gene Expression

Loperamide treatment dramatically lowered the concentration of acylated ghrelin in plasma, whereas *Yeokwisan* (especially 400 mg/kg *Yeokwisan*) significantly ameliorated this change in concentration ($p < 0.05$, **Figure 6A**). This effect was supported by the gene expression of ghrelin in the stomach tissue ($p < 0.01$, **Figure 6B**). Loperamide also downregulated the gene expression of GHSR, GOAT and ADRB1 but upregulated the expression of SSTR in the stomach, while these alterations were significantly attenuated by *Yeokwisan* pretreatment ($p < 0.05$ or $p < 0.01$, **Figure 6C**). As expected, the expression of these genes (GHSR and GOAT) in the small intestine tissue was not altered by loperamide or *Yeokwisan* (**Figure 6D**). Mosapride showed similar effects to *Yeokwisan* for almost all parameters, except for GHSR, ADRB1, and SSTR gene expression in stomach tissue.

DISCUSSION

To investigate the pharmaceutical potential of *Yeokwisan* in the treatment of FD and its underlying mechanisms, we herein used a loperamide-induced FD mouse model. Loperamide, a μ2-opioid receptor agonist, suppresses the activity of the GI myenteric plexus, which decreases the tone of the circular and longitudinal smooth muscles of the GI tract (Katzung et al., 2004; Chen et al., 2012). Clinically, loperamide is used to treat diarrhea, and its adverse effects include abdominal pain, nausea, dyspepsia, and constipation (Hanauer, 2008). Thus, high doses of loperamide have been used to establish animal models of FD and constipation in preclinical studies (Jeon et al., 2019; Li et al., 2021).

As expected, our study showed that a single dose of loperamide injection (10 mg/kg, peritoneally) notably delayed both gastric emptying and intestinal transit (**Figures 2**, **3**). Moreover, the administration of *Yeokwisan* (especially 200 and 400 mg/kg

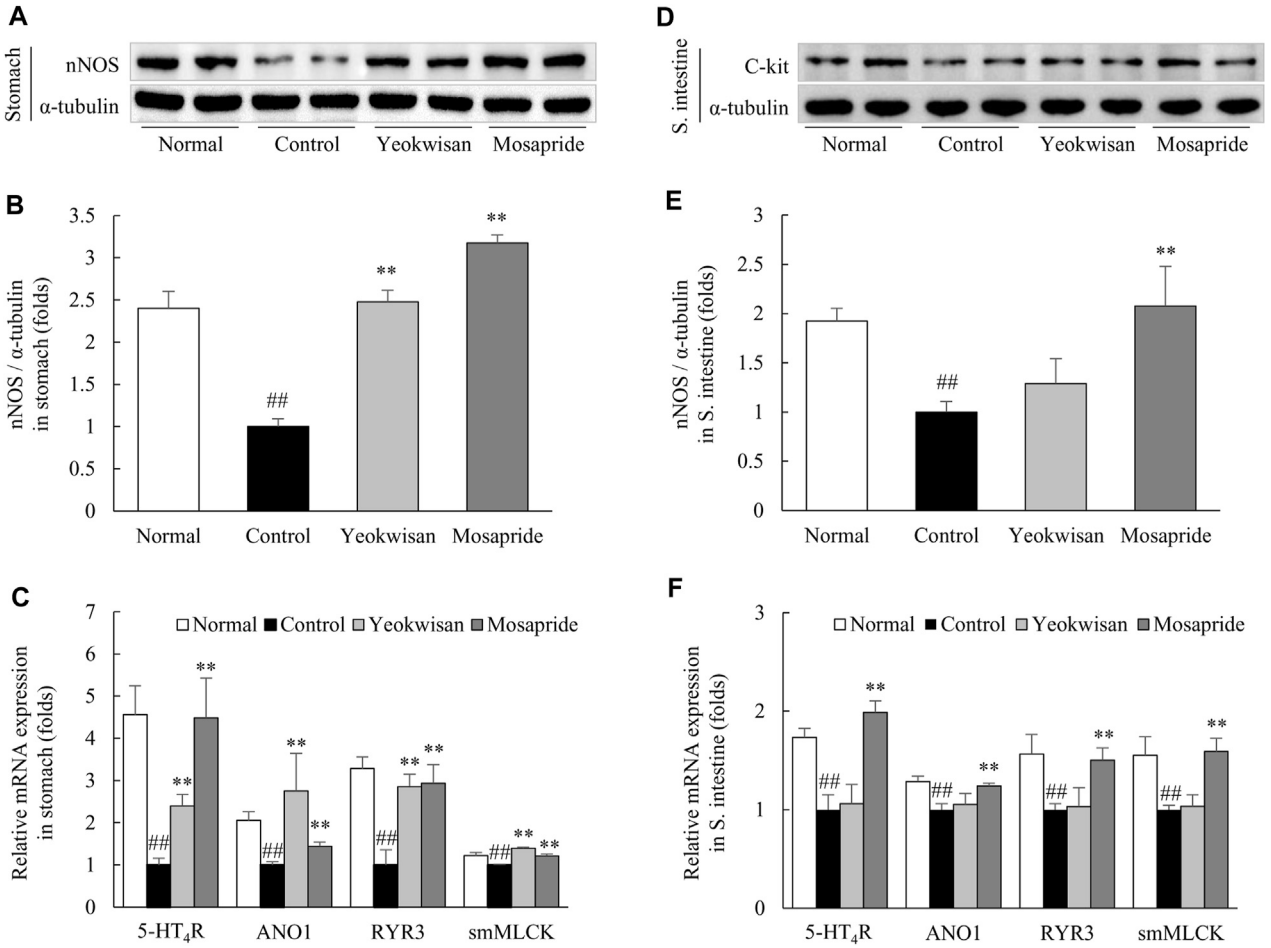

FIGURE 5 | Effects of *Yeokwisan* on the expression of the nNOS protein and contraction-related genes in stomach and small intestine tissues. Western blotting analysis of nNOS and semiquantification of the data were performed in stomach **(A,B)** and small intestine **(D,E)** tissues. mRNA expression analyses for four GI motility-associated genes were conducted on stomach **(C)** and small intestine **(F)** tissues. The *Yeokwisan* group was treated with a dose of 400 mg/kg in these results. The data are presented as the mean ± SEM. ##$p < 0.01$ compared with the normal group; **$p < 0.01$ compared with the control group. nNOS, neuronal nitric oxide synthase; 5-HT_4R, 5-HT_4 receptor; ANO1, anoctamin-1; RYR3, ryanodine receptor 3; smMLCK, smooth muscle myosin light chain kinase.

Yeokwisan) significantly attenuated this delayed gastric emptying, as evidenced by stomach weight, extended stomach volume and quantification of the amount of phenol red retained in the stomach (**Figures 2A–E**). These effects were very similar to those of mosapride, a positive control agent in the present study. 5-HT and its receptors are involved in the regulation of smooth muscle contraction, and 5-HT_4R agonists such as mosapride are the main options for the treatment of functional disorders with impaired GI motility (Yang et al., 2017). In our results, both *Yeokwisan* and mosapride significantly restored the loperamide-induced downregulation of 5-HT_4R gene expression in stomach tissue (**Figure 5C**). Abnormally suppressed gastric motility is one of the main causes of FD, and it has a negative impact, particularly on the PDS type of FD compared to the EPS type (Tack et al., 1998; Tack et al., 2002). Approximately 30% of all FD patients and 66% of all PDS patients showed delayed gastric emptying that was related to symptoms of postprandial fullness and early satiety and sometimes to gastroparesis-like symptoms, including vomiting and nausea (Talley et al., 2001; Sarnelli et al., 2003).

On the other hand, ghrelin, called a "hunger hormone", has attracted attention as a key player in GI motility and as a therapeutic target for FD treatment (Yagi et al., 2013). Several studies found that ghrelin levels were significantly lower in patients with FD than in healthy volunteers (Takamori et al., 2007; Lee et al., 2009b). Both clinical studies (Murray et al., 2005; Binn et al., 2006) and animal studies (Trudel et al., 2002; Qiu et al., 2008) have shown that ghrelin binds to its receptor, GHSR, which consequently leads to the promotion of gastric peristalsis and passage of a meal. Ghrelin cells (G cells) of the stomach produce ghrelin in the form of des-acyl ghrelin, which is then converted into the active form (acyl-ghrelin) by ghrelin O-acyltransferase (GOAT) before being released into the blood (Yagi et al., 2013). As expected, loperamide injection drastically lowered the plasma level of acyl-ghrelin, while the reduction of acyl-ghrelin was significantly normalized by *Yeokwisan*

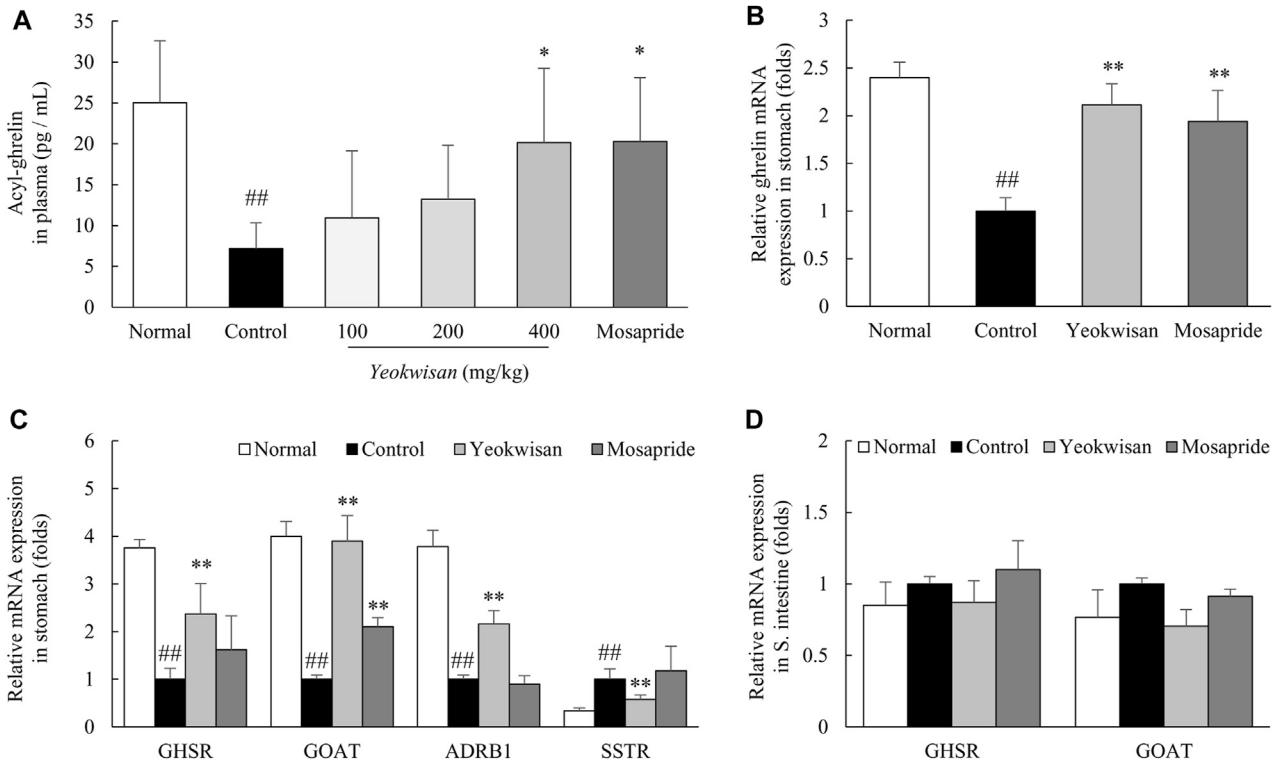

FIGURE 6 | Effects of *Yeokwisan* on the level of ghrelin in plasma, and ghrelin-related genes in stomach and small intestine tissues. The level of acyl-ghrelin in plasma was determined using ELISA **(A)**. mRNA expression analyses of ghrelin in stomach tissue **(B)** and ghrelin-associated genes in the stomach **(C)** and small intestine **(D)** were performed. The *Yeokwisan* group was treated with a dose of 400 mg/kg in **(B–F)**. The data are presented as the mean ± SEM. ##$p < 0.01$ compared with the normal group; *$p < 0.05$, **$p < 0.01$ compared with the control group. GHSR, growth hormone secretagogue receptor; GOAT, ghrelin-O-acyltransferase; ADRB1, adrenergic receptor β1; SSTR, somatostatin receptor.

(especially 400 mg/kg) (**Figure 6A**). This effect was also supported by the expression levels of genes related to the production of ghrelin (**Figure 6B**) and its acylation enzyme (GOAT) in stomach tissue (**Figure 6C**). The production and secretion of ghrelin is stimulated by various hormones, such adrenaline and somatostatin, which bind to receptors of the G cell membrane (Engelstoft et al., 2013). We confirmed that *Yeokwisan* activated a representative excitatory receptor (ADRB1) but suppressed an inhibitory receptor (SSTR) related to ghrelin production (**Figure 6C**).

It is well-known that GI motility is a continuous and repetitive process of segmental and peristaltic contractions and relaxations, in which interstitial cells of Cajal (ICCs) play a central role as pacemakers that generate electrical slow waves then transfer the these slow wave to the smooth muscle cells (Sanders et al., 2014). Some clinical studies have suggested that dysfunction or loss of ICCs causes abnormal GI motility-related diseases, including FD (Forster et al., 2005; Farrugia, 2008). To explore the involvement of ICCs in the gastric emptying effect of *Yeokwisan,* we evaluated the protein expression level of C-kit, a representative parameter of ICCs, in stomach tissue. As expected, administration of *Yeokwisan* significantly normalized the loperamide-induced loss of C-kit signal as shown by immunohistological findings and protein assays (**Figures 4A–D**). In fact, ghrelin binds to its receptor (GHSR) on ICCs and sequentially activates ICCs-derived electrical slow waves, as evidenced by *in vivo* and *in vitro* experiments (Yang et al., 2014; Kim and Kim, 2019). We also found that *Yeokwisan* upregulated the gene expression of GHSR in stomach tissue (**Figure 6C**). Slow wave generation and delivery by activated ICCs are regulated by several key molecules; ANO1 and RYR3 increase Ca^{2+} concentrations inside ICCs and generate intracellular Ca^{2+} waves, respectively (Sanders et al., 2006; Sanders et al., 2012). Then, the generated Ca^{2+} waves deliver electric signals to neighboring smooth muscle cells via gap junctions, which causes the contraction of smooth muscle by active smMLCK (Garcia et al., 1997). *Yeokwisan* administration attenuated the loperamide-induced changes in the expression of above-mentioned genes in stomach tissue (**Figure 5C**). In addition, regarding the relaxation process of smooth muscle in the GI tract, the nNOS-mediated production of nitric oxide (NO) is vitally important, as NO is retrograde neurotransmitter in synapses of vagus nerves (Terauchi et al., 2005). In clinical and animal studies, the administration of the NOS inhibitor, N^G-nitro-L-arginine methyl ester, delayed gastric emptying, and $nNOS^{-/-}$ mice also exhibited delayed gastric emptying (Plourde et al., 1994; Tack et al., 2002; Micci et al., 2005). In our study, *Yeokwisan* treatment significantly restored the loperamide-induced downregulation of nNOS protein

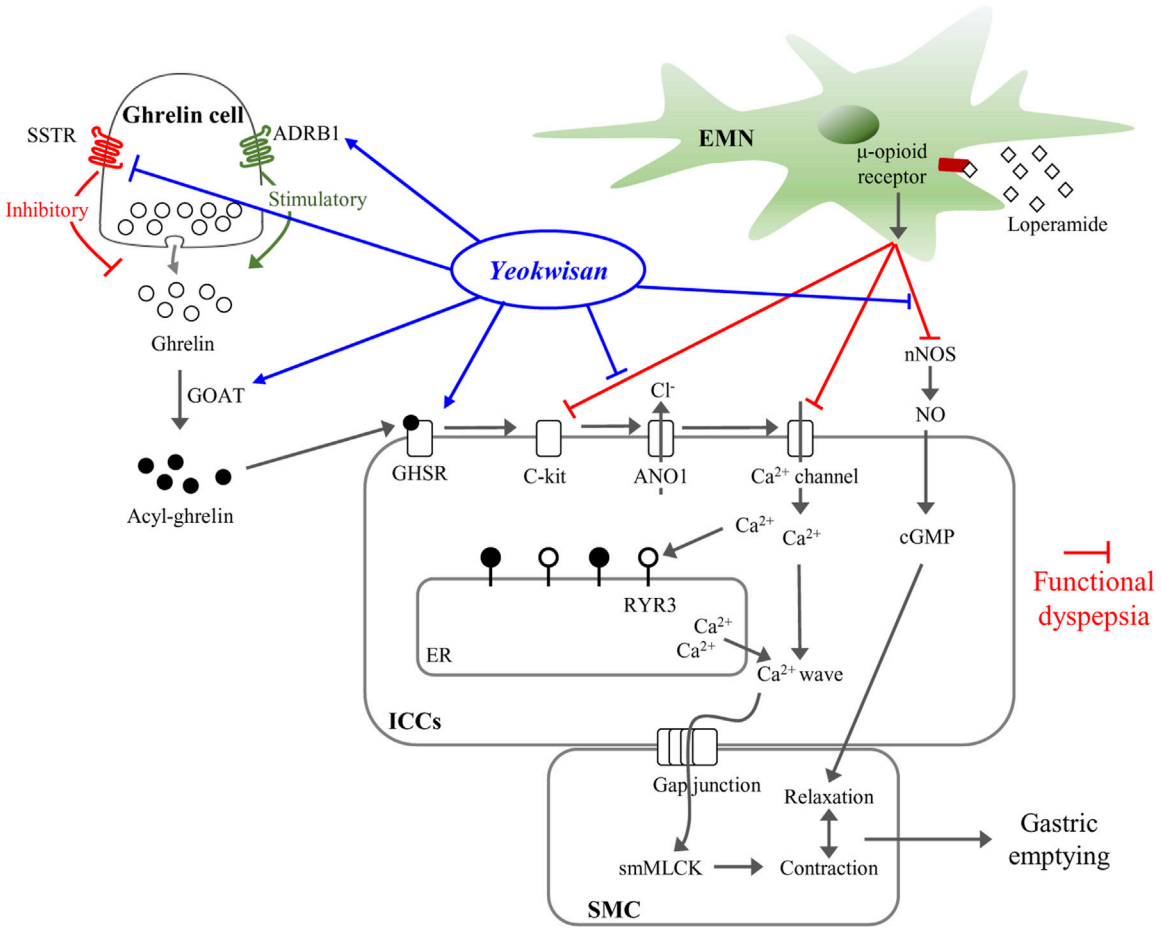

FIGURE 7 | Summary for mechanism of *Yeokwisan* on stomach tissue in loperamide-induced functional dyspepsia model. ADRB1, adrenergic receptor β1; ANO1, anoctamin-1; cGMP, cyclic guanosine monophosphate; EMN, enteric motor neuron; ER, endoplasmic reticulum; GHSR, growth hormone secretagogue receptor; GOAT, ghrelin-O-acyltransferase; ICCs, interstitial cells of Cajal; nNOS, neuronal nitric oxide synthase; NO, nitric oxide; RYR3, ryanodine receptor 3; SSTR, somatostatin receptor; smMLCK, smooth muscle myosin light chain kinase; SMC, smooth muscle cell.

expression in stomach tissue (**Figures 5A,B**). These results suggest that the pharmacological function of *Yeokwisan* is mainly associated with the modulation of ghrelin and ICCs activity in stomach tissue.

On the other hand, *Yeokwisan* did not improve intestinal transit as different from stomach (**Figures 3A,B**). These effects of *Yeokwisan* was very intriguing because prokinetics, such as mosapride, cisapride and acotiamide, generally work on the whole GI tract, both stomach and intestine (Tack et al., 2019). These results might indicate the not involvement of μ2-opioid receptor as the main mechanisms of *Yeokwisan,* because loperamide is an agonist of μ2-opioid receptor, suppressing the motility both in intestine and stomach (Chen et al., 2012). In the present study, we found *Yeokwisan* only promotes gastric motility via ghrelin-related pathway, but not intestinal transit (**Figures 2**, **3**, **6**). So, we propose the μ2-opioid receptor might not be markedly changed by *Yeokwisan*. In our study, mosapride accelerated the transit in the stomach (**Figure 2**) and small intestine (**Figure 3**). In our previous study, an herbal formula, *Banha-sasim-tang*, also promoted motility in both the stomach and small intestine (Jeon et al., 2019). Nevertheless, *Yeokwisan* changed potential GI motility-related proteins and genes as a different pattern between stomach and intestine. Briefly, *Yeokwisan* did not recover the GI motility-related proteins (C-kit and nNOS, **Figures 4E–H**, **5D,E**) and genes (5-HT_4R, ANO1, RYR3, and smMLCK, **Figure 5F**) expression, ghrelin-related genes (GHSR and GOAT, **Figure 6D**) expression in intestine, rather than stomach. As we known, G cells dominantly exist in stomach (Sakata and Sakai, 2010). Our data also showed that *Yeokwisan* significantly elevated ghrelin gene expression in stomach as compared to loperamide-treated group (**Figure 6B**). Therefore, it was proposed that ghrelin might be a key modulator on prokinetic effects in stomach by *Yeokwisan*. From the perspective of diarrhea-inducing adverse effects or clinical limitations of prokinetics (Quigley, 2015; Tack et al., 2019), these pharmacological characteristics of *Yeokwisan* may indicate the proper applicable spectrum of FD patients. Both FD and irritable bowel syndrome (IBS) are functional GI disorders (FGIDs) that are frequently comorbid. According to one study, 32% of patients with FD had overlapping IBS, and 37%

of patients with IBS had FD symptoms (Suzuki and Hibi, 2011). IBS includes two major subtypes, the constipation-dominant or diarrhea-dominant type, and 16.6% of patients with diarrhea-dominant type (but 11% of patients with the constipation type) also had FD (Choi et al., 2017). In present study, Yeokwisan promote the gastric motility via modulation of GI-motility-related molecules (**Figures 2**, **4A–D**, **5A–C**), not in the small intestine (**Figures 3**, **4E–H**, **5D–F**). Because of these gastric-specific properties of *Yeokwisan,* it may be further beneficial for FD patients with overlapping diarrhea-type IBS.

Due to the clinical limitations of currently available drugs for FD including the relatively high recurrence rate after cessation of 51% (Shinozaki et al., 2020), herbal resources have received attention in drug development (Tan et al., 2020). We herein proved the anti-FD activity of *Yeokwisan,* a standardized formula consisting of a six-herbal mixture including *P. trifoliata*, *S. baicalensis, G. uralensis,* Massa medicata fermentata, *P. bambusoides, O. gigas* (**Table 1**). Previous animal studies reported beneficial effects of two composing herbs, *P. trifoliata,* and *S. baicalensis,* on dysfunction of GI motility in atropine-induced (Lee et al., 2005), and ritonavir-induced (Mehendale et al., 2007) conditions, respectively. In particular, *G. uralensis* significantly improved the symptoms of patients with FD in a clinical study (Raveendra et al., 2012). According to the Korean herbal pharmacopoeia (Food and Adiministration, 2012), *Yeokwisan* has been standardized using six compounds: baicalein and baicalin from *S. baicalensis*, naringin and poncirin from *P. trifoliata*, and glycyrrhizic acid and wogonin from *G. uralensis* (**Figures 1A–C**). Among these compounds, baicalin and baicalein showed antidepressive effects in stress-induced depression rodent models (Lee et al., 2013; Liu et al., 2019). The depressive mood or dysregulation of 5-HT is well-known to inhibit peristatic movement in the GI tract (Kheder et al., 2018), while patients with FD complain of high comorbidity of depression (Esterita et al., 2021). Gastroprotective effects of naringin, wogonin and poncirin were also reported in gastric ulcer, mucosal damage, and gastritis rat models (Park et al., 2004; Lee JH. et al., 2009; Emin and Volkan, 2019). In particular, naringin improved delayed GI transit by activating ghrelin receptor in a laparotomy-induced rat model (Jang et al., 2013). These previous data support our beneficial effects of *Yeokwisan*.

Accordingly, we expected the synergistic effects of *Yeokwisan*, a mixture of six herbs on gastric emptying, may supporting the clinical relevance of this drug for treatment of patients with dyspepsia and GERD (**Figure 7**). Although we cannot explain the underlying mechanisms, we propose that the stomach-specific effect on peristaltic movement resulted from the mixture of multiple herbs or compounds, which modulate the expression of ghrelin-related genes (Ghrelin, GHSR, GOAT, ADRB1, and SSTR) only in the stomach (**Figures 6B,C**) but not in the small intestine (**Figure 6D**). The lack of identification of active compounds is a limitation of the present study. Further research is needed to address these issues. In addition, we have to further investigate the ideal formulation of these multi-herbal combinations to maximize stomach-specific activity and its underlying mechanisms.

Taken together, our present data showed the clinical effect of *Yeokwisan* on FD in a loperamide-induced functional dyspepsia mouse model. The main mechanisms corresponding to these effects may involve the modulation of the ghrelin pathway, including activation of ICCs in stomach tissue. In particular, we found that *Yeokwisan* improves gastric emptying via stomach-specific effects on GI motility.

DATA AVAILABILITY STATEMENT

The original contributions presented in the study are included in the article/**Supplementary Material**, further inquiries can be directed to the corresponding authors.

ETHICS STATEMENT

The animal study was reviewed and approved by The Institutional Animal Care and Use Committee of Daejeon University (Daejeon, Republic of Korea; Approval No. DJUARB 2021-013).

AUTHOR CONTRIBUTIONS

S-JH conducted experiments and wrote the manuscript. J-HW and J-SL supported the revision of manuscript and participated in the discussion. H-DL constructed the fingerprinting of Yeokwisan. T-JC discussed the manuscript. S-HC and C-GS supervised the whole process of this study and contributed to the initial design. All the authors read and approved the final manuscript.

FUNDING

This research was supported by the National Research Foundation of Korea (NRF) grant funded by the Ministry of Science, ICT and Future Planning (NRF-2018R1A6A1A03025221).

SUPPLEMENTARY MATERIAL

The Supplementary Material for this article can be found online at: https://www.frontiersin.org/articles/10.3389/fphar.2021.753153/full#supplementary-material

REFERENCES

Asano, T., Aida, S., Suemasu, S., and Mizushima, T. (2016). Anethole Restores Delayed Gastric Emptying and Impaired Gastric Accommodation in Rodents. *Biochem. Biophys. Res. Commun.* 472, 125–130. doi:10.1016/j.bbrc.2016.02.078

Binn, M., Albert, C., Gougeon, A., Maerki, H., Coulie, B., Lemoyne, M., et al. (2006). Ghrelin Gastrokinetic Action in Patients with Neurogenic Gastroparesis. *Peptides* 27, 1603–1606. doi:10.1016/j.peptides.2005.12.008

Chen, W., Chung, H. H., and Cheng, J. T. (2012). Opiate-induced Constipation Related to Activation of Small Intestine Opioid μ2-receptors. *World J. Gastroenterol.* 18, 1391–1396. doi:10.3748/wjg.v18.i12.1391

Choi, Y. J., Kim, N., Yoon, H., Shin, C. M., Park, Y. S., Kim, J. W., et al. (2017). Overlap between Irritable Bowel Syndrome and Functional Dyspepsia Including Subtype Analyses. *J. Gastroenterol. Hepatol.* 32, 1553–1561. doi:10.1111/jgh.13756

De Maeyer, J. H., Lefebvre, R. A., and Schuurkes, J. A. (2008). 5-HT4 Receptor Agonists: Similar but Not the Same. *Neurogastroenterol Motil.* 20, 99–112. doi:10.1111/j.1365-2982.2007.01059.x

Emin, S., and Volkan, G. (2019). Protective Effects of Naringin in Indomethacin-Induced Gastric Ulcer in Rats. *GSC Biol. Pharm. Sci.* 8.

Enck, P., Azpiroz, F., Boeckxstaens, G., Elsenbruch, S., Feinle-Bisset, C., Holtmann, G., et al. (2017). Functional Dyspepsia. *Nat. Rev. Dis. Primers* 3, 1–20. doi:10.1038/nrdp.2017.81

Engelstoft, M. S., Park, W. M., Sakata, I., Kristensen, L. V., Husted, A. S., Osborne-Lawrence, S., et al. (2013). Seven Transmembrane G Protein-Coupled Receptor Repertoire of Gastric Ghrelin Cells. *Mol. Metab.* 2, 376–392. doi:10.1016/j.molmet.2013.08.006

Esterita, T., Dewi, S., Suryatenggara, F. G., Glenardi, G., et al. (2021). Association of Functional Dyspepsia with Depression and Anxiety: A Systematic Review. *Journal of Gastrointestinal and Liver Diseases* 30.

Farrugia, G. (2008). Interstitial Cells of Cajal in Health and Disease. *Neurogastroenterology Motil.* 20, 54–63. doi:10.1111/j.1365-2982.2008.01109.x

Food, and Administration, D (2005).Guidance for Industry: Estimating the Maximum Safe Starting Dose in Initial Clinical Trials for Therapeutics in Adult Healthy Volunteers, *Cent. Drug Eval. Res. (Cder)* 7. .

Food, K., and Adiministration, D (2012).The Korean Herbal Pharmacopoeia. *The KFDA Notification*.

Ford, A. C., Marwaha, A., Sood, R., and Moayyedi, P. (2015). Global Prevalence of, and Risk Factors for, Uninvestigated Dyspepsia: a Meta-Analysis. *Gut* 64, 1049–1057. doi:10.1136/gutjnl-2014-307843

Ford, A. C., Mahadeva, S., Carbone, M. F., Lacy, B. E., and Talley, N. J. (2020). Functional Dyspepsia. *The Lancet*. doi:10.1016/s0140-6736(20)30469-4

Forster, J., Damjanov, I., Lin, Z., Sarosiek, I., Wetzel, P., and Mccallum, R. W. (2005). Absence of the Interstitial Cells of Cajal in Patients with Gastroparesis and Correlation with Clinical Findings. *J. Gastrointest. Surg.* 9, 102–108. doi:10.1016/j.gassur.2004.10.001

Garcia, J. G., Lazar, V., Gilbert-Mcclain, L. I., Gallagher, P. J., and Verin, A. D. (1997). Myosin Light Chain Kinase in Endothelium: Molecular Cloning and Regulation. *Am. J. Respir. Cel Mol Biol* 16, 489–494. doi:10.1165/ajrcmb.16.5.9160829

Haj Kheder, S., Heller, J., Bär, J. K., Wutzler, A., Menge, B. A., and Juckel, G. (2018). Autonomic Dysfunction of Gastric Motility in Major Depression. *J. Affect Disord.* 226, 196–202. doi:10.1016/j.jad.2017.09.049

Hanauer, S. B. (2008). The Role of Loperamide in Gastrointestinal Disorders. *Rev. Gastroenterol. Disord.* 8, 15–20.

Jang, Y., Kim, T. K., and Shim, W. S. (2013). Naringin Exhibits *In Vivo* Prokinetic Activity via Activation of Ghrelin Receptor in Gastrointestinal Motility Dysfunction Rats. *Pharmacology* 92, 191–197. doi:10.1159/000354579

Jeon, Y. J., Lee, J. S., Cho, Y. R., Lee, S. B., Kim, W. Y., Roh, S. S., et al. (2019). Banha-sasim-tang Improves Gastrointestinal Function in Loperamide-Induced Functional Dyspepsia Mouse Model. *J. Ethnopharmacol* 238, 111834. doi:10.1016/j.jep.2019.111834

Katzung, B. G., Masters, S. B., and Trevor, A. J. (2004). *Basic & Clinical Pharmacology*.

Kim, J. B., Shin, J. W., Kang, J. Y., Son, C. G., Kang, W., Lee, H. W., et al. (2014). A Traditional Herbal Formula, Hyangsa-Pyeongwi San (HPS), Improves Quality of Life (QoL) of the Patient with Functional Dyspepsia (FD): Randomized Double-Blinded Controlled Trial. *J. Ethnopharmacol* 151, 279–286. doi:10.1016/j.jep.2013.10.033

Kim, J. N., and Kim, B. J. (2019). The Mechanism of Action of Ghrelin and Motilin in the Pacemaker Potentials of Interstitial Cells of Cajal from the Murine Small Intestine. *Mol. Cell* 42, 470–479. doi:10.14348/molcells.2019.0028

Kim, S. K., Joung, J. Y., Ahn, Y. C., Jung, I. C., and Son, C. G. (2021). Beneficial Potential of Banha-Sasim-Tang for Stress-Sensitive Functional Dyspepsia via Modulation of Ghrelin: A Randomized Controlled Trial. *Front. Pharmacol.* 12, 636752. doi:10.3389/fphar.2021.636752

Lacy, B. E., Weiser, K. T., Kennedy, A. T., Crowell, M. D., and Talley, N. J. (2013). Functional Dyspepsia: the Economic Impact to Patients. *Aliment. Pharmacol. Ther.* 38, 170–177. doi:10.1111/apt.12355

Lahner, E., Bellentani, S., Bastiani, R. D., Tosetti, C., Cicala, M., Esposito, G., et al. (2013). A Survey of Pharmacological and Nonpharmacological Treatment of Functional Gastrointestinal Disorders. *United Eur. Gastroenterol J* 1, 385–393. doi:10.1177/2050640613499567

Lee, B., Sur, B., Park, J., Kim, S. H., Kwon, S., Yeom, M., et al. (2013). Chronic Administration of Baicalein Decreases Depression-like Behavior Induced by Repeated Restraint Stress in Rats. *Korean J. Physiol. Pharmacol.* 17, 393–403. doi:10.4196/kjpp.2013.17.5.393

Lee, H. T., Seo, E. K., Chung, S. J., and Shim, C. K. (2005). Effect of an Aqueous Extract of Dried Immature Fruit of Poncirus Trifoliata (L.) Raf. On Intestinal Transit in Rodents with Experimental Gastrointestinal Motility Dysfunctions. *J. Ethnopharmacol* 102, 302–306. doi:10.1016/j.jep.2005.08.015

Lee, J. H., Lee, S. H., Kim, Y. S., and Jeong, C. S. (2009a). Protective Effects of Neohesperidin and Poncirin Isolated from the Fruits of Poncirus Trifoliata on Potential Gastric Disease. *Phytother Res.* 23, 1748–1753. doi:10.1002/ptr.2840

Lee, K. J., Cha, D. Y., Cheon, S. J., Yeo, M., and Cho, S. W. (2009b). Plasma Ghrelin Levels and Their Relationship with Gastric Emptying in Patients with Dysmotility-like Functional Dyspepsia. *Digestion* 80, 58–63. doi:10.1159/000215389

Lee, M. C., Ha, W., Park, J., Kim, J., Jung, Y., and Kim, B. J. (2016). Effects of Lizhong Tang on Gastrointestinal Motility in Mice. *World J. Gastroenterol.* 22, 7778–7786. doi:10.3748/wjg.v22.i34.7778

Lee, Y. Y., and Chua, A. S. (2012). Investigating Functional Dyspepsia in Asia. *J. Neurogastroenterol Motil.* 18, 239–245. doi:10.5056/jnm.2012.18.3.239

Li, T., Hu, M., Jiang, C., Zhang, D., Gao, M., Xia, J., et al. (2021). Laxative Effect and Mechanism of Tiantian Capsule on Loperamide-Induced Constipation in Rats. *J. Ethnopharmacol* 266, 113411. doi:10.1016/j.jep.2020.113411

Liu, B., Piao, X., and Guo, L. (2013). Effect of Herbal Formula Xiao Pi-II on Functional Dyspepsia. *J. Tradit Chin. Med.* 33, 298–302. doi:10.1016/s0254-6272(13)60168-5

Liu, L., Dong, Y., Shan, X., Li, L., Xia, B., and Wang, H. (2019). Anti-depressive Effectiveness of Baicalin *In Vitro* and *In Vivo*. *Molecules* 24, 326. doi:10.3390/molecules24020326

Mahadeva, S., and Goh, K. L. (2006). Epidemiology of Functional Dyspepsia: a Global Perspective. *World J. Gastroenterol.* 12, 2661–2666. doi:10.3748/wjg.v12.i17.2661

Marona, H. R., and Lucchesi, M. B. (2004). Protocol to Refine Intestinal Motility Test in Mice. *Lab. Anim.* 38, 257–260. doi:10.1258/002367704323133637

Mehendale, S., Aung, H., Wang, C. Z., Tong, R., Foo, A., Xie, J. T., et al. (2007). Scutellaria Baicalensis and a Constituent Flavonoid, Baicalein, Attenuate Ritonavir-Induced Gastrointestinal Side-Effects. *J. Pharm. Pharmacol.* 59, 1567–1572. doi:10.1211/jpp.59.11.0015

Micci, M. A., Kahrig, K. M., Simmons, R. S., Sarna, S. K., Espejo-Navarro, M. R., and Pasricha, P. J. (2005). Neural Stem Cell Transplantation in the Stomach Rescues Gastric Function in Neuronal Nitric Oxide Synthase-Deficient Mice. *Gastroenterology* 129, 1817–1824. doi:10.1053/j.gastro.2005.08.055

Mittelstadt, S. W., Hemenway, C. L., and Spruell, R. D. (2005). Effects of Fasting on Evaluation of Gastrointestinal Transit with Charcoal Meal. *J. Pharmacol. Toxicol. Methods* 52, 154–158. doi:10.1016/j.vascn.2005.04.017

Murray, C. D., Martin, N. M., Patterson, M., Taylor, S. A., Ghatei, M. A., Kamm, M. A., et al. (2005). Ghrelin Enhances Gastric Emptying in Diabetic Gastroparesis: a Double Blind, Placebo Controlled, Crossover Study. *Gut* 54, 1693–1698. doi:10.1136/gut.2005.069088

Nair, A. B., and Jacob, S. (2016). A Simple Practice Guide for Dose Conversion between Animals and Human. *J. Basic Clin. Pharm.* 7, 27–31. doi:10.4103/0976-0105.177703

Park, S., Hahm, K. B., Oh, T. Y., Jin, J. H., and Choue, R. (2004). Preventive Effect of the Flavonoid, Wogonin, against Ethanol-Induced Gastric Mucosal Damage in Rats. *Dig. Dis. Sci.* 49, 384–394. doi:10.1023/b:ddas.0000020490.34220.6d

Plourde, V., Quintero, E., Suto, G., Coimbra, C., and Taché, Y. (1994). Delayed Gastric Emptying Induced by Inhibitors of Nitric Oxide Synthase in Rats. *Eur. J. Pharmacol.* 256, 125–129. doi:10.1016/0014-2999(94)90236-4

Qiu, W. C., Wang, Z. G., Wang, W. G., Yan, J., and Zheng, Q. (2008). Gastric Motor Effects of Ghrelin and Growth Hormone Releasing Peptide 6 in Diabetic Mice with Gastroparesis. *World J. Gastroenterol.* 14, 1419–1424. doi:10.3748/wjg.14.1419

Quigley, E. M. (2015). Prokinetics in the Management of Functional Gastrointestinal Disorders. *J. Neurogastroenterol Motil.* 21, 330–336. doi:10.5056/jnm15094

Raveendra, K. R., Srinivasa, V., Sushma, K. R., Allan, J. J., Goudar, K. S., Shivaprasad, H. N., et al. (2012). An Extract of Glycyrrhiza Glabra (GutGard) Alleviates Symptoms of Functional Dyspepsia: a Randomized, Double-Blind, Placebo-Controlled Study. *Evidence-Based Complement. Altern. Med.* 2012.

Sakata, I., and Sakai, T. (2010). Ghrelin Cells in the Gastrointestinal Tract. *Int. J. peptides* 2010. doi:10.1155/2010/945056

Sanders, K. M., Koh, S. D., and Ward, S. M. (2006). Interstitial Cells of Cajal as Pacemakers in the Gastrointestinal Tract. *Annu. Rev. Physiol.* 68, 307–343. doi:10.1146/annurev.physiol.68.040504.094718

Sanders, K. M., Zhu, M. H., Britton, F., Koh, S. D., and Ward, S. M. (2012). Anoctamins and Gastrointestinal Smooth Muscle Excitability. *Exp. Physiol.* 97, 200–206. doi:10.1113/expphysiol.2011.058248

Sanders, K. M., Ward, S. M., and Koh, S. D. (2014). Interstitial Cells: Regulators of Smooth Muscle Function. *Physiol. Rev.*. doi:10.1152/physrev.00037.2013

Sarnelli, G., Caenepeel, P., Geypens, B., Janssens, J., and Tack, J. (2003). Symptoms Associated with Impaired Gastric Emptying of Solids and Liquids in Functional Dyspepsia. *Am. J. Gastroenterol.* 98, 783–788. doi:10.1111/j.1572-0241.2003.07389.x

Shah, N. H., Lependu, P., Bauer-Mehren, A., Ghebremariam, Y. T., Iyer, S. V., Marcus, J., et al. (2015). Proton Pump Inhibitor Usage and the Risk of Myocardial Infarction in the General Population. *PloS one* 10, e0124653. doi:10.1371/journal.pone.0124653

Shinozaki, S., Osawa, H., Sakamoto, H., Hayashi, Y., Kobayashi, Y., Miura, Y., et al. (2020). Timing and Predictors of Recurrence of Dyspepsia Symptoms after Cessation of Acotiamide Therapy for Functional Dyspepsia: a Long-Term Observational Study. *Digestion* 101, 382–390. doi:10.1159/000500134

Stanghellini, V., Chan, F. K., Hasler, W. L., Malagelada, J. R., Suzuki, H., Tack, J., et al. (2016). Gastroduodenal Disorders. *Gastroenterology* 150, 1380–1392. doi:10.1053/j.gastro.2016.02.011

Suzuki, H., and Hibi, T. (2011). Overlap Syndrome of Functional Dyspepsia and Irritable Bowel Syndrome - Are Both Diseases Mutually Exclusive?. *J. Neurogastroenterol Motil.* 17, 360–365. doi:10.5056/jnm.2011.17.4.360

Tack, J., Demedts, I., Meulemans, A., Schuurkes, J., and Janssens, J. (2002). Role of Nitric Oxide in the Gastric Accommodation Reflex and in Meal Induced Satiety in Humans. *Gut* 51, 219–224. doi:10.1136/gut.51.2.219

Tack, J., Piessevaux, H., Coulie, B., Caenepeel, P., and Janssens, J. (1998). Role of Impaired Gastric Accommodation to a Meal in Functional Dyspepsia. *Gastroenterology* 115, 1346–1352. doi:10.1016/s0016-5085(98)70012-5

Tack, J., Van Den Houte, K., and Carbone, F. (2019). The Unfulfilled Promise of Prokinetics for Functional Dyspepsia/postprandial Distress Syndrome. *Am. J. Gastroenterol.* 114, 204–206. doi:10.14309/ajg.0000000000000072

Takamori, K., Mizuta, Y., Takeshima, F., Akazawa, Y., Isomoto, H., Ohnita, K., et al. (2007). Relation Among Plasma Ghrelin Level, Gastric Emptying, and Psychologic Condition in Patients with Functional Dyspepsia. *J. Clin. Gastroenterol.* 41, 477–483. doi:10.1097/01.mcg.0000225614.94470.47

Talley, N. J., Verlinden, M., and Jones, M. (2001). Can Symptoms Discriminate Among Those with Delayed or normal Gastric Emptying in Dysmotility-like Dyspepsia?. *Am. J. Gastroenterol.* 96, 1422–1428. doi:10.1111/j.1572-0241.2001.03683.x

Tan, N., Gwee, K. A., Tack, J., Zhang, M., Li, Y., Chen, M., et al. (2020). Herbal Medicine in the Treatment of Functional Gastrointestinal Disorders: A Systematic Review with Meta-Analysis. *J. Gastroenterol. Hepatol.* 35, 544–556. doi:10.1111/jgh.14905

Terauchi, A., Kobayashi, D., and Mashimo, H. (2005). Distinct Roles of Nitric Oxide Synthases and Interstitial Cells of Cajal in Rectoanal Relaxation. *Am. J. Physiol. Gastrointest. Liver Physiol.* 289, G291–G299. doi:10.1152/ajpgi.00005.2005

Trudel, L., Tomasetto, C., Rio, M. C., Bouin, M., Plourde, V., Eberling, P., et al. (2002). Ghrelin/motilin-related Peptide Is a Potent Prokinetic to Reverse Gastric Postoperative Ileus in Rat. *Am. J. Physiol. Gastrointest. Liver Physiol.* 282, G948–G952. doi:10.1152/ajpgi.00339.2001

Yagi, T., Asakawa, A., Ueda, H., Miyawaki, S., and Inui, A. (2013). The Role of Ghrelin in Patients with Functional Dyspepsia and its Potential Clinical Relevance (Review). *Int. J. Mol. Med.* 32, 523–531. doi:10.3892/ijmm.2013.1418

Yang, C. G., Liao, Z. F., Qiu, W. C., Yan, J., and Wang, Z. G. (2014). Function of Ghrelin and Ghrelin Receptors in the Network Regulation of Gastric Motility. *Mol. Med. Rep.* 10, 2453–2458. doi:10.3892/mmr.2014.2571

Yang, Y. J., Bang, C. S., Baik, G. H., Park, T. Y., Shin, S. P., Suk, K. T., et al. (2017). Prokinetics for the Treatment of Functional Dyspepsia: Bayesian Network Meta-Analysis. *BMC Gastroenterol.* 17, 83–11. doi:10.1186/s12876-017-0639-0

Conflict of Interest: T-JC is employed by Wooje IM Inc.

The remaining authors declare that the research was conducted in the absence of any commercial or financial relationships that could be construed as a potential conflict of interest.

Publisher's Note: All claims expressed in this article are solely those of the authors and do not necessarily represent those of their affiliated organizations, or those of the publisher, the editors and the reviewers. Any product that may be evaluated in this article, or claim that may be made by its manufacturer, is not guaranteed or endorsed by the publisher.

frontiers in Pharmacology

SYSTEMATIC REVIEW
published: 11 October 2021
doi: 10.3389/fphar.2021.742978

Efficacy and Safety of Tongxinluo Capsule as Adjunctive Treatment for Unstable Angina Pectoris: A Systematic Review and Meta-Analysis of Randomized Controlled Trials

Pengqi Li[1,2†], Qiqi Xin[1,2†], Jiaqi Hui[1,2], Rong Yuan[1,2], Ya Wang[1,2], Yu Miao[1,2], Simon Ming-Yuen Lee[3], Sean X. Leng[4], Weihong Cong[1,2*] and BPNMI Consortium*

[1]Laboratory of Cardiovascular Diseases, Xiyuan Hospital, China Academy of Chinese Medical Sciences, Beijing, China, [2]National Clinical Research Center for Chinese Medicine Cardiology, Xiyuan Hospital, Beijing, China, [3]State Key Laboratory of Quality Research in Chinese Medicine, Institute of Chinese Medical Sciences, University of Macau, Taipa, Macao, SAR China, [4]Division of Geriatric Medicine and Gerontology, Department of Medicine, Johns Hopkins University School of Medicine, Baltimore, MD, United States

OPEN ACCESS

Edited by:
X. Y. Zhang,
University of Minho, Portugal

Reviewed by:
Wei Mao,
Zhejiang Chinese Medical University, China
Lian-Sheng Wang,
Nanjing Medical University, China
Diraviyam Thirumalai,
SASTRA University, India

***Correspondence:**
Weihong Cong
congcao@188.com
Sean X. Leng
sleng1@jhmi.edu

[†]These authors have contributed equally to this work and share first authorship

Specialty section:
This article was submitted to Ethnopharmacology, a section of the journal Frontiers in Pharmacology

Received: 17 July 2021
Accepted: 20 September 2021
Published: 11 October 2021

Citation:
Li P, Xin Q, Hui J, Yuan R, Wang Y, Miao Y, Lee SM-Y, Leng SX, Cong W and BPNMI Consortium (2021) Efficacy and Safety of Tongxinluo Capsule as Adjunctive Treatment for Unstable Angina Pectoris: A Systematic Review and Meta-Analysis of Randomized Controlled Trials. Front. Pharmacol. 12:742978. doi: 10.3389/fphar.2021.742978

Tongxinluo capsule (TXLC) is a commonly used Chinese medicine for unstable angina pectoris (UA). This article aimed to clarify the safety and efficacy of TXLC as an adjunctive treatment for UA. Two reviewers searched 7 databases from inception to August 2021, and performed literature screening and information extraction independently. The meta-analysis was implemented after evaluating the methodological quality of each randomized controlled trial (RCT) by the Cochrane Risk of Bias tool. Sensitivity analyses were conducted for testing the stability of the results, and the Begg and Egger tests were performed for any potential publication bias. After eligibility assessment, 42 RCTs with a total of 5,421 participants were included. Evidence showed that TXLC reduced the rate of cardiovascular events [RR = 0.29, 95% CI (0.19, 0.45), $p < 0.00001$, $I^2 = 0\%$] {including cardiovascular mortality [RR = 0.16, 95% CI (0.03, 0.88), $p = 0.03$, $I^2 = 20\%$], the incidence of acute myocardial infarction [RR = 0.27, 95% CI (0.13, 0.57), $p = 0.0006$, $I^2 = 0\%$] and the occurrence of revascularization [RR = 0.28, 95% CI (0.15,0.54), $p = 0.0001$, $I^2 = 0\%$]}, all-cause mortality [RR = 0.25, 95% CI (0.06, 0.99), $p = 0.05$, $I^2 = 19\%$], recurrence of angina [RR = 0.25, 95% CI (0.11, 0.61), $p = 0.002$, $I^2 = 0\%$], the number of ST-segment depression [MD = −0.45, 95% CI (−0.69, −0.20), $p = 0.0005$, $I^2 = 0\%$], the summation of ST-segment depression [MD = −0.70, 95% CI (−1.08, −0.32), $p = 0.0003$, $I^2 = 70\%$] and the hypersensitive C-reactive protein level [MD = −2.86, 95% CI (−3.73, −1.99), $p < 0.00001$, $I^2 = 86\%$], increased the nitric oxide level [MD = 11.67, 95% CI (8.33, 15.02), $p < 0.00001$, $I^2 = 33\%$], improved the electrocardiogram change [RR = 1.23, 95% CI (1.16, 1.30), $p < 0.00001$, $I^2 = 0\%$] and the clinical efficacy in UA [RR = 1.26, 95% CI (1.21, 1.32), $p < 0.00001$, $I^2 = 24\%$], and relieved the symptoms of angina pectoris {including chest pain or tightness [RR = 1.13, 95% CI (0.97, 1.32), $p = 0.12$, $I^2 = 30\%$], palpitations [RR = 1.47, 95% CI (1.18, 1.84), $p = 0.0007$, $I^2 = 0\%$], shortness of breath [RR = 1.53, 95% CI (1.24, 1.88), $p < 0.0001$, $I^2 = 0\%$], and asthenia [RR = 1.69, 95% CI (0.83, 3.43), $p = 0.15$, $I^2 = 90\%$]}. The most common adverse effect was gastrointestinal symptoms

which could be relieved and eliminated through dose reduction, medication time adjustment and symptomatic remedy. Collectively, TXLC was effective and considerably safe for UA. However, due to the unavoidable risk of bias, these results must be interpreted with caution and further verified by large-scale and high-quality RCTs.

Systematic Review Registration: www.crd.york.ac.uk/PROSPERO/, identifier CRD42021232771.

Keywords: unstable angina pectoris, Tongxinluo capsule, Chinese medicine, efficacy, safety, systematic review, meta-analysis

INTRODUCTION

The World Health Organization (WHO) reported that the global number of individuals with cardiovascular diseases (CVDs) had doubled from 271 million in 1990 to 523 million in 2019. In China, the number of CVD patients reached approximately 330 million in 2019. Ischemic heart disease (IHD), the most common CVD, was currently the largest international cause of death, bringing heavy economic burdens and health threats to the world (Roth et al., 2020; The Writing Committee of the Report on Cardiovascular Health Diseases in China., 2020). As one of the most common and typical IHD, unstable angina pectoris (UA) was manifested as a significant exacerbation of angina symptoms (Cannon et al., 2001), and often progressed rapidly, even to acute myocardial infarction (AMI) or sudden death.

Local coronary artery lesions including unstable plaques, thrombosis, vasospasm, and intravascular inflammation are regarded as the pathological basis of UA, which cause vascular stenosis or blockage and lead to myocardial ischemia. Accordingly, the conventional treatments (CTs) for UA mainly include anti-platelet, anti-coagulation, blood lipids regulation, angina control, and anti-myocardial ischemia. However, the currently available treatment regimens for UA represent an unmet medical need, such as the clinical resistance to antiplatelet agents or lipid-lowing drugs (Helgeson et al., 1994; Chessman et al., 2004; Serebruany et al., 2005; Münzel et al., 2011) and the adverse effects during long-term medication. Given the great variability in individual efficacy and poor patient compliance of the currently available treatment regimens, it is difficult to obtain satisfactory therapeutic effects against UA. Therefore, finding potential approaches for alleviating limitations on CTs of UA is warranted. Tongxinluo capsule (TXLC), a Chinese medicinal product composed of *Panax ginseng* C.A.Mey. (Ren Shen), *Hirudo nipponica* Whitman (Shui Zhi), *Scolopendra subspinipes mutilans* L. Koch (Wu Gong), *Eupolyphaga sinensis* Walker (Tu Bie Chong), *Buthus martensii* Karsch (Quan Xie), *Cryptotympana pustulata* Fabricius (Chan Tui), *Paeonia lactiflora* Pall. (Chi Shao), *Dryobalanops aromatica* C.F.Gaertn. (Bing Pian), *Santalum album* L. (Tan Xiang), *Boswellia carterii* Birdw. (Ru Xiang), *Dalbergia odorifera* T.C.Chen (Jiang Xiang), *Ziziphus jujuba* Mill. (Suan Zao Ren), etc., is widely used in China and has been recommended by several guidelines and expert consensuses for the treatment of angina pectoris [e.g., the Guidelines for Rational Use of Drugs for Coronary Heart Disease (Second Edition): TXLC can reduce the adhesion of platelets to collagen fibers and significantly relieve clopidogrel resistance during DAPT treatment]. In high-performance liquid chromatography analysis, the similarity of the fingerprints of each batch of TXLC was above 95%, indicating that the product quality was stable and controllable (Meng et al., 2014; Li Q. et al., 2018). Clinical and laboratory researches have been conducted since 1995, indicating that TXLC plays a positive role in enhancing cardiac systolic function, protecting the vascular endothelium, delaying the progression of atherosclerosis, preventing coronary embolism after PCI in patients with AMI, reducing vascular endothelial damage, preventing heart failure caused by pressure overload and regulating cytokine levels with multiple targets (Ma et al., 2009; Chen et al., 2016; Wang et al., 2019; Zhang et al., 2019; Li et al., 2020). The previous meta-analyses showed that TXLC had a good secondary preventive effect against AMI, the addition of TXLC to conventional western medicine might prevent the recurrence of restenosis and cardiovascular events in patients with coronary heart disease after PCI. It also effectively reduced the symptoms of angina pectoris in Cardiac Syndrome X and seemed to be more effective than β-blockers in the treatment of angina pectoris (Jia and Leung., 2015; Mao et al., 2015; Li Q. et al., 2018; Mao et al., 2018). At present, TXLC is widely used for UA as an adjuvant treatment. Nevertheless, some adverse effects, such as digestive tract reactions, bleeding gums and blood biochemical changes, have been reported (Xu, 2013; Xu and Shao., 2020). Given that, the efficacy and safety of TXLC for UA need to be reassessed, for providing new inspiration for UA's current therapeutic regimen.

METHODS

Protocol and Registration

The systematic review protocol was registered in the International Prospective Register of Systematic Reviews (PROSPERO) (No. CRD42021232771). All projects, including the design, implementation, analysis, and report, were determined following the PRISMA guidelines (Page et al., 2021). See **Supplementary Material S1** for the PRISMA 2020 Checklist.

Search Strategies

Two reviewers (PL and JH) independently completed the literature search without restrictions on language, race or literature scope. The search aimed at all related studies published on Cochrane Central Register of Controlled Trials (CENTRAL), PubMed, EMBASE Database, China National

Knowledge Infrastructure (CNKI), Chinese Biomedical Literature Service System (SinoMed), Wanfang Database and Chinese Scientific Journal Database (VIP) as of August 31, 2021. "Angina, Unstable" was used as the Medical Subject Heading and matched with corresponding free words for enhancing accuracy, and various expressions of "tong xin luo" were connected with truncation characters for describing the intervention part. Given the discrepancy between databases, the keywords were adjusted flexibly for "randomized controlled trial, RCT or semi-randomized controlled trial". Finally, all retrieval expressions were formed by logically connecting AND or OR. For example, EMBASE Database was searched as ('tongxinluo capsule': ab, ti OR 'tong xin luo*': ab, ti OR 'tong-xin-luo*': ab, ti OR 'txl*': ab, ti OR 'tongxinluo*': ab, ti) AND ('random': ab, ti OR 'placebo': ab, ti OR 'double-blind': ab, ti). See **Supplementary Material S2** for the complete search strategies.

Study Selection Criteria

Study Design and Participants

All randomized controlled trials (RCTs) or semi-randomized controlled trials evaluating the efficacy or safety of TXLC for the treatment of UA were included regardless of blinding. The sample sizes of selected studies were all greater than 100. There were no restrictions on participants' gender, race, age, nationality, course, or severity of disease. Participants had to meet available diagnostic criteria such as the "2000 WHO diagnostic criteria for unstable angina pectoris", "2000 Chinese Medical Association recommendations for diagnosis and treatment of UA", "1979 WHO nomenclature and diagnostic criteria of IHD" and other standards or consensuses, and accompanied by recent angina pectoris attacks and electrocardiogram (ECG) ischemic ST-T changes. Patients in any of the following conditions were excluded: severe disease of the brain, lung, liver, kidney, or other organs; active bleeding, infections, tumors, or immune system diseases; history of drug allergic reactions; pregnancy or lactation; and chest pain from other etiologies at the time of the study.

Interventions

Patients treated with CTs, including isosorbide dinitrate, low molecular weight heparin, β-blockers, aspirin, angiotensin-converting enzyme inhibitors and angiotensin receptor blockers, were classified in the control group, while the intervention of the trial group was TXLC combined with CTs. Patients with hyperlipidemia, diabetes, hypertension or certain complications were treated accordingly. Except for TXLC, trials involving any other traditional Chinese medicine interventions (such as qigong, acupuncture, other herbs, and moxibustion) were excluded.

Outcome Measures

Preset primary or secondary outcome indicators must have been reported in the included trials. The primary outcome indicators were defined as the incidence of all-cause mortality, the incidence of cardiovascular events, and adverse effects. The incidence of cardiovascular events was a comprehensive outcome of AMI, cardiac death and revascularization [including percutaneous coronary intervention (PCI), percutaneous transluminal coronary angioplasty (PTCA) and coronary artery bypass grafting (CABG)]. Any adverse effect and withdrawal of patients due to intolerances was recorded.

Secondary outcome indicators comprised the relapse of angina, the number of ST-segment depression (NST), summation of ST-segment depression (∑ST), ECG improvement, clinical efficacy in UA, symptom improvement (chest pain or tightness, palpitation, shortness of breath and asthenia), hypersensitive C-reactive protein (hs-CRP) level, and level of nitric oxide (NO). The ECG improvement was defined as a recovery of ST-segment depression exceeding 0.05 mV. The clinical efficacy of UA was considered meeting one of the following conditions as effective (otherwise it was invalid): 1) the frequency, duration or nitroglycerin dose of UA decreased by more than 50% compared with previously; 2) Canadian Cardiovascular Society classification of angina pectoris improved 1 level or above; and 3) cardiac load grew without increasing angina frequency. Outcomes were evaluated at the point of longest follow-up time when more than one follow-up time was mentioned.

Data Extraction and Quality Assessment

All records were imported into reference management software (EndNote X7) to eliminate duplicates. Study eligibility was independently assessed by 2 reviewers (PL and QX) according to the inclusion/exclusion criteria. Irrelevant literatures, such as reviews and pharmacological trials, were eliminated by reading titles and abstracts. Full texts were read before confirming inclusion. The reviewers further clarified studies with unclear titles or abstracts for potential inclusion (PL and QX). If repeated data were published by the same author across studies, the latest published or the one with the largest sample size was selected. To facilitate data statistics, a standard form was used for data extraction which including the following: 1) study ID, 2) sample size, 3) baseline characteristics of participants (sex, age, etc.), 4) interventions (dosage of administration), 5) duration of therapy, 6) UA diagnostic criteria, and 7) outcomes and adverse effects. Authors of the original studies were consulted for unclear or missing information when necessary. Any disagreement was resolved through discussion between two reviewers or with another author.

Risk of Bias Assessment

Two investigators (PL and QX) independently assessed the quality of the included studies according to the Cochrane Collaboration tool, which included 7 areas of low, high and undefined risks: 1) random sequence generation, 2) allocation concealment, 3) blinding of participants and personnel, 4) blinding of outcome assessment, 5) incomplete outcome data, 6) selective reporting, and 7) other bias. An item was judged as "unclear" when it encountered ambiguous information or could not be determined to be "high" or "low".

Statistical Synthesis and Analysis

Meta-analysis was performed with the Review Manager Software package (RevMan, v.5.3; The Cochrane Collaboration). The relative risk (RR) of dichotomic variables and the mean difference (MD) of the continuous variables were calculated

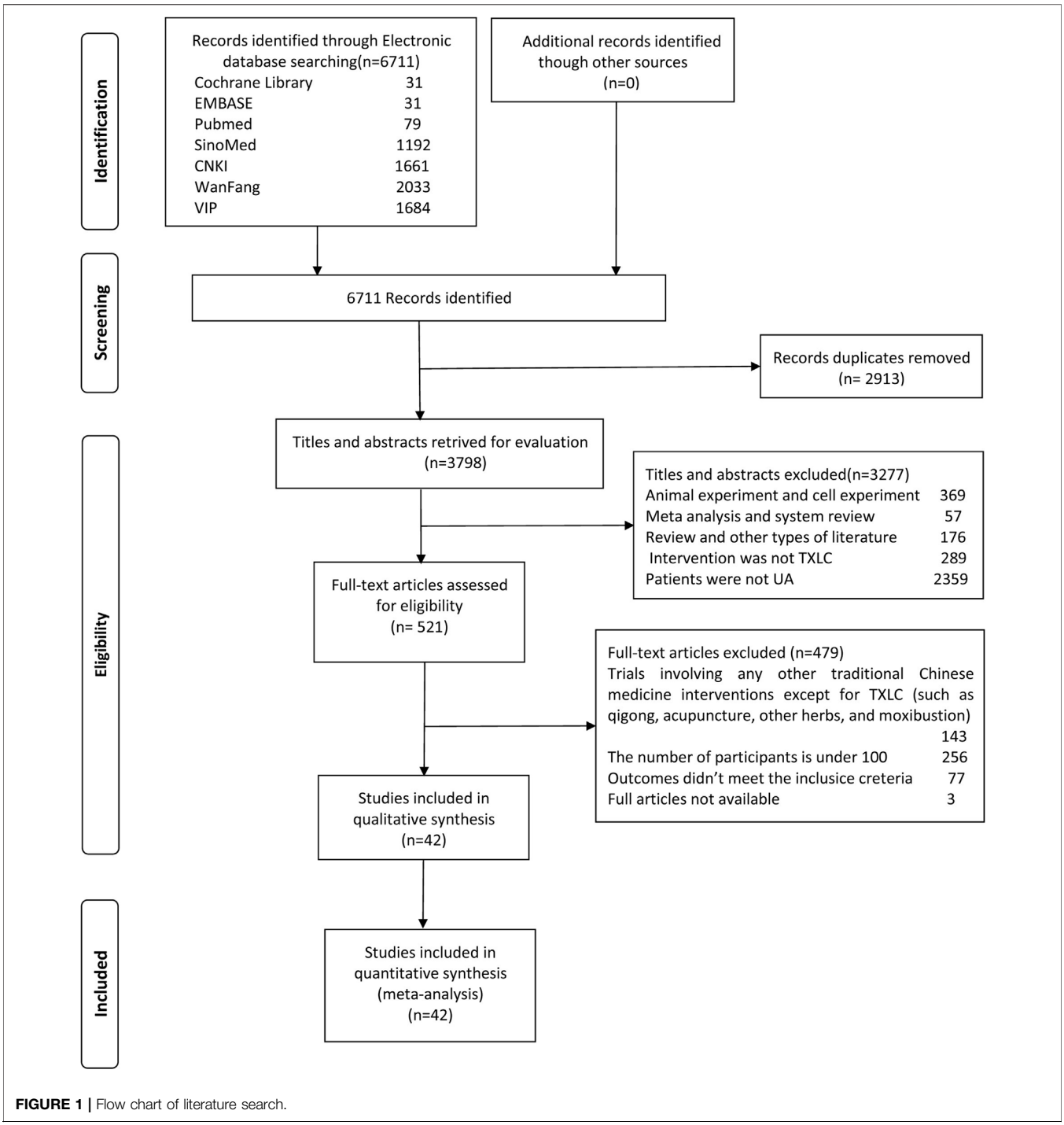

FIGURE 1 | Flow chart of literature search.

with 95% CIs, and the results were presented as forest maps. Skewed data and nonquantitative data were presented with descriptions. All reported p values were two-tailed and considered statistically significant when $p < 0.05$. The I^2 statistic was applied for heterogeneity assessment. $I^2 \geq 50\%$ showed significant heterogeneity, with a random effect model being applied; otherwise, a fixed effect model was adopted instead. Sensitivity analysis was used to test the robustness of the results. If an indicator was reported in more than 10 included trials, potential publication bias would be assessed by an inverted funnel plot (Sterne and Egger., 2001). Meanwhile, the Begg rank correlation (Begg and Mazumdar., 1994) and Egger regression asymmetry test (Egger et al., 1997) performed by STATA v.12.0 (Stata Corp LP, College Station, TX, United States) were used to assess the dissymmetry degree of the funnel plot ($p < 0.05$).

RESULTS

Search Results

A total of 6,711 studies were identified from preliminary searches according to the above retrieval strategy. After removing 2,913 duplicates and 3,277 substandard studies by browsing titles and abstracts, 521 papers were retained for further assessment. After screening based on the inclusion and exclusion criteria, 42 standard-compliant RCTs were included in the final analysis. **Figure 1** presents the detailed screening flow of eligible studies.

Characteristics of the Included Studies

Ultimately, 5,421 patients from 42 trials (Cai and Li., 2010; Chang et al., 2018; Chang and Zhao, 2004; Chen and Li, 2009; Cui, 2008; Ding et al., 2013; Du, 2016; Gao et al., 2002; Hao, 2015; Hui et al., 2018; Jiang et al., 2019; Li Q. et al., 2018; Li, 2013; Liu and An., 2016; Liu, 2011; Luo, 2013; Ma et al., 2011; Ren et al., 2018; Shi, 2013; Song et al., 2008; Sun et al., 2011; Tian and Xu., 2005; Tian et al., 2007; Wang and Li., 2007; Wang, 2017; Wang et al., 2013; Wang et al., 2010; Wang, 2015; Wang et al., 2009; Wang et al., 2012; Wu, 2011; Wu S. J. et al., 2006; Wu et al., 2010; Xin et al., 2008; Xing, 2013; Yang, 2008; Yang et al., 2019; Yu and Chen., 2015; Yu and Hu., 2012; Yuan, 2019; Zhang and Li, 2009; Zhou, 2013) (published between 2002 and 2019) were included. All selected studies were single center, parallel design, and conducted in China. There were 2,867 participants in the trial group (TXLC combined with CTs) and 2,554 participants in the control group (CTs only). The age of participants ranged from 30 to 90 years old. Six trials (Yang, 2008; Liu., 2011; Sun et al., 2011; Shi., 2013; Hao., 2015; Chang et al., 2018) had more female participants than males, 4 trials (Chang and Zhao, 2004; Wu S. J. et al., 2006; Song et al., 2008; Ren et al., 2018) did not report the gender ratio, and the remaining trials had more male participants. Both trial and control groups received CTs including nitrate, aspirin, statins, low molecular weight heparin, β-blockers, and so on. TXLCs were purchased from Shijiazhuang Yiling Pharmaceutical Co., Ltd., with a specification of 30 capsules per box, 0.26 g per pill. For the dosages of TXLC taken in the included trials, 4 capsules three times per day was the most frequently dosage used, which was implemented in 21 studies (Chen and Li, 2009; Cai and Li, 2010; Ding et al., 2013; Hao, 2015; Du, 2016; Liu and An., 2016; Ren et al., 2018; Jiang et al., 2019; Shi, 2013; Sun et al., 2011; Tian et al., 2007; Wang and Li, 2007; Wang, 2017; Wang et al., 2013; Wang, 2015; Wang et al., 2009; Wang et al., 2012; Wu et al., 2010; Xin et al., 2008; Xing, 2013; Zhang and Li, 2009). In addition, there were 9 cases (Chang and Zhao, 2004; Cui, 2008; Yang., 2008; Cai and Li., 2010; Wang et al., 2010; Zhou., 2013; Du., 2016; Chang et al., 2018; Hui et al., 2018) of 3 capsules three times per day, 4 cases (Yu and Hu., 2012; Li., 2013; Yu and Chen., 2015; Li Q. et al., 2018) of 2 capsules three times per day, 3 cases (Liu., 2011; Jiang et al., 2019; Yang et al., 2019) of 4 capsules twice per day, and 1 case (Song et al., 2008) of 2 capsules twice per day, and dosages in the rest of the studies were adjusted between the maximum and the minimum according to the actual conditions. The trial duration ranged from 2 weeks to 1 year. Seventeen studies (Cai and Li., 2010; Chang et al., 2018; Du., 2016; Gao et al., 2002; Hui et al., 2018; Li Q. et al., 2018; Li., 2013; Liu and An., 2016; Shi., 2013; Wang., 2017; Wang et al., 2013; Wang., 2015; Wang et al., 2012; Xing., 2013; Yang., 2008; Yu and Hu., 2012; Zhang and Li., 2009) mentioned the course of disease, ranging from 2 days to 21 years. Eight studies (Song et al., 2008; Xin et al., 2008; Wang et al., 2009; Cai and Li., 2010; Wu., 2011; Li., 2013; Wang et al., 2013; Hui et al., 2018) reported comorbidities in UA patients, including at least one case of diabetes, hypertension, or hyperlipidemia. The details of all studies were summarized in **Table 1**. See the TXLC quality control data of all included studies in **Supplementary Material S3**.

Risk of Bias in Included Studies

The qualities of 42 RCTs were evaluated from 7 aspects following the risk of bias scale in the Cochrane handbook of the Cochrane Collaboration. All selected trials reported randomized allocation of participants but rarely referred to randomization methods in sequence generation; hence, this situation was judged as unclear risk. Seven studies (Wu S. J. et al., 2006; Li., 2013; Shi., 2013; Du., 2016; Li Q. et al., 2018; Yang et al., 2019; Yuan, 2019) used random number tables to generate sequences and were rated as low risk, while the risk for allocation concealment was deemed a high level. Only 1 study (Yu and Hu., 2012) mentioned blinding without further information on specific methods, therefore other studies were considered at a high risk of bias due to unsearchable blind details. Two studies (Tian and Xu., 2005; Wu., 2011) reported 10 patient withdrawals due to the intolerance of side effects and consequently obtained a high likelihood of incomplete result. The rest of the participants finished all treatments except for 1 dropout from the control group. Selective reporting was found in 12 studies (Chen and Li, 2009; Cui, 2008; Ding et al., 2013; Gao et al., 2002; Hao., 2015; Hui et al., 2018; Liu., 2011; Tian et al., 2007; Wang et al., 2013; Wang et al., 2009; Wang et al., 2012; Yu and Chen., 2015). Beyond that, no studies mentioned attrition bias or reporting bias. Although the above information demonstrated a consistent between-group baseline, the potential sources of bias such as differences in CTs options, intent-to-treat and other adherence difference might still exist. After trying to contact the authors to clarify the unreported information *via* e-mail and receiving no reply, other biases were assessed as unclear risks. The risk of bias assessments for overall and individual studies are presented in **Figures 2**, **3**.

Effects of Interventions

Primary Outcome Measures

Rate of Cardiovascular Events

Cardiovascular events were defined as cardiovascular death, AMI and revascularization (including PCI, PTCA, CABG). A fixed effect model was used after the heterogeneity test ($\chi^2 = 2.61$, $p = 0.76$; $I^2 = 0$). Strong evidence across 909 participants in 6 studies (Wu et al., 2010; Ma et al., 2011; Wu., 2011; Yu and Hu., 2012; Wang et al., 2013; Yu and Chen., 2015) showed that taking TXLC as adjuvant therapy had a lower rate of cardiovascular events than CTs did, and a significant difference between the two groups was observed [RR = 0.29, 95% CI (0.19, 0.45), $p < 0.00001$, **Figure 4A**].

TABLE 1 | The basic information of the 42 included articles (sorted by the first letter of author's name).

Studies	Sample size (T/C)	Sex M/F	Age, Mean ± SD (year)	Intervention			Course of treatment	Diagnostic criteria	Outcomes
				T	TXLC dosage	C			
Cai and Li (2010)	120 (61/59)	73/47	NR	TXLC + CT	4 capsules, Tid	CT (isosorbide dinitrate, diltiazem hydrochloride tables, metoprolartrate tables, sublingual nitroglycerin if angina attach, no details)	4 weeks	2000 CMA recommendations for diagnosis and treatment of UA	(6) (8) (9)
Chang et al. (2018)	108 (54/54)	53/55	T 57.2 ± 2.8 C 57.7 ± 2.4	TXLC + CT	3 capsules, Tid	CT (aspirin 100 mg Qd, atorvastatin 20 mg Qd, isosorbide mononitrate 40 mg Qd, subcutaneous injection of enoxaparine 0.6 mg Q12h if necessary)	30 days	2007 CMA Guidelines for the diagnosis and management of UA and non-ST-segment elevation myocardial infarction	(11) (12) (13) (14) (15) (17)
Chang and Zhao (2004)	114 (68/46)	NR	T 65 ± 4 C 64 ± 6	TXLC + CT	3 capsules, Tid	CT (isosorbide dinitrate, aspirin, calcium antagonists, β-blocker, no details)	6 weeks	WHO Diagnostic criteria for UA	(10)
Chen and Li (2009)	118 (60/58)	79/39	NR	TXLC + CT	4 capsules, Tid	CT (aspirin 100 mg, Qd; simvastatin 10 mg, Qd; subcutaneous injection of LMWH 5000U, Q12h; metoprolol)	4 weeks	2000 CMA recommendations for diagnosis and treatment of UA (except for variantangina vectoris)	(6) (10)
Cui (2008)	144 (76/68)	82/62	T:55 ± 2 C:55 ± 3	TXLC + CT	3 capsules, Tid	CT (β-blocker, calcium antagonists, aspirin, etc.; nitroglycerin, ivgtt; LMWH Calcium Injection, iH, 5–7 d)	1 month	1979 WHO nomenclature and diagnostic criteria of IHD	(6) (10)
Ding et al. (2013)	120 (60/60)	77/43	NR	TXLC + CT	4 capsules, Tid	CT (aspirin, 100 mg, Qd; metoprolol 12.5 mg, Bid; nitroglycerin for angina attack 0.5–1 sublingual; simvastatin 10 mg, Qd; LMWH 5000U, iH, Q12h)	4 weeks	2000 WHO Diagnostic criteria for UA	(10) (11)
Du (2016)	100 (50/50)	51/49	T 63.3 ± 5.4 C 62.9 ± 5.1	TXLC + CT	4 capsules, Tid	CT (ACEI; nitrates; lipid-altering drugs; β-blocker; aspirin, 100 mg, Qd)	4 weeks	2000 WHO Diagnostic criteria for UA	(6) (10) (11)
Gao et al. (2002)	100 (60/40)	63/37	NR	TXLC + CT	2–4 capsules, Tid	CT (nitroglycerin, metoprolol, aspirin, etc., no details)	4 weeks	WHO Nomenclature and diagnostic criteria of IHD and the clinical research guidelines for new traditional Chinese medicines for the treatment of chest pain formulated by the Ministry of Health in 1993	(10)
Hao (2015)	110 (55/55)	53/57	T 48.1 ± 3.8 C 49.3 ± 3.3	TXLC + CT	4 capsules, Tid	CT (aspirin, nitrates, metoprolol, simvastatin, etc., no details)	2 months	Diagnostic criteria of UA in "Internal medicine"	(10)
Hui et al. (2018)	100 (50/50)	55/45	T 56.20 ± 6.75 C 56.56 ± 6.32	TXLC + CT	3 capsules, Tid	CT (aspirin, β-blocker, statins, nitrates, atients with diabetes were also given hypoglycemic therapy, isosorbide mononitrate for angina attack)	2 weeks	Diagnostic criteria for UA	(11)

(Continued on following page)

TABLE 1 | (*Continued*) The basic information of the 42 included articles (sorted by the first letter of author's name).

Studies	Sample size (T/C)	Sex M/F	Age, Mean ± SD (year)	Intervention			Course of treatment	Diagnostic criteria	Outcomes
				T	TXLC dosage	C			
Jiang et al. (2019)	160 (80/80)	90/ 70	T 58.5 ± 6.4 C 59.1 ± 6.2	TXLC + CT	4 capsules, Tid	CT (antiplatelet aggregation, calcium antagonist and anticoagulant therapy. astatin tablets 20 mg/ times, Qd, daily bedtime oral)	3 months	Relevant standards formulated by the South China International Cardiovascular Symposium	(16)
Li Q. et al. (2018)	128 (64/64)	74/ 54	T: 68.11 ± 7.29 C: 68.11 ± 7.29	TXLC + CT	2 capsules, Tid	CT (conventional treatment and a torvastatin calcium tablets 20 mg, Qd)	2 months	2009 edition of "Coronary Heart Disease with Integrated Traditional Chinese and Western Medicine"	(16)
Li (2013)	110 (55/55)	81/ 29	T: 55.4 ± 9.6 C: 57.0 ± 9.2	TXLC + CT	2 capsules,Tid	CT (atorvastatin, 20 mg, Qd; oral nitrates, β-receptor blockers, calcium antagonists, anti-platelet aggregation drugs and LMWH, etc.)	8 weeks	Diagnostic criteria for UA in the 1979 WHO standards and the standards of the National Symposium on the Diagnosis and Treatment of UA in August 2000	(11)
Liu and An (2016)	160 (80/80)	101/ 59	51.1 ± 1.4	TXLC + CT	4 capsules, Tid	CT (sublingual nitroglycerin; aspirin antiplatelet therapy; heparin anticoagulation therapy; thrombolysis; β-blockers (propranolol) and ACEI (angiotensin II), attovastatin calcium tablets, 20 mg, Qd)	3 months	The relevant diagnostic criteria for coronary heart disease and angina pectoris formulated by the WHO; all are diagnosed as UA of coronary heart disease through clinical symptoms, laboratory examinations, and imaging data	(6)
Liu (2011)	102 (51/51)	47/ 54	NR	TXLC + CT	4 capsules, Bid	CT (conventional treatment and LMWH 5000U, iH, Q12h, continuous use of 5–7 d)	4 weeks	The diagnostic criteria for unstable myocardial infarction in the "Guidelines for the Diagnosis and Treatment of Elevated Myocardial Infarction" formulated by the Cardiovascular Branch of the CMA in 2007	(8) (9)
Luo (2013)	120 (60/60)	63/ 57	T:58.88 ± 14.37 C:59.12 ± 15.01	TXLC + CT	2–4 capsules, Tid	CT [rest, oxygen inhalation, low-fat diet, give nitrate vinegar drugs, aspirin, lipid-lowering drugs, calcium antagonists, LMWH, metoprolol tartrate (start from the minimum dose of 6 t 25 mg, Bid, every 1–2 weeks to gradually increase, and finally increase to the target value of 50–150 mg, Qd, for 14 consecutive days)]	3 months	"Naming and Diagnostic Standards for Coronary Heart Disease" developed by WHO	(11)
Ma et al. (2011)	318 (159/159)	194/ 124	60.6 ± 12.8	TXLC + CT	3–4 capsules, Tid	CT (aspirin, nitroglycerin, heparin, calcium antagonists, β-blockers, no details)	NR	Diagnosis based on the characteristics of angina pectoris and the dynamic evolution of the S-T segment of the ECG at the onset (s-T segment downward shift ≥0.1 mv)	(1) (2) (3) (4) (5) (6)

(Continued on following page)

TABLE 1 | (*Continued*) The basic information of the 42 included articles (sorted by the first letter of author's name).

Studies	Sample size (T/C)	Sex M/F	Age, Mean ± SD (year)	Intervention			Course of treatment	Diagnostic criteria	Outcomes
				T	TXLC dosage	C			
Ren et al. (2018)	100 (50/50)	NR	NR	TXLC + CT	4 capsules, Tid	CT (nitrate drugs, β-blockers, aspirin orally, 100 mg, Qd)	4 weeks	Evidence for the diagnosis of UA	(6) (11)
Shi (2013)	112 (56/56)	45/67	65.38 ± 10.57	TXLC + CT	4 capsules, Tid	CT (rest on bed, low-salt diet, low-flow oxygen inhalation, etc. nifedipine tablets, 10 mg, Tid; aspirin enteric-coated tablets 112 mg, Qd; angiotensin converting enzyme inhibitor benazepril 5 mg, Qd; trimetazidine, 20 mg, Tid; isosorbide dinitrate tablets 10 mg, Tid; take isosorbide dinitrate tablets when angina pectoris attacks, 10 mg/time)	14 days	Diagnostic criteria for UA developed by experts from the ACC and the American Association of Cardiology (AHA)	(6) (10) (11)
Song et al. (2008)	176 (106/70)	NR	NR	TXLC + CT	2 capsules, Bid	CT (nitroglycerin 5mg, added to 5% glucose injection 250 ml intravenous infusion, first start at 10 μg/min, increase by 5–10 μg every 15 min, maintain the systolic blood pressure at about 100 mmHg)	2 weeks	Standards established by WHO in 1979	(6) (10) (11)
Sun et al. (2011)	128 (66/62)	62/66	68.26 ± 10.17	TXLC + CT	4 capsules, Tid	CT (aspirin 100 mg, Qd; atorvastatin 20 mg, Qn; isosorbide mononitrate 20 mg, Bid; oral ACEI and calcium antagonists, β-blockers. intravenous nitrates and subcutaneous injection of LMWH if necessary)	4 weeks	WHO recommended diagnostic criteria for UA	(16)
Tian and Xu (2005)	118 (77/41)	82/36	NR	TXLC + CT	TXLC group 1: 45 cases, 2 capsules, Tid; TXLC group 2: 32 cases, 4 capsules, Tid	CT (isosorbide 10 mg, tid; enteric-coated aspirin 0.1 g, Qd; captopril 6.25–25 mg, Tid; and add β-blockers or calcium antagonists, statins lipid-lowering drugs, intravenous nitrates and subcutaneous injection of LMWH if necessary)	8 weeks	1997 WHO Diagnostic criteria for IHD	(5) (6)
Tian et al. (2007)	120 (60/60)	69/51	57.4 ± 4.7	TXLC + CT	4 capsules, Tid	CT (Conventional coronary artery dilation, anticoagulation, and oxygen consumption reduction therapy)	4 weeks	WHO standard for UA	(6)

(Continued on following page)

TABLE 1 | (*Continued*) The basic information of the 42 included articles (sorted by the first letter of author's name).

Studies	Sample size (T/C)	Sex M/F	Age, Mean ± SD (year)	Intervention			Course of treatment	Diagnostic criteria	Outcomes
				T	TXLC dosage	C			
Wang and Li (2007)	180 (90/90)	124/56	T:56 ± 6 C:56 ± 7	TXLC + CT	4 capsules, Tid	CT [enteric-coated aspirin (changed to 100 mg/d after 300 mg/d, 3 days), nitrate, β-blockers, LMWH sodium (5000 IU subcutaneous injection, Q12h) (LMWH for 1 week)]	8 weeks	Selection criteria: 1. initial exertional angina pectoris; 2. deteriorating exertional angina pectoris; 3. resting angina pectoris; 4. angina after infarction. At the same time: 1.96 h of sudden exacerbation of angina, activity tolerance decreased significantly; 2. spontaneous angina attack at least once within 24 h; 3. ST-segment moved down more than 1 mm at the time of the attack, and it recovered significantly after the attack was relieved	(6) (11)
Wang (2017)	120 (60/60)	62/58	T:63.1 ± 5.2 C: 62.8 ± 4.3	TXLC + CT	4 capsules, Tid	CT (nitrate drugs, ACEI, β-blockers, aspirin, 100 mg/time)	4 weeks	All patients meet the clinical diagnostic criteria for UA established by the Cardiovascular Branch of the CMA in 2000; ASA Cardiac Function Classification I~II	(6) (11)
Wang et al. (2013)	150 (100/50)	85/65	T: 74.28 ± 5.14 C: 72.80 ± 4.98	TXLC + CT	4 capsules, Tid	CT (antiplatelet aggregation and anticoagulant drugs, antiangina drugs; in special circumstances, quick-acting anti-angina pectoris can be added temporarily)	4 weeks	The diagnostic criteria for UA in the 2007 "Guidelines for the Diagnosis and Treatment of UA and Non-ST Segment Elevation Myocardial Infarction". The angina pectoris classification adopts the angina pectoris classification of the CCS	(4) (10) (11) (12) (13) (14) (15)
Wang et al., 2010	110 (56/54)	74/36	63.3 ± 7.2	TXLC + CT	3 capsules, Tid	CT (aspirin + simvastatin + nitrate)	12 weeks	UA risk stratification of Brauwald in 1989	(11)
Wang (2015)	100 (50/50)	62/38	T: 75.3 ± 2.7 C: 74.8 ± 3.1	TXLC + CT	4 capsules, Tid	CT (antiangina drugs, antiplatelet aggregation drugs and anticoagulant drugs)	1 month	clinical diagnostic criteria for UA	(11)
Wang et al. (2009)	126 (66/60)	88/38	T:54.3 C:53.8	TXLC + CT	4 capsules, Tid	CT (isosorbide, 10 mg, Tid)	2 months	The naming and diagnostic criteria of IHD developed by WHO	(6) (11)
Wang et al. (2012)	144 (72/72)	80/64	T:68.6 ± 8 C: 67.6 ± 10	TXLC + CT	4 capsules, Tid	CT (nitrates, lipid-lowering drugs, β-receptor blockers, enteric-coated aspirin, calcium channel blockers, ACEI, angiotensin receptor inhibitors)	8 weeks	The "Nomenclature and Diagnostic Criteria for IHD" recommended by WHO and the diagnostic criteria in "Recommendations for the Diagnosis and Treatment of UA" issued by the Cardiovascular Branch of the CMA in 2000	(6) (10) (11)

(Continued on following page)

TABLE 1 | (*Continued*) The basic information of the 42 included articles (sorted by the first letter of author's name).

Studies	Sample size (T/C)	Sex M/F	Age, Mean ± SD (year)	Intervention			Course of treatment	Diagnostic criteria	Outcomes
				T	TXLC dosage	C			
Wu (2011)	109 (59/50)	75/ 34	T:66.6 ± 11.35 C:63.8 ± 10.57	TXLC + CT	2 or 4 capsules, Tid	CT (clopidogrel 75 mg, Qn; LMWH calcium 5000 U, iH, Q12h, 7 days; isosorbide mononitrate, 20 mg, Bid; betaloc 12.5 mg, Bid: simvastatin, 20 mg, Qn; enalapril, 5 mg, Bid, as long as hypotension does not occur; calciumion antagonists, etc. Patients with arrhythmia, hypertension, and diabetes are given symptomatic treatments such as antihypertensive, hypoglycemic, and antiarrhythmic treatment at the same time)	10 months	"Acc/A—HA2007 UA/Non-ST-segment Elevation Myocardial Infarction Treatment Guidelines Diagnostic Criteria"	(6)
Wu S. J. et al. (2006)	180 (120/60)	NR	NR	TXLC + CT	TXLC low dose group 2 capsules, Tid; TXLC high dose group 4 capsules, Tid	CT (antithrombotic, nitrate vinegar drugs, β-blockers, ACEI)	4 weeks	UA diagnostic criteria in the guidelines and recommendations for the treatment of cardiovascular diseases	(6)
Wu et al. (2010)	110 (57/53)	63/ 47	T: 71.4 ± 4.5 C: 69.8 ± 4.3	TXLC + CT	4 capsules, Tid	CT (routinely give clopidogrel 75 mg/d and aspirin 100 mg/d for at least 7 days before PCI; routine treatment after PCI (such as aspirin, clopidogrel, β-blockers, nitrates, angiotensin conversion) enzyme inhibitors, LMWH, etc.)	6 months	Guidelines for the diagnosis and treatment of UA and non-ST-segment elevation myocardial infarction formulated by the Cardiovascular Branch of the CMA in 2007	(3) (4) (7)
Xin et al. (2008)	128 (66/62)	73/ 55	T:64 ± 10 C:63 ± 8	TXLC + CT	4 capsules, Tid	CT (enteric-coated aspirin, nitrate esters, β-blocker, containing nitroglycerin at the time of disease)	4 weeks	The naming and diagnostic criteria for IHD recommended by the International Society of Cardiology and WHO	(6) (8) (9)
Xing (2013)	120 (60/60)	71/ 29	NR	TXLC + CT	4 capsules, Tid	CT (Low-fat diet, recorde resting ECG once a day; isosorbide, 10 mg, Tid; enteric-coated aspirin, 100 mg, qd; oxygen inhalation, sublingual nitroglycerin for angina pectoris, intravenous nitroglycerin, subcutaneous injection of tid LMWH, etc. if necessary)	4 weeks	WHO diagnosis and classification criteria of coronary heart disease and angina pectoris in 1979	(9)
Yang (2008)	100 (50/50)	49/ 51	T: 62.4 ± 10.9 C: 58.2 ± 12.0	TXLC + CT	3 capsules, Tid	CT (nitrates, calcium antagonists, β-receptor blockers, ACEI, enteric-coated aspirin, statins)	1 month	In line with the WHO diagnosis of UA patients	(11) (17)

(Continued on following page)

TABLE 1 | (*Continued*) The basic information of the 42 included articles (sorted by the first letter of author's name).

Studies	Sample size (T/C)	Sex M/F	Age, Mean ± SD (year)	Intervention			Course of treatment	Diagnostic criteria	Outcomes
				T	TXLC dosage	C			
Yang et al. (2019)	100 (50/50)	61/39	T: 66.2 ± 4.8 C: 66.6 ± 4.7	TXLC + CT	4 capsules, Bid	CT (5-isosorbate mononitrate, 40 mg, Bid; aspirin,100 mg, Qn, before bedtime; betaloc, 25 mg, Bid)	3 months	According to the WHO diagnostic criteria for angina pectoris of coronary heart disease: typical symptoms of angina pectoris; ECG showed obvious changes of myocardial ischemia	(6) (10) (11)
Yu and Chen (2015)	122 (68/54)	69/53	T:56.6 ± 3.5 C: 57.2 ± 2.9	TXLC + CT	2 capsules, Tid	CT (aspirin, clopidogrel, ACEI, β-blockers, statins, nitrates, and subcutaneous injection of LMWH and other drugs)	1 year	On the basis of typical clinical manifestations, dynamic changes of ECG ST-segment elevation and depression, myocardial enzyme spectrum during angina pectoris attack, troponin was clearly diagnosed as UA patient	(3) (7)
Yu and Hu (2012)	120 (60/60)	66/54	T: 55.3 ± 6.5 C: 54.7 ± 6.2	TXLC + CT	2 capsules, Tid	CT (betalox 50 mg, Bid; antiplatelet aggregation drugs, ACEI and lipid lowering drugs)	NR	According to the Braunwald grade, there were 46 cases in grade I, 40 cases in grade II and 34 cases in grade III.	(2) (5) (6)
Yuan (2019)	100 (50/50)	53/47	T: 63.14 ± 5.79 C: 62.78 ± 5.42	TXLC + CT	3 capsules, Qd	CT (adjusting blood glucose and controlling blood pressure; simvastatin 4 tablets/time, Qd)	4 months	The relevant diagnostic criteria for coronary heart disease UA in the Guidelines for the Diagnosis and Treatment of UA and Non-ST-Segment Elevation Myocardial Infarction formulated by the Chinese Society of Cardiology, etc.	(16)
Zhang et al. (2009)	166 (86/80)	114/52	T:55 C:54	TXLC + CT	4 capsules, Tid	CT (nitrates, aspirin, β-blockers, etc.)	3 months	International Society of Cardiology and WHO Diagnostic Criteria	(6) (10)
Zhou (2013)	152 (78/74)	98/54	T:67 C:68	TXLC + CT	3 capsules, Tid	CT (rest on bed for 7 days, oxygen inhalation, blood pressure control; isosorbide tablets, 10 mg, Tid; atorvastatin calcium tablets, 20 mg, Qn; enteric-coated aspirin tablets, 150 mg, Qd, change to 100 mg Qd after 3 days)	1 month	The standard of the middle and high risk group for the risk stratification of UA by the Cardiovascular Branch of the CMA	(6) (10)

Note: CT, conventional treatment; T, trial; C, control; M, male; F, female; SD, standard deviation; TXLC, Tongxinluo capsule; CMA, Chinese Medical Association; UA, unstable angina; WHO, World Health Organization; IHD, ischemic heart disease; LMWH, low molecular weight heparin; ACEI, angiotension converting enzyme inhibitors; ECG, electrocardiogram; ASC, American Society of Cardiology; AHA, American Heart Association; CCS, Canadian Cardiovascular Society; PCI, percutaneous coronary intervention; Bid, twice a day; Tid, three times a day; Qd, once a day; iH, hypodermic injection; Qn, every night; Q12h, every 12 h. (1) Rate of cardiovascular events; (2) Mortality due to any cardiovascular event; (3) Incidence of acute myocardial infarction (AMI); (4) Revascularization (including percutaneous coronary intervention (PCI), percutaneous transluminal coronary angioplasty (PTCA) and coronary artery bypass grafting (CABG)); (5) All-cause mortality; (6) Adverse effect; (7) Recurrence of angina; (8) NST; (9) ∑ST; (10) ECG Improvement; (11) Clinical efficacy in UA; (12) Chest pain or tightness; (13) Palpitation; (14) Shortness of breath; (15) Asthenia; (16) Hypersensitive C-reactive protein (hs-CRP) Level; (17) Nitric oxide (NO) Level.

Except for adverse effects, the meta-analysis results of each outcome indicator is shown in **Table 2**.

Two trials (Ma et al., 2011; Yu and Hu., 2012) with a total of 438 participants compared the efficacy of two interventions on cardiovascular mortality. The merged result indicated that TXLC combined with CT showed a better potential for reducing cardiovascular mortality which with low heterogeneity [χ^2 = 1.26, p = 0.26; I^2 = 20%; RR = 0.16, 95% CI (0.03, 0.88), p = 0.03, **Figure 4B**].

The incidence of AMI was evaluated in 550 participants of 3 trials (Wu et al., 2010; Ma et al., 2011; Yu and Chen., 2015). The meta-analysis result showed that adding TXLC to CT reduced the onset of AMI [RR = 0.27, 95% CI (0.13, 0.57), p = 0.0006], and no statistical heterogeneity was detected (χ^2 = 0.45, p = 0.80; I^2 = 0, **Figure 4C**).

Three trials (Wu et al., 2010; Ma et al., 2011; Wang et al., 2013) with 578 participants reported the occurrence of revascularization. Among them, Ma et al. (2011) observed the implementation of

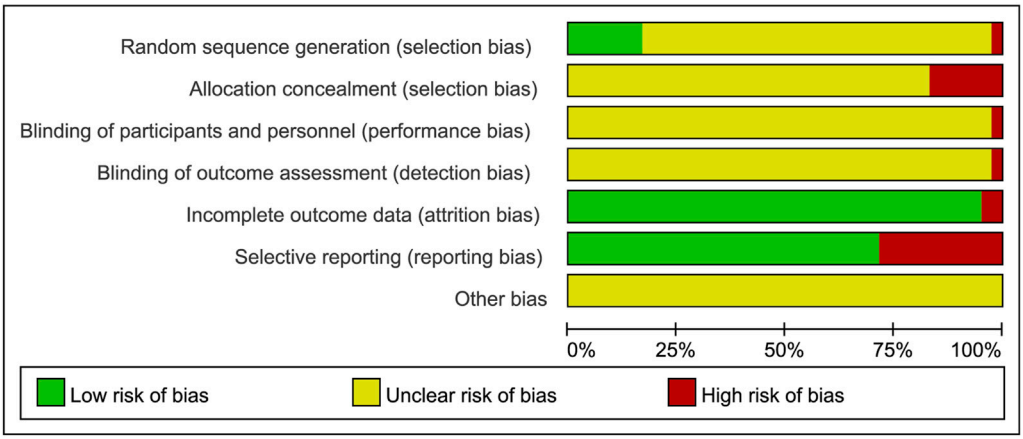

FIGURE 2 | Risk of bias graph.

PTCA/CABG, Wang et al. (2013) did not mention the type of emergency revascularization, and Wu et al. (2010) recorded the patients who received PCI. Meta-analysis demonstrated a lower incidence of revascularization in the trial group [$\chi^2 = 1.50$, $p = 0.47$; $I^2 = 0$, RR = 0.28, 95% CI (0.15, 0.54), $p = 0.0001$, **Figure 4D**].

All-Cause Mortality

Three trials (Tian and Xu., 2005; Ma et al., 2011; Yu and Hu., 2012) involving 556 participants reported the all-cause mortality in both trial and control groups. In consideration of the low heterogeneity ($\chi^2 = 2.47$, $p = 0.29$; $I^2 = 19\%$), we performed a fixed effect model for the meta-analysis. The pooled result showed that the all-cause mortality in the trial group was significantly lower than that in the control group [RR = 0.25, 95% CI (0.06, 0.99), $p = 0.05$, **Figure 5**].

Adverse Effect

Twenty-two studies mentioned adverse reactions during therapy (Tian and Xu., 2005; Wu S. J. et al., 2006; Tian et al., 2007; Wang and Li., 2007; Cui., 2008; Song et al., 2008; Xin et al., 2008; Chen and Li., 2009; Wang et al., 2009; Zhang and Li., 2009; Cai and Li., 2010; Ma et al., 2011; Wu., 2011; Wang et al., 2012; Yu and Hu., 2012; Shi., 2013; Zhou., 2013; Du., 2016; Liu and An, 2016; Wang., 2017; Ren et al., 2018; Yang et al., 2019), and 12 of them presented with adverse effects from 12 trial groups and 2 control groups. Two trials (Wang and Li., 2007; Ma et al., 2011) recorded 1 gingival bleeding case from the trial group; comparatively, no case of bleeding gums was found in the control group. One study (Yang et al., 2019) found 3 cases of hypotension from both trial and control groups, and only 1 case used TXLC as an auxiliary treatment. They also observed 1 case of bradycardia in both groups.

A total of 11 trials reported 41 patients treated with TXLC as an auxiliary therapy who showed gastrointestinal symptoms (Tian and Xu., 2005; Wu S. J. et al., 2006; Wang and Li., 2007; Cui., 2008; Xin et al., 2008; Wang et al., 2009; Ma et al., 2011; Wu., 2011; Zhou., 2013; Du., 2016; Liu and An., 2016), mainly manifested as bloating, belching, nausea, loss of appetite, acid reflux or dull pain, while only 5 participants from the control group in 1 trial experienced the same discomforts (Liu and An, 2016). Two trials (Tian and Xu., 2005; Wu., 2011) recorded 9 TXLC supplementary cases that stopped the trial due to gastrointestinal reactions. One case (Du., 2016) with TXLC had mild discomfort in the upper abdomen, and symptoms disappeared after being given gastric mucosal protective agents. Two trials (Cui., 2008; Wang et al., 2009) reported 5 cases of epigastric discomfort, acid reflux, nausea or dull pain, and symptoms disappeared when TXLC was taken after meals. A trial (Zhou., 2013) reported that the participants experienced epigastric discomforts after TXLC and aspirin were treated combinedly, which disappeared when treated separatedly at an hour's interval.

There were no withdrawals from the trials due to hypotension, bradycardia or gum bleeding. No other adverse effect was reported. In summary, it is premature to conclude that TXLC is safe based on existing data. The details of adverse effects are shown in **Table 3**.

Secondary Outcomes

Recurrence of Angina

Two included (Wu et al., 2010; Yu and Chen., 2015) trials reported recurrences of angina. A fixed effect model was performed due to zero between-trial heterogeneity ($\chi^2 = 0.33$, $p = 0.57$; $I^2 = 0\%$). A total of 232 participants were followed for 6 months and angina frequency was recorded during this period. The forest plot showed that adding TXLC to CTs reduced the recurrence of angina pectoris. There was a significant difference between the 2 groups [RR = 0.25, 95% CI (0.11, 0.61), $p = 0.002$, **Figure 6**].

NST

Three trials (Xin et al., 2008; Cai and Li., 2010; Liu., 2011) measured the number of ST-segment depressions in UA patients. After testing heterogeneity ($\chi^2 = 0.14$, $p = 0.93$; $I^2 = 0\%$), a fixed effect model was used. Under the 2 different treatments, the depression number in the trial group was less than that in the control group among 350 participants, indicating that TXLC improved the ECG characterization of myocardial ischemia [MD = −0.45, 95% CI (−0.69, −0.20), $p = 0.0005$, **Figure 7**].

FIGURE 3 | Risk of bias summary.

$\sum ST$

The summation of ST-segment depression reflects the degree of myocardial ischemia. It was evaluated in 470 participants from 4 trials (Xin et al., 2008; Cai and Li., 2010; Liu., 2011; Xing., 2013). The heterogeneity was more than 50% ($\chi^2 = 10.10$, $p = 0.02$; $I^2 = 70\%$), and a random effect model was chosen. Meta-analysis showed that the total declines of ST-segment in the trial group was lower than the control group, and the difference between the 2 groups was statistically significant [MD = −0.70, 95% CI (−1.08, −0.32), $p = 0.0003$, **Figure 8**].

ECG Improvement

Thirteen studies (Chang and Zhao, 2004; Chen and Li, 2009; Cui., 2008; Ding et al., 2013; Du., 2016; Gao et al., 2002; Hao., 2015; Shi., 2013; Song et al., 2008; Wang et al., 2013; Wang et al.,2012; Yang et al., 2019; Zhou., 2013) mentioned ECG improvement. Using a fixed effect model was reasonable owing to nonexistent between-trial heterogeneity ($\chi^2 = 9.42$, $p = 0.67$; $I^2 = 0\%$). The meta-analysis result showed that combined with CTs, TXLC showed an improvement in the effectiveness of the ECG. There was a statistically significant difference between the 2 groups [RR = 1.23, 95% CI (1.16, 1.30), $p < 0.00001$, **Figure 9**].

Clinical Efficacy in UA

Nineteen RCTs (Wang and Li., 2007; Song et al., 2008; Yang., 2008; Wang et al., 2009; Zhang and Li 2009; Wang et al., 2010; Wang et al., 2012; Ding et al., 2013; Li., 2013; Luo., 2013; Shi., 2013; Wang et al., 2013; Wang., 2015; Du., 2016; Wang., 2017; Chang et al., 2018; Hui et al., 2018; Ren et al., 2018; Yang et al., 2019) reported the clinical efficacy for UA. A fixed effect model was adopted for merging data after testing heterogeneity ($\chi^2 = 23.80$, $p = 0.16$; $I^2 = 24\%$). The merged results suggested that TXLC combined with CTs was better than CTs alone in improving the clinical efficacy of angina pectoris. A significant difference was observed between groups [RR = 1.26, 95% CI (1.21, 1.32), $p < 0.00001$, **Figure 10**].

Symptom Improvement

Two studies (Wang et al., 2013; Chang et al., 2018) compared symptom improvement. Unlike the clinical efficacy for UA, which has specific diagnostic criteria and consensus, symptom improvement includes remissions of chest pain or tightness, palpitation, shortness of breath and asthenia. In contrast with these quantifiable indicators, such as ECG, consumption of nitroglycerine, and frequency and duration of angina attack, the symptoms here emphasized the patient's overall disease state. Because low between-trial heterogeneity for chest pain or tightness ($\chi^2 = 1.43$, $p = 0.23$; $I^2 = 30\%$) was shown, and no heterogeneity for palpitation ($\chi^2 = 0.33$, $p = 0.57$; $I^2 = 0\%$) or shortness of breath ($\chi^2 = 0.35$, $p = 0.56$; $I^2 = 0\%$) were found, fixed effect models were selected. However, a random effect model was used for asthenia due to its high heterogeneity ($\chi^2 = 10.06$, $p = 0.002$; $I^2 = 90\%$). The meta-analyses indicated that the trial group had more remissions of palpitation [RR = 1.47, 95% CI (1.18, 1.84), $p = 0.0007$, **Figure 11A**] and shortness of breath [RR = 1.53, 95% CI (1.24, 1.88), $p < 0.0001$, **Figure 11B**], the difference between groups was statistically significant. Further, the trial group showed an improvement of chest pain or tightness and asthenia, but there was no significant difference compared with the control group [RR = 1.13, 95% CI (0.97, 1.32), $p = 0.12$, **Figure 11C**; RR = 1.69, 95% CI (0.83, 3.43), $p = 0.15$, **Figure 11D**].

Hs-CRP Level

Hs-CRP was evaluated in a total of 4 studies (Sun et al., 2011; Li Q. et al., 2018; Jiang et al., 2019; Yuan., 2019). As

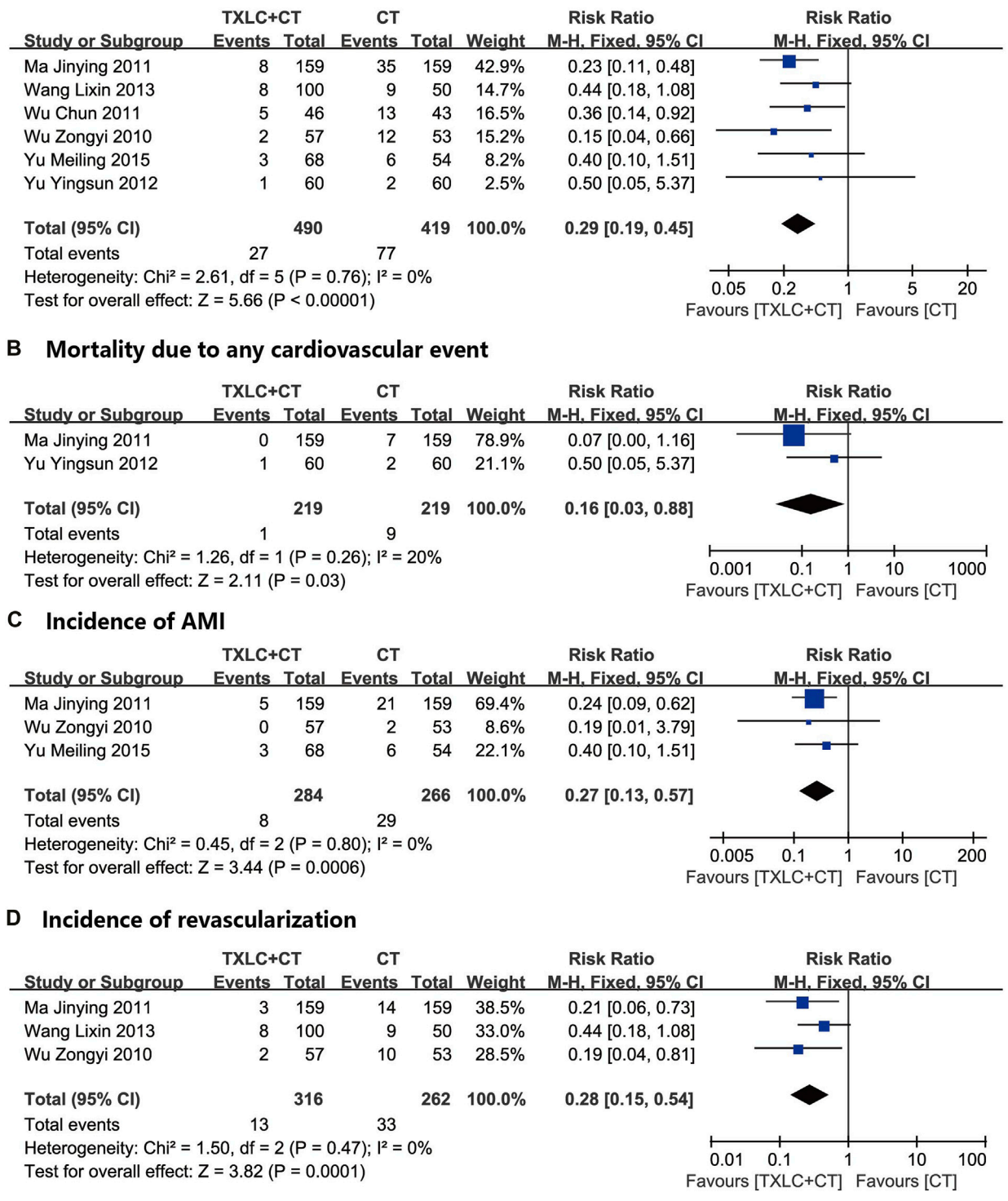

FIGURE 4 | Meta-analysis of the rate of cardiovascular events (including cardiovascular mortality incidence of AMI, and incidence of revascularization) using TXLC Plus CT vs. CT.

TABLE 2 | Summary of meta-analysis results of outcome indicators.

Outcome/indicators		No. (RCTs)	No. (participants)	MD/RR [95%CI]	I^2 value	Model
Rate of cardiovascular events		6	909	RR = 0.29, [0.19, 0.45]	0	Fixed
Cardiovascular events	Cardiovascular mortality	2	438	RR = 0.16, [0.03, 0.88]	20%	Fixed
	Incidence of AMI	3	550	RR = 0.27, [0.13, 0.57]	0	Fixed
	Occurrence of revascularization	3	578	RR = 0.28, [0.15,0.54]	0	Fixed
All-cause mortality		3	556	RR = 0.25, [0.06, 0.99]	19%	Fixed
Recurrence of angina		2	232	RR = 0.25, [0.11, 0.61]	0	Fixed
NST		3	350	MD = −0.45, [−0.69, −0.20]	0	Fixed
∑ST		4	470	MD = −0.70, [−1.08, −0.32]	70%	Random
ECG Improvement		13	1,640	RR = 1.23, [1.16, 1.30]	0	Fixed
Clinical efficacy in UA		19	2,342	RR = 1.26, [1.21, 1.32]	24%	Fixed
Hs-CRP Level		4	516	MD = −2.86, [−3.73, −1.99]	86%	Random
NO Level		2	208	MD = 11.67, [8.33,15.02]	33%	Fixed
Symptom improvement	Chest pain or tightness	2	220	RR = 1.13, [0.97, 1.32]	30%	Fixed
	Palpitation	2	191	RR = 1.47, [1.18,1.84]	0	Fixed
	Shortness of breath	2	193	RR = 1.53, [1.24,1.88]	0	Fixed
	Asthenia	2	221	RR = 1.69, [0.83, 3.43]	90%	Random

Note: AMI, acute myocardial infarction; CI, confidence interval; MD, mean difference; NST, number of ST-segment depression; RCT, randomized controlled trial; RR, risk ratio; UA, unstable angina.

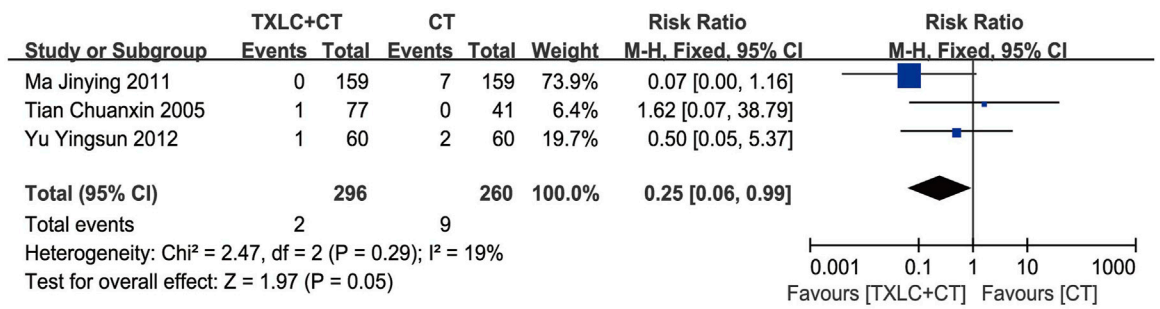

FIGURE 5 | Meta-analysis of the all-cause mortality using TXLC Plus CT vs. CT.

TABLE 3 | The incidences of main adverse effects and of TXLC Plus CTs *vs.* CTs

Adverse effects	TXLC plus CTs		Studies	CTs		Studies
	Adverse effect (n)	Trials(n)		Adverse effect (n)	Trials(n)	
Gastrointestinal symptoms such as bloating, belching, nausea, loss of appetite, acid reflux, and dull pain	41	11	Cui (2008), Du (2016), Liu and An (2016), Ma et al. (2011), Tian and Xu (2005), Wang and Li (2007), Wang et al. (2009), Wu (2011), Wu S. J. et al. (2006), Xin et al. (2008), Zhou (2013)	5	1	Liu and An (2016)
Hypotension	1	1	Yang et al. (2019)	2	1	Yang et al. (2019)
Bleeding gums	2	2	Ma et al. (2011), Wang and Li (2007)	0	0	no
Bradycardia	1	1	Yang et al. (2019)	1	1	Yang et al. (2019)

Note: TXLC, Tongxinluo capsule; CTs, conventional treatments.

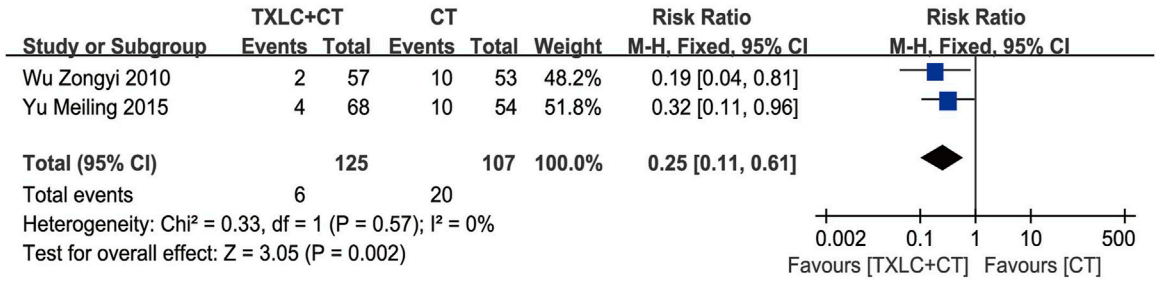

FIGURE 6 | Meta-analysis of recurrence of angina using TXLC Plus CT vs. CT.

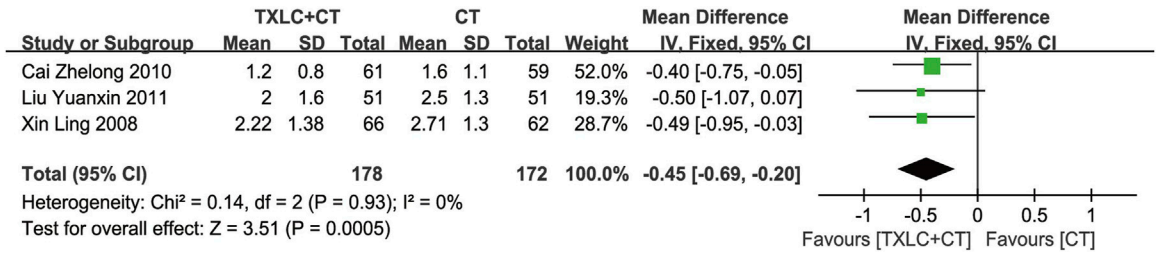

FIGURE 7 | Meta-analysis of NST using TXLC Plus CT vs. CT.

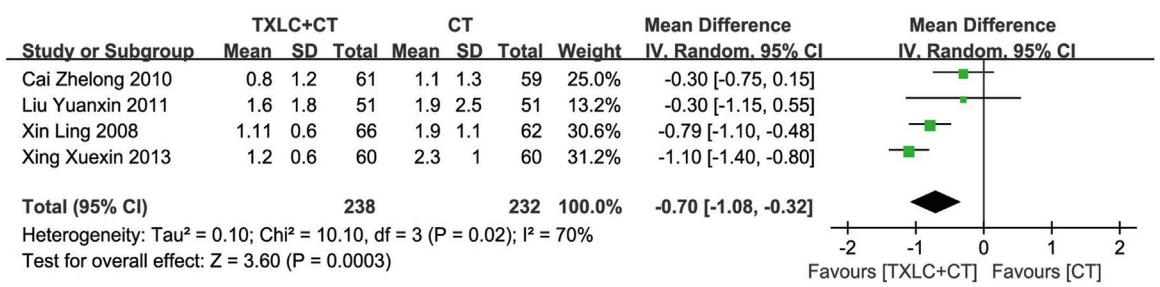

FIGURE 8 | Meta-analysis of ∑ST using TXLC Plus CT vs. CT.

high between-trial heterogeneity was shown (χ^2 = 21.01, p = 0.0001; I^2 = 86%), a random effect model was performed. Meta-analysis showed that conventional drugs combined with TXLC significantly reduced serum hs-CRP [MD = -2.86, 95% CI (−3.73, −1.99), p < 0.00001, **Figure 12**].

NO Level

Evidence from pooled analysis across two studies (Yang., 2008; Chang et al., 2018) showed that TXLC plus CTs produced greater increase of the plasma level of NO over CTs [MD = 11.67, 95% CI (8.33, 15.02), p < 0.00001, **Figure 13**] with no significant heterogeneity (χ^2 = 1.50, p = 0.22; I^2 = 33%).

Sensitivity Analysis

When discussing hs-CRP and ∑ST, the analysis results showed high between-trial heterogeneities, so sensitivity analyses were implemented by excluding each study. After inspecting, the heterogeneity of hs-CRP decreased from I^2 = 86% to I^2 = 29% after excluding Li Q. et al. (2018). When Xing (2013) was excluded in ∑ST, the heterogeneity decreased from I^2 = 70% to I^2 = 45%. Both indicators' heterogeneities were reduced from a high level to less than 50%, indicating that the results of hs-CRP and ∑ST were not stable enough.

After rechecking the data, the possible sources of heterogeneities of the two indicators were discovered. The serum hs-CRP concentration before treatment recorded by Li Q. et al. (2018) was not significantly different from the other three studies. After treatment, the average hs-CRP concentration of the two groups was lower than other included trials, the average concentration of the trial group even dropped to 2.41 mg/L. After excluding the influence of the patients' baseline and medication course, three possible sources of heterogeneity were inferred: 1) The total daily dose of TXLC in Li Q. et al. (2018) was 6, which was the lowest of

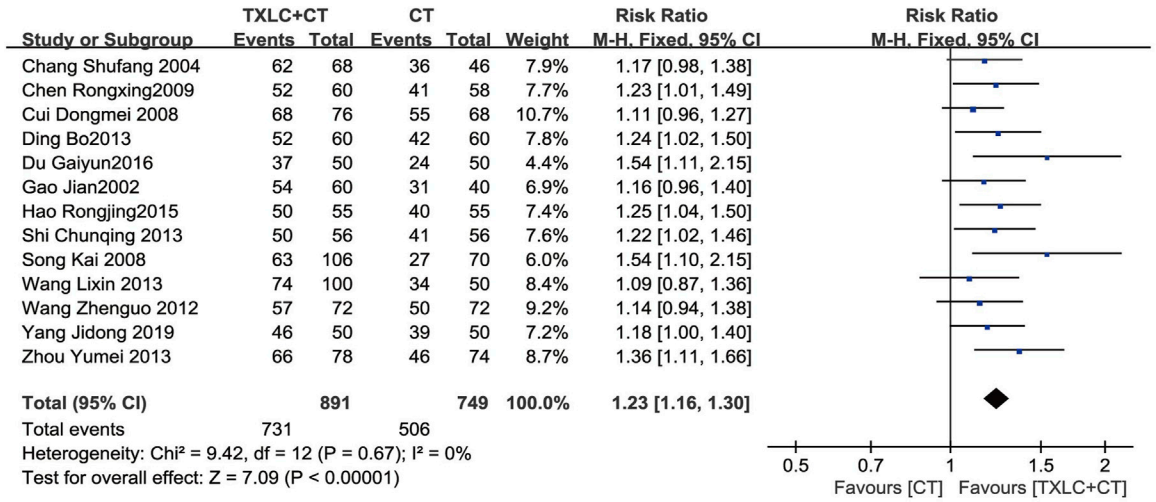

FIGURE 9 | Meta-analysis of ECG improvement using TXLC Plus CT vs. CT.

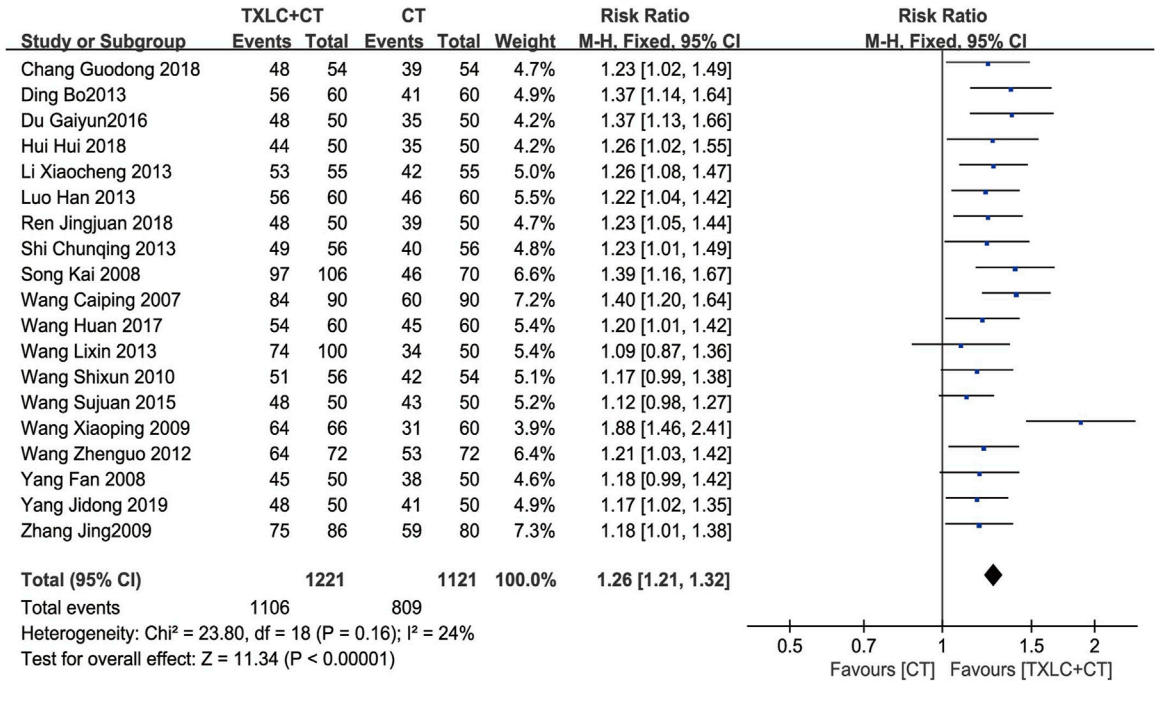

FIGURE 10 | Meta-analysis of the clinical efficacy in UA using TXLC Plus CT vs. CT.

the three groups; 2) Specific CTs programs were not mentioned, and there were differences in the version and content of the diagnostic criteria between the 4 RCTs; 3) Errors occurred in the process of testing and data recording. It is known that the hs-CRP level in patients with coronary heart disease is relatively high, while the average value of the Li Q. et al. (2018) treatment group was very close to the normal standard. As the authors of the original article were uncontactable, the main source of the heterogeneity has not yet been determined. Regarding ∑ST, no obvious source of heterogeneity was found except for the differences in the UA diagnostic criteria of the 4 RCTs. The forest plot was shown in **Supplementary Material S4**.

Publication Bias

The number of RCTs included in the ECG improvement and clinical efficacy in UA were 13 and 19, which were greater than

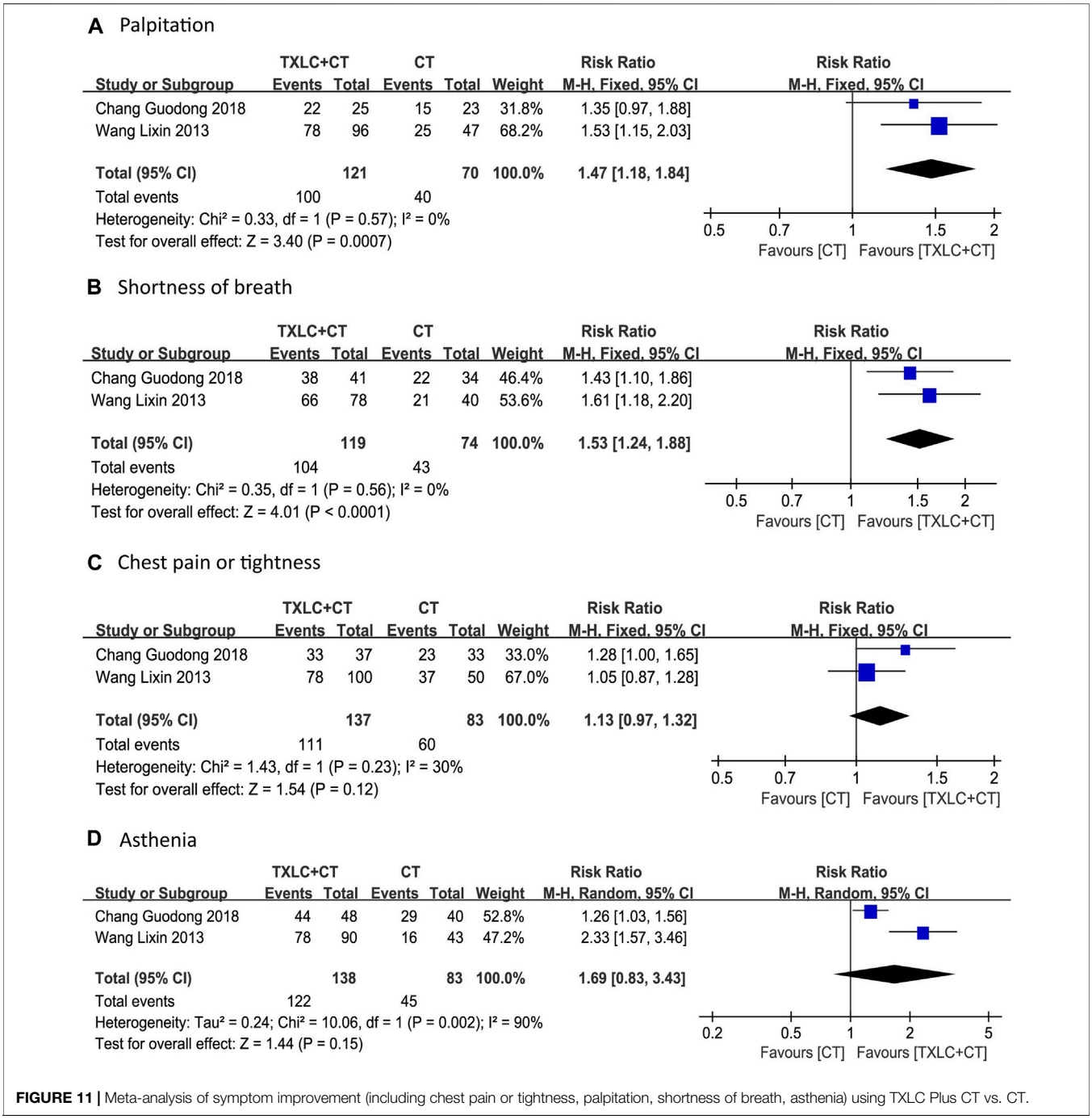

FIGURE 11 | Meta-analysis of symptom improvement (including chest pain or tightness, palpitation, shortness of breath, asthenia) using TXLC Plus CT vs. CT.

10, so funnel plots were constructed to assess potential publication bias. Since funnel plots of both indicators showed slight asymmetries in the scatter distribution, it was considered that certain degree of publication biases might exist. This conclusion was consistent with the Begg (ECG improvement: Z = 2.01, $p = 0.044$; angina pectoris efficacy: Z = 1.61, $p = 0.108$) and Egger tests (ECG improvement: t = 3.45, $p = 0.005$; angina pectoris efficacy: t = 2.62, $p = 0.018$), which indicated that there should be publication biases to a certain extent. Factors such as insufficient sample sizes and the lack of reporting on negative results were the possible causes of publication biases (**Figures 14A–C**, **Figures15A–C**).

DISCUSSION

Summary of Main Results (Benefits and Harms)

A total of 5421 UA patients in 42 RCTs were included in this systematic review. Meta-analysis showed that TXLC, as an

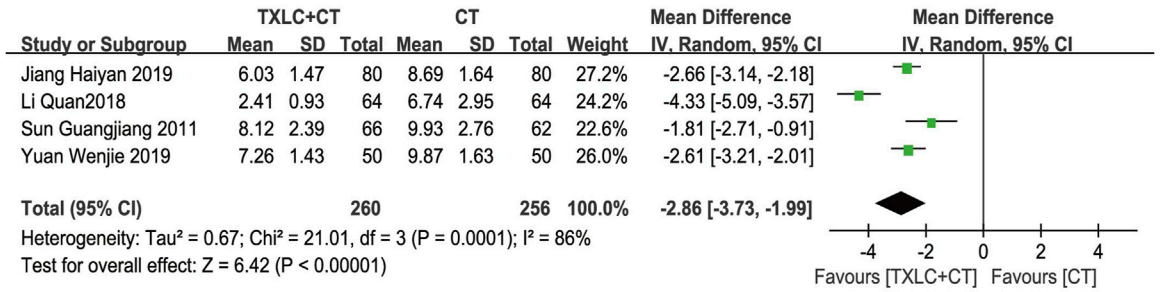

FIGURE 12 | Meta-analysis of hs-CRP level using TXLC Plus CT vs. CT.

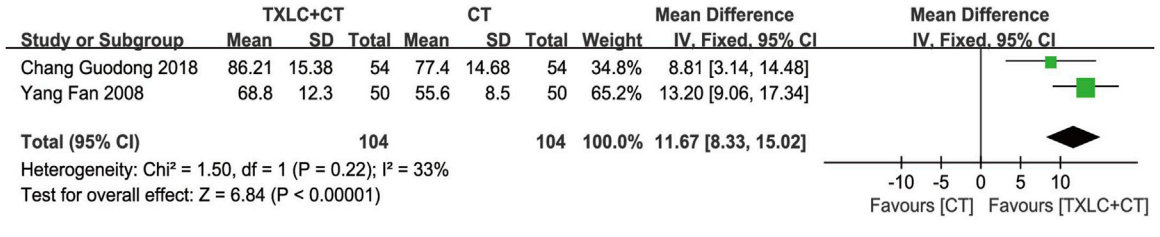

FIGURE 13 | Meta-analysis of NO level using TXLC Plus CT vs. CT.

adjunct to CT, reduced the incidence of cardiovascular events and all-cause mortality, improved ECG performance, and relieved angina symptoms and other accompanying symptoms. It also showed beneficial effects on regulating serum hs-CRP level and plasma NO concentration. Oral TXLC medication caused few adverse effects with mild symptoms, which were mostly eliminated by adjusting the medication course, reducing the dose, or giving symptom-relieving drugs. Few patients chose to withdraw from the clinical trials on account of unbearable adverse effects. Among all the results, only the concentrations of hs-CRP (I^2 = 86%) and ∑ST (I^2 = 70%) demonstrated high heterogeneities. Except for the improvement of chest pain and tightness and asthenia, all intergroup differences of the remaining results showed statistical significance.

Meta-analysis revealed that TXLC was beneficial to reducing UA endpoint events. The general incidence of cardiovascular events in the trial group was lower than that in the control group without between-trial heterogeneity, and the result manifested good stability in the sensitivity analysis. It is noteworthy that except for two studies (Ma et al., 2011; Yu and Hu., 2012) not recording the duration of treatment, the follow-up times of the other 4 studies (Wu et al., 2010; Wu., 2011; Wang et al., 2013; Yu and Chen., 2015) were 6 months, 10 months, 4 weeks and 1 year. Further comparison showed that the endpoint event rate of UA patients with a 1 year course of treatment was 3.3%, which was the lowest among the 4 trials, and notably, the trial with 6 months course of treatment had 5.5 times end point event rate in the control group higher than that of the trial group (Wu et al., 2010). Based on this, it was speculated that TXLC had the potential to reduce endpoint events in both long-term and short-term adjuvant treatments. In this meta-analysis, 6 months and above TXLC treatment showed better effect in reducing cardiovascular events. However, under the limitation of incomplete data, it was hard to fully conclude that the curative effect was proportional to the treatment time. When analyzing all-cause mortality and cardiovascular mortality, two analogical results appeared. After comparing all included RCTs, it was found that one RCT reported an accidental death case in the trial group, which was the only difference between all cases of the two indicators. Thus, no definitive conclusions could be drawn on TXLC reducing all-cause mortality of UA when it worked as an adjunct to CTs.

Additionally, TXLC had a good performance in reducing UA recurrence, improving ECG parameters and alleviating angina symptoms. Two RCTs showed that the rate of UA recurrence in the trial group was only 25% of that in the control group, suggesting that TXLC might better prevent UA recurrence. In terms of ECG parameters, TXLC was found to significantly reduced the degree of myocardial ischemia in UA by reducing the ST-segment depression number and the total depression distance with an average of 0.45 and 0.70 mm, respectively. The ECG improvement was defined as an elevation of the ST-segment over 0.05 millivolt. Among 13 RCTs, 731 (82.0%) of 891 patients undergoing TXLC treatment showed improvement in ECG, while 506 (67.6%) of 749 patients treated with conventional drugs exhibited effective responses, indicating striking differences in efficacy between groups. As the clinical efficacy in UA was the most frequently reported indicator, the results showed that 1,106 out of 1,221 patients treated with TXLC demonstrated reduced

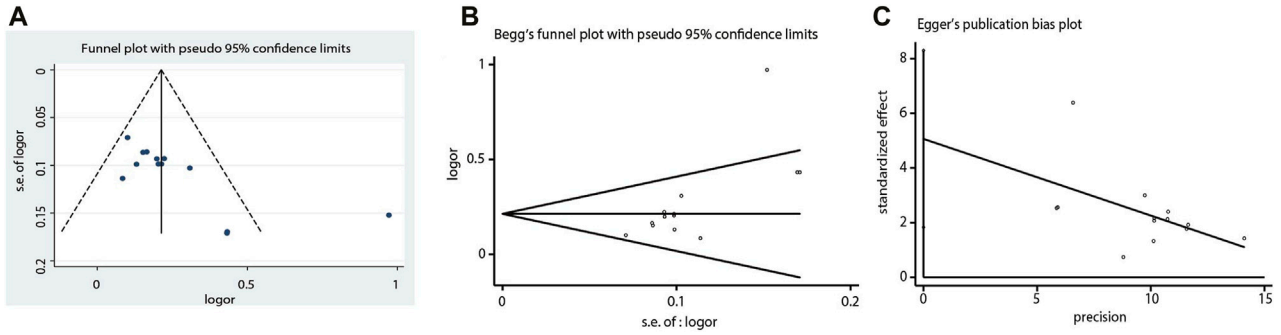

FIGURE 14 | Funnel plot, Begg's funnel plot and Egger's publication bias plot of the ECG improvement.

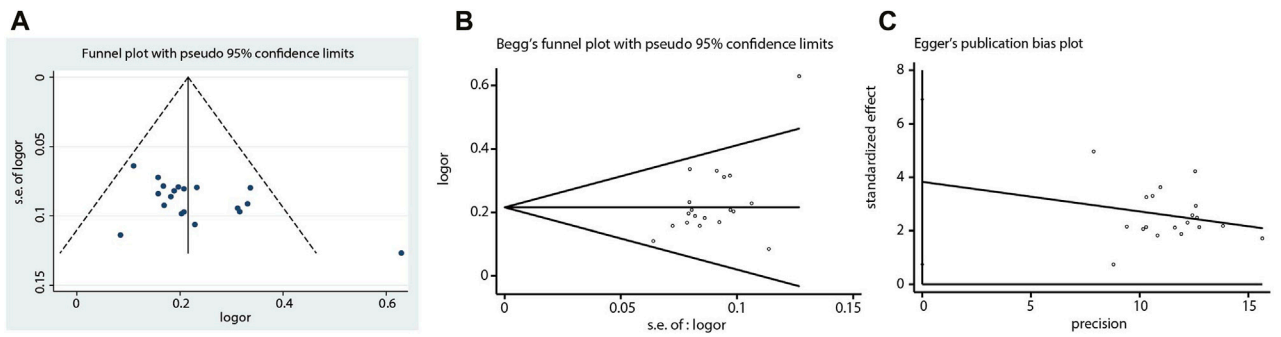

FIGURE 15 | Funnel plot, Begg's funnel plot and Egger's publication bias plot of the clinical efficacy in UA.

symptoms of angina, which reached 90.58% effective rate and better than 72.17% in the control group. It was also found that taking TXLC based on CTs significantly improved a series of symptoms of UA including chest pain or tightness, palpitations, shortness of breath, and asthenia. However the improvement of chest pain or tightness and asthenia presented a high degree of heterogeneity, which might attribute to the inconsistency of the baseline. Based on the above analysis, TXLC showed improvement on the overall efficacy as an auxiliary treatment, which might rely on its multitarget and multichannel mode of action (Wang et al., 2021).

Another valuable finding was the effects of TXLC on regualating hs-CRP and NO levels. As an acute-phase protein synthesized under an inflammatory state, hs-CRP is of diagnostic and prognostic value for acute coronary syndrome. In this study, the trial group supplemented with TXLC reduced the serum hs-CRP level in UA patients by 2.86 mg/L compared with that of the control group. However, the results showed high heterogeneity ascribed to low trial quality and unmeasured hs-CRP baselines. Nitrates are known to exert their vasodilation and anti-angina effects by converting to NO in the body, and traditional Chinese medicine may regulate NO concentration through multiple pathways. Experimental evidence has shown that TXLC regulates NO synthesis by changing the activity of endothelial NO synthase, thereby protecting the myocardium from ischemia/reperfusion injury. Two RCTs included in this study recorded plasma NO levels. Compared with the control group, the plasma NO level of the trial group increased 11.67 μmol/L, showing that TXLC could regulate NO synthesis, which related to its effects of promoting vascular endothelial repair, improving endothelial cell function, reducing vascular tone and ameliorating coronary blood supply (Liu et al., 1996).

Safety of TXLC is of great concern because of its wide application. No serious adverse effect were mentioned in the included studies, while 4 adverse effects were described in 22 RCTs, including gastrointestinal reactions, hypotension, gum bleeding and palpitation. Gastrointestinal discomfort was the most frequently reported adverse effect. Eleven RCTs reported gastrointestinal reactions in the trial group, and the treatment was interrupted in 9 patients in 2 trials (Yang., 2008; Wang et al., 2010) due to intolerance. Even though most of the side effects could be eliminated or alleviated through dose reduction, medication time adjustment and symptomatic remedy, the non-negligible proportion of the patients who discontinued treatment due to gastrointestinal reactions (9/41) deserve further attention. In addition, 1 RCT reported hypotension and bradycardia in both trial and control groups and there was no statistically significant difference in the total incidence of adverse effects between the two groups (Yang et al., 2019). Owing to the differences in age, gender, course of the disease, comorbidities in UA and the CT regimens among the included studies, the correlation between these factors and the incidence of adverse effects was analysized. But apart from the regimen of CTs,

no direct relationship between other factors and adverse effects has been found. It is worth noting that in 11 studies with gastrointestinal symptoms, aspirin was used as CTs in 8 studies (Tian and Xu., 2005; Wang and Li., 2007; Cui., 2008; Xin et al., 2008; Ma et al., 2011; Zhou., 2013; Du., 2016; Liu and An., 2016), clopidogrel was used as CT in 1 study (Wu., 2011), atorvastatin, simvastatin or other lipid-lowering drugs was used as CTs in another 5 studies (Tian and Xu., 2005; Cui., 2008; Wu., 2011; Zhou., 2013; Liu and An., 2016). Although gastrointestinal discomforts are the side effects of anticoagulants and lipid-lowering drugs (Sugisaki et al., 2018; Zhao, 2020), only 1 of the 11 RCTs (Liu and An., 2016) reported gastrointestinal discomforts in the control group, indicating the occurrence of gastrointestinal discomforts in the trial group might not be attributed to the CTs intervention. Similarly, bleeding, another side effects in UA treatment, did not reported in the control group of the included studies. In summary, the difference in CTs composition might not be a source of bias on adverse effects for this meta-analysis.

Consistency and Disagreement with Other Researches or Reviews

Three previous meta-analyses (one in English and 2 in Chinese) of TXLC for UA patients were retrieved (Wu T. et al., 2006; Wu et al., 2018; Yang et al., 2021). After comparing the previous work with the present one vertically and horizontally, all studies indicated that UA patients treated with TXLC as an auxiliary therapy had better clinical outcomes on angina and ECG than those treated with CTs only, and most of the results showed low heterogeneity despite the low quality of the studies included.

The difference between the 4 meta-analyses was first reflected in the changes in the number, quality, and outcome indicators of the included studies. The meta-analysis published in the Cochrane Library in 2006 compared the incidence of cardiovascular events, sudden death, and angina pectoris scores between TXLC and CTs for the first time (Wu T. et al., 2006). The analysis showed TXLC had no advantages over conventional drugs in reducing the incidence of cardiovascular events, decreasing the risk of sudden death, or improving the angina pectoris score, which were different from the positive results in the present study. These inconsistencies might be partially due to the small sample size, high heterogeneity, and the limited number of included studies. This meta-analysis also reported that TXLC alleviated the onset of acute angina pectoris, and reduced the consumption of nitroglycerin as well despite the high heterogeneity (Wu T. et al., 2006). Besides, both TXLC and isosorbide mononitrate showed a reduced effect on endothelin level, and no significant quantitative difference was found between them (Wu T. et al., 2006). The meta-analysis published in 2018 only reported the efficacies of TXLC on angina pectoris and ECG, but included more high-quality studies compared with the previous one (Wu T. et al., 2006; Wu et al., 2018). Both meta-analyses confirmed that the combination of TXLC and CTs showed better effects than CTs alone on reducing the degree of angina and improving ECG. In 2020, a meta-analysis further expanded the number of included studies (Yang et al., 2021), which included indicators of hs-CRP, vascular endothelial cytokines, blood lipids and hemodynamics, indicating that TXLC might play a macroscopic role in treating UA through mechanisms of anti-inflammatory, anticoagulant, antioxidant, or endothelial protection. Today, based on a large amount of clinical data, this article investigated TXLC's impact on UA endpoint events, and comprehensively summarized its adverse effects and the corresponding mitigation methods as well as the effects of TXLC on the recurrence of angina pectoris after recovery, the improvement of the overall symptoms, and NO level. The results confirmed that TXLC could reduce the occurrence of UA endpoint events and angina recurrence after recovery, improve the symptoms of UA, and increase the level of serum NO. Compared with 3 previous meta-analyses, this meta-analysis not only overturned the previous conclusion that TXLC was not effective for UA cardiovascular events, but also indicated the improvement of TXLC on angina pectoris sypmtoms, ECG, hs-CRP level, etc. New indicators were also observed, for example, symptoms of UA, providing additional evidence-based medicine data support for TXLC in the treatment of UA. However, a sample size of no less than 100 was set in this study in order to improve the accuracy of estimates. As a result, many of the indicators in the unqualified study were not selected, possibly leading to the limitations in this research.

Another rule found along the timeline was the change in follow-up times. In the meta-analysis of 2006, 15 of 18 studies on TXLC had a follow-up time no longer than 4 weeks, while the longest follow-up time was 8 weeks reported in 2018, which reached to 24 weeks in 2020. In the present study, the follow-up time was extended to as long as 10 months or even to 1 year. Therefore, although it still needs improvements on the scale and quality of long-term follow-up studies, the present work does contribute to the conclusion of long-term effects of TXLC intervention for UA. But it should not be neglected that the quality of RCTs in the above-mentioned 3 meta-analyses was an inescapable key weakness (Wu T. et al., 2006; Wu et al., 2018; Yang et al., 2021), which might directly affect the reliability of evidence-based medicine. High-quality and large-scale trials are essential for obtaining mature and stable evidence-based conclusions which will provide better guidance for clinical practice.

Limitations

1) Comprehensive searches was conducted in the designated database without restricting language, ethnicity, or literature type. Since proprietary Chinese medicines have not been promoted globally, all participants ultimately included were Chinese due to the limitation of application scope.
2) The sample size was strictly limited to no less than 100 people, which led to the abandonment of some observation indicators included in small-sample studies, and several preset outcome indicators were finally discarded for the absence of the corresponding research.
3) Among the 42 studies included, only 7 of them used the random sequence generation method with high allocation concealment risk, and 1 reported the use of blinding. The

related authors were contacted for details of allocation concealment and randomization methods, but no receivedwas responsed.

4) All participants had complete general information, and the between-group difference at baseline was not statistically significant. However, the difference in follow-up times and conventional prescriptions was likely to be one of the heterogeneity sources.
5) The patients from some of the included trials only received single-agent therapy which did not conform to standard treatment protocols (Wang et al., 2009; Li Q. et al., 2018). This might affect the efficacy of TXLC and lead to false-positive results.
6) Among all trials included, most of the follow-up times were within 3 months, and the longest one was only 1 year (Yu and Chen., 2015). The long-term benefit of TXLC for UA patients cannot be scaled.

CONCLUSION

Taken together, this meta-analysis showed that TXLC could reduce the rate of cardiovascular, all-cause mortality and the number and summation of ST-segment depression, decreased serum hs-CRP level, improved the ECG abnormalities and clinical efficacy in UA, relieved the UA symptoms, as well as increased plasma NO concentrations. As an adjunctive treatment for UA, TXLC had a wide range of clinical effects, remarkable efficacy and good stability. Nevertheless, even if no serious adverse effects have been found, discomforts such as gastrointestinal symptoms, bleeding gums, bradycardia, and hypotension still occurred at an inconvenient low frequency. Therefore, no definitive conclusions can be drawn on its absolute safety so far, and medical staff should pay close attention to its administration.

Currently, the clinical efficacy of TXLC for UA is mainly validated *via* randomized or semi-randomized controlled trials. Inherent problems such as the high risk of bias, low quality of evidence and small samples are likely to exist. The insufficient evidence in the clinical studies of TXLC can be ameliorated by expanding the sample size and carrying out multicenter studies. It is hoped the remedies for poor quality evidence will be found early, and that more attention will be paid to the quality of life, compliance and cost acceptance in future clinical trials.

DATA AVAILABILITY STATEMENT

The original contributions presented in the study are included in the article/**Supplementary Material**, further inquiries can be directed to the corresponding authors.

AUTHOR CONTRIBUTIONS

Study determination and scheme design: WC, QX, and PL. Literature screening and data extraction: PL, JH, YW, and YM. Data analysis and interpretation: PL, QX, RY, SM-YL, SL, and WC. Article writing: PL, QX, and WC. Article review and final approval: all authors.

FUNDING

This work was partially supported by the Joint Innovation Program of China Academy of Chinese Medical Sciences (CACMS, ZZ11-061); CACMS Innovation fund (CI2021A00914); Nursery Project of Xiyuan Hospital of CACMS (2019XYMP-10); National Natural Science Foundation of China (82004193). Joint Innovation Program of CACMS (ZZ11-061), project director: WC; CACMS Innovation fund (CI2021A00914), project director: WC; Nursery Project of Xiyuan Hospital of CACMS (2019XYMP-10), project director: QX; National Natural Science Foundation of China (82004193), project director: RY.

SUPPLEMENTARY MATERIAL

The Supplementary Material for this article can be found online at: https://www.frontiersin.org/articles/10.3389/fphar.2021.742978/full#supplementary-material

REFERENCES

Begg, C. B., and Mazumdar, M. (1994). Operating Characteristics of a Rank Correlation Test for Publication Bias. *Biometrics.* 50, 1088–1101. doi:10.2307/2533446

Cai, Z. L., and Li, M. F. (2010). Tongxinluo Capsule in Treating 61 Cases of Unstable Angina Pectoris. *Chin. Forgn. Med.* 29, 107. doi:10.3969/j.issn.1674-0742.2010.33.081

Cannon, C. P., Battler, A., Brindis, R. G., Cox, J. L., Ellis, S. G., Every, N. R., et al. (2001). American College of Cardiology Key Data Elements and Definitions for Measuring the Clinical Management and Outcomes of Patients With Acute Coronary Syndromes. A Report of the American College of Cardiology Task Force on Clinical Data Standards (Acute Coronary Syndromes Writing Committee). *J. Am. Coll. Cardiol.* 38, 2114–2130. doi:10.1016/s0735-1097(01)01702-8

Chang, G. D., Chen, Y. W., Xu, X. S., and Wang, Y. (2018). Study on the Efficacy and Mechanism of Tongxinluo Capsule in the Treatment of Coronary Heart Disease. *Chin. J. Evid. Bas. Cardiol. Med.* 10, 729–732. doi:10.3969/j.issn.1674-4055.2018.06.24

Chang, S. F., and Zhao, M. (2004). Clinical Observation on Treatment of 68 Cases of Unstable Angina With Tongxinluo Capsule. *Mod. J. Int. Tradit. Chin. West. Med.* 13, 189. doi:10.3969/j.issn.1008-8849.2004.02.040

Chasman, D. I., Posada, D., Subrahmanyan, L., Cook, N. R., Stanton, V. P., and Ridker, P. M. (2004). Pharmacogenetic Study of Statin Therapy and Cholesterol Reduction. *JAMA.* 291, 2821–2827. doi:10.1001/jama.291.23.2821

Chen, R. X., and Li, L. L. (2009). Intervention Effect of Tongxinluo Capsule on Unstable Angina Pectoris. *Guiz Med.* 33, 923–924. doi:10.3969/j.issn.1000-744X.2009.10.030

Chen, Z. Q., Hong, L., Wang, H., and Yin, Q. L. (2016). Effects of Tongxinluo Capsule on Platelet Activating Factor, Vascular Endothelial Function, Blood Flow of Thrombolysis in Myocardial Infarction in Acute Myocardial Infarction

Patients after Delayed Percutaneous Coronary Intervention. *Zhongguo Zhong Xi Yi Jie He Za Zhi.* 36, 415–420. doi:10.7661/CJIM.2016.04.0415

Cui, D. M. (2008). Clinical Observation of Tongxinluo Capsule in the Treatment of Unstable Angina Pectoris. *Chin. Heal. Car.* 16, 594–595.

Ding, B., Fang, Z. G., and Ren, A. L. (2013). Observation of Therapeutic Effect of Tongxinluo Capsule on Unstable Angina Pectoris. *J. Med. Forum.* 34, 25–27.

Du, G. Y. (2016). The Clinical Effect of Aspirin Combined With Tongxinluo in the Treatment of Unstable Angina Pectoris. *Chin. Pres. Drug.* 14, 48–49. doi:10.3969/j.issn.1671-945X.2016.04.032

Egger, M., Davey Smith, G., Schneider, M., and Minder, C. (1997). Bias in Meta-Analysis Detected by a Simple, Graphical Test. *BMJ.* 315, 629–634. doi:10.1136/bmj.315.7109.629

Gao, J., Hui, B., Zhang, Y. C., and Zhao, H. L. (2002). Clinical Observation of Tongxinluo Capsule in the Treatment of 60 Cases of Unstable Angina Pectoris. *J. Binz. Med. Univ.* 25, 143–144. doi:10.3969/j.issn.1001-9510.2002.02.031

Hao, R. J. (2015). Clinical Observation of Tongxinluo Capsule in the Treatment of Coronary Heart Disease Complicated With Unstable Angina Pectoris. *Pro. 11th. Int. Symp. Coll. Dis. Theor.*, 212–213.

Helgason, C. M., Bolin, K. M., Hoff, J. A., Winkler, S. R., Mangat, A., Tortorice, K. L., et al. (1994). Development of Aspirin Resistance in Persons With Previous Ischemic Stroke. *Stroke.* 25, 2331–2336. doi:10.1161/01.str.25.12.2331

Hui, H., Zhang, M., Peng, Z. G., Liao, Mei., Ji, Meng., and Wu, G. P. (2018). The Effect of Tongxinluo Capsule on Myocardial Enzymes and Electrocardiogram in Patients with Unstable Angina Pectoris. *Chin. J. Ger.* 38, 2080–2082. doi:10.3969/j.issn.1005-9202.2018.09.014

Jia, Y., and Leung, S. W. (2015). Comparative Efficacy of Tongxinluo Capsule and Beta-Blockers in Treating Angina Pectoris: Meta-Analysis of Randomized Controlled Trials. *J. Altern. Complement. Med.* 21, 686–699. doi:10.1089/acm.2014.0290

Jiang, H. Y., Li, F., and Zhao, X. S. (2019). The Efficacy of Tongxinluo Combined With Atorvastatin in the Treatment of Unstable Angina Pectoris of Coronary Heart Disease and its Influence on High-Sensitivity C-Reactive Protein. *Chin. J. Mod. Drug App.* 13, 57–59. doi:10.14164/j.cnki.cn11-5581/r.2019.17.033

Li, G., Xu, Q., Han, K., Yan, W., and Huang, C. (2020). Experimental Evidence and Network Pharmacology-Based Analysis Reveal the Molecular Mechanism of Tongxinluo Capsule Administered in Coronary Heart Diseases. *Biosci. Rep.* 40, BSR20201349. doi:10.1042/BSR20201349

Li, M., Li, C., Chen, S., Sun, Y., Hu, J., Zhao, C., et al. (2018). Potential Effectiveness of Chinese Patent Medicine Tongxinluo Capsule for Secondary Prevention After Acute Myocardial Infarction: A Systematic Review and Meta-Analysis of Randomized Controlled Trials. *Front. Pharmacol.* 9, 830. doi:10.3389/fphar.2018.00830

Li, Q., Chen, G. N., and Gao, W. K. (2018). Effects of Tongxinluo Capsule Combined With Atorvastatin on Blood Lipids and Inflammatory Factors in Elderly Patients With Unstable Angina Pectoris of Coronary Heart Disease. *Chin. Pharm.* 27, 32–34. doi:10.3969/j.issn.1006-4931.2018.14.011

Li, X. C. (2013). Tongxinluo Combined With Atorvastatin in the Treatment of Unstable Angina Pectoris and its Effect on Blood Lipids and Coagulation. *Chin. J. Prim. Med. Pharm.* 20, 3635–3636. doi:10.3760/cma.j.issn.1008-6706.2013.23.054

Liu, H. X., Deng, X. R., Jin, M., Jin, J. S., Huang, L. J., and Xia, J. (1996). Plasma Endothelin and Nitric Oxide Levels in Patients With Unstable Angina Pectoris and the Effect of Traditional Chinese Medicine Treatment. *Chin. J. Int. Tradit. Chin. West. Med.* 10, 585–587.

Liu, S. G., and An, J. (2016). Observation of the Clinical Effect of Atorvastatin Combined With Tongxinluo Capsule in the Treatment of Unstable Angina Pectoris of Coronary Heart Disease. *Chin. J. Clin. Rat. Drug Us.* 9, 3–4. doi:10.15887/j.cnki.13-1389/r.2016.05.002

Liu, Y. X. (2011). Efficacy of Tongxinluo Combined With Heparin in the Treatment of Unstable Angina Pectoris. *Cont. Med.* 17, 12–13. doi:10.3969/j.issn.1009-4393.2011.8.007

Luo, H. (2013). Efficacy Observation of 60 Cases of Unstable Angina Pectoris Treated With Metoprolol Tartrate Combined With Tongxinluo Capsule. *Guid. Chin. Med.* 11, 588–589. doi:10.3969/j.issn.1671-8194.2013.21.455

Ma, J. Y., Liu, L. L., and Ru, C. (2011). Clinical Study of Tongxinluo Capsule in the Treatment of Unstable Angina Pectoris. *Jil. Med.* 32, 2154–2155. doi:10.3969/j.issn.1004-0412.2011.11.052

Ma, Q., Zhang, S., Ning, Y., Pu, X., Yu, G., Zheng, Z., et al. (2009). Effect of Tongxinluo on Endothelial Function and Hypersensitive C-Reactive Protein in Acute Coronary Syndrome Patients Undergoing Percutaneous Coronary Intervention. *Zhong Nan Da Xue Xue Bao Yi Xue Ban.* 34, 550–554. doi:10.3321/j.issn:1672-7347.2009.06.016

Mao, C., Fu, X. H., Yuan, J. Q., Yang, Z. Y., Chung, V. C., Qin, Y., et al. (2015). Tong-xin-Luo Capsule for Patients With Coronary Heart Disease After Percutaneous Coronary Intervention. *Cochrane Database Syst. Rev.* 21, CD010237–59. doi:10.1002/14651858

Mao, H. M., Liu, M., Qu, H., Wang, L. Q., and Shi, D. Z. (2018). Tongxinluo Capsule () for Cardiac Syndrome X: A Systematic Review and Meta-Analysis. *Chin. J. Integr. Med.* 24, 296–303. doi:10.1007/s11655-017-2762-8

Meng, Z. H., Jiang, X. G., Zhao, S. H., Li, Y. H., Jia, J. M., and Ma, Z. S. (2014). Study on UPLC Fingerprint of Tongxinluo Capsules. *Chin. J. Exp. Tradit. Med. Form.* 20, 56–58. doi:10.11653/syfj2014030056

Münzel, T., Daiber, A., and Gori, T. (2011). Nitrate Therapy: New Aspects Concerning Molecular Action and Tolerance. *Circulation.* 123, 2132–2144. doi:10.1161/CIRCULATIONAHA.110.981407

Page, M. J., McKenzie, J. E., Bossuyt, P. M., Boutron, I., Hoffmann, T. C., Mulrow, C. D., et al. (2021). The PRISMA 2020 Statement: An Updated Guideline for Reporting Systematic Reviews. *Int. J. Surg.* 88, 105906–105909. doi:10.1016/j.ijsu.2021.105906

Ren, J. J., Guo, P., and Li, X. L. (2018). Efficacy Analysis of Aspirin Combined With Tongxinluo in the Treatment of Unstable Angina Pectoris. *Electr. J. Clin. Med. Lit.* 5, 72. doi:10.3877/j.issn.2095-8242.2018.31.061

Roth, G. A., Mensah, G. A., Johnson, C. O., Addolorato, G., Ammirati, E., Baddour, L. M., et al. (2020). Global Burden of Cardiovascular Diseases and Risk Factors, 1990-2019: Update From the GBD 2019 Study. *J. Am. Coll. Cardiol.* 76, 2982–3021. doi:10.1016/j.jacc.2020.11.010

Serebruany, V. L., Steinhubl, S. R., Berger, P. B., Malinin, A. I., Bhatt, D. L., and Topol, E. J. (2005). Variability in Platelet Responsiveness to Clopidogrel Among 544 Individuals. *J. Am. Coll. Cardiol.* 45, 246–251. doi:10.1016/j.jacc.2004.09.067

Shi, C. Q. (2013). The Clinical Effect of Trimetazidine Combined with Tongxinluo Capsules on Unstable Angina Pectoris. *Chin. Med. Guid.* 15, 82–83. doi:10.3969/j.issn.1009-0959.2013.01.052

Song, K., Li, X. P., and Xu, G. Y. (2008). Efficacy of Tongxinluo in the Treatment of Unstable Angina Pectoris in the Elderly. *J. Changzh. Med. Col.* 22, 109–110. doi:10.3969/j.issn.1006-0588.2008.02.010

Sterne, J. A., and Egger, M. (2001). Funnel Plots for Detecting Bias in Meta-Analysis: Guidelines on Choice of Axis. *J. Clin. Epidemiol.* 54, 1046–1055. doi:10.1016/s0895-4356(01)00377-8

Sugisaki, N., Iwakiri, R., Tsuruoka, N., Sakata, Y., Shimoda, R., Fujimoto, S., et al. (2018). A Case-Control Study of the Risk of Upper Gastrointestinal Mucosal Injuries in Patients Prescribed Concurrent NSAIDs and Antithrombotic Drugs Based on Data from the Japanese National Claims Database of 13 Million Accumulated Patients. *J. Gastroenterol.* 53, 1253–1260. doi:10.1007/s00535-018-1483-x

Sun, G. J., Wang, Y., and Gao, H. (2011). The Effect of Tongxinluo Capsule on Unstable Angina Pectoris and its Effect on High-Sensitivity C-Reactive Protein. *Mod. J. Int. Tradit. Chin. West. Med.* 20, 1613–1614. doi:10.3969/j.issn.1008-8849.2011.13.030

The Writing Committee of the Report on Cardiovascular Health Diseases in China (2020). Summary of China Cardiovascular Health and Disease Report 2019. *Chin. Circ.* 35, 833–854. doi:10.3969/j.issn.1000-3614.2021.06.001

Tian, C. X., and Xu, Y. (2005). The Effect of Tongxinluo Capsule on C-Reactive Protein in Patients with Unstable Angina Pectoris. *J. Bethune Mil. Med. Coll. J. Beth. Med. Sci.* 3, 93–94. doi:10.3969/j.issn.1672-2876.2005.02.012

Tian, F. X., Wu, K. J., and Zhu, H. C. (2007). Efficacy of Tongxinluo Capsule in Treating 60 Cases of Unstable Angina Pectoris of Coronary Heart Disease. *Chin. Prac. Med.* 36, 158–159. doi:10.3969/j.issn.1673-7555.2007.36.110

Wang, B., Yang, Q., Bai, W. W., Xing, Y. F., Lu, X. T., Sun, Y. Y., et al. (2019). Correction: Tongxinluo Protects Against Pressure Overload-Induced Heart Failure in Mice Involving VEGF/Akt/eNOS Pathway Activation. *PLoS One.* 14, e0220845. doi:10.1371/journal.pone.0220845

Wang, C. P., and Li, Y. (2007). Analysis of 90 Cases of Unstable Angina Pectoris Treated by Tongxinluo. *Chin. Prac Med.* (33), 124–125. doi:10.3969/j.issn.1673-7555.2007.33.085

Wang, H. (2017). The Effect of Aspirin Combined With Tongxinluo in the Treatment of Unstable Angina Pectoris. *Front. Med.* 7, 221–222. doi:10.3969/j.issn.2095-1752.2017.04.199

Wang, L. X., Li, F. J., and Li, Y. (2013). Tongxinluo Capsule in the Treatment of 100 Cases of Elderly Unstable Angina Pectoris. *Proc. 9th. Int. Conf. Coll. Dis.*, 136-139.

Wang, S. J. (2015). Clinical Observation of Tongxinluo Capsule in the Treatment of Unstable Angina Pectoris in the Elderly. *AP. Tradit. Med.* 11, 114–115. doi:10.11954/ytctyy.201505060

Wang, S. X., Mou, Y. G., Liu, T. X., and Tan, L. (2010). Tongxinluo Capsule Treatment of Unstable Angina Pectoris and its Effect on Serum MMP-2. *Hain. Med.* 21, 34–35. doi:10.3969/j.issn.1003-6350.2010.15.012

Wang, X. P., Gao, M. Y., and Deng, Wei. (2009). Efficacy Observation of Tongxinluo Capsule in Treating Unstable Angina Pectoris With Hyperlipidemia. *J. Gann. Med. Col.* 29, 397–398. doi:10.3969/j.issn.1001-5779.2009.03.035

Wang, Y. L., and Xu, D. J. (2010). Mechanism and the Therapy of Unstable Angina Pectoris. *Guid. China Med.* 8, 33–34. doi:10.3969/j.issn.1671-8194.2010.32.018

Wang, Z. G., Feng, W. J., and Pang, J. J. (2012). Clinical Observation of 72 Cases of Unstable Angina Pectoris in the Elderly Treated With Tongxinluo Capsule Combined with Conventional Therapy. *Heal Mus. Read.* 11, 192–193.

Wang, Z. X., Gao, S. W., Liu, Z. C., Ma, J. L., and Wang, B. H. (2021). Research Progress of Tongxinluo Capsule in Treating Coronary Heart Disease and Angina Pectoris. *Guid. Chin. Med.* 27, 134–137. doi:10.13862/j.cnki.cn43-1446/r.2021.01.032

Wu, C. (2011). Clinical Efficacy of Tongxinluo Capsule in the Treatment of Unstable Angina Pectoris. *Chin. Heal Mthly.* 30, 51–52.

Wu, S. J., Mo, Y. Q., He, J. S., Wei, B., and Wang, Q. (2006). Effect of Tongxinluo on Interleukin-18 and Endothelin in Patients With Unstable Angina Pectoris. *Int. Symp. Coll. Dis.* 3, 299–301.

Wu, T., Harrison, R. A., Chen, X., Ni, J., Zhou, L., Qiao, J., et al. (2006). Tongxinluo (Tong Xin Luo or Tong-xin-Luo) Capsule for Unstable Angina Pectoris. *Cochrane Database Syst. Rev.* 4, CD004474. doi:10.1002/14651858.CD004474

Wu, X. Q., Li, J., and Chen, Y. (2018). Meta Analysis of the Efficacy of Tongxinluo Capsule in the Treatment of Unstable Angina Pectoris. *Hun. J. Tradit. Chin. Med.* 34, 154–157. doi:10.16808/j.cnki.issn1003-7705.2018.07.071

Wu, Z. Y., Yang, D. C., Bin., H, and Chen, Y. G. (2010). The Role of Tongxinluo Capsules in Interventional Therapy for Patients with Unstable Angina Pectoris. *Chin. Med. Hera.* 7, 17–20. doi:10.3969/j.issn.1673-7210.2010.20.008

Xin, L., Li, J. Y., Wang, Y., and Huang, W. J. (2008). Clinical Observation of Tongxinluo Capsules in the Treatment of Unstable Angina Pectoris. *Pract. J. Card. Cer. Vasc. Dis.* 16, 256–259. doi:10.3969/j.issn.1008-5971.2008.04.005

Xing, X. X. (2013). Observation on the Efficacy of Tongxinluo Capsules in the Treatment of Unstable Angina Pectoris. *Proc. 9th. Int. Symp. Coll. Dis.*, 140-141.

Xu, C. Y. (2013). Safety Analysis of Combined Application of Tongxinluo and Cardiovascular Drugs. Modern Diagnosis and Treatment. *Mod. Diag Treat.* 24, 558. doi:10.3969/j.issn.1001-8174.2013.03.054

Xu, J. B., and Shao, L. F. (2020). Clinical Study of Tongxinluo Capsule Combined with Trimetazidine in the Treatment of Senile Myocardial Ischemia. *Drug Eval. Res.* 43, 2065–2068. doi:10.7501/j.issn.1674-6376.2020.10.025

Yang, F. (2008). Effect of Tongxinluo Capsule on Vascular Endothelial Function in Patients With Unstable Angina Pectoris. *Chin. Foreign Heal. Dig. Clin. Edit.* 5, 206–208.

Yang, J. D., Zhu, S. G., and Ma, Y. (2019). Efficacy of Tongxinluo Combined With Western Medicine in the Treatment of Unstable Angina Pectoris in the Elderly. *Clin. Med. Res. Prac.* 4, 122–123+138. doi:10.19347/j.cnki.2096-1413.201902055

Yang, J., Zhang, Y., Zhang, Y. J., Gao, D., Chen, S. F., Pang, J. Z., et al. (2021). Meta-Analysis of the Efficacy and Safety of Tongxinluo Capsules Combined With Conventional Western Medicine in the Treatment of Unstable Angina Pectoris. *Drug Eval. Res.* 44, 830–847. doi:10.7501/j.issn.1674-6376.2021.04.026

Yu, M. L., and Chen, Q. (2015). Clinical Study on the Treatment of Unstable Angina Pectoris With Integrated Traditional Chinese and Western Medicine. *Cardiol. Dis. Electr. J. Int. Tradit. Chin. West. Med.* 8, 39–40. doi:10.16282/j.cnki.cn11-9336/r.2015.08.024

Yu, Y. S., and Hu, Na. (2012). Efficacy Analysis of Betaloc Combined With Tongxinluo Capsules in the Treatment of Unstable Angina Pectoris. *Chin. Med. Inno.* 9, 17–18. doi:10.3969/j.issn.1674-4985.2012.35.009

Yuan, W. J. (2019). Effects of Tongxinluo Capsule Combined with Simvastatin on Inflammatory Factors in Patients With Unstable Angina Pectoris. *Hen Med. Res.* 28, 3954–3955. doi:10.3969/j.issn.1004-437X.2019.21.063

Zhang, J., and Li, G. W. (2009). Observation on the Curative Effect of Tongxinluo Capsule in the Treatment of Unstable Angina Pectoris. *West. Med.* 21, 1352–1353. doi:10.3969/j.issn.1672-3511.2009.08.045

Zhang, M., Liu, Y., Xu, M., Zhang, L., Liu, Y., Liu, X., et al. (2019). Carotid Artery Plaque Intervention With Tongxinluo Capsule (CAPITAL): A Multicenter Randomized Double-Blind Parallel-Group Placebo-Controlled Study. *Sci. Rep.* 9, 45. doi:10.1038/s41598-019-41118-z

Zhao, M. (2020). Analysis and Countermeasures of Adverse Reactions in Clinical Use of Statins. *Chin. Rem Clin.* 20, 632–633. doi:10.11655/zgywylc2020.04.066

Zhou, Y. M. (2013). Observation on the Efficacy of Tongxinluo in the Treatment of Unstable Angina Pectoris in the High-Risk Group. *Front. Med.* 27, 171. doi:10.3969/j.issn.2095-1752.2013.27.161

Conflict of Interest: The authors declare that the research was conducted in the absence of any commercial or financial relationships that could be construed as a potential conflict of interest.

Publisher's Note: All claims expressed in this article are solely those of the authors and do not necessarily represent those of their affiliated organizations, or those of the publisher, the editors and the reviewers. Any product that may be evaluated in this article, or claim that may be made by its manufacturer, is not guaranteed or endorsed by the publisher.

frontiers in Plant Science

ORIGINAL RESEARCH
published: 16 November 2021
doi: 10.3389/fpls.2021.736332

Morus alba L. Leaves – Integration of Their Transcriptome and Metabolomics Dataset: Investigating Potential Genes Involved in Flavonoid Biosynthesis at Different Harvest Times

Ding-Qiao Xu[1†], Shu-Yan Cheng[2†], Jun-Qing Zhang[3], Han-Feng Lin[2], Yan-Yan Chen[1], Shi-Jun Yue[1], Meng Tian[1], Yu-Ping Tang[1] and Yu-Cheng Zhao[2]**

[1] Key Laboratory of Shaanxi Administration of Traditional Chinese Medicine for TCM Compatibility, School of Pharmacy, Shaanxi University of Chinese Medicine, Xi'an, China, [2] Department of Resources Science of Traditional Chinese Medicines, State Key Laboratory of Natural Medicines, School of Traditional Chinese Pharmacy, China Pharmaceutical University, Nanjing, China, [3] Department of Metabolism, Digestion and Reproduction, Faculty of Medicine, Imperial College London, London, United Kingdom

OPEN ACCESS

Edited by:
X. Y. Zhang,
University of Minho, Portugal

Reviewed by:
Bing Hao,
Yunnan Agricultural University, China
Fei Qiao,
Chinese Academy of Tropical Agricultural Sciences, China

***Correspondence:**
Yu-Ping Tang
yupingtang@sntcm.edu.cn
Yu-Cheng Zhao
zhaoyucheng1986@126.com

[†] These authors have contributed equally to this work

Specialty section:
This article was submitted to Plant Metabolism and Chemodiversity, a section of the journal Frontiers in Plant Science

Received: *05 July 2021*
Accepted: *07 October 2021*
Published: *16 November 2021*

Citation:
Xu D-Q, Cheng S-Y, Zhang J-Q, Lin H-F, Chen Y-Y, Yue S-J, Tian M, Tang Y-P and Zhao Y-C (2021) Morus alba L. Leaves – Integration of Their Transcriptome and Metabolomics Dataset: Investigating Potential Genes Involved in Flavonoid Biosynthesis at Different Harvest Times. Front. Plant Sci. 12:736332. doi: 10.3389/fpls.2021.736332

The mulberry leaf is a classic herb commonly used in traditional Chinese medicine. It has also been used as animal feed for livestock and its fruits have been made into a variety of food products. Traditionally, mulberry (*Morus alba* L.) leaf harvesting after frost is thought to have better medicinal properties, but the underlying mechanism remains largely unsolved. To elucidate the biological basis of mulberry leaves after frost, we first explored the content changes of various compounds in mulberry leaves at different harvest times. Significant enrichment of flavonoids was observed with a total of 224 differential metabolites after frost. Subsequently, we analyzed the transcriptomic data of mulberry leaves collected at different harvest times and successfully annotated 22,939 unigenes containing 1,695 new genes. Kyoto Encyclopedia of Genes and Genomes (KEGG) analysis revealed 26, 20, and 59 unigenes related to flavonoids synthesis in three different groups harvested at different times. We found that the expression levels of flavonoid biosynthesis-related unigenes also increased when harvested at a delayed time, which was consistent with the flavonoid accumulation discovered by the metabolomic analysis. The results indicated that low temperature may be a key trigger in flavonoid biosynthesis of mulberry leaves by increasing the expression of flavonoid biosynthesis-related genes. This study also provided a theoretical basis for the optimal harvest time of mulberry leaves.

Keywords: *Morus alba* L., transcriptome, metabolomics, harvest time, flavonoid biosynthesis

INTRODUCTION

Mulberry leaves, the dried leaves of *Morus alba* L. which belongs to the family *Moraceae* and genus *Morus* (Wei, 2015), are among the most used traditional Chinese medicine material (Yang et al., 2010). Moreover, it is also an excellent source of functional nutraceutical food. Mulberry leaves contain carbohydrates, amino acids, fatty acids, and other bioactive compounds with

good anti-oxidation, antibacterial, anti-inflammatory, anti-hypoglycemic, and anti-aging effects (Srivastava et al., 2006; Cho et al., 2007; Hunyadi et al., 2012; Park et al., 2013; Wang et al., 2015; Mahboubi, 2019). Several value-added products are developed from mulberry leaves such as mulberry tea, salads, and supplement capsules. Mulberry leaf has been successfully used as a medicinal and edible resource for over 4,000 years. Traditional Chinese pharmacists have always believed that the pharmacological effect of medicinal herbs is closely related to harvest time. Chinese pharmacopeia also suggested that it would be better to harvest the mulberry leaves after than before the winter frost (Commission, 2020), which may improve their pharmacological effects. The study of Zhang et al. (2015) found that after frost, mulberry leaves have the effects of resolving exterior with pungent and cool natured drugs, which are weakened to a certain extent when harvested before frost. However, there are few reports that focus on its underlying mechanisms.

It is generally accepted that biosynthesis and accumulation of plant secondary metabolites are largely influenced by various environmental factors (Li et al., 2020). In general, genetic background determines the secondary metabolite profile of species, whereas environmental factors can cause prominent qualitative and quantitative changes to the metabolite composition. For instance, a previous study concluded that *Fragaria vesca* L. grew in natural habitats contained significantly more flavonoids and phenolic acids in its fruits, compared with those harvested from cultivation (Najda et al., 2014). The study of Jochum et al. (2007) studied the temperature effect on the saponin content of *Panax quinquefolium*, and the results showed that the saponin content of *P. quinquefolium* root significantly increased when the temperature increased. The research of Wang on *Ginkgo biloba* also showed that low temperature and moist conditions induced the expression of key enzymes in flavonoid biosynthesis in *G. biloba* leaves, leading to an increasing of flavonoid contents (Wang et al., 2013). Thus, we speculated that temperature change would be an important factor affecting secondary metabolites in mulberry leaves.

Previous, studies have shown that the mulberry leaves are rich in flavonoids (Wei, 2015; Chan et al., 2016), which account for up to 1–3% of the dry weight of mulberry leaves (Yang et al., 2003). Flavonoids form a group of phenolic secondary metabolites ubiquitously present in higher plants (Zhao et al., 2015). The basic structure of flavonoids is 2-phenyl-benzo[α]pyrane, which consists of fifteen carbon atoms arranged in three rings (C6-C3-C6) (Nijveldt et al., 2001). Due to the different patterns of the substitution of the ring, there are many derivatives, such as isoflavones, flavonols, flavanones, and chalcones (Park et al., 2013; Wei, 2015). Flavonoids are produced by the phenylpropanoid metabolic pathway, which is a common metabolic pathway in plants (Saito et al., 2013; Tohge et al., 2017). Phenylalanine ammonia-lyase (PAL) is the first enzyme in the phenylpropionate pathway, which catalyzes the non-oxidative deamination of phenylalanine to *trans*-cinnamic acid (Fang et al., 2005). Cinnamate 4-hydroxylase (C4H) then converts cinnamic acid to p-coumaric acid, which is then converted by 4-coumaroyl-CoA ligase (4CL) enzyme to 4-coumaroyl coenzyme A and, finally, leads different subgroups by enzymatic catalysis (Rodriguez et al., 2017). Among subgroups, chalcone is an important flavonoid class, which is produced by chalcone synthase (CHS). Some other important enzymes also have vital effects in this pathway. For instance, molecular characterization of isoliquiritigenin 3′-dimethylallyltransferase (MaIDT) in mulberry leaves has been reported, and the results showed that MaIDT might be used for the regiospecific prenylation of flavonoids to produce bioactive compounds (Wang et al., 2014). Furthermore, the decreased temperature has also been confirmed to elevate the flavonoid accumulation in plants. The total accumulation of flavonoids (genistein, daidzein, and genistein) in soybean (*Glycine max*) roots was increased after being treated at a low temperature for 24 h (Janas et al., 2002). Low temperature-induced anthocyanin accumulation in leaves and stems of *Arabidopsis thaliana* and facilitated anthocyanin synthesis through the phenylpropanoid pathway associated with increased transcripts of flavonoid biosynthetic genes including PAL and CHS (Leyva et al., 1995). The expression of the UDP-glucose flavonoid 3-O-glucosyltransferase (UFGT) in mulberry leaves could be induced by low temperature and resulted in the accumulation of flavonoid glycosides (Yu et al., 2017). Thus, we hypothesized that flavonoid synthesis in mulberry leaves increases under conditions of low temperature, as a stress response to resist chilling.

Metabolomics is defined as the study of the complete set of metabolites synthesized by an organism in response to genetic or environmental changes, aiming to provide a link between genotypes and phenotypes (Fiehn, 2002). Transcriptomics can be used to analyze the differences in gene expression levels of medicinal plants under abiotic pressure, which lays the foundation for the regulation of plant secondary metabolism (Patra et al., 2013). By combining the two kinds of analyses strategy, the difference of metabolites in different groups, as well as their gene expression level, can be illustrated. For example, the molecular mechanism of anthocyanin accumulation in *Solanum melongena* L. was determined by combined transcriptome and metabolome analysis (Zhang et al., 2014). Integrated analyses were also used in the studies of the biosynthesis pathway of the podophyllotoxin in *Podophyllum hexandrum* (Lau and Sattely, 2015). The results revealed that flavonoids were the main differential accumulative metabolites (mDAMs), and their contents increased with the temperature decrease. In this study, using metabolomics and transcriptomics analysis, we proved the importance of temperature in the regulation of secondary metabolites production and its relationship with the quality of medicinal plants. This paper also provided guidance for the preference of harvesting time of mulberry leaves. Additionally, considering that mulberry leaf constitutes a functional food and medicinal plant commercialized for the treatment of hyperlipidemia, the identification of low temperature modulating the biosynthesis of these metabolites could benefit in the development of reliable commercial products.

MATERIALS AND METHODS

Plant Material and Grouping Omics Analyzed Samples

Fresh mulberry leaves were picked from mulberry trees [located in Hanzhong City (106.21°E, 32.53°N), Shaanxi Province, China] at different times. From mulberry leaves A (MbLA) to E (MbLE), the temperature gradually dropped as there was a delay in harvesting time (on October 9th, 23rd, November 6th, 20th, and December 5th in the Beijing time zone and the average temperature are 20, 13, 10, 6, and 4°C, respectively) (**Figure 1A**). The descent of the frost was on October 23rd. Each leaf was split into two equal parts along with the midvein: one-half was used for metabolomic analysis, and the other half was used for transcriptomic analysis. For transcriptomic analysis, three biological replicas were conducted, whereas for metabolomics analysis, additional six biological replicas were needed which up to nine replicas. All materials were immediately frozen in liquid nitrogen to prevent RNA degradation.

Sample Extraction

For the metabolomics experiments, every nine samples from each group were used for separate analysis. Then, 60 mg of leave samples were weighed, and 20 μL of 2-chloro-l-phenylalanine (0.3 mg/ml, dissolved in methanol as internal standard) and 0.6 ml of mixed solution [methanol/water = 7/3 (*v:v*)] were added. The samples were homogenized for 2 min and were extracted for 30 min by sonication. They were then placed at −20°C for 20 min and centrifuged at 13,000 × *g* for 15 min. Afterward, 100 μL supernatant from each tube was collected, filtered through 0.22 μm microfilters, and transferred to liquid chromatography (LC) vials. Quality control (QC) samples were prepared by mixing aliquots of all samples to be a pooled sample and then analyzed using the same method with the analytic samples. The QCs were injected at regular intervals (every 10 samples) throughout the analytical run to provide a data set from which repeatability could be assessed.

Metabolite Profiling Using Ultra-High-Performance Liquid Chromatography-Quadrupole Time-of-Flight Mass Spectrometry

Analyses were performed using a Waters UPLC I-class system equipped with a binary solvent delivery manager and a sample manager, coupled with a Waters VION IMS Q-TOF Mass Spectrometer equipped with an electrospray ionization source (Waters Corporation, Milford, MA, United States). Samples were analyzed using an ACQUITY UPLC BEH C18 column (2.1 mm × 100 mm, 1.7 μm, Waters Corporation, Milford, MA, United States) in positive and negative modes. The column temperature was maintained at 45°C and the flow rate of the mobile phase was 0.4 ml/min, accompanied by an injection volume of 3 μL. Mobile phase A was aqueous formic acid [0.1% (*v/v*) formic acid], while mobile phase B was acetonitrile [0.1% (*v/v*) formic acid]. The separation was achieved using the following gradient: 5–20% B over 0–2 min, 20–60% B over 2–8 min, and 60–100% B over 8–12 min. The composition was held at 100% B for 2 min, then 14–14.5 min, 100% to 5% B, and 14.5–15.5 min holding at 5% B. The automatic sampler was set at 4°C during the analysis of all samples.

All data were collected in MS^E mode, and the parameters were as follows: Capillary voltage was 3 kV for positive mode. Source temperature was set at 150°C with a cone gas flow of 50 L/h, and desolvation temperature was set at 500°C with a desolvation gas flow of 900 L/h. Leucine enkephalin (Waters Co., Manchester, United Kingdom) was used as the lock mass generating a reference ion at *m/z* 556.2771 in positive mode or *m/z* 554.2615 in negative mode, which was introduced by a lock spray at 5 μL/min for data calibration. The MS^E data were acquired in centroid mode using ramp collision energy in two scan functions. For Function 1 (low energy), scan range 50–1,000 Da, scan time 0.25 s, and collision energy 10 V were set. In the case of Function 2 (high energy), scan range 50–1,000 Da, scan time 0.25 s, and a collision energy ramp 20–50 V were employed.

Data Processing and Analysis of Metabolites

The UPLC-Q-TOF/MS raw data were imported into Progenesis QI V2 (Waters Corporation, Milford, MA, United States) to the clean background noise, be normalized by a reference sample, correct the retention time, pick the peak, and identify compounds with databases such as METLIN, HMDB, and Lipid Maps. The resulting matrix was further reduced by removing any peaks with missing values (ion intensity = 0) in more than 60% of samples. The internal standard was used for data QC (reproducibility). The positive and negative data were combined to get a combined data set, which was imported into SIMCA-P^+14.0 software (Umetrics, Umeå, Sweden). Principle component analysis (PCA) and (orthogonal) partial least-squares-discriminant analysis (O) PLS-DA were performed to visualize the metabolic alterations among experimental groups, after mean centering and unit variance scaling. OPLS-DA concentrated group discrimination in the X block related to Y into the first component, with the remaining unrelated variations orthogonal to Y in subsequent components. MS data of the second independent experiment of leaves were used as the test data to objectively assess R^2, Q^2, and misclassification rate of established models based on permutation test (2,000 times) that was performed to further validate the supervised model. The significant different metabolites were determined based on the combination of a statistically significant threshold of variable importance in the projection (VIP) values obtained from the OPLS-DA model and two-tailed Student's *t*-test (*p*-value) on the raw data, and the metabolites with VIP values larger than 1 and *p*-values <0.05 were considered significantly different between the compared groups.

Total RNA Extraction

For every three samples at different harvest times, the total RNA of mulberry leave samples was isolated once using TransZol Plant reagent (TransGen Biotech, Beijing, China) according to the recommendations of the manufacturer. The quantity

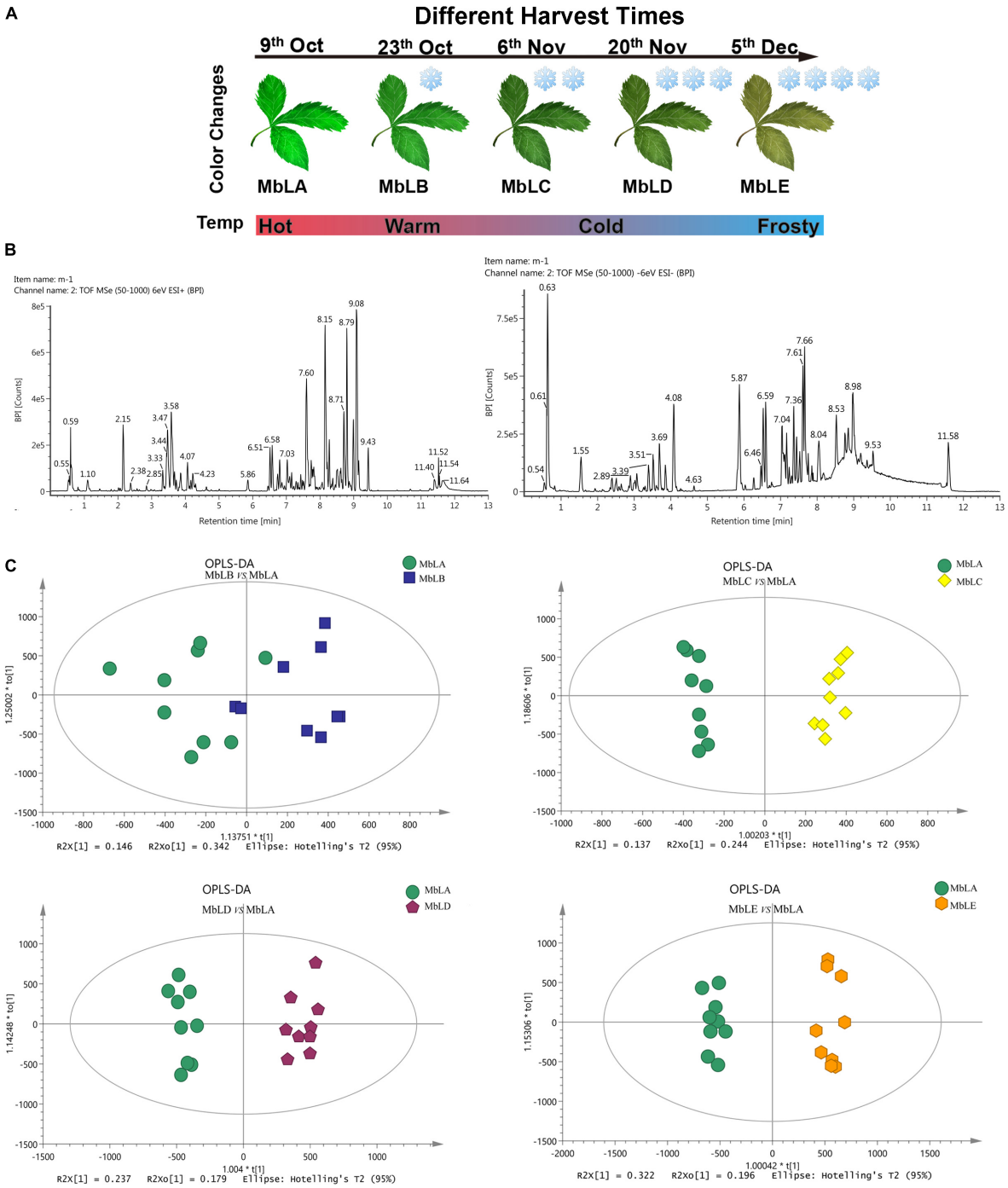

FIGURE 1 | Metabolite accumulation in the mulberry leaves at five periods. **(A)** Mulberry leaves picked on October 6th were recorded as MbLA group; those picked on October 23th were recorded as MbLB group; those picked on November 6th were recorded as MbLC group; those picked on November 20th as MbLD group, and those picked on December 5th were recorded as MbLE group. **(B)** Analysis of compounds extracted from the sample of mulberry leaves using UPLC-Q-TOF/MS. Base peak intensity (BPI) chromatogram of extract analyzed by UPLC-Q-TOF-MS in positive and negative ion mode. **(C)** Score plots for OPLS-DA analysis based on UPLC-Q-TOF-MS data of mulberry leaves extracts obtained from the MbLB to MbLE, with MbLA as the control group. Each point represents an independent biological replicate, and each ellipse represents the 95% CI.

and quality of RNA were determined using a SpectraMax Plus 384 spectrophotometer (Molecular Devices, Sunnyvale, CA, United States) and 1% agarose gels. In addition, the quantity and quality of RNA were determined by Agilent 2100 Bioanalyzer system (Agilent Technologies, Santa Clara, CA, United States) and the one representative result is listed in

Supplementary Figure 1. The RIN, 28S/18S, OD260/280, and OD260/OD230 ratios of all samples are listed in **Supplementary Table 3**. All samples were treated with DNase I (Takara, Dalian, China) at a concentration of 1 unit/μg of total RNA for 30 min to remove the potential DNA.

cDNA Library Construction and Transcriptome Sequencing

A cDNA library was prepared with a kit provided by Illumina according to the recommendations of the manufacturer and previously used methods (Yuan et al., 2015). Then, poly (A) mRNA was purified from the total RNA using oligo(dT) beads. After purification, mRNA was sheared into small pieces using fragmentation buffer. The first-strand cDNA was annealed with random primers using cleaved mRNA fragments as templates. The second-strand cDNA was synthesized with DNA polymerase I and RNase H. Subsequently, the cDNA fragments were purified and ligated to index adapters. Finally, the cDNA library was constructed and subjected to Illumina HiSeq 2500 system for high-throughput sequencing. The raw data were converted into fastaq format and then compressed as.gz files to be transferred to the National Center for Biotechnology Information (NCBI). The Sequence Read Achieve (SRA) sequence database under project accession number was PRJNA533997.

Due to the error rate in the raw data, low-quality-sequence fragments were removed *via* slip-window sampling using the following parameters: quality threshold of 20 (error rate = 1%), a window size of 5 bp, and length threshold of 35 bp. To adjust the pollution of the reads, 10^5 sequences were randomly selected for sequence alignment of the nr reads at an *E*-value of $<1e^{-10}$ and a coverage level of >80%. After the pollution of the reads being cleaned, the good reads were used to assemble transcripts and unigenes using Trinity software (version trinityrnaseq_r2013-02-25)[1]. The unigenes representing the longest transcripts at each locus were assembled using the Chrysalis cluster module in Trinity program. To normalize the abundance of the transcripts, a *k*-mer value of 25 reads per kilobase per million mapped reads (RPKM) (Wagner et al., 2012) was applied and defined in this way:

$$\mathrm{RPKM} = \frac{\text{total exon read}}{\text{mapped reads(millions)} * \text{exon length(KB)}} \quad (1)$$

Functional Annotation and Classification

To find the most descriptive annotation for each transcript sequence, The Basic Local Alignment Search Tool (BLAST) searches (Altschul et al., 1997) were conducted based on sequence similarities using a series of databases (Kanehisa et al., 2002; Dimmer et al., 2012), with the significance threshold set at an *e*-value of $\leq 1e^{-5}$. The functional categories of these unique sequences were analyzed using the Gene Ontology (GO)[2] database, AGI codes and the TAIR GO slim program were provided by TAIR (Lamesch et al., 2012). Pathway assignments were conducted based on the Kyoto Encyclopedia of Genes and Genomes (KEGG) mapping results, and enzyme commission (EC) numbers were assigned to the unique sequences (Aoki-Kinoshita and Kanehisa, 2007). The KOG/COGs (clusters of orthologous groups) of the proteins were aligned to the entries in the EggNOG database to predict and classify the possible functions of the unigene products[3].

Integrative Analysis of Metabolomics and Transcriptome

Metabolites and differentially expressed genes (DEGs) involved in flavonoid biosynthesis and metabolism in KEGG pathways were selected for integrative analysis. Metabolites used for correlation analysis were filtered according to VIP > 1, *p*-value <0.05, and $|\ \mathrm{Log_2}^{\mathrm{FoldChange}}| \geq 2$. Pearson correlation coefficients and *p*-values were calculated for metabolomics and transcriptome data integration using the Spearman method (Kyoungwon et al., 2016).

RESULTS

Metabolomics Analysis Revealed Abundant and Diverse Flavonoid Enrichment in Mulberry Leaves Under Cold Stress

To explore changes of the metabolites in mulberry leaves under cold stress, the base peak intensity (BPI) chromatogram of mulberry leaves extract was analyzed by UPLC-Q-TOF-MS in positive and negative ion modes (**Figure 1B**). Efficient metabolomics data processing was performed by Progenesis QI, while pattern-recognition chemometrics was applied for species classification and potential markers discovery (Wang et al., 2014). The differences between samples in different groups were reflected by the PCA score charts (**Supplementary Figure 2A**). The points of the QC samples in this experiment were closely clustered together, indicating that the whole experimental process had good repeatability and there was no abnormal situation in the data (**Supplementary Figure 3**). The final statistics showed that 18,598 and 10,239 metabolites were obtained by the positive and negative modes, respectively, 9,016 and 4,699 of which were annotated. With the temperature decreasing, there were more differences of metabolites among groups, which were also verified by the heat map (**Figure 2A**). In the OPLS-DA score plots, four groups were divided according to different periods clustered with MbLA (**Figure 1C**). MbLA and MbLB groups exhibited clear separation in OPLS-DA score plots with satisfactory goodness of fit ($R^2 = 0.98$; $Q^2 = 0.9$) (**Supplementary Figure 2**). The two-values associated with fold changes of metabolites before and after the Benjamini-Hochberg method indicating significantly altered metabolites in leaf extracts, which were listed in **Table 1**. With the temperature decreasing, the number of differential metabolites increased (**Figure 2B**). We compared all the differential metabolites in mulberry leaves at four temperatures and obtained a total of 27 common differential

[1]http://trinityrnaseq.sf.net

[2]http://www.geneontology.org/

[3]http://www.ncbi.nlm.nih.gov/COG/

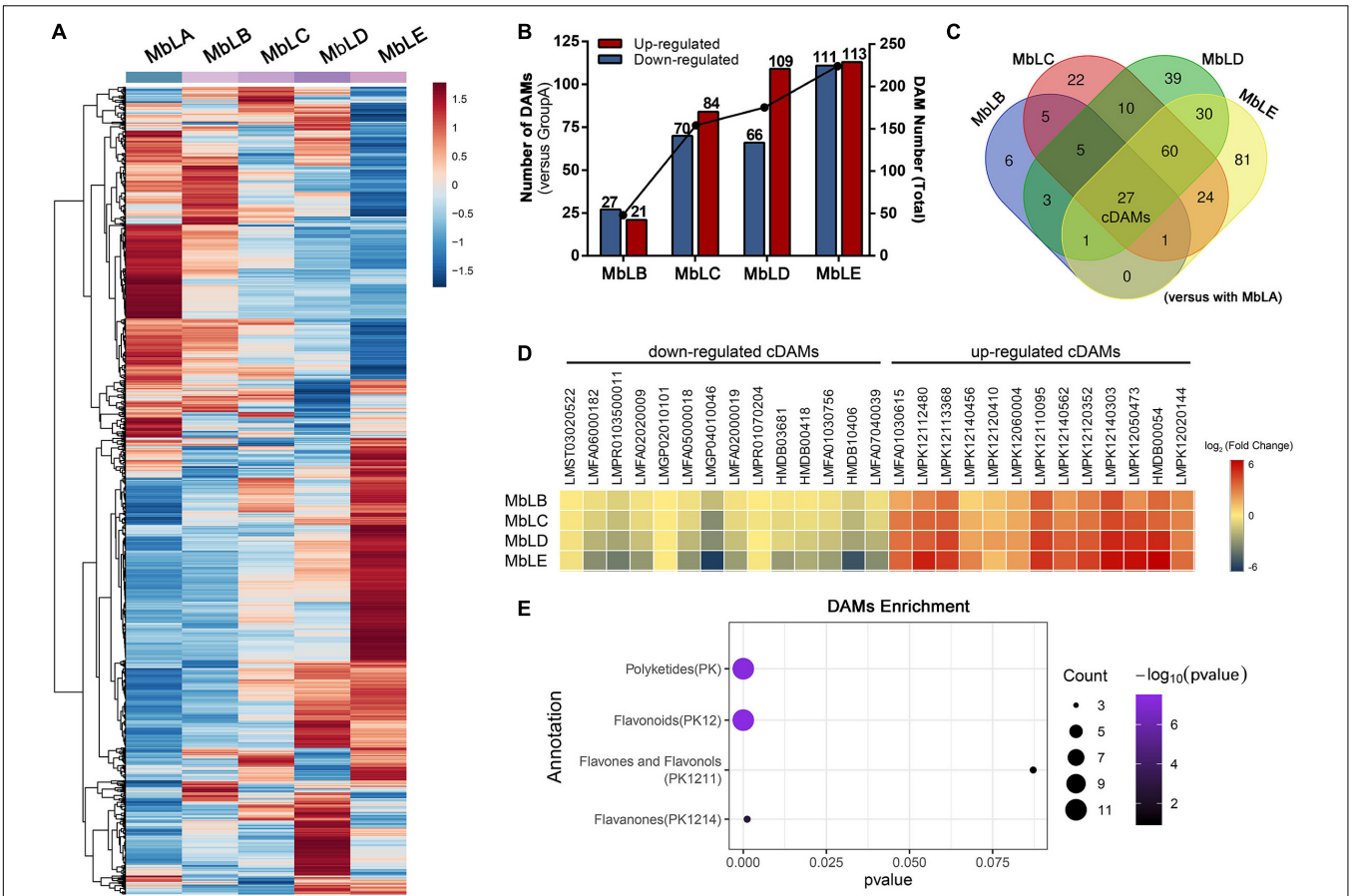

FIGURE 2 | Differential metabolite accumulation in the mulberry leaves at different periods. **(A)** Heat map of all metabolites for MbLA to MbLE. **(B)** The changes of the significantly differentially accumulated metabolites (DAMs) at different periods. **(C)** Venn diagram for all DAMs in MbLB, MbLC, MbLD, and MbLE, with MbLA as the control group. cDAMs refers to common differential accumulation metabolites. **(D)** Heat map of the cDAMs in MbLB, MbLC, MbLD, and MbLE. **(E)** Metabolites annotation enrichment of upregulated cDAMs. The number of DAMs is represented by the circle size.

metabolites (cDAMs; **Figure 2C**). The heat map of cDAMs showed that from all the upregulation, cDAMs had obvious accumulations and change trends (**Figure 2D**). mDAMs were annotated and enriched, and 11 compounds were annotated as flavonoids (**Figure 2E**). From the comparison of upregulated cDAMs, almost all compounds were accumulated while the temperature decreased. These results laid the foundation for our subsequent validation.

Sequencing and Functional Annotation

In this study, the metabolomics analysis indicated that flavonoids were important differential metabolites in mulberry leaves under different periods. This difference might be regulated by temperature-related genes. To further explore the mechanism of flavonoid enrichment, transcriptomic analysis was performed to identify key genes involved in flavonoid biosynthesis in mulberry leaves. As a result, high quality of data with the average percentage of Q30 bases above 94.24% was obtained, and its comparative efficiency ranged from 71.45 to 77.32%. As we can see from the statistics of sequencing data listed in **Supplementary Tables 1, 2**, the total clean data reached 103.13 GB with an average clean data of each sample of 5.98 GB. The BLAST was used to perform sequence alignment with RefSeq non-redundant proteins, Swiss-Prot, GO, COG, KOG, PFAM, and KEGG databases to functional annotation. Eventually, a total of 22,939 unigenes containing 1,695 new genes were functional annotations. Additionally, the differentially expressed genes were also identified according to their expression levels in different samples (**Supplementary Figure 4**). The mapped reads were pieced with StringTie software and compared with the original genetic annotation information to supplement and improve the original genetic annotation information. In addition, several analyses were also performed, including alternative splicing prediction analysis, gene structure optimization analysis, and discovery of new genes.

Differential Expression of Genes Among Mulberry Leaves Under Different Periods

To select the DEGs in different groups (**Supplementary Table 4**), $|\log_2^{\text{FoldChange}}| \geq 2$ and false discovery rate (FDR) <0.01 were used as the screening criteria. The conclusion was that both upregulated and downregulated genes increased with the delay of picking time, which was similar to the differential

metabolites accumulation. In groups MbLC and MbLD, the number of DEGs compared with MbLB began to increase, and it reached the maximum in the MbLE (**Figure 3A**). Specifically, there are 33 DEGs in MbLB, 885 DEGs in MbLC, 987 DEGs in MbLD, and 3,908 DEGs in MbLE, compared with MbLA. The statistical significance of the gene expression level differences in mulberry leaves at different periods was also represented in the volcano plots (**Figure 3B**). Interestingly, despite the number of DEGs increased, the DEGs in different groups seem various. For instance, by comparing the numbers of common differential genes (**Figure 3C**) among the groups, we found that there were only six common differential genes. They were *gene 21769*, *gene 8596*, *gene 8678*, *new gene 6800*, *new gene 7715,* and *new gene 7831*. The results also indicated that MbLE maybe has enormous DEGs. Then we compared the DEGs from MbLE with MbLA, and 68 downregulated DEGs and 149 upregulated DEGs were found. All these results indicated that the temperature might had an important role in the gene expression of mulberry leaves.

Analysis of the Differential Expressed Genes in the Flavonoid Synthesis Pathway

The recent reports suggested that the main active ingredient of mulberry was flavonoids (Zhang et al., 2018). Hence, we mainly focused on the DEGs involved in flavonoid biosynthesis. To predict individual protein function, we performed COG of protein function classification of the consensus sequence. The annotation of COG indicated that the biosynthetic function of the secondary metabolites of MbLC, MbLD, and MbLE groups was relatively stronger (**Figure 4A**). KEGG analysis revealed that 26, 20, and 59 genes related to flavonoids synthesis in MbLC,

TABLE 1 | Identified the main common differential accumulative metabolites with fold changes in MbLA, MbLB, MbLC, MbLD, and MbLE groups in their *p*-values of mulberry leaves.

Metabolites	*m/z*	Formula	MbLB vs. MbLA		MbLC vs. MbLA		MbLD vs. MbLA		MbLE vs. MbLA	
			FC	*P*	FC	*P*	FC	*P*	FC	*P*
PG(12:0/14:1(9Z))	637.4041	$C_{32}H_{61}O_{10}P$	0.29	*	0.1	**	0.1	**	0.02	**
LysoPC(24:1(15Z))	628.4264	$C_{32}H_{64}NO_7P$	0.38	*	0.25	**	0.17	**	0.03	***
5-(1-oxopropan-2-yl)isolongifol-5-ene	305.2112	$C_{18}H_{28}O$	0.44	*	0.3	**	0.17	***	0.07	***
9Z,11E,13-Tetradecatrienal	251.1643	$C_{14}H_{22}O$	0.59	*	0.43	**	0.24	***	0.11	***
12,13-Dimethyl-5,14-dioxabicyclo[9.2.1]-tetradeca-1(13),11-dien-4-one	235.1329	$C_{14}H_{20}O_3$	0.62	*	0.48	**	0.23	***	0.1	***
1,3S-dihydroxy-8E-decen-5-one	185.1173	$C_{10}H_{18}O_3$	0.62	*	0.5	**	0.26	***	0.12	***
Norlinolenic acid	309.2062	$C_{17}H_{28}O_2$	0.63	*	0.52	**	0.31	***	0.15	***
9S-hydroxy-10S,11S-epoxy-12Z,15Z-octadecadienoic acid	309.2062	$C_{18}H_{30}O_4$	0.65	*	0.51	**	0.31	***	0.15	***
cis-Jasmone	209.1174	$C_{11}H_{16}O$	0.65	*	0.53	**	0.31	***	0.13	***
4-Acetamidobutanoic acid	146.0811	$C_6H_{11}NO_3$	0.68	**	0.52	***	0.48	***	0.14	***
18-Hydroxycortisol	377.1937	$C_{21}H_{30}O_6$	0.71	*	0.58	**	0.39	***	0.2	***
1alpha-hydroxy-2beta-(5-hydroxypentoxy)vitamin D3	520.4358	$C_{32}H_{54}O_4$	0.77	***	0.7	***	0.65	***	0.63	***
6′-Hydroxysiphonaxanthin	617.4176	$C_{40}H_{56}O_5$	0.79	*	0.65	***	0.79	*	0.7	***
PE(10:0/10:0)	541.3654	$C_{25}H_{50}NO_8P$	0.81	**	0.77	***	0.75	***	0.76	***
Peruvianoside I	539.1384	$C_{23}H_{26}O_{12}$	1.28	*	2.38	***	2.93	***	5.69	***
Carthamone	447.0928	$C_{21}H_{20}O_{11}$	1.74	*	1.88	*	3.57	***	1.89	*
Dalpanol O-glucoside	573.1975	$C_{29}H_{34}O_{12}$	2.44	*	2.75	*	3.6	***	3.49	***
7-undecynoic acid	205.1223	$C_{11}H_{18}O_2$	2.77	*	6.68	***	7.75	***	9.86	***
Eriodictyol 5,4′-dimethyl ether 7-O-glucoside	477.1411	$C_{23}H_{26}O_{11}$	3.54	*	5.21	**	10.57	***	11.55	***
(+)-Dihydrowighteone	341.1384	$C_{20}H_{20}O_5$	4.34	***	13.63	***	26.78	***	48.92	***
Plumerubroside	509.1665	$C_{24}H_{30}O_{12}$	4.77	*	5.78	**	5.92	***	8.51	***
Larycitrin 3-alpha-L-arabinofuranoside	465.1027	$C_{21}H_{20}O_{12}$	5.17	*	10.19	**	11.05	***	35.79	*
2,3,4,5,2′,3′,4′,6′-Octamethoxychalcone	493.1711	$C_{23}H_{28}O_9$	6.12	*	7.41	**	12.43	***	19.95	**
3′-Hydroxy-3,5,6,7,8,4′,5′-heptamethoxyflavone	493.1348	$C_{22}H_{24}O_{10}$	8.72	*	10.84	***	18.66	***	22.34	**
Bilirubin	629.2616	$C_{33}H_{36}N_4O_6$	9.3	*	10.2	***	31.26	***	103.08	***
5,6,2′,3′,5′,6′-Hexamethoxyflavone	447.129	$C_{21}H_{22}O_8$	12.3	*	11.77	***	21.24	***	25.47	***
3-Methylnaringenin	287.0913	$C_{16}H_{14}O_5$	14.99	*	16.95	***	32.26	***	48.8	**

*P-value: *p < 0.05, **p < 0.01, and ***p < 0.001. Color coded according to fold change using color* bar 

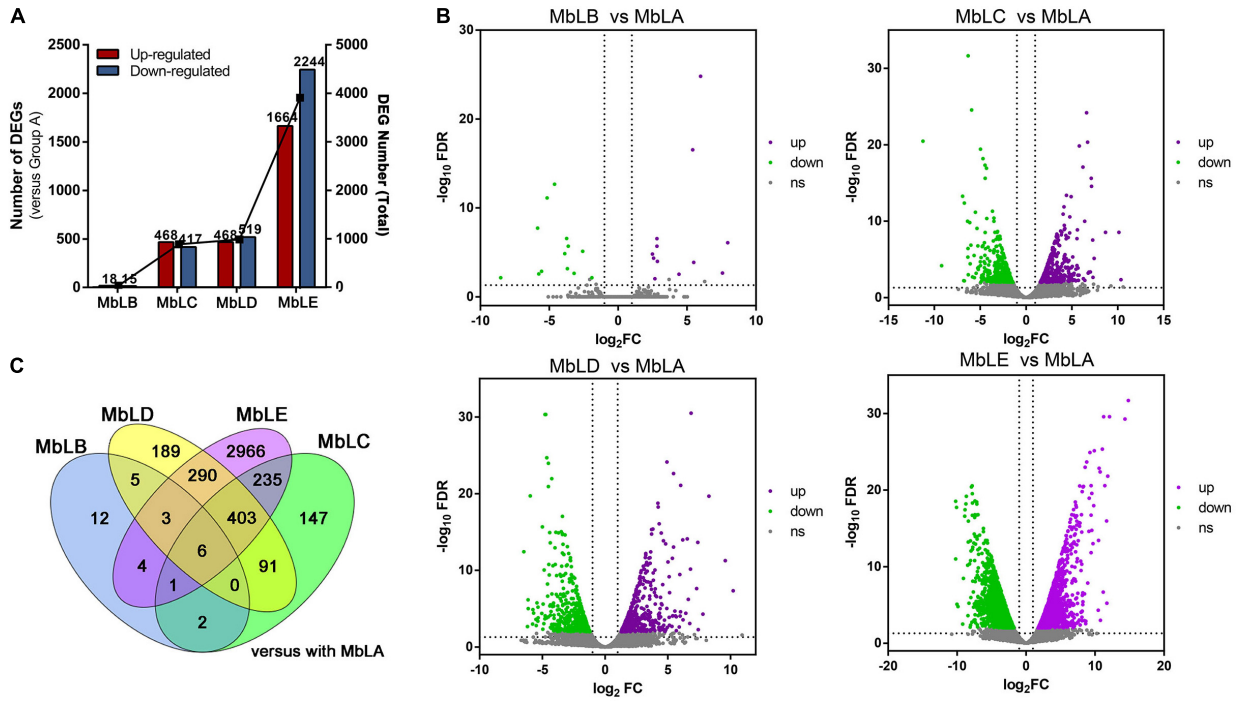

FIGURE 3 | Analysis of the differentially expressed genes (DEGs) at different periods. **(A)** The changes of upregulated DEGs and downregulated DEGs in different groups, with MbLA as control groups. **(B)** Volcano plots for DEGs in the MbLB vs. MbLA, MbLC vs. MbLA, MbLD vs. MbLA, and MbLE vs. MbLA groups. **(C)** Venn diagram for all DEGs in MbLB, MbLC, MbLD, and MbLE, with MbLA as the control group.

MbLD, and MbLE, respectively. However, the ratio of differential expressed genes decreased owing to the number of flavonoid-related genes increased (**Figure 4B**).

Enrichment analysis was performed to seek the pathways that involved the DEGs. The pathway enrichment charts (**Supplementary Figure 5**) show the top 20 pathways with the most reliable enrichment significance (i.e., the lowest *Q*-value). In the top three groups, proteins related to the flavonoid biosynthesis pathway were enriched. For the fourth group, despite such pathways were not in the top 20 pathways with the lowest *Q*-value, there are more metabolic genes were enriched, such as the photosynthesis-antenna pathway. Hence, it was concluded that the flavonoid synthesis in mulberry leaves and the enrichment of their related genes were related to temperature.

Putative Flavonoid Biosynthesis Pathway in Mulberry Leaves

In organisms, different gene products coordinate with each other to perform related biological functions. Pathway annotation analysis of differentially expressed genes is helpful for further understanding gene function. Combined with the KEGG pathway annotation, we compared and displayed these different genes screened above in the pathway (**Figure 5**). From **Figure 5**, we could see that the expression of genes related to flavonoid synthesis is highly correlated with temperature. For example, compared with the expression level of chalcone synthase *gene* 7,356 in MbLE and MbLA, the value of $\log_2^{\text{Fold Change}}$ was 4, indicating that the expression level of this gene was significantly different in the two groups of the mulberry leaves. Additionally, compared the expression level of 4-coumaroyl-CoA ligase gene 11,910 in MbLD and MbLA, $\log_2^{\text{Fold Change}}$ value was 2, indicating that the expression level of this gene in the mulberry leaves of the two groups was also different to some extent. As can be seen from the figure, the number of genes encoding key enzymes of flavonoid synthesis is large, and the expression levels significantly vary at different periods (**Supplementary Table 5**). It was concluded that the flavonoid synthesis in mulberry leaves and the enrichment of their related genes were related to temperature. Interestingly, expression patterns do not vary in one direction as compared to metabolites and it may due to the insufficient transcription factors, since the process from gene to protein expression is complex. In addition, we analyzed the very top and bottom of our list of the DEGs, and we found that the bottom of the list is a cytochrome P450 71D9-like which is involved in secondary metabolites biosynthesis, transport, and catabolism, while the bottom of the list is a zinc finger BED domain-containing protein involved in replication, recombination, and repair (Kajikawa et al., 2004; Dai et al., 2015; AbuZayed et al., 2019; Wang et al., 2021). This indicated that at an extremely low temperature, mulberry needs to fight against the hostile environment and at the same time, the biosynthesis process of metabolites may be blocked. These results partly agree with the data in **Figure 5** and **Supplementary Figure 4**, in which the gene expression level of flavonoid-related genes was decreased. All the new findings had been added in the article which may provide

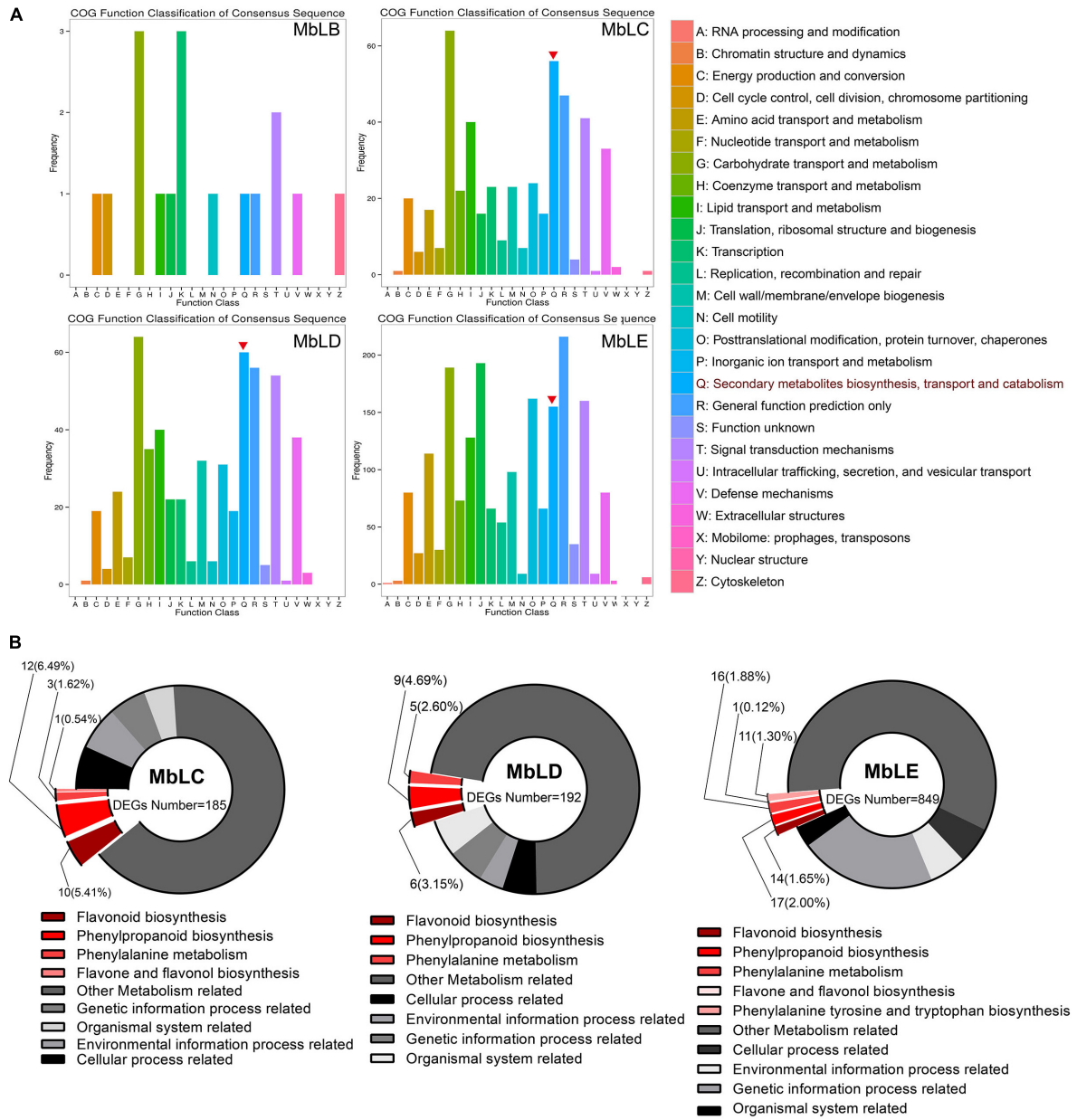

FIGURE 4 | Rich distribution map of differentially expressed genes based on functional annotation. **(A)** COG function classification. The vertical axis represents the gene frequency, and the horizontal axis represents the function class. The red inverted triangles indicated the genes involved in secondary metabolites biosynthesis, transport, and catabolism. **(B)** The enrichment factor represents the ratio of the genes' proportion annotated to a certain pathway in different genes to the genes' proportion annotated to this pathway in all genes. The circle's color represents the *Q*-value, which is the *P*-value after the correction of multiple hypothesis tests. The smaller the *Q* value, the more reliable the enrichment significance of differentially expressed genes in this pathway. The circle's size indicates the genes' number enriched in the pathway, and the larger the circle, the more the number of genes.

new evidence in the conclusion that temperature exerted a great influence on the flavonoid biosynthesis in mulberry leaves.

DISCUSSION

Mulberry leaf is an excellent source of nutrients and phytochemicals. In this study, we explored the changes in relevant compounds and their respective genes at different harvest times through metabolic profiling and transcriptome analyses. The results show that mulberry leaves at different harvest times expressed different flavonoids biosynthesis genes, which results in increasing amounts of flavonoids.

Gene expression associated with flavonoid synthesis was higher at lower temperatures according to the results. However, according to the comparison of the 20 pathways with the highest

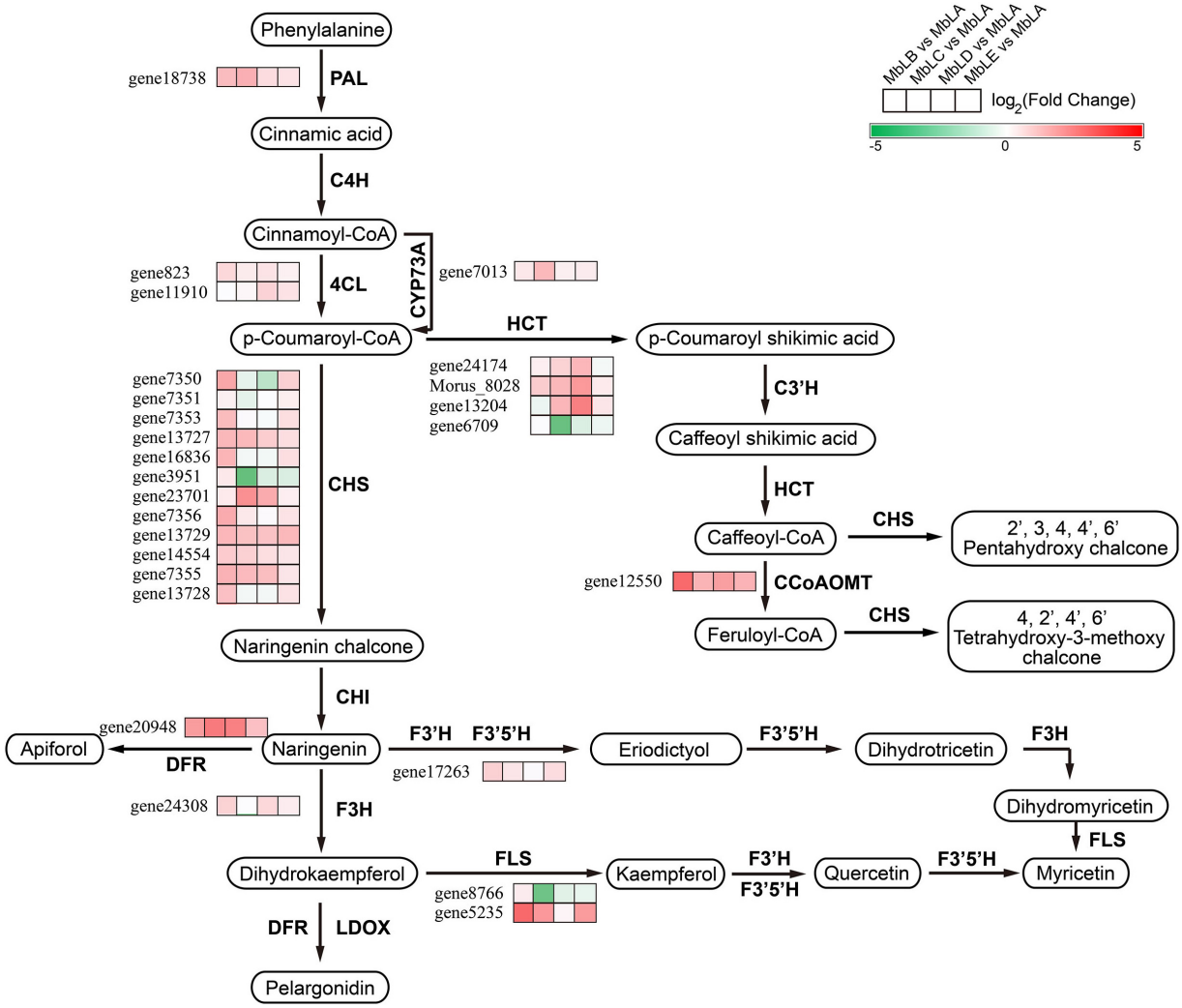

FIGURE 5 | Putative flavonoid biosynthesis pathway in mulberry leaves and gene expression profile of the key enzymes. PAL, Phenylalanine ammonia-lyase; C4H, Cinnamate 4-hydroxylase; 4CL, 4-coumaroyl-CoA ligase; CHS, Chalcone synthase; CHI, Chalcone isomerase; DFR, Dihydroflavonol reductase; F3H, Flavanone 3-hydroxylase; F3′H, Flavonoid 3′-hydroxylase; F3′5′H, Flavonoid 3′5′ hydroxylase; LDOX, leucoanthocyanidin dioxygenase; FLS, Flavonol synthase; HCT, hydroxycinnamoyl transferase.

enrichment significance, we found fewer differentially expressed genes associated with the flavonoid synthesis pathway at the lowest temperature (**Supplementary Figure 6**). This suggests that genes affecting flavonoid synthesis may not be present in the DEGs lists, or that our criteria for DEGs were too strict. If lower down the criteria, genes affecting flavonoid synthesis may be present in the DEGs lists. However, it is known that when the criteria are lower, the DEGs may become more and more. In order to make the criteria unification, we used the same criteria for the four groups. It is also possible that the plants have higher metabolic demands at low temperatures. For example, the study Guy et al. (1992) studied the influence of growth temperature on the free sugar and sucrose phosphate synthase content of spinach (*Spinacia oleracea*) leaf tissue. They found that the enzyme levels involved in sugar synthesis increased at lower temperatures. In this case, although the expression of genes involved in the flavonoid biosynthesis increased, their proportion decreased. Based on this, we infer that there may be a suitable temperature range for mulberry leaves that will have the greatest effect. The effects of different environmental temperatures on the entire mulberry tree should also be considered.

This study could also be used to verify previous studies on the changes in the levels of flavonoid biosynthesis enzymes and the increased expression of related genes after the weather got cold. We knew that there are many important enzymes affecting flavonoid content from previous studies, such as PAL, CHS, and UDP glucose flavonoid-3-o-glycosyltransferase (UFGT; Qian et al., 2012). Compared with previous studies, we found more genes related to certain key enzymes in flavonoid synthesis. Also, we are inclined to show the rule of metabolites in mulberry leaves with temperature changes and study-related genes on this basis, making the conclusion more convincing.

Additionally, using the annotation information of all genes, we found that certain genes related to the flavonoid biosynthesis pathway were annotated as *iron ion binding* in GO annotation and "flavonoid biosynthesis" in KEGG annotation, such as *Gene 17264, Gene 5235, Gene 5234, Gene 8766, Gene 17263,* and *Gene 5236*. Earlier studies have shown that flavonoids can bind to metal ions and have special effects because of the conjugation and spatial configuration (De Souza and De Giovani, 2004). Based on this, we speculated that enzymes related to flavonoid synthesis have metal ion binding ability, which could be proven through gene annotation. De Souza and De Giovani (2004) found that complexes of metal ions with quercetin, rutin, galangin, and catechin had antioxidant properties. To a certain extent, this confirmed the relationship between flavonoids and metal ions and could invite future investigation.

If we focused on the genes involved in flavonoid synthesis, we could find that genes encoding flavonol synthase (FLS), hydroxycinnamoyl transferase (HCT), dihydroflavonol reductase (DFR), catechol-*O*-methyltransferase (COMT), and CHS showed a relatively higher difference. On the other hand, by analyzing the pathways, we found that the pathways with the greatest degree of gene change were those related to plant metabolism. The synthesis pathway of flavonoids also increased with temperature decrease trend. However, in MbLE, the synthesis pathway enrichment of flavonoids was not in the top 20, the main enrichment pathways were photosynthesis, respiration, amino acid synthesis pathway, and amino acid synthesis pathway. It was possible that genes related to flavonoid synthesis were still enriched and upregulated, but the changes were smaller than those in other basic metabolic pathways.

In summary, we investigated the metabolomics and transcriptome of mulberry leaves and compared DEGs and DAMs at different periods. Using the functional group analysis of GO and KEGG pathway annotations, compounds and genes related to the flavonoid biosynthesis pathway at different periods were identified and used to speculate that lower temperatures induce the expression of flavonoid-related genes. We also compared and displayed the screened differential genes in the pathways as a preliminary exploration of the biosynthesis pathway of the flavonoids in mulberry leaves, which requires further study. Finally, our study could serve as a reference for the analysis of metabolomic and transcriptomic data from other medicinal plants.

DATA AVAILABILITY STATEMENT

The datasets presented in this study can be found in online repositories. The names of the repository/repositories and accession number(s) can be found below: NCBI SRA BioProject, accession no: PRJNA533997.

AUTHOR CONTRIBUTIONS

D-QX, S-YC, Y-CZ, and Y-PT conceived the experiments and helped to coordinate support and funding. D-QX, J-QZ, S-YC, S-JY, and MT performed the research, drafted, and revised the manuscript. J-QZ, H-FL, and Y-YC participated in the experiments. D-QX and Y-CZ analyzed the data and edited the manuscript. All authors read and approved the final manuscript.

FUNDING

This research was funded by the National Key R&D Program of China (2019YFC1711000), Basic Research Program for Natural Science of Shaanxi Province (2020JQ-862). It was also funded by the Scientific Research Project of Shaanxi Provincial Department of Education (20JK0602), Youth Innovation Team of Shaanxi Universities (2020), and Subject Innovation Team of Shaanxi University of Chinese Medicine (2019-YL10). This Project was funded by the Fundamental Research Funds for the Central Universities of China Pharmaceutical University (2632020ZD09).

ACKNOWLEDGMENTS

The authors thank AiMi Academic Services (www.aimieditor.com) for English language editing and review services.

SUPPLEMENTARY MATERIAL

The Supplementary Material for this article can be found online at: https://www.frontiersin.org/articles/10.3389/fpls.2021.736332/full#supplementary-material

REFERENCES

AbuZayed, R., Bulatova, N., Kasabri, V., Suyagh, M., Halaseh, L., and AlAlawi, S. (2019). Correlates of zinc finger BED domain-containing protein 3 and ghrelin in metabolic syndrome patients with and without prediabetes. *Horm. Mol. Biol. Clin. Investig.* 37:20180052. doi: 10.1515/hmbci-2018-0052

Altschul, S. F., Madden, T. L., Schäffer, A. A., Zhang, J., Zhang, Z., Miller, W., et al. (1997). Gapped BLAST and PSI-BLAST: a new generation of protein database search programs. *Nucleic Acids Res.* 25, 3389–3402. doi: 10.1093/nar/25.17.3389

Aoki-Kinoshita, K. F., and Kanehisa, M. (2007). Gene annotation and pathway mapping in KEGG. *Methods Mol. Biol.* 396, 71–91. doi: 10.1007/978-1-59745-515-2_6

Chan, E. W., Lye, P. Y., and Wong, S. K. (2016). Phytochemistry, pharmacology, and clinical trials of Morus alba. *Chin. J. Nat. Med.* 14, 17–30.

Cho, Y. S., Shon, M. Y., and Lee, M. K. (2007). Lipid-lowering action of powder and water extract of mulberry leaves in C57BL/6 mice fed high-fat diet. *J. Kor. Soc. Food Sci. Nutr.* 36, 405–410. doi: 10.3746/jkfn.2007.36.4.405

Commission, C. P. (2020). *Pharmacopoeia of the People's Republic of China*. Beijing: Chinese Medical Science and Technology Press.

Dai, F., Wang, Z., Luo, G., and Tang, C. (2015). Phenotypic and transcriptomic analyses of autotetraploid and diploid mulberry (Morus alba L.). *Int. J. Mol. Sci.* 16, 22938–22956. doi: 10.3390/ijms160922938

De Souza, R. F., and De Giovani, W. F. (2004). Antioxidant properties of complexes of flavonoids with metal ions. *Redox Rep.* 9, 97–104. doi: 10.1179/135100004225003897

Dimmer, E. C., Huntley, R. P., Alam-Faruque, Y., Sawford, T., O'Donovan, C., Martin, M. J., et al. (2012). The UniProt-GO annotation database in 2011. *Nucleic Acids Res.* 40, D565–D570. doi: 10.1093/nar/gkr1048

Fang, C. B., Wan, X. C., and Jiang, C. J. (2005). The research progress of flavonoids biosynthesis. *J. Anhui Agric. Univ.* 32, 498–504.

Fiehn, O. (2002). Metabolomics – the link between genotypes and phenotypes. *Plant Mol. Biol.* 48, 155–171. doi: 10.1023/A:1013713905833

Guy, C. L., Huber, J. L., and Huber, S. C. (1992). Sucrose phosphate synthase and sucrose accumulation at low temperature. *Plant Physiol.* 100, 502–508.

Hunyadi, A., Martins, A., Hsieh, T. J., Seres, A., and Zupkó, I. (2012). Chlorogenic acid and rutin play a major role in the in vivo anti-diabetic activity of Morus alba leaf extract on type II diabetic rats. *PLoS One* 7:e50619.

Janas, K. M., Cvikrová, M., Pa Agiewicz, A., Szafranska, K., and Posmyk, M. M. (2002). Constitutive elevated accumulation of phenylpropanoids in soybean roots at low temperature. *Plant Sci.* 163, 369–373.

Jochum, G. M., Mudge, K. W., and Thomas, R. B. (2007). Elevated temperatures increase leaf senescence and root secondary metabolite concentrations in the understory herb Panax quinquefolius (Araliaceae). *Am. J. Bot.* 94, 819–826. doi: 10.3732/ajb.94.5.819

Kajikawa, M., Yamato, K. T., Kohzu, Y., Sakata, R., Fukuzawa, H., Uchida, H., et al. (2004). Expressed sequence tags from callus of Euphorbia tirucalli: a resource for genes involved in triterpenoid and sterol biosynthesis. *Plant Biotechnol.* 21, 349–353. doi: 10.5511/plantbiotechnology.21.349

Kanehisa, M., Goto, S., Kawashima, S., and Nakaya, A. (2002). The KEGG databases at GenomeNet. *Nucleic Acids Res.* 30, 42–46. doi: 10.1093/nar/30.1.42

Kyoungwon, C., Kwang-Soo, C., Hwang-Bae, S., Jin, H. I., Su-Young, H., and Hyerim, L. (2016). Network analysis of the metabolome and transcriptome reveals novel regulation of potato pigmentation. *J. Exp. Bot.* 67, 1519–33. doi: 10.1093/jxb/erv549

Lamesch, P., Berardini, T. Z., Li, D., Swarbreck, D., Wilks, C., Sasidharan, R., et al. (2012). The Arabidopsis information resource (TAIR): improved gene annotation and new tools. *Nucleic Acids Res.* 40, D1202–D1210.

Lau, W., and Sattely, E. S. (2015). Six enzymes from mayapple that complete the biosynthetic pathway to the etoposide aglycone. *Science* 349, 1224–1228. doi: 10.1126/science.aac7202

Leyva, A., Jarillo, J. A., Salinas, J., and Martinez-Zapater, J. M. (1995). Low temperature induces the accumulation of phenylalanine ammonia-lyase and chalcone synthase mRNAs of Arabidopsis thaliana in a light-dependent manner. *Plant Physiol.* 108, 39–46. doi: 10.1104/pp.108.1.39

Li, Y., Kong, D., Fu, Y., Sussman, M. R., and Wu, H. (2020). The effect of developmental and environmental factors on secondary metabolites in medicinal plants. *Plant Physiol. Biochem.* 148, 80–89. doi: 10.1016/j.plaphy.2020.01.006

Mahboubi, M. (2019). Morus alba (mulberry), a natural potent compound in management of obesity. *Pharmacol. Res.* 146:104341. doi: 10.1016/j.phrs.2019.104341

Najda, A., Dyduch, J., Dyduch-Siemińska, M., and Gantner, M. (2014). Comparative analysis of secondary metabolites contents in Fragaria vesca L. fruits. *Ann. Agric. Environ. Med.* 21, 339–343. doi: 10.5604/1232-1966.1108601

Nijveldt, R. J., Van Nood, E. L. S., Van Hoorn, D. E., Boelens, P. G., Van Norren, K., and Van Leeuwen, P. A. (2001). Flavonoids: a review of probable mechanisms of action and potential applications. *Am. J. Clin. Nutr.* 74, 418–425. doi: 10.1093/ajcn/74.4.418

Park, E., Lee, S. M., Lee, J., and Kim, J. H. (2013). Anti-inflammatory activity of mulberry leaf extract through inhibition of NF-κB. *J. Funct. Foods* 5, 178–186. doi: 10.1016/j.jff.2012.10.002

Patra, B., Schluttenhofer, C., Wu, Y., Pattanaik, S., and Ling, Y. (2013). Transcriptional regulation of secondary metabolite biosynthesis in plants - sciencedirect. *Biochim. Biophys. Acta* 1829, 1236–1247. doi: 10.1016/j.bbagrm.2013.09.006

Qian, J. Z., Wang, B. C., Tan, J., and Liu, W. Q. (2012). Pharmacological activities and metal complexes for the flavonoids. *Chin. Pharmacol. Bull.* 28, 1058–1062.

Rodriguez, A., Strucko, T., Stahlhut, S. G., Kristensen, M., Svenssen, D. K., Forster, J., et al. (2017). Metabolic engineering of yeast for fermentative production of flavonoids. *Bioresour. Technol.* 245, 1645–1654.

Saito, K., Yonekura-Sakakibara, K., Nakabayashi, R., Higashi, Y., Yamazaki, M., Tohge, T., et al. (2013). The flavonoid biosynthetic pathway in Arabidopsis: structural and genetic diversity. *Plant Physiol. Biochem.* 72, 21–34. doi: 10.1016/j.plaphy.2013.02.001

Srivastava, S., Kapoor, R., Thathola, A., and Srivastava, R. P. (2006). Nutritional quality of leaves of some genotypes of mulberry (Morus Alba). *Int. J. Food Sci. Nutr.* 57, 305–313. doi: 10.1080/09637480600801837

Tohge, T., de Souza, L. P., and Fernie, A. R. (2017). Current understanding of the pathways of flavonoid biosynthesis in model and crop plants. *J. Exp. Bot.* 68, 4013–4028. doi: 10.1093/jxb/erx177

Wagner, G. P., Kin, K., and Lynch, V. J. (2012). Measurement of mRNA abundance using RNA-seq data: RPKM measure is inconsistent among samples. *Theory Biosci.* 131, 281–285. doi: 10.1007/s12064-012-0162-3

Wang, G. B., Guo, X. Q., Chang, L., and Cao, F. L. (2013). Effects of air temperature and soil moisture on flavonoids accumulation in Ginkgo biloba leaves. *J. Appl. Ecol.* 24, 3077–3083.

Wang, G. Q., Zhu, L., Ma, M. L., Chen, X. C., Gao, Y., Yu, T. Y., et al. (2015). Mulberry 1-deoxynojirimycin inhibits adipogenesis by repression of the ERK/PPARγ signaling pathway in porcine intramuscular adipocytes. *J. Agric. Food Chem.* 63:6212. doi: 10.1021/acs.jafc.5b01680

Wang, R., Chen, R., Li, J., Liu, X., Xie, K., Chen, D., et al. (2014). Molecular characterization and phylogenetic analysis of two novel regio-specific flavonoid prenyltransferases from Morus alba and Cudrania tricuspidata. *J. Biol. Chem.* 289, 35815–35825. doi: 10.1074/jbc.M114.608265

Wang, R., Ren, C., Dong, S., Chen, C., Xian, B., Wu, Q., et al. (2021). Integrated metabolomics and transcriptome analysis of flavonoid biosynthesis in Safflower (Carthamus tinctorius L.) with different colors. *Front. Plant Sci.* 12:712038. doi: 10.3389/fpls.2021.712038

Wei, H. (2015). *Morus Alba L. (Sang, White Mulberry)*. Vienna: Springer. 721–730. doi: 10.1007/978-3-211-99448-1_81

Yang, H. X., Zhu, X. R., and Sheng, L. H. (2003). Research progress on exploiting and utilizing of mulberry leaves in the field of health care. *Bull. Sci. Technol.* 19, 72–76.

Yang, X., Yang, L., and Zheng, H. (2010). Hypolipidemic and antioxidant effects of mulberry (Morus alba L.) fruit in hyperlipidaemia rats. *Food Chem. Toxicol.* 48, 2374–2379. doi: 10.1016/j.fct.2010.05.074

Yu, X., Zhu, Y., Fan, J., Wang, D., Gong, X., and Ouyang, Z. (2017). Accumulation of flavonoid glycosides and UFGT gene expression in mulberry leaves (Morus alba L.) before and after frost. *Chem. Biodivers.* 14:e1600496. doi: 10.1002/cbdv.201600496

Yuan, F., Lyu, M. J. A., Leng, B. Y., Zheng, G. Y., Feng, Z. T., Li, P. H., et al. (2015). Comparative transcriptome analysis of developmental stages of the Limonium bicolor leaf generates insights into salt gland differentiation. *Plant Cell Environ.* 38, 1637–1657. doi: 10.1111/pce.12514

Zhang, H., Zheng, M., Luo, X., and Li, X. (2018). Effects of mulberry fruit (Morus alba L.) consumption on health outcomes: a mini-review. *Antioxidants* 7:69. doi: 10.3390/antiox7050069

Zhang, W., Ouyang, Z., Zhao, M., Yuan, W., Yang, S., Wang, Z., et al. (2015). Differential expression of secondary metabolites in mulberry leaves before and after frost. *Food Sci.* 36, 109–114.

Zhang, Y., Hu, Z., Chu, G., Huang, C., Tian, S., Zhao, Z., et al. (2014). Anthocyanin accumulation and molecular analysis of anthocyanin biosynthesis-associated genes in eggplant (Solanum melongena L.). *J. Agric. Food Chem.* 62, 2906–2912. doi: 10.1021/jf404574c

Zhao, S., Park, C. H., Li, X., Kim, Y. B., Yang, J., Sung, G. B., et al. (2015). Accumulation of rutin and betulinic acid and expression of phenylpropanoid and triterpenoid biosynthetic genes in mulberry (Morus alba L.). *J. Agric. Food Chem.* 63, 8622–8630. doi: 10.1021/acs.jafc.5b03221

Conflict of Interest: The authors declare that the research was conducted in the absence of any commercial or financial relationships that could be construed as a potential conflict of interest.

Publisher's Note: All claims expressed in this article are solely those of the authors and do not necessarily represent those of their affiliated organizations, or those of the publisher, the editors and the reviewers. Any product that may be evaluated in this article, or claim that may be made by its manufacturer, is not guaranteed or endorsed by the publisher.

frontiers in Pharmacology

ORIGINAL RESEARCH
published: 22 November 2021
doi: 10.3389/fphar.2021.730416

Regulation of Cytochrome P450 2a5 by *Artemisia capillaris* and 6,7-Dimethylesculetin in Mouse Hepatocytes

Sangsoo Daniel Kim[1], *Larry Morgan*[1], *Elyse Hargreaves*[1], *Xiaoying Zhang*[1,2], *Zhihui Jiang*[3], *Monica Antenos*[1], *Ben Li*[2] *and Gordon M. Kirby*[1]*

[1]*Department of Biomedical Sciences, Ontario Veterinary College, University of Guelph, Guelph, ON, Canada,* [2]*Chinese-German Joint Institute for Natural Product Research, College of Biological Science and Engineering, Shaanxi University of Technology, Hanzhong, China,* [3]*He'nan Joint International Research Laboratory of Veterinary Biologics Research and Application, Anyang Institute of Technology, Anyang, China*

Jaundice is a potentially fatal condition resulting from elevated serum bilirubin levels. For centuries, herbal remedies containing *Artemisia capillaris* Thunb. including the compound 6,7-dimethylesculetin (DE) have been used in Asia to prevent and treat jaundice in neonates. DE activates an important regulator of bilirubin metabolism, the constitutive androstane receptor (CAR), and increases bilirubin clearance. In addition, murine cytochrome P450 2a5 (Cyp2a5) is known to be involved in the oxidative metabolism of bilirubin. Moreover, treatment of mice with phenobarbital, a known inducer of both CAR and Cyp2a5, increases expression of Cyp2a5 suggesting a potential relationship between CAR and Cyp2a5 expression. The aim of this study is to investigate the influence of *Artemisia capillaris* and DE on the expression and regulatory control of Cyp2a5 and the potential involvement of CAR. Treatment of mouse hepatocytes in primary culture with DE (50 μM) significant increased Cyp2a5 mRNA and protein levels. In mice, *Artemisia capillaris* and DE treatment also increased levels of hepatic Cyp2a5 protein. Luciferase reporter assays showed that CAR increases *Cyp2a5* gene transcription through a CAR response element in the *Cyp2a5* gene promoter. Moreover, DE caused nuclear translocation of CAR in primary mouse hepatocytes and increased Cyp2a5 transcription in the presence of CAR. These results identify a potential CAR-mediated mechanism by which DE regulates *Cyp2a5* gene expression and suggests that DE may enhance bilirubin clearance by increasing Cyp2a5 levels. Understanding this process could provide an opportunity for the development of novel therapies for neonatal and other forms of jaundice.

Keywords: Artemisia capillaris thunb, cytochrome P450, mouse, gene regulation, liver, jaundice

OPEN ACCESS

Edited by:
Yibin Feng,
The University of Hong Kong, Hong Kong, SAR China

Reviewed by:
Charles Awortwe,
Stellenbosch University, South Africa
Ayman El-Kadi,
University of Alberta, Canada

***Correspondence:**
Gordon M. Kirby
gkirby@uoguelph.ca

Specialty section:
This article was submitted to Ethnopharmacology, a section of the journal Frontiers in Pharmacology

Received: *24 June 2021*
Accepted: *08 November 2021*
Published: *22 November 2021*

Citation:
Kim SD, Morgan L, Hargreaves E, Zhang X, Jiang Z, Antenos M, Li B and Kirby GM (2021) Regulation of Cytochrome P450 2a5 by Artemisia capillaris *and 6,7-Dimethylesculetin in Mouse Hepatocytes. Front. Pharmacol. 12:730416. doi: 10.3389/fphar.2021.730416*

Abbreviations: AhR, aryl hydrocarbon receptor; CAR, constitutive androstane receptor; CCRP, cytoplasmic CAR-retaining protein; C/EBP, CCAAT/enhancer-binding protein; CYP, cytochrome P450; Cyp2a5, murine cytochrome P450 2a5; DE, dimethylesculetin; DR-4, direct repeat elements separated by 4 base pairs; ERα, Estrogen receptor alpha; HNF-4, hepatocyte nuclear factor 4; HSP90, heat shock protein 90; NF-1, nuclear factor 1; NRF-4α, nuclear factor 4 alpha; Nrf2, nuclear factor (erythroid-derived 2)-like 2; OATP, organic anion transporting polypeptides; PPARα, peroxisome proliferator-activated receptor alpha; PPP1R16A (a regulatory subunit of protein phosphatase 1β); PXR, pregnane X receptor; RXR, retinoid X receptor; TCPOBOP, 1, 4-bis [2-(3, 5-dichloropyridyloxy)]benzene; TBST, Tris-buffered saline with 0.5% Tween-20; UGT1A1, uridine diphosphate 5′-glucuronosyltransferase.

INTRODUCTION

Jaundice is a condition that is particularly common in neonates resulting from an imbalance in the production and elimination of bilirubin (BR) that is characteristically observed during the transitional period following birth (Dennery et al., 2001; Mitra and Rennie, 2017; Chee et al., 2018). BR is produced during normal heme catabolism and displays cytoprotective capacities at physiological levels and toxicity at supra-physiological concentrations (Tomaro and Batlle, 2002; McDonagh, 2010; Abu-Bakar et al., 2011; Takeda et al., 2015). To prevent excessive accumulation of BR, hepatic uridine diphosphate 5′-glucuronosyltransferase 1A1 (UGT1A1) catalyzes the conjugation of BR to glucuronic acid to produce a water-soluble product suitable for biliary excretion. However, deficiencies in this process result in elevated serum bilirubin concentrations that is manifested clinically as jaundice (Huang et al., 2003; Mitra and Rennie, 2017; Chee et al., 2018).

Due to a more rapid turnover of erythrocytes, newborns produce bilirubin at much higher rates than adults (Mitra and Rennie, 2017; Chee et al., 2018). Additionally, infants are relatively deficient in UGT1A1, causing them to have a limited capacity to conjugate and excrete bilirubin (Yang et al., 2011; Rets et al., 2019). The primary concern and consequence of this imbalance is the ability of lipophilic bilirubin to concentrate in the central nervous system and elicit neurotoxicity, a condition called kernicterus (Mitra and Rennie, 2017). Neonatal jaundice is conventionally treated with phototherapy, a process which involves exposure of affected babies to UV light causing photoisomerization of bilirubin to an excretable form (Mitra and Rennie, 2017; Chee et al., 2018). Pharmacological therapies such as phenobarbital have been shown to enhance bilirubin excretion, however adverse effects persist (Dennery et al., 2001; Huang et al., 2003). Consequently, phototherapy remains widely used to effectively reduce bilirubin levels in infants (Mitra and Rennie, 2017).

In Asia, Yin Zhi Huang and other herbal decoctions containing *Artemisia capillaris* Thunb. Such as Yin Chen Hao have long been used to prevent and treat neonatal jaundice (Li et al., 2001; Li et al., 2017; Hui et al., 2020) and other liver diseases. Both Yin Zhi Huang and phenobarbital have been shown to enhance bilirubin clearance, however Yin Zhi Huang displays a more potent effect (Huang et al., 2003). The major constituent of *Artemisia capillaris* Thunb. 6,7-dimethylesculetin (DE; also known as scoparone), has been shown to accelerate bilirubin clearance in mice *in vivo* and activate an important regulator of bilirubin metabolism, the constitutive androstane receptor (CAR), in primary mouse hepatocytes (Huang et al., 2003; Elferink, 2004).

As a member of the nuclear receptor superfamily, CAR is a ligand-responsive transcription factor that is predominantly expressed in the liver (Baes et al., 1994; Pustylnyak et al., 2020). Inactive CAR is restricted to the cytoplasm where it forms a complex with heat shock protein 90 (HSP90), cytoplasmic CAR-retaining protein (CCRP), and PPP1R16A (a regulatory subunit of protein phosphatase 1β) (Savas et al., 1999; Kachaylo et al., 2011; Pustylnyak et al., 2020). Upon ligand activation, CAR is released from the protein complex to allow for nuclear translocation. Within the nucleus, CAR forms a heterodimer with the retinoid X receptor (RXR) which then binds to specific DNA-responsive elements to mediate transcriptional activation of target genes (Savas et al., 1999; Kachaylo et al., 2011). CAR is an important regulator of the expression of enzymes involved in xenobiotic metabolism including proteins involved in the metabolism and elimination of bilirubin (Huang et al., 2003; Kachaylo et al., 2011; Pustylnyak et al., 2020).

In a study conducted by Huang *et al.* (2004), treatment of humanized CAR transgenic mice with the herbal decoction Yin Zhi Huang resulted in an increased expression of functional components of the bilirubin clearance pathway and accelerated bilirubin elimination (Huang et al., 2004). This effect was absent in CAR knockout mice. Because there is evidence to suggest that several other nuclear receptors may be involved in the regulation of bilirubin clearance, Huang *et al.* (2004) compared the roles of four receptors [CAR, pregnane X receptor (PXR), aryl hydrocarbon receptor (AhR) and peroxisome proliferator-activated receptor alpha (PPARα)] (Huang et al., 2004). Following treatment with specific activators for each nuclear receptor, the most significant increase in bilirubin clearance was observed in mice treated with the CAR activator, 1, 4-bis [2-(3, 5-dichloropyridyloxy)]benzene (TCPOBOP). A more recent study has confirmed the role of CAR as an important regulator of bilirubin clearance (Wang et al., 2017).

The cytochrome P450 (CYP) enzymes comprise a superfamily of metabolically active hemoproteins. Murine Cyp2a5, and its human ortholog CYP2A6, are important hepatic enzymes involved in the metabolism of a variety of compounds including the endogenous substrate bilirubin (Seubert et al., 2002; Abu-Bakar et al., 2005; Abu-Bakar et al., 2011; Lämsä et al., 2012; Kim et al., 2013). Regulatory control of the expression of Cyp2a5 is distinct from that of other CYP enzymes as it is induced by a broad range of structurally diverse compounds and by pathophysiological states that reduce the expression of other CYPs (Abu-Bakar et al., 2007; Kirby et al., 2011; Muhsain et al., 2015). For example, hepatic Cyp2a5 is induced during liver injury caused by several hepatotoxins including phenobarbital, pyrazole, chloroform, various heavy metals and 1,4-bis [2-(3,5-dichloropyridyloxy)]benzene (TCPOBOP) (Kirby et al., 2011). Cyp2a5 expression is also upregulated by heme, bilirubin, and porphyrinogenic compounds such as aminotriazole and griseofulvin (Abu-Bakar et al., 2011; Kirby et al., 2011). Several transcription factors including the albumin D-site-binding protein (Lavery et al., 1999), the hepatocyte nuclear factor 4 (HNF-4), the nuclear factor 1 (NF-1) [5], the aryl hydrocarbon receptor (AhR) [6], and the nuclear factor (erythroid-derived 2)-like 2 (Nrf2) [2] have been implicated in the expression of Cyp2a5 (Kirby et al., 2011). CAR has also been linked to the regulation of Cyp2a5 expression. Mice treated with the CAR inducer phenobarbital displayed increased expression of Cyp2a5, an effect that was absent in CAR knockout mice (Simonsson et al., 2006; Kirby et al., 2011). Although these findings suggest that CAR may be involved in the regulation

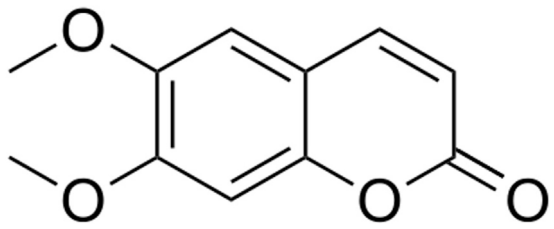

FIGURE 1 | Chemical structure of 6,7-dimethylesculetin.

of Cyp2a5, no CAR-responsive elements have been positively identified within the promoter of the CYP enzyme.

We hypothesize that *Artemisia capillaris* Thunb. and DE induce Cyp2a5 expression through a transcriptional mechanism involving CAR. The aims of this study are to assess the effect of *Artemisia capillaris* and DE on Cyp2a5 expression in mouse liver and DE-treated hepatocytes in primary culture and to determine the role of CAR in transcriptional regulation of Cyp2a5 by DE.

MATERIALS AND METHODS

Reagents. UPLC-MS-grade acetonitrile and formic acid were purchased from Thermo Fisher Scientific (Waltham, MA, United States), Sigma-Aldrich (Darmstadt, Germany), respectively. Ultrapure water with a resistivity of 18 MΩ cm at 25°C was generated with Microporous system (Ulu pure, Xian, Shaanxi, China). The analytical standards were purchased from Yuanye Bio-Technology (Shanghai, China): 6,7-dimethylesculetin (purity >98%, MW: 206.1, CAS: 120-08-1) was purchased from Chengdu Biopurify Phytochemicals Ltd. (Chengdu, Sichuan, China). The chemical structure of 6,7-dimethylesculetin is shown in **Figure 1**. The plant material of *Artemisia capillaris* Thunb. originating from Shangluo, Shaanxi province, was purchased from Yikang Pharmacy (Yangling, Shaanxi, China) and was authenticated by Dr Xiaoying Zhang (Pharmacologist). A voucher specimen (No. 200701) was deposited in the Shaanxi University of Technology, Anyang, China.

Preparation of *Artemisia capillaris* samples. The sample of *Artemisia capillaris* was washed twice with distilled water and dried in oven at 60°C. Sample preparation for animal treatment involved preparing a decoction by boiling 40 g of *Artemisia capillaris* in distilled water for 30 min which was then filtered and adjusted to a final volume of 40 ml. Sample preparation for HPLC analysis involved extracting 5 g of dried *Artemisia capillaris* in 100 ml of 53% ethanol in water for 6 h. After filtration, ethanol was removed by evaporation, water was removed by lyophilization and the extracts were stored at −80°C for future use.

HPLC analysis of *Artemisia capillaris* extracts. The various constituents in the decoction of *Artemisia capillaris* were determined by UHPLC by dissolving 5 mg of extract in 1 ml of 50% methanol and 0.1 mg of 6,7-dimethylesculetin standard in 1 ml of 50% methanol. Chromatographic separations were achieved using a Shimadzu UHPLC, LC-30 system (Shimadzu Corporation, Kyoto, Japan) and a UV-Vis photodiode array detector. Ten microliters of each dissolved extract sample was injected onto a Shimadzu InertSustain C18 liquid chromatography column (100 mm × 2.1 mm, 2 μm particles). Mobile phase A was acetonitrile and mobile phase B was ultrapure water containing 0.1% formic acid. The gradient elution program was set as follows: 5–50% (A) for 0–7 min, 50%–95% (A) for 7–9 min, 95%–95% (A) for 9–10 min. The flow rate was 1.0 ml/min. The column was maintained at 35°C. HPLC chromatograms were produced using a wavelength of 345 nm (**Figure 2A,B**).

Mass spectrometry of *Artemisia capillaris* extracts. Mass spectrometry analysis of *Artemisia capillaris* extracts was achieved by Hybrid Quadrupole-TOF LC/MS/MS Mass Spectrometry using a TripleTOF® 5,600 + system (Sciex, Framingham, MA). Electrospray ionization (ESI) was used to detect positive ions. The ESI source conditions were as follows: Ion Source Gas1(Gas 1):50, Ion Source Gas2(Gas 2):50, Curtain Gas (CUR): 25, Source Temperature: 500°C (positive ion), Ion Spray Voltage Floating (ISVF) 5500V (positive ion), TOF MS scan range: 100–1,200 Da, product ion scan range: 50–1,000 Da, TOF MS scan accumulation time 0.2 s, product ion scan accumulation time 0.01 s, The secondary mass spectrum was obtained by information dependent acquisition (IDA) with high sensitivity mode ±60V, Collision Energy: 35 ± 15 eV. The mass spectra of the first-order isotope (**Figures 3A,B**) and the secondary mass spectrum of the main fragment (**Figures 3C,D**) of extracts of *Artemisia capillaris* and 6,7-dimethylesculetin are presented.

Animals. Twelve adult male Kunming mice (20–25 g) (The Experimental Animal Center of the Medical University of the Air Force, Xi'an, China) were fed *ad libitum* and exposed to a 12-h light/dark cycle in a 23°C climate. Twelve adult male mice were divided into three groups (i.e., four controls, four *Artemisia capillaris*-treated and four DE-treated) and were gavaged daily for 3 days with either distilled water, the *Artemisia capillaris* decoction (10 ml/kg) or DE dissolved in distilled water (100 mg/kg). Mice were then euthanized by CO_2 inhalation and liver samples were collected.

Isolation and Culturing of Primary Mouse Hepatocytes. Primary mouse hepatocytes were isolated from male C57Bl/6 mice using a modified two-step retrograde collagenase perfusion method as previously described (Gilmore and Kirby, 2004). Mice were first anesthetized with an intraperitoneal injection (100 mg/kg) of pentobarbital sodium (Euthanyl® 240 mg/ml, Bimeda-MTC Animal Health Inc. Cambridge, ON, Canada). A catheter was inserted into the inferior vena cava and the liver was perfused with Hank's balanced salt solution (pH 7.4), containing 0.1 M EGTA and 1 M HEPES, for 2.5 min (3 ml/min). The liver was subsequently perfused with collagenase (100 U/mL) in William's E medium (pH 7.4), supplemented with 1 M HEPES and 7.5% (v/v) bovine serum albumin, for 5–8 min (4 ml/min) to allow for hepatocyte dissociation. The liver was excised, then rinsed and scored in fresh attachment media containing William's E medium, pH 7.4, supplemented with 10 mM

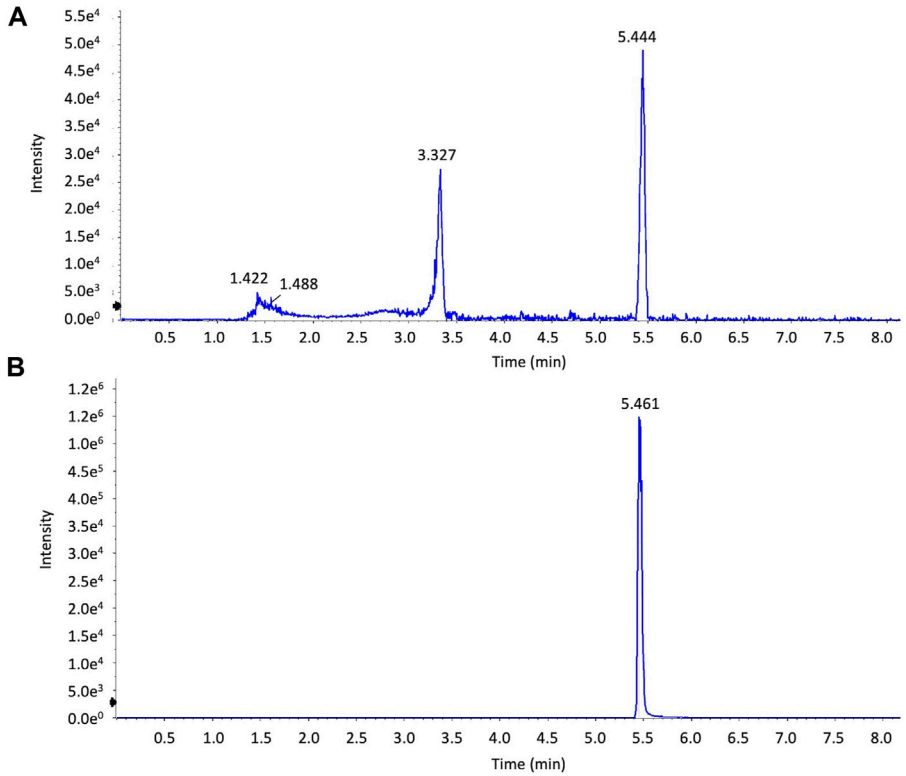

FIGURE 2 | HPLC analysis of extracts of Artemisia capillaris. Extracts of *Artemisia capillaris* and the standard compound 6,7-dimethylesculetin were subjected to HPLC analysis (Panels **(A)** and **(B)** respectively).

dexamethasone, ITS (5 mg/L, insulin, 5 mg/L transferrin, 5 μg/L sodium selenite), 10 μg/ml gentamicin, and 10% (v/v) fetal bovine serum. The dissociated hepatocytes were filtered, centrifuged (50 g for 2 min) and resuspended in attachment medium. Hepatocytes were plated at various densities described below and maintained in a humidified incubator (5% CO_2, 37°C). After 8 h, the attachment medium was replaced with serum-free William's E medium, supplemented with 1 M HEPES, ITS and 7.5 μg/ml gentamycin, and the cells were left to incubate overnight.

Treatment of Primary Mouse Hepatocytes. Cultured primary mouse hepatocytes were plated at a density of 9×10^5 cells per well in 6-well plates and were treated with variable concentrations of DE (10, 25, 50 μM) or the vehicle dimethyl sulfoxide (DMSO, 0.1%) in serum-free William's E medium. Hepatocytes were then maintained in a humidified incubator for 24 h for the experiment with variable doses of DE or for 1, 3, 6 or 24 h at a single dose of 50 μM.

RNA Extraction, Reverse Transcription and Comparative Real-time RT-PCR Analysis. Comparative real-time reverse transcription polymerase chain reaction (real time RT-PCR) was performed to assess *Cyp2a5* expression in DE-treated primary mouse hepatocytes. Following treatments described above, total cellular RNA was isolated using TRIzol® reagent (Thermo Fisher Scientific, Waltham, MA, United States) as per the manufacturer's instructions. RNA was quantified using a NanoDrop ND-1000 spectrophotometer (Thermo Fisher Scientific, Waltham, MA, United States). The RNA (1 μg) was then treated with 1 unit of DNase I (RQ1 RNase-Free DNase; Promega, Madison, WI, United States). cDNA was produced from the DNase-treated RNA by reverse transcription using 0.1 μg of random primers, 20 units of RNase inhibitor (RNase-OUT; Thermo Fisher Scientific, Waltham, MA, United States), and 200 units of Moloney murine leukemia virus reverse transcriptase (M-MLV RT; Thermo Fisher Scientific, Waltham, MA, United States). A LightCycler 2.0 apparatus (Roche Life Science, Indianapolis, IN, United States) was used to perform real-time PCR using 1 μl SYBR Green I, 2 mM Mg+ (DNA Master SYBR Green I kit; Applied Biosystems-Thermo Fisher Scientific, Waltham, MA, United States) and 5 μM of each following primers:

Cyp2a5 Forward 5′-GGACAAAGAGTTCCTGTCACTGCTTC-3′

Reverse 5′-GTGTTCCACTTTCTTGGTTATGAAGTCC-3′

GAPDH Forward 5′-ACAGTCCATGCCATCACTGCC-3′

Reverse 5′-GCCTGCTTCACCACCTTCTTG-3′

The PCR program parameters included an initial denaturation period (95°C for 10 min) followed by 45 amplification cycles consisting of denaturation (95°C for 15 s), annealing (70°C for 5 s), and elongation (72°C for 15 s) steps. Relative *Cyp2a5* mRNA levels of the treatment groups were determined by comparing the amplification threshold cycles at which the fluorescent signal

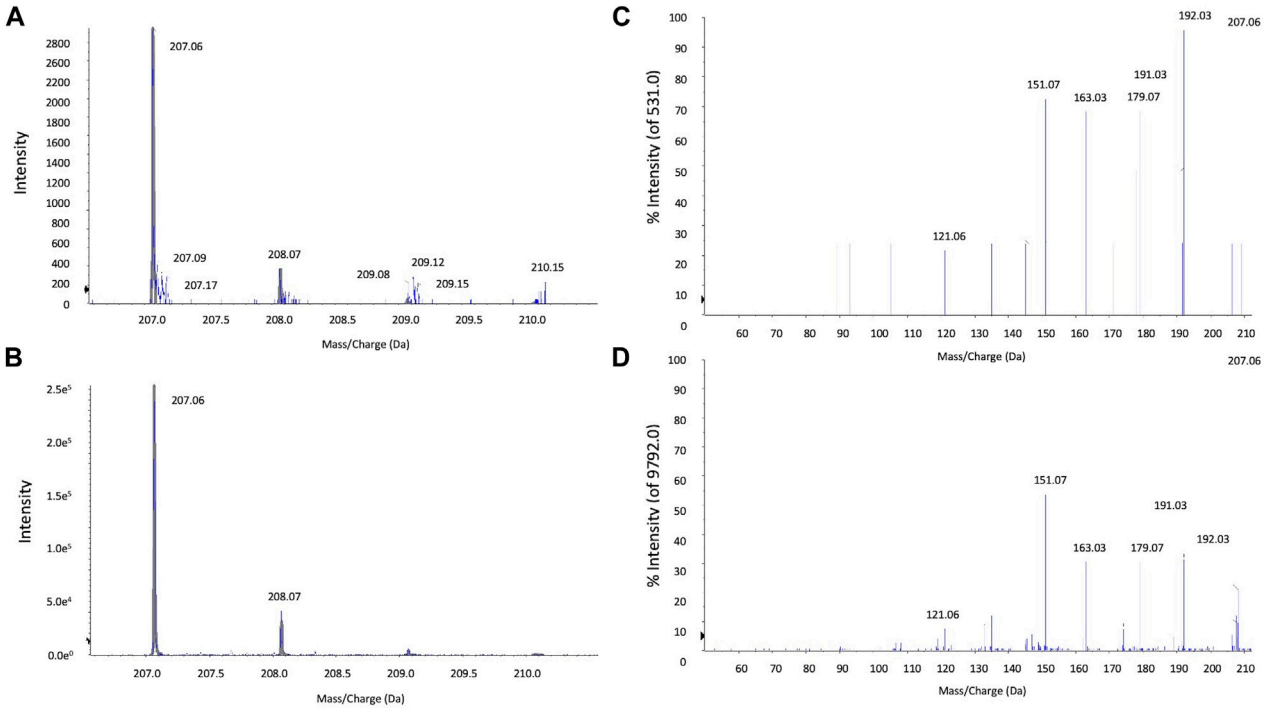

FIGURE 3 | LC-MS/MS analysis of extracts of Artemisia capillaris. The major HPLC peak (5.4 min) from extracts of *Artemisia capillaris* and the standard compound 6,7-dimethylesculetin were subjected to tandem mass spectrometry. Primary isotope mass spectrometry of *Artemisia capillaris* extract and 6,7-dimethylesculetin (Panels **(A)** and **(B)** respectively) and the secondary mass spectrum of *Artemisia capillaris* extract and 6,7-dimethylesculetin (Panels **(C)** and **(D)** respectively) from precursor 207.1 Da are shown.

exceeded the background level. *Cyp2a5* mRNA quantities were normalized against the housekeeping gene, glyceraldehyde-3-phosphate dehydrogenase (GAPDH), to correct for sample-to-sample variation.

Protein Extraction and Western Blot Analysis. Western blot analysis was performed to assess Cyp2a5 protein expression in DE-treated primary mouse hepatocytes and in DE- and *Artemisia capillaris*-treated mouse liver. Primary hepatocytes were plated at a density of 1×10^6 cells per well in 12-well plates. Following a 48 h treatment with DE (5, 10, 25 and 50 μM), primary mouse hepatocytes were harvested and cell extracts were prepared in lysis buffer (50 mM Tris-HCl, pH 7.4, 250 mM sucrose, 25 mM KCl, 5 mM $MgCl_2$, and 1 Roche cOmplete Mini Protease Inhibitor Cocktail™ tablet (Sigma-Aldrich, Oakville, ON, Canada) per 10 ml as we have previously described (Nichols and Kirby, 2008). Microsomes were prepared from mouse liver by differential centrifugation according to our protocol (Kirby et al., 1993) and protein concentrations were determined by the Bradford method. Nuclear protein was isolated from primary mouse hepatocytes as we have previously described (Kim et al., 2013). Proteins from nuclear extracts (25 μg) and microsomes (50 μg) were separated by size via SDS-PAGE (4% acrylamide stacking gel, 10% acrylamide separating gel) and transferred to a nitrocellulose membrane. The membrane was blocked for 1 h at room temperature in 5% skim milk dissolved in Tris-buffered saline with 0.5% Tween-20 (TBST). Following an overnight incubation (4°C) with either chicken anti-mouse Cyp2a5 polyclonal antibody (1:10,000) (a kind gift of Dr. H. Raunio; University of Kuopio, Finland) or rabbit anti-mouse constitutive androstane receptor polyclonal antibody (ab228767, 1:2000) (Abcam, Cambridge, United Kingdom), the membrane was incubated with rabbit anti-chicken peroxidase-conjugated secondary antibody (1:5,000) (Sigma-Aldrich, Oakville, ON, Canada) for 1 h at room temperature. Chemiluminescence detection of the secondary antibody was performed by the ECL + Plus™ Western blotting method (GE Healthcare Sciences, Waltham, MA, United States) using a Typhoon 9,410 scanner (GE Healthcare Sciences, Waltham, MA, United States). The membrane was then blocked and subject to incubation with mouse anti-β-actin polyclonal antibody (1:5,000) (Sigma-Aldrich, Oakville, ON, Canada), followed by goat anti-mouse peroxidase conjugated secondary antibody (1:2000) (Sigma-Aldrich, Oakville, ON, Canada). After chemiluminescence detection, ImageJ2® software was used to quantify Cyp2a5 by densitometry, relative to the housekeeping protein, β-actin (Rueden et al., 2017).

Transfection and Dual-Luciferase Reporter Assays. Transfections and dual-luciferase reporter assays were conducted to determine whether the DE-mediated induction of Cyp2a5 in primary mouse hepatocytes occurs via a transcriptional mechanism. First, primary mouse hepatocytes dispersed in attachment media were plated at a density of 2.5×10^5 cells per well in 24-well plates. The attachment media was replaced with serum-free media 8 h later and the cells were left to

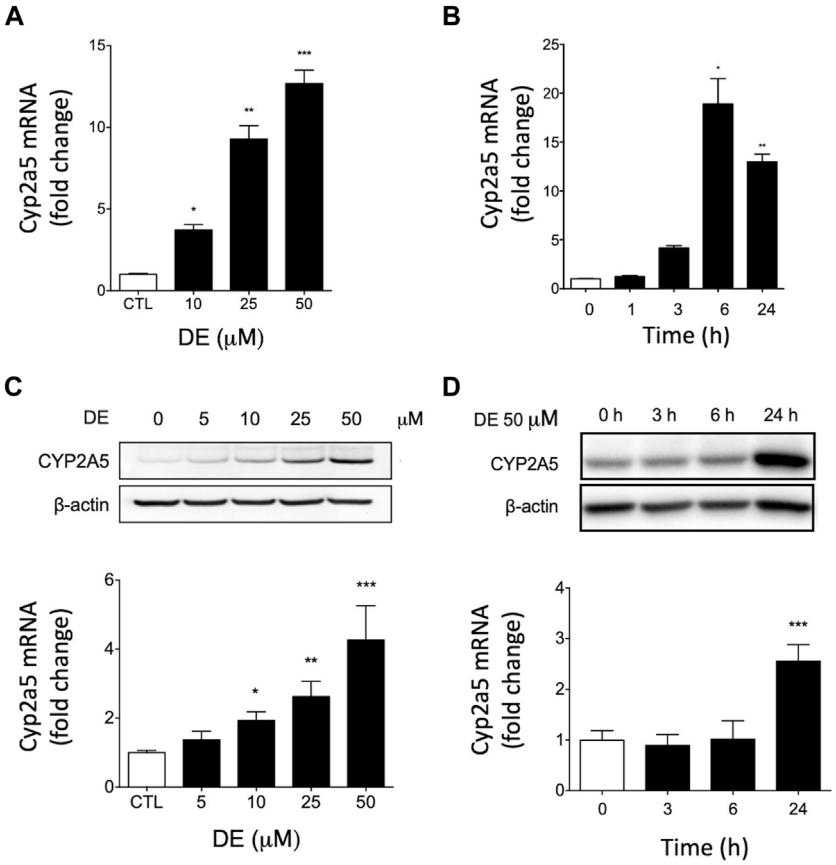

FIGURE 4 | DE increases Cyp2a5 mRNA and protein levels in primary mouse hepatocytes. Primary mouse hepatocytes were treated with increasing doses of DE or the vehicle for 24 h or at 50 μM for specific times up to 24 h Cyp2a5 mRNA (Panels **(A)** and **(B)**) and protein levels (Panels **(C)** and **(D)**) were determined. Densitometric quantification of Cyp2a5 and β-Actin protein levels is presented as the mean fold-change ± SEM of the Cyp2a5/β-actin ratio relative to the control. Values represent means ± SEM of data generated from three independent experiments (n = 3) performed in triplicate. The mean difference is significant from controls at $p \leq 0.05$ *, $p \leq 0.01$ ** and $p \leq 0.001$ ***.

incubate overnight. Hepatocytes were then transiently transfected using Lipofectamine 2000 (Thermo Fisher Scientific, Waltham, MA, United States) in Opti-MEM reduced serum media (Thermo Fisher Scientific, Waltham, MA, United States) as per the manufacturer's instructions. All cells were transfected with the phRL-TK reporter plasmid (*Renilla reniformis*, Promega, Madison, WI, United States) (50 ng/well) to control for variability in cell numbers and transfection efficiency (Shifera and Hardin, 2010). As a positive control, hepatocytes were co-transfected with pGL3 control plasmid (Promega, Madison, WI, United States) (500 ng/well) which constitutively expresses the luciferase gene. Co-transfection with the empty pGL3 basic plasmid (Promega, Madison, WI, United States) (500 ng/well) served as a negative control. The remaining hepatocytes were co-transfected with a Cyp2a5 reporter construct (500 ng/well), which contained a 3,033 bp segment of the Cyp2a5 5′ proximal promoter [p*Cyp2a5*-3,033 + 10luc; (a kind gift of Dr. Jukka Hakkola, University of Oulu, Finland)]. To assess whether DE-induced Cyp2a5 promoter activity involves CAR, cells were also co-transfected with a murine CAR plasmid (pCR3-mCAR, 300 ng/well) kindly provided by Dr. Masahiko Negishi (NIEHS, NIH, United States)). At 24 h after transfection, the media was replaced with serum-free media supplemented with DE (50 μM) or the vehicle (DMSO). After an additional 24 h of incubation, the media was removed and the cells were lysed using a passive lysis buffer (Promega) (110 μl/well) for 1 h at −80°C. Luciferase activity was then measured with a FLUOstar OPTIMA luminometer (BMG LABTECH, Ortenberg, Germany) using a dual-luciferase reporter assay system (Promega) as per the manufacturer's instructions. Relative luciferase activities were determined through normalization against *Renilla* luciferase activities. The data are presented as a ratio of luminescence relative to the control.

Statistical Analysis. Data are presented as the mean ± standard error of the mean (SEM). One-way analysis of variance (ANOVA) and Tukey's post-hoc test were conducted to determine the statistical significance of the data generated from Cyp2a5 mRNA and protein analyses. Two-way ANOVA and Bonferroni's post-hoc test were utilized for analysis of the luciferase assay data. *p*-values ≤ 0.05 were considered significant.

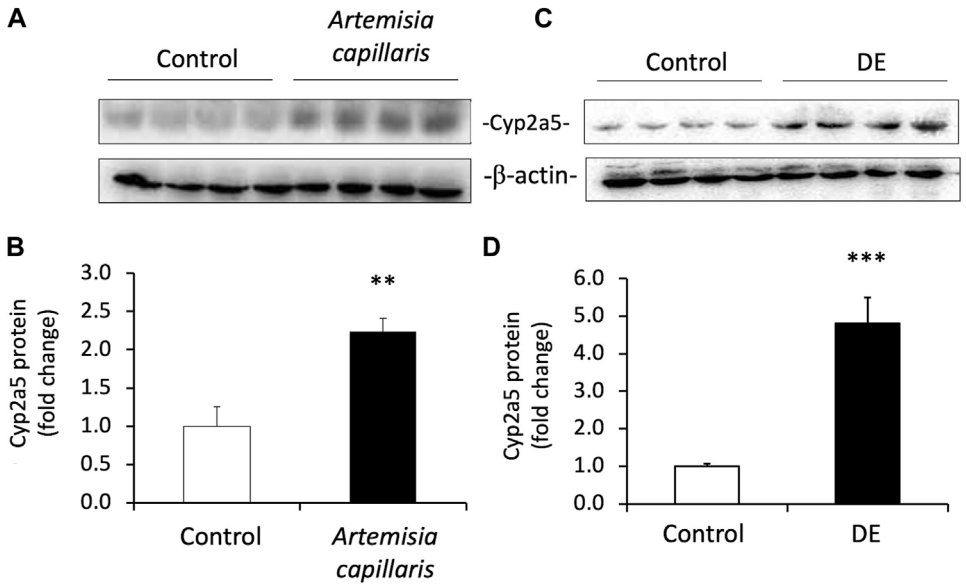

FIGURE 5 | Artemisia capillaris and DE increase hepatic Cyp2a5 protein in mice**.** Groups of 4 mice were gavaged daily for 3 days with either saline (controls), *Artemisia capillaris* (10 ml/kg) or DE (100 mg/kg). Panels **(A)** and **(B)**, western blots of hepatic Cyp2a5 protein from *Artemisia capillaris*- or DE-treated mice. Panels **(C)** and **(D)**, densitometric quantification of western blots. The mean difference is significant from controls at $p \leq 0.01$ ** and $p \leq 0.001$ ***.

RESULTS

HPLC and MS Analysis of *Artemisia capillaris* Extracts

The various constituents in the decoction of *Artemisia capillaris* were analyzed by UHPLC and mass spectrometry. Analysis of extracts of *Artemisia capillaris* by UHPLC revealed a major peak with a retention time of 5.444 (**Figure 2A**). A similar retention time (5.461) was obtained for the standard compound 6,7-dimethylesculetin (**Figure 2B**).

Mass spectrometry analysis of *Artemisia capillaris* extract revealed a main fragment of the first-order isotope with a mass-to charge ratio of 207.06 m/z for both *Artemisia capillaris* and 6,7-dimethylesculetin (**Figures 3A,B**). The secondary mass spectrum of the main fragment for both *Artemisia capillaris* and 6,7-dimethylesculetin had identical mass-to-charge ratios (i.e., 121.06, 151.07, 163.03, 179.07, 191.03, 192.03 and 207.06 m/z) for the most abundant ion peaks (**Figures 3C,D**).

6,7-Dimethylesculetin Increases Cyp2a5 mRNA and Protein Levels in Mouse Hepatocytes

Real-time RT-PCR of mRNA from primary mouse hepatocytes revealed dose-dependent increases in Cyp2a5 mRNA by DE to a maximum change of 12.7-fold at a concentration of 50 μM, ($p \leq 0.001$; **Figure 4A**). In a time-course experiment, treatment of primary mouse hepatocytes with 50 μM DE resulted in a significant induction of Cyp2a5 mRNA that peaked at 18-fold at 6 h ($p \leq 0.05$; **Figure 4B**).

Western blot analysis of microsomal protein from primary mouse hepatocytes showed that DE caused dose-dependent increases in Cyp2a5 protein levels to a maximum of approximately 4-fold at a concentration of 50 μM, ($p \leq 0.001$; **Figure 4C**). In a time-course experiment, Cyp2a5 protein was significantly elevated 2.5-fold by 24 h following treatment with 50 μM DE, ($p \leq 0.001$; **Figure 4D**).

Artemisia capillaris Thunb. And DE Induce Murine Hepatic Cyp2a5 Protein Levels *in vivo*

Because *Artemisia capillaris* is the active herb in Yin Chen Hao and DE is the major constituent of *Artemisia capillaris* comprising up to 2% by dry weight, we determined the capacity of both *Artemisia capillaris* and DE to induce murine Cyp2a5 protein *in vivo* (**Figure 5**). Both *Artemisia capillaris* and DE increased Cyp2a5 protein levels by 2.2-fold ($p \leq 0.01$, **Figure 5**, Panels A and B) and 4.8-fold ($p \leq 0.001$, **Figure 5**, Panels C and D) respectively.

DE Induces Constitutive Androstane Receptor Translocation Into Nucleus

To ascertain whether CAR is involved in DE-mediated upregulation of Cyp2a5, we first determined if DE activates CAR translocation to the nucleus. Western blot analysis of nuclear extracts from primary mouse hepatocytes demonstrated that DE treatment caused progressive increases in nuclear CAR levels in a time-dependent manner to a level significantly higher than controls by 2-fold ($p \leq 0.05$) by 24 h (**Figure 6**).

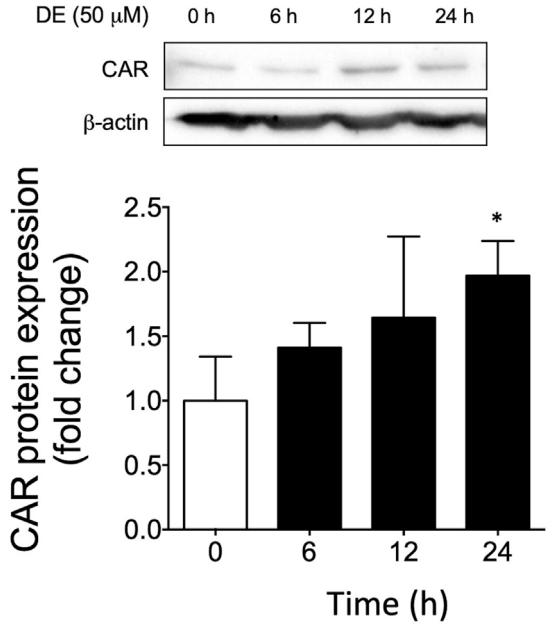

FIGURE 6 | DE causes nuclear translocation of CAR protein. Primary mouse hepatocytes were treated with 50 μM DE for 0, 6, 12, and 24 h. **(A)** Western blot analysis of nuclear CAR protein from DE-treated primary mouse hepatocytes. β-actin protein levels are shown as a control for protein loading. The western blot represents one replicate of three samples. All values represent the mean ± SEM (n = 3 hepatocyte cultures from different mice) normalized against the control levels and quantified by densitometry. Mean difference is significant from the control group at $*p \leq 0.05$.

Constitutive Androstane Receptor Regulates *Cyp2a5* Transcription Through a CAR Response Element in the *Cyp2a5* Promoter

To investigate the regulatory mechanism by which Cyp2a5 is induced by *Artemisia capillaris* and DE and the involvement of CAR in this process, we first identified two potential CAR-responsive DR-4 elements within the 5′-UTR of the *Cyp2a5* gene through MatInspector analysis, one located proximally within positions -366 to -390, and the other distally within positions 2,702 to 2,726 (**Figure 7**). To localize the CAR response element, luciferase activity was measured in mouse hepatocytes co-transfected with the mCAR expression plasmid and various truncation constructs of the *Cyp2a5* promoter (**Figure 8**). CAR overexpression significantly induced luciferase activity in the reporter constructs containing −3,033/+10 and −2,603/+10 fragments by approximately 16.5-fold and 10-fold respectively ($p \leq 0.05$) but had no effect on the constructs of shorter length.

To determine the role of the distal CAR-responsive element in Cyp2a5 transactivation, we transfected primary mouse hepatocytes with the wild-type full-length luciferase reporter plasmid p*Cyp2a5*-3,033 + 10-luc or with a reporter construct with the full-length 5′UTR in which the CAR-responsive element was mutated i.e. p*Cyp2a5*-ΔCAR (**Figure 9A**). Co-transfection with a mCAR expression plasmid revealed that CAR overexpression increased the wild-type Cyp2a5 promoter activity two-fold ($p \leq 0.05$), compared to hepatocytes transfected with an empty vector (**Figure 9B**). However, mutation of the CAR response element significantly reduced the CAR-mediated increase in reporter activity to 30% of the level observed in wild-type transfectants ($p \leq 0.05$).

Dimethylesculetin Increases *Cyp2a5* Transcription in the Presence of Constitutive Androstane Receptor

To further investigate the mechanism by which DE increases Cyp2a5 mRNA levels through a transcriptional mechanism involving CAR, a luciferase reporter assay was performed using primary mouse hepatocytes transfected with the wild-type *Cyp2a5*-3,033 + 10-luc construct with or without mCAR co-transfection in the presence or absence of DE (50 μM). A 3-fold increase in Cyp2a5 promoter activity ($p \leq 0.05$) was observed following treatment with DE (50 μM) alone (**Figure 10**). Cyp2a5 promoter activity increased 4.2-fold ($p \leq 0.05$) in hepatocytes co-transfected with mCAR and a 5-fold increase ($p \leq 0.05$) in Cyp2a5 promoter activity was observed in DE-treated hepatocytes co-transfected with mCAR.

DISCUSSION

Herbal decoctions such as Yin Zhi Huang and Yin Chen Hao containing *Artemisia capillaris* Thunb. and essential constituent 6,7-dimethylesculetin (DE) have been used for centuries in Asia to prevent and treat neonatal jaundice (Hui et al., 2020). While Yin Zhi Huang increases clearance and elimination of bilirubin via a process involving the transcription factor CAR and induction of hepatic glucuronosyl transferase (Huang et al., 2003; Huang et al., 2004), the detailed mechanism underlying this therapeutic effect is not entirely clear. CAR and other xenobiotic nuclear receptors are key intermediators by which xenobiotics regulate the expression of enzyme and transporters involved in their own absorption, metabolism and eventual elimination (Yan and Xie, 2016; Negishi et al., 2020). Moreover, the elimination of potentially toxic endogenous substances, such as bilirubin, is facilitated by CAR. For example, stimulation of CAR increases expression of hepatic organic anion transporting polypeptides (OATP) 1A1 and 1A4 thereby increasing uptake of bilirubin by the liver and also induces hepatic UDP-glucuronosyltransferase (UGT) 1A1, the only transferase capable of conjugating bilirubin to increase its hydrophilicity and excretion (Wagner et al., 2005; Wang et al., 2017; Weber et al., 2021). Accordingly, exposure to DE stimulates CAR in primary mouse hepatocytes and enhances bilirubin clearance (Huang et al., 2003; Huang et al., 2004). Because CAR stimulation induces Cyp2a5 (Kirby et al., 2011), an enzyme involved in the oxidative metabolism of bilirubin (Abu-Bakar et al., 2005; Kirby et al., 2011; Kim et al., 2013), we hypothesized that DE and *Artemisia capillaris* cause overexpression of Cyp2a5 via a molecular mechanism involving transcriptional activation by CAR.

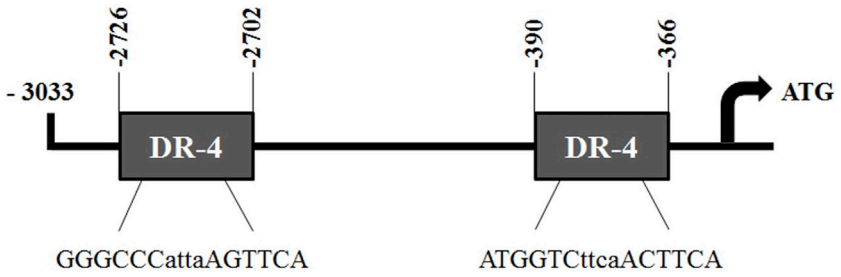

FIGURE 7 | Putative CAR responsive DR-4 elements in the Cyp2a5-3,033 + 10-luc promoter construct. Two potential CAR-responsive DR-4 elements identified within the Cyp2a5-3,033 + 10-luc construct through MatInspector analysis. Core sequences are shown below each site.

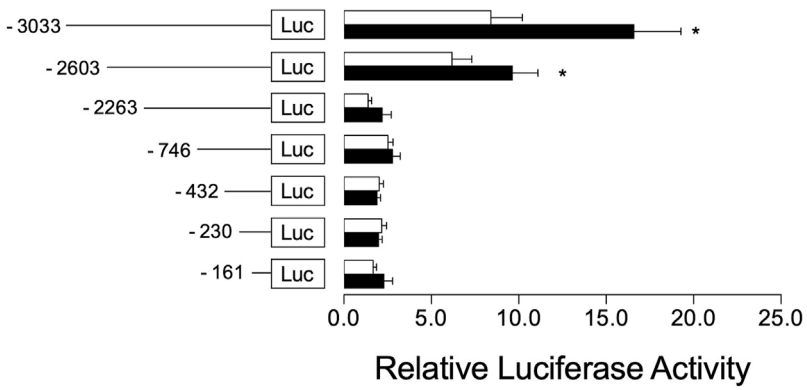

FIGURE 8 | CAR co-transfection increases Cyp2a5 transcriptional activation. Mouse Cyp2a5 promoter reporter assays were conducted in primary mouse hepatocytes transfected with progressively truncated luciferase reporter constructs (white bars) and co-transfected with a CAR expression plasmid (black bars). Luciferase activities were measured 24 h after transfection. The measured activities were normalized against Renilla (pR-TK) activities. All values represent the mean ± SEM derived from n = 3 hepatocyte cultures from different mice. The effect of CAR on each reporter construct is indicated by fold activity relative to control hepatocytes co-transfected with pcDNA3.1. Mean difference is significant from the control group at $^*p \leq 0.05$.

To test this hypothesis, Cyp2a5 mRNA and protein levels were first measured in *Artemisia capillaris*- and DE-treated mouse liver and DE-treated hepatocytes using quantitative real-time polymerase chain reaction (qRT-PCR) and Western blot analysis. Cyp2a5-luciferase reporter assays were then performed to investigate the involvement of CAR in the DE-mediated regulation of Cyp2a5 expression. The dose of DE (100 mg/kg) administered to mice was chosen based on the study by Huang et al., 2004 that demonstrated CAR activation and increased bilirubin clearance in mice treated with i. p. injections of DE at a dose of 100 mg/kg (Huang et al., 2004). An approximation of the human equivalent dose (HED) of DE can be derived by allometric scaling from mice to humans (HED = 100 mg/kg X 0.08 = 8 mg/kg) (USFDA et al., 2005; Nair and Jacob, 2016). The *in vitro* concentration of DE (50 μM) was also derived from the same study (Huang et al., 2004) that showed increased Cyp2b10 mRNA levels in cultured hepatocytes from wild-type mice but not from CAR knockout mice. An approximate extrapolation of this concentration of DE used in our cultured mouse hepatocyte experiments revealed it to be 14-fold lower than the HED.

Our findings show a dose-dependent relationship between DE treatment and increased Cyp2a5 expression at the mRNA and protein levels in primary mouse hepatocytes. An increase in hepatic Cyp2a5 protein levels was also observed in mice treated with both *Artemisia capillaris* and DE *in vivo*. A recent study using mouse and human liver microsomes has shown that both Cyp2a5 and CYP2A6 contribute to the O-demethylation of DE to scopoletin, the primary route of DE metabolism (Fayyaz et al., 2018). Collectively, this suggests that DE-mediated induction of Cyp2a5 would expedite DE metabolism as well as that of bilirubin, however, this was not investigated in the current study.

To determine whether DE regulates *Cyp2a5* at the transcriptional level, a luciferase reporter assay was conducted in DE-treated primary hepatocytes co-transfected with the Cyp2a5-3,033 + 10-luc promoter and the mCAR expression plasmid. DE significantly increased *Cyp2a5* promoter activity in mouse hepatocytes that overexpressed CAR indicating that DE transactivation of *Cyp2a5* occurs through a transcriptional mechanism involving CAR. We also confirmed previous studies that demonstrate DE-mediated translocation of CAR to

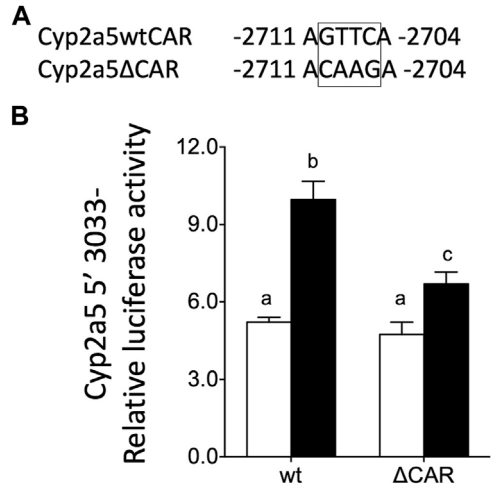

FIGURE 9 | Murine CAR overexpression increases Cyp2a5 transcription via a CAR response element in the murine Cyp2a5 promoter region. **(A)** The sequence of a CAR response element within the *Cyp2a5* promoter region showing site-directed mutation. **(B)** Cyp2a5-5′-3,033 luciferase reporter activities were assessed in primary mouse hepatocytes co-transfected with a CAR expression plasmid (black bars) or without co-transfection (white bars). In addition, the effect of site-directed mutation of the CAR response element (ΔCAR) on Cyp2a5 transcriptional activation of Cyp2a5 was tested. The measured activities were normalized against Renilla (pRL-TK) activities. All values represent the mean ± SEM (n = 4 hepatocyte cultures from different mice). Bars with different letters are significantly different ($p \leq 0.05$).

the nucleus of mouse hepatocytes in primary culture (Huang et al., 2004; Yang et al., 2011). Within the nucleus, CAR-RXR heterodimers interact with *cis*-elements in CAR-regulated genes. Although no CAR-responsive elements have been positively identified within the Cyp2a5 gene, analysis of the Cyp2a5 5′-UTR sequence using a transcription factor binding site search (MatInspector, Genomatix), revealed two putative CAR-responsive elements. Both identified sites were direct repeat elements separated by 4 base pairs (DR-4). Our luciferase reporter results including deletion analysis and site-directed mutagenesis of these sites indicate that the more distal site represents a DR-4 motif by which CAR regulates Cyp2a5 transcriptional activity. To the best of our knowledge, this is the first time that a functional CAR-responsive DR-4 motif has been identified in the promoter region of Cyp2a5. It has previously been shown that phenobarbital causes CAR-RXR heterodimers to bind to DR-4 motifs resulting in up-regulation of CYP2B genes and other genes involved drug metabolism (Kakizaki et al., 2003). CAR also interacts with DR-4 motifs in the promoters of several other CYP genes including the murine CYP2B10 (Honkakoski et al., 1998), CYP2C29 (Ferguson et al., 2005), and CYP2C37 (Jackson et al., 2006), and human CYP2B6 (Sueyoshi et al., 1999), CYP2C9 (Gerbal-Chaloin et al., 2002), CYP2C19 (Chen et al., 2003), and CYP2C8 (Ferguson et al., 2005). These previous findings corroborate the results of this study as they highlight the potential for CAR-mediated regulation of the *Cyp2a5* gene.

It is not surprising that DE and *Artemisia capillaris* induce Cyp2a5 via CAR considering that CAR is xenobiotic sensor and Cyp2a5 plays an important cytoprotective role in protecting against liver injury and hepatoxicity (Kirby et al., 2011; Abu-Bakar et al., 2013; Hong et al., 2016). CAR is also involved in enhancing CYP2B10-mediated detoxification of ethanol in the liver (Cederbaum, 2012). In addition to CAR, *Cyp2a5* is regulated by other transcription factors including Nrf2 (Abu-Bakar et al., 2007; Lämsä et al., 2010; Kirby et al., 2011), AhR (Arpiainen et al., 2005) and hepatic nuclear factor 4 alpha (NRF-4a) and NF-1 (Ulvila et al., 2004) and functional response elements for these transcription factors have been identified in the *Cyp2a5* promoter region. In addition, we have also shown that bilirubin causes Nrf2-mediated transactivation of *Cyp2a5* thus providing protection against bilirubin hepatotoxicity (Kim et al., 2013).

CYPs are known to be induced and inhibited by various drugs, herbal remedies, and toxic compounds (Hakkola et al., 2020). Interestingly, Artemisinin, an extract from the plant *Artemisia annua,* used as a medication to treat malaria, is also an activator of CAR and an inducer of Cyp2b10 and Cyp2a5 in mouse liver (Simonsson et al., 2006). Moreover, human CYP2A6 is induced by various natural products including genistein and quercetin (Hakkola et al., 2020). While CYP2A6 is also induced by CAR and other transcription factors including, PXR, ERα, NRF2, HNF-4alpha, C/EBPalpha and beta, and Oct-1 (Pitarque et al., 2005; Raunio and Rahnasto-Rilla, 2012), it not is not known whether DE or *Artemisia capillaris* are capable of inducing CYP2A6. However, coumarin is the marker substrate for human CYP2A6 and mouse Cyp2a5 as they both have coumarin 7-hydroxylase activity (Kaipainen et al., 1984; Pelkonen et al., 2000; Raunio and Rahnasto-Rilla, 2012). Interestingly, DE and esculetin (6,7 dihydroxycoumarin) are both coumarin derivatives and have antioxidative and cytoprotective properties against hepatotoxicity and liver injury (Atmaca et al., 2011). It is possible that the

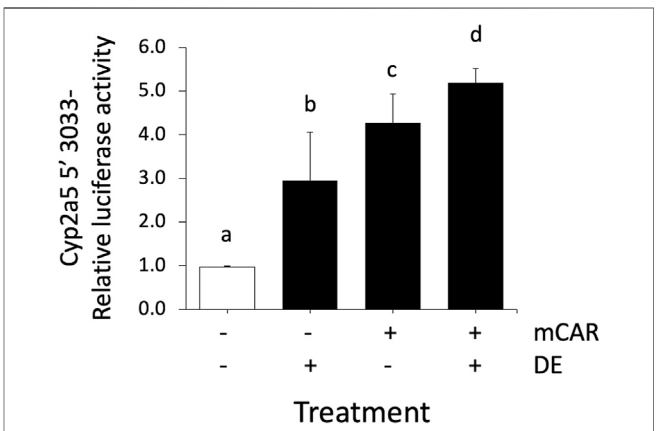

FIGURE 10 | Cyp2a5 induction by DE is increased by CAR overexpression. Cyp2a5-5′-luciferase reporter activities were assessed in primary mouse hepatocytes 24 h after CAR co-transfection, CAR co-transfection followed by 50 μM DE or DE treatment alone for 24 h. The measured activities were normalized against Renilla (pRL-TK) activities. All values represent the mean ± SEM (n = 4). Bars with different letters are significantly different ($p \leq 0.05$).

hepatoprotective qualities of Yin Zhi Huang and Yin Chen Hao in humans and other species are due, in part, to induction of CYP2A enzymes.

In conclusion, the results of this study indicate that *Artemisia capillaris* and DE induce Cyp2a5 expression at both mRNA and protein levels. Additionally, the current findings show that 6,7-dimethylesculetin significantly increases *Cyp2a5* expression at the transcriptional level through transactivation by CAR. These findings contribute to our understanding of Cyp2a5 regulation and may also provide further insight into the mechanism by which DE enhances bilirubin clearance. While it has been well established that CAR increases bilirubin clearance by inducing hepatic UGT1A1 and various ion transporters that increase bilirubin clearance, it is possible that DE-mediated upregulation of Cyp2a5 may also be involved in view of the role of Cyp2a5 in the oxidative metabolism of bilirubin (Abu-Bakar et al., 2011; Kim et al., 2013). Future *in vivo* studies could assess the role of Cyp2a5 and CYP2A6 in the oxidative metabolism of bilirubin in DE-mediated bilirubin clearance. This may ultimately provide an opportunity for the development of novel therapies for neonatal and other forms of jaundice.

DATA AVAILABILITY STATEMENT

The raw data supporting the conclusions of this article will be made available by the authors, without undue reservation.

ETHICS STATEMENT

The animal study was reviewed and approved by Animal Care Committee of the University of Guelph, Animal Utilization Protocol number 3243.

AUTHOR CONTRIBUTIONS

GK and XZ designed the overall study. SDK, LM, EH, MA, BL and ZJ performed the experiments. XZ and ZJ provided samples essential to the study. SDK, GK, and XZ wrote the manuscript. All authors contributed to the article and approved the submitted version.

FUNDING

This research was supported by funding from "The Incubation Project on State Key Laboratory of Biological Resources and Ecological Environment of Qinba Areas" (grant number SLGPT2019KF04-04).

ACKNOWLEDGMENTS

We would like to thank Meghan Larin for creating the luciferase reporter construct with site-directed mutation of the CAR response element (ΔCAR) in the Cyp2a5 5′ proximal promoter.

REFERENCES

Abu-Bakar, A., Arthur, D. M., Aganovic, S., Ng, J. C., and Lang, M. A. (2011). Inducible Bilirubin Oxidase: a Novel Function for the Mouse Cytochrome P450 2A5. *Toxicol. Appl. Pharmacol.* 257 (1), 14–22. doi:10.1016/j.taap.2011.08.011

Abu-Bakar, A., Hakkola, J., Juvonen, R., Rahnasto-Rilla, M., Raunio, H., and Lang, M. A. (2013). Function and Regulation of the Cyp2a5/CYP2A6 Genes in Response to Toxic Insults in the Liver. *Curr. Drug Metab.* 14 (1), 137–150. doi:10.2174/138920013804545223

Abu-Bakar, A., Lämsä, V., Arpiainen, S., Moore, M. R., Lang, M. A., and Hakkola, J. (2007). Regulation of CYP2A5 Gene by the Transcription Factor Nuclear Factor (Erythroid-derived 2)-like 2. *Drug Metab. Dispos* 35 (5), 787–794. doi:10.1124/dmd.106.014423

Abu-Bakar, A., Moore, M. R., and Lang, M. A. (2005). Evidence for Induced Microsomal Bilirubin Degradation by Cytochrome P450 2A5. *Biochem. Pharmacol.* 70 (10), 1527–1535. doi:10.1016/j.bcp.2005.08.009

Arpiainen, S., Raffalli-Mathieu, F., Lang, M. A., Pelkonen, O., and Hakkola, J. (2005). Regulation of the Cyp2a5 Gene Involves an Aryl Hydrocarbon Receptor-dependent Pathway. *Mol. Pharmacol.* 67 (4), 1325–1333. doi:10.1124/mol.104.008078

Atmaca, M., Bilgin, H. M., Obay, B. D., Diken, H., Kelle, M., and Kale, E. (2011). The Hepatoprotective Effect of Coumarin and Coumarin Derivates on Carbon Tetrachloride-Induced Hepatic Injury by Antioxidative Activities in Rats. *J. Physiol. Biochem.* 67 (4), 569–576. doi:10.1007/s13105-011-0103-5

Baes, M., Gulick, T., Choi, H. S., Martinoli, M. G., Simha, D., and Moore, D. D. (1994). A New Orphan Member of the Nuclear Hormone Receptor Superfamily that Interacts with a Subset of Retinoic Acid Response Elements. *Mol. Cel Biol* 14 (3), 1544–1552. doi:10.1128/mcb.14.3.1544

Cederbaum, A. I. (2012). Alcohol Metabolism. *Clin. Liver Dis.* 16 (4), 667–685. doi:10.1016/j.cld.2012.08.002

Chee, Y. Y., Chung, P. H., Wong, R. M., and Wong, K. K. (2018). Jaundice in Infants and Children: Causes, Diagnosis, and Management. *Hong Kong Med. J.* 24 (3), 285–292. doi:10.12809/hkmj187245

Chen, Y., Ferguson, S. S., Negishi, M., and Goldstein, J. A. (2003). Identification of Constitutive Androstane Receptor and Glucocorticoid Receptor Binding Sites in the CYP2C19 Promoter. *Mol. Pharmacol.* 64 (2), 316–324. doi:10.1124/mol.64.2.316

Dennery, P. A., Seidman, D. S., and Stevenson, D. K. (2001). Neonatal Hyperbilirubinemia. *N. Engl. J. Med.* 344 (8), 581–590. doi:10.1056/NEJM200102223440807

Elferink, R. O. (2004). Yin Zhi Huang and Other Plant-Derived Preparations: where Herbal and Molecular Medicine Meet. *J. Hepatol.* 41 (4), 691–693. doi:10.1016/j.jhep.2004.08.001

Fayyaz, A., Makwinja, S., Auriola, S., Raunio, H., and Juvonen, R. O. (2018). Comparison of *In Vitro* Hepatic Scoparone 7-O-Demethylation between Humans and Experimental Animals. *Planta Med.* 84 (5), 320–328. doi:10.1055/s-0043-119886

Ferguson, S. S., Chen, Y., LeCluyse, E. L., Negishi, M., and Goldstein, J. A. (2005). Human CYP2C8 Is Transcriptionally Regulated by the Nuclear Receptors Constitutive Androstane Receptor, Pregnane X Receptor, Glucocorticoid Receptor, and Hepatic Nuclear Factor 4alpha. *Mol. Pharmacol.* 68 (3), 747–757. doi:10.1124/mol.105.013169

Gerbal-Chaloin, S., Daujat, M., Pascussi, J. M., Pichard-Garcia, L., Vilarem, M. J., and Maurel, P. (2002). Transcriptional Regulation of CYP2C9 Gene. Role of Glucocorticoid Receptor and Constitutive Androstane Receptor. *J. Biol. Chem.* 277 (1), 209–217. doi:10.1074/jbc.M107228200

Gilmore, W. J., and Kirby, G. M. (2004). Endoplasmic Reticulum Stress Due to Altered Cellular Redox Status Positively Regulates Murine Hepatic CYP2A5 Expression. *J. Pharmacol. Exp. Ther.* 308 (2), 600–608. doi:10.1124/jpet.103.060111

Hakkola, J., Hukkanen, J., Turpeinen, M., and Pelkonen, O. (2020). Inhibition and Induction of CYP Enzymes in Humans: an Update. *Arch. Toxicol.* 94 (11), 3671–3722. doi:10.1007/s00204-020-02936-7

Hong, F., Si, C., Gao, P., Cederbaum, A. I., Xiong, H., and Lu, Y. (2016). The Role of CYP2A5 in Liver Injury and Fibrosis: Chemical-specific Difference. *Naunyn Schmiedebergs Arch. Pharmacol.* 389 (1), 33–43. doi:10.1007/s00210-015-1172-8

Honkakoski, P., Zelko, I., Sueyoshi, T., and Negishi, M. (1998). The Nuclear Orphan Receptor CAR-Retinoid X Receptor Heterodimer Activates the Phenobarbital-Responsive Enhancer Module of the CYP2B Gene. *Mol. Cel Biol* 18 (10), 5652–5658. doi:10.1128/mcb.18.10.5652

Huang, W., Zhang, J., Chua, S. S., Qatanani, M., Han, Y., Granata, R., et al. (2003). Induction of Bilirubin Clearance by the Constitutive Androstane Receptor (CAR). *Proc. Natl. Acad. Sci. U S A.* 100 (7), 4156–4161. doi:10.1073/pnas.0630614100

Huang, W., Zhang, J., and Moore, D. D. (2004). A Traditional Herbal Medicine Enhances Bilirubin Clearance by Activating the Nuclear Receptor CAR. *J. Clin. Invest.* 113 (1), 137–143. doi:10.1172/JCI18385

Hui, Y., Wang, X., Yu, Z., Fan, X., Cui, B., Zhao, T., et al. (2020). Scoparone as a Therapeutic Drug in Liver Diseases: Pharmacology, Pharmacokinetics and Molecular Mechanisms of Action. *Pharmacol. Res.* 160, 105170. doi:10.1016/j.phrs.2020.105170

Jackson, J. P., Ferguson, S. S., Negishi, M., and Goldstein, J. A. (2006). Phenytoin Induction of the Cyp2c37 Gene Is Mediated by the Constitutive Androstane Receptor. *Drug Metab. Dispos* 34 (12), 2003–2010. doi:10.1124/dmd.106.012005

Kachaylo, E. M., Pustylnyak, V. O., Lyakhovich, V. V., and Gulyaeva, L. F. (2011). Constitutive Androstane Receptor (CAR) Is a Xenosensor and Target for Therapy. *Biochemistry (Mosc)* 76 (10), 1087–1097. doi:10.1134/S0006297911100026

Kaipainen, P., Nebert, D. W., and Lang, M. A. (1984). Purification and Characterization of a Microsomal Cytochrome P-450 with High Activity of Coumarin 7-hydroxylase from Mouse Liver. *Eur. J. Biochem.* 144 (3), 425–431. doi:10.1111/j.1432-1033.1984.tb08483.x

Kakizaki, S., Yamamoto, Y., Ueda, A., Moore, R., Sueyoshi, T., and Negishi, M. (2003). Phenobarbital Induction of Drug/steroid-Metabolizing Enzymes and Nuclear Receptor CAR. *Biochim. Biophys. Acta* 1619 (3), 239–242. doi:10.1016/s0304-4165(02)00482-8

Kim, S. D., Antenos, M., Squires, E. J., and Kirby, G. M. (2013). Cytochrome P450 2A5 and Bilirubin: Mechanisms of Gene Regulation and Cytoprotection. *Toxicol. Appl. Pharmacol.* 270 (2), 129–138. doi:10.1016/j.taap.2013.04.013

Kirby, G. M., Nichols, K. D., and Antenos, M. (2011). CYP2A5 Induction and Hepatocellular Stress: an Adaptive Response to Perturbations of Heme Homeostasis. *Curr. Drug Metab.* 12 (2), 186–197. doi:10.2174/138920011795016845

Kirby, G. M., Wolf, C. R., Neal, G. E., Judah, D. J., Henderson, C. J., Srivatanakul, P., et al. (1993). *In Vitro* metabolism of Aflatoxin B1 by normal and Tumorous Liver Tissue from Thailand. *Carcinogenesis* 14 (12), 2613–2620. doi:10.1093/carcin/14.12.2613

Lämsä, V., Levonen, A. L., Leinonen, H., Ylä-Herttuala, S., Yamamoto, M., and Hakkola, J. (2010). Cytochrome P450 2A5 Constitutive Expression and Induction by Heavy Metals Is Dependent on Redox-Sensitive Transcription Factor Nrf2 in Liver. *Chem. Res. Toxicol.* 23 (5), 977–985. doi:10.1021/tx100084c

Lämsä, V., Levonen, A. L., Sormunen, R., Yamamoto, M., and Hakkola, J. (2012). Heme and Heme Biosynthesis Intermediates Induce Heme Oxygenase-1 and Cytochrome P450 2A5, Enzymes with Putative Sequential Roles in Heme and Bilirubin Metabolism: Different Requirement for Transcription Factor Nuclear Factor Erythroid- Derived 2-like 2. *Toxicol. Sci.* 130 (1), 132–144. doi:10.1093/toxsci/kfs237

Lavery, D. J., Lopez-Molina, L., Margueron, R., Fleury-Olela, F., Conquet, F., Schibler, U., et al. (1999). Circadian Expression of the Steroid 15 Alpha-Hydroxylase (Cyp2a4) and Coumarin 7-hydroxylase (Cyp2a5) Genes in Mouse Liver Is Regulated by the PAR Leucine Zipper Transcription Factor DBP. *Mol. Cel Biol* 19 (10), 6488–6499. doi:10.1128/mcb.19.10.6488

Li, G., Zhu, J., and Wu, L. (2001). Study on Hepatic-Protective Effect of "yinzhihuang" Granula. *Zhong Yao Cai* 24 (5), 353–355.

Li, J. Y., Cao, H. Y., Sun, L., Sun, R. F., Wu, C., Bian, Y. Q., et al. (2017). Therapeutic Mechanism of Yin-Chén-Hāo Decoction in Hepatic Diseases. *World J. Gastroenterol.* 23 (7), 1125–1138. doi:10.3748/wjg.v23.i7.1125

McDonagh, A. F. (2010). The Biliverdin-Bilirubin Antioxidant Cycle of Cellular protection: Missing a Wheel. *Free Radic. Biol. Med.* 49 (5), 814–820. doi:10.1016/j.freeradbiomed.2010.06.001

Mitra, S., and Rennie, J. (2017). Neonatal Jaundice: Aetiology, Diagnosis and Treatment. *Br. J. Hosp. Med. (Lond)* 78 (12), 699–704. doi:10.12968/hmed.2017.78.12.699

Muhsain, S. N., Lang, M. A., and Abu-Bakar, A. (2015). Mitochondrial Targeting of Bilirubin Regulatory Enzymes: An Adaptive Response to Oxidative Stress. *Toxicol. Appl. Pharmacol.* 282 (1), 77–89. doi:10.1016/j.taap.2014.11.010

Nair, A. B., and Jacob, S. (2016). A Simple Practice Guide for Dose Conversion between Animals and Human. *J. Basic Clin. Pharm.* 7 (2), 27–31. doi:10.4103/0976-0105.177703

Negishi, M., Kobayashi, K., Sakuma, T., and Sueyoshi, T. (2020). Nuclear Receptor Phosphorylation in Xenobiotic Signal Transduction. *J. Biol. Chem.* 295 (45), 15210–15225. doi:10.1074/jbc.REV120.007933

Nichols, K. D., and Kirby, G. M. (2008). Expression of Cytochrome P450 2A5 in a Glucose-6-Phosphate Dehydrogenase-Deficient Mouse Model of Oxidative Stress. *Biochem. Pharmacol.* 75 (5), 1230–1239. doi:10.1016/j.bcp.2007.10.032

Pelkonen, O., Rautio, A., Raunio, H., and Pasanen, M. (2000). CYP2A6: a Human Coumarin 7-hydroxylase. *Toxicology* 144 (1-3), 139–147. doi:10.1016/s0300-483x(99)00200-0

Pitarque, M., Rodríguez-Antona, C., Oscarson, M., and Ingelman-Sundberg, M. (2005). Transcriptional Regulation of the Human CYP2A6 Gene. *J. Pharmacol. Exp. Ther.* 313 (2), 814–822. doi:10.1124/jpet.104.081570

Pustylnyak, Y. A., Gulyaeva, L. F., and Pustylnyak, V. O. (2020). Noncanonical Constitutive Androstane Receptor Signaling in Gene Regulation. *Int. J. Mol. Sci.* 21 (18). doi:10.3390/ijms21186735

Raunio, H., and Rahnasto-Rilla, M. (2012). CYP2A6: Genetics, Structure, Regulation, and Function. *Drug Metabol Drug Interact* 27 (2), 73–88. doi:10.1515/dmdi-2012-0001

Rets, A., Clayton, A. L., Christensen, R. D., and Agarwal, A. M. (2019). Molecular Diagnostic Update in Hereditary Hemolytic Anemia and Neonatal Hyperbilirubinemia. *Int. J. Lab. Hematol.* 41 (Suppl. 1), 95–101. doi:10.1111/ijlh.13014

Rueden, C. T., Schindelin, J., Hiner, M. C., DeZonia, B. E., Walter, A. E., Arena, E. T., et al. (2017). ImageJ2: ImageJ for the Next Generation of Scientific Image Data. *BMC Bioinformatics* 18, 529. doi:10.1186/s12859-017-1934-z

Savas, U., Griffin, K. J., and Johnson, E. F. (1999). Molecular Mechanisms of Cytochrome P-450 Induction by Xenobiotics: An Expanded Role for Nuclear Hormone Receptors. *Mol. Pharmacol.* 56 (5), 851–857. doi:10.1124/mol.56.5.851

Seubert, J. M., Webb, C. D., and Bend, J. R. (2002). Acute Sodium Arsenite Treatment Induces Cyp2a5 but Not Cyp1a1 in the C57Bl/6 Mouse in a Tissue (Kidney) Selective Manner. *J. Biochem. Mol. Toxicol.* 16 (2), 96–106. doi:10.1002/jbt.10023

Shifera, A. S., and Hardin, J. A. (2010). Factors Modulating Expression of Renilla Luciferase from Control Plasmids Used in Luciferase Reporter Gene Assays. *Anal. Biochem.* 396 (2), 167–172. doi:10.1016/j.ab.2009.09.043

Simonsson, U. S., Lindell, M., Raffalli-Mathieu, F., Lannerbro, A., Honkakoski, P., and Lang, M. A. (2006). *In Vivo* and Mechanistic Evidence of Nuclear Receptor CAR Induction by Artemisinin. *Eur. J. Clin. Invest.* 36 (9), 647–653. doi:10.1111/j.1365-2362.2006.01700.x

Sueyoshi, T., Kawamoto, T., Zelko, I., Honkakoski, P., and Negishi, M. (1999). The Repressed Nuclear Receptor CAR Responds to Phenobarbital in Activating the Human CYP2B6 Gene. *J. Biol. Chem.* 274 (10), 6043–6046. doi:10.1074/jbc.274.10.6043

Takeda, T. A., Mu, A., Tai, T. T., Kitajima, S., and Taketani, S. (2015). Continuous De Novo Biosynthesis of Haem and its Rapid Turnover to Bilirubin Are Necessary for Cytoprotection against Cell Damage. *Sci. Rep.* 5, 10488. doi:10.1038/srep10488

Tomaro, M. L., and Batlle, A. M. (2002). Bilirubin: its Role in Cytoprotection against Oxidative Stress. *Int. J. Biochem. Cel Biol* 34 (3), 216–220. doi:10.1016/s1357-2725(01)00130-3

USFDA (2005). *Guidance for Industry: Estimating the Maximum Safe Starting Dose in Adult Healthy Volunteers*. Rockville, MD: DHHS.

Ulvila, J., Arpiainen, S., Pelkonen, O., Aida, K., Sueyoshi, T., Negishi, M., et al. (2004). Regulation of Cyp2a5 Transcription in Mouse Primary Hepatocytes:

Roles of Hepatocyte Nuclear Factor 4 and Nuclear Factor I. *Biochem. J.* 381 (3), 887–894. doi:10.1042/BJ20040387

Wagner, M., Halilbasic, E., Marschall, H. U., Zollner, G., Fickert, P., Langner, C., et al. (2005). CAR and PXR Agonists Stimulate Hepatic Bile Acid and Bilirubin Detoxification and Elimination Pathways in Mice. *Hepatology* 42 (2), 420–430. doi:10.1002/hep.20784

Wang, X., Zheng, L., Wu, J., Tang, B., Zhang, M., Zhu, D., et al. (2017). Constitutive Androstane Receptor Activation Promotes Bilirubin Clearance in a Murine Model of Alcoholic Liver Disease. *Mol. Med. Rep.* 15 (6), 3459–3466. doi:10.3892/mmr.2017.6435

Weber, A. A., Mennillo, E., Yang, X., van der Schoor, L. W. E., Jonker, J. W., Chen, S., et al. (2021). Regulation of Intestinal UDP-Glucuronosyltransferase 1A1 by the Farnesoid X Receptor Agonist Obeticholic Acid Is Controlled by Constitutive Androstane Receptor through Intestinal Maturation. *Drug Metab. Dispos* 49 (1), 12–19. doi:10.1124/dmd.120.000240

Yan, J., and Xie, W. (2016). A Brief History of the Discovery of PXR and CAR as Xenobiotic Receptors. *Acta Pharm. Sin B* 6 (5), 450–452. doi:10.1016/j.apsb.2016.06.011

Yang, D., Yang, J., Shi, D., Deng, R., and Yan, B. (2011). Scoparone Potentiates Transactivation of the Bile Salt export Pump Gene and This Effect Is Enhanced by Cytochrome P450 Metabolism but Abolished by a PKC Inhibitor. *Br. J. Pharmacol.* 164 (5), 1547–1557. doi:10.1111/j.1476-5381.2011.01522.x

Conflict of Interest: The authors declare that the research was conducted in the absence of any commercial or financial relationships that could be construed as a potential conflict of interest.

Publisher's Note: All claims expressed in this article are solely those of the authors and do not necessarily represent those of their affiliated organizations, or those of the publisher, the editors and the reviewers. Any product that may be evaluated in this article, or claim that may be made by its manufacturer, is not guaranteed or endorsed by the publisher.

frontiers in Pharmacology

ORIGINAL RESEARCH
published: 26 November 2021
doi: 10.3389/fphar.2021.761551

HPLC-DAD Fingerprints Combined With Multivariate Analysis of Epimedii Folium From Major Producing Areas in Eastern Asia: Effect of Geographical Origin and Species

Ben Li[1], Marta R. M. Lima[2†], Yuhao Nie[1], Long Xu[1,3], Xiang Liu[1], Hongchao Yuan[4], Chen Chen[1], Alberto CP Dias[1,3,5] and Xiaoying Zhang[1,3,6]**

[1]Chinese-German Joint Laboratory for Natural Product Research, Qinling-Bashan Mountains Bioresources Comprehensive Development C.I.C., College of Biological Science and Engineering, Shaanxi University of Technology, Hanzhong, China, [2]Department of Agriculture Nutrition and Food Systems, University of New Hampshire, Durham, NH, United States, [3]Centre of Molecular and Environmental Biology (CBMA), Department of Biology, University of Minho, Campus de Gualtar, Braga, Portugal, [4]Jinhuifang Traditional Chinese Medicine Technology Co., Ltd, Hanzhong, China, [5]Centre of Biological Engineering (CEB), University of Minho, Campus de Gualtar, Braga, Portugal, [6]Department of Biomedical Sciences, Ontario Veterinary College, University of Guelph, Guelph, ON, Canada

The growth location and plant variety may influence the active components and biological activities of plants used in phytomedicine. In this study, nine sets of different Epimedii Folium, from different representative cultivation locations and Epimedium species, were collected for comparison, using HPLC-DAD combined with multivariate analysis. The objective was to investigate the influence of geographical origin and Epimedium species on the quality of Epimedii Folium, and provide applicable guidance for cultivation and quality control of Epimedii Folium. Several Epimedium spp. sets were used to establish the HPLC-DAD fingerprints and 91 peaks (compounds) were selected for the multivariate analysis. Major compounds were analyzed by HPLC-DAD combined with principal component analysis (PCA). HPLC quantitative analysis of known bioactive compounds was performed. Application of PCA to HPLC data showed that Epimedium samples sharing the same geographical origin or species clustered together, indicating that both species and geographical origin have impacts on the quality of Epimedii Folium. The major bioactive flavonoid compounds, epimedin C, icariin and baohuoside I, were identified and quantified. The concentration of bioactive compounds was significantly influenced both by species and geographical origin. *E. sagittatum* from Sichuan showed the highest content of bioactive compounds. The results showed that both Epimedium species and geographical origin have strong impact into quality of Epimedii Folium. HPLC data combined with multivariate analysis is a suitable approach to inform the selection of cultivation areas and choose Epimedium spp. most suitable for different geographical areas, resulting in improved quality of Epimedii Folium.

Keywords: Epimedium sp, high performance liquid chromatography (HPLC), principal component analysis (PCA), epimedin C, icariin, baohuoside I

OPEN ACCESS

Edited by:
George Qian Li, Western Sydney University, Australia

Reviewed by:
Hossein Hashempour, Azarbaijan Shahid Madani University, Iran
Abuzar Kabir, Florida International University, United States

***Correspondence:**
Alberto CP Dias
acpdias@bio.uminho.pt
Xiaoying Zhang
zhang@bio.uminho.pt

†Present address:
Marta R. M. Lima, School of Plant and Environmental Sciences, Virginia Tech, Blacksburg, VA, United States

Specialty section:
This article was submitted to Ethnopharmacology, a section of the journal Frontiers in Pharmacology

Received: *20 August 2021*
Accepted: *09 November 2021*
Published: *26 November 2021*

Citation:
Li B, Lima MRM, Nie Y, Xu L, Liu X, Yuan H, Chen C, Dias ACP and Zhang X (2021) HPLC-DAD Fingerprints Combined With Multivariate Analysis of Epimedii Folium From Major Producing Areas in Eastern Asia: Effect of Geographical Origin and Species. Front. Pharmacol. 12:761551. doi: 10.3389/fphar.2021.761551

INTRODUCTION

Epimedii Folium, "淫羊藿 (Yin Yang Huo)" in Chinese - also known as Herba Epimedii, barrenwort, bishop's hat, fairy wings, horny goat weed, and rowdy lamb herb - is an important medicinal herb ingredient used in traditional Chinese medicine (TCM) to treat osteoporosis and sexual dysfunction, among other conditions (Ma et al., 2011). Epimedii Folium has been used for more than 2000 years with the major functions of "tonifying kidney Yang, strengthening muscles and bones, dispelling wind and dampness" (Chen et al., 2015b). Epimedium sp. improved osteoporosis condition and strengthening bones in human studies (Indran et al., 2016), and has been used to treat sexual dysfunction (Shindel et al., 2010) and cardiovascular diseases (Li et al., 2015b). Nowadays, Chinese Pharmacopeia accepts four Epimedium species as a source of Epimedii Folium, including *Epimedium brevicornum* Maxim, *Epimedium sagittatum* (Siebold and Zucc.) Maxim, *Epimedium pubescens* Maxim, and *Epimedium koreanum* Nakai. Its dried leaves have spicy and sweet tastes, and have been used for further dosage preparations (Chinese Pharmacopoeia, 2020).

Many active compounds, including epimedin A, epimedin B, epimedin C, icariin and baohuoside I, have been identified from Epimedium (Wu et al., 2012). Among them, the prenylflavonoids flavonoids icariin, epimedin C and baohuoside I, are considered as the major bioactive components and used as marker compounds for quality control (Zhao et al., 2010). Icariin, a flavonol glycoside obtained from the aerial part of the plant (Indran et al., 2016), could enhance the osteogenic effect of bone morphogenetic protein 2 (BMP2) which induces osteoblast differentiation and stimulate bone or cartilage formation and cyclic adenosine monophosphate (cAMP) signaling pathway which regulates osteogenic differentiation and mineralization (Chen et al., 2019). Additionally, icariin has been reported to have anti-tumorigenic activity. Icariin significantly inhibited the proliferation of several cancer cells, like ovarian cancer cells (Li et al., 2015a), medulloblastoma cells (Sun et al., 2016), and human neural cells (Yang et al., 2016).

Epimedium brevicornum Maxim is widely distributed in northwest China, including Gansu, Shaanxi, Ningxia and He'nan provinces, whilst *Epimedium pubescens* Maxim grows in the south provinces of Sichuan, Guizhou and Anhui (Guo and Xiao, 2003). These two species have been regarded having higher quality with consistent higher levels of major active components (He et al., 2019). Quality of commercial Epimedii Folium is mainly controlled by its icariin content, with the minimal content of 0.5% (g/g DW) in dried products, according to Chinese Pharmacopoeia (Chinese Pharmacopoeia, 2015). However, icariin contents of Epimedium on the markets remain uneven, even undetectable in some batches of commercial Epimedium, possibly due to the regional and varietal differences. According to a survey performed in 2014, the ranges of icariin contents in 104 batches from different species were 0.01–0.17% (g/g DW) and all of them were substandard (Ma et al., 2014). Other studies support such observation (Pei et al., 2007; Polat and Coskun, 2016).

TABLE 1 | Sources and species of Epimedii Folium samples.

Sample	Origin	Species
S1	Wanyuan, Sichuan	*E. pubescens* Maxim
S2	Wanyuan, Sichuan	*E. sagittatum* (Siebold and Zucc.) Maxim
S3	Linjiang, Jilin	*E. pubescens* Maxim
S4	Linjiang, Jilin	*E. koreanum* Nakai
S5	Longnan, Gansu	*E. pubescens* Maxim
S6	Longnan, Gansu	*E. brevicornum* Maxim
S7	Weiyuan, Gansu	*E. brevicornum* Maxim
S8	Daqiu, South Korea	*E. koreanum* Nakai
S9	Shangluo, Shaanxi	*E. brevicornum* Maxim

This study aimed to investigate the influence of the cultivation location (province) and Epimedium species on the phytocomposition and quality of Epimedii Folium, namely the major relevant bioactive components, using HPLC-DAD and multivariate statistical analysis, since these issues are highly relevant for cultivation and quality control of Epimedii Folium.

MATERIALS AND METHODS

Chemicals

HPLC-grade ethanol, acetonitrile and formic acid were purchased from Chron chemicals (Chengdu, Sichuan, China), Damao chemical (Tianjin, China) and Kermel Chemical (Tianjin, China), respectively. Ultrapure water with a resistivity of 18 M^{Ω}.cm at 25°C was generated with Microporous system (Ulu pure, Xian, Shaanxi, China). The analytical standards were purchased from Desite (Chengdu, Sichuan, China): Epimedin C (purity >98%), icariin (purity >98%) and Baohuoside I (purity >99%).

Collection and Preparation of Epimedium sp. Samples

Leaves of *E. pubescens* and *E. sagittatum* were collected at a cultivation field located at Wanyuan (Sichuan) (S1 and S2 samples, **Table 1**). Other Epimedium samples were purchased directly from local certified TCM markets, with a valid and clear certificate of origin, provided by Chinese official regulators (State Administration for Market Regulation). All the samples were further verified and confirmed by experts and voucher specimens were deposited in the herbarium collection of College of Biological Science and Engineering, Shaanxi University of Technology, Hanzhong, China. The species and respective origin are listed in **Table 1** and geographical locations are shown in **Figure 1**. From each location/species, five independent samples were obtained based on batch leaves from individual plants, to account for normal *in vivo* variability.

The leaves were dried by lyophilization to constant weight, milled into powder, and stored in the dark at room temperature until use. Aliquots (0.2 g) of powder samples of Epimedium were weighed and added to 8 ml of 70% aqueous ethanol. Extraction was done using sonication for 2 min × 30 min. After this, solutions were centrifuged at 13,500 *g* for 5 min, the

FIGURE 1 | Geographical distribution of Epimedium samples collected in this study.

supernatant was filtered through 0.22 μm Nylon six microporous filter membrane, and the filtrate was collected in amber borosilicate glass vials for HPLC-DAD analysis.

HPLC-DAD Analysis

Samples were injected into a liquid chromatograph system UltiMate 3000 (Thermo, Waltham, MA, United States). Chromatographic separations were achieved using gradient elution on an Inertsil ODS-3 column (150 mm × 4.6 mm, 4 μm). Mobile phase A was acetonitrile containing 0.1% formic acid and mobile phase B was ultrapure water containing 0.1% formic acid. The gradient elution program was set as follows: 80% (B) for 0–3 min, 80%–70% (B) for 3–15 min, 70% (B) for 10–15 min, 70%–10% (B) for 15–30 min, 10% (B) for 30–35 min, 10%–80% (B) for 35–40 min. The flow rate was 0.75 ml/min. The column was maintained at 30°C and the sample injection volume was 10 μL. The detection wavelength was recorded between 230 and 600 nm, and chromatograms were recorded at 274 nm. Quantification of epimedin C, icariin and baohuoside I was made at 274 nm based on the external standard method using standard curves of commercial pure compounds.

The HPLC chromatograms were exported as txt ASCII files and the chromatographic fingerprint process was drew using Origin Lab Pro version 9.4 (Origin Lab software, Northampton, MA, United States).

Statistical Analysis

A total of 91 peaks in the HPLC chromatograms of the nine Epimedium sets (45 independent samples in total) were selected for multivariate statistical analysis. Peaks were manually aligned based on their retention time and UV spectra, to assure common identity, and named 1 to 91. Peak areas (274 nm) were corrected by the amount of biomass extracted. The resulting table was imported into GraphPad Prism version 9.1.1 for Windows (GraphPad Software, San Diego, CA, United States, www.graphpad.com). Data was standardized prior to principal component analysis (PCA). The R-statistical software version 4.1.0 (R Core Team, 2021), ggplot2 version 3.3.5 (Wickham, 2016), and ggrepel version 0.9.1 (https://cran.r-project.org/web/packages/ggrepel/index.html) packages were used to display the corresponding plots. The amounts of epimedin C, icariin and baohuoside I from the different Epimedium species cultivated in different regions were plotted and compared in GraphPad Prism using one-way ANOVA followed Tuckey's test or t-test, to compare three or two groups, respectively. One outlier of *E. sagittatum*, one of *E. pubescens* from Sichuan, and two outliers of *E. brevicornum* from Weiyuan Gansu were removed prior to comparison. Data normality was assessed using the Kolmogorov-Smirnov test. Statistical significance was considered at $p < 0.05$. All matrices were also imported into the SIMCA14.0 software (Umetrics, Umea, Västerbotten, Sweden). The obtained quantification data were scaled with unit variance scaling, and sample subgroups (*E. koreanum* and Sichuan) were subjected to PCA.

RESULTS AND DISCUSSION

Epimedii Folium HPLC-DAD Analysis

The chemical quality of plants is influenced by both biotic and abiotic environmental factors and known to exhibit extensive geographic variation (Chen et al., 2013). Epimedium is native to China with wide distribution in He'nan, Shanxi, Shaanxi, Gansu, and Ningxia Provinces (although Epimedium spp. can be found in other regions of East Asia such as *E. koreanum* in Japan and

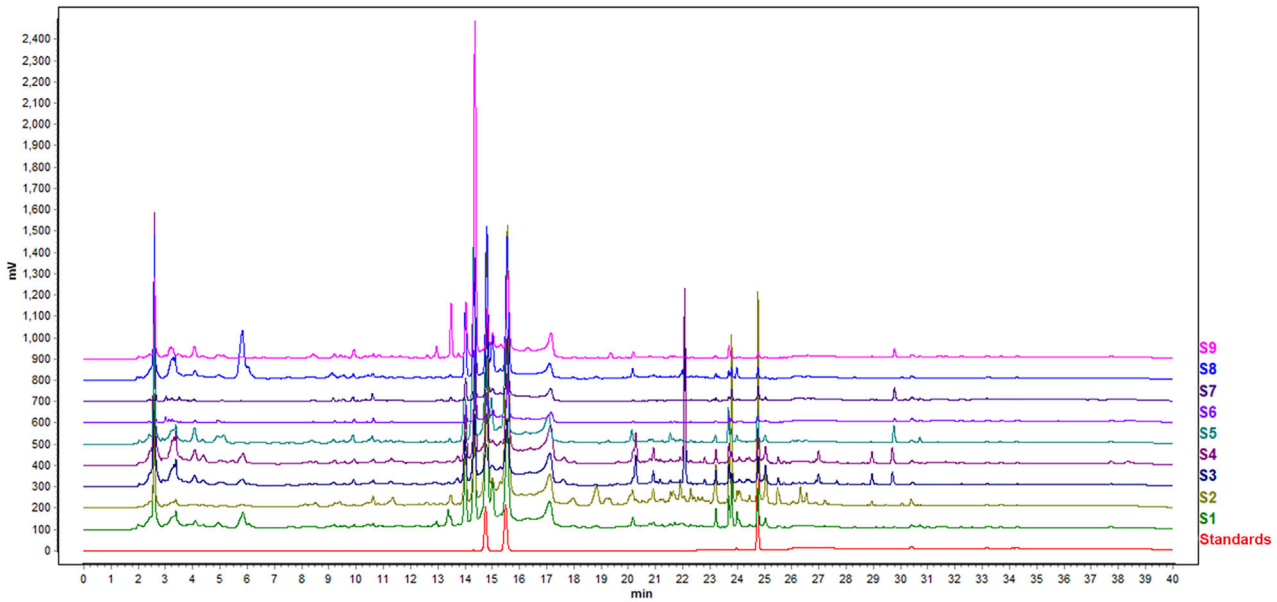

FIGURE 2 | HPLC fingerprints of nine sets of Epimedium samples studied and standards (epimedin C, icariin and baohuoside I, from left to right).

North Korea), and has abundant pharmacological functions (Xu et al., 2013; Li et al., 2018). However, safe and effective use of Epimedium has been limited by variation of Epimedium quality, and identification of plant location and variation (Han et al., 2012).

Typical chromatograms resulting from the HPLC analysis of nine sets of Epimedium from different geographical origin and species are shown in **Figure 2**. There were good chromatogram resolutions in the fingerprint of all Epimedium samples, namely for the standards epimedin C, icariin and baohuoside I, considered quality marker compounds for Epimedii Folium, and the other major compounds found. Differences between the different Epimedium samples could not be easily detected in the chromatograms by simple visual inspection. Hence, HPLC data was subjected to PCA, with the purpose of uncovering an effect related to geographical origin and/or species on the quality of Epimedium.

PCA Analysis

The use of Multivariate Analysis, like Principal Component Analysis (PCA), is nowadays commonly used for better understanding metabolite diversity, namely of phenolics, and link it with adulterations (Windarsih et al., 2019), biotic stress (Lima et al., 2010), and different geographical and species variation (Chen et al., 2015a).

In this work, PCA was used to investigate how different species and geographical origin are relevant (or not) for differences and quality of Epimedii Folium. The best discriminating principal components (PCs), PC1 and PC2, cumulatively accounted to the explanation of 42.01% of the total variance in the data. The PC1 and PC2 scores scatter plot (**Figure 3A**) clearly shows the separation of *E. sagittatum* species from the other Epimedium species along PC1, with *E. sagittatum* samples clustering towards higher positive values of PC1 (orange ellipse in **Figure 3A**), and all other species grouping towards lower and negative values of PC1.

Additionally, PC2 clearly separates Epimedium samples based on geographical origin. Samples from South Korea clustered towards the highest values of PC2 (green ellipse in **Figure 3A**), the samples from central China provinces (Gansu, Sichuan, and Shaanxi) clustered at lower values of PC2 (blue ellipse in **Figure 3A**), and the samples from the Jilin province, in northeast China, clustered towards negative values of PC2 (purple ellipse in **Figure 3A**).

The PC1 and PC2 loadings plot (**Figure 3B**) shows the compounds contributing to the separation of Epimedium samples into different groups. The pharmacologically active compounds epimedin C, icariin and baohuoside I, were among the compounds that most contribute to sample separation, because they are associated with higher PC1 values and positive PC2 values. To further confirm the importance of these bioactive compounds in separating Epimedium samples, the data points in the scores scatter plot were colored according to a gradient based on epimedin C concentration (**Figure 3A**). The *E. sagittatum* samples contained higher amounts of Epidemium C (orange ellipse), followed by the *E. koreanum* samples from South Korea with medium-high amounts (green ellipse), then the *E. pubescens* and *E. brevicornum* samples from central China with medium-low concentration of epimedin C (blue ellipse), and finally the *E. koreanum* and *E. pubescens* samples from the Jilin province containing the lowest amounts of epimedin C (purple ellipse).

Some isolated studies indicated that the compounds of Epimedium from neighboring locations were similar (Huang et al., 2007; Xu et al., 2013; Xu et al., 2017). This study included samples from a wide geographical area and from different species (**Table 1**; **Figure 1**), as a way to offer a more comprehensive view of how location and species may affect

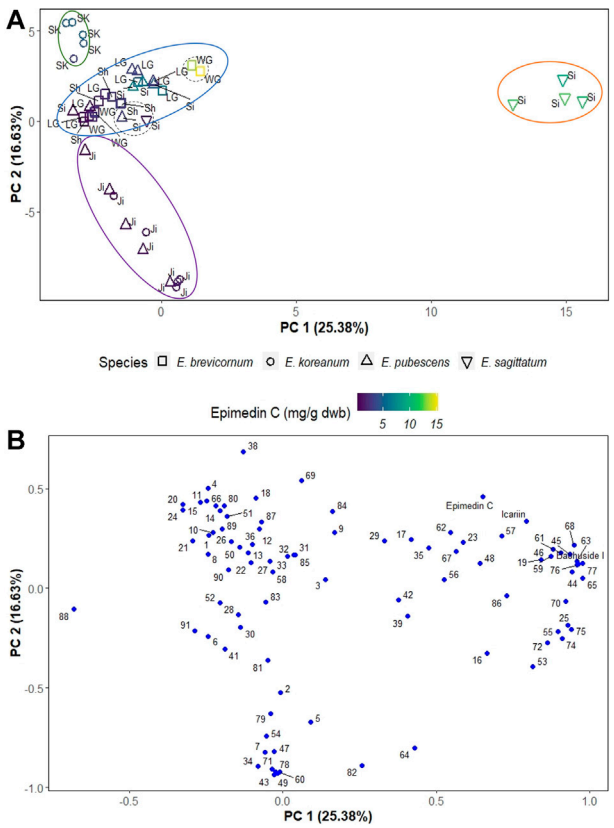

FIGURE 3 | PCA scores plot **(A)** and loadings plot **(B)** of Epimedium samples. In the scores plot, Epimedium species are represented by different shapes, and each data point is colored according to its amount of epimedin C and labeled with its geographical origin (SK—South Korea, LG—Longnan Gansu, WG—Weiyuan Gansu, Ji—Jilin, Si—Sichuan, Sh—Shaanxi). Ellipses indicate sample groups based on species or geographical origin; dashed-line circles indicate outliers (two *E. brevicornum* outliers from Weiyuan Gansu, one E. sagittatum outlier and another E. pubescens both from Sichuan). The loadings plot **(B)** shows the compounds responsible for the group separation; for clarity, the peak numbers corresponding to epimedin C, icariin and baohuoside I were substituted by their name.

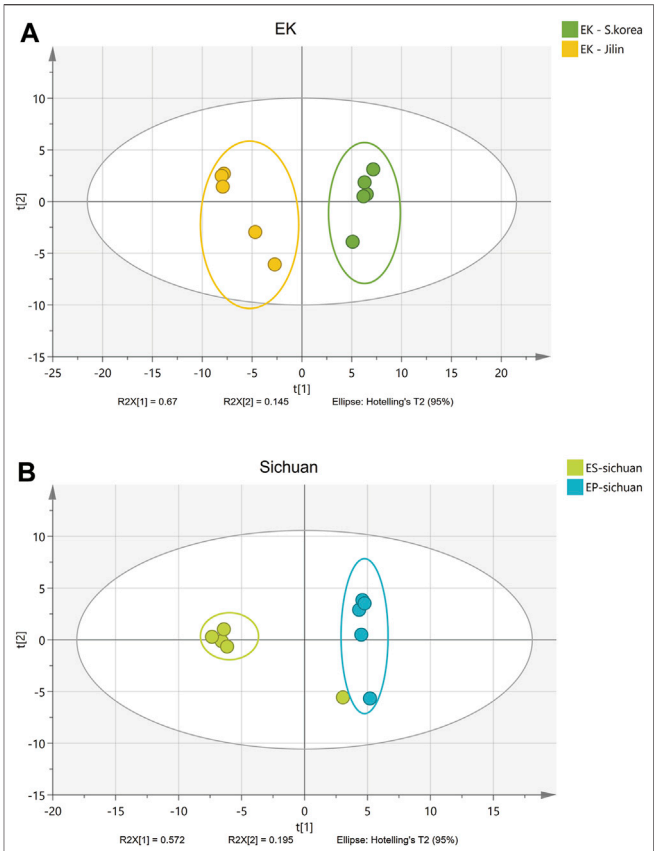

FIGURE 4 | PCA scores plot **(A)** for same Epimedium species (*E. koreanum*, EK) collected in different locations (Daqiu, South Korea and Jilin, China)—A; and PCA scores plot **(B)** for different species (*E. sagittatum*, EK, and *E. pubescens*, EP) cultivated in the same field (Wanyuan, Sichuan).

biomass quality. In fact, using PCA analysis, it was easy to distinguish Epimedii Folium from the same species but from different provenience (**Figure 4A**), and from different species grown in the same cultivated field, under the same abiotic and biotic stressors (**Figure 4B**). It is clear that, both Epimedium species and provenience have strong impact on the phenolic contents and quality of Epimedii Folium.

Content Differences of Bioactive Components in Epimedium Sets

The relevant bioactive compounds to Epimedii Folium (or Herba Epimedii) used in TCM, epimedin C, icariin, and baohuoside I, were quantified in the samples studied (**Figures 5**, **6**). *E. sagittatum* contained the highest amounts of epimedin C (10.88 ± 0.83 mg/g dwb), icariin (11.21 ± 1.12 mg/g dwb), and baohuoside I (3.23 ± 0.24 mg/g dwb). The bioactive amounts in the other Epimedium species were lower and varied according to geographical origin (**Figure 5**). For *E. pubescens* (**Figure 5A**), average epimedin C concentration was significantly higher when cultivated in Sichuan (5.43 ± 1.87 mg/g dwb) compared to *E. pubescens* samples from Longnan Gansu (2.54 ± 1.05 mg/g dwb) and Jilin (0.65 ± 0.36 mg/g dwb). Average *E. pubescens* icariin concentration was significantly higher in samples from Longnan Gansu (4.42 ± 1.79 mg/g dwb) when compared to samples from Jilin (1.28 ± 0.73 mg/g dwb), but not significantly different from Sichuan samples (3.07 ± 1.22 mg/g dwb). Average *E. pubescens* baohuoside I concentration was significantly higher in samples from Sichuan (0.63 ± 0.07 mg/g dwb) when compared to samples from Jilin (0.30 ± 0.14 mg/g dwb), but not significantly different from Longnan Gansu samples (0.51 ± 0.17 mg/g dwb). It is noteworthy to mention that some of the species indicated by producers as having the highest contents in bioactive contents might be different. As an example, *E. pubescens* was considered to have the highest contents in bioactives (He et al., 2019). Nevertheless, for *E. sagittatum* and *E. pubescens* plants cultivated in the same field location, under the same abiotic and biotic environment, the bioactive contents (icariin, epimedin C, baohuoside I) were significantly higher for *E. sagittatum* (**Figure 6**).

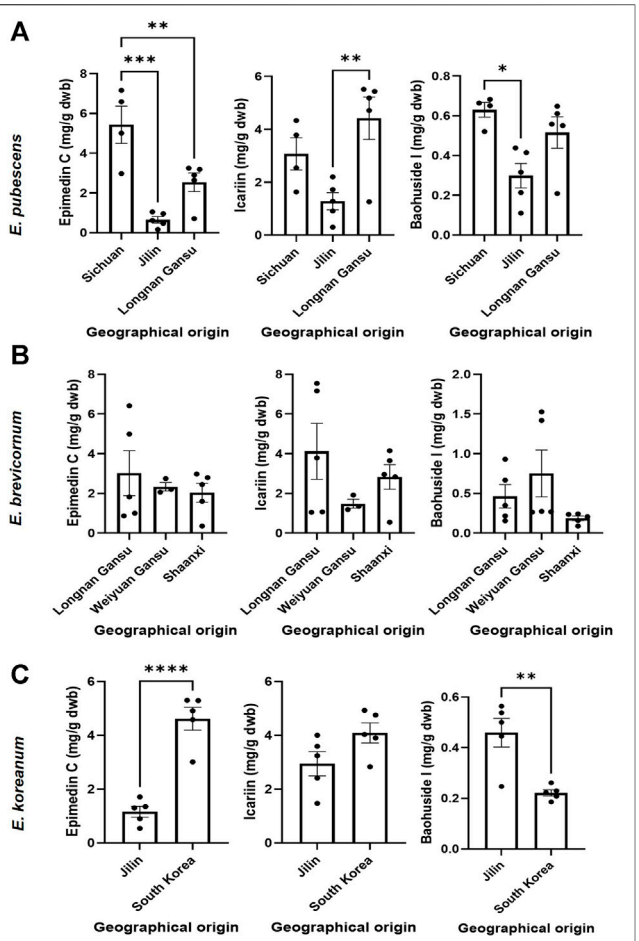

FIGURE 5 | Amount (mg/g dry weight biomass) of epimedin C, icariin and baohuoside I in *E. pubescens* **(A)**, *E. brevicornum* **(B)** and *E. koreanum* **(C)** cultivated in different geographical locations. Bars represent average ±SEM; dots represent individual data points. Statistically significant differences are represented by asterisks (*$p < 0.05$, **$p < 0.01$, ***$p < 0.001$, ****$p < 0.0001$).

For *E. brevicornum* (**Figure 5B**) the amount of the identified bioactive components varied, on average, between 2.04 and 3.02 mg/g dwb for epimidium C, between 1.49 and 4.12 mg/g dwb for icariin, and between 0.19 and 0.75 mg/g dwb for baohuoside I. No significant differences were detected among the different geographical regions, likely because all the *E. brevicornum* samples analyzed in this study were cultivated in regions exclusively located to central China. For *E. koreanum* (**Figure 5C**), average epimedin C concentration was significantly higher when cultivated in South Korea (4.62 ± 0.95 mg/g dwb) compared to *E. koreanum* samples from Jilin (1.16 ± 0.45 mg/g dwb). Average E. koreanum icariin content was not significantly different in samples from South Korea (4.10 ± 0.83 mg/g dwb) compared to samples from Jilin (2.94 ± 1.01 mg/g dwb). Average *E. koreanum* baohuoside I concentration was significantly higher in samples from Jilin (0.46 ± 0.13 mg/g dwb) compared to samples from South Korea (0.22 ± 0.03 mg/g dwb).

In our current study, the contents of icariin in *E. sagittatum* from Sichuan and *E. brevicornum* from Gansu Wanyuan were above standard according to the 2015 Chinese Pharmacopoeia (Chinese Pharmacopoeia, 2015). However, in the current Chinese Pharmacopoeia released in 2020 (Chinese Pharmacopoeia, 2020), the standard for Epimedium quality control has been changed to the analysis of the icariin content and calculation of the total amount of Epimedium A, B, C and icariin based on the correction factor, that means, *E. pubescens* from Jilin and *E. brevicornum* from Shaanxi were below standard. There is clear difference between the two editions of the pharmacopoeia standards, despite the content of icariin has been the major quality consideration in both editions. It is noteworthy that, according to the results of the recent studies, the contents of icariin in Epimedium were easily affected by external factors (Chen et al., 2015b; Deng et al., 2018; Li et al., 2020). Therefore, finding the variation patterns of the content of various components in Epimedium herbs of different origins and varieties and screening the appropriate content determination index are the keys to solve the current Epimedium quality control issue.

Overall, both species variant and geographical location influence the contents of bioactive components in Epimedii Folium, and so the pharmacology quality of the biomass (Wei et al., 2017; Yuan et al., 2017). Therefore, it is necessary to explore the geo-herbalism of Herba epimedii by the characteristic component variation and chromatographic fingerprint among different sets. *E. koreanum* belongs to large-flowered taxa and *E. pubescens, E. sagittatum* and *E. brevicornum* all belong to small-flowered taxa (Xu and He, 2005). However, the icariin content of *E. sagittatum* was significantly higher compared with *E. pubescens* cultivated in the same region (**Figure 6**). *E. sagittatum* also showed relatively independent from *E. pubescens*, *E. koreanum* and *E. brevicornum* through PCA scores plot compared with *E. wushanense* (Xie et al., 2010), which proved that Epimedium species variation is a factor in the interspecific differences, and indicated that the differences between different species of Epimedium should be explored.

As a conclusion, the use of HPLC-DAD combined with multivariate analysis (PCA) is an effective methodology to discriminate different Epimedii Folium samples from different epimedium species and geographical origins. Our results provide applicable guidance to the geographical location and plant species selection of GAP (Good Agricultural Practices) production for Epimedii Folium. Both species and geographical location variations have impacts on the quality and composition of Epimedii Folium. However, the components of herbal products are diverse and complex, and their pharmacological activities are always affected by unique component constituents as well as their combinations, instead of a single component (Zhang et al., 2013). Therefore, associations between the variation of plant species and geographical locations with pharmacological activity of Epimedii Folium need to be further explored for providing better evaluation criteria for geo-herbalism of Epimedii Folium.

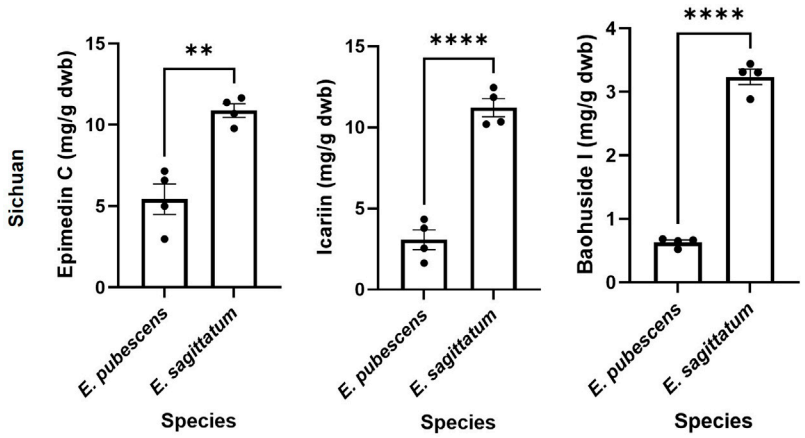

FIGURE 6 | Amount (mg/g dry weight biomass) of epimedin C, icariin and baohuoside I of different plant species cultivated in same place (Wanyuan, Sichuan). Bars represent average ±SEM; dots represent individual data points. Statistically significant differences are represented by asterisks (**$p < 0.01$, ****$p < 0.0001$).

DATA AVAILABILITY STATEMENT

The original contributions presented in the study are included in the article/Supplementary Material, further inquiries can be directed to the corresponding authors.

AUTHOR CONTRIBUTIONS

AD and XZ contributed to conception and design of the study. BL and ML performed the statistical analysis. BL and ML wrote the first draft of the manuscript. HN, LX, HY, CC, AD, and XZ wrote sections of the manuscript. All authors contributed to manuscript revision, read, and approved the submitted version.

FUNDING

This work was supported by Incubation Project on State Key Laboratory of Biological Resources and Ecological Environment of Qinba Areas (SLGPT2019KF04-04), China, and the ERDF through the COMPETE2020—Programa Operacional Competitividade e Internacionalização (POCI), Portugal.

REFERENCES

Chen, J., Li, Z., Maiwulanjiang, M., Zhang, W. L., Zhan, J. Y., Lam, C. T., et al. (2013). Chemical and Biological Assessment of Ziziphus Jujuba Fruits from China: Different Geographical Sources and Developmental Stages. *J. Agric. Food Chem.* 61 (30), 7315–7324. doi:10.1021/jf402379u

Chen, J., Xu, Y., Wei, G., Liao, S., Zhang, Y., Huang, W., et al. (2015a). Chemotypic and Genetic Diversity in Epimedium Sagittatum from Different Geographical Regions of China. *Phytochemistry* 116, 180–187. doi:10.1016/j.phytochem.2015.04.005

Chen, M., Cui, Y., Li, H., Luan, J., Zhou, X., and Han, J. (2019). Icariin Promotes the Osteogenic Action of BMP2 by Activating the cAMP Signaling Pathway. *Molecules* 24 (21), 3875. doi:10.3390/molecules24213875

Chen, X. J., Tang, Z. H., Li, X. W., Xie, C. X., Lu, J. J., and Wang, Y. T. (2015b). Chemical Constituents, Quality Control, and Bioactivity of Epimedii Folium (Yinyanghuo). *Am. J. Chin. Med.* 43 (5), 783–834. doi:10.1142/s0192415x15500494

Chinese Pharmacopoeia (2015). *Pharmacopoeia of the People's Republic of China*. Beijing: China Medical Science Press.

Chinese Pharmacopoeia (2020). *Pharmacopoeia of the People's Republic of China*. Beijing: China Medical Science Press.

Deng, A. P., Fang, W. T., Zhou, Q. G., Yang, H. J., Wang, L., Nan, T. G., et al. (2018). Research Actuality and Quality-Influencing Factor of Epimedii Folium. *Zhongguo Zhong Yao Za Zhi* 43 (5), 1062–1070. doi:10.19540/j.cnki.cjcmm.2018.0037

Guo, B., and Xiao, P. (2003). Review on Main Species of Herba Epimedii. *Zhongguo Zhong Yao Za Zhi* 04, 18–22.

Han, S., Xie, Y. Y., Wang, Y. M., Liang, Q. L., and Luo, G. A. (2012). Comparative Study on Chemical Quality of Main Species of Epimedium. *Yao Xue Xue Bao* 47 (4), 502–507. doi:10.16438/j.0513-4870.2012.04.007

He, L., Huang, N., Yan, Y., Lin, W., Gao, L., and Lin, X. (2019). Identification and Determination of Components in Five Kinds of Yinyanghuo. *Clin. J. Chin. Med.* 11 (22), 139–144.

Huang, H., Liang, M., Zhang, X., Zhang, C., Shen, Z., and Zhang, W. (2007). Simultaneous Determination of Nine Flavonoids and Qualitative Evaluation of Herba Epimedii by High Performance Liquid Chromatography with Ultraviolet Detection. *J. Sep. Sci.* 30 (18), 3207–3213. doi:10.1002/jssc.200700262

Indran, I. R., Liang, R. L., Min, T. E., and Yong, E. L. (2016). Preclinical Studies and Clinical Evaluation of Compounds from the Genus Epimedium for Osteoporosis and Bone Health. *Pharmacol. Ther.* 162, 188–205. doi:10.1016/j.pharmthera.2016.01.015

Li, J., Jiang, K., and Zhao, F. (2015a). Icariin Regulates the Proliferation and Apoptosis of Human Ovarian Cancer Cells through microRNA-21 by Targeting PTEN, RECK and Bcl-2. *Oncol. Rep.* 33 (6), 2829–2836. doi:10.3892/or.2015.3891

Li, R., Guo, M., and Pang, X. (2018). Identification and Classification of Medicinal Plants in Epimedium. *Chin. Herbal Medicines* 10 (03), 249–254. CNKI:SUN:CHME.0.2018-03-004. doi:10.1016/j.chmed.2018.07.001

Li, W. X., Deng, Y. Y., Li, F., Liu, B., Liu, H. Y., Shi, J. S., et al. (2015b). Icariin, a Major Constituent of Flavonoids from Epimedium Brevicornum, Protects against Cognitive Deficits Induced by Chronic Brain Hypoperfusion via its

Anti-amyloidogenic Effect in Rats. *Pharmacol. Biochem. Behav.* 138, 40–48. doi:10.1016/j.pbb.2015.09.001

Li, X. M., Pan, J. Q., Luo, Y. J., Yang, Q. R., Xu, C. Q., Shen, G. A., et al. (2020). Effects of Light Quality on Growth and Icariin Flavonoid Content of Epimedium Pseudowushanense under Different Light Intensity. *Zhongguo Zhong Yao Za Zhi* 45 (11), 2502–2508. doi:10.19540/j.cnki.cjcmm.20200329.113

Lima, M. R., Felgueiras, M. L., Graça, G., Rodrigues, J. E., Barros, A., Gil, A. M., et al. (2010). NMR Metabolomics of Esca Disease-Affected Vitis vinifera Cv. Alvarinho Leaves. *J. Exp. Bot.* 61 (14), 4033–4042. doi:10.1093/jxb/erq214

Ma, H., He, X., Yang, Y., Li, M., Hao, D., and Jia, Z. (2011). The Genus Epimedium: an Ethnopharmacological and Phytochemical Review. *J. Ethnopharmacol.* 134 (3), 519–541. doi:10.1016/j.jep.2011.01.001

Ma, Q., Wang, J., Han, L., Lv, C., Jia, L., and Lu, J. (2014). Simultaneous Determination of 8 Flavonoids in Epimedium by HPLC. *Shenyang Pharm. Univ.* 31 (12), 970–978. doi:10.14066/j.cnki.cn21-1349/r.2014.12.008

Pei, L. K., Huang, W. H., He, T. G., and Guo, B. L. (2007). Systematic Studies on Quality of Main Species of Herba Epimedii. *Zhongguo Zhong Yao Za Zhi* 32 (21), 2217–2222.

Polat, D. C., and Coskun, M. (2016). Quantitative Determination by HPLC-DAD of Icariin, Epimedin A, Epimedin B, and Epimedin C in Epimedium (Berberidaceae) Species Growing in Turkey. *Nat. Prod. Commun.* 11 (11), 1665–1666. doi:10.1177/1934578x1601101110

R Core Team (2021). *R: A Language and Environment for Statistical Computing*. Vienna, Austria): R Foundation for Statistical Computing.

Shindel, A. W., Xin, Z. C., Lin, G., Fandel, T. M., Huang, Y. C., Banie, L., et al. (2010). Erectogenic and Neurotrophic Effects of Icariin, a Purified Extract of Horny Goat weed (Epimedium spp.) *In Vitro* and *In Vivo*. *J. Sex. Med.* 7 (4 Pt 1), 1518–1528. doi:10.1111/j.1743-6109.2009.01699.x

Sun, Y., Sun, X. H., Fan, W. J., Jiang, X. M., and Li, A. W. (2016). Icariin Induces S-phase Arrest and Apoptosis in Medulloblastoma Cells. *Cell. Mol. biol.* 62 (4), 123–129. doi:10.14715/cmb/2016.62.4.21

Wei, Q., He, M., Chen, M., Chen, Z., Yang, F., Wang, H., et al. (2017). Icariin Stimulates Osteogenic Differentiation of Rat Bone Marrow Stromal Stem Cells by Increasing TAZ Expression. *Biomed. Pharmacother.* 91, 581–589. doi:10.1016/j.biopha.2017.04.019

Wickham, H. (2016). *ggplot2: Elegant Graphics for Data Analysis*. New York: Springer-Verlag.

Windarsih, A., Rohman, A., and Swasono, R. T. (2019). Application of 1H-NMR Based Metabolite Fingerprinting and Chemometrics for Authentication of Curcuma Longa Adulterated with C. Heyneana. *J. Appl. Res. Med. Aromatic Plants* 13, 100203. doi:10.1016/j.jarmap.2019.100203

Wu, B., Chen, Y., Huang, J., Ning, Y., Bian, Q., Shan, Y., et al. (2012). Icariin Improves Cognitive Deficits and Activates Quiescent Neural Stem Cells in Aging Rats. *J. Ethnopharmacol* 142 (3), 746–753. doi:10.1016/j.jep.2012.05.056

Xie, P. S., Yan, Y. Z., Guo, B. L., Lam, C. W., Chui, S. H., and Yu, Q. X. (2010). Chemical Pattern-Aided Classification to Simplify the Intricacy of Morphological Taxonomy of Epimedium Species Using Chromatographic Fingerprinting. *J. Pharm. Biomed. Anal.* 52 (4), 452–460. doi:10.1016/j.jpba.2010.01.025

Xu, N., Zhou, G., Li, X., Lu, H., Meng, F., and Zhai, H. (2017). Geographical Classification of Epimedium Based on HPLC Fingerprint Analysis Combined with Multi-Ingredients Quantitative Analysis. *Biomed. Chromatogr.* 31 (5), e3871. doi:10.1002/bmc.3871

Xu, W., and He, S. (2005). Species and Geographic Distribution of Large-Flowered Taxa of Epimedium in China. *Zhong Yao Cai* 28 (4), 267–271. doi:10.13863/j.issn1001-4454.2005.04.005

Xu, Y., Li, Z., Yuan, L., Zhang, X., Lu, D., Huang, H., et al. (2013). Variation of Epimedins A - C and Icariin in Ten Representative Populations of Epimedium Brevicornu Maxim., and Implications for Utilization. *Chem. Biodivers* 10 (4), 711–721. doi:10.1002/cbdv.201100424

Yang, P., Guan, Y. Q., Li, Y. L., Zhang, L., Zhang, L., and Li, L. (2016). Icariin Promotes Cell Proliferation and Regulates Gene Expression in Human Neural Stem Cells *In Vitro*. *Mol. Med. Rep.* 14 (2), 1316–1322. doi:10.3892/mmr.2016.5377

Yuan, X. Y., Wang, M., Lei, S., Yang, Q. X., and Liu, Y. Q. (2017). Rapid Screening of Active Components with an Osteoclastic Inhibitory Effect in Herba Epimedii Using Quantitative Pattern-Activity Relationships Based on Joint-Action Models. *Molecules* 22 (10), 1767. doi:10.3390/molecules22101767

Zhang, M. H., Feng, L., Hu, S. Y., and Jia, X. B. (2013). Essence of Material Base in Geoherbs: Specificality of Constituent Structure. *Zhongguo Zhong Yao Za Zhi* 38 (1), 136–140.

Zhao, H., Fan, M., Fan, L., Sun, J., and Guo, D. (2010). Liquid Chromatography-Tandem Mass Spectrometry Analysis of Metabolites in Rats after Administration of Prenylflavonoids from Epimediums. *J. Chromatogr. B Analyt Technol. Biomed. Life Sci.* 878 (15), 1113–1124. doi:10.1016/j.jchromb.2010.03.023

Conflict of Interest: Author HY was employed by the Jinhuifang Traditional Chinese Medicine Technology Co., Ltd.

The remaining authors declare that the research was conducted in the absence of any commercial or financial relationships that could be construed as a potential conflict of interest.

Publisher's Note: All claims expressed in this article are solely those of the authors and do not necessarily represent those of their affiliated organizations, or those of the publisher, the editors and the reviewers. Any product that may be evaluated in this article, or claim that may be made by its manufacturer, is not guaranteed or endorsed by the publisher.

frontiers in Pharmacology

ORIGINAL RESEARCH
published: 06 December 2021
doi: 10.3389/fphar.2021.754554

Antioxidant Effects of *Sophora davidi* (Franch.) Skeels on D–Galactose–Induced Aging Model in Mice *via* Activating the SIRT1/p53 Pathway

Beibei Lin[1†], Dingqiao Xu[2†], Sanqiao Wu[1], Shanshan Qi[1], Youmei Xu[1], Xiang Liu[1], Xiaoying Zhang[1,3] and Chen Chen[1]**

[1]Chinese-German Joint Laboratory for Natural Product Research, College of Biological Science and Engineering, Shaanxi University of Technology, Hanzhong, China, [2]Key Laboratory of Shaanxi Administration of Traditional Chinese Medicine for TCM Compatibility, Shaanxi University of Chinese Medicine, Xi'an, China, [3]Centre of Molecular and Environmental Biology, Department of Biology, University of Minho, Campus de Gualtar, Braga, Portugal

OPEN ACCESS

Edited by:
SubbaRao V. Madhunapantula, JSS Academy of Higher Education and Research, India

Reviewed by:
Santhepete Manjula, JSS College of Pharmacy, India
Haci Ahmet Deveci, University of Gazisantep, Turkey

***Correspondence:**
Xiaoying Zhang
zhang@bio.uminho.pt
Chen Chen
cchen@snut.edu.cn

[†]These authors have contributed equally to this work

Specialty section:
This article was submitted to Ethnopharmacology, a section of the journal Frontiers in Pharmacology

Received: 06 August 2021
Accepted: 17 November 2021
Published: 06 December 2021

Citation:
Lin B, Xu D, Wu S, Qi S, Xu Y, Liu X, Zhang X and Chen C (2021) Antioxidant Effects of Sophora davidi (Franch.) Skeels on D–Galactose–Induced Aging Model in Mice via Activating the SIRT1/p53 Pathway. Front. Pharmacol. 12:754554. doi: 10.3389/fphar.2021.754554

This study investigated the protective effect of *Sophora davidi* (Franch.) Skeels fruits extract (SDE) on D–galactose–induced acute aging in mice. Ultra performance liquid chromatography coupled with tine-of-flight mass spectrometry (UPLC-Q-TOF/MS) was performed to identify the composition of compounds in SDE. KM mice were divided stochastically into the normal control group (NC, saline), D–galactose (D-gal) model group, vitamin C (Vc) group (positive control), low–, medium–and high–dose SDE treat groups. After 28 days administration and fasting overnight, the serum, liver, and brain samples of mice were collected. The levels of inducible nitric oxide synthase (iNOS), acetylcholinesterase (AChE) activity in the brain, malondialdehyde (MDA) and reduced glutathione (GSH) content, superoxide dismutase (SOD) and total antioxidant capacity (T–AOC) activity in the liver and brain were measured. Immunohistochemistry was applied to detect silent information regulator 1 (SIRT1) and p53 protein expression in the liver and brain, and quantitative real-time polymerase chain reaction (qRT-PCR) was used to detect the expression of nuclear factor κB (NF–κB), tumor necrosis factor (TNF–α), interleukin–6 (IL–6), interleukin-1β (IL–1β), and anti-aging factor Klotho in the liver and brain. The results showed that UPLC-Q-TOF/MS identified 78 compounds in SDE. SDE could reduce the iNOS activity in serum and AChE activity in the brain, upregulate the levels of SOD, T–AOC and GSH in liver and brain, and debase the MDA content in liver and brain. SDE could downregulate the mRNA expressions of TNF–α, NF–kB, IL–1β, and IL–6 in the liver and brain, and elevate the mRNA expression of Klotho. SDE improved the pathological changes of the liver and brain induced by D–gal, increased the expression of SIRT1 protein in the liver and brain, and inhibited the expression of p53 protein induced by D–gal. To summarize, SDE demonstrated clear anti–aging effect, and its mechanism may be relevant to the activation of the SIRT1/p53 signal pathway.

Keywords: SIRT1, p53, D-galactose, anti-aging, *Sophora davidi* (franch.) skeels fruits extract

INTRODUCTION

Aging is a progressive, physiological impairment involving various organs and tissues, which can lead to normal cell regulatory dysfunction; can affect nervous system, respiratory system, immune system and other systems; and is a risk factor for many chronic diseases, such as cancers, cardiovascular diseases, and neurodegenerative diseases (Zhu et al., 2017; Bektas et al., 2018; Mahmut et al., 2020). With the increase of aging population and life expectancy, screening on natural and synthetic bioactive constituents with potential anti-aging pharmacological activity acquires research priority.

The construction of aging mice by long–term administration of D–gal is a classic model in aging related study (Zhou et al., 2013; Li et al., 2015). D–galactose (D–gal) is a type of reduced aldose, which exists naturally in the body, including the brain (Nagy and Pohl, 2015; Qing et al., 2018; Zhao et al., 2020; Mu et al., 2021). Under normal conditions, D–gal is metabolized into glucose, however, the host will produce excessive reactive oxygen species (ROS) and increase the oxidative stress under the challenge of excessive amount of D–gal. This pathological change can be used for the development of aging animal model for pharmacological investigation, as ROS will destroy the dynamic balance of oxidation and antioxidation, reduce the activity of antioxidant enzymes in the body, damage mitochondria and neurons, and cause cognitive, learning, and memory disorders, and aging phenomenon (Zhou et al., 2013; Kong et al., 2018).

Sophora davidi (Franch.) Skeels (*S. davidi*) is a semi–evergreen deciduous shrub species of the Leguminosae family, it has been used in the treatment of sore throat, hematochezia, lung heat cough, dysentery, gonococcal disease, edema, hematuria, and so forth (Tai et al., 2011; Huang et al., 2018; Lin et al., 2019). *S. davidi* is widely distributed, with dense flowers and light aromatic taste. Therefore, *S. davidi* is one of the main honey source plants in China. The flower, leaves, stem, fruit and root of *S. davidi* contain polyphenols, flavonoids, alkaloids, and other active substances that these components have anti–inflammatory, antitumor, hypoglycemic, and antioxidant effects (Ping et al., 1999; Wang et al., 2016; Xie et al., 2017; Lin et al., 2019). Previous reports indicated that polyphenols, flavonoids, alkaloids from *S. davidi* have anti-aging effects (Rosa et al., 2009; Ma et al., 2018; Hano and Tungmunnithum, 2020). Our previous studies have proved that the *S. davidi* extract showed good anti–oxidation activity *in vitro* (Lin et al., 2019), this study aimed to explore the anti–aging effect of *S. davidi* fruits extract (SDE) against D–gal–induced acute aging mice.

MATERIALS AND METHODS

Materials

The fruits of *Sophora davidi* (Franch.) Skeels were gathered in the south of Qinling Mountains in September 2017 (110°54′ east longitude, 33°32′ north latitude), and authenticated by Prof. Sanqiao Wu from the College of Biological Science and Engineering, Shaanxi University of Technology.

D–galactose, rapid extraction kit of total RNA and ascorbic acid (Vc) were purchased from Sangon Biotech Co., Ltd (Shanghai, China). AChE, iNOS, MDA, SOD, T–AOC and GSH kits were purchased from Jiancheng Bioengineering Institute (Nanjing, China). BSA protein assay kit was purchased from Beyotime Biotechnology (Shanghai, China). DAB reagent kit was purchased from Zhongshan Jinqiao Biotechnology Co., Ltd (Beijing, China). SIRT1 antibody and p53 antibody were acquired from Biosynthesis Biotechnology Co., Ltd. (Beijing, China). cDNA reverse transcription kit and PCR kit were purchased from Takara Biomedical Technology Co., Ltd. (Dalian, China). Hematoxylin, eosin, and immunohistochemistry pen were obtained from Dingguo Changsheng Biotechology Co., Ltd. (Beijing, China).

Preparation of SDE

The fruits were dried at 45°C and then smashed, a total of 40 ml ethanol (60%) was added to the smashed fruits (1 g) (fruit: solvent = 1 : 40, g: mL) for ultrasonic wave extraction under 100 W power (KQ5200DE CNC ultrasonic instrument, Jiangsu, China) for 30 min, subjected to suction filtration, and the residue was extracted repeatedly once. The two extracts were combined and concentrated by rotary evaporator. The resulting mixtures were filtered and dried in a lyophilizer. The SDE extract ratio is 1: 0.257 (g: g). The plant extracts were kept at 4°C until further analysis.

UPLC-Q-TOF/MS Analysis

The sample analysis was performed with a Waters Acquity™ ultra-performance liquid chromatography (UPLC) system (Waters Corporation, Milford, MA, United States) coupled with a Synapt G2 mass spectrometer (MS; Waters Corp, Manchester, United Kingdom) equipped with an electrospray ion (ESI) source. An Acquity UPLC BEH C_{18} column (2.1 × 100 mm, 1.7 mm) was applied for all analyses. The mobile phase was composed of A (0.1% formic acid water solution) and B (acetonitrile) with a gradient elution: 0–2 min, 5% B; 2–3 min, 5%–15% B; 3–4 min, 15%–25% B; 4–5 min, 25%–26% B; 5–6 min, 26%–35% B; 6–7 min, 35%–60% B; 7–8.5 min, 60%–95% B; 8.5–13 min, 95% B; 13–14 min, 95%–15% B; 14–15 min, 15%–5% B. The flow rate was set at 0.3 ml/min. The column temperature was set at 35°C. The detector was PDA and detection wavelength was 200–400 nm. Mass spectrometry detection was performed using an electrospray ionization source (ESI), positive and negative ion mode detection. The conditions of MS analysis were designed with positive as follows: the capillary voltage at 3 kV, the desolvation gas flow rate set to 600 L/h at a temperature of 350°C, the cone gas flow rate set at 50 L/h and the source temperature at 100°C. The scan range was 50–1,200 (*m/z*). The conditions of MS analysis were designed with negative as follows: the capillary voltage at 2 kV, the desolvation gas flow rate set to 600 L/h at a temperature of 350°C, the cone gas flow rate set at 50 L/h and the source temperature at 100 °C. The scan range was 50–1,200 (*m/z*). The data was acquired through Waters MassLynx v4.2 software (Waters Corporation, Milford, MA, United States)

UPLC Quantitative Analysis

The quantitative analysis of SDE was performed on a Thermo UltiMate 3000 UPLC system (Thermo Scientific, Waltham, MA, United States) with diode-array detector (DAD). For the content determination of polyphenols according to the method described our previously report (Lin et al., 2019). The Inertsil/WondaSil C_{18} phase-HPLC column (250 mm × 4.6 mm i. d, 4 μm particles) was used to separate and quantify individual alkaloids, and the detection wavelength is 205 nm. Acetonitrile (A), 0.05 M potassium phosphate monobasic (B, acetic acid adjusted to pH 4.5) and ultrapure water (C) were used as mobile phase. The following linear gradient elution: 0–30 min, 2:88:10%–3:87:10% (A: B: C) was used to analyze samples. The injection volume was 10 μL with 1 ml/min flow rate. The detection temperature is 35°C. Each sample was paralleled three times.

Animals and Treatments

A total of 48 male and female Kunming mice (SPF level) were obtained from Chengdu Dasuo experimental animal Co., Ltd (Chengdu, China). The mice with weight of 22 ± 5 g, were kept at 25 ± 2°C with a humidity of 55 ± 5%, and 12 h light and dark cycle. They were allowed to access to feed and water freely and were fed adaptively during the experiments. Mice were divided into six groups (n = 8): normal control group (treated with normal saline everyday); D–gal model group (treated with D–gal 200 mg/kg BW/day); low–, medium–, and high–dose groups (SL, SM, and SH group, treated with SDE 125, 250, and 500 mg/kgBW/day, respectively); and Vc positive control group (treated with D–gal, Vc 50 mg/kg BW/day). In the next 4 weeks, the growth and mental state of mice were observed. After 28 days into the experiment, the mice were fasted overnight, weighed and then their blood, liver and brain were collected. Liver and brain were weighed and the organ indexes were calculated. The blood was centrifuged at 3,000 rpm at 4°C for 10 min to obtain the serum, which was then kept at −80°C for further analysis. Parts of the liver and brain of each mouse were fixed in 4% paraformaldehyde solution for histomorphology observation. The remaining liver and brain tissues were stored at −80°C.

All animal procedures were performed in accordance with the Animal Ethics Committee of Shaanxi University of Technology (2019–007, Chinese–German Joint Laboratory for Natural Product Research).

Histomorphological Observation of Liver and Brain

The mice liver and brain tissues fixed with paraformaldehyde solution were embedded in paraffin, then sectioned with a 5 μm tissue slicer (Leica, Wetzlar, Germany) and stained with hematoxylin–eosin (H&E). The pathological changes of the tissues were observed under microscope (Leica, Wetzlar, Germany) (Li et al., 2019).

Determination of iNOS Activity in Serum

The activity of iNOS in serum was measured by ELISA kit according to the manufacturer's instructions.

Measurement of the Biochemical Indicators in Liver and Brain of Mice

To determine the activity of AChE in the brain and the activity of SOD, T–AOC, the content of GSH and MDA in the liver and brain, we took the liver and brain tissue, added ice and normal saline in the proportion of 1:9, homogenate (OMNI, Kenneesaw, GA, United States), centrifuged at 4°C, 3,000 rpm for 10 min, and then took the supernatant and packed it separately at −20°C for storage (Zhao et al., 2018).

Immunohistochemistry

The expressions of SIRT1 and p53 proteins in the liver and brain were detected by immunohistochemistry. The liver and brain sections were dewaxed with xylene and gradient alcohol, triton X–100 broke the membrane for 30 min, followed by incubation with 3% H_2O_2 for 30 min, 3% BSA sealed for 20 min, anti–SIRT1 and anti–p53 antibody incubated for 2 h (1:250), horseradish perioxidase (HRP) incubated for 1.5 h (1: 200), DAB stained (liver 20 min, brain 10 min), neutral gum sealed and counterstained with hematoxylin. The expressions of SIRT1 and p53 protein in liver and brain of mice in each group were analyzed and photographed under the same setting.

Quantitative Real–Time PCR

Rapid extractions of total RNA from liver and brain tissues were conducted with a total RNA extraction kit. The first-strand cDNA was reverse-transcribed using the PrimeScript RT reagent kit. The transcription levels of TNF–α, NF–kB, IL–1β, IL–6, and Klotho were quantified by qRT-PCR with GAPDH Gene as internal reference. The qRT-PCR was analyzed on real time PCR detection system with SYBR green (StepOnePlus, ABI, Carlsbad, CA, United States). The primer sequences of the targets and reference genes are summarized in **Table 1**.

After qRT-PCR, the relative expression level of each gene was calculated using GAPDH as the internal reference gene (Li et al., 2019), and the formula was $2^{-(\triangle\triangle Ct)}$.

Statistical Analysis

Data were analyzed using SPSS 19.0 software (SPSS Inc, Chicago, IL, United States). GraphPad Prism 5 (GraphPad Software, San Diego, California, United States) was used for drawing. Mass spectral data were collected and analyzed using MassLynx V 4.2 software (Waters, Milford, MA, United States). The one–way analysis of variance (ANOVA) with Duncan's multiple range tests and $p < 0.05$ was considered statistically significant. Three repetitions in each experiment were displayed as mean ± standard deviation (SD).

RESULTS

Chemical Composition of SDE

A total of 78 compounds were identified in the SDE, which belong to phenols, alkaloids, flavonoids, etc., the flavonoids include prenylated flavonols, prenylated isoflavonoids, isoflavone and chalcone, etc (**Figure 1** and **Table 2**).

TABLE 1 | qRT-PCR amplification primer.

Target gene	Upstream primer (5′–3′)	Downstream primer (5′–3′)
TNF–α	TATGGCTCAGGGTCCAACTC	GCTCCAGTGAATTCGGAAAG
NF–kB	ACGATCTGTTTCCCCTCATCT	TGGGTGCGTCTTAGTGGTATC
IL–1β	TCCAGGATGAGGACATGAGCAC	GAACGTCACACACCAGCAGGTTA
IL–6	CAAAGCCAGAGTCCTTCAGAG	GTCCTTAGCCACTCCTTCTG
Klotho	GGGACACTTTCACCCATCACT	TGGGTGCGTCTTAGTGGTATC
GAPDH	ACAGTCCATGCCATCACTGCC	GCCTGCTTCACCACCTTCTTG

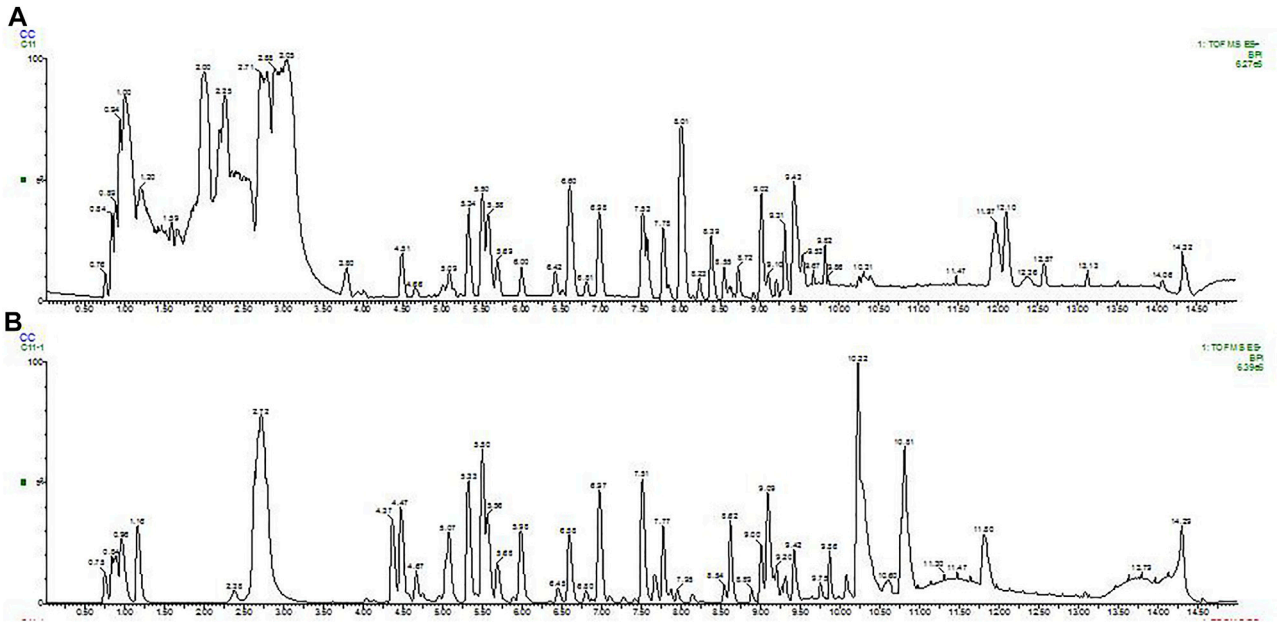

FIGURE 1 | BPI (base peak intensity) diagram of fruit. A: Positive ion BPI (base peak intensity) diagram of fruit; B: Negative ion BPI (base peak intensity) diagram of fruit.

The UPLC based quantitative analysis of polyphenols and alkaloids further indicated that the contents of oxysophocarpine and caffeic acid were the highest among the alkaloids and polyphenols, respectively (**Table 3**).

Mice Body Weight Change and Organ Index

During the D–gal–induction, the growth and development of mice (**Table 4**) and their health condition were documented. There were no difference in the weights among groups at the beginning of the experiment, while after 4 weeks of continuous feeding, the weight gain in each group increased in varying degrees, in which, D–gal group mice slowed the increase, accompanied with mental atrophy, slow movement, rough hair, reduced activity, and other general behavioral states; mice in the SL-, SM-, SH- and Vc group had significant weight gains, and in a dose-dependent manner among SDE groups.

The organ index is calculated by dividing the weight of the organ by the weight of the mouse. The liver and brain indexes of mice in the D–gal group were dramatically lower than those in the NC group ($p < 0.05$), while the indexes were significantly higher in SM, SH and Vc groups than in D–gal group ($p < 0.05$, **Table 5**).

Histological Changes

As shown in **Figure 2A**, the normal structure and obvious boundary of hepatocytes appeared without congestion in the liver of normal mice. The liver cells in D–gal group were disorganized; the intercellular space was enlarged (indicated by the arrow) and ballooning degeneration; the nuclear staining was deepened; some hepatocytes were missing; and there was obvious liver damage. After treatment, the SL and SM groups have basically improved, SH and Vc groups have no significant difference compared with the NC group, indicating that SDE had an improving effect on the D–gal–induced liver injury in aging mice.

Figure 2B shows the pathological changes of the hippocampus in the brain of mice. The neurons in the hippocampus of the normal group were closely arranged, with a large number, complete morphology and no necrosis. In the D–gal group, the neurons in the hippocampus were sparse (indicated by the arrow) and stained deeply, and necrotic cells appeared. The arrangement of cells in SL group and SM group was loose, with a small amount of necrosis and damage of hippocampal cells, the arrangement of hippocampal cells in SH group and Vc

TABLE 2 | The retention time and MS data of 78 compounds in fruit detected by UPLC–MS/MS.

No	Compounds	RT (min)	Molecular formula	Molecular weight	[M + H]	[M–H]	[M + Na]
1	Sophoramine	0.726	$C_{15}H_{21}N_2O$	245.1654	√	—	—
2	Alopecurone A	0.780	$C_{39}H_{37}O_9$	649.2438	—	√	—
3	Kushenol W	0.815	$C_{21}H_{21}O_7$	385.1287	—	√	—
4	Cinnamic acid	0.841	$C_9H_7O_2$	147.0446	—	√	—
5	Alopecurone B	0.866	$C_{39}H_{37}O_9$	649.2438	—	√	—
6	Quercetin	0.892	$C_{15}H_{11}O_7$	303.0505	√	—	—
7	Sophocarpine	0.936	$C_{15}H_{23}N_2O$	247.1810	√	—	—
8	Kaushenol N	0.954	$C_{26}H_{31}O_7$	455.2070	√	—	—
9	Daidzein	0.963	$C_{15}H_{13}O_4$	257.0814	—	√	—
10	Sparteine	0.989	$C_{15}H_{27}N_2$	235.2174	√	—	—
11	Aloperine	1.049	$C_{15}H_{25}N_2$	233.2018	√	—	—
12	Secundiflorol A	1.155	$C_{21}H_{23}O_8$	403.1393	√	—	—
13	Kushenol L	1.312	$C_{25}H_{29}O_7$	441.1913	—	√	—
14	Leachianone G	1.460	$C_{20}H_{21}O_6$	357.1338	√	—	—
15	Sophoraisoflavanone A	1.521	$C_{20}H_{18}O_6$	353.1025	√	—	—
16	Kushenol B	1.547	$C_{30}H_{37}O_6$	493.2590	√	—	—
17	Caffeic acid	1.573	$C_9H_9O_4$	181.0501	√	—	—
18	Gallic acid	1.609	$C_7H_5O_5$	169.0137	—	√	—
19	Luteoloside	1.686	$C_{21}H_{21}O_{11}$	449.1084	—	√	—
20	Kaushenol H	2.018	$C_{26}H_{31}O_7$	455.2070	√	—	—
21	Benzoic acid	2.237	$C_7H_5O_2$	121.0290	—	√	—
22	Ferulic acid	2.534	$C_{10}H_9O_4$	193.0501	—	√	—
23	N-Methylaytisine	3.773	$C_{12}H_{16}N_2O$	205.1341	√	—	—
24	LupinifoLin	3.957	$C_{25}H_{25}O_5$	405.1702	—	√	—
25	Secundiflorol D	4.035	$C_{21}H_{23}O_6$	371.1495	√	—	—
26	Kushenol Q	4.183	$C_{25}H_{29}O_7$	441.1913	—	√	—
27	Rutin	4.315	$C_{27}H_{29}O_{16}$	609.1456	—	√	—
28	Daidzin	4.324	$C_{21}H_{21}O_9$	417.1186	√	—	—
29	Matrine	4.375	$C_{15}H_{25}N_2O$	249.1967	√	—	—
30	Sophoraisoflavanone D	4.402	$C_{30}H_{37}O_6$	493.2590	√	—	—
31	Vicenin–2	4.428	$C_{27}H_{29}O_{15}$	593.1509	—	√	—
32	Sophoricoside	4.515	$C_{21}H_{19}O_{10}$	431.0978	—	√	—
33	Isokurarinone	4.550	$C_{26}H_{29}O_6$	437.1964	—	√	—
34	Kurarinol	4.576	$C_{26}H_{31}O_7$	455.2070	—	√	—
35	Saponarin	4.585	$C_{27}H_{29}O_{15}$	593.1509	—	√	—
36	Isosakuranin	4.594	$C_{22}H_{23}O_{10}$	447.1291	—	√	—
37	Sophoridine	4.595	$C_{15}H_{25}N_2O$	249.1967	√	—	—
38	Kushenol X	4.638	$C_{25}H_{29}O_7$	441.1913	—	√	—
39	Echinoisoflavanone	4.655	$C_{22}H_{25}O_7$	401.1600	√	—	—
40	(^{2}S) –2′–methoxykurarinone	4.733	$C_{27}H_{33}O_6$	453.2277	√	—	—
41	Chlorogenic acid	4.917	$C_{16}H_{17}O_9$	353.0873	—	√	—
42	Kushenol C	4.934	$C_{25}H_{25}O_7$	437.1600	—	√	—
43	Triterpene	4.943	$C_{22}H_{21}O_{10}$	445.1135	—	√	—
44	Kurarinone	4.943	$C_{26}H_{29}O_6$	437.1964	—	√	—
45	Alopecurone D	4.952	$C_{40}H_{39}O_9$	663.2594	—	√	—
46	Epicatechin	4.978	$C_{15}H_{13}O_6$	289.0712	—	√	—
47	Erythrabrssin II	4.987	$C_{25}H_{29}O_4$	393.2066	√	—	—
50	Kuraridinol	5.178	$C_{26}H_{31}O_7$	455.2070	—	√	—
51	Diosmetin	5.589	$C_{16}H_{13}O_6$	301.0712	√	—	—
52	Cytisine	5.702	$C_{11}H_{14}N_2ONa$	213.1004	—	—	√
53	Isoquerctrin	5.807	$C_{21}H_{19}O_{12}$	463.0877	—	√	—
54	Exiguaflavanone D	6.042	$C_{30}H_{37}O_7$	509.2539	—	√	—
55	Sophpraflavanone B	6.504	$C_{20}H_{19}O_5$	339.1232	—	√	—
56	Kushenol K	6.889	$C_{27}H_{31}O_6$	483.2019	—	√	—
57	Kushenol U	7.099	$C_{25}H_{29}O_5$	409.2015	—	√	—
58	Luteolin	7.508	$C_{15}H_9O_6$	285.0399	—	√	—
59	Alopecurone J	8.198	$C_{39}H_{37}O_9$	649.2438	—	√	—
60	Alopecurone K	8.609	$C_{39}H_{37}O_9$	649.2438	—	√	—
61	Sophoraflavanone I	8.949	$C_{39}H_{37}O_9$	649.2438	—	√	—
62	Sophoranone	8.992	$C_{30}H_{35}O_5$	475.2484	—	√	—
63	Maackiain	9.323	$C_{16}H_{11}O_5$	283.0606	—	√	—
64	Kushenol T	9.324	$C_{25}H_{31}O_6$	427.2121	√	—	—
65	Norkurarinone	9.630	$C_{25}H_{29}O_6$	425.1964	√	—	—
66	Leachianone B	9.672	$C_{26}H_{29}O_6$	437.1964	—	√	—
67	Leachianone A	9.962	$C_{26}H_{29}O_6$	437.1964	—	√	—

(Continued on following page)

TABLE 2 | (*Continued*) The retention time and MS data of 78 compounds in fruit detected by UPLC–MS/MS.

No	Compounds	RT (min)	Molecular formula	Molecular weight	[M + H]	[M–H]	[M + Na]
68	Sophoraflavanone H	10.179	$C_{34}H_{31}O_9$	583.1968	√	—	—
69	Alopecurone G	10.240	$C_{26}H_{29}O_5$	421.1025	—	√	—
70	Flavenochromane C	10.764	$C_{24}H_{25}O_6$	421.1615	—	√	—
71	Secundiflorol E	10.765	$C_{22}H_{25}O_7$	401.1600	√	—	—
72	Isosophoranone	10.807	$C_{26}H_{29}O_6$	437.1964	—	√	—
73	8–Lavandulylkaempferol	10.948	$C_{24}H_{25}O_6$	421.1615	—	√	—
74	Orientin	11.514	$C_{21}H_{19}O_{11}$	447.0927	—	√	—
75	Sophpraflavanone G	12.073	$C_{25}H_{27}O_6$	423.1808	—	√	—
76	Desmethylanhydroicaritin	12.222	$C_{20}H_{17}O_6$	353.1025	—	√	—
77	Daucosterol	13.984	$C_{35}H_{59}O_6$	575.4312	—	√	—
78	Kushenol S	14.289	$C_{20}H_{19}O_5$	339.1232	—	√	—

TABLE 3 | Quantification of major polyphenols and alkaloids in SDE.

Compound	Content (mg/g·SDE)
p-Hydroxybenzoic acid	0.026 ± 0.07^{ab}
Caffeic acid	1.911 ± 0.29^{g}
Epicatechin	0.101 ± 0.65^{cd}
Rutin	0.077 ± 0.10^{bcd}
Ferulic acid	0.011 ± 0.03^{a}
Quercetin	1.248 ± 0.43^{f}
Cytisine	2.142 ± 0.01^{abcd}
Oxysophoridine	0.070 ± 0.00^{abc}
Matrine	0.127 ± 0.01^{d}
Sophoridine	0.363 ± 0.01^{e}
Sophocarpine	0.116 ± 0.00^{d}
Oxymatrine	17.736 ± 0.23^{g}
Oxysophocarpine	24.951 ± 0.52^{h}

Different lowercase letters represent significant differences (p < 0.05). mg/g: Milligrams of a certain compound contained in each Gram of dry SDE.

group was orderly and compact, with complete morphology. SDE could inhibit the apoptosis of hippocampal neurons and improve the D–gal–induced brain aging.

iNOS Activity in Serum

Compared with the NC group, the level of iNOS in the D–gal group increased significantly ($p < 0.01$; **Figure 3**) and the activity of iNOS in the SL group decreased, but there was a significant difference between the NC group and SL group ($p < 0.01$). Compared to the D–gal group, the iNOS activity in the SH group and the Vc group decreased significantly ($p < 0.01$).

AChE Activity in the Brain

AChE activity increased significantly in the D–gal group ($p < 0.05$; **Figure 4**), indicating the success of modeling. The AChE activity in the midbrain of the SH group and the Vc group decreased

TABLE 4 | Changes in body weight during feeding.

Group	Weight (g)					
	0 weeks	1 week	2 weeks	3 weeks	4 weeks	Weight Gain
NC	31.79 ± 1.50	31.93 ± 1.06	33.24 ± 1.07	33.92 ± 1.35	34.29 ± 1.68	2.50 ± 0.72
D–gal	32.33 ± 1.26	33.27 ± 2.35	33.40 ± 2.32	34.42 ± 2.18	34.00 ± 1.95	1.67 ± 0.23
SL	32.97 ± 0.81	33.57 ± 1.16	34.22 ± 1.66	34.29 ± 1.58	34.90 ± 2.66	1.93 ± 0.99
SM	30.76 ± 1.13	31.40 ± 1.28	31.73 ± 1.77	32.33 ± 2.17*	32.86 ± 2.01	2.10 ± 0.26
SH	31.50 ± 0.79	32.02 ± 0.91	32.39 ± 0.94	33.14 ± 1.43	34.17 ± 1.31	2.67 ± 0.72*
Vc	31.40 ± 0.75	32.29 ± 1.48	32.88 ± 1.60	33.07 ± 1.43	34.31 ± 1.40	2.91 ± 0.86*

*Compared with D–gal group, *: p < 0.05. NC, normal control group; D–gal, D–gal model group; SL, low–dose SDE, group; SM, medium–dose SDE, group; SL, high–dose SDE, group; Vc, Vc positive control group.*

TABLE 5 | Mice organ index.

Group	Liver index (%)	Brain index (%)
NC	4.001 ± 0.141	1.098 ± 0.038
D–gal	3.514 ± 0.465#	0.999 ± 0.073#
SL	3.773 ± 0.187	1.018 ± 0.055
SM	3.861 ± 0.161*	1.087 ± 0.096
SH	4.141 ± 0.157*	1.087 ± 0.082
Vc	4.007 ± 0.341*	1.089 ± 0.061

*Compared with normal group, #: p < 0.05; Compared with D–gal group, *: p < 0.05. NC, normal control group; D–gal, D–gal model group; SL, low–dose SDE, group; SM, medium–dose SDE, group; SL, high–dose SDE, group; Vc, Vc positive control group.*

significantly and returned to the normal level ($p < 0.05$). However, AChE activities decreased in the SL and SM groups, despite no significant differences compared with the NC group. These results suggest that SDE may delay brain aging by improving the function of the cholinergic system.

MDA in the Liver and Brain

D–gal could induce the increase of MDA content in liver and brain ($p < 0.01$; **Figure 5**). The MDA content in the liver and brain decreased after the treatment with SDE, and there was a significant difference between the SH group, Vc group, and D–gal group ($p < 0.01$).

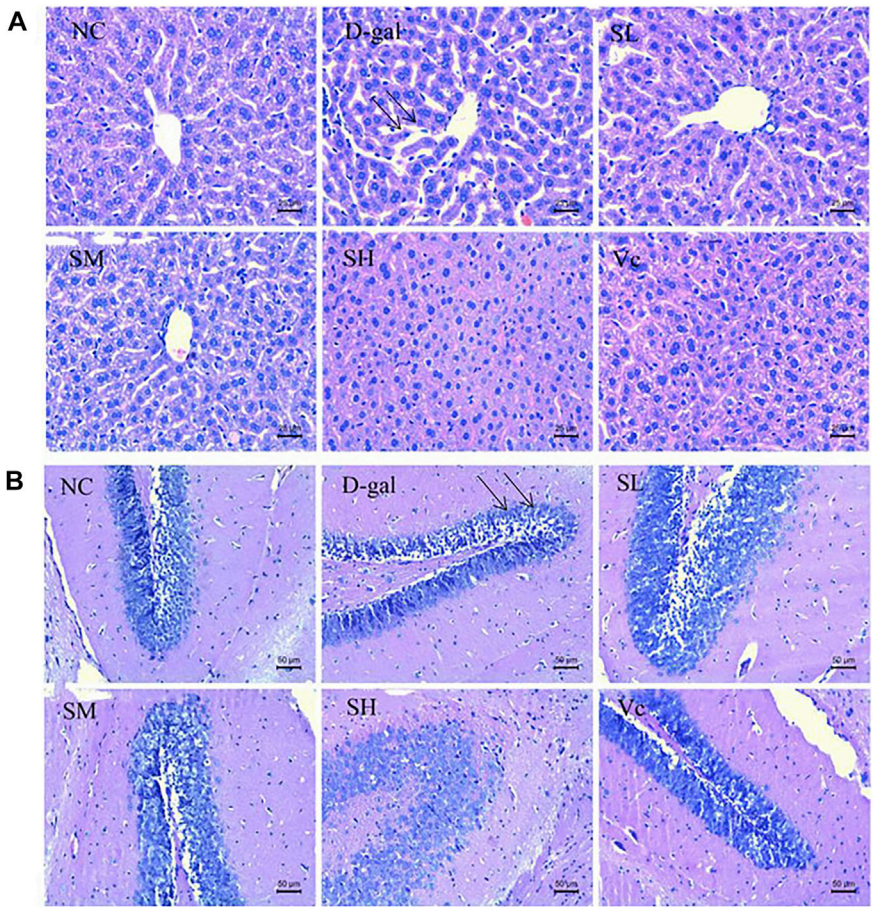

FIGURE 2 | Histopathological changes of liver **(A)** and brain **(B)** in mice (×400). NC: normal control group; D–gal: D–gal model group; SL: low–dose SDE group; SM: medium–dose SDE group; SL: high–dose SDE group; Vc: Vc positive control group. The arrow indicates the injury site.

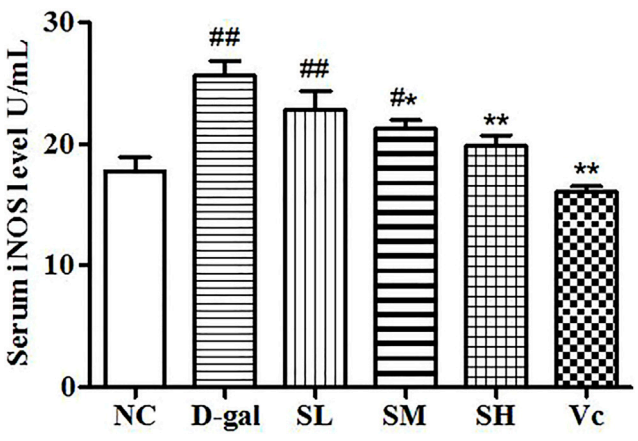

FIGURE 3 | Serum iNOS level. Compared with normal group, #: $p < 0.05$, ##: $p < 0.01$; Compared with model group, *: $p < 0.05$, **: $p < 0.01$. NC: normal control group; D–gal: D–gal model group; SL: low–dose SDE group; SM: medium–dose SDE group; SL: high–dose SDE group; Vc: Vc positive control group.

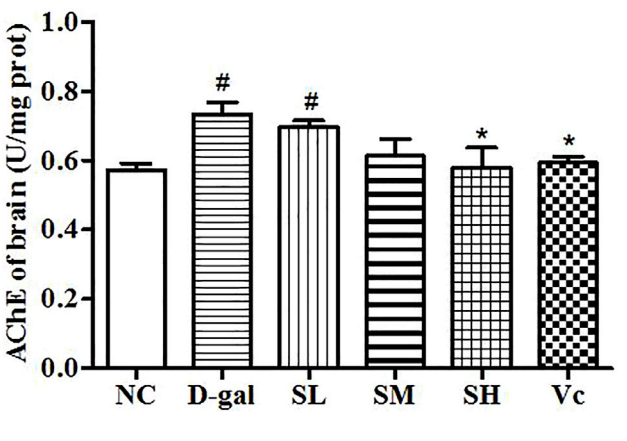

FIGURE 4 | Activity of AChE in mice brain. Compared with normal group, #: $p < 0.05$; Compared with D–gal group, *: $p < 0.05$. NC: normal control group; D–gal: D–gal model group; SL: low–dose SDE group; SM: medium–dose SDE group; SL: high–dose SDE group; Vc: Vc positive control group.

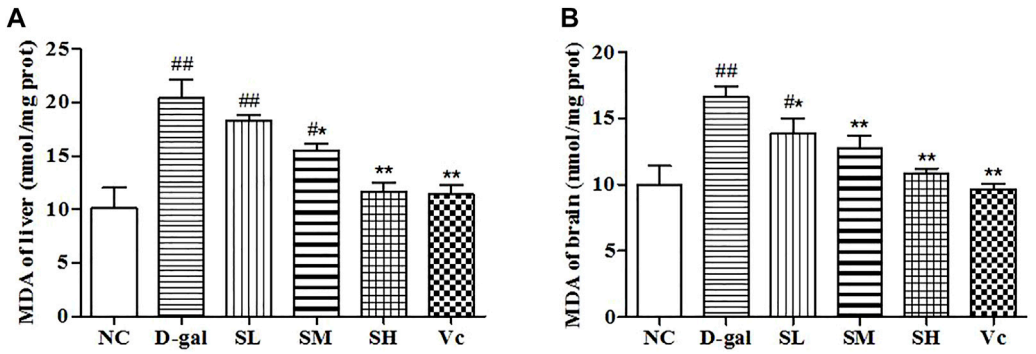

FIGURE 5 | The MDA content of liver **(A)** and brain **(B)** in mice. Compared with normal group, #: $p < 0.05$, ##: $p < 0.01$; Compared with D–gal group, *: $p < 0.05$, **: $p < 0.01$. NC: normal control group; D–gal: D–gal model group; SL: low–dose SDE group; SM: medium–dose SDE group; SL: high–dose SDE group; Vc: Vc positive control group.

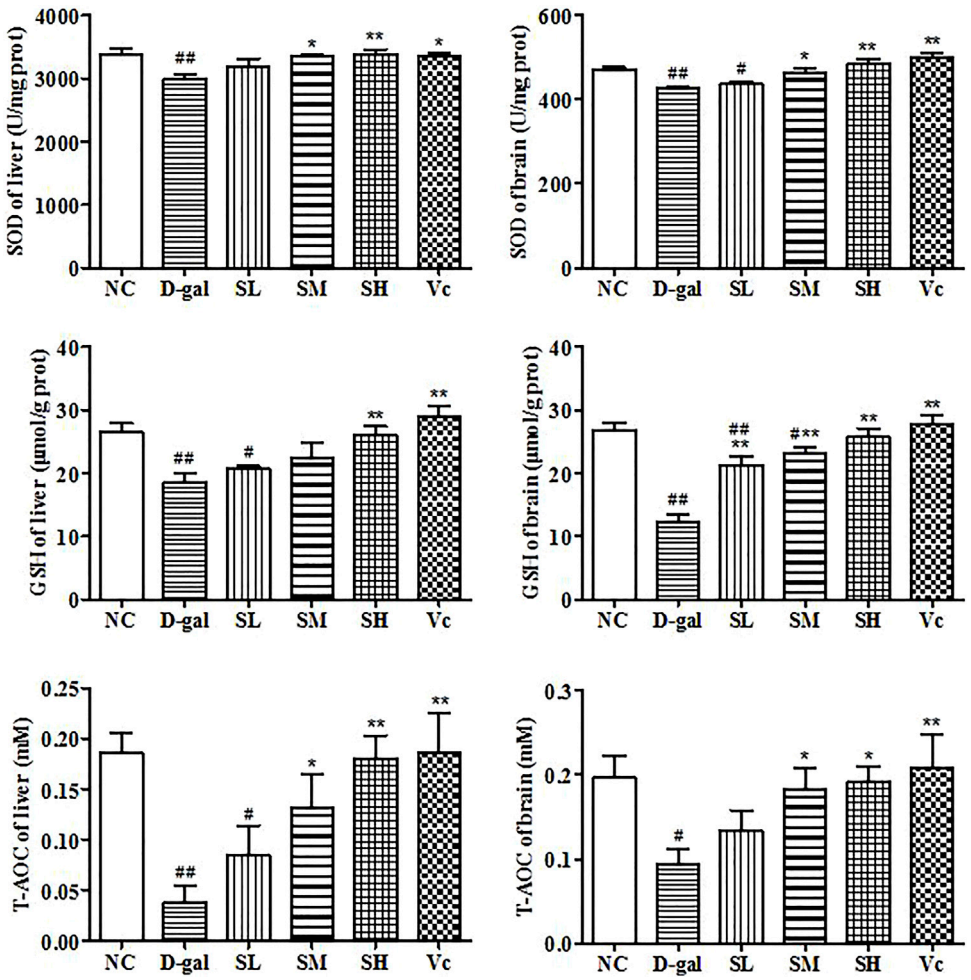

FIGURE 6 | Antioxidant enzyme activity in liver and brain. Compared with normal group, #: $p < 0.05$, ##: $p < 0.01$; Compared with D–gal group, *: $p < 0.05$, **: $p < 0.01$. NC: normal control group; D–gal: D–gal model group; SL: low–dose SDE group; SM: medium–dose SDE group; SL: high–dose SDE group; Vc: Vc positive control group.

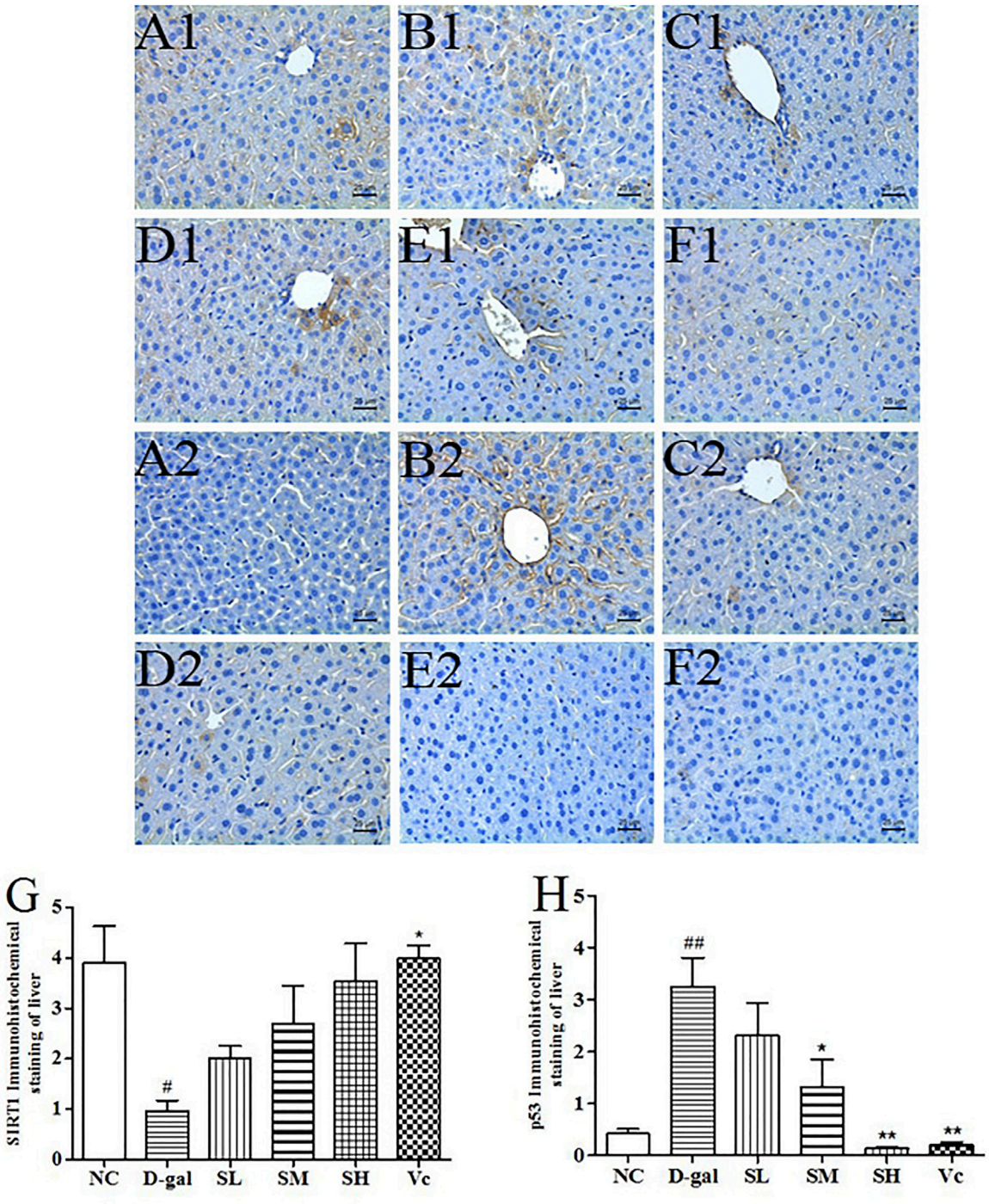

FIGURE 7 | The SIRT1 and p53 protein expressions in the liver tissues of each group (×400). SIRT1 (A1–F1), A1: NC group, B1: D–gal group, C1: low–dose group, D1: medium–dose group, E1: high–dose group, F1: Vc group; p53 (A2–F2), A2: NC group, B2: D–gal group, C2: low–dose group, D2: medium–dose group, E2: high–dose group, F2: Vc group. G: The SIRT1 positive staining area in each group; H: The p53 positive staining area in each group. Compared with normal group, #: $p < 0.05$; ##: $p < 0.01$; Compared with D–gal group, *: $p < 0.05$, **: $p < 0.01$. NC: normal control group; D–gal: D–gal model group; SL: low–dose SDE group; SM: medium–dose SDE group; SL: high–dose SDE group; Vc: Vc positive control group.

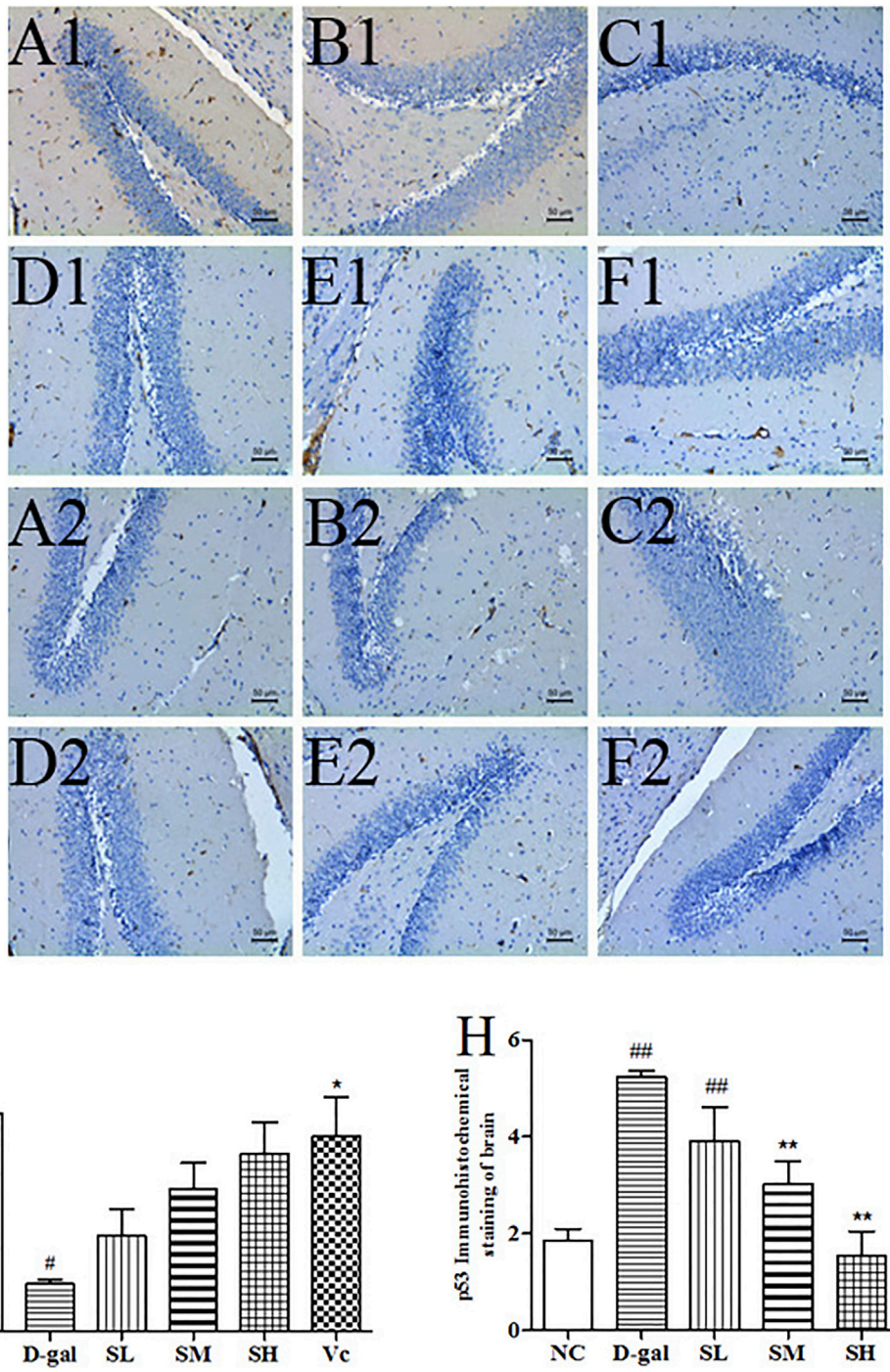

FIGURE 8 | The SIRT1 and p53 proteins expression in the brain tissues of each group (×200). SIRT1 (A1–F1), A1: NC group, B1: D–gal group, C1: low–dose group, D1: medium–dose groups, E1: high–dose group, F1: Vc group; p53 (A2–F2), A2: NC group, B2: D–gal group, C2: low–dose group, D2: medium–dose group, E2: high–dose group, F2: Vc group. G: The SIRT1 positive staining area in each group; H: The p53 positive staining area in each group. Compared with normal group, #: $p < 0.05$, ##: $p < 0.01$; Compared with D–gal group, *: $p < 0.05$, **: $p < 0.01$. NC: normal control group; D–gal: D–gal model group; SL: low–dose SDE group; SM: medium–dose SDE group; SL: high–dose SDE group; Vc: Vc positive control group with normal group, #: $p < 0.05$, ##: $p < 0.01$; Compared with D–gal group, *: $p < 0.05$, **: $p < 0.01$. NC: normal control group; D–gal: D–gal model group; SL: low–dose SDE group; SM: medium–dose SDE group; SL: high–dose SDE group; Vc: Vc positive control group.

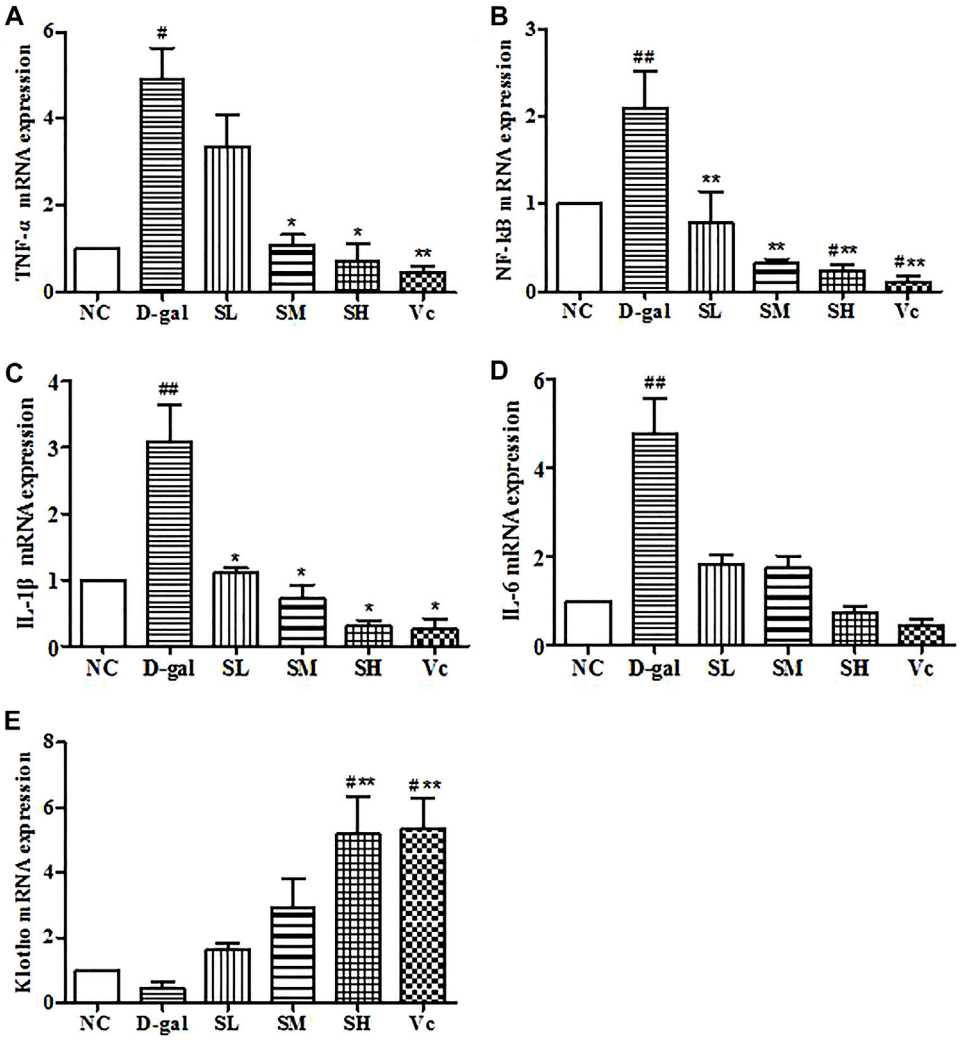

FIGURE 9 | mRNA levels of TNF–α, NF–kB, IL–1β, IL–6 and Klotho in mice liver. Compared with normal group, #: $p < 0.05$, ##: $p < 0.01$; Compared with D–gal group, *: $p < 0.05$, **: $p < 0.01$. NC: normal control group; D–gal: D–gal model group; SL: low–dose SDE group; SM: medium–dose SDE group; SL: high–dose SDE group; Vc: Vc positive control group.

GSH, SOD and T–AOC Level in the Liver and Brain

In this study, we investigated the activities of SOD, T–AOC and GSH (**Figure 6**). Long-term injection of D–gal in the liver and brain reduced significantly GSH level ($p < 0.01$), SOD and T–AOC activity ($p < 0.05$). However, when the mice were treated with SDE, antioxidant enzyme levels in mice gradually return to normal. These results suggested that SDE treatment could improve significantly the antioxidant stress of the liver and brain.

SIRT1 and p53 Protein Expression in the Liver

The SIRT1 protein expression levels in the D–gal group were significantly reduced ($p < 0.05$), as compared with those of the mice in the NC group (**Figure 7G**). After treatment with SDE, the SIRT1 protein expression levels was increased in the mice of SL and SM and SH groups, and a dose-dependent manner. The p53 protein expression levels in the D–gal group were 676.19% higher than that of the NC group (**Figure 7H**). The SL, SM, SH and Vc groups can significantly reduce the expressions of p53 protein in the liver of aging mice. The anti-aging effect of SDE may be related to the activation of a SIRT1/p53 signal pathway.

SIRT1 and p53 Protein Expression in the Brain

D–gal significantly decreased SIRT1 levels (**Figure 8G**, $p < 0.05$) and increased the expression of p53 protein in the brain (**Figure 8H**, $p < 0.01$). The SIRT1 protein expression significantly reduced ($p < 0.05$) in the D-gal group, while SDE treatment significantly increased SIRT1 in a dose-dependent

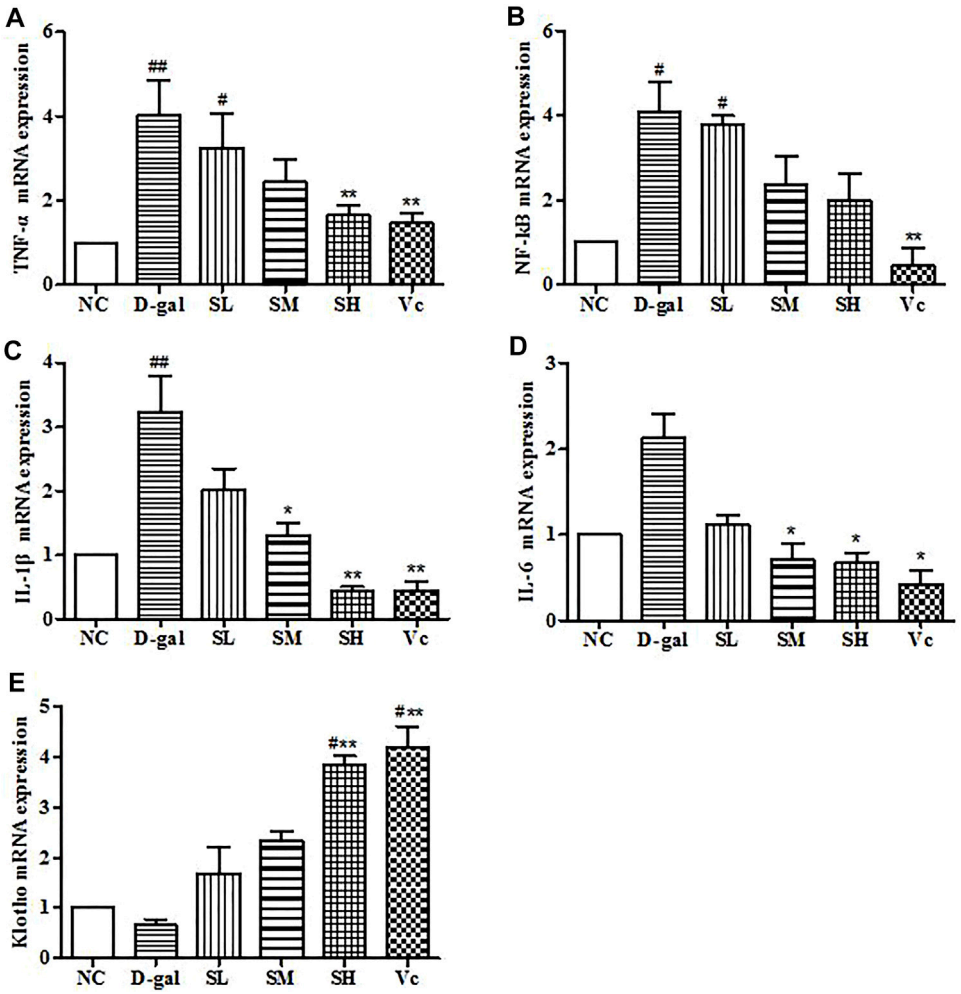

FIGURE 10 | mRNA levels of TNF–α, NF–kB, IL–1β, IL–6 and Klotho in mice brain. Compared with normal group, #: $p < 0.05$, ##: $p < 0.01$; Compared with D–gal group, *: $p < 0.05$, **: $p < 0.01$. NC: normal control group; D–gal: D–gal model group; SL: low–dose SDE group; SM: medium–dose SDE group; SL: high–dose SDE group; Vc: Vc positive control group.

manner. After Vc treatment, SIRT1 protein expression was higher than in the SH groups, and there was significant difference compared with the D–gal group ($p < 0.05$). The expression of p53 protein was attenuated by SDE in a dose-dependent manner.

mRNA Expressions of TNF–α, NF–kB, IL–1β, IL–6 and Klotho in the Liver

The mRNA expression of TNF–α, NF–kB, IL–1β and IL–6 significantly increased ($p < 0.05$) in the D-gal group, while SDE treatments remarkably decreased TNF–α, NF–kB, and IL–1β levels (**Figures 9A–C**). The expression of Klotho mRNA decreased in the D–gal group (**Figure 9E**). After SDE treatments, the expression of Klotho mRNA increased in the SL and the SM groups. There was a significant difference among SH, Vc, and NC groups ($p < 0.05$), and there was a very significant difference compared with the D–gal group ($p < 0.01$). These results indicate that SDE can reverse the high expression of inflammatory factors in the liver of aging mice.

mRNA Expressions of TNF–α, NF–kB, IL–1β, IL–6 and Klotho in the Brain

In the D–gal group, the mRNA expressions of TNF–α, NF–kB, and IL–1β increased significantly ($p < 0.05$). The mRNA expression of IL–6 increased, but the difference was not significant, which indicating that there was neuroinflammation in the brain. After treatment with SDE, the mRNA of TNF–α, NF–kB, IL–1β, and IL–6 were reduced significantly ($p < 0.05$; **Figures 10A–D**). Klotho mRNA expression in the D–gal group decreased, but the difference was not significant compared with the normal group (**Figure 10E**). The mRNA expression of Klotho increased in the SL group and the Vc group, which was different from the NC group ($p < 0.05$), and significantly different from the

D–gal group ($p < 0.01$). The above shows that SDE can reduce neuroinflammation in the brain of aged mice.

DISCUSSION

S. davidi is a medicinal plant used in Chinese ethnic minorities. In our study, 78 compounds were initially identified in SDE, including flavonoids, polyphenols and alkaloids, in which, desmethlyanhydroicaritin, 8-lavandulylkeampferol and kushenol C had been confirmed with clear antioxidant activity *in vivo* (Boozari et al., 2018).

The iNOS can be induced or stimulated by various cytokines such as TNF-α, IL–1β, and IL-6. Under inflammatory conditions and oxidative stress, iNOS protein expression and iNOS gene transcription can be upregulated and remain active to produce enormous NO (Abdul et al., 2021). NO has been associated with the pathogenesis and progression of several diseases, such as liver diseases, insulin resistance, obesity and diseases of the cardiovascular system (Anavi and Tirosh, 2020). Therefore, inhibiting the production of iNOS and NO can inhibit the production of pro-inflammatory mediator factors. The iNOS activity in the D–gal group increased, and the mRNA expression of TNF–α and IL–1β in liver and brain tissues increased significantly, indicating that the mRNA expression of TNF–α and IL–1β increased. The body produces an inflammatory response, which raises the iNOS level, causing damage to the body. Excessive iNOS levels in the body can also trigger an inflammatory response. Our results suggested that SDE can reduce iNOS levels in mice, and consistent with previous reports (Zeng et al., 2018). AChE is a hydrolytic enzyme present mainly in the nervous system, which catalyzes the hydrolysis of the neurotransmitter acetylcholine (ACh). The cognitive ability of human and animal brain learning and memory are closely related to the function of the cholinergic system. AChE is a specific protease reflecting the function of the cholinergic system. It can degrade ACh in synaptic space and reduce its content. Therefore, increasing the level of ACh in the brain and decreasing the activity of AChE, thus enhancing the function of the cholinergic system in the brain may be one of the mechanisms of action against anti-aging and improving the brain's ability for learning and memory. In the D–gal group, the AChE activity in the brain tissue significantly increased, which is consistent with the results of the study by Zhou (Zhou et al., 2013) and his colleagues. After treatment with SDE and Vc, AChE activity in the SH and the Vc group were significantly lower. Decreased AChE activity in brain, suggests that SDE may slow brain aging by improving the cholinergic system.

MDA is a product of lipid peroxidation caused by free radicals in the body, which is often used as an index to evaluate aging (Kong et al., 2018); T–AOC can reflect the total antioxidant capacity of the human body (Zhao et al., 2018). SOD is an important antioxidant enzyme *in vivo*, which can effectively eliminate superoxide anion free radicals, reduce the production of MDA and free radical metabolites, and protect cells from damage (Kong et al., 2018). GSH is the most important non–enzymatic antioxidant in the body, and the amount of GSH is also an important measure of the antioxidant capacity. After the D–gal group was treated with SDE, MDA, GSH content, T–AOC level and SOD activity in the liver and brain were significantly different from the normal group. The content of MDA in liver and brain was downregulated and the content of GSH, the level of T–AOC, and the activity of SOD were upregulated. The results of this study are consistent with a recent publication (Zhao et al., 2018), indicating that SDE has the same anti-aging effect as compound walnut oil capsule.

SIRT1 is a nucleohistone deacetylase dependent on nicotinamide adenine dinucleotide (NAD+), which is involved in the regulation of many physiological processes such as aging, stress cells, DNA repair, and metabolism, etc. Under normal circumstances, SIRT1 protein is highly expressed *in vivo*. p53 is a tumor suppressor that can be activated by many stressors and induces apoptosis, cell cycle arrest, or aging, and also plays a major role in the aging process (Nicole and Ulrich, 2008; Tian et al., 2019). Studies have shown that the activation of SIRT1 has a significant inhibitory effect on the senescence regulator p53, thereby reducing apoptosis and delaying senescence (Li et al., 2018). In our study, we used the immunohistochemical method analyze the expression of SIRT1 and p53 proteins induced by D–gal in the liver and brain of aging mice. The experimental results showed that SDE could increase significantly the expression of SIRT1 protein in the liver and brain of aging mice and inhibit effectively the overexpression of p53 caused by D–gal. The results are similar to those of Tian and his colleagues (Tian et al., 2019). The above results indicated that SDE has good anti-aging effects, and its mechanism may be associated with the activation of a SIRT1/p53 signaling pathway.

Kim et al. found that the expressions of TNF–α, NF–kB, IL–1β and IL–6 are upregulated in the liver and brain tissue of aging mice, indicating the body had an inflammatory reaction (Kim et al., 2020). A previous study (Ruan et al., 2013) demonstrated for the first time that D–gal induces liver cell senescence accompanied by upregulation of pro-inflammatory cytokines. SDE can downregulate the high expression of four kinds of proinflammatory factors, alleviate the inflammatory reaction in liver and brain tissues, and thus play an anti–aging role. Klotho is a type of anti-aging gene. Deficiency of Klotho leads to shortened life span, atherosclerosis, osteoporosis, cognitive and memory impairment, and aging characteristics. In contrast, overexpression of Klotho can prolong life (Wang and Sun, 2009). In addition, studies have shown that Klotho is an important factor in regulating oxidative stress, apoptosis, and cell proliferation. The results of our study show that SDE can increase significantly the expression of the Klotho gene in the liver and brain and protect them from oxidative stress.

CONCLUSIONS

The extract of *S. davidi* fruit has anti-aging effect by reducing the activity of iNOS in serum and AChE in the brain, increasing the activity of antioxidant enzymes in liver and brain tissue, weakening the inflammatory response, upregulating the expression of SIRT1 protein, and inhibiting the over expression of p53 protein. The activation of a SIRT/p53 signal pathway was observed. As a

promising medicinal and functional plant, further exploration on SDE chemical compositions and their pharmacological basis are expected.

DATA AVAILABILITY STATEMENT

The datasets presented in this study can be found in online repositories. The names of the repository/repositories and accession number(s) can be found in the article/Supplementary Material.

ETHICS STATEMENT

The animal study was reviewed and approved by the institutional ethics committee, Shaanxi University of Technology.

AUTHOR CONTRIBUTIONS

BL and DX carried out experimental study. XL and YX guided data analysis. SQ and SW designed the study. XZ proof-read the manuscript. CC supervised the study and checked the final manuscript.

FUNDING

This study was funded by the Shaanxi Province Key Research and Development Plan (grant number 2016NY–161), Innovation Capability Support Program of Shaanxi (grant number 2019XY–04) and Scientific Research Program Funded by Shaanxi Provincial Education Department (grant number 19JC012), China.

REFERENCES

Abdul Rahim, R., Jayusman, P. A., Muhammad, N., Mohamed, N., Lim, V., Ahmad, N. H., et al. (2021). Potential Antioxidant and Anti-inflammatory Effects of *Spilanthes Acmella* and its Health Beneficial Effects: a Review. *Int. J. Environ. Res. Public Health* 18, 3532. doi:10.3390/ijerph18073532

Anavi, S., and Tirosh, O. (2020). iNOS as a Metabolic Enzyme under Stress Conditions. *Free Radic. Biol. Med.* 146, 16–35. doi:10.1016/j.freeradbiomed.2019.10.411

Bektas, A., Schurman, S. H., Sen, R., and Ferrucci, L. (2018). Aging, Inflammation and the Environment. *Exp. Gerontol.* 105, 10–18. doi:10.1016/j.exger.2017.12.015

Boozari, M., Soltani, S., and Iranshahi, M. (2018). Biologically Active Prenylated Flavonoids from the Genus Sophora and Their Structure-Activity Relationship-A Review. *Phytotherapy Res.* 33, 546–560. doi:10.1002/ptr.6265

Hano, C., and Tungmunnithum, D. (2020). Plant Polyphenols, More Than Just Simple Natural Antioxidants: Oxidative Stress, Aging and Age-Related Diseases. *Medicines (Basel)* 7, 26. doi:10.3390/medicines7050026

Huang, Y., Hao, J., Tian, D., Wen, Y., Zhao, P., Chen, H., et al. (2018). Antidiabetic Activity of a Flavonoid–Rich Extract from *Sophora Davidii* (Franch.) Skeels in KK–Ay Mice via Activation of AMP–Activated Protein Kinase. *Front. Pharmacol.* 9, 5–6. doi:10.3389/fphar.2018.00760

Kim, Y., Gautam, S., Aseer, K. R., Kim, J., Chandrasekaran, P., Mazucanti, C. H., et al. (2020). Hepatocyte Cannabinoid 1 Receptor Nullification Alleviates Toxin-Induced Liver Damage via NF-kappaB Signaling. *Cell Death Dis* 11, 1044. doi:10.1038/s41419-020-03261-8

Kong, S.-Z., Li, J.-C., Li, S.-D., Liao, M.-N., Li, C.-P., Zheng, P.-J., et al. (2018). Anti–aging Effect of Chitosan Oligosaccharide on D–Galactose–Induced Subacute Aging in Mice. *Mar. Drugs* 16, 7–8. doi:10.3390/md16060181

Li, J.-J., Zhu, Q., and Lu, Y.-P. (2015). Ligustilide Prevents Cognitive Impairment and Attenuates Neurotoxicity in D–Galactose Induced Aging Mice Brain. *Brain Res.* 1595, 19–28. doi:10.1016/j.brainres.2014.10.012

Li, Q.-S., Zeng, J.-C., Su, M.-L., He, Y., and Zhu, B.-H. (2018). Acetylshikonin from *Zicao Attenuates* Cognitive Impairment and hippocampus Senescence in D–Galactose–Induced Aging Mouse Model via Upregulating the Expression of SIRT1. *Brain Res. Bull.* 137, 311–318. doi:10.1016/j.brainresbull.2018.01.007

Li, X.-X., Jiang, Z.-H., Zhou, B., Chen, C., and Zhang, X.-Y. (2019). Hepatoprotective Effect of Gastrodin against Alcohol–Induced Liver Injury in Mice. *J. Physiolo. Biochem.* 75, 29–37. doi:10.1007/s13105-018-0647-8

Lin, B.-B., Liu, X., Wu, S.-Q., Zheng, H.-X., Huo, K.-K., Qi, S.-S., et al. (2019). Phytochemicals Content, Antioxidant and Antibacterial Activities of *Sophora Viciifolia*. *Chem. Biodivers.* 16, e19000080. doi:10.1002/cbdv.201900080

Ma, Y.-J., Ma, B., Shang, Y.-Y., Yin, Q.-Q., Wang, D.-J., Xu, S., et al. (2018). Flavonoid–rich Ethanol Extract from the Leaves of *Diospyros Kaki* Attenuates D–Galactose–Induced Oxidative Stress and Neuroinflammation–Mediated Brain Aging in Mice. *Oxid. Med. Cel Longev.* 2018, 1–2. doi:10.1155/2018/8938207

Mahmut, M., Valentina, C., Antonio, M., Fernanda, A., and Antonio, G. (2020). Role of P53 in the Regulation of Cellular Senescence. *Biomolecules* 10, 420–430. doi:10.3390/biom10030420

Mu, J.-F., Yang, F.-P., Tan, F., Zhou, X.-R., Pan, Y.-N., Long, X.-Y., et al. (2021). Determination of Polyphenols in *Ilex Kudingcha* and *Insect Tea* (Leaves Altered by Animals) by Ultra-high-performance Liquid Chromatography-Triple Quadrupole Mass Spectrometry (UHPLC-QqQ-MS) and Comparison of Their Anti-aging Effects. *Front. Pharmacol.* 11, 3. doi:10.3389/fphar.2020.600219

Nagy, G., and Pohl, N. L. (2015). Complete Hexose Isomer Identification with Mass Spectrometry. *J. Am. Soc. Mass. Spectrom.* 26, 677–685. doi:10.1007/s13361-014-1072-z

Nicole, E., and Ulrich, M. (2008). Aging and Anti–aging: Unexpected Side Effects of Everyday Medication through Sirtuin1 Modulation. *Int. J. Mol. Med.* 21, 223–232. doi:10.3892/ijmm.21.2.223

Ping, X., Hajime, K., Hideaki, K., Yan, Y.-N., Li, J.-S., Ohmiya, S., et al. (1999). Lupin Alkaloids from Seeds of *Sophora Viciifolia*. *Phytochemistry* 50, 189–193. doi:10.1002/chin.199920196

Qing, W.-X., Li, F., Wang, X.-P., Quan, C.-X., Wen, O.-Y., and Liao, Q. (2018). Inhibiting RIP1 Improves Chronic Stress-Induced Cognitive Impairments in D-Galactose-Induced Aging Mice. *Front. Behav. Neurosci.* 12, 1–2. doi:10.3389/fnbeh.2018.00234

Rosa, T., Federica, M., Filomena, C., Monica, R. L., Marco, B., Giancarlo, S., et al. (2009). Potential Role of Alkaloid Extracts from *Salsola* Species (*Chenopodiaceae*) in the Treatment of Alzheimer`s Disease. *J. Enzym. Inhib.* 24, 818–824. doi:10.1080/14756360802399662

Ruan, Q., Liu, F., Gao, Z., Kong, D., Hu, X., Shi, D., et al. (2013). The Anti–inflamm–aging Andhepatoprotective Effects of Huperzine A in D–Galactose–Treated Rats. *Mech. Ageing Dev.* 134, 89–97. doi:10.1016/j.mad.2012.12.005

Tai, Z.-G., Cai, L., Dai, L., Dong, L.-H., Wang, M.-F., Yang, Y.-B., et al. (2011). Antioxidant Activity and Chemical Constituents of Edible Flower of *Sophora Viciifolia*. *Food Chem.* 126, 1648–1654. doi:10.1016/j.foodchem.2010.12.048

Tian, Y., Zhi, Q., Li, F.-X., Li, F.-H., Zhao, J.-C., Zeng, K.-F., et al. (2019). Optimization of Extraction Process of Water–Soluble Flavonoids from *Coreopsis Tinctoria* Buds and its Effect on Expression of SIRT1 and P53 in Liver Tissues of Aging Mice. *Food Sci.* 40, 300–303. doi:10.15255/KUI.2013.027

Wang, Y.-H., and Sun, Z.-J. (2009). Current Understanding of Klotho. *Aging Res. Rev.* 8, 43–51. doi:10.1016/j.arr.2008.10.002

Wang, Z., Xu, W., Lin, Z., Li, C.-Y., Wang, Y.-H., Yang, L.-W., et al. (2016). Reduced Apurinic/apyrimidinic Endonuclease Activity Enhances the Antitumor Activity of Oxymatrine in Lung Cancer Cells. *Int. J. Oncol.* 49, 2331–2340. doi:10.3892/ijo.2016.3734

Xie, Y.-X., Chen, J., Xiao, A.-P., and Liu, L.-L. (2017). Antibacterial Activity of Polyphenols: Structure–Activity Relationship and Influence of Hyperglycemic Condition. *Molecules* 22, 1–10. doi:10.3390/molecules22111913

Zeng, L.-L., Ding, C.-B., Yang, S., She, X.-X., Liu, X.-L., Li, Z.-Q., et al. (2018). Anti–aging Effects and Mechanism of Red Ginseng Extract on D–Galactose Induced Aging Mice. *Chin. Pharm. J.* 53, 1470–1475. doi:10.11669/cpj.2018.17.009

Zhao, H.-D., Chen, Y.-X., Li, J., Chen, Y., Zhao, J., and Ren, C.-P. (2018). Antioxidant Effects of Compound walnut Oil Capsule in Mice Aging Model Induced by D–Galactose. *J. Food Nutr. Res.* 62, 1–10. doi:10.29219/fnr.v62.1371

Zhao, M.-H., Tang, X.-Q., Gong, D.-Y., Xia, P., Wang, F.-S., and Xu, S.-J. (2020). Bungeanum Improves Cognitive Dysfunction and Neurological Deficits in D-Galactose-Induced Aging Mice via Activating PI3K/Akt/Nrf2 Signaling Pathway. *Front. Pharmacol.* 11, 1–2. doi:10.3389/fphar.2020.00071

Zhou, X.-X., Yang, Q., Xie, Y.-H., Sun, J.-Y., Qiu, P.-C., Cao, W., et al. (2013). Protective Effect of Tetrahydroxystilbene Glucoside against D–Galactose Induced Aging Process in Mice. *Phytochem. Lett.* 6, 372–378. doi:10.1016/j.phytol.2013.05.002

Zhu, S.-Y., Jiang, N., Tu, J., Yang, J., and Zhou, Y. (2017). Antioxidant and Anti–aging Activities of *Silybum Marianum* Protein Hydrolysate in Mice Treated with D–Galactoseactose. *Biomed. Environ. Sci.* 30, 623–631. doi:10.3967/bes2017.083

Conflict of Interest: The authors declare that the research was conducted in the absence of any commercial or financial relationships that could be construed as a potential conflict of interest.

Publisher's Note: All claims expressed in this article are solely those of the authors and do not necessarily represent those of their affiliated organizations, or those of the publisher, the editors and the reviewers. Any product that may be evaluated in this article, or claim that may be made by its manufacturer, is not guaranteed or endorsed by the publisher.

frontiers in Pharmacology

SYSTEMATIC REVIEW
published: 21 February 2022
doi: 10.3389/fphar.2022.744928

Red Yeast Rice Preparations Reduce Mortality, Major Cardiovascular Adverse Events, and Risk Factors for Metabolic Syndrome: A Systematic Review and Meta–analysis

Rong Yuan[1,2†], Yahui Yuan[1,2†], Lidan Wang[1,2], Qiqi Xin[1,2], Ya Wang[1,2], Weili Shi[1,2], Yu Miao[1,2], Sean Xiao Leng[3], Keji Chen[1,2]* and Weihong Cong[1,2]* and BPNMI Consortium*

[1]Laboratory of Cardiovascular Diseases, Xiyuan Hospital, China Academy of Chinese Medical Sciences, Beijing, China, [2]National Clinical Research Center for Chinese Medicine Cardiology, Xiyuan Hospital, China Academy of Chinese Medical Sciences, Beijing, China, [3]Division of Geriatric Medicine and Gerontology, Department of Medicine, Johns Hopkins University School of Medicine, Baltimore, MD, United States

OPEN ACCESS

Edited by:
Norberto Peporine Lopes, University of São Paulo, Brazil

Reviewed by:
Bunleu Sungthong, Mahasarakham University, Thailand
Željko Reiner, University Hospital Centre Zagreb, Croatia

***Correspondence:**
Weihong Cong
congcao@188.com
Keji Chen
kjchenvip@163.com
Sean Xiao Leng
sleng1@jhmi.edu

[†]These authors have contributed equally to this work

Specialty section:
This article was submitted to Ethnopharmacology, a section of the journal Frontiers in Pharmacology

Received: 21 July 2021
Accepted: 01 February 2022
Published: 21 February 2022

Citation:
Yuan R, Yuan Y, Wang L, Xin Q, Wang Y, Shi W, Miao Y, Leng SX, Chen K and Cong W (2022) Red Yeast Rice Preparations Reduce Mortality, Major Cardiovascular Adverse Events, and Risk Factors for Metabolic Syndrome: A Systematic Review and Meta–analysis. Front. Pharmacol. 13:744928. doi: 10.3389/fphar.2022.744928

Background: Metabolic syndrome (MetS) is characterized by the cooccurrence of obesity, insulin resistance, dyslipidaemia, and hypertension. Red yeast rice (RYR) preparations might be beneficial for the prevention and treatment of MetS.

Objective: To implement a systematic review and meta–analysis to determine whether RYR preparations improve clinical endpoints and reduce risk factors for MetS.

Methods: The PubMed, Cochrane Library, EMBASE, Scopus, China National Knowledge Infrastructure, Chinese VIP Information, and WanFang databases were searched for randomized controlled trials (published up to September 2020), and a meta–analysis was performed using fixed– or random–effects models. The primary outcome measures were mortality and major adverse cardiovascular events (MACEs), and the secondary outcome measures were biochemical parameters of blood glucose, blood lipids, and blood pressure. The registration number is CRD42020209186.

Results: A total of 921 articles were identified, of which 30 articles were included in this article. RYR preparations group demonstrated significant improvements in MetS compared with control group. RYR preparations reduced the mortality and MACEs (RR = 0.62, 95% CI [0.49, 0.78]; RR = 0.54, 95% CI [0.43, 0.66]). In terms of blood glucose metabolism, fasting plasma glucose (FPG) (MD = −0.46 mmol/L, 95% CI [−0.71, −0.22]), haemoglobin A1c (HbA1c) (MD = −0.49, 95% CI [−0.71, −0.26]) and the homeostasis model assessment of insulin resistance (HOMA–IR) (MD = −0.93, 95% CI [−1.64, −0.21]) were decreased. Regarding the lipid metabolism, total cholesterol (TC) (MD = −0.74 mmol/L, 95% CI [−1.02, −0.46]), triglycerides (TG) (MD = −0.45 mmol/L, 95% CI [−0.70, −0.21]), and low–density lipoprotein cholesterol (LDL) (MD = −0.42 mmol/L, 95% CI [−0.78, −0.06]) were decreased, while high–density lipoprotein cholesterol (HDL) (MD = 0.14 mmol/L, 95% CI [0.09, 0.20]) was increased. Regarding blood pressure, the mean arterial pressure (MAP) (MD

= –3.79 mmHg, 95% CI [–5.01, –2.57]) was decreased. In addition, RYR preparations did not increase the incidence of adverse reactions (RR = 1.00, 95% CI [0.69, 1.43]).

Conclusion: RYR preparations reduce mortality, MACEs, and multiple risk factors for MetS without compromising safety, which supports its application for the prevention and treatment of MetS. However, additional high–quality studies are needed to provide more evidence for the effect of RYR on MetS due to the heterogeneity in this study.

Systematic Review Registration: www.crd.york.ac.uk/PROSPERO, identifier CRD42020209186

Keywords: red yeast rice, metabolic syndrome, clinical endpoints, risk factors, dyslipidaemia, hypertension, diabetes

INTRODUCTION

Metabolic syndrome (MetS) comprises atherogenic dyslipidaemia, hypertension, obesity, and insulin resistance (Hu et al., 2020), and is associated with an increased risk of type 2 diabetes mellitus, nonalcoholic fatty liver disease, myocardial infarction, and stroke (Prasun, 2020). MetS has become increasingly prevalent with the improvement of people's lives, and it is associated with an increased risk for cardiovascular disease (CVD) and all–cause mortality (Hirode and Wong, 2020). At present, MetS is an urgent global health problem that is unresolved, and there is no single drug that simultaneously treats the multiple diseases or regulates complex underlying mechanisms of MetS yet (Hu et al., 2020). Therefore, it is important to identify therapies that impede the development of metabolic diseases from a preventive perspective.

Red yeast rice (RYR), also known as Hong Qu, Hon–Chi, Anka and red Koji, is a functional food containing monacolin K (lovastatin), monacolin KA, citrinin (ppb), and so on (Halber et al., 2010), and active ingredient monacolin K is the first statin drug (lovastatin) to be approved for treatment of high cholesterol levels (Hunter and Hegele, 2017). RYR is made by fermenting steamed rice with an edible fungus, *Monascus purpureus* Went. RYR products included RYR powders, dietary supplements, and Chinese proprietary medicines (Xuezhikang and Zhibituo), and ingredients were controllable (Klingelhöfer, and Morlock, 2019). Substantial evidence suggests a strong biochemical effect of RYR on plasma lipid levels and it is frequently consumed to lower low–density lipoprotein (LDL) as an alternative to statins (Loubser et al., 2019).

Several meta–analyses have shown that RYR is an effective and relatively safe therapy for dyslipidaemia (Xiong et al., 2017; Sungthong et al., 2020). Increasing evidence also suggests that RYR has antidyslipidaemia, antidiabetic, antiatherosclerotic, antiobesity, and antihypertensive activities (Zhu et al., 2019), leading to a growing interest in the hypothesis that RYR has beneficial health effects on MetS and its adverse clinical outcomes. Thus, we aimed to evaluate the efficacy and safety of RYR preparations in MetS through a systematic review and meta–analysis of randomized controlled trials (RCTs).

METHODS

This study was conducted and reported based on the guidelines of PRISMA and was registered in PROSPERO (the registration number is CRD42020209186).

Search Strategies

We identified articles by searching the following electronic databases from database inception until September 2020: PubMed, Cochrane Library, EMBASE, Scopus, China National Knowledge Infrastructure, Chinese VIP Information, and WanFang. The search strategy included population and intervention keywords (MetS and RYR preparations) as well as synonyms of these terms (**Supplementary Material S1**). We also manually searched the reference lists of the included articles. Authors of relevant studies were contacted to obtain additional and missing data. Two reviewers (RY, YY) independently identified relevant studies, and any disagreement was resolved through discussion or consultation with a third reviewer.

Selection of Studies

The inclusion criteria were as follows: a) Populations: participants meeting at least one of the international or domestic diagnostic criteria for MetS with no restrictions of age, sex, race, course; b) Interventions: patients in the treatment group were given RYR preparations alone or combined with conventional treatment (hypoglycemic drugs, lipid–lowering drugs, and antihypertensive drugs alone or the combination of these drugs), defining RYR preparations as involving Xuezhikang interventions or other relevant preparations; c) Comparators: patients in the control group were given conventional treatment or placebo; d) Outcomes: reported data for at least one of the interest outcomes: the primary outcomes of interest were mortality and MACEs, the secondary outcomes of interest included MetS risk factors, such as blood sugar parameters [fasting plasma glucose (FPG), haemoglobin A1c (HbA1c), homeostasis model assessment of insulin resistance (HOMA–IR), insulin sensitivity index (ISI)], blood lipid parameters [total cholesterol (TC), triglycerides (TG), LDL, high–density lipoprotein (HDL)], and blood pressure [mean arterial pressure (MAP), systolic blood pressure (SBP), and diastolic blood pressure (DBP)]. In addition, adverse reactions were also assessed; e) Study designs: RCTs.

The exclusion criteria were as follows: a) included patients with severe abnormal heart, liver and kidney function, severe infections, tumor or other serious primary disease; b) included patients with special populations such as lactating woman or pregnant women; c) patients in the treatment group were given nutraceuticals combination compound; d) no clinical data could be extracted; e) reviews, retrospective studies, observational studies, letters, case reports, and animal/cell experiments.

Data Extraction

The Cochrane Data Collection form was applied for the data extraction. Two independent investigators (RY and YY) reviewed the studies and extracted the data. The following data were extracted for each study: participant characteristics, such as the number of participants in each group, age, sex, drug and control treatment, intervention duration, outcomes (major adverse cardiovascular events (MACEs), mortality, and the biochemical parameters of blood glucose, blood lipids, and blood pressure), and adverse events.

Quality Assessment

Two reviewers (YR, YY) independently evaluated the quality of included studies according to the Physiotherapy Evidence Database (PEDro) scale (Moseley et al., 2020), which is exclusively applied to assess the risk of bias in RCTs. The PEDro criteria items include eligibility criteria, random allocation, concealed allocation, group similarity at baseline, participant/therapist/assessor blinding, dropout number, intention–to–treat analysis, between–group differences, and point estimate and variability. The PEDro scale awards 1 point per criterion (the first criterion is not scored): a score of less than 4 is considered "poor", 4 to 5 is considered "fair", 6 to 8 is considered "good" and 9 to 10 is considered 'excellent' (Cashin and Mcauley, 2020). In addition, we assessed the quality of included evidence using the Grading of Recommendations, Assessment, Development and Evaluations (GRADE) approach, which classifies the evidence as high, moderate, low, or very low.

Data Analysis

RevMan 5.3.0 was utilized to analyse the results. Continuous variables were calculated by the mean difference (MD) and 95% confidence interval (CI). Dichotomous variables were expressed as relative risk (RR) with 95% CI. According to the Cochrane Handbook for Systematic Reviews of Interventions, once the multiple treatment groups were included from one study, the shared control group were split into two or more groups with smaller sample sizes, and two or more (reasonably independent) comparisons were included (Higgins et al., 2019). The heterogeneity of the results across the studies was evaluated using the I^2 statistic: $I^2 < 50\%$ were considered to have low heterogeneity and the results were estimated by a fixed–effects model, while $I^2 \geq 50\%$ were considered to have moderate and high heterogeneity and the results were estimated by a random–effects model. In cases of heterogeneity, we investigated the potential causes by performing subgroup and meta–regression analyses. When there were high levels of heterogeneity, study characteristics and data–related factors (such as age, sex, intervention duration and intervention type) were explored to identify the cause of the heterogeneity. Stata 15.1 was utilized to draw funnel plots, and we conducted Egger's test to detect publication bias when the number of studies for each outcome was above or equal to 10.

RESULTS

Study Selection

A total of 921 articles were searched, and 805 articles were screened by the title and abstract after the removal of duplicates. A total of 139 articles were identified for review based on the full text, and 30 articles were eligible to be included in the review (**Figure 1**). Data were only included once in meta–analysis when participant data reported in more than one publication.

Study Characteristics

In this meta–analysis, Li et al., 2017 contained two treatment groups and presented the results separately for Xuezhikang or Xuezhikang + Daixiefang compared with Daixiefang (a traditional Chinese medicine prescription). Two articles (Li et al., 2010) (Li et al., 2009) reported data from one trial. The clinical studies were published in English and Chinese from 1997 to 2019, and all of the studies were conducted in China except for one from Italy. A total of 5440 patients were included, and the mean age of the participants ranged from 41 to 76. Interventions included Xuezhikang and lovastatin, and trial duration ranged from 1 month to 4.5 years. The detailed characteristics of the included trials are shown in **Table 1**. The detailed information of RYR preparations in the included trials is described in **Supplementary Table S1**. The PEDro score ranged from 4 (Shen, 2011; Zhang and Wu, 2014) to 9 (Li et al., 2009; Li et al., 2010; Li et al., 2017) (**Supplementary Table S2**).

Risk of Bias

The median score on the PEDro (on a scale of 0–10) for the included trials was 6. Among the 30 original trials, ten (33.3%) trials were considered "fair" quality and had a medium risk of bias (PEDro score ranging from 4 to 5). Seventeen (56.7%) trials were considered "good" quality and had a low risk of bias (PEDro score ranging from 6 to 8). Three (10.0%) trials were considered "excellent" quality and had a low risk of bias (PEDro score of 9) (**Table 1**). The main reasons for the risk of bias were nonblinded therapists (24 trials [80.0%]), nonblinded assessors (30 trials [100.0%]), not performing concealed allocation (27 trials [90.0%]), and withdrawal rates higher than 15% (8 trials [26.7%]) (**Supplementary Table S2**).

Effects of RYR Preparations on Mortality and MACEs

Two trials (Zhao et al., 2007; Li et al., 2010) including 3297 participants reported therapeutic effects of RYR on mortality, and three trials (Zhao et al., 2007; Li et al., 2010; Shen, 2011) including 3360 participants reported its therapeutic effects on MACEs. RYR

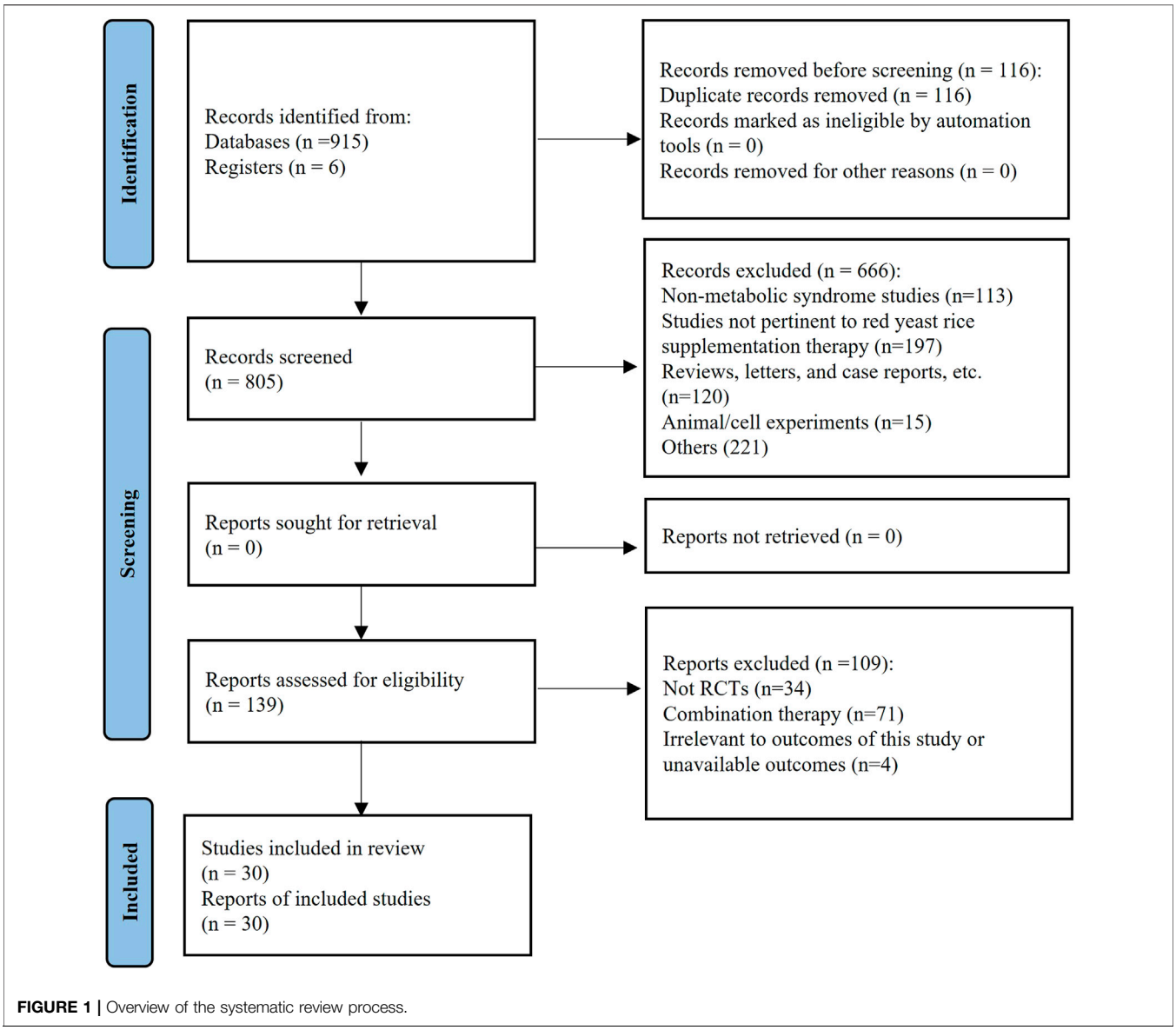

FIGURE 1 | Overview of the systematic review process.

preparations significantly reduced the mortality (RR = 0.62, 95% CI [0.49, 0.78]), and MACEs (RR = 0.54, 95% CI [0.43, 0.66]) compared with control group. Furthermore, there was no heterogeneity among the studies (**Figure 2**).

Effects of RYR Preparations on MetS Risk Factors

Blood Glucose Parameters (FPG, HbA1c, HOMA-IR, and ISI)

Ten trials including 646 participants reported therapeutic effects of RYR on FPG, and RYR preparations significantly reduced FPG level (−0.46 mmol/L, 95% CI [−0.71, −0.22]) compared with control group (**Figure 3A**). There was high heterogeneity among the studies of FPG and subgroup analysis was performed. RYR preparations significantly reduced FPG level (−0.92 mmol/L, 95% CI [−1.26, −0.58], $p < 0.00001$, $I^2 = 41\%$) in 40- to 50-year-old patients with more notable effects and low heterogeneity, while other subgroups had high heterogeneity. Besides, compared with conventional therapy, RYR plus conventional therapy reduced FPG level (−0.53 mmol/L, 95% CI [−0.93, −0.12], $p = 0.01$, $I^2 = 67\%$) with medium heterogeneity, while other subgroups had high heterogeneity (**Supplementary Figure S1**). Five trials including 392 participants reported its therapeutic effects on HbA1c, and RYR preparations reduced HbA1c level (−0.49, 95% CI [−0.71, −0.26]) compared with control group (**Figure 3B**). There was high heterogeneity among the studies of HbA1c, hence subgroup analysis was performed. However, compared with conventional therapy, RYR plus conventional therapy reduced HbA1c level (−1.48 mmol/L, 95% CI [−2.13, −0.84], $p < 0.00001$, $I^2 = 94\%$) with high heterogeneity, and the heterogeneity remains unexplained in other subgroups (**Supplementary Figure S2**). Two trials including 102 participants reported therapeutic

TABLE 1 | Study characteristics.

Study (country)	Population	PEDro score	Participants (int:cont)	Male: Female (int/cont)	Age range	Trial intervention	Control intervention	Period of treatment	Outcomes
Zhang, (2019)	Diabetes + hyperlipidaemia	6	67:67	33:34/ 36:31	int: 45.19 ± 3.84 cont: 45.18 ± 1.91	Lovastatin + metformin	Metformin	8 weeks	TC, TG, FPG, HbA1c
Xiao, (2019)	Hyperlipidaemia + prehypertension	6	42:42	23:19/ 25:17	int: 67.53 ± 5.76 cont: 68.24 ± 6.13	Xuezhikang	Atorvastatin calcium	4 weeks	TC, TG, HDL–C, LDL–C SBP, DBP, MAP
Li et al. (2017)	MetS	9	20:21	5:15/ 11:10	int: 68.25 ± 10.92/cont: 62.38 ± 9.90	Xuezhikang	Daixiefang*	12 weeks	TC, TG, HDL–C, LDL–C, FPG, HbA1c, HOMA–IR
			21:21	7:14/ 11:10	int: 66.10 ± 8.85 cont: 62.38 ± 9.90	Xuezhikang + Daixiefang			
Wang and Wang, (2016)	Hyperlipidaemia + prehypertension	6	62:62	48:14/ 46:16	int: 66.7 ± 7.9 cont: 67.6 ± 8.1	Xuezhikang	Atorvastatin calcium	8 weeks	TC, TG, HDL–C, LDL–C, SBP, DBP, MAP
Zhao, (2015)	Diabetes + dyslipidaemia	5	32:33	17:15/ 15:18	int: 59.6 ± 4.7 cont: 57.6 ± 5.3	Xuezhikang	Placebo	8 weeks	TC, TG, HDL–C, LDL–C
Ke, (2015)	Diabetes + dyslipidaemia	6	29:29	18:11/ 16:13	int: 62.3 ± 6.6 cont: 62.9 ± 7.1	Xuezhikang	Simvastatin	12 weeks	TC, TG, HDL–C, LDL–C, FPG
Zhang and Wu, (2014)	MetS	4	20:20	24:16	76 ± 10	Xuezhikang + routine treatment	Routine treatment	12 weeks	TG, HDL–C, SBP, DBP, FPG, HOMA–IR
Chen, (2013)	Diabetes + hyperlipidaemia	7	45:44	Not reported	45–70	Xuezhikang	Simvastatin	12 weeks	TC, TG, HDL–C, LDL–C
Wang and Liu, (2013)	Diabetes + dyslipidaemia	6	32:30	18:14/ 13:17	int: 59 ± 7.6 cont: 61 ± 9.3	Xuezhikang	Simvastatin	8 weeks	TG
Wu and Wei, (2011)	Hypertension + dyslipidaemia	5	75:75	48:27/ 49:26	int: 54.8 ± 10.2 cont: 55.26 ± 9.8	Xuezhikang	Atorvastatin calcium	8 weeks	TC, TG, HDL–C, LDL–C
Ma and Qian, (2011)	Diabetes + dyslipidaemia	6	37:37	22:15/ 24:13	int: 42–66 cont: 41–65	Xuezhikang	Simvastatin	6 weeks	TC, TG, HDL–C
Shen, (2011)	Diabetes + dyslipidaemia	4	40:25	35:30	45–65	Xuezhikang + routine treatment	Routine treatment	18 weeks	TG, HDL–C, LDL–C, MACEs
Li et al., 2010	Hypertension + dyslipidaemia	9	1363:1341	1093:270/ 1054:287	int: 59.4 ± 9.2 cont: 59.2 ± 9.5	Xuezhikang	Placebo	4.5 years	TC, TG, HDL–C, LDL–C, SBP, DBP, mortality, MACEs
Zhai and Li, (2010)	Diabetes + hyperlipidaemia	5	48:38	28:20/ 21:17	int: 50.6 cont: 51.8	Xuezhikang + routine treatment	Routine treatment	12 weeks	TG, TC
Li et al, (2009)	Hypertension + dyslipidaemia	9	772:758	1143/387	int: 66 ± 4 cont: 66 ± 4	Xuezhikang	Placebo	4.5 years	SBP, DBP, TG, TC, LDL–C, HDL–C
He and Zhan, (2009)	Diabetic nephropathy	6	72:72	56:16/ 58:14	int: 53.3 ± 9.4 cont: 51.3 ± 11.6	Xuezhikang	Atorvastatin calcium	48 weeks	TC, TG
Zhang, (2009)	Diabetes + dyslipidaemia	8	45:43	33:12/ 29:14	int: 61.2 ± 4.6 cont: 58.8 ± 6.2	Xuezhikang + routine treatment	Routine treatment	16 weeks	TC, TG, HDL–C
Jin et al. (2007)	Diabetic nephropathy + dyslipidaemia	6	30:30	21:9/ 19:11	int: 52.81 ± 9.39 cont: 54.96 ± 7.98	Xuezhikang + routine treatment	Routine treatment	12 weeks	TC, TG, HDL–C, FPG
		7	306:285		int: 60.5 ± 8.7	Xuezhikang	Placebo	4 years	

(Continued on following page)

TABLE 1 | (*Continued*) Study characteristics.

Study (country)	Population	PEDro score	Participants (int:cont)	Male: Female (int/cont)	Age range	Trial intervention	Control intervention	Period of treatment	Outcomes
Zhao et al. (2007)	Diabetes + dyslipidaemia			226:80/ 198:87	cont: 61.6 ± 8.0				TC, TG, HDL–C, LDL–C, mortality, MACEs
Wang et al. (2005)	Diabetes + hyperlipidaemia	5	32:30	17:15/ 16:14	int: 54.2 ± 10.4 cont: 55.1 ± 9.5	Xuezhikang	Pravastatin	8 weeks	TC, TG, HDL–C, LDL–C
Zhu and Yao, (2005)	Diabetes + hyperlipidaemia	6	31:31	40:22	51–75	Xuezhikang	Routine treatment	4 weeks	TC, TG, FPG
Li et al. (2005)	Diabetes + hyperlipidaemia	6	24:24	Not reported	40–50	Xuezhikang + routine treatment	Routine treatment	8 weeks	TC, TG, HDL–C, LDL–C, FPG, HbA1c
Yao et al. (2004)	Diabetes + hyperlipidaemia	6	24:22	12:12/ 12:10	int: 56.87 cont: 57.37	Xuezhikang + routine treatment	Routine treatment	8 weeks	TC, TG, HDL–C, LDL–C, FPG
Sui, (2003)	Diabetes + hyperlipidaemia	5	48:32	24:24/ 22:10	int: 45–73 cont: 42–70	Xuezhikang	Amaranth capsules	8 weeks	TC, TG, HDL–C, FPG, ISI, HbA1c
Deng et al. (2003)	Diabetes + hyperlipidaemia	6	30:26	34:22	52.6 ± 7.3	Xuezhikang + routine treatment	Routine treatment	weeks	TC, TG, HDL–C, LDL–C
Zeng et al. (2001)	Diabetes + hyperlipidaemia	5	22:24	12:10/ 12:12	int: 47–71 cont: 52–74	Xuezhikang + routine treatment	Routine treatment	8 weeks	TC, TG, HDL–C, LDL–C, FPG, HbA1c
Gentile et al. (2000)	Diabetes + hypercholesterolemia	6	80:86	54:26/ 63:23	int: 58 ± 5 cont: 61 ± 6	Lovastatin	Placebo	24 weeks	TC, TG, HDL–C, LDL–C
Peng et al. (2000)	Diabetes + hyperlipidaemia	5	34:34	22:12/ 25:9	int: 44.1 ± 9.0 cont: 46.7 ± 9.6	Xuezhikang + routine treatment	Routine treatment	24 weeks	TC, TG, FPG, HbA1c
Chang et al. (1998)	Hypertension + hyperlipidaemia	6	32:30	30:32	56.7 ± 6.2	Lovastatin	Inositol nicotinate	2 months	TC, TG, HDL–C
Wang et al. (1997)	Diabetes + hyperlipidaemia	5	17:17	9:25	60 ± 4	Xuezhikang	Gemfibrozil	4 weeks	TC, TG, HDL–C, ISI

*Note:*Daixiefang: a prescription of traditional Chinese medicine is used to improve the metabolism, including Prunus persica (L.) batsch, Rheum officinale Baill., Alisma plantago–aquatica Linn., trichosanthis radix, Dendranthema indicum(L) Des Moul., and Crataegus pinnatifida, Sargassum.*

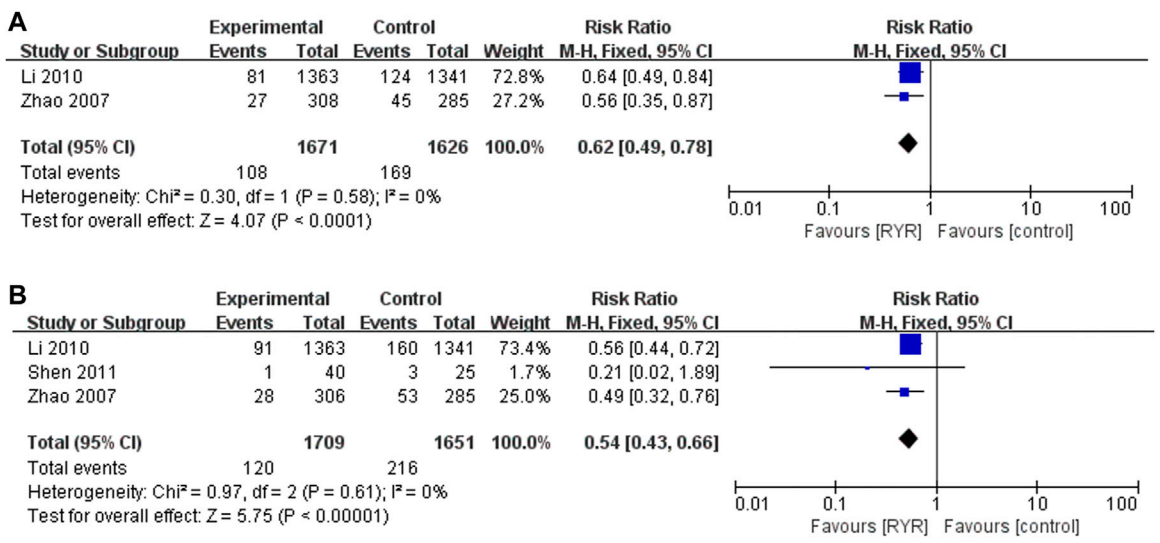

FIGURE 2 | Forest plots of the risk of **(A)** mortality and **(B)** MACEs.

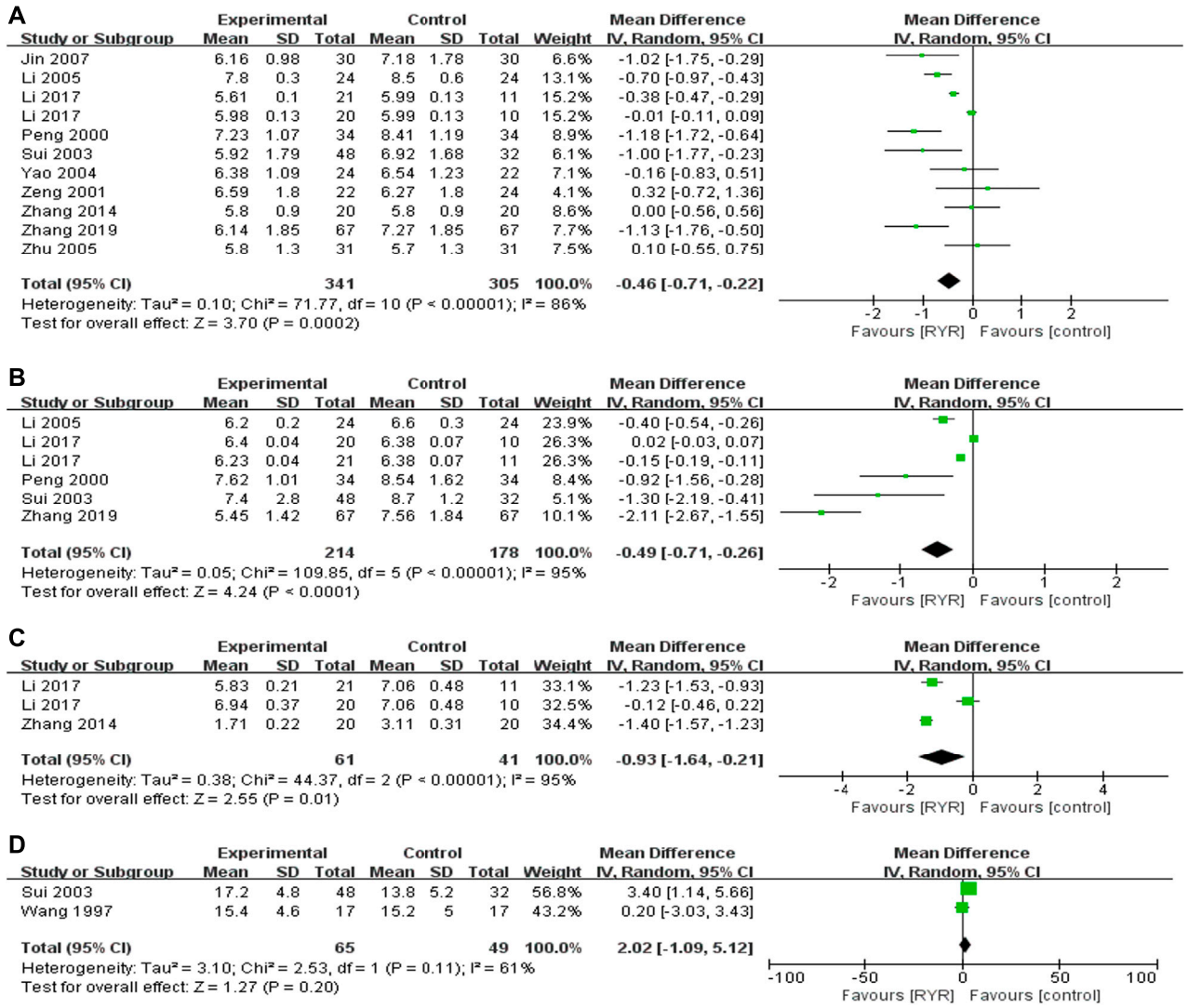

FIGURE 3 | Forest plots of **(A)** FPG, **(B)** HbA1c, **(C)** HOMA–IR, and **(D)** ISI.

effects on HOMA–IR, and two trials including 114 participants reported therapeutic effects on ISI. RYR preparations lowered HOMA–IR (−0.93, 95% CI [−1.64, −0.21]) while did not increase ISI (2.02, 95% CI [−1.09, 5.12]) compared with control group (**Figures 3C,D–**). There was high heterogeneity among the studies of HOMA-IR and ISI, yet subgroup analysis could not be performed and the heterogeneity could not be fully investigated due to the limited number of studies and the small sample sizes. Therefore, further validation on existing results is required.

Lipid Profile Parameters (TC, TG, LDL-C, and HDL-C)

Twenty–three trials including 5084 participants reported therapeutic effects of RYR on TC, 26 trials including 5234 participants on TG, 16 trials including 4391 participants on LDL, and 19 trials including 4653 participants on HDL. RYR preparations reduced the levels of TC (−0.74 mmol/L, 95% CI [−1.02, −0.46]), TG (−0.45 mmol/L, 95% CI [−0.70, −0.21]) and LDL–C (−0.42 mmol/L, 95% CI [−0.78, −0.06]), while increased HDL–C level (0.14 mmol/L, 95% CI [0.09, 0.20]) compared with control group (**Figure 4**). There was high heterogeneity among the studies of TC, TG, LDL–C and HDL–C, hence subgroup analysis was performed. RYR preparations significantly reduced the levels of TC (−1.55 mmol/L, 95% CI [−1.85, −1.25], $p < 0.00001$, $I^2 = 0\%$) and TG (−0.70 mmol/L, 95% CI [−0.90, −0.50], $p < 0.00001$, $I^2 = 24\%$) in 40– to 50–year–old patients with more notable effects and low heterogeneity, while other subgroups had high heterogeneity. It also significantly reduced TG level (−0.59 mmol/L, 95% CI [−0.66, −0.52], $p < 0.00001$, $I^2 = 0\%$) in a higher proportion of women (male: female = 1:1.5) with more notable effects and low heterogeneity, while other subgroups had high heterogeneity. Moreover, RYR preparations significantly reduced the levels of TC (−0.19 mmol/L, 95% CI [−0.23, −0.15], $p < 0.00001$, $I^2 = 26\%$), TG (−0.12 mmol/L, 95% CI

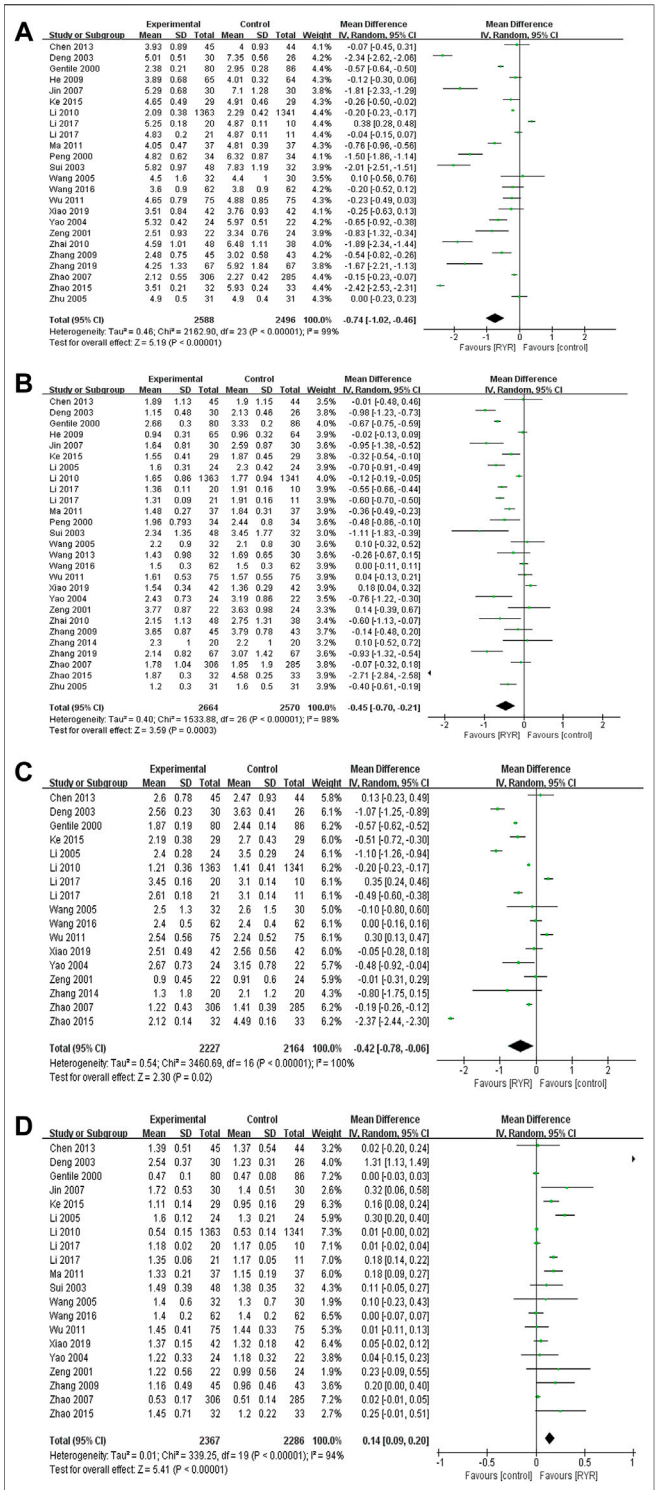

FIGURE 4 | Forest plots of **(A)** TC, **(B)** TG, **(C)** LDL–C, and **(D)** HDL–C.

[−0.18, −0.05], $p = 0.0005$, $I^2 = 0\%$), LDL (−0.20 mmol/L, 95% CI [−0.23, −0.17], $p < 0.00001$, $I^2 = 0\%$), and increased the level of HDL (0.01 mmol/L, 95% CI [0.00, 0.02], $p = 0.02$, $I^2 = 0\%$) in the intervention duration of >12 months with mild effects and low heterogeneity, while other subgroups had high heterogeneity. However, compared with conventional therapy, RYR plus conventional therapy reduced the levels of TC (−1.48 mmol/L, 95% CI [−2.13, −0.84], $p < 0.00001$, $I^2 = 94\%$), TG (−0.53 mmol/L, 95% CI [−0.78, −0.28], $p < 0.0001$, $I^2 = 75\%$) and LDL (−0.70 mmol/L, 95% CI [−1.12, −0.28], $p < 0.001$, $I^2 = 91\%$), while increased HDL level (0.40 mmol/L, 95% CI [0.03, 0.78], $p = 0.03$, $I^2 = 96\%$) with high heterogeneity; compared with lipid–lowing drugs, RYR preparations increased HDL level (0.07 mmol/L, 95% CI [0.01, 0.12], $p = 0.01$, $I^2 = 67\%$) with medium heterogeneity; compared with placebo, RYR preparations reduced the levels TC (−0.83 mmol/L, 95% CI [−1.58, −0.09], $p = 0.03$, $I^2 = 100\%$) and LDL (−0.83 mmol/L, 95% CI [−1.64, −0.03], $p = 0.04$, $I^2 = 100\%$) with high heterogeneity **(Supplementary Figures S3–S6)**. In addition, meta−regression analysis revealed that age was a significant moderator of TC ($p = 0.017$) **(Supplementary Table S3)**.

Blood Pressure Parameters (MAP, SBP, and DBP)

Two trials (Wang and Wang, 2016; Xiao 2019) including 208 participants reported therapeutic effects of RYR on MAP, and RYR preparations reduced MAP level (−3.79 mmHg, 95% CI [−5.01, −2.57]) compared with control group **(Figure 5A)**. There was high heterogeneity among the studies of MAP, while subgroup analysis could not be performed and the heterogeneity could not be fully investigated due to the limited number of studies and the small sample sizes. Therefore, further validation on existing results is required. Four trials including 2952 participants reported its therapeutic effects on SBP and DBP, while RYR preparations did not reduce SBP or DBP levels compared with control group **(Figures 5B,C–)**. There was high heterogeneity among the studies of SBP and DBP and subgroup analysis was performed. RYR preparations significantly reduced SBP level (−8.59 mmHg, 95% CI [−12.28, −4.91], $p < 0.00001$, $I^2 = 62\%$) and DBP level (−7.02 mmHg, 95% CI [−8.82, −5.22], $p < 0.00001$, $I^2 = 0\%$) in 60 to 70-year-old patients with more notable effects and low to medium heterogeneity, while other subgroups had high heterogeneity. RYR preparations significantly reduced SBP level (−6.72 mmHg, 95% CI [−11.31, −2.14], $p = 0.004$, $I^2 = 74\%$) and DBP level (−6.36 mmHg, 95% CI [−8.93, −3.79], $p < 0.00001$, $I^2 = 39\%$) in the intervention duration of ≤3 months with more notable effects and low to medium heterogeneity, while other subgroups had high heterogeneity. Furthermore, compared with lipid–lowing drugs, RYR preparations significantly reduced SBP level (−8.59 mmHg, 95% CI [−12.28, −4.91], $p < 0.00001$, $I^2 = 62\%$) and DBP level (−7.02 mmHg, 95% CI [−8.82, −5.22], $p < 0.00001$, $I^2 = 0\%$) with more notable effects and low to medium heterogeneity, while other subgroups had high heterogeneity **(Supplementary Figures S7–S8)**.

Effects of RYR Preparations on Adverse Reactions

Twelve trials including 4164 participants reported adverse reactions, including gastrointestinal disorders (nausea, abdominal pain, diarrhoea, flatulence, etc.), mental−neurological symptoms (depression, etc.), oedema, myalgia, dizziness, and allergic reactions. RYR preparations

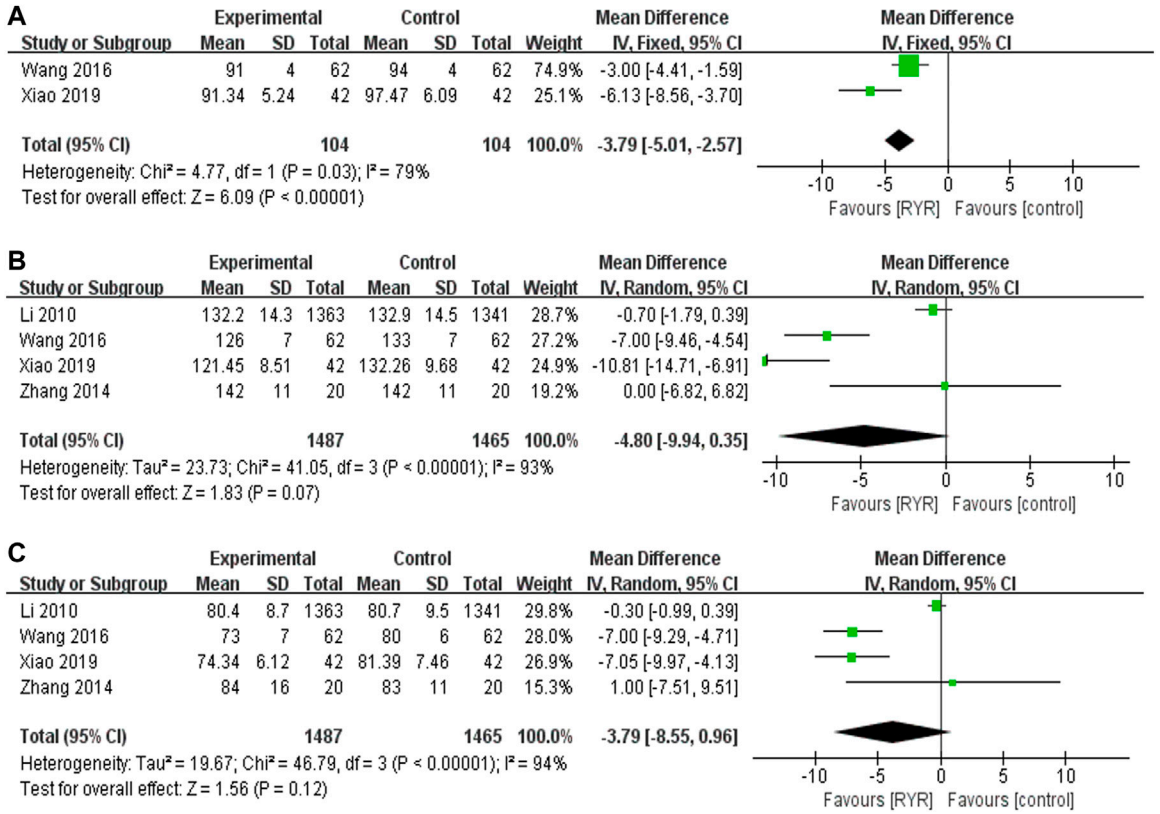

FIGURE 5 | Forest plots of **(A)** MAP, **(B)** SBP, and **(C)** DBP.

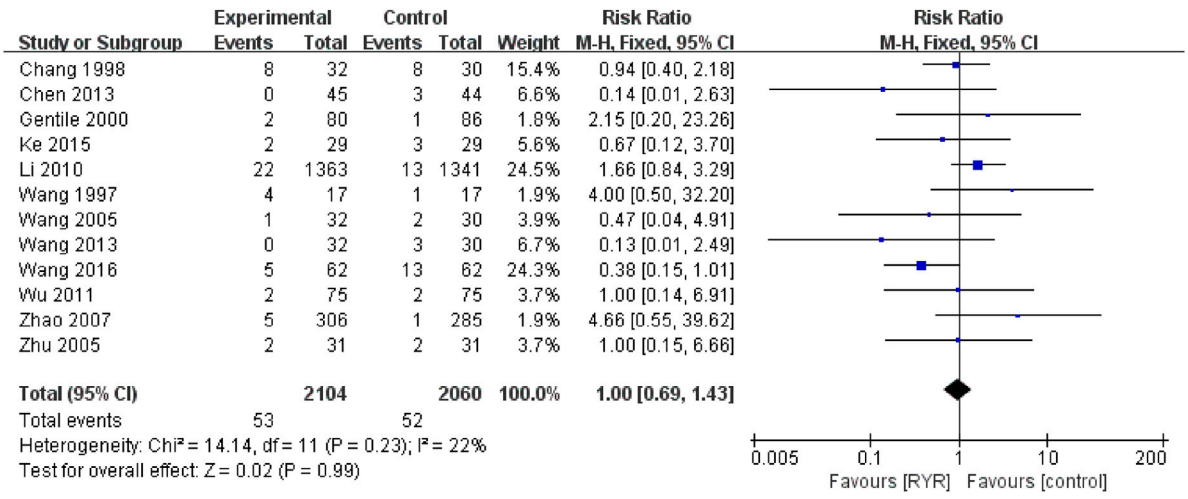

FIGURE 6 | Forest plot of the adverse reactions.

did not increase the incidence of adverse reactions compared with control group (1.00, 95% CI [0.69, 1.43]) and there was low heterogeneity (I^2 = 22%) among the studies (**Figure 6**).

Sensitivity Analysis

Sensitivity analysis demonstrated the pooled effect estimates of mortality, MACEs, FPG, HbA1c, TC, TG, LDL-C, HDL-C, MAP,

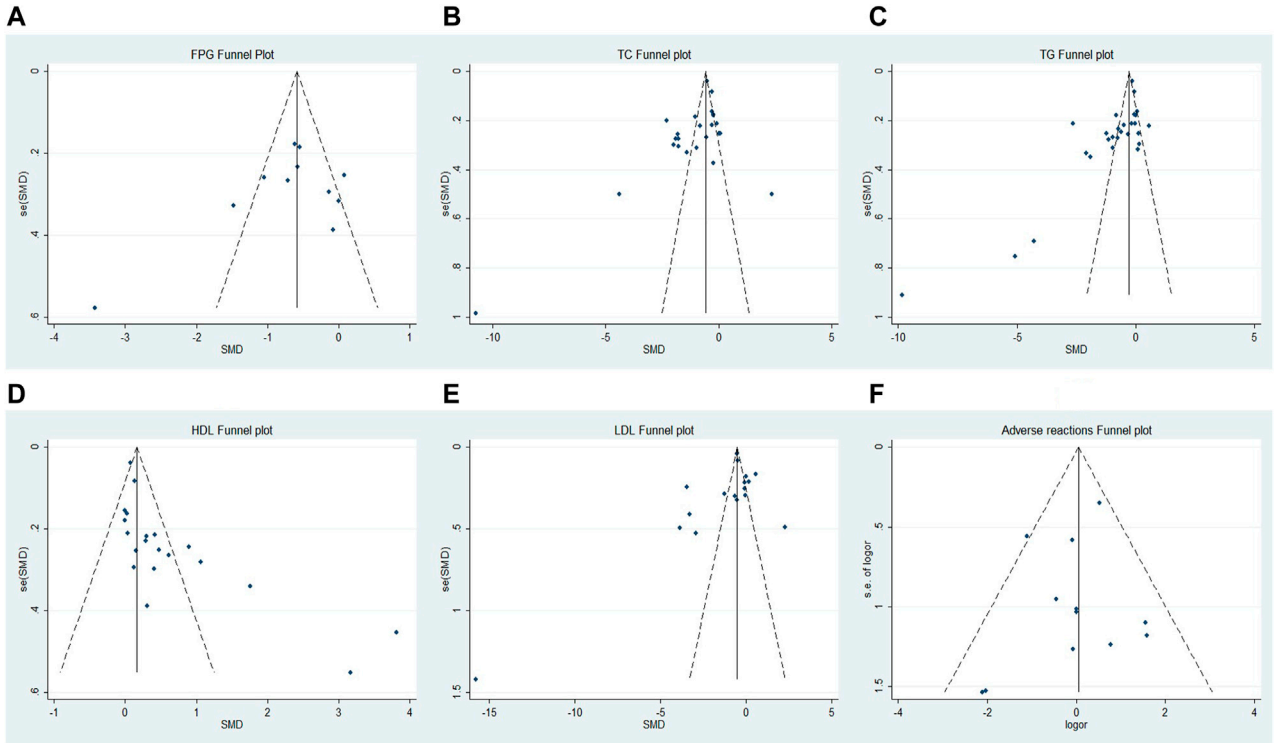

FIGURE 7 | Funnel plots of **(A)** FPG, **(B)** TC, **(C)** TG, **(D)** HDL–C, **(E)** LDL–C, and **(F)** adverse reactions.

and adverse reactions did not substantially modify, and these results are robust. However, the pooled effect estimates showed no significant differences for HOMA–IR after excluding the study by Zhang and Wu, 2014, which indicated that this result was not robust. The reason might be related to low methodological quality of Zhang and Wu, 2014 (PEDro score = 4) with no concealed allocation and blinding, and the high risk of selection bias might exaggerate the effect of RYR preparations in lowering HOMA–IR. Furthermore, the pooled effect estimates showed significant differences in SBP and DBP after excluding the study by Li et al., 2010a, which also indicated that this result was not robust. The reason might be related to long duration of treatment in Li et al., 2010b (4.5 years), and the effects of RYR preparations on SBP and DBP might not be significant in the long follow–up time.

Publication Bias

Both visual inspection of the funnel plot and Egger's test demonstrated no evidence of publication bias in FPG (p = 0.265), LDL-C (p = 0.241) and adverse reactions (p = 0.573). However, there was publication bias for TC (p = 0.040), TG (p = 0.001) and HDL–C (p = 0.002) (**Figure 7** and **Supplementary Table S4**).

Quality of the Evidence

All of the outcomes of interest were assessed with GRADE and evidence profiles are shown in **Table 2**. There was high-quality evidence on mortality, MACEs and adverse reactions; medium–quality evidence on FPG, HbA1c, HOMA-IR, TC, LDL-C, MAP and DBP; low-quality evidence on TG, HDL-C and SBP; and very low–quality evidence on ISI. The certainty of the evidence ranged from very low to high, which might be attributed to the risk of bias, reporting bias, inconsistency, and imprecision, indicating that these estimates are uncertain and that future studies are likely to influence our confidence in the results.

DISCUSSION

Summary of Main Results

This systematic review and meta-analysis showed robust and consistent findings that RYR preparations reduce mortality, MACEs, and risk factors of MetS. Therefore, RYR preparations might be an effective treatment to improve health outcomes and might assist in decreasing the MetS risk factors and preventing progression to CVD. Taken together, the results of these studies support the beneficial effects of RYR preparations across different clinical settings.

Clinical Benefits and Mechanism of Improving MetS Biochemical Parameter

Blood glucose parameters are related to diabetes. A recent nationwide epidemiological data demonstrated that elevated FPG increase the risk of CVD (Kaneko et al., 2021); each 1%

TABLE 2 | GRADE quality assessment.

		Bias	Inconsistency	Indirectness	Imprecision	Publication bias	Rating
Mortality, 2 RCTs (*n* = 3297)	RR 0.62, 95%CI 0.49 to 0.78, I^2 0%	0	0	0	0	0[d]	4: high
MACEs, 3 RCTs (*n* = 3360)	RR 0.54, 95%CI 0.43 to 0.66, I^2 0%	0	0	0	0	0[d]	4: high
FPG, 10 RCTs (*n* = 646)	MD −0.46, 95% CI −0.71to −0.22, I^2 86%	0	−1[b]	0	0	0	3: medium
HbAc1, 5 RCTs (*n* = 392)	MD −0.49, 95%CI −0.71 to −0.26, I^2 95%	0	−1[b]	0	0	0[d]	3: medium
HOMA–IR, 2 RCTs (*n* = 102)	MD −0.93, 95%CI −1.64 to −0.21, I^2 95%	0	−1[b]	0	0	0[d]	3: medium
ISI, 2 RCTs (*n* = 114)	MD 2.02, 95%CI −1.09 to 5.12, I^2 61%	−1[a]	−1[b]	0	−1[c]	0[d]	1: very low
TC, 23 RCTs (*n* = 5114)	MD −0.74, 95%CI −1.02 to −0.46, I^2 99%	0	0	0	0	−1[e]	3: medium
TG, 26 RCTs (*n* = 5264)	MD −0.45, 95%CI −0.70 to −0.21, I^2 98%	0	−1[b]	0	0	−1[e]	2: low
LDL, 16 RCTs (*n* = 4421)	MD −0.42, 95%CI −0.78 to −0.06, I^2 100%	0	−1[b]	0	0	0	3: medium
HDL, 19 RCTs (*n* = 4683)	MD 0.14, 95%CI 0.09 to 0.20, I^2 94%	0	−1[b]	0	0	−1[e]	2: low
MAP, 2 RCTs (*n* = 208)	MD −3.79, 95%CI −5.01 to −2.57, I^2 79%	0	−1[b]	0	0	0[d]	3: medium
SBP, 4 RCTs (*n* = 2952)	MD −4.80, 95%CI −9.94 to 0.35, I^2 93%	0	−1[b]	0	−1[c]	0[d]	2: low
DBP, 4 RCTs (*n* = 2952)	MD −3.79, 95%CI −8.55 to 0.96, I^2 94%	0	0	0	−1[c]	0[d]	3: medium
Adverse reactions, 12 RCTs (*n* = 4194)	RR 1.00, 95%CI 0.69 to 1.43, I^2 22%	0	0	0	0	0	4: high

[a]*Downgraded one place due to the majority of trials scoring <6 on the PEDro scale.*
[b]*Downgraded one place due to unexplained heterogeneity.*
[c]*Downgraded one place due to the small sample size or the combined effect size passing the invalid line.*
[d]*Funnel plots not completed due to <10 studies in the meta–analysis.*
[e]*Downgraded one place due to publication bias.*

higher HbA1c, independent of diabetes status, is associated with an 18% greater risk of myocardial infarction (de Jong et al., 2020); HOMA–IR is positive correlation with CVD risk (Lu et al., 2020). This meta–analysis observed that RYR preparations significantly reduced the levels of FPG, HbA1c and HOMA–IR, indicating its promising application in improving diabetes and CVD. Previous studies indicated that RYR could stimulate muscarinic M3 receptors in pancreatic cells and augment insulin release to lower plasma glucose (Chen and Liu, 2006); and inhibit high glucose–induced proangiogenic cells senescence and oxidative stress, thereby decreasing the vascular complications of diabetes (Liu et al., 2017), which might partly account for the improved blood glucose parameters after RYR preparations treatment.

Blood lipid profiles play a critical role in arteriosclerotic CVD. A cross–sectional study in T2 diabetes found that a lower TG was associated with a reduced CVD risk in the short term (Ren et al., 2018); Mortality and morbidity from CVD were reduced via primary and secondary prevention through lipid–lowering therapy targeting LDL–C (Collins et al., 2016, Serban et al., 2016); HDL has antidiabetic functions by increasing insulin sensitivity and β–cell function (Cochran et al., 2021). As the results of the present study, the reductions of TC, TG, LDL–C and the increase of HDL–C are likely to be clinically significant in improving glucose and lipid metabolism and then reducing CAD risk. Previous studies indicated that RYR could lower lipid by inhibiting HMG–CoA reductase (Banach et al., 2018), which might partly account for the improved blood lipid profiles after RYR preparations treatment.

High blood pressure can result in heart failure, heart attack, stroke, and kidney disease (Desai, 2020), and MAP is a predictor of all–cause and CVD mortality in the middle–aged and elderly populations (Sun et al., 2020). In the present study, RYR preparations significantly reduced MAP level of 3.79 mmHg, it also significantly reduced SBP and DBP level in 60–70 years old patients and in the intervention duration of ≤3 months. In addition, previous studies indicated that RYR could improve artery stiffness, endothelial dysfunction and inflammation by promoting and stabilizing the expression of endothelial nitric oxide synthase (eNOS) (Hu et al., 2020; Cicero et al., 2021). Therefore, the mechanism of RYR on lowering blood pressure might be due to improving endothelial dysfunction and inflammation.

Consistency and Disagreement With Other Studies

Up to now, used as assistance for CVD prevention, nutraceuticals has mainly been focusing on lipid-lowering, as referred in the documents produced by the International Lipid Expert Panel (ILEP). As lipid-lowering nutraceuticals, RYR plays an important role in the reduction of inflammation-related residual CVD risk (Ruscica et al., 2021). Recent studies suggested that RYR could be

used in patients at cardiovascular risk who had not reached the LDL-C target, but not eligible for statins or unable to tolerate statins (Banach et al., 2019). RYR has been validated to decrease blood sugar, lower cholesterol, control high blood pressure, and inhibit inflammation (Patel, 2016). Therefore, these findings indicated that RYR could treat MetS and improve the prognosis of CVD, which is consistent with our findings. Recent reports identified a low prevalence of suspected adverse effects associated with RYR (Banach et al., 2021), confirmed its safety in hypercholesterolemic patients, even in patients with statin intolerance (Fogacci et al., 2019; Cicero et al., 2021), and our findings also supported the safety of RYR.

Previous study indicated that the lipid–lowering effect of RYR was not influenced by age or gender in physicians (Verhoeven et al., 2013). However, in the subgroup analysis of the present study, RYR preparations significantly reduced the levels of FPG, TC and TG in 40–50 years old patients, SBP and DBP in 60–70 years old patients, and TG in women with more notable effects and low to medium heterogeneity, which suggested that RYR preparations might have better therapeutic advantages in these populations. The different results on age and gender might be related to the basal metabolic rate, vascular dysfunction, and sex differences in TG metabolism: previous studies indicated that basal metabolic rate was significantly higher in middle age (40–50 years old) compared with old age (60–70 years old) (St–Onge and Gallagher, 2010); blood pressure has an increasingly positive association with vascular dysfunction and vascular stiffness as age increases (Wen et al., 2015); women have better clearance of meal–related TG and estrogen is acting directly in the liver to reduce TG level (Palmisano et al., 2018). Therefore, RYR preparations might have better effects on blood glucose and blood lipid in middle–aged people by regulating basal metabolic rate, have better effect on SBP and DBP in old–aged people by improving vascular dysfunction and artery stiffness, and have better effect on TG in women by virtue of better TG clearance. Previous clinical trials showed that MAP, SBP, or DBP were not significantly different between Xuezhikang and placebo at 6, 12, 24, and 48 months (Li et al., 2010). While the present study found that RYR preparations could reduce MAP level, it also reduced SBP and DBP levels in the intervention duration of ≤3 months, which indicated that short duration of RYR preparations intervention might be beneficial to reducing blood pressure. Previous studies indicated that nutraceuticals (berberine, RYR, policosanol) significantly reduced the levels of TC, LDL and HOMA–IR after a 12-months treatment (Marazzi et al., 2011). Nevertheless, in the subgroup analysis of the present study, RYR preparations had a small but significant improvement on TC, TG, LDL and HDL in the intervention duration of >12 months with low heterogeneity, which provided more evidence on long–term use of RYR preparations on reducing blood lipid. Previous systematic review showed that RYR plus conventional therapy lowered the levels of TC, LDL, and SBP compared with conventional therapy, and the levels of TC and LDL compared with placebo plus conventional therapy, while RYR plus statins lowered the levels of TC, TG, LDL, SBP, and DBP compared with statins (Xiong et al., 2017). However, the I^2 ranged from 47 to 98%, suggesting the medium to high heterogeneity among the included studies. In the present study, RYR preparations reduced the levels of SBP and DBP, while increased HDL level compared with lipid–lowing drugs (I^2 ranged from 0 to −95%); RYR preparations plus conventional therapy reduced the levels of FPG, HbA1c, TC, TG and LDL, while increased HDL level compared with conventional therapy (I^2 ranged from 58 to −96%); RYR preparations reduced TC and LDL levels compared with placebo (I^2 = 100%), which was partly consistent with the previous study. Additionally, the present study further indicated that RYR preparations showed positive effect on DBP with low heterogeneity (I^2 = 0%), and it also beneficially regulate FPG, HbA1c and HDL levels, which have not been reported in the systematic review of Xiong et al., 2017.

Strengths and Limitations

There have been many previous meta-analyses and reviews about RYR preparations, while these analyses mainly focused on lipid profiles and safety (Dujovne, 2017; Banach et al., 2019). The present meta-analysis mainly focused on the efficacy and safety of RYR preparations on MetS, showed the association between biochemical parameters and clinical benefits, all of which might provide the evidence base for clinical practice. Moreover, the results showed promising effects of RYR preparations on improving glucose and lipid metabolism, modifying cardiovascular risk, effectively reducing the occurrence of mortality and MACEs, which have not been evaluated in the previous meta–analysis. Furthermore, the results demonstrated that RYR preparations were well tolerated with a favourable safety profile.

There are some limitations of our study. First, most of the studies included were of low and moderate methodological quality, which might increase the risk of bias, and therefore, only low- and medium-level evidence can be established. Second, most of the included studies focused on the Chinese population, except for one study conducted in Italy, thus, it is not clear whether the effect of RYR preparations could be extended to other populations. Third, although some of the outcomes in subgroup analysis showed more notable effects and low heterogeneity, sample sizes of these studies were small, thus the efficacy needs further investigation. Finally, regarding the high heterogeneity, different patient ages and sexes, different intervention durations and intervention types were taken into account; however, although subgroup analysis and meta–regression analyses were conducted, the heterogeneities were not eliminated for HbA1c, HOMA–IR, ISI and MAP, and differences remained among the studies in terms of the limited number of studies, sample sizes, race, religious beliefs, and concern regarding the disease; thus, these results should be interpreted with caution. Therefore, more large–sample and high–quality RCTs in broader populations are needed to provide additional data support for the efficacy of RYR on MetS.

CONCLUSION

The evidence of the current review suggests that RYR preparations significantly reduce the occurrence of mortality

and MACEs in MetS and improve blood glucose, lipid profiles, and blood pressure. Taken over the long term, RYR preparations could improve clinical endpoints, prevent metabolic diseases, and reduce the risk of CAD. However, due to the low– and moderate–quality evidence of the included studies and the heterogeneity among the different studies, the results of our study should be evaluated with prudence, and more high–quality clinical studies are required to provide stronger evidence for RYR in the treatment of MetS. These findings suggest that RYR preparations should be taken into consideration for the prevention and treatment of MetS due to its favourable effects on multiple risk factors for hyperglycaemia, dyslipidaemia, and hypertension and its acceptable safety profile.

DATA AVAILABILITY STATEMENT

The original contributions presented in the study are included in the article/**Supplementary Material**, further inquiries can be directed to the corresponding authors.

AUTHOR CONTRIBUTIONS

RY and YY contributed equally to this work. RY and WC contributed to the concept and design of the systematic review. RY and YY performed the literature search, data collection, and data analysis. RY, YY, LW, QX, YW, WS, and YM performed data interpretation. RY, YY, LW contributed to the manuscript preparation. SL, WC, and KC critically revised the systematic review. All authors contributed to the article and approved the submitted version.

FUNDING

This work was partially supported by the CACMS Innovation Fund (CI 2021A00914), the Opening Project of the Key Laboratory of Integrative Chinese and Western Medicine for the Diagnosis and Treatment of Circulatory Diseases of Zhejiang Province (2C32001), the National Natural Science Foundation of China (82004193) and the Fundamental Research Funds for the Central public welfare research institutes (ZZ14–YQ–007).

SUPPLEMENTARY MATERIAL

The Supplementary Material for this article can be found online at: https://www.frontiersin.org/articles/10.3389/fphar.2022.744928/full#supplementary-material

REFERENCES

Banach, M., Bruckert, E., Descamps, O. S., Ellegård, L., Ezhov, M., Föger, B., et al. (2019). The Role of Red Yeast rice (RYR) Supplementation in Plasma Cholesterol Control: A Review and Expert Opinion. *Atheroscler. Suppl.* 39, e1–e8. doi:10.1016/j.atherosclerosissup.2019.08.023

Banach, M., Katsiki, N., Latkovskis, G., Rizzo, M., Pella, D., Penson, P. E., et al. (2021). Postmarketing Nutrivigilance Safety Profile: a Line of Dietary Food Supplements Containing Red Yeast rice for Dyslipidemia. *Arch. Med. Sci.* 17 (4), 856–863. doi:10.5114/aoms/133716

Banach, M., Patti, A. M., Giglio, R. V., Cicero, A. F. G., Atanasov, A. G., Bajraktari, G., et al. (2018). The Role of Nutraceuticals in Statin Intolerant Patients. *J. Am. Coll. Cardiol.* 72 (1), 96–118. doi:10.1016/j.jacc.2018.04.040

Cashin, A. G., and Mcauley, J. H. (2020). Clinimetrics: Physiotherapy Evidence Database (PEDro) Scale. *J. Physiother.* 66 (1), 59. doi:10.1016/j.jphys.2019.08.005

Chang, Y. H., Wang, M., Li, S. J., Yang, Q. Z., Zhang, Y. M., and Zhao, H. L. (1998). Clinical Observation of Lipid–Lowering Effect of Lovastatin on Essential Hypertension with Hyperlipidemia. *Chin. J. Intern. Med.* 37 (4), 277–280. doi:10.3760/j.issn:0578–1426.1998.04.025

Chen, C. C., and Liu, I. M. (2006). Release of Acetylcholine by Hon–Chi to Raise Insulin Secretion in Wistar Rats. *Neurosci. Lett.* 404 (1–2), 117–121. doi:10.1016/j.neulet.2006.05.024

Chen, G. J. (2013). Clinical Observation of Xuezhikang and Simvastatin in the Treatment of Type 2 Diabetes Mellitus with Hyperlipidemia. *Chin. J. Mod. Drug Appl.* 7 (19), 142–144. doi:10.3969/j.issn.1673–9523.2013.19.118

Cicero, A. F. G., Fogacci, F., and Zambon, A. (2021). Red Yeast Rice for Hypercholesterolemia: JACC Focus Seminar. *J. Am. Coll. Cardiol.* 77 (5), 620–628. doi:10.1016/j.jacc.2020.11.056

Cochran, B. J., Ong, K.–L., Manandhar, B., and Rye, K.–A. (2021). High Density Lipoproteins and Diabetes. *Cells* 10 (4), 850. doi:10.3390/cells10040850

Collins, R., Reith, C., Emberson, J., Armitage, J., Baigent, C., Blackwell, L., et al. (2016). Interpretation of the Evidence for the Efficacy and Safety of Statin Therapy. *Lancet* 388 (10059), 2532–2561. doi:10.1016/S0140–6736(16)31357–5

de Jong, M., Woodward, M., and Peters, S. A. E. (2020). Diabetes, Glycated Hemoglobin, and the Risk of Myocardial Infarction in Women and Men: A Prospective Cohort Study of the UK Biobank. *Diabetes Care* 43 (9), 2050–2059. doi:10.2337/dc19–2363

Deng, Y. X., Zhang, J., Dong, Y. G., and Duan, Q. L. (2003). Therapeutic Effect of Xuezhikang on 56 Cases of Type 2 Diabetes Mellitus. *Mod. J Integr Tradit Chin West. Med* 12 (13), 1376–1377. doi:10.3969/j.issn.1008–8849.2003.13.016

Desai, A. N. (2020). High Blood Pressure. *JAMA* 324 (12), 1254–1255. doi:10.1001/jama.2020.11289

Dujovne, C. A. (2017). Red Yeast Rice Preparations: Are They Suitable Substitutions for Statins. *Am. J. Med.* 130 (10), 1148–1150. doi:10.1016/j.amjmed.2017.05.013

Fogacci, F., Banach, M., Mikhailidis, D. P., Bruckert, E., Toth, P. P., Watts, G. F., et al. (2019). Safety of Red Yeast rice Supplementation: A Systematic Review and Meta–Analysis of Randomized Controlled Trials. *Pharmacol. Res.* 143, 1–16. doi:10.1016/j.phrs.2019.02.028

Gentile, S., Turco, S., Guarino, G., Sasso, C. F., Amodio, M., Magliano, P., et al. (2000). Comparative Efficacy Study of Atorvastatin vs Simvastatin, Pravastatin, Lovastatin and Placebo in Type 2 Diabetic Patients with Hypercholesterolaemia. *Diabetes Obes. Metab.* 2 (6), 355–362. doi:10.1046/j.1463–1326.2000.00106.x

Halbert, S. C., French, B., Gordon, R. Y., Farrar, J. T., Schmitz, K., Morris, P. B., et al. (2010). Tolerability of Red Yeast rice (2,400 Mg Twice Daily) versus Pravastatin (20 Mg Twice Daily) in Patients with Previous Statin Intolerance. *Am. J. Cardiol.* 105 (2), 198–204. doi:10.1016/j.amjcard.2009.08.672

He, L., and Zhan, J. F. (2009). The Early Intervention and Clinic Effect of Xuezhikang on Diabetic Nephropathy Patients. *J. Kunming Med. Univ.* 30 (12), 78–82. doi:10.3969/j.issn.1003–4706.2009.12.021

Higgins, J., Thomas, J., Chandler, J., Cumpston, M., Li, T., Page, M., et al. (Editors) (2019). Cochrane Handbook for Systematic Reviews of Interventions Version 6. *Cochrane part 4 section 23-3-4*. Available at: www.training.cochrane.org/handbook/archive/v6.

Hirode, G., and Wong, R. J. (2020). Trends in the Prevalence of Metabolic Syndrome in the United States, 2011–2016. *JAMA* 323 (24), 2526–2528. doi:10.1001/jama.2020.4501

Hu, J., Wang, J., Gan, Q. X., Ran, Q., Lou, G. H., Xiong, H. J., et al. (2020). Impact of Red Yeast Rice on Metabolic Diseases: A Review of Possible Mechanisms of Action. *J. Agric. Food Chem.* 68 (39), 10441–10455. doi:10.1021/acs.jafc.0c01893

Hunter, P. M., and Hegele, R. A. (2017). Functional Foods and Dietary Supplements for the Management of Dyslipidaemia. *Nat. Rev. Endocrinol.* 13 (5), 278–288. doi:10.1038/nrendo.2016.210

Jin, J., Zhang, W. W., He, Y, J., Peng, Z., and Yu, M. (2007). 60 Cases Clinical Observation of Xuezhikang on Diabetic Nephropathy with Abnormal Blood Lipid. *Zhejiang Med. J.* 29 (9), 973–974. doi:10.3969/j.issn.1006–2785.2007.09.034

Kaneko, H., Itoh, H., Kiriyama, H., Kamon, T., Fujiu, K., Morita, K., et al. (2021). Fasting Plasma Glucose and Subsequent Cardiovascular Disease Among Young Adults: Analysis of a Nationwide Epidemiological Database. *Atherosclerosis* 319, 35–41. doi:10.1016/j.atherosclerosis.2020.12.024

Ke, M. J. (2015). A Clinical Observation of the Efficacy of Xuezhikang in the Treatment of Type 2 Diabetes with Dyslipidemia. *China Med. Pharm.* 5 (21), 98–100. doi:10.34038/jpp.2019.01.003

Klingelhöfer, I., and Morlock, G. E. (2019). Lovastatin in Lactone and Hydroxy Acid Forms and Citrinin in Red Yeast rice Powders Analyzed by HPTLC–UV/FLD. *Anal. Bioanal. Chem.* 411 (25), 6655–6665. doi:10.1007/s00216–019–02039–y

Li, C. Y., Chen, Z. S., Hu, J. W., Yu, J., and Luo, Y. (2017). The Intervention Effect of Daixiefang on the Patients of Metabolic Syndrome with Dyslipidemia, Insulin Resistance. *J. Tianjin Univ. Tradit Chin. Med.* 36 (4), 258–262. doi:10.11656/j.issn.1673–9043.2017.04.06

Li, H., Zheng, Q. G., and Lv, S. G. (2005). Observation of Therapeutic Effect of Xuezhikang on Hyperlipidemia of Type 2 Diabetes Mellitus with Microalbuminuria. *Fujian Med. J.* 27 (5), 60–61. doi:10.3969/j.issn.1001–7585.2003.08.077

Li, J. J., Lu, Z. L., Kou, W. R., Chen, Z., Wu, Y. F., Yu, X. H., et al. (2009). Beneficial Impact of Xuezhikang on Cardiovascular Events and Mortality in Elderly Hypertensive Patients with Previous Myocardial Infarction from the China Coronary Secondary Prevention Study (CCSPS). *J. Clin. Pharmacol.* 49 (8), 947–956. doi:10.1177/0091270009337509

Li, J. J., Lu, Z. L., Kou, W. R., Chen, Z., Wu, Y. F., Yu, X. H., et al. (2010). Long–term Effects of Xuezhikang on Blood Pressure in Hypertensive Patients with Previous Myocardial Infarction: Data from the Chinese Coronary Secondary Prevention Study (CCSPS). *Clin. Exp. Hypertens.* 32 (8), 491–498. doi:10.3109/10641961003686427

Li, J. J., Lu, Z. L., Kou, W. R., Chen, Z., Wu, Y. F., Yu, X. H., et al. (2010a). Impact of Xuezhikang on Coronary Events in Hypertensive Patients with Previous Myocardial Infarction from the China Coronary Secondary Prevention Study (CCSPS). *Ann. Med.* 42 (3), 231–240. doi:10.3109/07853891003652534

Li, J. J., Lu, Z. L., Kou, W. R., Wu, Z. Y. F., Yu, X. H., and Zhao, Y. C. (2010b). Impact of Xuezhikang on Coronary Events in Hypertensive Patients with Previous Myocardial Infarction from the China Coronary Secondary Prevention Study (CCSPS). *Ann. Med.* 42 (3), 231–240. doi:10.3109/07853891003652534

Liu, J. T., Chen, H. Y., Chen, W. C., Man, K. M., and Chen, Y. H. (2017). Red Yeast Rice Protects Circulating Bone Marrow–Derived Proangiogenic Cells against High–Glucose–Induced Senescence and Oxidative Stress: The Role of Heme Oxygenase–1. *Oxid. Med. Cel. Longev.* 2017, 3831750. doi:10.1155/2017/3831750

Loubser, L., Weider, K. I., and Drake, S. M. (2019). Acute Liver Injury Induced by Red Yeast rice Supplement. *BMJ Case Rep.* 12 (3), e227961. doi:10.1136/bcr–2018–227961

Lu, M. C., Fang, W. C., Li, W. C., Yeh, W. C., Shieh, Y. H., and Chen, J. Y. (2020). The Association between Insulin Resistance and Cardiovascular Disease Risk: A Community–Based Cross–Sectional Study Among Taiwanese People Aged over 50 Years. *Int. J. Environ. Res. Public Health* 17 (19), 7195. doi:10.3390/ijerph17197195

Ma, X, L., and Qian, Z. (2011). Clinical Observation on the Effect of Xuezhikang and Simvastatin on Dyslipidemia in Type 2 Diabetes Mellitus. *J. Qiqihaer Univ. Med.* 32 (18), 2979–2980. doi:10.3969/j.issn.1002–1256.2011.18.045

Marazzi, G., Cacciotti, L., Pelliccia, F., Iaia, L., Volterrani, M., Caminiti, G., et al. (2011). Long–term Effects of Nutraceuticals (Berberine, Red Yeast rice, Policosanol) in Elderly Hypercholesterolemic Patients. *Adv. Ther.* 28 (12), 1105–1113. doi:10.1007/s12325–011–0082–5

Moseley, A. M., Elkins, M. R., Van der Wees, P. J., and Pinheiro, M. B. (2020). Using Research to Guide Practice: The Physiotherapy Evidence Database (PEDro). *Braz. J. Phys. Ther.* 24 (5), 384–391. doi:10.1016/j.bjpt.2019.11.002

Palmisano, B. T., Zhu, L., Eckel, R. H., and Stafford, J. M. (2018). Sex Differences in Lipid and Lipoprotein Metabolism. *Mol. Metab.* 15, 45–55. doi:10.1016/j.molmet.2018.05.008

Patel, S. (2016). Functional Food Red Yeast rice (RYR) for Metabolic Syndrome Amelioration: a Review on Pros and Cons. *World J. Microbiol. Biotechnol.* 32 (5), 87. doi:10.1007/s11274–016–2035–2

Peng, W. H., Qu, Q., and Chen, J. (2000). The Effects of Xuezhikang on Microalbuminuria in Non–dependent Diabetes Mellitus with hyperlipidemiaCNKI:SUN:FZZY. *J. Fuzhou Gen. Hosp.* 7 (4), 17–19. doi:10.1177/000456329303000504

Prasun, P. (2020). Mitochondrial Dysfunction in Metabolic Syndrome. *Biochim. Biophys. Acta Mol. Basis Dis.* 1866 (10), 165838. doi:10.1016/j.bbadis.2020.165838

Ren, Y., Ren, Q., Lu, J., Guo, X., Huo, X., Ji, L., et al. (2018). Low Triglyceride as a Marker for Increased Risk of Cardiovascular Diseases in Patients with Long–Term Type 2 Diabetes: A Cross–Sectional Survey in China. *Diabetes Metab. Res. Rev.* 34 (2), e2960. doi:10.1002/dmrr.2960

Ruscica, M., Penson, P. E., Ferri, N., Sirtori, C. R., Pirro, M., Mancini, G. B. J., et al. (2021–). Impact of Nutraceuticals on Markers of Systemic Inflammation: Potential Relevance to Cardiovascular Diseases – A Position Paper from the International Lipid Expert Panel (ILEP). *Prog. Cardiovasc. Dis.* 67, 40–52. doi:10.1016/j.pcad.2021.06.010

Shen, H. X. (2011). Clinical Observation of Xuezhikang in Treating Diabetic Patients with Dyslipidemia. *Contemp. Med.* 17 (6), 66–67. doi:10.3969/j.issn.1009–4393.2011.6.048

St–Onge, M. P., and Gallagher, D. (2010). Body Composition Changes with Aging: the Cause or the Result of Alterations in Metabolic Rate and Macronutrient Oxidation. *Nutrition* 26 (2), 152–155. doi:10.1016/j.nut.2009.07.004

Sui, L. (2003). Clinical Effect of Xuezhikang on Type 2 Diabetes Mellitus Complicated with Hyperlipidemia. *Liaoning Pharm. Clin.* 6 (2), 73–74. doi:10.3969/j.issn.1673–0070.2003.02.009

Sun, S., Lo, K., Liu, L., Huang, J., Feng, Y. Q., Zhou, Y. L., et al. (2020). Association of Mean Arterial Pressure with All–Cause and Cardiovascular Mortality in Young Adults. *Postgrad. Med. J.* 96 (1138), 455–460. doi:10.1136/postgradmedj–2019–137354

Sungthong, B., Yoothaekool, C., Promphamorn, S., and Phimarn, W. (2020). Efficacy of Red Yeast rice Extract on Myocardial Infarction Patients with Borderline Hypercholesterolemia: A Meta–Analysis of Randomized Controlled Trials. *Sci. Rep.* 10 (1), 2769. doi:10.1038/s41598–020–59796–5

Verhoeven, V., Lopez Hartmann, M., Remmen, R., Wens, J., Apers, S., and Van Royen, P. (2013). Red Yeast rice Lowers Cholesterol in Physicians – a Double Blind, Placebo Controlled Randomized Trial. *BMC Complement. Altern. Med.* 13, 178. doi:10.1186/1472–6882–13–178

Wang, G. H., Luo, Y., and Ren, H, Q. (2005). Clinical Observation of Xuezhikang in the Treatment of Type 2 Diabetes Mellitus Complicated with Hyperlipidemia. *Chin. Hosp. Pharm. J.* 25 (12), 1160–1161. doi:10.3321/j.issn:1001–5213.2005.12.030

Wang, X. J., and Wang, J. (2016). Comparative Study for Clinical Effect in Treating Elderly Lacunar Infarction Patients Complicated with Hyperlipidaemia and Prehypertension between Xuezhikang Capsule and Atorvastatin Calcium Tablets. *Pract. J. Card. Cereb. Pneu Vasc. Dis.* 24 (6), 67–71. doi:10.3969/j.issn.1008–5971.2016.06.017

Wang, Y. F., Yang, C. K., Xu, W. J., Sun, L., Liu, B., and Wang, G. G. (1997). Regulation of Xuezhikang and Jiferozil on Hyperlipidemia and Insulin Sensitivity in Senile Patients. *Chin. Med. News* 12 (19), 22–23.

Wang, Y. X., and Liu, X, W. (2013). Clinical Effect Analysis of Xuezhikang in the Treatment of Type 2 Diabetes Mellitus with Dyslipidemia. *Med. J. Chin. Peopl Health* 25 (18), 2–3. doi:10.3969/j.issn.1672–0369.2013.18.016

Wu, W. X., and Wei, R, Q. (2011). Clinical Observation of Xuezhikang and Atorvastatin on Hypertensive Patients with Dyslipidemia. *J. Youjiang Med. Univ. Natl.* 33 (6), 760–762. doi:10.3969/j.issn.1001–5817.2011.06.0091

Xiao, J. (2019). Comparison of Clinical Efficacy of Xuezhikang Capsule and Atorvastatin Calcium Tablets in the Treatment of Senile Lacunar Cerebral Infarction with Hyperlipidemia and Prehypertension. *Yao Pin Ping Jia* 16 (10), 41–43. doi:10.3969/j.issn.1672–2809.2019.10.013

Xiong, X., Wang, P., Li, X., Zhang, Y., and Li, S. (2017). The Effects of Red Yeast rice Dietary Supplement on Blood Pressure, Lipid Profile, and C–Reactive Protein in Hypertension: A Systematic Review. *Crit. Rev. Food Sci. Nutr.* 57 (9), 1831–1851. doi:10.1080/10408398.2015.1018987

Yao, Z., Yu, F. H., and Ding, X. P. (2004). Clinical Observation of Jiangzhi Decoction on Type 2 Diabetes Mellitus with Hyperlipemia. *Shanghai J. Tradit Chin. Med.* 38 (11), 11–12. doi:10.16305/j.1007–1334.2004.11.005

Zeng, X. Y., Pan, J., and Zhao, Z. G. (2001). Endothelial protection of Xuezhikang in Type 2 Diabetes Mellitus Complicated with Hyperlipemia. *J. Third Mil. Med.* 23 (6), 726–728. doi:10.3321/j.issn:1000–5404.2001.06.034

Zhai, W. J., and Li, A. Q. (2010). Effect of Xuezhikang on the Serum High – Sensitivity C – Reactive Protein and Blood Lipid in Patients with Type 2 Diabetes Mellitus and Hyperlipidemia. *Xuzhou Acta Academ Med.* 30 (2), 102–103. doi:10.3969/j.issn.1000–2065.2010.02.012

Zhang, L. L. (2009). Observation of Therapeutic Effect of Xuezhikang on Type 2 Diabetes Mellitus with Dyslipidemia. *J. China Tradit Chin. Med. Inform.* 1 (3), 10–11.

Zhang, X. L. (2019). Study on Combination of Two Drugs in Treating Diabetes Mellitus with Hyperlipidemia. *China Contin. Med. Educ.* 11 (25), 138–140. doi:10.3969/j.issn.1674–9308.2019.25.056

Zhang, Z. H., and Wu, Ping. S. (2014). Effect of Xuezhikang on Metabolic Syndrome in the Elderly. *Chin. J. Gerontol.* 34 (13), 3597–3599. doi:10.3969/j.issn.1005–9202.2014.13.040

Zhao, J. X. (2015). Clinical Observation of Xuezhikang on Type 2 Diabetes with Dyslipidemia. *Continuing Med Educ* 29 (1), 115–116. doi:10.3969/j.issn.1004–6763.2015.01.075

Zhao, S. P., Lu, Z. L., Du, B. M., Chen, Z., Wu, Y. F., Yu, X. H., et al. (2007). Xuezhikang, an Extract of Cholestin, Reduces Cardiovascular Events in Type 2 Diabetes Patients with Coronary Heart Disease: Subgroup Analysis of Patients with Type 2 Diabetes from China Coronary Secondary Prevention Study (CCSPS). *J. Cardiovasc. Pharmacol.* 49 (2), 81–84. doi:10.1097/FJC.0b013e31802d3a58

Zhu, B., Qi, F., Wu, J., Yin, G., Hua, J., Zhang, Q., et al. (2019). Red Yeast Rice: A Systematic Review of the Traditional Uses, Chemistry, Pharmacology, and Quality Control of an Important Chinese Folk Medicine. *Front. Pharmacol.* 10, 1449. doi:10.3389/fphar.2019.01449

Zhu, C. C., and Yao, Z. L. (2005). The Clinical Research of XuezhiKang in Treatment of the Geriatric Patients Who Had Hyperlipidemia and Type 2 Diabetes Mellitus. *Chin. J. Pract. Chin. Mod. Med.* 18 (15), 521–522.

Conflict of Interest: The authors declare that the research was conducted in the absence of any commercial or financial relationships that could be construed as a potential conflict of interest.

Publisher's Note: All claims expressed in this article are solely those of the authors and do not necessarily represent those of their affiliated organizations, or those of the publisher, the editors and the reviewers. Any product that may be evaluated in this article, or claim that may be made by its manufacturer, is not guaranteed or endorsed by the publisher.

frontiers in Pharmacology

ORIGINAL RESEARCH
published: 25 February 2022
doi: 10.3389/fphar.2022.729605

Pantao Pill Improves the Learning and Memory Abilities of APP/PS1 Mice by Multiple Mechanisms

Qiqi Xin[1,2†], *Weili Shi*[1,2†], *Yan Wang*[1,2†], *Rong Yuan*[1,2], *Yu Miao*[1,2], *Keji Chen*[1,2*] and *Weihong Cong*[1,2*]

[1]*Laboratory of Cardiovascular Diseases, Xiyuan Hospital of China Academy of Chinese Medical Sciences, Beijing, China,* [2]*National Clinical Research Center for Chinese Medicine Cardiology, Xiyuan Hospital, China Academy of Chinese Medical Sciences, Beijing, China*

Background: To explore the effect and mechanisms of Pantao Pill (PTP) on cognitive impairment.

Methods: Network pharmacology was performed to analyze the mechanism of PTP treating cognitive impairment. The targets of PTP and cognitive impairment were predicted and used to construct protein-protein interaction (PPI) networks. The intersection network was selected, and the core network was obtained through topological analysis. Enrichment analysis was conducted to obtain the GOBP terms and KEGG pathways. We then performed experiments to validate the results of the network pharmacology by using an APP/PS1 transgenic mouse model. The APP/PS1 mice were divided into four groups: the model group, the high-dose PTP (3.6 g/kg·d) group, the low-dose PTP (1.8 g/kg·d) group, and the positive control group (donepezil hydrochloride, 2 mg/kg·d). Wild-type (WT) C57 mice served as a normal control group. PTP and donepezil were administered by gavage for 8 weeks.

Results: Network pharmacology showed that PTP might improve cognitive impairment by regulating autophagy, apoptosis, and oxidative stress. For the Morris water maze test, a significant difference was shown in the total swimming distance among groups ($p < 0.05$) in the positioning navigation experiment, and with training time extension, the swimming speed increased ($p < 0.01$). In the space probe test, PTP administration significantly reduced the swimming path length and the escape latency of APP/PS1 mice ($p < 0.05$ or $p < 0.01$), whereas it had no effect on the swimming speed ($p > 0.05$). PTP (3.6 g/kg/d) rescued the reduction of norepinephrine and acetylcholine levels ($p < 0.05$), and increased the acetylcholinesterase concentration ($p < 0.05$) in the brain tissue. PTP (1.8 g/kg/d) increased the norepinephrine level ($p < 0.01$). PTP rescued the activity reduction of superoxide dismutase in the brain tissue ($p < 0.01$) and the neuron cell pyknosis in the hippocampal CA region ($p < 0.05$). PTP reduced ATG12 and PS1 expression ($p < 0.05$ or $p < 0.01$), and increased Bcl-2 expression in the brain tissue ($p < 0.05$).

Conclusion: PTP can significantly improve the learning and memory abilities of APP/PS1 mice, and the mechanism may be related to the increase of neurotransmitter acetylcholine and norepinephrine levels, the reduction of the excessive autophagic activation, and the suppression of oxidative stress and excessive apoptotic activity.

Keywords: cognitive impairment, oxidative stress, autophagy, apoptosis, neurotransmitter, pantao pill

OPEN ACCESS

Edited by:
Xy Zhang,
University of Minho, Portugal

Reviewed by:
Yao-Hsiang Shih,
Kaohsiung Medical University Hospital, Taiwan
Haidong Xu,
Soochow University Medical College, China
Chandramani Pathak,
Lan Zhang,
Capital Medical University, China

***Correspondence:**
Weihong Cong
congcao@188.com
Keji Chen
kjchenvip@163.com

[†]*These authors have contributed equally to this work and share first authorship*

Specialty section:
This article was submitted to Ethnopharmacology, a section of the journal Frontiers in Pharmacology

Received: *23 June 2021*
Accepted: *20 January 2022*
Published: *25 February 2022*

Citation:
Xin Q, Shi W, Wang Y, Yuan R, Miao Y, Chen K and Cong W (2022) Pantao Pill Improves the Learning and Memory Abilities of APP/PS1 Mice by Multiple Mechanisms. Front. Pharmacol. 13:729605. doi: 10.3389/fphar.2022.729605

INTRODUCTION

Cognitive impairment is one of the characteristics of human aging and often manifests as declines in attention, reasoning ability, learning ability, short-term and long-term memory, executive ability, and the perception of the surrounding environment (Kennedy et al., 2017). In China, the incidence of mild cognitive impairment alone is estimated to be as high as 15% among people over 60 years of age (Xue et al., 2018). Alzheimer's disease (AD) is the most common cause of cognitive dysfunction, which has been reported to cause 50–75% of dementia cases. The number of AD patients in China is approaching 10 million. According to the Alzheimer's Association Report 2021, more than 12 million people in the United States will suffer from Alzheimer's and other dementias by 2050 (Alzheimer's and association, 2021). The main pathological manifestations of AD are the formation of senile plaques caused by the deposition of amyloid β protein (Aβ) and the neurofibrillary tangling caused by the hyperphosphorylation of tau protein. The CA region of the hippocampus is a commonly affected area (Morrone et al., 2020). The occurrence of AD is related to a variety of pathological mechanisms. Mutations in the amyloid precursor protein (APP) and presenilin1 (PS1) genes can increase the production and accumulation of Aβ. The decrease in cellular autophagy leads to the accumulation of misfolded proteins and autophagosomes and further accelerate neurodegeneration (Nobili et al., 2021). Excessive Aβ deposition inhibits the activity of antioxidant enzymes, continuously enhances intracellular oxidative stress, and ultimately induces neuronal apoptosis (Chen et al., 2020).

Pantao Pill (PTP), is composed of traditional Chinese medicines including *Panax ginseng* C. A. Mey. [Araliaceae; Ginseng Radix et Rhizoma], *Asparagus cochinchinensis* (Lour.) Merr. [Liliaceae; Asparagi Radix], *Ophiopogon japonicus* (L. f). Ker-Gawl. [Liliaceae; Ophiopogonis Radix], *Lycium barbarum* L. [Solanaceae; Lycii Fructus], *Rehmannia glutinosa* Libosch. [Scrophulariaceae; Rehmanniae Radix], *Angelica sinensis* (Oliv.) Diels [Umbelliferae; Angelicae Sinensis Radix], *Alpinia oxyphylla* Miq. [Zingiberaceae; Alpiniae Oxyphyllae Fructus], *Ziziphus jujuba* Mill. var. *spinosa* (Bunge) Hu ex H.F. Chou [Rhamnaceae; Ziziphi Spinosae Semen], *Bombyx mori* Linnaeus [Bombycidae; Bombyx Mori Faeces], and *Juglans regia* L. [Juglandaceae; Juglandis Fructus Diaphragma]. PTP is an anti-aging prescription used by Chinese Emperor Qianlong of the Qing Dynasty and was previously awarded to officials who performed great feats, which now has been developed as Qinggong shoutao Pill. It can be used to treat dizziness, fatigue, memory decline, tinnitus, deafness, nocturia, and other diseases caused by aging. Clinical studies have shown that PTP induces significant improvements in amnestic mild cognitive impairment and can prevent 8.85% of amnestic mild CI patients from progressing to AD (Tian et al., 2019). PTP can significantly alleviate fatigue, dizziness, tinnitus, deafness, nocturia, and other clinical symptoms, reduce plasma lipid peroxide level, increase plasma estradiol and testosterone concentrations, and significantly improve transient and long-term memory in patients (≥45 years old) with manifestations of aging (Chen et al., 1984; Chen et al., 1985). PTP also inhibited the formation of lipid peroxide in rat liver homogenate *in vitro* and significantly increased the survival rate of quails (Chen et al., 1984; Chen et al., 1985). However, the mechanism by which PTP improves cognitive impairment in elderly patients is not fully understood. To further clarify the role and mechanism of PTP in improving cognitive impairment, this study used network pharmacology to predict its mechanism of action and further used an APP/PS1 double transgenic mouse model to explore the effect and mechanism of PTP on learning and memory abilities.

MATERIALS AND METHODS

Network Pharmacology

The ingredients of PTP were retrieved from the Traditional Chinese Medicine Systems Pharmacology Database and Analysis Platform (TCMSP, https://tcmspw.com/tcmsp.php) and Traditional Chinese Medicines Integrated Database (TCMID, http://119.3.41.228:8000/tcmid/search/) databases (Xue et al., 2013; Ru et al., 2014). The absorption, distribution, metabolism, and excretion (ADME) system of the TCMSP database was used to select the active ingredients. The oral bioavailability ≥30%, drug-likeness ≥ 0.18, and blood brain barrier ≥ −0.3 were chosen as the boundaries, and the targets of the active ingredients were further predicted by the TCMSP and the Encyclopedia of Traditional Chinese Medicine (ETCM, http://www.tcmip.cn/ETCM/) databases (Xu et al., 2018). For components not included in the TCMSP database, the Bioinformatics Analysis Tool for Molecular mechanism of TCM (BATMAN-TCM) database was used to predict their active targets (Liu et al., 2016).

Effective targets of cognitive impairment were retrieved from the Online Mendelian Inheritance in Man (OMIM, https://www.omim.org/), the Pharmacogenomics knowledgebase (PharmGKB, https://www.pharmgkb.org/), the Genetic Association Database (GAD, https://geneticassociationdb.nih.gov/), and the Therapeutic Target Database (TTD, https://db.idrblab.org/ttd/) databases. Cytoscape 3.8 software was used to construct the PTP-drug-ingredient-target network and cognitive impairment-targets network. By using the Bisogenet plugin, the protein-protein interaction (PPI) network of PTP and related targets associated with cognitive impairment were further constructed, and the intersection of the two PPI networks was obtained. The intersection network was topologically analyzed with the CytoNCA plugin (Tang et al., 2015), and a new network was constructed by screening targets with a more than 2-fold increase in the median degree. Topological analysis was performed on the new network. The core network was built based on six topological features, including "degree centrality (DC)", "betweenness centrality (BC)", "closeness centrality (CC)", "eigenvector centrality (EC)", "network centrality (NC)", and "local average connectivity-based method (LAC)". All six algorithms are calculated for centralities and used to identify candidate targets. BC was calculated based on the total number of shortest paths from a target node to another node and the number of those paths that pass through a third

node. CC determined a protein's essentiality based on the number of the target node's neighbors and the distance of the shortest path from the target node to another node. DC value was calculated based on the number of the target node's neighbors and the weight of the edge connecting the node and another node. EC was calculated based on the eigenvector corresponding to the largest eigenvalue of the adjacency matrix. LAC determined a protein's essentiality by evaluating the relationship between a protein and its neighbors, which was calculated based on the node-set containing all the neighbors of a target node. NC considered both the centrality of a node and the relationship between it and its neighbors, and a node's essentiality was determined by the sum of the edge clustering coefficients of interactions connecting it and its neighbors.

The targets of the core network were enriched and analyzed by the Database for Annotation, Visualization and Integrated Discovery (DAVID, https://david.ncifcrf.gov/home.jsp) database to obtain Gene Ontology Biological Process (GOBP) and Kyoto Encyclopedia of Genes and Genomes (KEGG) information. In GO and KEGG prediction, the rich factor refers to the ratio of the number of target genes in the pathway to the number of all genes annotated. The larger the rich factor is, the greater the degree of enrichment. The *p*-value represents the significance of the focus gene enrichment. The GO and KEGG terms were considered for inclusion in outcomes as long as the corresponding *p* value was less than 0.05 and correlated to cognitive impairment pathology. The enrichment analysis results were visualized by the OmicShare platform (https://www.omicshare.com/tools/Home/Soft/getsoft) (Huang da et al., 2009).

Drugs and Reagents

PTP refined powder (batch number P004) was provided by Darentang Pharmaceutical Factory (Tianjin, China). The preparation process of PTP refined powder is as below: the raw materials of the TCMs are mixed, dried, and crushed into fine powders; then, the fine powders are sieved and sterilized to be refined powder. The UPLC-LTQ-Orbitrap fingerprint results of PTP are shown in the Supplementary material (**Supplementary Material S1**). Donepezil hydrochloride (Arricent, national drug approval number H20050978) was purchased from Eisai Pharmaceutical Co., Ltd. (Shanghai, China). Malondialdehyde (MDA), superoxide dismutase (SOD), norepinephrine (NE), 5-hydroxytryptamine (5-HT), acetylcholine (Ach), and acetylcholinesterase (AchE) detection kits were purchased from Nanjing Jiancheng Institute of Biological Engineering (Nanjing, China). B-cell lymphoma 2 (Bcl-2) antibodies were purchased from Abcam (Shanghai) Trading Co., Ltd. (Shanghai, China). Antibodies against PS1, autophagy-related protein-12 (ATG12), beclin-1, glyceraldehyde-3-phosphate dehydrogenase (GAPDH) were purchased from CST (Shanghai) Biological Reagents Co., Ltd. (Shanghai, China). Horseradish peroxidase-labeled goat anti-mouse and goat anti-rabbit antibodies were purchased from Shanghai Beyotime Biotechnology Co., Ltd. (Shanghai, China).

Instruments

The Morris water maze video tracking analysis system 2.0 was purchased from Chengdu Taimeng Technology Co., Ltd. (Chengdu, China). The automatic microplate reader was purchased from BioTek Instruments, Inc. (Vermont, United States). The BH-2 optical microscope was obtained from Olympus Corporation (Tokyo, Japan). The HPIAS-1000 pathology image analyzer was obtained from Zhongke Company (Beijing, China).

Animals and Groups

Mice were purchased from the Institute of Experimental Animals of the Chinese Academy of Medical Sciences. Mice were assigned to five groups, including the normal control group, the model group, the low-dose PTP group, the high-dose PTP group, and the positive control group. Nine-month-old APP/PS1 transgenic mice were used in the model group, and C57BL/6 wild-type (WT) mice were used in the control group. The low-dose PTP (1.8 g/kg/d), high-dose PTP (3.6 g/kg/d) and donepezil (2 mg/kg/d) groups were administered the indicated treatments by intragastric gavage for 8 weeks. The 1.8 g/kg/d, and 3.6 g/kg/d dose of PTP are equivalent to the amount of drug administered using the approved PTP 14 g/kg/d, and 28 g/kg/d dose in a 70-kg patient, respectively. The normal control group and the model group were administered an equal amount of normal saline.

Morris Water Maze

The Morris water maze test was designed to evaluate the spatial learning and memory abilities of mice according to previous studies and included a 4-day positioning navigation experiment and a 1-day space probe test (Vorhees and Williams, 2006). The Morris water maze test was conducted in a round white pool 120 cm in diameter and 40 cm deep. During the training and the formal experiment, the references outside the maze remained unchanged. In the first 4 days of the navigation experiments, a platform with a diameter of 10 cm was placed in the target quadrant and hidden 1 cm underwater. The mice were placed in the water facing the wall of the pool. The time mice spent on finding the platform was recorded as the escape latency. If the platform was not found within 120 s, the mice were led to the platform and made to stand on the platform for 30 s to generate memory. On day 5, the space probe test was performed. Mice were placed in water, the automatic video recording system recorded the time (swimming duration) and swimming path length each mouse took to find the platform, and the spatial memory abilities of the mice were evaluated.

Measurement of Cholinergic and Monoaminergic Neurotransmitters and Related Enzymes in Brain Tissue

The brains were quickly removed on an ice platform after the mice were sacrificed. The hippocampus and cerebral cortex tissues were quickly frozen with liquid nitrogen and stored at −80°C. The concentrations of Ach, AchE, NE, and 5-HT were determined according to the instructions of the kits.

The Ach content was determined by a colorimetric method. The brain tissue was homogenized with the extraction reagent at a

ratio of 1:9 and centrifuged at 2500 rpm for 10 min, and the supernatant was retained. The substrate solution was added to the supernatant and mixed. After being incubated at room temperature for 15 min, the terminating solution was added to stop the reaction, and the chromogenic solution was added and mixed. After being incubated for 10 min, the absorbance value of each tube was measured at a wavelength of 550 nm.

The activity of AchE was determined by an optical method. The brain tissue was homogenized with normal saline at a ratio of 1:9 and centrifuged at 2500 rpm for 10 min, and the supernatant was retained. The substrate buffer solution and color application solution were added successively, mixed, and reacted at 37°C for 6 min. The inhibitor and transparent agent were added, mixed, and incubated for 15 min, and the absorbance value of each tube was measured at a wavelength of 412 nm.

The concentrations of NE and 5-HT were measured by enzyme-linked immunoassay. Brain tissue samples were added to enzyme-labeled wells that were precoated with NE or 5-HT monoclonal antibodies. After incubation, biotin-labeled NE or 5-HT antibodies was added, bound with streptomycin-HRP to form an immune complex. After incubation and washing, the unbound enzyme was removed, and the substrate was added to produce a blue color, which was converted to yellow under the action of an acid. The intensity of the color positively correlated with the concentration of NE or 5-HT in the sample.

Measurement of the Oxidative Stress Index in Brain Tissue

A 10% brain homogenate was prepared to measure the MDA level and total SOD activity. The MDA level was detected by the thiobarbituric acid method. Tissue homogenate supernatant was transferred to the measuring tube, and equal amounts of standard material, anhydrous ethanol and tissue supernatant were added to the standard tube, blank tube and control tube, respectively. Appropriate amounts of detection reagent were added to all tubes successively and mixed well. The tubes were heated in a water bath at 95°C for 40 min, then cooled to room temperature, and centrifuged at 3000 rpm for 10 min. The absorbance of the supernatant was measured at 532 nm to calculate the concentration of MDA. The activity of SOD was determined by the hydroxylamine method. The supernatant of the tissue homogenate and distilled water were added to the measuring tube and the control tube, respectively, and the detection reagents were added successively. After the solution was mixed following incubated in a water bath at 37°C for 40 min, the absorbance was measured at a wavelength of 550 nm, and the total SOD activity was calculated.

HE Staining

Brain tissues were fixed in 10% formaldehyde, dehydrated, paraffin-embedded, and sliced continuously at a thickness of 5 μm. After gradient dewaxing with xylene and ethanol, the paraffin sections were stained with hematoxylin for 5 min, washed with distilled water, differentiated with hydrochloric acid and ethanol for 30 s, soaked in a warm water bath for 5 min, and redyed with eosin for 5 min. After conventional dehydration, the slices were sealed with transparent neutral resin. The sections were randomly selected, observed, and photographed.

Western Blotting

After the mice were sacrificed, the cerebral cortex was quickly removed on an ice platform. Precooled RIPA protein extraction reagent and a protease inhibitor were added to extract the proteins. The slurry was homogenized with an electric homogenizer and incubated on ice for 20 min, followed by ultrasonic oscillation and centrifugation. After measuring the protein concentration by the BCA method, RIPA buffer was used to adjust all samples to the lowest sample concentration, and the samples were denatured in a 95°C water bath for 5 min. An SDS-PAGE gel was prepared. After gelation was complete, sample loading, electrophoresis, and membrane transfer processes were performed. The membrane was blocked with 5% bovine serum protein and incubated with primary and secondary antibodies. An ECL luminescence kit was used for staining, photos were taken, and gray values were calculated.

Statistical Analysis

The results are expressed as the mean ± SD. The variance among multiple groups was assessed by a one- or two-way analysis of variance with/without repeated measures followed by a post hoc test. SPSS 17.0 statistical software was used for data analysis. $p < 0.05$ was considered statistically significant.

RESULTS

Network Pharmacological Analysis of the Mechanism by Which PTP Improves Cognitive Impairment

Sixty possible active components of PTP were identified (**Table 1**), and a total of 151 targets were obtained through prediction analysis (**Figure 1**). A total of 956 possible targets associated with cognitive impairment were retrieved (**Supplementary Figure S2**, **Supplementary Material S3**). The PTP target PPI network and the cognitive impairment target PPI network were constructed with the Bisogenet plugin (**Supplementary Figure S3A**, **Supplementary Material S4**). Then, the intersection of the PTP and cognitive impairment PPI networks was obtained (**Supplementary Figure S3B**, **Supplementary Material S5**). Topology analysis of the intersection PPI network was carried out, and a new network was constructed after screening with a DC > 48 as the threshold. Topology analysis of the new network was performed to obtain the core PPI network. Bounded by BC > 0.00021355, CC > 0.48908, DC > 124, EC > 0.013344, LAC >13.08955, NC > 14.446487, the core PPI network was built, which contained a total of 275 targets (**Supplementary Figure S3C**, **Supplementary Material S5**).

In GO and KEGG prediction, both *p*-value and the rich-factor are essential indicators for possible mechanisms which could reflect the significance and degree of the target genes enriched in specific GO or KEGG terms. The GOBP enrichment analysis of the core PPI network targets

TABLE 1 | PTP active ingredient prediction.

Drug	Ingredient	Drug	Ingredient
Alpiniae Oxyphyllae Fructus	sitosterol	Lycii Fructus	4,24-methyllophenol
	Stigmasterol		Lophenol
	Daucosterol		4alpha,14alpha,24-trimethylcholesta-8,24-dienol
Angelicae Sinensis Radix	beta-sitosterol		4alpha,24-dimethylcholesta-7,24-dienol
	Stigmasterol		4alpha-methyl-24-ethylcholesta-7,24-dienol
Asparagi Radix	beta-sitosterol		6-Fluoroindole-7-Dehydrocholesterol
	sitosterol		(E,E)-1-ethyl octadeca-3,13-dienoate
	Stigmasterol		lanost-8-en-3beta-ol
	diosgenin		lanost-8-enol
	7-Methoxy-2-methyl isoflavone		Obtusifoliol
Bombyx Mori Faeces	CLR	Ginseng Radix et	beta-sitosterol
	beta-carotene	Rhizoma	Stigmasterol
Juglandis Fructus	oleanolic acid		Fumarine
Diaphragma	dibutyl phthalate		Diop
	oleic acid		Inermin
Lycii Fructus	beta-sitosterol		Aposiopolamine
	Stigmasterol		Deoxyharringtonine
	CLR		arachidonate
	Sitosterol alpha1		Frutinone A
	Mandenol		Ginsenoside-Rh4_qt
	Ethyl linolenate		Girinimbin
	LAN		Panaxadiol
	Cycloartenol		suchilactone
	atropine		alexandrin_qt
	campesterol	Ophiopogonis	Stigmasterol
	cyanin	Radix	Ophiopogonanone A
	24-methylidenelophenol		Orchinol
	daucosterol_qt		Ophiopogonone B
	glycitein	Rehmanniae Radix	sitosterol
	14b-pregnane		Stigmasterol
	24-ethylcholest-22-enol	Ziziphi Spinosae	Mairin
	24-ethylcholesta-5,22-dienol	Semen	(S)-Coclaurine
	24-methyl-31-norlanost-9 (11)-enol		Daucosterol
	24-methylenelanost-8-enol		phytosterol
	Fucosterol		sanjoinenine
	31-norlanost-9 (11)-enol		zizyphusine
	31-norlanosterol		

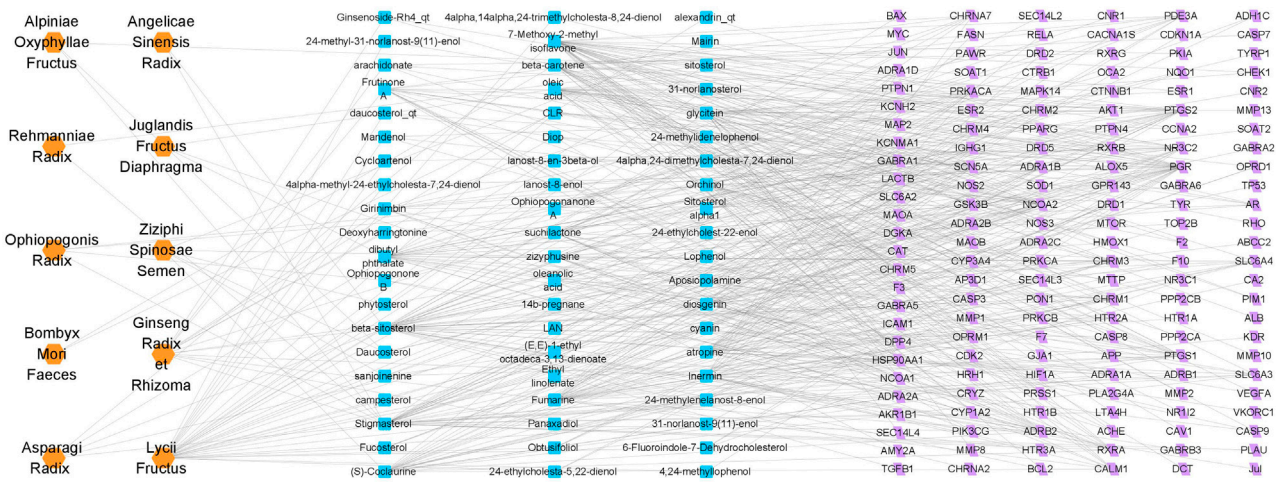

FIGURE 1 | Drug-ingredient-target network of PTP. The orange nodes represent drugs, the blue nodes represent active ingredients, and the purple nodes represent possible targets of the active ingredients.

indicated that PTP might play a role in improving cognitive impairment by acting on biological processes such as oxidative stress, apoptotic process, autophagy, aging, and neuron death (**Figure 2A**). The KEGG enrichment analysis showed that PTP might exert its cognitive improvement effects by regulating apoptosis, mTOR, PI3K-Akt, and MAPK signaling pathways (**Figure 2B**). In the present study, we verified some of the terms related to the pathology of cognitive impairment as examples with animal experiments.

Effects of PTP on the Spatial Learning and Memory Abilities of APP/PS1 Transgenic Mice

There was a significant difference in the total swimming distance among groups ($F = 3.287$, $p = 0.028$) in the positioning navigation experiment. However, no difference was shown in swimming speed ($F = 1.182$, $p = 0.344$) or escape latency ($F = 0.976$, $p = 0.439$). With training time extension, the swimming speed showed an upward trend ($F = 5.285$, $p = 0.009$). The total swimming distance ($F = 1.014$, $p = 0.409$) and escape latency ($F = 2.890$, $p = 0.064$) showed downward trend, however, these trends were not statistically significant (**Figures 3A–C**).

For the space probe test, the escape latency ($p < 0.01$) and total swimming distance ($p < 0.01$) of the APP/PS1 group were significantly longer than those of the WT group. Compared with the model group, PTP (3.6 g/kg/d) administration for 8 weeks significantly reduced the swimming path length ($p = 0.014$) and escape latency ($p = 0.006$) of APP/PS1 mice. The escape latency ($p = 0.006$) and swimming path length ($p = 0.012$) in the PTP (1.8 g/kg) group were significantly reduced (**Figure 3**). Donepezil reduced both the swimming path length ($p < 0.01$) and escape latency ($p < 0.01$) significantly (**Figures 3D,E**). All treatment groups had no effect on the swimming speed ($F = 0.279$, $p = 0.890$) (**Figure 3F**).

Effects of PTP on Neurotransmitters and Related Enzymes in the Brain

Compared with WT mice, APP/PS1 mice exhibited no significant changes in the brain 5-HT levels. PTP treatment for 8 weeks showed no effect on the 5-HT concentrations ($p > 0.05$) (**Figure 4A**). NE levels were decreased in APP/PS1 mice ($p < 0.05$), which were significantly improved by PTP and donepezil treatment ($p < 0.05$ or $p < 0.01$) (**Figure 4B**). Compared with that in the WT group, the Ach level in APP/PS1 mice was significantly decreased ($p < 0.05$), but AchE activity was not significantly changed ($p = 0.801$). After 8 weeks of treatment, the level of Ach and the activity of AchE in the brain tissue in the high-dose PTP group were significantly increased compared with those in the APP/PS1 group ($p < 0.05$). There were no significant changes in Ach levels ($p = 0.622$) or AchE activity ($p = 0.766$) in the low-dose PTP group. Donepezil significantly increased the Ach level ($p < 0.05$) but showed no effects on AchE activity (**Figures 4C,D**).

Effects of PTP on Oxidative Stress in Brain Tissue

There were no differences between the WT group and the APP/PS1 group on the MDA level. After 8 weeks of treatment, there was no significant change in the MDA level in the positive control group or PTP group compared with the APP/PS1 group ($F = 1.256$, $p = 0.307$) (**Figure 5A**).

Compared with that in WT mice, the activity of SOD in APP/PS1 mice was significantly decreased ($p < 0.01$). After 8 weeks of treatment, compared with that in APP/PS1 mice, the activity of SOD in the PTP groups was significantly increased ($p < 0.01$), while there was no change in the donepezil group ($p = 0.392$) (**Figure 5B**).

Effects of PTP on the Pathological Manifestations in the Hippocampal CA Region

Under a microscope, pyramidal cells in the hippocampal CA region of WT mice were densely arranged, with neat and plump cells. The nuclear membrane was smooth and uninterrupted, and the nucleoli were visible. In the APP/PS1 transgenic mouse group, pyramidal cells in the hippocampal CA region were loosely arranged. A small fraction of cells showed signs of neurodegeneration, such as wrinkled nuclei, hyperchromatic, and shrunken triangulated neuronal bodies. Some cells appeared structurally less intact, and a few cells were lost. Compared with those in the model group, the pyramidal cells in the donepezil and PTP groups were regularly arranged, the cytoplasmic and nuclear membranes appeared to be smooth and uninterrupted, and the nuclear pyknosis and deep staining were reduced (**Figure 6A**).

Quantitative analysis showed that the number of pyknotic cells per field was significantly higher in the APP/PS1 group than in the WT group ($p < 0.05$). PTP (1.8 g/kg and 3.6 g/kg) ($p < 0.05$) and donepezil ($p < 0.01$) treatment could rescue the cell pyknosis (**Figure 6B**).

Effects of PTP on Autophagy and Apoptosis

Compared with those in the WT group, the protein level of Bcl-2 was significantly decreased ($p = 0.002$), and the beclin-1 ($p = 0.004$), PS1 ($p = 0.011$), and ATG12 ($p = 0.028$) protein levels were significantly increased in the APP/PS1 transgenic mice. After 8 weeks of PTP (3.6 g/kg) treatment, the expression of Bcl-2 ($p = 0.018$) increased, and the expression of ATG12 ($p = 0.027$) and PS1 ($p = 0.005$) decreased significantly. PTP (1.8 g/kg) increased Bcl-2 ($p = 0.049$) expression, reduced PS1 ($p = 0.011$) expression, and whereas has no significant effect on ATG12 ($p = 0.178$) expression. Donepezil treatment increased the level of Bcl-2 ($p = 0.027$), reduced the expression of ATG12 ($p = 0.002$), whereas showed no significant effect on PS1 ($p = 0.139$) expression. The protein expression of beclin-1 decreased slightly in the PTP groups (PTP 3.6 g/kg, $p = 0.111$; PTP 1.8 g/kg, $p = 0.202$) and donepezil group ($p = 0.209$), but this reduction was not statistically significant (**Figure 7**).

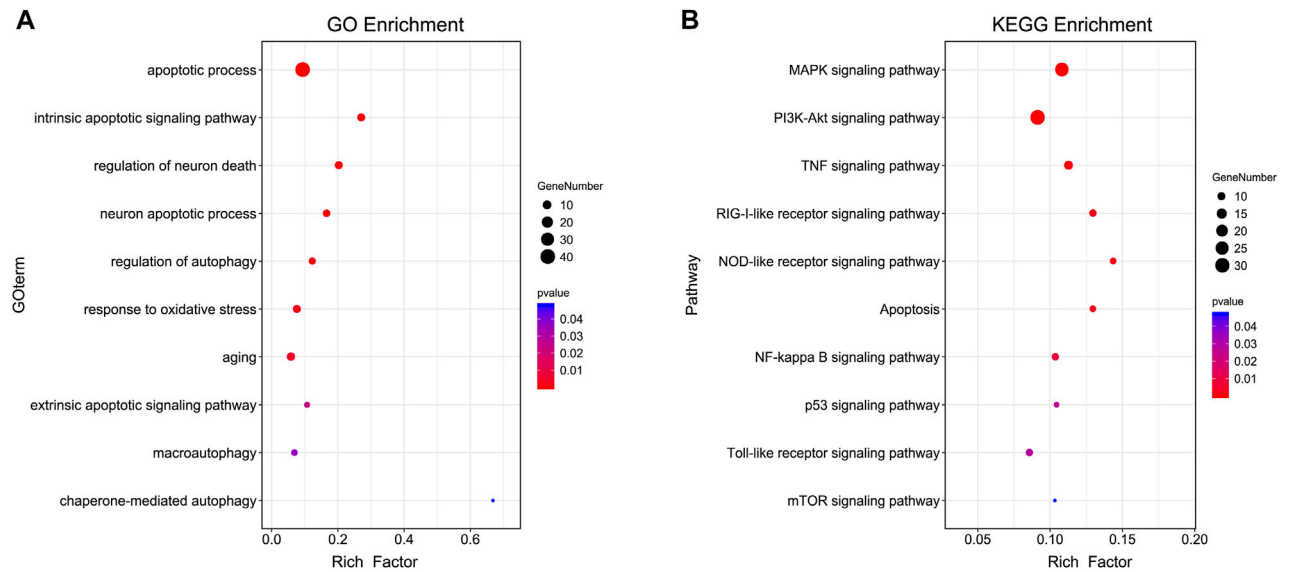

FIGURE 2 | GOBP and KEGG analysis of core targets. **(A)** GOBP terms. **(B)** KEGG terms. The genes used for GO analysis were the core targets obtained from the top analysis of the merged PPI network. The *y*-axis represents GOBP or KEGG terms, the *x*-axis represents the rich factor, the dot size represents the number of genes, and the dot colors represent the *p*-value. The *p*-value represents the significance of the focus gene enrichment. The rich factor refers to the ratio of the number of target genes in the pathway to the number of all genes annotated. The larger the rich factor is, the greater the degree of enrichment.

DISCUSSION

This study showed that PTP could significantly improve the learning and memory abilities of APP/PS1 mice. The PTP groups showed increased neurotransmitters Ach and NE levels, reduced excessive autophagic activation, and suppressed oxidative stress and apoptotic activity.

Given the complexity of active components in PTP, it is difficult to characterize the pharmacological mechanisms of PTP for cognitive impairment by conventional methods. Therefore, we utilized a network pharmacological approach to analyze the active compounds and therapeutic targets of PTP. Having identified candidate targets, we further annotated their functions by GO and KEGG functional analysis with the DAVID database. This analysis highlighted that PTP might rescue cognitive impairment by several mechanisms, such as regulating apoptosis, autophagy, oxidative stress biological processes, and modulating apoptotic pathway, PI3K-Akt, signaling pathway, and MAPK signaling pathway. Since the number of GO and KEGG terms that meet the inclusion criteria is large and even up to several hundred, it is impossible to verify all the terms with pharmacology experiments. In the present study, we confirmed some of the terms related to the pathology of cognitive impairment as examples with animal experiments, including apoptosis, autophagy, and oxidative stress.

The APP/PS1 transgenic mouse model was used in this study. APP/PS1 transgenic mice express a mutated fusion of human presenilin (DeltaE9) and human amyloid precursor protein (AppSwe), leading to cognitive impairment. APP/PS1 transgenic mice showed cognitive-behavioral changes at 3 months of age, plaques at 5 months of age, and a large number of plaques at 12 months of age. In APP/PS1 transgenic mice, the distribution of Aβ protein deposition is largely similar to that of human AD and senile cognitive impairment. APP/PS1 transgenic mouse model can be used to simulate cognitive impairment in AD (Zha et al., 2020).

The Morris water maze is an important tool for testing the memory abilities of animals (Mifflin et al., 2021). The classic Morris water maze test evaluates the ability of mice trained to find a hidden platform in a fixed position and achieve stable spatial recognition. This kind of memory is a type of spatial reference memory, and its storage location mainly involves the limbic system, and related cerebral cortex regions. In this study, APP/PS1 transgenic mice were used as models, and the swimming duration and swimming path length of mice in the water maze within 2 min were used as the main indexes to observe the effects of PTP on the swimming performance of the mice. The results showed that after treatment with PTP for 8 weeks, the swimming performance of APP/PS1 transgenic mice in the water maze was significantly improved, suggesting that PTP could improve the spatial learning and memory abilities of APP/PS1 mice. The escape latency and distance were evoked on day 4 in the APP/PS1 group, which is different from the other groups. Researchers still do not have a clear explanation on the candidate reasons for this issue, although a similar phenomenon has also been reported by several other studies (D'Agostino et al., 2013; Lu et al., 2014; Zhou et al., 2016; Banks et al., 2018). Theoretically and empirically, it might be related to the pathological processes of cognitive impairment and the specific characteristics of the APP/PS1 transgenic mouse model.

Brain monoamine neurotransmitters are closely related to mental activity, emotion, behavior, and body movement, and

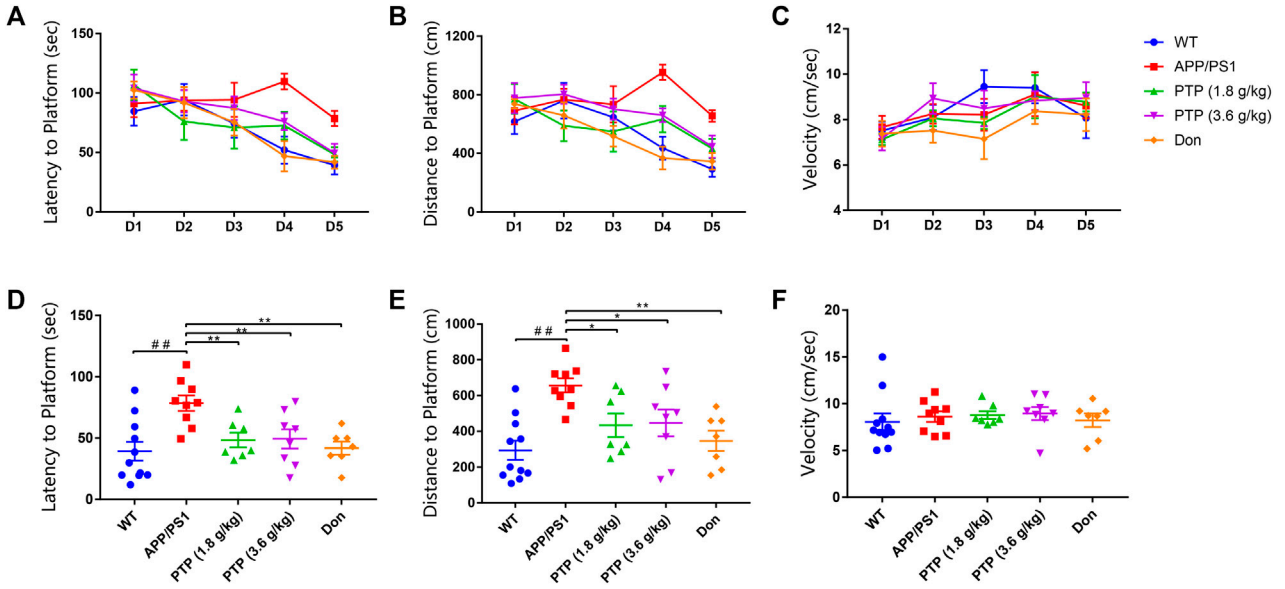

FIGURE 3 | Evaluation of mice learning and memory in the Morris water maze. **(A)** Escape latency in the positioning navigation experiment. **(B)** Total swimming distance in the positioning navigation experiment. **(C)** Swimming speed to the platform in the positioning navigation experiment. **(D)** Escape latency to the platform in the space probe test. **(E)** Total swimming distance in the space probe test. **(F)** Swimming speed in the space probe test. Compared with the wild-type group: $^{\#\#}p < 0.01$; compared with the APP/PS1 group: $^{*}p < 0.05$, $^{**}p < 0.01$. ($n \geq 7$).

there is also a certain correlation with learning and memory (Bekdash, 2021). Abnormal NE and 5-HT levels can lead to decreased brain excitability, resulting in memory loss and depressive symptoms. The lesions associated with AD often involve the locus ceruleus and dorsal raphe nucleus and are characterized by abnormal levels of NE and 5-HT in the corresponding brain regions and decreased learning and memory abilities (Trillo et al., 2013; Šimić et al., 2017). Modulating the levels of monoamine transmitters in the brain may help improve learning and memory abilities. In this study, APP/PS1 transgenic mice showed no reduction in 5-HT levels, and PTP failed to regulate the 5-HT level, which still needs to be further explored. APP/PS1 mice showed significantly decreased NE levels, and after 8 weeks of PTP administration, the level of NE in the brain tissue increased significantly, suggesting that PTP may play a role in regulating certain monoamine neurotransmitters. The NE level of the PTP (1.8 g/kg) group increased more than that of the PTP (3.6 g/kg) group. Such phenomenon shown in this study was probably due to the complex composition of PTP. Unlike the pharmacological characterization of an individual compound, complex compound preparations often do not show a dose-effect relationship and sometimes even show reversed dose-effect relationships. Results showed that donepezil also evokes the NE level. NE and Ach belong to different neurotransmitter systems. Although donepezil is well known as the AchE inhibitor, evidence from animals (Sakr et al., 2014; Kaundal et al., 2018), and humans (Ma et al., 2020) showed donepezil could also enhance the NE level in cognitive impairments. However, the underlying mechanisms have not yet been fully elucidated.

The brain cholinergic system is closely related to cognitive function and is usually damaged in AD patients (Cheng et al., 2021). As an essential transmitter in the human and mammalian brain, Ach is involved in the physiological and pathological processes of learning and memory, sleep and wake, as well as a variety of nervous system diseases, such as AD, and Parkinson's disease. One of the main clinical manifestations of AD is decreased Ach synthesis in the brain. The Ach concentration becomes an important parameter to measure learning and memory abilities (Dineley et al., 2015). A change in the Ach level before and after medication can reflect the effect of drugs on the cholinergic system more intuitively than AchE activity. The low levels of Ach in the brains of APP/PS1 transgenic mice were similar to those seen in AD patients. The prominent pathological manifestations of AD are abnormalities in the cholinergic system, including AchE hyperactivity and decreased Ach levels. The administration of an AchE inhibitor is an effective method to increase the level of Ach in the brains of patients. In this study, compared with WT mice, APP/PS1 transgenic mice showed significant decreases in brain Ach levels and no significant changes in AchE activity. The results might indicate the reduced brain Ach synthesis but not the enhancement of brain Ach degradation, which led to a decrease in cholinergic system function. This finding is consistent with the reduction in Ach synthesis in AD patients. After 8 weeks of PTP administration, the levels of Ach and the activity of AchE in the brains of the APP/PS1 transgenic mice were significantly increased, suggesting that PTP may increase the level of Ach by increasing its synthesis. It implies that PTP may improve the abnormal function of the brain cholinergic system in AD by regulating the abnormal metabolic state of Ach, thus improving the learning and memory abilities.

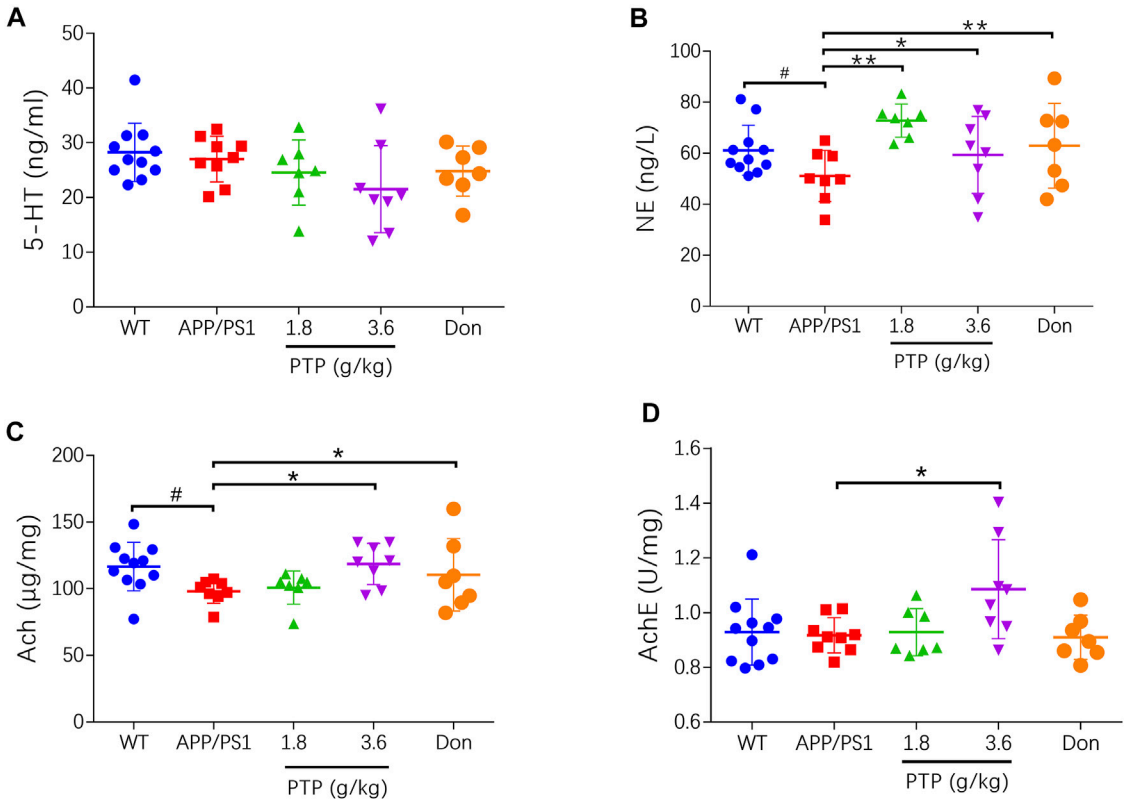

FIGURE 4 | Effects of PTP on neurotransmitters and related enzyme in brain tissue. **(A)** 5-HT, **(B)** NE, **(C)** Ach, and **(D)** AchE. Compared with the wild-type group: $^{\#}p < 0.05$; compared with the APP/PS1 group: $^{*}p < 0.05$, $^{**}p < 0.01$. ($n \geq 7$).

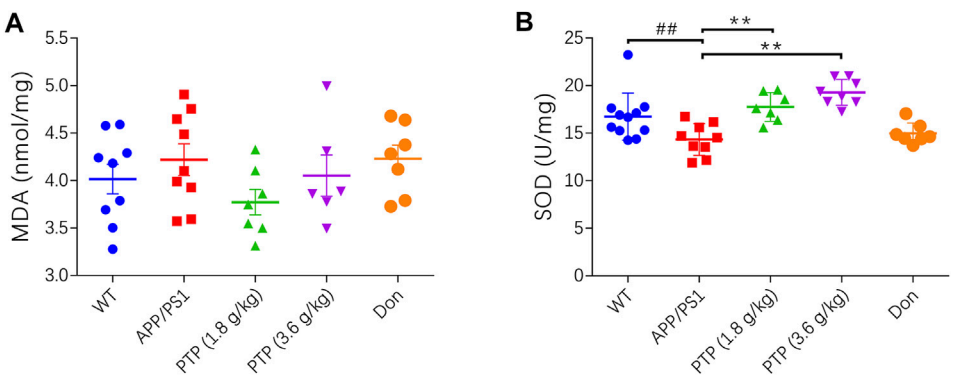

FIGURE 5 | Effects of PTP on oxidative stress in brain tissue. **(A)** The effect of PTP on the concentration of MDA in brain tissue. **(B)** The effect of PTP on SOD activity in brain tissue. Compared with the wild-type group: $^{\#\#}p < 0.01$; compared with the APP/PS1 group: $^{**}p < 0.01$. ($n \geq 7$).

Although it seems unreasonable that the AchE activity didn't change in the donepezil treatment group, previous studies of the effect of donepezil on AchE activity in APP/PS1 showed controversial results (Ye et al., 2015; Shi et al., 2018). As shown in the previous study (Abe et al., 2003), the maximal AchE inhibition of donepezil occurs at about 1 hour after drug administration in mice, and the inhibition diminishes with time passing. The above finding of the inhibitory effect of donepezil on AchE may be associated with its pharmacodynamic characteristics, as donepezil was reported to have a half-life of about 3 hours in rats (Goh et al., 2011; Nirogi et al., 2012). The results showed that PTP modulated the function of the brain cholinergic system via a mechanism distinct from that of donepezil which maintains Ach levels by inhibiting Ach

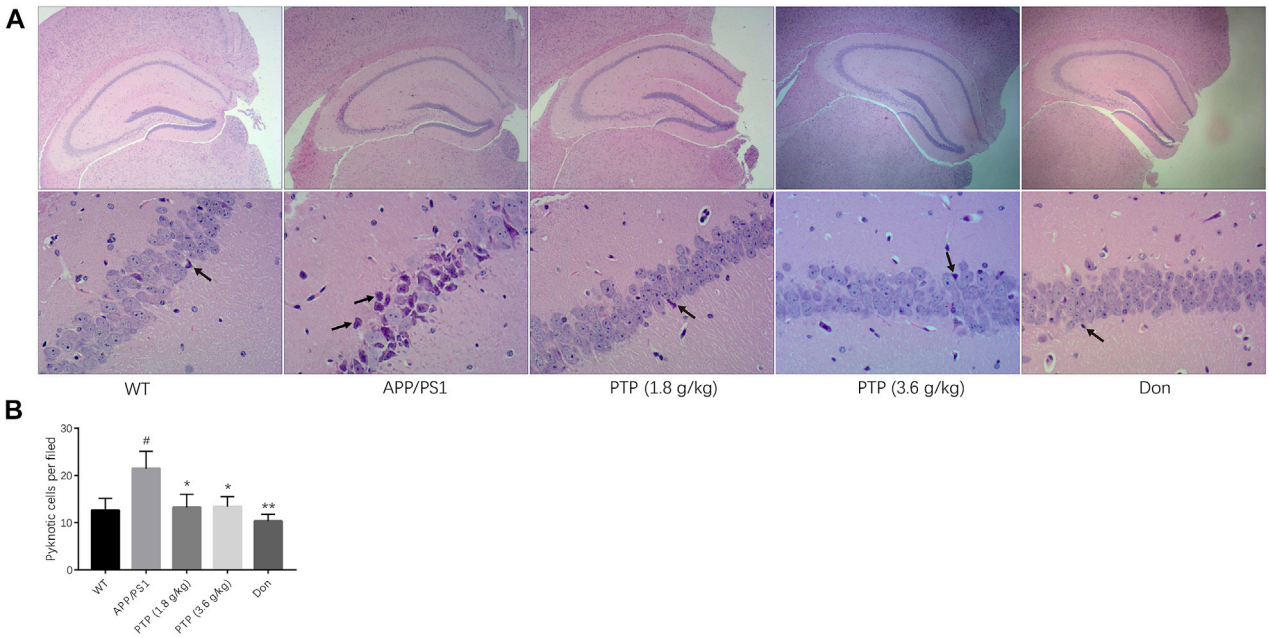

FIGURE 6 | Evaluation of mice pathological manifestations in the hippocampal CA region. **(A)** Effects of PTP on pathological manifestations in the hippocampal CA region. The black arrow indicates pyknosis of the nerve cell nucleus. (HE staining, ×40 & ×200). **(B)** Quantitative analysis of the pyknotic cells in the hippocampal CA region. Compared with the wild-type group: $^{\#}p < 0.05$; compared with the APP/PS1 group: $^{*}p < 0.05$, $^{**}p < 0.01$. ($n = 3$).

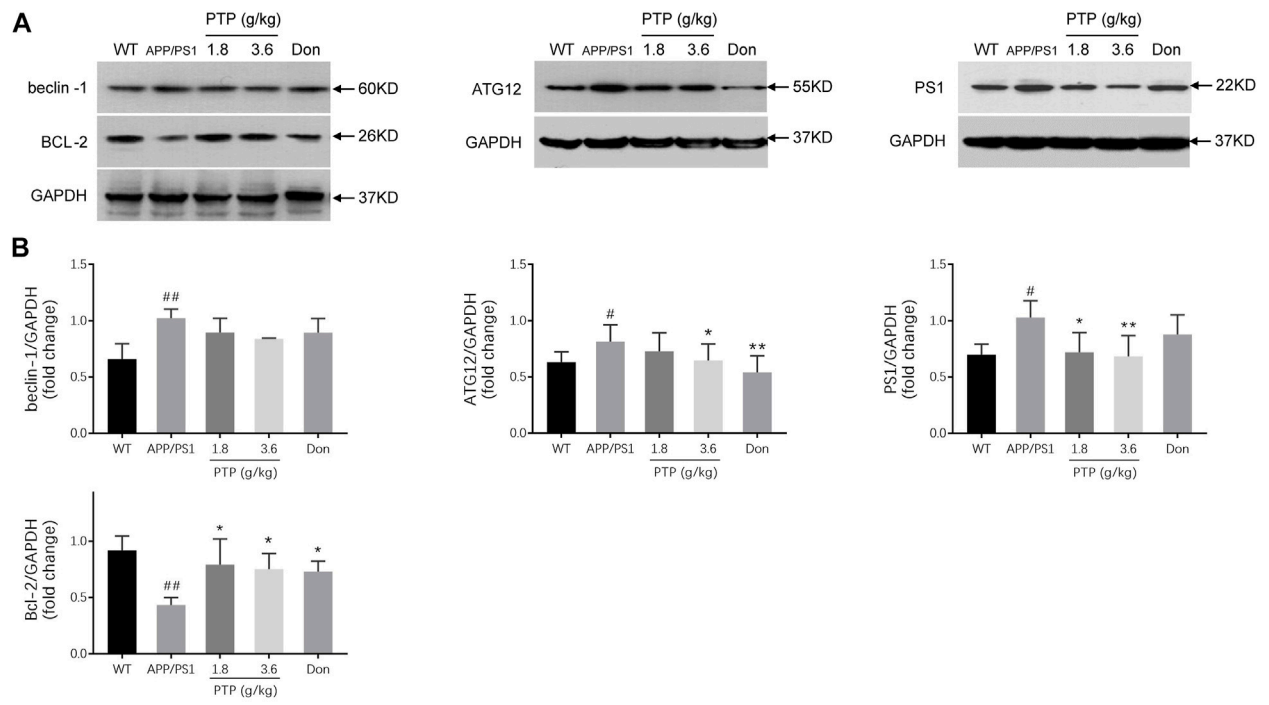

FIGURE 7 | Effects of PTP on autophagy- and apoptosis-related proteins in the cerebral cortex **(A)** Western blotting was performed to detect the protein expression of beclin-1, Bcl-2, ATG12, and PS1. **(B)** The quantitative analysis of the protein expression of beclin-1, Bcl-2, ATG12, and PS1. Compared with the wild-type group: $^{\#}p < 0.05$, $^{\#\#}p < 0.01$; compared with the APP/PS1 group: $^{*}p < 0.05$, $^{**}p < 0.01$. ($n = 3$).

degradation rather than increasing Ach synthesis, whereas this effect has been shown to be time-limited in clinical practice. The high dose PTP increased the AchE activity as well as Ach level. Since PTP is a complex compound preparation, it might have the effect of increasing both the concentrations of Ach and AchE, and the elevated AchE was not sufficient to completely degrade the increased Ach.

The toxic effects of oxidative stress and free radical damage on nerve cells have been well established (Mattson and Arumugam, 2018). Previous studies have shown that oxidative stress and free radical damage significantly increase with aging (Cochemé et al., 2011; Upadhyay et al., 2020). The nervous system is particularly sensitive to free radical damage due to its rich lipid composition, relative lack of antioxidant enzymes, and high oxygen consumption. Mitochondrial function declines during aging, and excessive free radicals accumulate, attacking the body, causing oxidative stress, resulting in the peroxidation of lipids, proteins, and DNA and eventually leading to nerve cell death. SOD and MDA are two classical indexes reflecting systemic redox homeostasis. SOD is the most important antioxidant enzyme, and MDA is an oxidative product produced when reactive oxygen species attack fat tissue. The level of MDA can reflect the degree of lipid peroxidation and reflect the degree of cell damage better than reactive oxygen species. The activity of SOD in the brains of APP/PS1 transgenic mice was significantly decreased, indicating decreased antioxidant capacity, and which was consistent with the clinical lesions of aging and senile patients with cognitive impairment. After the administration of PTP, the activity of SOD in brain tissue was significantly increased. The results showed an opposite trend for the MDA and SOD results, although some of the results did not show significant differences, indicating that PTP may significantly improve free radical scavenging in the brain, which may be helpful in anti-aging by preventing or delaying age-related pathological processes.

The integrity of the brain tissue structure is the basis of normal function. Physical or pathological factors, such as aging and AD, lead to morphological and functional abnormalities of the brain tissue. The hippocampal CA region is a common brain region affected by aging and AD (Zeier et al., 2011). In this study, APP/PS1 transgenic mice exhibited neuronal loss, apoptosis, and disordered arrangement in the hippocampal CA area, indicating functional impairment of the corresponding region. PTP and donepezil rescued the apoptosis and neuron loss, suggesting their protective effects on cognitive impairment.

Autophagy is a lysosomal-dependent physiological process that helps the body remove and degrade damaged and denatured proteins, aging and dysfunctional cells and organelles to maintain the balance of protein metabolism and the stability of the intracellular environment (Cai et al., 2016). The autophagic activity of APP/PS1 mice is various at different age. At 4–5 months old, the autophagy process is initiated in the brain tissue; at 6–8 months old, the autophagic activity was excessively activated; at 10 months old, large amounts of autophagic vacuoles and lysosome were observed in the brain of APP/PS1 mice. The formation of autophagosomes is a complex biological process. Beclin-1 and ATG12 are involved in the formation of autophagosomes. Once the autophagosome fuses with the lysosome, the autophagosome can be degraded by the lysosome. This study showed that compared with that in WT mice, the protein expression of beclin-1 and ATG12 in APP/PS1 transgenic mice was significantly increased, which indicated that autophagic activity of APP/PS1 transgenic mice was excessively increased and reflected the increased pathology severity indirectly. After 8 weeks of PTP administration, the protein expression of beclin-1 and ATG12 decreased. Although it is unclear the cause-and-effect relationship between the effect of PTP on autophagy and the other pathology changes, the results suggest that PTP may effectively alleviate the pathology severity of the brain tissue, and suppress the hyperactivated autophagy levels in the brain. Furthermore, since the autophagy flow is the primary indicator in determining the autophagy activity, which is a dynamic process, further research on the effect of PTP in regulating autophagy flow-related proteins is needed. For the issue of donepezil's effect on ATG12, no relevant literature has been reported so far. The effect of donepezil on autophagy is rarely reported in APP/PS1 mouse model. A rat model of vascular dementia showed that donepezil could inhibit autophagy, whereas evidence from a cardiac ischemia/reperfusion injury gave opposite conclusions (Jiang et al., 2019; Khuanjing et al., 2021). Thus, the effect and mechanism of donepezil on autophagy still require further investigation.

Apoptosis is one of the main pathogeneses of neurodegenerative diseases. A decrease in apoptosis is related to the stability of cognitive function (Friedlander, 2003; Wingo et al., 2019). Inhibiting brain cell apoptosis may be beneficial in ameliorating age-related cognitive decline (Ramos-Miguel et al., 2017). Bcl-2 is an anti-apoptotic protein that can significantly inhibit apoptosis. Abnormal PS1 can induce neuronal apoptosis, resulting in neuronal loss. This study showed that the expression of Bcl-2 in APP/PS1 mice was decreased, and the expression of PS1 was increased, suggesting that apoptosis was up-regulated in brain cells. PTP up-regulated the expression of the anti-apoptotic protein Bcl-2 and downregulated the expression of the apoptosis-related proteins PS1 in APP/PS1 mice, suggesting that PTP could inhibit neuronal apoptosis in the brain. Multiple studies have documented donepezil could enhance the Bcl-2 level (Takada-Takatori et al., 2006; He et al., 2018; Zaitone et al., 2020). The possible mechanism may be that donepezil inhibited apoptosis by activating the PI3K/Akt/Bcl-2 pathway (Zaitone et al., 2020). Donepezil affords excess Ach, which binds to α7 nicotinic acetylcholine receptor and then activates its channels, permitting sodium and calcium influx. Then, calcium binds to calcium reliant enzymatic reactions that elicit the PI3K/Akt/Bcl-2 pathway.

In this study, the existing positive results could support the conclusion effectively, including the efficacy indicators, such as behavioral parameters, neurotransmitters, and HE staining result, and those related to the key mechanisms, including autophagy oxidative stress, and apoptosis. However, this study also had some limitations. Firstly, Aβ accumulation is one of the most important hypothetical pathologies for AD, and there are several key fragments of Aβ peptides concerning AD pathology hypothetically. However,

from an alternative perspective, although Aβ has been the prime suspect for driving pathology in AD, its effect on AD treatment is still controversial. Recently, a meta-analysis showed anti-Aβ interventions are unlikely to have an important impact on slowing cognitive or functional decline (Lu et al., 2020). Basic research also indicates that these proteins have been highly conserved throughout evolution and may have crucial physiological roles, and Aβ-targeting therapies may unintentionally disrupt such functions. A balanced consideration of both the physiological and pathological roles of Aβ will be essential for designing safe and effective therapeutics (Kent et al., 2020). This study investigated the effect of PTP on PS1 protein but did not further verify whether PTP regulated the production of APP and Aβ or tau protein phosphorylation. Future studies still need to examine the regulatory effect of PTP on biological markers related to Aβ and its mechanism. Secondly, autophagy is another critical mechanism of AD. We found the autophagy-related protein ATG12 was down-regulated in the PTP group. However, since the autophagy flow is the primary indicator in determining the autophagy activity, which is a dynamic process, and further research on the effect of PTP in regulating autophagy flow-related proteins is needed. Thus, further research on the effect of PTP in regulating more autophagy flow-related proteins is needed.

The effect of PTP on cognitive impairment has been confirmed in clinical and basic studies. However, the composition of PTP is complex. How to simplify its components to obtain effective and relatively low-cost alternative formulas or compound preparations will be the focus of future work.

CONCLUSION

The present work showed that PTP could improve the cognitive function of APP/PS1 mice. The mechanism may be related to the improvement of neurotransmitter Ach and NE levels; the reduction of the excessive autophagic activation, which manifests as ATG12 decrease; the suppression of oxidative stress by increasing SOD level; and inhibiting apoptosis process by up-regulating Bcl-2 and down-regulating PS1.

The present study is the first systematic research of the effect of PTP in treating cognitive impairment by network pharmacology approach and verified by conducting a wide range of animal experiments. This work effectively confirmed the effect and mechanisms of PTP on cognitive impairment and provided an exemplar for similar studies in pharmacological research of traditional Chinese medicine compound preparations.

Despite these important discoveries, this study has limitations. The Aβ accumulation and tau protein phosphorylation are important hypothetical pathologies for AD. However, the effect of PTP on the production of Aβ or tau protein phosphorylation was not verified in the present study, which needs to be further explored in the future. Autophagy is another critical mechanism of AD, and the autophagy flow is the primary indicator in determining autophagy activity. We only observed the effect of PTP on some particular autophagy-related proteins but did not verify the effect of PTP on the whole autophagy flow.

DATA AVAILABILITY STATEMENT

The original contributions presented in the study are included in the article/**Supplementary Material**, further inquiries can be directed to the corresponding authors.

ETHICS STATEMENT

The animal study was reviewed and approved by the Ethics Committee of Xiyuan Hospital of China Academy of Chinese Medical Sciences.

AUTHOR CONTRIBUTIONS

WC, KC, and QX contributed to study design, trial. WS, YW, RY, and YM contributed to the trial. WC and QX wrote the original draft. All the authors read and approved the final version.

FUNDING

This work was partially supported by the National Natural Science Foundation of China (81373821); China Postdoctoral Science Foundation (2015T80206); Merit-based Funding Program for Returned Overseas Researchers supported by Ministry of Human Resources and Social Security (WC). National Natural Science Foundation of China (81373821), project director: WC; China Postdoctoral Science Foundation (2015T80206), project director: WC; Merit-based Funding Program for Returned Overseas Researchers supported by Ministry of Human Resources and Social Security (WC), project director: WC.

SUPPLEMENTARY MATERIAL

The Supplementary Material for this article can be found online at: https://www.frontiersin.org/articles/10.3389/fphar.2022.729605/full#supplementary-material

REFERENCES

Abe, Y., Aoyagi, A., Hara, T., Abe, K., Yamazaki, R., Kumagae, Y., et al. (2003). Pharmacological Characterization of RS-1259, an Orally Active Dual Inhibitor of Acetylcholinesterase and Serotonin Transporter, in Rodents: Possible Treatment of Alzheimer's Disease. *J. Pharmacol. Sci.* 93 (1), 95–105. doi:10.1254/jphs.93.95

Alzheimer's and association (2021). 2021 Alzheimer's Disease Facts and Figures. *Alzheimers. Dement.* 17 (3), 327–406. doi:10.1002/alz.12328

Banks, G., Lassi, G., Hoerder-Suabedissen, A., Tinarelli, F., Simon, M. M., Wilcox, A., et al. (2018). A Missense Mutation in Katnal1 Underlies Behavioural,

Neurological and Ciliary Anomalies. *Mol. Psychiatry* 23 (3), 713–722. doi:10.1038/mp.2017.54

Bekdash, R. A. (2021). The Cholinergic System, the Adrenergic System and the Neuropathology of Alzheimer's Disease. *Int. J. Mol. Sci.* 22 (3), 1273. doi:10.3390/ijms22031273

Cai, Y., Arikkath, J., Yang, L., Guo, M. L., Periyasamy, P., and Buch, S. (2016). Interplay of Endoplasmic Reticulum Stress and Autophagy in Neurodegenerative Disorders. *Autophagy* 12 (2), 225–244. doi:10.1080/15548627.2015.1121360

Chen, K. J., Zhou, W. Q., Li, C. S., Shi, T. R., Lei, S. P., Li, X. H., et al. (1984). Clinical Study of Qinggong Shoutao Pill on Delaying Senility - Clinical Effect and Effect on Plasma Lipid Peroxidation Level. *Chin. J. Integr. Trad. West. Med.* 4 (11), 658–659+642.

Chen, K. J., Zhou, W. Q., Li, C. S., Shi, T. R., Wang, W., Wang, J. S., et al. (1985). Clinical and Experimental Study of Qinggong Shoutao Pill on Delaying Senility. *J. Trad. Chin. Med.* 26 (7), 25–28.

Chen, S. Y., Gao, Y., Sun, J. Y., Meng, X. L., Yang, D., Fan, L. H., et al. (2020). Traditional Chinese Medicine: Role in Reducing β-Amyloid, Apoptosis, Autophagy, Neuroinflammation, Oxidative Stress, and Mitochondrial Dysfunction of Alzheimer's Disease. *Front. Pharmacol.* 11, 497. doi:10.3389/fphar.2020.00497

Cheng, Y. J., Lin, C. H., and Lane, H. Y. (2021). Involvement of Cholinergic, Adrenergic, and Glutamatergic Network Modulation with Cognitive Dysfunction in Alzheimer's Disease. *Int. J. Mol. Sci.* 22 (5), 2283. doi:10.3390/ijms22052283

Cochemé, H. M., Quin, C., McQuaker, S. J., Cabreiro, F., Logan, A., Prime, T. A., et al. (2011). Measurement of H_2O_2 within Living Drosophila during Aging Using a Ratiometric Mass Spectrometry Probe Targeted to the Mitochondrial Matrix. *Cell Metab.* 13 (3), 340–350. doi:10.1016/j.cmet.2011.02.003

D'Agostino, G., Kim, J. D., Liu, Z. W., Jeong, J. K., Suyama, S., Calignano, A., et al. (2013). Prolyl Endopeptidase-Deficient Mice Have Reduced Synaptic Spine Density in the CA1 Region of the hippocampus, Impaired LTP, and Spatial Learning and Memory. *Cereb. Cortex* 23 (8), 2007–2014. doi:10.1093/cercor/bhs199

Dineley, K. T., Pandya, A. A., and Yakel, J. L. (2015). Nicotinic ACh Receptors as Therapeutic Targets in CNS Disorders. *Trends. Pharmacol. Sci.* 36 (2), 96–108. doi:10.1016/j.tips.2014.12.002

Friedlander, R. M. (2003). Apoptosis and Caspases in Neurodegenerative Diseases. *N. Engl. J. Med.* 348 (14), 1365–1375. doi:10.1056/NEJMra022366

Goh, C. W., Aw, C. C., Lee, J. H., Chen, C. P., and Browne, E. R. (2011). Pharmacokinetic and Pharmacodynamic Properties of Cholinesterase Inhibitors Donepezil, Tacrine, and Galantamine in Aged and Young Lister Hooded Rats. *Drug Metab. Dispos.* 39 (3), 402–411. doi:10.1124/dmd.110.035964

He, L., Deng, Y., Gao, J., Zeng, L., and Gong, Q. (2018). Icariside II Ameliorates Ibotenic Acid-Induced Cognitive Impairment and Apoptotic Response via Modulation of MAPK Pathway in Rats. *Phytomedicine* 41, 74–81. doi:10.1016/j.phymed.2018.01.025

Huang, da. W., Sherman, B. T., and Lempicki, R. A. (2009). Systematic and Integrative Analysis of Large Gene Lists Using DAVID Bioinformatics Resources. *Nat. Protoc.* 4 (1), 44–57. doi:10.1038/nprot.2008.211

Jiang, X., Niu, X., Guo, Q., Dong, Y., Xu, J., Yin, N., et al. (2019). FoxO1-mediated Autophagy Plays an Important Role in the Neuroprotective Effects of Hydrogen in a Rat Model of Vascular Dementia. *Behav. Brain Res.* 356, 98–106. doi:10.1016/j.bbr.2018.05.023

Kaundal, M., Deshmukh, R., and Akhtar, M. (2018). Protective Effect of Betulinic Acid against Intracerebroventricular Streptozotocin Induced Cognitive Impairment and Neuronal Damage in Rats: Possible Neurotransmitters and Neuroinflammatory Mechanism. *Pharmacol. Rep.* 70 (3), 540–548. doi:10.1016/j.pharep.2017.11.020

Kennedy, G., Hardman, R. J., Macpherson, H., Scholey, A. B., and Pipingas, A. (2017). How Does Exercise Reduce the Rate of Age-Associated Cognitive Decline? A Review of Potential Mechanisms. *J. Alzheimers. Dis.* 55 (1), 1–18. doi:10.3233/JAD-160665

Kent, S. A., Spires-Jones, T. L., and Durrant, C. S. (2020). The Physiological Roles of Tau and Aβ: Implications for Alzheimer's Disease Pathology and Therapeutics. *Acta Neuropathol.* 140 (4), 417–447. doi:10.1007/s00401-020-02196-w

Khuanjing, T., Palee, S., Kerdphoo, S., Jaiwongkam, T., Anomasiri, A., Chattipakorn, S. C., et al. (2021). Donepezil Attenuated Cardiac Ischemia/reperfusion Injury through Balancing Mitochondrial Dynamics, Mitophagy, and Autophagy. *Transl. Res.* 230, 82–97. doi:10.1016/j.trsl.2020.10.010

Liu, Z., Guo, F., Wang, Y., Li, C., Zhang, X., Li, H., et al. (2016). BATMAN-TCM: a Bioinformatics Analysis Tool for Molecular Mechanism of Traditional Chinese Medicine. *Sci. Rep.* 6, 21146. doi:10.1038/srep21146

Lu, C. L., Tang, S., Meng, Z. J., He, Y. Y., Song, L. Y., Liu, Y. P., et al. (2014). Taurine Improves the Spatial Learning and Memory Ability Impaired by Sub-chronic Manganese Exposure. *J. Biomed. Sci.* 21 (1), 51. doi:10.1186/1423-0127-21-51

Lu, L., Zheng, X., Wang, S., Tang, C., Zhang, Y., Yao, G., et al. (2020). Anti-Aβ Agents for Mild to Moderate Alzheimer's Disease: Systematic Review and Meta-Analysis. *J. Neurol. Neurosurg. Psychiatry* 91 (12), 1316–1324. doi:10.1136/jnnp-2020-323497

Ma, X. X., Quan, Q. K., Tian, Y., Zhang, H., and Guo, L. Y. (2020). Effects of Paroxetine on Alzheimer's Disease Combined with Depression on Serum NE and 5-HT Expression. *Prog. Mod. Biomed.* 20 (21), 4080–4083. doi:10.13241/j.cnki.pmb.2020.21.017

Mattson, M. P., and Arumugam, T. V. (2018). Hallmarks of Brain Aging: Adaptive and Pathological Modification by Metabolic States. *Cell Metab.* 27 (6), 1176–1199. doi:10.1016/j.cmet.2018.05.011

Mifflin, M. A., Winslow, W., Surendra, L., Tallino, S., Vural, A., and Velazquez, R. (2021). Sex Differences in the IntelliCage and the Morris Water Maze in the APP/PS1 Mouse Model of Amyloidosis. *Neurobiol. Aging* 101, 130–140. doi:10.1016/j.neurobiolaging.2021.01.018

Morrone, C. D., Bazzigaluppi, P., Beckett, T. L., Hill, M. E., Koletar, M. M., Stefanovic, B., et al. (2020). Regional Differences in Alzheimer's Disease Pathology Confound Behavioural rescue after Amyloid-β Attenuation. *Brain* 143 (1), 359–373. doi:10.1093/brain/awz371

Nirogi, R., Bhyrapuneni, G., Kandikere, V., Benade, V., Muddana, N., Saralaya, R., et al. (2012). Concurrent Administration of Atypical Antipsychotics and Donepezil: Drug Interaction Study in Rats. *Eur. J. Drug Metab. Pharmacokinet.* 37, 155–161. doi:10.1007/s13318-012-0081-1

Nobili, A., La Barbera, L., and D'Amelio, M. (2021). Targeting Autophagy as a Therapeutic Strategy to Prevent Dopamine Neuron Loss in Early Stages of Alzheimer Disease. *Autophagy* 17 (5), 1278–1280. doi:10.1080/15548627.2021.1909409

Ramos-Miguel, A., García-Sevilla, J. A., Barr, A. M., Bayer, T. A., Falkai, P., Leurgans, S. E., et al. (2017). Decreased Cortical FADD Protein Is Associated with Clinical Dementia and Cognitive Decline in an Elderly Community Sample. *Mol. Neurodegener.* 12 (1), 26. doi:10.1186/s13024-017-0168-x

Ru, J., Li, P., Wang, J., Zhou, W., Li, B., Huang, C., et al. (2014). TCMSP: a Database of Systems Pharmacology for Drug Discovery from Herbal Medicines. *J. Cheminform.* 6, 13. doi:10.1186/1758-2946-6-13

Sakr, H. F., Khalil, K. I., Hussein, A. M., Zaki, M. S., Eid, R. A., and Alkhateeb, M. (2014). Effect of Dehydroepiandrosterone (DHEA) on Memory and Brain Derived Neurotrophic Factor (BDNF) in a Rat Model of Vascular Dementia. *J. Physiol. Pharmacol.* 65 (1), 41–53.

Shi, Y., Huang, W., Wang, Y., Zhang, R., Hou, L., Xu, J., et al. (2018). Bis(9)-(-)-Meptazinol, a Novel Dual-Binding AChE Inhibitor, Rescues Cognitive Deficits and Pathological Changes in APP/PS1 Transgenic Mice. *Transl. Neurodegener.* 7, 21. doi:10.1186/s40035-018-0126-8

Šimić, G., Babić Leko, M., Wray, S., Harrington, C. R., Delalle, I., Jovanov-Milošević, N., et al. (2017). Monoaminergic Neuropathology in Alzheimer's Disease. *Prog. Neurobiol.* 151, 101–138. doi:10.1016/j.pneurobio.2016.04.001

Takada-Takatori, Y., Kume, T., Sugimoto, M., Katsuki, H., Sugimoto, H., and Akaike, A. (2006). Acetylcholinesterase Inhibitors Used in Treatment of Alzheimer's Disease Prevent Glutamate Neurotoxicity via Nicotinic Acetylcholine Receptors and Phosphatidylinositol 3-kinase cascade. *Neuropharmacology* 51 (3), 474–486. doi:10.1016/j.neuropharm.2006.04.007

Tang, Y., Li, M., Wang, J., Pan, Y., and Wu, F. X. (2015). CytoNCA: a Cytoscape Plugin for Centrality Analysis and Evaluation of Protein Interaction Networks. *Biosystems* 127, 67–72. doi:10.1016/j.biosystems.2014.11.005

Tian, J., Shi, J., Wei, M., Ni, J., Fang, Z., Gao, J., et al. (2019). Chinese Herbal Medicine Qinggongshoutao for the Treatment of Amnestic Mild Cognitive Impairment: A 52-week Randomized Controlled Trial. *Alzheimers Dement (N Y)* 5, 441–449. doi:10.1016/j.trci.2019.03.001

Trillo, L., Das, D., Hsieh, W., Medina, B., Moghadam, S., Lin, B., et al. (2013). Ascending Monoaminergic Systems Alterations in Alzheimer's Disease. Translating Basic Science into Clinical Care. *Neurosci. Biobehav. Rev.* 37 (8), 1363–1379. doi:10.1016/j.neubiorev.2013.05.008

Upadhyay, M., Milliner, C., Bell, B. A., and Bonilha, V. L. (2020). Oxidative Stress in the Retina and Retinal Pigment Epithelium (RPE): Role of Aging, and DJ-1. *Redox Biol.* 37, 101623. doi:10.1016/j.redox.2020.101623

Vorhees, C. V., and Williams, M. T. (2006). Morris Water Maze: Procedures for Assessing Spatial and Related Forms of Learning and Memory. *Nat. Protoc.* 1 (2), 848–858. doi:10.1038/nprot.2006.116

Wingo, A. P., Dammer, E. B., Breen, M. S., Logsdon, B. A., Duong, D. M., Troncosco, J. C., et al. (2019). Large-scale Proteomic Analysis of Human Brain Identifies Proteins Associated with Cognitive Trajectory in Advanced Age. *Nat. Commun.* 10 (1), 1619. doi:10.1038/s41467-019-09613-z

Xu, H. Y., Zhang, Y. Q., Liu, Z. M., Chen, T., Lv, C. Y., Tang, S. H., et al. (2018). ETCM: an Encyclopaedia of Traditional Chinese Medicine. *Nucleic Acids Res.* 47 (D1), D976–D982. doi:10.1093/nar/gky987

Xue, J., Li, J., Liang, J., and Chen, S. (2018). The Prevalence of Mild Cognitive Impairment in China: A Systematic Review. *Aging Dis.* 9 (4), 706–715. doi:10.14336/AD.2017.0928

Xue, R., Fang, Z., Zhang, M., Yi, Z., Wen, C., and Shi, T. (2013). TCMID: Traditional Chinese Medicine Integrative Database for Herb Molecular Mechanism Analysis. *Nucleic Acids Res.* 41 (Database issue), D1089–D1095. doi:10.1093/nar/gks1100

Ye, C. Y., Lei, Y., Tang, X. C., and Zhang, H. Y. (2015). Donepezil Attenuates Aβ-Associated Mitochondrial Dysfunction and Reduces Mitochondrial Aβ Accumulation *In Vivo* and *In Vitro*. *Neuropharmacology* 95, 29–36. doi:10.1016/j.neuropharm.2015.02.020

Zaitone, S. A., Alshaman, R., Alattar, A., Elsherbiny, N. M., Abogresha, N. M., El-Kherbetawy, M. K., et al. (2020). Retinoprotective Effect of Donepezil in Diabetic Mice Involves Mitigation of Excitotoxicity and Activation of PI3K/mTOR/BCl2 Pathway. *Life Sci.* 262, 118467. doi:10.1016/j.lfs.2020.118467

Zeier, Z., Madorsky, I., Xu, Y., Ogle, W. O., Notterpek, L., and Foster, T. C. (2011). Gene Expression in the hippocampus: Regionally Specific Effects of Aging and Caloric Restriction. *Mech. Ageing. Dev.* 132 (1-2), 8–19. doi:10.1016/j.mad.2010.10.006

Zha, L., Yu, Z., Fang, J., Zhou, L., Guo, W., and Zhou, J. (2020). NLRC3 Delays the Progression of AD in APP/PS1 Mice via Inhibiting PI3K Activation. *Oxid. Med. Cell. Longev.* 2020, 5328031. doi:10.1155/2020/5328031

Zhou, D., Zhou, W., Song, J. K., Feng, Z. Y., Yang, R. Y., Wu, S., et al. (2016). DL0410, a Novel Dual Cholinesterase Inhibitor, Protects Mouse Brains against Aβ-Induced Neuronal Damage via the Akt/JNK Signaling Pathway. *Acta Pharmacol. Sin.* 37 (11), 1401–1412. doi:10.1038/aps.2016.87

Conflict of Interest: The authors declare that the research was conducted in the absence of any commercial or financial relationships that could be construed as a potential conflict of interest.

Publisher's Note: All claims expressed in this article are solely those of the authors and do not necessarily represent those of their affiliated organizations, or those of the publisher, the editors and the reviewers. Any product that may be evaluated in this article, or claim that may be made by its manufacturer, is not guaranteed or endorsed by the publisher.

frontiers in Pharmacology

CLINICAL TRIAL
published: 09 March 2022
doi: 10.3389/fphar.2022.843469

Anti-Wrinkle Efficacy of Edible Bird's Nest Extract: A Randomized, Double-Blind, Placebo-Controlled, Comparative Study

Hyung Mook Kim[1,2†], Yong Moon Lee[2], Ee Hwa Kim[1], Sang Won Eun[3], Hyun Kyung Sung[4], Heung Ko[5], Sang Jun Youn[6], Yong Choi[6], Wakana Yamada[7] and Seon Mi Shin[5†]*

[1]Global Cosmeceutical Center, Cheongju-si, South Korea, [2]College of Pharmacy, Chungbuk National University, Cheongju-si, South Korea, [3]Daehan Chemtech Co., Ltd., Seoul, South Korea, [4]Department of Pediatrics, College of Korean Medicine, Semyung University, Jecheon-si, South Korea, [5]Department of Internal Medicine, College of Korean Medicine, Semyung University, Jecheon-si, South Korea, [6]RnBS Corp., Seoul, South Korea, [7]New Products Development Department, Oryza Oil & Fat Chemical Co., Ltd., Ichinomiya, Japan

OPEN ACCESS

Edited by:
X. Y. Zhang,
University of Minho, Portugal

Reviewed by:
Wei Hsum Yap,
Taylor's University, Malaysia
Mustapha Umar Imam,
Zhengzhou University, China
Karl Tsim,
Hong Kong University of Science and Technology, Hong Kong SAR, China

***Correspondence:**
Seon Mi Shin
bunggujy21@hanmail.net

[†]These authors have contributed equally to this work and share first authorship

Specialty section:
This article was submitted to Ethnopharmacology, a section of the journal Frontiers in Pharmacology

Received: 26 December 2021
Accepted: 14 February 2022
Published: 09 March 2022

Citation:
Kim HM, Lee YM, Kim EH, Eun SW, Sung HK, Ko H, Youn SJ, Choi Y, Yamada W and Shin SM (2022) Anti-Wrinkle Efficacy of Edible Bird's Nest Extract: A Randomized, Double-Blind, Placebo-Controlled, Comparative Study. Front. Pharmacol. 13:843469. doi: 10.3389/fphar.2022.843469

This study aimed to evaluate skin health's functional improvement, such as wrinkles, elasticity, moisture, and whitening, and safety following the consumption of "edible bird's nest extract" for 12 weeks by women. This single-center, double-blinded, parallel-group, placebo-controlled study included women aged 40–60 years. Our primary purpose was to assess improvement in skin wrinkles, elasticity, and moisture after 12 weeks using an SV700, cutometer, and corneometer, respectively, compared to baseline measurements. Our secondary purpose was to evaluate skin wrinkle, elasticity, and moisture changes at 4 and 8 weeks from baseline using the aforementioned equipment, and measure transdermal water loss and melanin and erythema indexes using a tewameter and mexameter, respectively. Experts performed the visual evaluation of skin wrinkles at 4, 8, and 12 weeks from baseline. The participants were randomly allocated in a 1:1 ratio into the edible bird's nest extract or the placebo group with 43 participants each, where they consumed 100 mg of the extract or placebo, respectively, daily for 12 weeks. The outcomes were measured at every visit. In this study, upon comparing changes in the skin elasticity value between the two intake groups at 12 weeks of ingestion, skin elasticity in the edible bird's nest extract group decreased significantly compared with that in the placebo group. Adverse reactions were absent in both groups. In the case of laboratory test results, changes before and after the ingestion of the extract were within the normal range, thus indicating no clinically significant difference. The edible bird's nest extract was effective in improving skin wrinkles. Moreover, it is beneficial for skin health and can be used as a skin nutritional supplement. Compared with the placebo, the edible bird's nest extract was identified as safe.

Clinical Trial Registration: https://cris.nih.go.kr/cris/search/detailSearch.do?search_lang=E&search_page=M&pageSize=10&page=undefined&seq=21007&status=5&seq_group=20330, identifier KCT0006558.

Keywords: bird nest extract, placebo-controlled study, randomized trial, skin health, nutritional supplements

INTRODUCTION

Edible bird's nest (EBN) is the swift's nest that is made from its saliva and contains sialylglycoconjugates. The composition of the swift's saliva resembles that of salivary mucin. Many studies have been carried out on the tonic effects of EBN, and it has been shown that EBN stimulates mitosis hormones and the epidermal growth factor, resulting in the repair of cells and stimulation of the immune system (Guo et al., 2017). In China, it is termed "Yan Woo (燕窩)" and was used to maintain the beauty and youth of court and upper-class ladies. In addition, according to the ancient Chinese literature, "Bencao gangmu shiyi (本草綱目拾遺) and Bencao qiu zhen (本草求眞)," it is effective in curing tuberculosis, chronic diarrhea, and lung infections (Dictionary of Chinese Traditional Drugs, 1985). According to Chinese medical books, it brightens the skin, nourishes the stomach and lungs, and improves complexion. Although previous studies showed that EBN contains sialic acid, is effective in brain development, and is used for the treatment of various chronic inflammatory diseases, studies on its effects on skin health are still lacking (Kim et al., 2021). Sialic acid is a generic term for acyl derivatives of neuraminic acid, and there are more than 30 kinds of this derivative in nature (Kiefel and von Itzstein, 2002). N-acetylneuraminic acid is present in the EBN extract, which improves learning ability (Morgan and Winick, 1980), strengthens immunity (Bagriaçik and Miller, 1999), prevents influenza infection (Biddle and Belyavin, 1963), and acts as an important ingredient at the ends of cell membrane glycoproteins and glycolipids, in addition to improving skin elasticity and moisturizing effect. Antioxidants and skin health are areas of interest to all ages, and the functionality of health functional food materials has been consistently prioritized. As the skin ages, the number of elastic fibers and the skin regeneration rate decrease and wrinkles increase. In addition, active oxygen generated as a by-product of metabolic activity, harmful external substances, and exposure to ultraviolet rays may damage the elastic fibers, advancing skin aging. Food intake can improve skin health; however, daily meals are often deficient in nutrients, and eating only certain foods can be detrimental to health. Epidermal growth factor (EGF) has been found in EBN, which has been proposed to correspond with the proliferative effect of EBN in epidermal tissues (Kong et al., 1987). In addition, N-acetylneuraminic acid, which is present in EBN, possesses a skin-whitening function (Chan et al., 2015), and additionally, EBN was shown to reduce water loss, wrinkle area, and dermal thickness of skin (Terazawa and Shimoda, 2020). Herein, we have provided a different evidence to reveal the signaling pathway of EBN extract and its regulation of the expressions of filaggrin and filaggrin-2, two important skin barrier proteins of the SFTP family playing roles in water balance of the skin surface. The EBN-mediated regulation of filaggrin and filaggrin-2 is demonstrated to be triggered by the p38-MAPK signaling pathway and various transcriptional factors, for example, GATA3, PPARα, PPARβ, and PPARγ (Lai et al., 2021).Therefore, we conducted this clinical trial to explore the effect of EBN on improving skin wrinkles, elasticity, moisture, and whitening to obtain evidence of the extract as a functional material for skin health.

METHODS AND DESIGN

Study Participants

We recruited healthy participants through a written notice posted on the hospital's homepage and bulletin board of the Chungbuk Cosmetics Clinical Research Support Center (Cheongju, Chungcheongbuk-do, the Republic of Korea) until the target sample size was reached. Women willing to participate in the study voluntarily visited the Chungbuk Cosmetics Clinical Research Support Center. After obtaining informed consent, we enrolled women who met the inclusion criteria. The first participant was enrolled in January 2021. The duration of the recruitment period was 8 months. The total sample size was 105. This clinical trial protocol (IRB No. SMCJH 2021-06) was approved by the Institutional Review Board of the Chungju Semyung University Korean Medicine Hospital and registered at the Korean Clinical Research Information Service (KCT0006558). Details of the eligibility and exclusion criteria are provided in **Table 1**.

Interventions

EBN extract, the primary ingredient of the test food, was obtained from Japan's Oryza Oil & Fat Chemical Co., Ltd. and is similar to the product commercially sold by EBN extract-PK, which contains 20% of the hydrolyzed swiftlet nest extract. Therefore, one capsule of this test food contains 20 mg of the hydrolyzed swiftlet nest extract (**Supplementary Table S2**). The HPLC analysis for sialic acid was included in the test food and is presented in **Supplementary Table S1** and **Figures 1B,C**. The active and placebo capsules were identical in shape, size, and color (**Figure 1**). The standardization of this test food capsule was guaranteed by strict process controls during manufacture and analysis of the hydrolyzed bird's nest extract. EBN extract is a powder that is dried by adding maltodextrin after enzymatic treatment of edible bird's nest with protease; the difference is that it has been subjected to enzyme treatment to increase absorption efficiency in the body and has been standardized with sialic acid, an indicator and functional ingredient (Kim et al., 2021). The participants were orally administered either an active or placebo tablet per dose once a day for 12 weeks. They received a 1-month supply of the investigational product at baseline and during weeks 4 and 8, following which they were encouraged to continue the prescribed dosage regimen. At weeks 4, 8, and 12, the unused capsules were returned and counted to evaluate participant compliance. We advised the participants to maintain their usual diet and exercise levels during the study. They were prohibited from consuming medicines or foods that could affect their skin during the study, and during the screening visit (visit 1), the subjects taking such medicines or foods were excluded so as not to affect the results of the outcome. Medicines, foods, exercise therapy, and diets maintained prior to their enrollment were allowed at the discretion of the principal investigator. Information regarding all concomitant

TABLE 1 | Eligibility and exclusion criteria.

Eligibility criteria
1) Women aged 40–60 years
2) Women with wrinkles around their eyes and a Global Photo Damage Score of 2–6
3) Women not currently consuming health functional foods or similar products for improving skin health, such as skin wrinkles, elasticity, moisturize, and whitening
4) Able to provide written informed consent
Exclusion criteria
1) Women with severe acute kidney disease, heart disease, liver disease, or other chronic diseases that may affect the test results within the last 6 months
2) Women with a history of stroke or transient ischaemic heart attack
3) Women with a history of malignancy or lung disease within 5 years of screening
4) Women with uncontrolled hypertension (systolic blood pressure >160 mmHg or diastolic blood pressure >100 mmHg, measured after 10 min of rest) or uncontrolled diabetes (fasting blood sugar >180 mg/dl)
5) Women with a neurological or psychological history or currently suffering from schizophrenia, epilepsy, alcoholism, drug addiction, anorexia, or bulimia
6) Women with skin abnormalities, such as spots, acne, tattoos, scars, erythema, capillary dilatation, and burn marks on the measurement site
7) Women who have consumed oral or applied retinoids/steroids within 6 months prior to the beginning of the test, or who have undergone skin peeling or skin wrinkle removal procedures
8) Women with irritation or allergy to cosmetics, pharmaceuticals, health functional foods, and daily exposure to sunlight
9) Women with a history of hypersensitivity (allergy) to bird nest extract
10) Pregnant women, lactating women, planning for pregnancy, and those under contraceptives or female hormones
11) Women receiving other prohibited treatment, such as insulin, antidepressant, antiserotonin, barbiturate, antipsychotic, drug with potential for abuse, absorption inhibitor, and appetite suppressant
12) Women who have consumed steroid-containing skin external agents for ≥2 weeks for the treatment of skin diseases
13) Women who have consumed steroids (oral and injection), hormones, or drugs that affect the absorption, distribution, metabolism, and the excretion of drugs within the past 3 months, and drugs that may affect the skin
14) Women with abnormalities in the general opinion of the specialist because of blood and urine tests, namely, AST, ALT, ALP, γ-GT, and total bilirubin levels greater than thrice UNL, and serum creatinine levels greater than twice the UNL
15) Within 3 months of participating in the clinical trial for skin health
16) Others considered unsuitable for the study at the discretion of the principal investigator

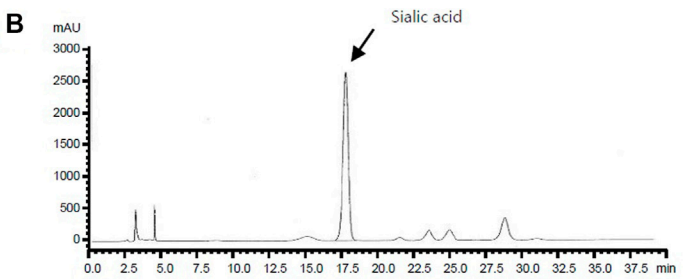

C

Retention time and content of EBN components	
	Sialic acid
N	3
Retention time (min)	17.992
Mean (μM/g of EBN)	17.132
SD	7.09

FIGURE 1 | (A) EBN tablet and placebo. **(B,C)** Fingerprinting analysis of EBN. **(B)** Chromatogram of sialic acid HPLC specifications (x: time, y: sialic acid concentration). **(C)** The retention time of sialic acid in EBN components.

medications, including the product or ingredient name, dosage, and duration, was recorded at every visit. We discontinued the intervention under the following conditions: a severe adverse event; a participant had used a drug or underwent a physical procedure that could affect the skin; a participant wished to discontinue study participation; difficulties in assessment for administrative reasons, such as violations of the dosage method or the visit schedule; and difficulties in follow-up owing to personal reasons.

Randomization and Blinding

In this clinical trial, we performed block randomization. During screening, participants who met the eligibility criteria and were judged suitable for the clinical trial were assigned to the EBN and placebo groups. The randomization table is a sequence of random number permutations generated by the randomization program of the SAS 9.4 (SAS Institute, Cary, NY, the United States), beginning from number 1 for human subjects. The sponsor attached the food label for the human application test according to the randomization table during food packaging and supplied it to the testing institution before the commencement of this clinical trial.

The randomization codes were not disclosed until the end of the trial, except when it was unavoidably necessary to read the code. The clinical trial tester supplied the intervention that matched the registration number assigned to the selected participant.

Outcome Measures and Endpoints

The primary endpoint comprised changes in skin wrinkles (in R1: skin roughness, R2: maximum roughness, R3: average roughness, R4: smoothness depth, and R5: arithmetic roughness average), skin elasticity (in R2: total elasticity, R5: real elasticity, and R7: the ratio of elasticity to the entire curve), and skin moisture, each after 12 weeks from the baseline.

The secondary endpoint comprised changes in skin wrinkles (in R1, R2, R3, R4, and R5), skin elasticity (in R2, R5, and R7), and skin moisture, each at 4 and 8 weeks from the baseline. Moreover, it comprised changes in the amount of transdermal water loss, melanin and erythema index, and visual evaluation of skin wrinkles measured by experts, each at 4, 8, and 12 weeks from the baseline. The visual evaluation was analyzed as one result by discussion among two experts.

Experts performed a visual evaluation of skin wrinkles at visits 1 (screening visit), 2 (week 0), 3 (week 4), 4 (week 8), and 5 (week 12), and after visits 1 and 2. The results of visit 1 could be recorded for visit 2 conducted within a week. At visit 1, the selection criteria were confirmed by identifying the presence of wrinkles around the eyes and the Global Photo Damage Score (approximately 2–6 points), visually or by photographs. The SV700 evaluated skin wrinkles, the Cutometer MPA 5809 evaluated skin elasticity values, the Corneometer CM 825 evaluated skin moisture values, the Tewameter TM 300 evaluated transdermal moisture loss, and the Mexameter MX 18 evaluated skin whitening. The evaluation time comprised four visits, including baseline, visit 3 (week 4), visit 4 (week 8), and visit 5 (week 12). Skin wrinkle evaluation using the SV700 measured the area 2–3 cm away from the left eye, and the remaining techniques measured the right-angle intersection of the corner of the eye and the tip of the nose. The test site was kept clean and dry to ensure similar measurement conditions in all participants. In addition, the skin was stabilized in a place with constant temperature and humidity (22 ± 2°C, R.H. 40–60%) for at least 30 min before proceeding. Water intake was restricted 1 h before the measurement.

Safety

Safety was evaluated through adverse reactions, laboratory tests (hematology, blood chemistry, and urine), and vital signs (systolic blood pressure, diastolic blood pressure, pulse, and body temperature).

Sample Size

We referred to the article by Hwang et al. (2015) and used the amount of change in the average depth of skin wrinkles (R4 smoothness depth) using a micro-wrinkle analyzer. More than 104 people who met the inclusion and exclusion criteria were recruited to be allocated to the investigational product for human clinical research. Furthermore, it was planned to analyze more than 41 people per group with the number of subjects who completed the study as per the protocol and have no major protocol deviations that may affect the interpretation of the primary endpoint.

The formula for calculating the number of subjects in the human application test was as follows:

$$n_c = \frac{2\left(Z_{1-\alpha/2} + Z_{1-\beta}\right)^2 \sigma^2}{\left(D_t - D_c\right)^2} = \frac{2\left(1.960 + 1.036\right)^2 0.03^2}{\left(-0.02\right)^2} \approx 41,$$
$$H_0 : D_t - D_c = 0 \quad vs \quad H_1 : D_t - D_c \neq 0.$$

D_t: Amount of change in R4 after the ingestion of BNE
D_c: Amount of change in R4 after the ingestion of placebo

Statistical Analyses

A statistical hypothesis test was conducted at a significance level of 0.05 (two-sided). The number of subjects, mean, and standard deviation were presented for primary and secondary endpoints. In addition, depending on whether the data normality assumption was satisfied, analysis of covariate (ANCOVA) used baselines as a covariate, or the Wilcoxon rank-sum test was performed to compare the difference between the groups. For demographic characteristics and laboratory test results, mean and standard deviation were presented, and a two-sample t-test or the Wilcoxon rank-sum test was used for inter-group comparison for continuous data. However, for categorical data, frequency and percentage were calculated, and Pearson's chi-square test or Fisher's exact test was used for inter-group comparison. Intra-group analysis was performed using the paired t-test or the Wilcoxon signed-rank test. Per-protocol set was used as the analysis for primary and secondary

TABLE 2 | Demographic characteristics of subjects.

		EBN (n = 43)	Placebo (n = 43)	*p*-Value
Mean age (year)		46.1	46.8	0.3762*
Mean height (cm)		161.1	160.1	0.3380*
Mean weight (kg)		59.5	60.7	0.4969*
Dietary habit (regular/irregular)		37/6	35/8	0.5591†
Exercise (times/week)	None	19	18	0.6135‡
	1–2	14	12	
	3–4	7	12	
	5–6	2	1	
	Everyday	1	0	
Smokers (non-smoker/ex-smoker/smoker)	42/0/1		41/1/1	1.0000‡
Drinking (non-drinker/quit drinking/current drinker)	31/1/11		34/0/9	0.6164‡

*Two-sample t-test.
†Chi-square test.
‡Fisher's exact test.

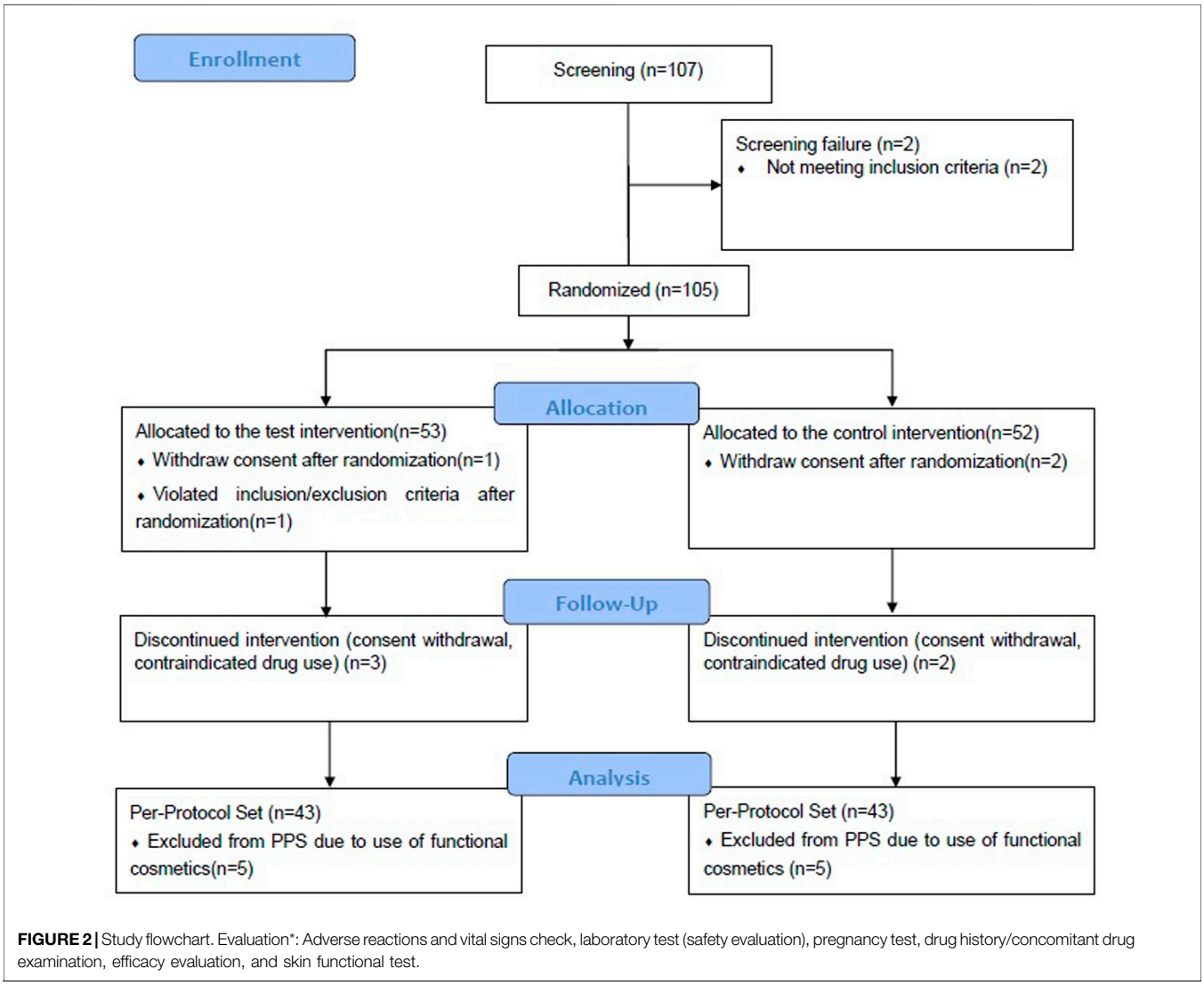

FIGURE 2 | Study flowchart. Evaluation*: Adverse reactions and vital signs check, laboratory test (safety evaluation), pregnancy test, drug history/concomitant drug examination, efficacy evaluation, and skin functional test.

endpoints. Per-protocol set included all subjects who completed the study per the protocol and had no major protocol deviations. Moreover, a safety set that included all subjects who received at least one capsule of the investigational product and had at least one safety assessment was used as the safety analysis.

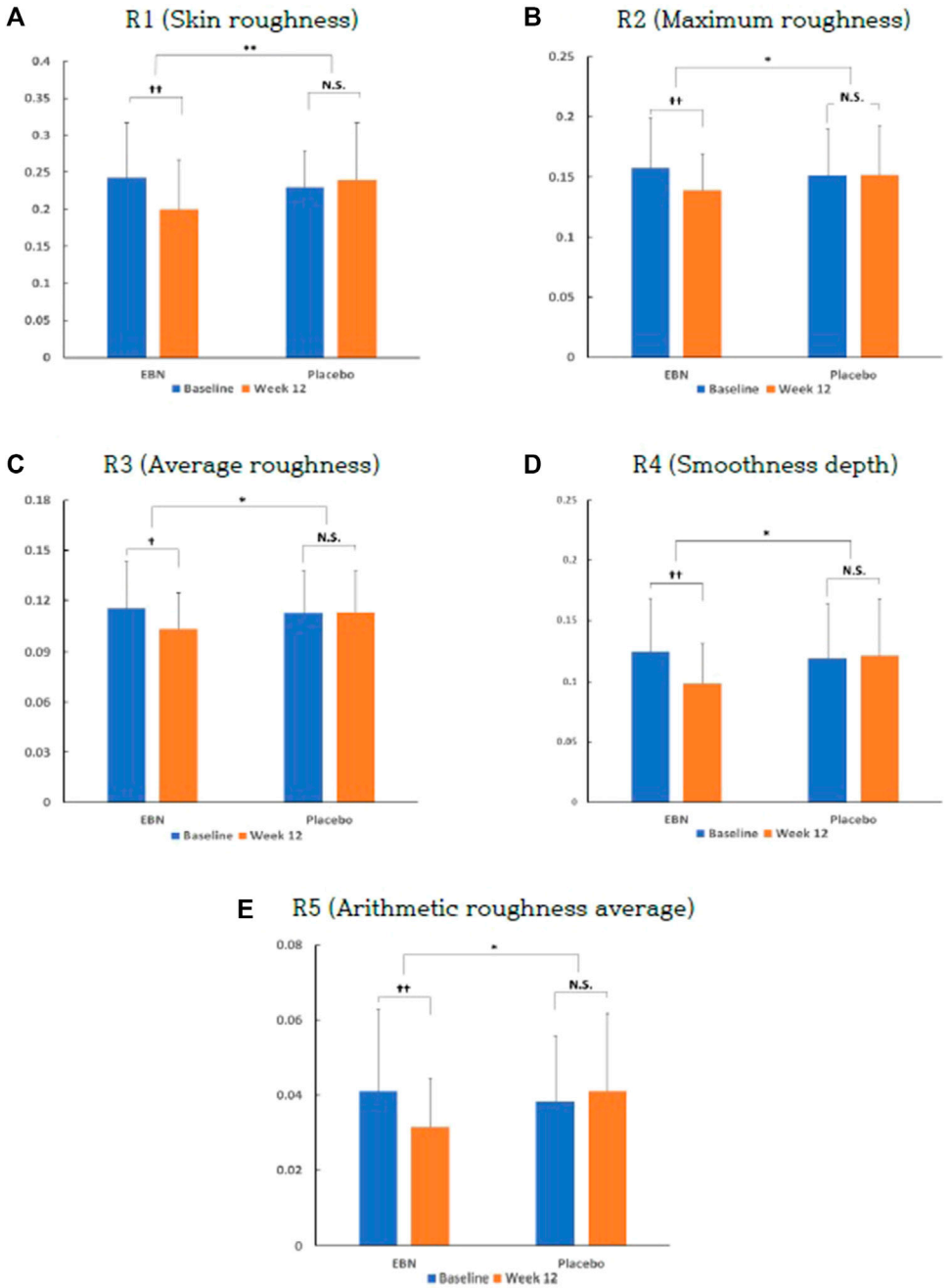

FIGURE 3 | Effect of EBN on skin wrinkle parameters at baseline and week 12. Data are presented as the means ± SD. *Indicates that the *p*-value between the two groups is <0.05. **Indicates that the *p*-value between the two groups is <0.01. †Indicates that the *p*-value compared within groups is <0.05. † indicates that the *p*-value compared within groups is <0.01. N.S. is an abbreviation for not significant.

RESULTS

For this clinical trial, the first participant for the human application trial was screened on 11th January 2021, whereas the last participant was screened on 23rd April 2021.

A total of 105 participants were enrolled for the clinical trial, and the per-protocol set comprised 86 participants (**Table 2**), 43 each in the EBN and placebo groups (**Figure 2** and **Supplementary Table S3**).

Primary Outcome

The EBN group showed a significant decrease in the skin wrinkle value compared to the placebo group at baseline and week 12. Elasticity decreased in both the groups; however, there was no

statistical significance. Regarding the amount of skin moisture change before and after intake, there was no statistically significant difference between the EBN and the placebo groups (**Figure 3** and **Supplementary Table S4**).

Secondary Outcomes

The skin elasticity value (R2: total elasticity, R5: real elasticity, and R7: ratio of elasticity to the entire curve) had decreased in both the EBN and placebo groups at baseline and week 12 (**Supplementary Table S4**).

Compared to the previous reading, there was no tendency for decrease or increase in the skin wrinkle value, skin elasticity value, and skin moisture value at week 4 and week 8 (**Supplementary Table S5**).

The change in transdermal water loss displayed a tendency to increase, and the melanin index and erythema index decreased in both groups at baseline and week 12 (**Supplementary Table S6**). However, there was no significant difference in secondary outcomes between the two groups.

Adverse Reaction

No adverse reactions occurred during this study. There was no minimally detectable change or minimal clinically significant change among the vital sign variables. Laboratory test results (hematology, blood chemistry, and urine) showed minimal clinically significant changes (**Supplementary Table S7**).

DISCUSSION

EBN is a swiftlets' (*Aerodramus fuciphagus*) residence made of their salivary gland secretions mixed with feathers or grass during breeding (Kew et al., 2014; Dai et al., 2021). The largest number of EBN was often found in caves or houses in Southeast Asia and the South Pacific, depending on the habitat distribution (Kew et al., 2014; Daud et al., 2021). EBN has been regarded as a high-grade healthy food that only privileged individuals can eat, with functions of moistening the lung, nourishing the stomach, relieving the liver, clearing the eyes, and tonifying the heart (Hwang et al., 2015). It is composed of protein, carbohydrate, ash, fat, and dietary elements (Quek et al., 2018), and has various effects, including antiviral effects and inhibitory hemagglutination (Guo et al., 2017); immunological enhancement (Zhao et al., 2016); improving intelligence and memory (Oliveros et al., 2018); improvement of neurodegenerative disease (Yew et al., 2014; Careena et al., 2018) and cardiovascular disease (Hun Lee et al., 2020); promoting cell division (Roh et al., 2012); antioxidant, anti-inflammatory, and anti-aging effects (Yida et al., 2015; Hun Lee et al., 2020) on epidermal growth factor-like activity (Kong et al., 1987); and stimulating collagen production and epithelial tissue proliferation (Park et al., 2017). EBN is expected to have various effects on skin health through these effects. Therefore, we tried to investigate the effect of EBN extract on skin wrinkles and whitening. We conducted this randomized, double-blind study to determine the effect of EBN extract on improving skin wrinkles, elasticity, moisture, and whitening. In a previous experimental study, the authors confirmed the safety of the extract (Haghani et al., 2016).

We observed a causal relationship between EBN and skin wrinkle improvement. We compared the amount of change in skin wrinkle (R1, R2, R3, R4, and R5) before (0 weeks) and after (12 weeks) the intake of EBN extract with the R1 value measured before the intake. Afterward, it was confirmed that the EBN group had significantly decreased the skin wrinkle value compared to the placebo group at baseline and week 12. In addition, R2, R3, R4, and R5 decreased significantly in the EBN group compared with those in the placebo group. In addition, the EBN and placebo groups demonstrated a statistically significant decrease in the skin wrinkle value before and after 12 weeks of the intervention. As a result, it was demonstrated that consumption of EBN extract positively affects skin wrinkle improvement.

There was no significant difference in secondary outcomes between the two groups. The skin elasticity value (R2: total elasticity, R5: real elasticity, and R7: ratio of elasticity to the entire curve) was decreased in both the EBN and placebo groups at baseline and week 12. The amount of change in transdermal water loss displayed a tendency to increase in both groups at baseline and week 12, and the melanin index and erythema index decreased in both groups at baseline and week 12.

There are studies that have documented that EBN containing EGF promotes and activates the synthesis of DNA, and thus promotes cell proliferation (Kong. et al., 1987). A further experiment was conducted to study the effects of EBN extract, with rich EGF, on human skin cell (epidermal keratinocytes and dermal fibroblasts) proliferation. The results showed that EBN extract promoted the proliferation of normal keratinocytes and fibroblasts dose-dependently (Kong et al., 1987). Keratinocytes play an important role in healthy skin barrier function, improved proliferation of keratinocytes directly improves skin barrier function, thus promoting skin suppleness and improving the overall skin texture. Meanwhile, fibroblasts synthesize extracellular matrix and collagen, and play a critical role in wound healing, influence skin elasticity, and physically apparent aging.

EGF plays an important role in the process of wound healing. Studies showed that wound healing is delayed in mice whose submandibular gland is removed as the submandibular gland produces EGF (Niall et al., 1982). Proliferation and migration of epithelial cells play a critical role in wound healing, and EGF is a known factor in promoting fibroblast proliferation and epithelial cells migration, thus promoting wound healing. The effect of EBN extract on wound healing was examined by a scratch test. Normal human keratinocytes were cultured in a petri dish. A damage model was induced by scratching a line in the center of the dish. Wound healing at the scratched area was observed after 24-h. Accelerated wound healing effect was observed in the dish treated with EBN extract, and the effect was dose-dependent. Thus, it is suggestive that EBN extract promotes wound healing (Niall et al., 1982).

Tight junctions (TJs) refer to a closely associated area of two adjacent cells whose membrane join together forming a

virtually impermeable barrier to fluid. In the epidermis, TJs play a crucial role in the formation and maintenance of epithelial barriers and prevent invasion of foreign particles. In the stratum corneum, ceramide acts as a first line of skin barrier. TJs in the stratum granulosum act as the second line of skin barrier. Occludin and claudin are integral plasma membrane proteins located at the TJs (Niessen, 2007). They form important barrier that protect the skin from external organism, prevent excessive water loss, and selectively transport small solutes through the skin (Yamamoto et al., 2008). This has prompted further understanding into the effect of EBN on skin barrier function where an experiment was conducted to evaluate the effect of EBN on skin TJs. Among the TJ proteins, claudin-1 (Cldn-1) and claudin-4 (Cldn-4) have been demonstrated to have a role in skin barrier function (Furuse et al., 2002; Yuki et al., 2011). The effect of EBN on the expression of TJ proteins was examined. Both genetic expression and protein expression of Cldn-1 and Cldn-4 was upregulated by EBN-P (PC) 0.1% *in vitro*. In addition, the effect of EBN on the protein expression of Cldn-4 of normal keratinocytes was examined and observed using fluorescence microscopy. The results showed that the protein expression of Cldn-4 was upregulated by EBN-P (PC) 0.1%.

Sialic acid is the major carbohydrate found in EBN and in several tissues and fluids in humans (Kim et al., 2021). A study demonstrated the antioxidant role of sialic acid as a hydroxyl radical scavenger (Ogasawara et al., 2007), and another study found that sialic acid from EBN has the effects of scavenging DPPH radicals and hydroxyl radicals (Wang et al., 2019). Several studies have demonstrated that sialic acid is essential for brain function, immune function, and cell proliferation and repair (Wang, 2009; Varki and Gagneux, 2012; Rashed et al., 2021); however, there was no statistically significant difference between the two groups in the amount of skin moisture change. Considering that the present trial was conducted during the COVID-19 pandemic, all participants routinely used medical masks. Therefore, the increase in skin moisture content and transdermal moisture loss was a possible outcome of using masks for a prolonged period. Furthermore, this is a single-center study, not a cross-over study; therefore, it is highly likely that only subjects from a specific region had participated, which may lead to consequential bias. It can be seen that there was a slightly negative effect as the mask dries the skin, which can lead to wrinkles and loss of moisture in the skin. In contrast, we evaluated skin wrinkles at a position 2–3 cm away from the left eye, which was not affected by long-term mask-wearing; therefore, it is considered an objective functional evaluation index and can be evaluated by excluding other external factors (wearing a mask). There were no adverse reactions or clinically meaningful changes in the laboratory test values following the ingestion of EBN extract. The consumption of EBN extract for 12 weeks objectively confirmed skin wrinkle improvement and a tendency to increase skin moisture and decrease the melanin and erythema index. In addition, there were no safety-associated problems. Therefore, EBN extract was effective in improving skin wrinkles. Moreover, it is beneficial for skin health and can be used as a skin nutritional supplement.

CONCLUSION

In this study, upon comparing changes in skin wrinkle values between the two intake groups at 12 weeks of ingestion, those in the EBN extract group decreased significantly compared with the placebo group. However, the skin elasticity value decreased and skin moisture value increased, but there was no statistical significance between the two groups. The change in transdermal water loss displayed a tendency to increase, and the melanin index and erythema index decreased in both groups at baseline and week 12. However, there was no significant difference in the secondary outcomes between the two groups.

No adverse reactions were recorded during the study. In the case of laboratory test results, changes before and after ingestion of the test food were within the normal range, and there was no minimally detectable change or minimal clinically significant change.

This study has several limitations, including that this is a single-center study, not a cross-over study. Moreover, there is no verum group in the study. However, if multicenter and cross-over studies are conducted in the future, it is expected that clearer and more reliable research results will be obtained. A verum group should be included in the next study, where a follow-up phase should be performed to assess skin wrinkle values of the EBN group after a period of no drug treatment. Furthermore, in future studies, it is thought that research and statistical analysis on the skin improvement effect by age should be performed.

DATA AVAILABILITY STATEMENT

The original contributions presented in the study are included in the article/**Supplementary Material**, further inquiries can be directed to SE: daehanchemtech@dhchemtech.com / SY: sjyoun@rnbs.co.kr / YC: choiy@rnbs.co.kr.

ETHICS STATEMENT

All patients voluntarily participated, and were informed prior so that they could withdraw from the study without penalty. This study was approved by the Institutional Review Boards of Chungju Semyung University Korean Medicine Hospital (IRB reference No.: SMCJH-2021-06, Protocol version 1.1) and registered at CRIS (KCT0006558). The patients/participants provided their written informed consent to participate in this study.

AUTHOR CONTRIBUTIONS

HMK: clinical trial progress and result report preparation; EK, YL, and HK: clinical trial supervision and editing; HS: editing, writing—reviewing, and editing; SE: clinical trial support; SY:

statistical processing, figure, and table creation; YC: statistical processing, figure, and table creation; WY: reviewing and raw material information advice; and SS: writing—original draft, editing, and reviewing.

FUNDING

This study received funding from Daehan Chemtech and Oryza Oil & Fat Chemical CO.,Ltd. The funder was not involved in the study design, collection, analysis, interpretation of data, the writing of this article, or the decision to submit it for publication.

SUPPLEMENTARY MATERIAL

The Supplementary Material for this article can be found online at: https://www.frontiersin.org/articles/10.3389/fphar.2022.843469/full#supplementary-material

REFERENCES

Bagriaçik, E. U., and Miller, K. S. (1999). Cell Surface Sialic Acid and the Regulation of Immune Cell Interactions: The Neuraminidase Effect Reconsidered. *Glycobiology*9, 267–275. doi:10.1093/glycob/9.3.267

Biddle, F., and Belyavin, G. (1963). The Haemagglutination Inhibitor in Edible Bird-Nest: Its Biological and Physical Properties. *J. Gen. Microbiol.*31, 31–44. doi:10.1099/00221287-31-1-31

Careena, S., Sani, D., Tan, S. N., Lim, C. W., Hassan, S., Norhafizah, M., et al. (2018). Effect of Edible Bird's Nest Extract on Lipopolysaccharide-Induced Impairment of Learning and Memory in Wistar Rats. *Evid. Based Complement. Alternat Med.*2018, 9318789. doi:10.1155/2018/9318789

Chan, G. K. L., Wong, Z. C. F., Lam, K. Y. C., Cheng, L. K. W., Zhang, L. M., Lin, H., et al. (2015). Edible Bird's Nest, an Asian Health Food Supplement, Possesses Skin Lightening Activities: Identification of N-Acetylneuraminic Acid as Active Ingredient. *Jcdsa*05, 262–274. doi:10.4236/jcdsa.2015.54032

Dai, Y., Cao, J., Wang, Y., Chen, Y., and Jiang, L. (2021). A Comprehensive Review of Edible Bird's Nest. *Food Res. Int.*140, 109875. doi:10.1016/j.foodres.2020.109875

Daud, N. A., Mohamad Yusop, S., Babji, A. S., Lim, S. J., Sarbini, S. R., and Hui Yan, T. (2021). Edible Bird's Nest: Physicochemical Properties, Production, and Application of Bioactive Extracts and Glycopeptides. *Food Rev. Int.*37, 177–196. doi:10.1080/87559129.2019.1696359

Dictionary of Chinese Traditional Drugs. (1985)(Shanghai Science and Technology Publisher, Shogakukan Inc.).

Furuse, M., Hata, M., Furuse, K., Yoshida, Y., Haratake, A., Sugitani, Y., et al. (2002). Claudin-based Tight Junctions Are Crucial for the Mammalian Epidermal Barrier: A Lesson from Claudin-1-Deficient Mice. *J.Cel Biol*156 (156), 1099–1111. doi:10.1083/jcb.200110122

Guo, C. T., Cao, Y., Hu, Z. P., Wo, E. K., Chen, S. S., You, J. B., et al. (2017). Effect of Edible Bird's Nest on Hemogram and Secondary Influenza Virus Infection of Mice with Aplastic Anemia. *Int. J. Epidemiol. Infect. Dis.*44, 228–232. doi:10.1016/j.foodres.2020.109875

Haghani, A., Mehrbod, P., Safi, N., Aminuddin, N. A., Bahadoran, A., Omar, A. R., et al. (2016). *In Vitro* and *In Vivo*Mechanism of Immunomodulatory and Antiviral Activity of Edible Bird's Nest (EBN) against Influenza A Virus (IAV) Infection. *J. Ethnopharmacol*185, 327–340. doi:10.1016/j.jep.2016.03.020

Hun Lee, T., Hau Lee, C., Alia Azmi, N., Kavita, S., Wong, S., Znati, M., et al. (2020). Characterization of Polar and Non-polar Compounds of House Edible Bird's Nest (EBN) from Johor, Malaysia. *Chem. Biodivers*17, e1900419. doi:10.1002/cbdv.201900419

Hwang, E., Park, S. Y., Jo, H., Lee, D. G., Kim, H. T., Kim, Y. M., et al. (2015). Efficacy and Safety of Enzyme-Modified Panax Ginseng for Anti-wrinkle Therapy in Healthy Skin: A single-center, Randomized, Double-Blind, Placebo-Controlled Study. *Rejuvenation Res.*18, 449–457. doi:10.1089/rej.2015.1660

Kew, P. E., Wong, S. F., Lim, P. K., and Mak, J. W. (2014). Structural Analysis of Raw and Commercial Farm Edible Bird Nests. *Trop. Biomed.*31, 63–76.

Kiefel, M. J., and von Itzstein, M. (2002). Recent Advances in the Synthesis of Sialic Acid Derivatives and Sialylmimetics as Biological Probes. *Chem. Rev.*102, 471–490. doi:10.1021/cr000414a

Kim, O. K., Kim, D., Lee, M., Park, S. H., Yamada, W., Eun, S., et al. (2021). Standardized Edible Bird's Nest Extract Prevents UVB Irradiation-Mediated Oxidative Stress and Photoaging in the Skin. *Antioxidants (Basel)*10, 1452. doi:10.3390/antiox10091452

Kong, Y. C., Keung, W. M., Yip, T. T., Ko, K. M., Tsao, S. W., and Ng, M. H. (1987). Evidence that Epidermal Growth Factor Is Present in Swiftlet's (Collocalia) Nest. *Comp. Biochem. Physiol. B*87, 221–226. doi:10.1016/030510.1016/0305-0491(87)90133-7

Lai, Q. W. S., Guo, M. S. S., Wu, K. Q., Liao, Z., Guan, D., Dong, T. T., et al. (2021). Edible Bird's Nest, an Asian Health Food Supplement, Possesses Moisturizing Effect by Regulating Expression of Filaggrin in Skin Keratinocyte. *Front. Pharmacol.*12, 685982. doi:10.3389/fphar.2021.685982

Morgan, B. L., and Winick, M. (1980). Effects of Administration of N-Acetylneuraminic Acid (NANA) on Brain NANA Content and Behavior. *J. Nutr.*110, 416–424. doi:10.1093/jn/110.3.416

Niall, M., Ryan, G. B., and O'Brien, B. M. (1982). The Effect of Epidermal Growth Factor on Wound Healing in Mice. *J. Surg. Res.*33 (2), 164–169. doi:10.1016/0022-4804(82)90024-5

Niessen, C. M. (2007). Tight Junctions/adherens Junctions: Basic Structure and Function. *J.Invest. Dermatol.*127 (11), 2525–2532. doi:10.1038/sj.jid.5700865

Ogasawara, Y., Namai, T., Yoshino, F., Lee, M. C., and Ishii, K. (2007). Sialic Acid Is an Essential Moiety of Mucin as a Hydroxyl Radical Scavenger. *FEBS Lett.*581, 2473–2477. doi:10.1016/j.febslet.2007.04.062

Oliveros, E., Vázquez, E., Barranco, A., Ramírez, M., Gruart, A., Delgado-García, J., et al. (2018). Sialic Acid and Sialylated Oligosaccharide Supplementation during Lactation Improves Learning and Memory in Rats. *Nutrients*10, 1519. doi:10.3390/nu10101519

Park, J. W., Hwang, S. R., and Yoon, I. S. (2017). Advanced Growth Factor Delivery Systems in Wound Management and Skin Regeneration. *Molecules*22, 1259. doi:10.3390/molecules22081259

Quek, M. C., Chin, N. L., Yusof, Y. A., Law, C. L., and Tan, S. W. (2018). Pattern Recognition Analysis on Nutritional Profile and Chemical Composition of Edible Bird's Nest for its Origin and Authentication. *Int. J. Food Properties*21, 1680–1696. doi:10.1080/10942912.2018.1503303

Rashed, A. A., Ahmad, H., Abdul Khalid, S. K., and Rathi, D.-N. G. (2021). The Potential Use of Sialic Acid from Edible Bird's Nest to Attenuate Mitochondrial Dysfunction by *In Vitro* Study. *Front. Pharmacol.*12, 633303. doi:10.3389/fphar.2021.633303

Roh, K. B., Lee, J., Kim, Y. S., Park, J., Kim, J. H., Lee, J., et al. (2012). Https:. Mechanisms of Edible Bird's Nest Extract-Induced Proliferation of Human Adipose-Derived Stem Cells. Evid. Based Complement. Alternat. *Med*2012, 797520. doi:10.1155/2012/797520

Terazawa, S., and Shimoda, H. (2020). Keratinocyte Proliferative and Wound Healing Effects of Edible Bird's Nest Extract on Human Skin. *Int. J. Biomed. Sci.*16, 43–51. Available at: http://ijbs.org/User/ContentFullText.aspx?VolumeNO=16&StartPage=43&Type=pdf (AccessedMar1, , 2021).

Varki, A., and Gagneux, P. (2012). Multifarious Roles of Sialic Acids in Immunity. *Ann. N. Y. Acad. Sci.*1253, 16–36. doi:10.1111/j.1749-6632.2012.06517.x

Wang, B. (2009). Sialic Acid Is an Essential Nutrient for Brain Development and Cognition. *Annu. Rev. Nutr.*29, 177–222. doi:10.1146/annurev.nutr.28.061807.155515

Wang, C.Y., Cheng, L.J., Shen, B., Yuan, Z.L., Feng, Y.Q., and Lu, S.H. (2019). Antihypertensive and Antioxidant Properties of Sialic Acid, the Major Component of Edible Bird's Nests. *Curr. Top. Nutraceutical Res.*17, 376–380. doi:10.37290/ctnr2641-452X.17:376-379

Yamamoto, T., Saeki, Y., Kurasawa, M., Kuroda, S., Arase, S., Sasaki, H., et al. (2008). Effect of RNA Interference of Tight junction-related Molecules on Intercellular Barrier Function in Cultured Human Keratinocytes. *Arch. Dermatol. Res.*300, 517–524. doi:10.1007/s00403-008-0868-8

Yew, M. Y., Koh, R. Y., Chye, S. M., Othman, I., and Ng, K. Y. (2014). Edible Bird's Nest Ameliorates Oxidative Stress-Induced Apoptosis in SH-Sy5yHuman Neuroblastoma Cells. *BMC Complement. Altern. Med.*14, 391. doi:10.1186/1472-6882-14-391

Yida, Z., Imam, M. U., Ismail, M., Hou, Z., Abdullah, M. A., Ideris, A., et al. (2015). Edible Bird's Nest Attenuates High Fat Diet-Induced Oxidative Stress and Inflammation via Regulation of Hepatic Antioxidant and Inflammatory Genes. *BMC Complement. Altern. Med.*15, 310. doi:10.1186/s12906-015-0843-9

Yuki, T., Hachiya, A., Kusaka, A., Sriwiriyanont, P., Visscher, M. O., Morita, K., et al. (2011). Characterization of Tight Junctions and Their Disruption by UVB in Human Epidermis and Cultured Keratinocytes. *J.Invest. Dermatol.*131, 744–752. doi:10.1038/jid.2010.385

Zhao, R., Li, G., Kong, X. J., Huang, X. Y., Li, W., Zeng, Y. Y., et al. (2016). The improvement effects of edible bird's nest on proliferation and activation of B lymphocyte and its antagonistic effects on immunosuppression induced by cyclophosphamide. *Drug Des Devel Ther.* 21(10), 371–381. doi:10.2147/DDDT.S88193

Conflict of Interest: Author SE was employed by Daehan Chemtech Co., Ltd. Authors SY and YC were employed by RnBS Corp. Author WY was employed by Oryza Oil & Fat Chemical Co., Ltd.

The remaining authors declare that the research was conducted in the absence of any commercial or financial relationships that could be construed as a potential conflict of interest.

frontiers in Pharmacology

REVIEW
published: 24 March 2022
doi: 10.3389/fphar.2022.766581

Isodon rubescens (Hemls.) Hara.: A Comprehensive Review on Traditional Uses, Phytochemistry, and Pharmacological Activities

Xufei Chen[1†], *Xufen Dai*[2†], *Yinghai Liu*[1], *Xirui He*[3*] *and Gu Gong*[1*]

[1]Department of Anesthesiology, The General Hospital of the Western Theater Command, Chengdu, China, [2]Shaanxi Institute for Food and Drug Control, Xi'an, China, [3]Department of Bioengineering, Zhuhai Campus, Zunyi Medical University, Zhuhai, China

Isodon rubescens is a medicinal and food plant, often eaten as a wild vegetable in ancient China, and has been widely used for decades to treat sore throats, tonsillitis, colds and headaches, bronchitis, chronic hepatitis, joint rheumatism, snake and insect bites, and various cancers. This comprehensive and systematic review of the ethnomedicinal uses, phytochemical composition, pharmacological activity, quality control and toxicology of *I. rubescens* provides updated information for the further development and application in the fields of functional foods and new drugs research. To date, a total of 324 substances have been isolated and identified from the plant, including terpenoids, flavonoids, polyphenols, alkaloids, amino acids, and volatile oils. Among these substances, diterpenoids are the most important and abundant bioactive components. In the past decades pharmacological studies have shown that *I. rubescens* has significant biological activities, especially in the modulation of antitumor and multidrug resistance. However, most of these studies have been conducted *in vitro*. In-depth *in vivo* studies on the quality control of its crude extracts and active ingredients, as well as on metabolite identification are still very limited. Therefore, more well-designed preclinical and clinical studies are needed to confirm the reported therapeutic potential of *I. rubescens*.

Keywords: ***Isodon rubescens*, traditional uses, chemical constituent, biological activity, toxicology**

OPEN ACCESS

Edited by:
X. Y. Zhang,
University of Minho, Portugal

Reviewed by:
Luping Qin,
Zhejiang Chinese Medical University, China
Taoufiq Benali,
Cadi Ayyad University, Morocco
Weihong Cong,
China Academy of Chinese Medical Sciences, China

***Correspondence:**
Xirui He
xiruihe6105194@163.com
Gu Gong
gonggu68@163.com

[†]These authors have contributed equally to this work

Specialty section:
This article was submitted to Ethnopharmacology, a section of the journal Frontiers in Pharmacology

Received: *29 August 2021*
Accepted: *28 January 2022*
Published: *24 March 2022*

Citation:
Chen X, Dai X, Liu Y, He X and Gong G (2022) Isodon rubescens (Hemls.) Hara.: A Comprehensive Review on Traditional Uses, Phytochemistry, and Pharmacological Activities. Front. Pharmacol. 13:766581. doi: 10.3389/fphar.2022.766581

INTRODUCTION

The genus *Isodon* (Lamiaceae family) consists of more than 150 species of perennial herbs that are widely distributed in tropical Africa, tropical and subtropical Asia, and East Central Siberia, with a few species in Malaysia, Australia, and the Pacific Islands. There are 90 species and 21 varieties in China, among which the largest number of species is found in the Southwest provinces. *I. rubescens* (Hemsl.) H. Hara is a perennial herb of the genus *Isodon* in the Labiaceae family. *I. rubescens* (**Figure 1**) is also known as *Rabdosia rubescens* var. *lushiensis*, *I. rubescens* var. *eglandulosus*, *Rabdosia rubescens* var. *taihangensis*, *Rabdosia dichromophylla* (The Plant List, 2013) as well as under local names such as "Donglingcao," "Binglingcao," "Xuehuacao," "Poxuedan," "Shanxiangcao," "Yehuoxiang," and "Liuyueling" in China (Wei, 2012).

I. rubescens is sweet and bitter in a prescription and slightly cold after the drug acting on the body, clears away heat, and has detoxifying, anti-inflammatory, analgesic, and antitumor effects. It has been used in the treatment of esophageal cancer in He'nan province in China for more than 50 years (Xiong, 2014). The aboveground parts of *I. rubescens* are commonly used in traditional Chinese

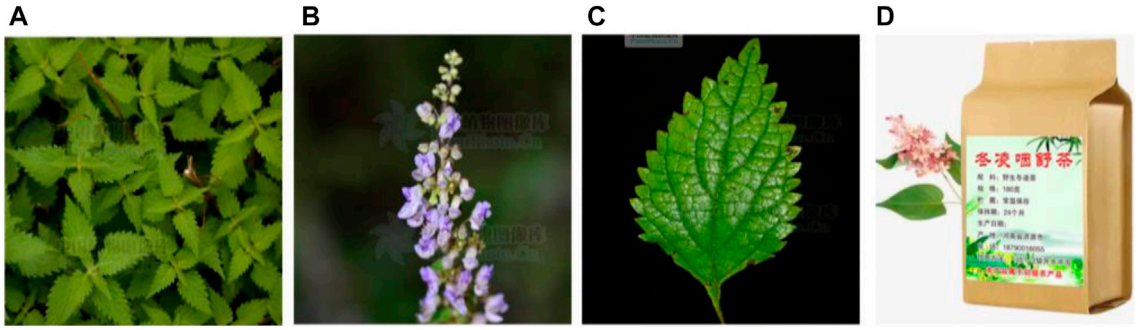

FIGURE 1 | The aerial part **(A)**, Plant flower **(B)**, Plant leaves **(C)** (http://ppbc.iplant.cn/), and *I. rubescens* tea **(D)**.

medicine (TCM) for sore throats, tonsillitis, laryngothralgia, colds, headaches, fever, heating, choking, nausea, tracheitis, chronic hepatitis, joint rheumatism, and snake and insect bites. It is also used alone or in combination with other herbs to treat cardiac cancer, liver cancer, lung cancer, prostate cancer, and bladder cancer in TCM (Feng et al., 2008). *I. rubescens* was first recorded in the "*Jiuhuang Bencao*" (simplified Chinese: 救荒本草) compiled by Zhu Xun in the Ming Dynasty (A.D. 1368–1644), it was often used as a wild vegetable in ancient China. In addition, many kinds of products related to *I. rubescens* such as *I. rubescens* tea, have been developed in the past decades.

In recent years, *I. rubescens* has received increasing attention due to the diverse chemical constituents and extensive biological activities, as well as its excellent clinical antitumor efficacy (Xue et al., 2007; Xiong, 2014). Previous phytochemical studies of *I. rubescens* have led to the identification of numerous diterpenoids, triterpenoids, phenols, alkaloids, volatile oils and other compounds. Its crude extract and some of its compounds have antitumor, anti-inflammatory, antibacterial, antioxidant, immunomodulatory, hypoglycemic, diarrheal and other biological activities (Han et al., 2003a). In particular, hundreds of enantio-kaurane and spirofo-kaurane diterpenes discovered in recent years are attracting increasing attention because of their novel structures and diverse biological activities. They have significant anti-proliferative, multidrug resistance (MDR) reversal properties as well as anti-inflammatory and anti-cardiovascular activities (Han, 2018).

To date, 324 compounds have been isolated and identified from *I. rubescens*. The main compound type are diterpenes of which the most representative one is oronidin (**1**). The results showed that oronidin has multiple biological activities and especially antitumor activity (Bae et al., 2014). However, the existing literature lacks a systematic review of traditional uses, toxicity, quality assessment, human studies, and newly discovered compounds of *I. rubescens*. In this review, in light of the widely recognized curative effect of *I. rubescens*, and hundreds of terpenoids with significant pharmacological activity have been isolated from *I. rubescens* in the past decades, we attempted to systematically and critically summarize the traditional uses, phytochemical constituents, pharmacological activity, quality evaluation, and toxicity of *I. rubescens* based on a database of scientific reports on human studies of *I. rubescens*. We believe that this review will provide important guidance for the further research and development of *I. rubescens* and its active components.

MATERIALS AND METHODS

Information for this review (until August 2021) was collected through several popular search engines and databases such as Web of Science, Scifinder Scholar, Google Scholar, ScienceDirect, ACS, PubMed, and classic texts of Chinese herbal medicines (e.g., *Jiuhuang Bencao*), and other web sources, such as the Flora of China, the Plant List, YaoZh website (https://db.yaozh.com/). The selection criteria of this article were: 1) Research involves the traditional application and modern pharmacological activity of *I. rubescens*; 2) research involves the preparation of crude extract and the separation and identification of monomer compounds; 3) research involves the determination of the activity of the crude extract and isolated compounds; 4) research involves the mechanism of action; 5) research involves the botany, toxicity, quality control, etc. Exclusion criteria of this review were: 1) Research did not properly address the topic of this review 2) research with obvious defects or unethical problems. Keywords used in the literature search were: "*I. rubescens,*" "冬凌草," "phytochemistry," "pharmacology," "biological activity," "traditional uses," "clinical trial," "safety," "quality control," "medicinal uses," "toxicology," and other related search terms. The chemical structures of these compounds isolated from *I. rubescens* were drawn using the software ChemBioDraw Ultra 14. 0 (The world's leading chemical structure drawing tool can draw various complex structural equations).

BOTANICAL DESCRIPTION AND TRADITIONAL USAGES

Botanical Description

According to the Flora of China, *I. rubescens* is a shrub of up to 1.2 m in height; Rootstock woody, stem erect, glabrous, branched with inflorescences, young branches very densely tomentose, purplish red. Cauline leaves opposite, base-wide cuneate, lateral veins on both sides very obvious, often purplish red;

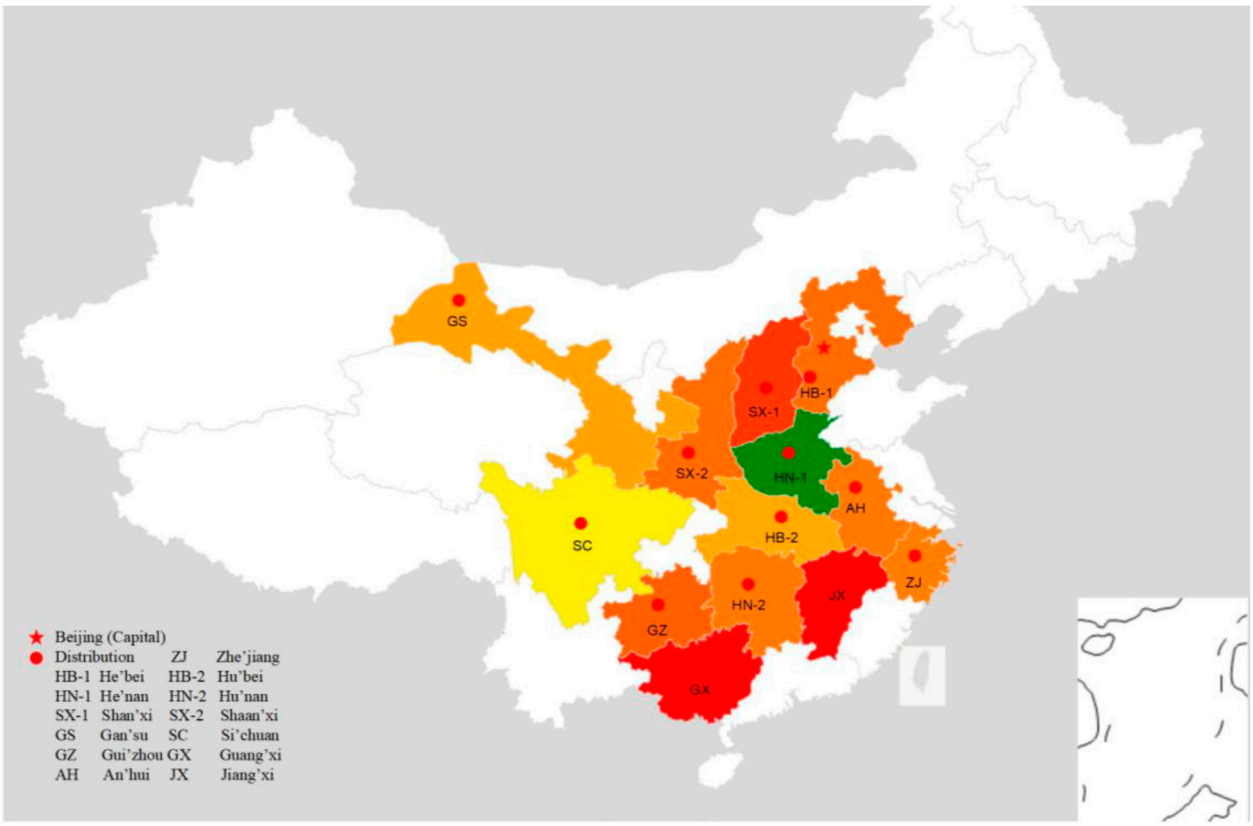

FIGURE 2 | The red spots in the map depicted the main region of *I. rubescens* distribution in China.

Petiole gradually shortening toward the top of stem and branch. Cymes, peduncles and peduncles, and rachis densely puberulent, but often purplish red; Bracts tapering upward, much beyond cyme in lower panicle, calyx campanulate, calyx teeth slightly two-lipped, fruity calyx enlarged, tubular campanulate, outer corolla sparsely puberulent and glandular, inner surface glabrous, shallow saccate above corolla tube, corolla eaves two-lipped, filaments flattened, styles filiform, disk annular. Obovate-trigonal nutlets flower from July to October, and bear fruits from August to November. *I. rubescens* is widely distributed in the Yellow River and Yangtze River basins in the provinces of Hu'bei, Si'chuan, Gui'zhou, Guang'xi, Shan'xi, Gan'su, Shaan'xi, He'nan, He'bei, Zhe'jiang, An'hui, Jiang'xi, and Hu'nan in China (**Figure 2**) (http://ppbc.iplant.cn/sp/222546). Its main production area is located in the southern part of the Taihang Mountain in Jiyuan, He'nan, with 1,400 hectares cultivation in 2015, and has been recognised as "National Geographical Indication Protected Product" since 2006. *I. rubescens* has been more used in the local owning to its high quality and clear efficacy. It may be related to the higher content of oridonin (**1**) and ponicidin (**2**) in the local *I. rubescens*.

Traditional Usages

The first known record of *I. rubescens* is found in "*Jiuhuang Bencao*" (simplified Chinese: 救荒本草) (Ming Dynasty, A.D. 1,406), which is an encyclopedia that specializes in endemic plants and combines edible aspects with famine relief. Moreover, *I. rubescens* is recorded in various versions of the Chinese Pharmacopoeia. In the Chinese pharmacopoeia 2020 edition, *I. rubescens* is sweet and bitter in a prescription and slightly cold after the drug acting on the body. To the lung, stomach, and liver meridian, it has the effects of clearing away heat, detoxification, activating blood and relieving pain, which are employed for the treatment of sore throats, scratches, snake bites and other diseases. In the Chinese Pharmacopoeia, the recommended dosage of *I. rubescens* is 30–60 g per day (China Pharmacopoeia, 2020). *I. rubescens* has also been included in many local herbal standards. For instance, according to the records of He'nan folks materia medica, *I. rubescens* is often used to treat sore throat, cold and headache, bronchitis, chronic hepatitis, rheumatism and joint pain, snake bites, as well as esophageal cancer, cardia cancer, liver cancer, lung cancer, prostate cancer, bladder cancer, colon cancer, cervical cancer and many other cancers.

According to the folk medicine from the Taihang Mountains area of China, "a bowl of *I. rubescens* can be consumed daily to prevent wrinkles, remove spots and nourish the appearance, brighten and clear the voice, and drive away the disease of the body and mind". Relatively few ancient prescriptions of *I. rubescens* are reported, but since the 1980s, the number of studies on *I. rubescens* has been increasing. *I. rubescens* related drugs and compatible formulations have emerged one after the

TABLE 1 | The prescriptions and efficacy indications of *I. rubescens* in China.

No	Preparation name	Main composition	Role of *I. rubescens* in prescription	Efficacy and indications	References
1	Donglingcao Diwan	*I. rubescens*	Leading role	Acute tonsillitis, acute pharyngitis, sore throat	Ren et al. (2009)
2	Donglingcao Pian	*I. rubescens*	Leading role	Tonsillitis, pharyngitis, stomatitis, hoarseness	Zhang et al. (2008)
3	Donglingcao Capsules	*I. rubescens*	Leading role	Acute and chronic tonsillitis, pharyngitis, laryngitis, stomatitis	Zhang, (2019)
4	Donglingcao Dispersible tablets	*I. rubescens*	Leading role	Acute and chronic tonsillitis, pharyngitis, laryngitis, stomatitis, cancer	Li et al. (2011)
5	Donglingcao tea	*I. rubescens*	Leading role	Pharyngitis, cancer prevention	Dai et al. (2015)
6	Fufang Donglingcao Lozenge	*I. rubescens, Mentha canadensis, Platycodon grandiflorus, Glycyrrhiza uralensis*	Leading role	Dryness, burning and pain in the pharynx, Chronic pharyngitis, oral ulcers	Deng and Lv, (2017)
7	Donglingcao Syrup	*I. Rubescens,* Sucrose, Sodium benzoate	Leading role	Chronic tonsillitis, pharyngitis, laryngitis, stomatitis	Li et al. (2001)
8	Yankang Lozenge	*I. Rubescens, Scrophularia ningpoensis*, *Ophiopogon japonicus, Platycodon grandiflorus, Glycyrrhiza uralensis*	Leading role	Acute and chronic pharyngitis caused by wind-heat in the lung meridian	Si et al. (1993)
9	Dongqie Granules	*Solanum melongena, I. rubescens*	Supporting role	Chronic bronchitis	Shi, (1984)
10	Donglingcao Toothpaste	*I. rubescens,* Glycerin, Sorbitol, Xylitol, Menthol	Leading role	Bleeding gums, periodontal abscess, caries	Yang and Shen, (1997)

other. The relevant ingredients and contents of the treatment of diseases are shown in **Table 1**. In clinical practice, *I. rubescens* is usually used alone or in combination with other TCM herbs. Many TCM herbs or classical prescriptions containing *I. rubescens* have been used in the form of decoction, powders, granules, tablets, pills and drop pills. For example, Fufang Donglingcao Lozenge, a representative classic formula containing *I. rubescens*, *Mentha canadensis*, *Platycodon grandiflorus,* and *Glycyrrhiza uralensis*, improves throat dryness, burning and pain, chronic pharyngitis, and oral ulcers (Deng and Lv, 2017). Overall, *I. rubescens* may be further studied and applied as a dietary supplement and therapeutic agent.

PHYTOCHEMICAL CONSTITUENTS

Many studies on the isolation and identification of *I. rubescens* have shown that *I. rubescens* contains a variety of secondary metabolites, including diterpenoids (**1**–**255**), triterpenoids (**256**–**266**), phenols (**267**–**301**), alkaloids (**302**–**311**), essential oils (**312**–**317**) and other compounds (**318**–**324**). The most important and abundant biologically active components isolated from *I. rubescens* are diterpenoids, which have excellent antitumor activity. These components should be considered as promising candidates for the future development. The phytochemicals present in *I. rubescens*, including their names, CAS numbers, formulas of the isolated compounds, are summarized in **Table 2**. The structures of compounds isolated from *I. rubescens* are illustrated in **Figure 3** showing that diterpenoids are the main components of *I. rubescens*. To document the advances in the pharmacological study of the listed compounds, these active compounds are shown in **Table 3**.

Diterpenoids

Diterpenoids are the main compounds identified from *I. rubescens*, and 255 diterpenoids have been isolated and identified from the whole plant of *I. rubescens*. Enantiokaurikane diterpenes are the most diverse type of terrestrial plant diterpenes with the most diverse molecular structures and biological activities among natural products. Recent studies have shown that some members of this family have antibacterial and antitumor activities. The structural feature of the enantiomer-kauritan type is that the rings A and B share two carbon atoms at positions 5 and 10, forming a bridged ring (Li et al., 2019). Such tetracyclic diterpene molecules can be transformed into complex molecular skeletons through intramolecular cyclization, oxidative cleavage and degradation rearrangement. Therefore, more than 1,500 natural enantiomer-kauritan diterpenoids have been isolated and identified. Among these enantiomer-kauritan diterpenoids, 7, 20-epoxy enantiomer kaureane diterpene has the largest number of isolated compounds and the best activity. The most widely studied enantiomer-kauritan diterpenoid is oridonin (**1**), and it has been reported that it has an inhibitory effect on a variety of tumor cells including liver cancer, laryngeal cancer, esophageal cancer, colon cancer, gastric cancer, breast cancer, leukemia, pancreatic cancer and other cancers. Oridonin also has anti-dementia, antidepressant, antibacterial and antiviral activities (Ding et al., 2016; Pi et al., 2017; Yang et al., 2018; Zhang D. et al., 2019). Among these bioactive constituents, oridonin (**1**), ponicidin (**2**), lushanrubescensin H (**46**), lushanrubescensin J (**48**), rabdosin A (**130**), isodocarpin (**135**), rabdoternin F (**152**), shikokianin (**153**), lasiodin (**154**), parvifoline AA (**161**), lasiodonin (**173**), lasiodoninacetonide (**175**), rosthorin (**203**), isojiangrubesin C (**227**), isojiangrubesin E (**229**), rabdoternin E (**234**), 11-O-acetylangustifolin (**236**), jaridonin (**246**), 14-O-acetyl-oridonin

TABLE 2 | The chemical constituents isolated from the *I. rubescens*.

No	Compounds	Molecular formula	CAS	Extracts	References
Diterpenoids					
1	rubescensin A	$C_{20}H_{28}O_6$	28957-04-2	EtOH	Cai, (2009)
2	rubescensin B	$C_{20}H_{26}O_6$	52617-37-5	EtOH	Cai, (2009)
3	rubescensin C	$C_{20}H_{30}O_6$	81661-34-9	EtOH	Cai, (2009)
4	rubescensin D	$C_{20}H_{26}O_6$	88907-93-1	EtOH	Cai, (2009)
5	rubescensin E	$C_{24}H_{34}O_7$	206659-93-0	EtOH	Cai, (2009)
6	rubescensin F	$C_{20}H_{30}O_7$	521930-43-8	EtOH	Cai, (2009)
7	rubescensin G	$C_{20}H_{30}O_7$	521930-45-0	EtOH	Cai, (2009)
8	rubescensin H	$C_{21}H_{30}O_7$	306996-29-2	EtOH	Cai, (2009)
9	rubescensin I	$C_{20}H_{32}O_4$	760948-08-1	Me_2CO	Feng et al. (2008)
10	rubescensin J	$C_{20}H_{30}O_3$	760948-09-2	Me_2CO	Feng et al. (2008)
11	rubescensin K	$C_{26}H_{39}NO_4$	760948-10-5	Me_2CO	Feng et al. (2008)
12	rubescensin L	$C_{26}H_{40}O_8$	760948-11-6	Me_2CO	Feng et al. (2008)
13	rubescensin M	$C_{40}H_{58}O_9$	760948-12-7	Me_2CO	Feng et al. (2008)
14	rubescensin N	$C_{19}H_{26}O_4$	602301-95-1	Me_2CO	Feng et al. (2008)
15	rubescensin O	$C_{21}H_{32}O_7$	602301-96-2	Me_2CO	Feng et al. (2008)
16	rubescensin P	$C_{20}H_{32}O_4$	760948-13-8	Me_2CO	Feng et al. (2008)
17	rubescensin Q	$C_{22}H_{32}O_6$	851868-64-9	Me_2CO	Feng et al. (2008)
18	rubescensin R	$C_{24}H_{34}O_8$	851868-65-0	Me_2CO	Feng et al. (2008)
19	rubescensin S	$C_{20}H_{28}O_7$	771485-56-4	Me_2CO	Feng et al. (2008)
20	rubescensin T	$C_{21}H_{30}O_7$	771531-48-7	Me_2CO	Feng et al. (2008)
21	rubescensin U	$C_{20}H_{28}O_6$	684278-34-0	Me_2CO	Feng et al. (2008)
22	rubescensin V	$C_{20}H_{28}O_6$	684278-35-1	Me_2CO	Feng et al. (2008)
23	xindongnin A	$C_2\ H_{32}O_7$	97230-44-9	Et_2O	Sun et al. (1985)
24	xindongnin B	$C_{22}H_{32}O_6$	97230-45-0	Et_2O	Sun et al. (1985)
25	xindongnin C	$C_{24}H_{34}O_7$	725718-96-7	Me_2CO	Feng et al. (2008)
26	xindongnin D	$C_{26}H_{38}O_8$	725718-97-8	Me_2CO	Feng et al. (2008)
27	xindongnin E	$C_{24}H_{36}O_7$	725718-98-9	Me_2CO	Feng et al. (2008)
28	xindongnin F	$C_{22}H_{32}O_6$	725718-99-0	Me_2CO	Feng et al. (2008)
29	xindongnin G	$C_{25}H_{38}O_8$	725719-00-6	Me_2CO	Feng et al. (2008)
30	xindongnin H	$C_{22}H_{30}O_6$	769923-93-5	Me_2CO	Feng et al. (2008)
31	xindongnin I	$C_{20}H_{28}O_5$	769923-94-6	Me_2CO	Feng et al. (2008)
32	xindongnin J	$C_{20}H_{28}O_5$	97230-60-9	Me_2CO	Feng et al. (2008)
33	xindongnin K	$C_{21}H_{32}O_6$	769923-95-7	Me_2CO	Feng et al. (2008)
34	xindongnin L	$C_{23}H_{34}O_7$	769923-96-8	Me_2CO	Feng et al. (2008)
35	xindongnin M	$C_{48}H_{70}O_{16}$	692740-04-8	Me_2CO	Feng et al. (2008)
36	xindongnin N	$C_{48}H_{68}O_{15}$	692740-05-9	Me_2CO	Feng et al. (2008)
37	xindongnin O	$C_{48}H_{68}O_{15}$	692740-06-0	Me_2CO	Feng et al. (2008)
38	xindongnin P	$C_{44}H_{64}O_{12}$	857642-15-0	Me_2CO	Feng et al. (2008)
39	lushanrubescensin A	$C_{28}H_{38}O_{10}$	93078-70-7	Et_2O	Liu et al. (2004a)
40	lushanrubescensin B	$C_{26}H_{36}O_9$	110325-77-4	Et_2O	Liu et al. (2004a)
41	lushanrubescensin C	$C_{28}H_{38}O_9$	110325-78-5	Et_2O	Liu et al. (2004a)
42	lushanrubescensin D	$C_{22}H_{32}O_6$	110325-79-6	Et_2O	Liu et al. (2004a)
43	lushanrubescensin E	$C_{24}H_{34}O_7$	114020-54-1	Et_2O	Liu et al. (2004a)
44	lushanrubescensin F	$C_2H_{32}O_7$	640284-51-1	Me_2CO	Feng et al. (2008)
45	lushanrubescensin G	$C_{20}H_{30}O_8$	640284-54-2	Me_2CO	Feng et al. (2008)
46	lushanrubescensin H	$C_{22}\ H_{30}O_6$	476640-22-9	Me_2CO	Feng et al. (2008)
47	lushanrubescensin I	$C_{22}H_{30}O_7$	640284-53-3	Me_2CO	Feng et al. (2008)
48	lushanrubescensin J	$C_{40}H_{52}O_{12}$	675603-42-6	Me_2CO	Feng et al. (2008)
49	taibairubescensin A	$C_{24}H_{34}O_7$	263910-37-8		Liu et al. (2004a)
50	taibairubescensin B	$C_{24}H_{34}O_7$	263910-38-9		Liu et al. (2004a)
51	taibairubescensin C	$C_{24}H_{34}O_7$	445256-93-9		Li et al. (2002)
52	hebeirubescensin A	$C_{26}H_{37}NO_8$	887333-23-5	Me_2CO	Huang et al. (2006)
53	hebeirubescensin B	$C_{25}H_{38}O_7$	887333-24-6	Me_2CO	Huang et al. (2006)
54	Hebeirubescensin C	$C_{25}H_{38}O_7$	887333-25-7	Me_2CO	Huang et al. (2006)
55	hebeirubescensin D	$C_{26}H_{34}O_7$	887333-26-8	Me_2CO	Huang et al. (2006)
56	hebeirubescensin E	$C_{25}H_{38}O_7$	887333-27-9	Me_2CO	Huang et al. (2006)
57	hebeirubescensin F	$C_{25}H_{40}O_7$	887333-28-0	Me_2CO	Huang et al. (2006)
58	hebeirubescensin G	$C_{20}H_{28}O_7$	887333-29-1	Me_2CO	Huang et al. (2006)
59	hebeirubescensin H	$C_{20}H_{28}O_7$	887333-30-4	Me_2CO	Huang et al. (2006)
60	hebeirubescensin I	$C_{21}H_{32}O_7$	887333-31-5	Me_2CO	Huang et al. (2006)
61	hebeirubescensin J	$C_{21}H_{32}O_6$	887333-32-6	Me_2CO	Huang et al. (2006)
62	hebeirubescensin K	$C_{20}H_{30}O_6$	887333-33-7	Me_2CO	Huang et al. (2006)

(Continued on following page)

TABLE 2 | (*Continued*) The chemical constituents isolated from the *I. rubescens*.

No	Compounds	Molecular formula	CAS	Extracts	References
63	hebeirubescensin L	$C_{26}H_{36}O_8$	887333-34-8	Me_2CO	Huang et al. (2006)
64	ludongnin A	$C_{20}H_{24}O_6$	93377-47-0	Et_2O	Liu et al. (2004a)
65	ludongnin B	$C_{20}H_{26}O_5$	110325-75-2	Et_2O	Liu et al. (2004a)
66	ludongnin C	$C_{20}H_{26}O_5$	609341-96-0	Et_2O	Liu et al. (2004a)
67	ludongnin D	$C_{20}H_{26}O_5$	609341-97-1	Et_2O	Liu et al. (2004a)
68	ludongnin E	$C_{20}H_{26}O_6$	100595-89-9	Et_2O	Liu et al. (2004a)
69	ludongnin F	$C_{21}H_{30}O_5$	623943-55-5	Me_2CO	Feng et al. (2008)
70	ludongnin G	$C_{21}H_{30}O_5$	623943-56-6	Me_2CO	Feng et al. (2008)
71	ludongnin H	$C_{21}H_{30}O_5$	623943-57-7	Me_2CO	Feng et al. (2008)
72	ludongnin I	$C_{21}H_{30}O_5$	623943-58-8	Me_2CO	Feng et al. (2008)
73	ludongnin J	$C_{21}H_{28}O_5$	623943-59-9	Me_2CO	Feng et al. (2008)
74	guidongnins A	$C_{20}H_{26}O_6$	119968-13-7	Me_2CO	Han et al. (2003b)
75	guidongnins B	$C_{20}H_{26}O_5$	596096-11-6	Me_2CO	Han et al. (2003b)
76	guidongnins C	$C_{20}H_{26}O_6$	93377-70-9	Me_2CO	Han et al. (2003b)
77	guidongnins D	$C_{20}H_{26}O_7$	596096-12-7	Me_2CO	Han et al. (2003b)
78	guidongnins E	$C_{20}H_{28}O_5$	102274-01-1	Me_2CO	Han et al. (2003b)
79	guidongnins F	$C_{20}H_{28}O_5$	596096-13-8	Me_2CO	Han et al. (2003b)
80	guidongnins G	$C_{20}H_{28}O_6$	596096-14-9	Me_2CO	Han et al. (2003b)
81	guidongnins H	$C_{21}H_{30}O_5$	596096-15-0	Me_2CO	Han et al. (2003b)
82	hebeiabinin A	$C_{20}H_{26}O_5$	934832-64-1	Me_2CO	Huang et al. (2007)
83	hebeiabinin B	$C_{20}H_{34}O_5$	934832-65-2	Me_2CO	Huang et al. (2007)
84	hebeiabinin C	$C_{20}H_{28}O_3$	934832-66-3	Me_2CO	Huang et al. (2007)
85	hebeiabinin D	$C_{40}H_{60}O_{11}$	934832-67-4	Me_2CO	Huang et al. (2007)
86	hebeiabinin E	$C_{40}H_{56}O_9$	934832-68-5	Me_2CO	Huang et al. (2007)
87	kaurine A	$C_{20}H_{27}NO_5$	1646821-73-9	EtOH	Liu, (2012)
88	kaurine B	$C_{20}H_{27}NO_5$	1646821-74-0	EtOH	Liu, (2012)
89	kaurine C	$C_{24}H_{33}NO_8$	1646821-75-1	EtOH	Liu, (2012)
90	jianshirubesin A	$C_{20}H_{28}O_7$	1476061-46-7	EtOH	Liu, (2012)
91	jianshirubesin B	$C_{20}H_{28}O_7$	1476061-47-8	EtOH	Liu, (2012)
92	jianshirubesin C	$C_{20}H_{28}O_8$	1476061-48-9	EtOH	Liu, (2012)
93	jianshirubesin D	$C_{20}H_{26}O_6$	1418183-49-9	EtOH	Liu, (2012)
94	jianshirubesin E	$C_{20}H_{28}O_6$	1418183-50-2	EtOH	Liu, (2012)
95	jianshirubesin F	$C_{20}H_{28}O_5$	1418183-51-3	EtOH	Liu, (2012)
96	jianshirubesin G	$C_{20}H_{32}O_4$	1621268-64-1	EtOH	Liu, (2012)
97	jianshirubesin H	$C_{26}H_{34}O_9$	1621268-65-2	EtOH	Liu, (2012)
98	jianshirubesin I	$C_{22}H_{30}O_7$	1621268-66-3	EtOH	Liu, (2012)
99	jianshirubesin J	$C_{20}H_{26}O_6$		EtOH	Liu, (2012)
100	jianshirubesin K	$C_{22}H_{30}O_6$		EtOH	Liu, (2012)
101	jianshirubesin L	$C_{24}H_{34}O_8$		EtOH	Liu, (2012)
102	jianshirubesin M	$C_{24}H_{36}O_8$		EtOH	Liu, (2012)
103	hubeirubesin A	$C_{22}H_{32}O_6$	1578156-49-6	EtOH	Liu, (2012)
104	hubeirubesin B	$C_{24}H_{32}O_6$	1578156-51-0	EtOH	Liu, (2012)
105	hubeirubesin C	$C_{28}H_{36}O_{10}$		EtOH	Liu, (2012)
106	hubeirubesin D	$C_{26}H_{34}O_{10}$		EtOH	Liu, (2012)
107	hubeirubesin E	$C_{28}H_{40}O_{10}$		EtOH	Liu, (2012)
108	hubeirubesin F	$C_{24}H_{34}O_9$		EtOH	Liu, (2012)
109	hubeirubesin G	$C_{23}H_{34}O_8$		EtOH	Liu, (2012)
110	hubeirubesin H	$C_{26}H_{36}O_8$		EtOH	Liu, (2012)
111	hubeirubesin I	$C_{26}H_{36}O_9$		EtOH	Liu, (2012)
112	hubeirubesin J	$C_{24}H_{34}O_8$		EtOH	Liu, (2012)
113	hubeirubesin K	$C_{24}H_{34}O_8$		EtOH	Liu, (2012)
114	hubeirubesin L	$C_{24}H_{34}O_7$		EtOH	Liu, (2012)
115	hubeirubesin M	$C_{24}H_{32}O_8$		EtOH	Liu, (2012)
116	hubeirubesin N	$C_{20}H_{30}O_7$		EtOH	Liu, (2012)
117	hubeirubesin O	$C_{20}H_{30}O_7$		EtOH	Liu, (2012)
118	hubeirubesin P	$C_{22}H_{33}O_6$		EtOH	Liu, (2012)
119	hubeirubesin Q	$C_{22}H_{32}O_5$		EtOH	Liu, (2012)
120	hubeirubesin R	$C_{20}H_{30}O_7$		EtOH	Liu, (2012)
121	hubeirubesin S	$C_{24}H_{34}O_8$		EtOH	Liu, (2012)
122	hubeirubesin T	$C_{20}H_{28}O_6$		EtOH	Liu, (2012)
123	hubeirubesin U	$C_{22}H_{32}O_6$		EtOH	Liu, (2012)
124	hubeirubesin V	$C_{20}H_{28}O_6$		EtOH	Liu, (2012)
125	hubeirubesin W	$C_{24}H_{34}O_9$		EtOH	Liu, (2012)
126	hubeirubesin X	$C_{20}H_{30}O_6$		EtOH	Liu, (2012)

(Continued on following page)

TABLE 2 | (*Continued*) The chemical constituents isolated from the *I. rubescens*.

No	Compounds	Molecular formula	CAS	Extracts	References
127	hubeirubesin Y	$C_{20}H_{32}O_6$		EtOH	Liu, (2012)
128	hubeirubesin Z	$C_{22}H_{32}O_6$		EtOH	Liu, (2012)
129	epinodosin	$C_{20}H_{26}O_6$	20086-60-6	EtOH	Liu, (2012)
130	rabdosin A	$C_{21}H_{28}O_6$	84304-91-6	EtOH	Liu, (2012)
131	enmein	$C_{20}H_{26}O_6$	3776-39-4	EtOH	Liu, (2012)
132	rabdosichuanin	$C_{20}H_{27}O_6$		EtOH	Liu, (2012)
133	taibaijaponicain A	$C_{21}H_{30}O_7$	C21H28O6	EtOH	Liu, (2012)
134	maoyecrystal K	$C_{21}H_{30}O_7$	791837-58-6	EtOH	Liu, (2012)
135	isodocarpin	$C_{20}H_{26}O_5$	10391-08-9	EtOH	Liu, (2012)
136	6β,15α-dihydroxy-6,7-seco-6,20-epoxy-1α, 7-olide-ent-kaur-16-ene	$C_{19}H_{28}O_6$		EtOH	Liu, (2012)
137	epinodosinol	$C_{20}H_{28}O_6$	27548-88-5	EtOH	Liu, (2012)
138	6α,15α-dihydroxy-20-aldehyde-6,7-seco-6, 11α-epoxy-ent-kaur 16-en-1α,7-olide	$C_{20}H_{25}O_6$		EtOH	Liu, (2012)
139	laxiflorin C	$C_{20}H_{26}O_5$	165337-72-4	EtOH	Liu, (2012)
140	laxiflorin D	$C_{20}H_{24}O_5$	319914-45-9	EtOH	Liu, (2012)
141	laxiflorin E	$C_{20}H_{26}O_5$	388122-19-8	EtOH	Liu, (2012)
142	rubescensin W	$C_{21}H_{30}O_6$	780773-93-5	EtOH	Liu, (2012)
143	6β,7β,14β,15β,tetrahy-droxy-7α,20-epoxy-ent-kaur-16-ene	$C_{20}H_{30}O_5$	167894-11-3	EtOH	Liu, (2012)
144	maoecrystal X	$C_{22}H_{32}O_6$	887471-86-5	EtOH	Liu, (2012)
145	maoyecrystal F	$C_{24}H_{34}O_7$	79854-99-2	EtOH	Liu, (2012)
146	acetonide of maoyecrystal F	$C_{22}H_{32}O_7$	664327-95-1	EtOH	Liu, (2012)
147	wikstroemioidin B	$C_{23}H_{34}O_6$	152511-36-9	EtOH	Liu, (2012)
148	rabdoternin A	$C_{20}H_{28}O_6$	128887-80-9	EtOH	Liu, (2012)
149	rabdoternin B	$C_{20}H_{28}O_7$	128887-81-0	EtOH	Liu, (2012)
150	rabdoternin C	$C_{24}H_{34}O_7$	128887-82-1	EtOH	Li et al. (2019)
151	rabdoternin D	$C_{22}H_{32}O_7$	155969-81-6	EtOH	Liu, (2012)
152	rabdoternin F	$C_{21}H_{30}O_7$	155977-87-0	EtOH	Liu, (2012)
153	shikokianin	$C_{24}H_{32}O_8$	24267-69-4	EtOH	Liu, (2012)
154	lasiodin	$C_{22}H_{30}O_7$	28957-08-6	EtOH	Liu, (2012)
155	lasiokaurinol	$C_{22}H_{32}O_7$	52718-05-5	EtOH	Liu, (2012)
156	enmenin	$C_{24}H_{34}O_7$	23811-50-9	EtOH	Liu, (2012)
157	enmenin monoacetate	$C_{26}H_{36}O_8$	23807-57-0	EtOH	Liu, (2012)
158	rabdolongin A	$C_{24}H_{34}O_8$	117229-55-7	EtOH	Liu, (2012)
159	parvifoline F	$C_{20}H_{26}O_6$	882673-14-5	EtOH	Liu, (2012)
160	odonicin	$C_{24}H_{30}O_7$	51419-51-3	EtOH	Liu, (2012)
161	parvifoline AA	$C_{20}H_{26}O_5$	934370-61-3	EtOH	Liu, (2012)
162	ent-abierubesin A	$C_{20}H_{32}O_5$	1578156-42-9	EtOH	Liu, (2012)
163	ent-abierubesin B	$C_{20}H_{34}O_5$	1578156-43-0	EtOH	Liu, (2012)
164	ent-abierubesin C	$C_{20}H_{32}O_4$	1578156-45-2	EtOH	Liu, (2012)
165	ent-abierubesin D	$C_{20}H_{32}O_4$	1578156-46-3	EtOH	Liu, (2012)
166	ent-abierubesin E	$C_{21}H_{32}O_7$	1578156-47-4	EtOH	Liu, (2012)
167	ent-abienervonin C	$C_{20}H_{32}O_5$	1132681-75-4	EtOH	Liu, (2012)
168	rabdoepigibberellolide	$C_{26}H_{34}O_9$	81398-21-2	EtOH	Liu, (2012)
169	neolaxiflorin U	$C_{22}H_{32}O_7$	1821199-19-2	EtOH	Shu et al. (2017)
170	epinodosinol	$C_{20}H_{28}O_6$	27548-88-5	EtOH	Shu et al. (2017)
171	rabdokaurin C	$C_{24}H_{34}O_8$	150148-80-4	EtOH	Lu et al. (2007)
172	lasiokaurinol	$C_{22}H_{32}O_7$	52718-05-5	EtOH	Lu et al. (2007)
173	lasiodonin	$C_{20}H_{28}O_6$	38602-52-7	EtOH	Lu et al. (2007)
174	lasiokaurin	$C_{22}H_{30}O_7$	28957-08-6	EtOH	Song et al. (2011)
175	lasiodonin acetonide	$C_{23}H_{32}O_6$	851860-25-8	EtOH	Feng et al. (2008)
176	bisrubescensin A	$C_{43}H_{60}O_{13}$	878481-77-7	Me_2CO	Feng et al. (2008)
177	bisrubescensin B	$C_{40}H_{58}O_{13}$	878481-78-8	Me_2CO	Feng et al. (2008)
178	bisrubescensin C	$C_{40}H_{56}O_{12}$	878481-79-9	Me_2CO	Feng et al. (2008)
179	bisrubescensin D	$C_{40}H_{56}O_{13}$	1052120-55-4	EtOH	Lu et al. (2008)
180	rubescrystal A	$C_{22}H_{28}O_7$		Me_2CO	Xie, (2012)
181	rubescrystal B	$C_{20}H_{24}O_6$		Me_2CO	Xie, (2012)
182	glaucocalactone	$C_{22}H_{26}O_7$	123086-85-1	Me_2CO	Xie, (2012)
183	rabdonervosin B	$C_{21}H_{30}O_6$	248256-56-6	Me_2CO	Xie, (2012)
184	acetonide of rubescensin J	$C_{20}H_{26}O_6$		Me_2CO	Xie, (2012)
185	maoyecrystal F	$C_{22}H_{32}O_7$	664327-95-1	Me_2CO	Xie, (2012)
186	1-α-O-β-D-glucopyran-osyl-enmenol	$C_{26}H_{40}O_6$		Me_2CO	Xie, (2012)
187	acetonide of maoyecrystal F	$C_{25}H_{36}O_7$		Me_2CO	Xie, (2012)

(Continued on following page)

TABLE 2 | (*Continued*) The chemical constituents isolated from the *I. rubescens*.

No	Compounds	Molecular formula	CAS	Extracts	References
188	melissoidesin G	$C_{24}H_{34}O_7$	256448-82-5	Me_2CO	Feng et al. (2008)
189	dawoensin A	$C_{26}H_{36}O_8$	137661-09-7	Me_2CO	Feng et al. (2008)
190	glabcensin V	$C_{24}H_{34}O_7$	197389-19-8	Me_2CO	Feng et al. (2008)
191	angustifolin	$C_{14}H_{14}O_3$	56881-08-4	Me_2CO	Feng et al. (2008)
192	6-epiangustifolin	$C_{21}H_{28}O_6$	369390-94-3	Me_2CO	Feng et al. (2008)
193	sculponeatin J	$C_{20}H_{24}O_5$	477529-69-4	Me_2CO	Feng et al. (2008)
194	enmenol	$C_{20}H_{30}O_6$	28957-06-4	EtOH	Cai, (2009)
195	dayecrystals B	$C_{21}H_{32}O_7$	926010-25-5	EtOH	Cai, (2009)
196	rabdosianin A	$C_{26}H_{36}O_9$	80138-69-8	MeOH	Li W et al. (2019)
197	parvifoline G	$C_{26}H_{34}O_9$	882673-16-7	MeOH	Li et al. (2019)
198	suimiyain A	$C_{22}H_{32}O_6$	143086-37-7	EtOH	Liu et al. (2004a)
199	effusanin E	$C_{20}H_{28}O_6$	76470-15-0	EtOH	Liu et al. (2004a)
200	jaridon 6	$C_{20}H_{24}O_5$		EtOH	Han, (2018)
201	16,17-exoepoxide-oridonin	$C_{20}H_{27}O_5$		EtOH	Bai N S. et al. (2010)
202	11,15-O,O-diacetyl-rabdoternins D	$C_{26}H_{36}O_9$		EtOH	Bai N S. et al. (2010)
203	rosthorin	$C_{20}H_{28}O_6$	93772-27-1	EtOH	Bai N S. et al. (2010)
204	isolushinin A	$C_{20}H_{28}O_3$	1233704-08-9	Me_2CO	Luo et al. (2010)
205	isolushinin B	$C_{22}H_{32}O_6$	1233704-09-0	Me_2CO	Luo et al. (2010)
206	isolushinin C	$C_{20}H_{30}O_5$	1233704-10-3	Me_2CO	Luo et al. (2010)
207	isolushinin D	$C_{23}H_{32}O_6$	1233704-11-4	Me_2CO	Luo et al. (2010)
208	isolushinin E	$C_{23}H_{34}O_6$	1233704-12-5	Me_2CO	Luo et al. (2010)
209	isolushinin F	$C_{21}H_{30}O_6$	1233704-13-6	Me_2CO	Luo et al. (2010)
210	isolushinin G	$C_{22}H_{32}O_7$	1233704-14-7	Me_2CO	Luo et al. (2010)
211	isolushinin H	$C_{22}H_{32}O_6$	1233704-15-8	Me_2CO	Luo et al. (2010)
212	isolushinin I	$C_{22}H_{32}O_7$	1233704-16-9	Me_2CO	Luo et al. (2010)
213	isolushinin J	$C_{20}H_{30}O_6$	1233704-17-0	Me_2CO	Luo et al. (2010)
214	luanchunin A	$C_{20}H_{28}O_5$	1242434-16-7	EtOH	Zhang et al. (2010a)
215	luanchunin B	$C_{20}H_{30}O_4$	1242434-17-8	EtOH	Zhang et al. (2010b)
216	rubluanin A	$C_{23}H_{34}O_6$	1252578-83-8	Me_2CO	Zhang et al. (2010a)
217	rubluanin B	$C_{21}H_{32}O_5$	1252578-85-0	Me_2CO	Zhang et al. (2010b)
218	rubluanin C	$C_{21}H_{32}O_5$	1252578-87-2	Me_2CO	Zhang et al. (2010a)
219	rubluanin D	$C_{21}H_{32}O_7$	1252578-88-3	Me_2CO	Zhang et al. (2010b)
220	rubesanolide A	$C_{20}H_{30}O_4$	1275523-36-8	MeOH	Zou et al. (2011)
221	rubesanolide B	$C_{20}H_{30}O4$	1275523-41-5	MeOH	Zou et al. (2011)
222	15α-acetoxyl-6,11α-epoxy-6α-hydroxy-20-oxo-6, 7-secoent-kaur-16-en-1,7-olide	$C_{22}H_{28}O_7$		Me_2CO	Xie et al. (2011)
223	15α-hydroxy-20-oxo-6,7-seco-ent-kaur-16-en-1, 7α(6,11α)-diolide	$C_{20}H_{24}O_6$		Me_2CO	Xie et al. (2011)
224	bisrubescensin E	$C_{40}H_{54}O_{13}$	1422357-49-0	MeOH	Lu and Liang, (2012)
225	isojiangrubesin A	$C_{22}H_{34}O_8$		Me_2CO	Zhang L et al. (2017)
226	isojiangrubesin B	$C_{21}H_{30}O_6$		Me_2CO	Zhang Y et al. (2017)
227	isojiangrubesin C	$C_{21}H_{30}O_6$		Me_2CO	Zhang L et al. (2017)
228	isojiangrubesin D	$C_{20}H_{30}O_6$		Me_2CO	Zhang Y et al. (2017)
229	isojiangrubesin E	$C_{24}H_{36}O_7$		Me_2CO	Zhang L et al. (2017)
230	isojiangrubesin F	$C_{24}H_{38}O_7$		Me_2CO	Zhang Y et al. (2017)
231	isojiangrubesin G	$C_{24}H_{38}O_7$		Me_2CO	Zhang L et al. (2017)
232	20(R)-6β,7β,15β-trihydroxy-20-methoxy-7α, 20-epoxy-entkaur-16-en-1α,11β-acetonide	$C_{24}H_{36}O_7$		Me_2CO	Zhang Y et al. (2017)
233	nervosanin A	$C_{21}H_{32}O_6$		Me_2CO	Zhang L et al. (2017)
234	rabdoternin E	$C_{21}H_{30}O_7$	155969-82-7	Me_2CO	Zhang Y et al. (2017)
235	6- epi-11-O-acetylangustifolin	$C_{23}H_{30}O_7$		MeOH	Luo et al. (2017)
236	11- O-acetylangustifolin	$C_{23}H_{30}O_7$		MeOH	Luo et al. (2017)
237	isodonrubescin A	$C_{22}H_{32}O_7$		EtOH	Wen et al. (2019)
238	isodonrubescin B	$C_{22}H_{32}O_7$		EtOH	Wen et al. (2019)
239	isodonrubescin C	$C_{22}H_{32}O_7$		EtOH	Wen et al. (2019)
240	isodonrubescin D	$C_{22}H_{32}O_7$		EtOH	Wen et al. (2019)
241	isodonrubescin E	$C_{22}H_{32}O_7$		EtOH	Wen et al. (2019)
242	isodonrubescin F	$C_{20}H_{28}O_5$		EtOH	Wen et al. (2019)
243	rubesanolide C	$C_{20}H_{30}O_4$		MeOH	Zou et al. (2012)
244	rubesanolide D	$C_{20}H_{30}O_3$		MeOH	Zou et al. (2012)
245	rubesanolide E	$C_{20}H_{30}O_2$		MeOH	Zou et al. (2012)
246	jaridonin	$C_{22}H_{32}O_5$	944826-54-4	Me_2CO	Ma et al. (2013)
247	14-O-acetyl-oridonin	$C_{22}H_{31}O_7$		EtOH	Bai N S. et al. (2010)
248	isodonoiol	$C_{22}H_{30}O_7$	82460-75-1	Me_2CO	Han et al. (2003d)

(Continued on following page)

TABLE 2 | (*Continued*) The chemical constituents isolated from the *I. rubescens*.

No	Compounds	Molecular formula	CAS	Extracts	References
249	isodonal	$C_{22}H_{28}O_7$	16964-56-0	Me_2CO	Han et al. (2003d)
250	rabdosin B	$C_{24}H_{32}O_8$	84304-92-7	Me_2CO	Han et al. (2003d)
251	effusanin A	$C_{20}H_{28}O_5$	30220-43-0	Me_2CO	Zhang L et al. (2017)
252	longikaurin A	$C_{20}H_{28}O_5$	75207-67-9	Me_2CO	Zhang Y et al. (2017)
253	xerophinoid B	$C_{21}H_{30}O_6$	946822-57-7	Me_2CO	Zhang L et al. (2017)
254	7,14-O-(1-methylethy-lidene) oridonin	$C_{23}H_{32}O_6$	331282-94-1	Me_2CO	Zhang Y et al. (2017)
255	3β-hydroxy-6β-methoxy-6,7-seco-6,20-epoxy-1α, 7-olide-ent-kaur-16-en-15-one	$C_{21}H_{28}O_6$		EtOH	Wen et al. (2019)
Triterpenes					
256	ursolic acid	$C_{30}H_{48}O_3$	77-52-1	EtOH	Cai, (2009)
257	oleanic acid	$C_{30}H_{48}O_3$	508-02-1	EtOH	Cai, (2009)
258	β-Sitosterol	$C_{29}H_{50}O$	64997-52-0	EtOH	Cai, (2009)
259	α-Amyrin	$C_{30}H_{50}O$	638-95-9	EtOH	Cai, (2009)
260	daucosterol	$C_{35}H_{60}O_6$	474-58-8	EtOH	Cai, (2009)
261	betulin	$C_{30}H_{50}O_2$	473-98-3	MeOH	Li et al. (2019)
262	betulinic acid	$C_{30}H_{48}O_3$	472-15-1	MeOH	Li W et al. (2019)
263	eryihrodiol	$C_{30}H_{50}O_2$	545-48-2	MeOH	Li et al. (2019)
264	friedelin	$C_{30}H_{50}O$	559-74-0	EtOH	Lu et al. (2013)
265	stigmasterol	$C_{29}H_{48}O$	83-48-7	EtOH	Yan et al. (2006)
266	2α,3α-dihydroxy-urs-12-en-28-oic acid	$C_{30}H_{48}O_4$		EtOH	Cai et al. (2008)
Polyphenols					
267	salicylic acid	$C_7H_6O_3$	69-72-7	Me_2CO	Feng et al. (2008)
268	caffeic acid	$C_9H_8O_4$	331-39-5	Me_2CO	Feng et al. (2008)
269	rosmarinic acid	$C_{18}H_{16}O_8$	20283-92-5	Me_2CO	Feng et al. (2008)
270	methyl rosmarinate	$C_{19}H_{18}O_8$	99353-00-1	Me_2CO	Feng et al. (2008)
271	danshensu	$C_9H_{10}O_5$	76822-21-4	Me_2CO	Feng et al. (2008)
272	chlorogenic acid	$C_{16}H_{18}O_9$	327-97-9	EtOH	Du, (2008)
273	p-Hydroxybenzalde-hyde	$C_7H_6O_2$	123-08-0	EtOH	Song et al. (2011)
274	acetovanillone	$C_9H_{10}O_3$	498-02-2	Me_2CO	Xie, (2012)
275	protocatechualdehyde	$C_7H_6O_3$	139-85-5	EtOH	Lu et al. (2007)
276	ferulic Acid	$C_{10}H_{10}O_4$	1,135-24-6	EtOH	Lu et al. (2007)
277	vanillic acid	$C_8H_8O_4$	121-34-6	EtOH	Lu et al. (2007)
Flavonoids					
278	cirsiliol	$C_{17}H_{14}O_7$	34334-69-5	EtOH	Cai, (2009)
279	pedalitin	$C_{16}H_{12}O_7$	22384-63-0	EtOH	Yan et al. (2006)
280	quercetin	$C_{15}H_{10}O_7$	117-39-5	Me_2CO	Gao and Wang, (2014)
281	sideritoflavone	$C_{18}H_{16}O_8$	70360-12-2	Me_2CO	Gao and Wang, (2014)
282	quercetin 3-O-rutinoside	$C_{27}H_{30}O_{16}$	949926-49-2	Me_2CO	Gao and Wang, (2014)
283	kaempferol 3,7-dirhamnoside	$C_{27}H_{30}O_{14}$	482-38-2	Me_2CO	Gao and Wang, (2014)
284	quercitrin	$C_{21}H_{20}O_{11}$	522-12-3	Me_2CO	Gao and Wang, (2014)
285	isorhamnetin	$C_{16}H_{12}O_7$	480-19–3	Me_2CO	Gao and Wang, (2014)
286	kaempferol 3-O-α-L-Rhamnoside	$C_{21}H_{20}O_{10}$	482-39-3	Me_2CO	Gao and Wang, (2014)
287	gardenin D	$C_{19}H_{18}O_8$	29202-00-4	Me_2CO	Gao and Wang, (2014)
288	5,3′,4′ -trihydroxy- 6,7,8 trimethoxy flavone	$C_{18}H_{16}O_8$		Me_2CO	Gao and Wang, (2014)
289	kaempferol - 3,7 -O-α-L -dirhamnoside	$C_{27}H_{30}O_{14}$	482-38-2	Me_2CO	Gao and Wang, (2014)
290	apigenin -6,8 -di -C-β-D-glucopyranoside	$C_{27}H_{30}O_{17}$		Me_2CO	Gao and Wang, (2014)
291	5-Hydroxyl-3′4′6,7-Tetramethoxyflavone	$C_{19}H_{18}O_7$		EtOH	Song et al. (2011)
292	5- Hydroxyl - 3′4′ 7 - Trimethoxyflavonoid	$C_{18}H_{16}O_6$		EtOH	Song et al. (2011)
293	4′, 5, 7 - Trimethoxy flavonoid	$C_{18}H_{16}O_5$		EtOH	Song et al. (2011)
294	5, 8, 4-trihydroxyl-6, 7, 3-trimethoxyl-flavone	$C_{18}H_{16}O_8$		EtOH	Lu et al. (2013)
295	Tricin	$C_{17}H_{14}O_7$	520-32-1	EtOH	Lu et al. (2013)
296	5, 3′, 4′ - trihydroxy-6, 7, 8-trimethoxyflavone	$C_{18}H_{16}O_8$		Me_2CO	Han et al. (2003c)
297	5, 4′ - trihydroxy-6,7, 8, 3′- trimethoxy- flavone	$C_{19}H_{18}O_8$		MeOH	Wang et al. (2010)
298	quercetin	$C_{15}H_{10}O_7$	117-39-5	EtOH	Lu et al. (2007)
299	nodifloretin	$C_{16}H_{12}O_7$	23494-48-6		Bai N et al. (2010)
300	penduletin	$C_{18}H_{16}O_7$	569-80-2		Bai N et al. (2010)
301	luteolin	$C_{15}H_{10}O_6$	491-70-3		Bai N et al. (2010)
Alkaloids					
302	donglingine	$C_{15}H_{19}N_3O_5$		Me_2CO	Guo et al. (2010)
303	aurantiamide acetate	$C_{28}H_{30}N_2O_4$		Me_2CO	Guo et al. (2010)
304	*N*-(2-Aminoformyl-Phenyl)-2-hydroxybenzamide-5- O-β-D-allopyranoside	$C_{20}H_{22}N_2O_9$		EtOH	Liu et al. (2004b)
305	2- amino-3-phenylpropyl-2-benzamido-3-phenylpropanoate	$C_{25}H_{26}N_2O_3$		Me_2CO	Guo et al. (2010)

(Continued on following page)

TABLE 2 | (*Continued*) The chemical constituents isolated from the *I. rubescens*.

No	Compounds	Molecular formula	CAS	Extracts	References
306	4-Acetamidobutyric acid	$C_6H_{11}NO_3$	3025-96-5	Me_2CO	Guo et al. (2010)
307	2,6-Dihydroxypurine	$C_5H_4N_4O_2$	69-89-6	Me_2CO	Guo et al. (2010)
308	7- Hydroxy-2-(1H)-quinolinone	$C_9H_9NO_2$	22246-18-0	Me_2CO	Guo et al. (2010)
309	pheophytin A	$C_{55}H_{74}N_4O_5$	603-17-8	EtOH	Lu and Xu (2008)
310	pheophytin B	$C_{55}H_{72}N_4O_6$	3147-18-0	EtOH	Lu and Xu (2008)
311	Urasil	$C_4H_4N_2O_2$	66-22-8	EtOH	Cai et al. (2008)
Monoterpenes and sesquiterpenes					
312	α-Pinene	$C_{10}H_{61}$	80-56-8	EtOH	Cai, (2009)
313	β-Pinene	$C_{10}H_{16}$	2437-95-8	EtOH	Cai, (2009)
314	cinene	$C_{10}H_{16}$	138-86-3	EtOH	Cai, (2009)
315	1,8-Cineole	$C_{10}H_{18}O$	470-82-6	EtOH	Cai, (2009)
316	p-Cymene	$C_{10}H_{14}$	99-87-6	EtOH	Cai, (2009)
317	β-Elemene	$C_{15}H_{24}$	515-13-9	EtOH	Cai, (2009)
Other Compounds					
318	nonanal	$C_9H_{18}O$	124-19-6	EtOH	Cai, (2009)
319	decanal	$C_{10}H_{20}O$	112-31-2	EtOH	Cai, (2009)
320	palmitic acid	$C_{16}H_{32}O_2$	57-10-3	EtOH	Cai, (2009)
321	inositol	$C_6H_{12}O_6$	87-89-8	EtOH	Cai, (2009)
322	a-D-fructofuranose	$C_6H_{12}O_6$	10489-79-9	Me_2CO	Feng et al. (2008)
323	tritriacontane	$C_{33}H_{68}$	630-05-7	EtOH	Liu et al. (2004a)
324	phytol	$C_{20}H_{40}O$	150-86-7	EtOH	Liu, (2012)

(**247**), isodonoiol (**248**), isodonal (**249**), rabdosin B (**250**), effusanin A (**251**), xerophinoid B (**253**), and 7,14-O-(1-methylethylidene) oridonin (**254**), are best known for their antitumor, antioxidant, anti-inflammatory, antibacterial, anti-cardiovascular, anti-dementia, and immune regulatory activities. The components of diterpenes and their derivatives are shown in **Table 2**, and their structures are shown in **Figure 3**.

Triterpenes

Triterpenes and their derivatives are well-known in the research of natural phytochemistry for their excellent antitumor activity. Before 2009, 11 triterpenoids (**256–266**), including ursolic acid (**256**), oleanic acid (**257**), β-sitosterol (**258**), α-amyrin (**259**), daucosterol (**260**), betulin (**261**), eryihrodiol (**263**), and stigmasterol (**265**), were isolated and identified from *I. rubescens*. Among these triterpenoids, ursolic acid is a common triterpenoid compound that exists in natural plants. It has sedative, anti-inflammatory, antibacterial, anti-diabetic, anti-ulcer, blood sugar lowering, and other pharmacological activities and can be used as medicine or emulsifier (Cai, 2009). However, few studies have been recently reported on the biological activities of other triterpenoids.

Phenols

Phenols are important secondary metabolites in nature with a wide range of pharmaceutical activities, such as antioxidant, anti-inflammatory, antibacterial, and antiviral activities. At present, 35 phenolic compounds (**267–301**) have been separated from the whole plant of *I. rubescens* and structurally characterized. Salicylic acid (**267**) is an important raw material for aspirin, salicylamide and other drugs, and can also be used as a disinfectant. Caffeic acid (**268**), danshensu (**271**), ferulic acid (**276**), and other compounds with catechol structure have strong antibacterial, antiviral, antioxidant, and anti-cardiovascular biological activities.

Flavonoids are an important component of phenols. The flavonoid structure is characterized by two benzene rings (A and B-rings) with phenolic hydroxyl groups connected with each other through the central three carbon atoms, with 2-phenylchromone as the basic nucleus. Biologically important secondary metabolites have attracted wide attention due to their extensive pharmacological activities. Up to date, 24 flavonoids (**278–301**) have been isolated and identified from the whole plant of *I. rubescens*. Some of these flavonoids form flavonoid glycosides with the hydroxyl groups of monosaccharides or disaccharides at positions 3, 5, 6 and 7 through O-glycosidic bonds. Compounds (**282–284**, **286**, and **289–290**) are flavonoids and compounds (**278–281**, **285**, **287–288**, and **291–301**) are flavonoid glycosides. Among these flavonoid glycosides, 5, 8, 4′-trihydroxyl-6, 7, 3′-trimethoxyl-flavone (**294**) and pedalitin (**279**) are modestly active in the inhibition of the nitrite production in macrophages, and 5, 4′-trihydroxy-6, 7, 8, 3′ trimethoxyflavone (**297**) was demonstrated to be selectively active against HL-60 cells with an IC_{50} value of 7.55 μM (Bai N. et al., 2010). Phenols are also an important material basis for the antioxidant effect of *I. rubescens*. A focus of future research should be on the phenols of *I. rubescens* and the promotion of their development for cosmetics, functional foods and medicine.

Alkaloids

Approximately nine alkaloids (**302–311**) have been isolated from the whole plant of *I. rubescens* (Guo et al., 2010). However, the pharmacological activity of most of these alkaloids is still unclear.

Essential Oil and Other Compounds

The stalks and leaves of *I. rubescens* also contain a series of essential oils. These volatile oils are mainly divided into monoterpenes and sesquiterpene compounds such as α-pinene (**312**), β-pinene (**313**), cinene (**314**), 1,8-cineole (**315**), p-cymene

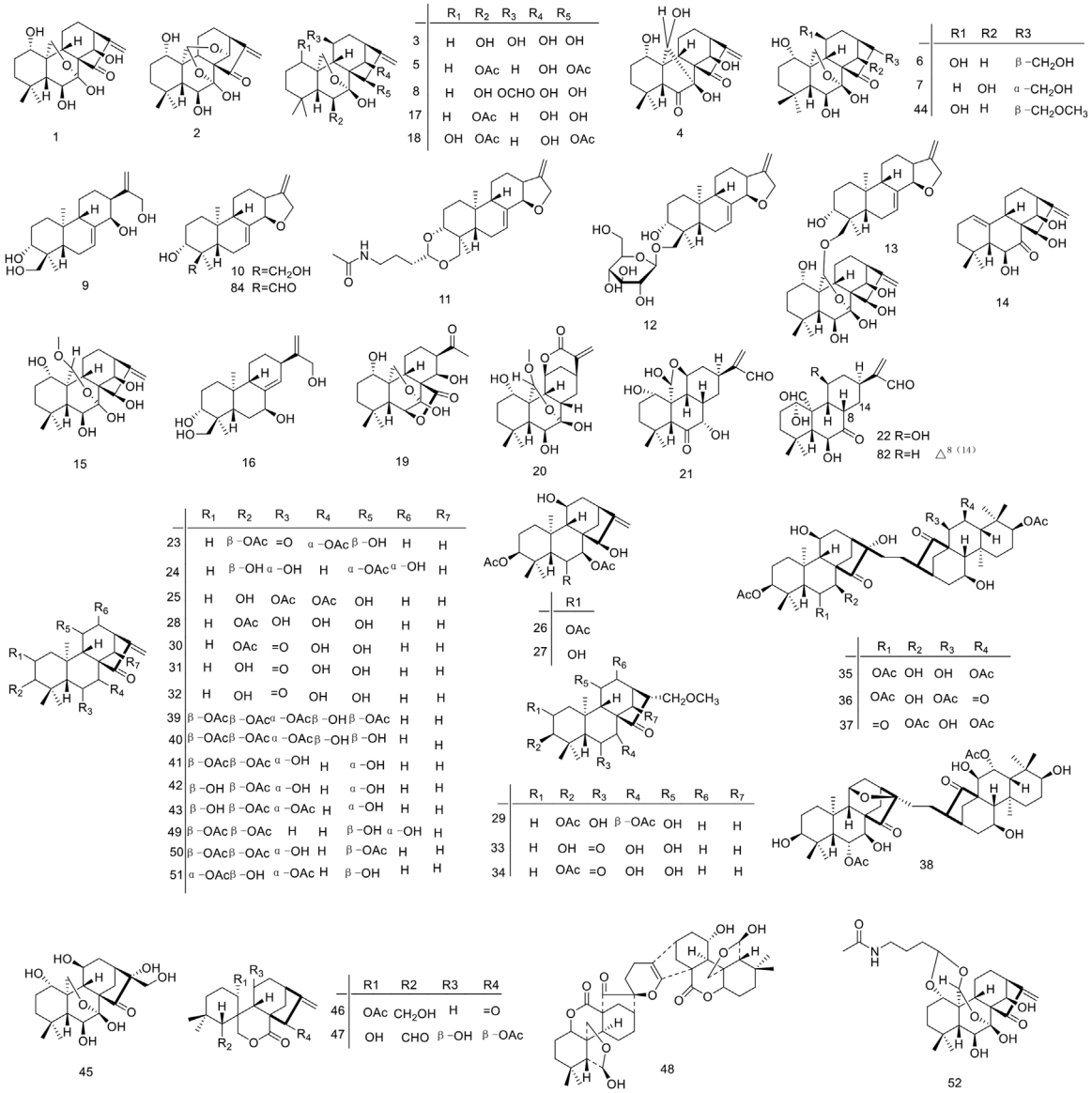

FIGURE 3 | The chemical structure of compounds from *I. rubescens*.

(**316**), and β-elemene (**317**) (Cai, 2009). In addition, fatty compounds (**318–320**, **323–324**) have also been identified from the essential oil of *I. rubescens* by GC-MS. Moreover, inositol (**321**) and α-D-fructofuranose (**322**) have also been identified from *I. rubescens* (Cai, 2009).

PHARMACOLOGICAL ACTIVITIES

The crude extracts and several compounds isolated from *I. rubescens* have been evaluated for their antitumor, antioxidant, anti-inflammatory, antibacterial, anti-dementia, and immune regulatory effects as well as their abilities in the prevention and treatment of cardiovascular and cerebrovascular diseases. Among these effects, the antitumor, antibacterial and anti-inflammatory activities of diterpenoids are the most important and also the most studied effects. Modern pharmacological studies are discussed below, and the main active ingredients are summarized in **Table 3**. In addition, the main molecular mechanism of the biological activity of *I. rubescens* is shown in **Figure 4**.

Antitumor Activity

In several published papers, aqueous and alcoholic extracts of *I. rubescens* have shown inhibitory activity against a variety of cancer cells, including esophageal, gastric, liver, bladder pain, pancreatic, intestinal, and breast cancers (Ding et al., 2016). The most widely studied and important anticancer active compound

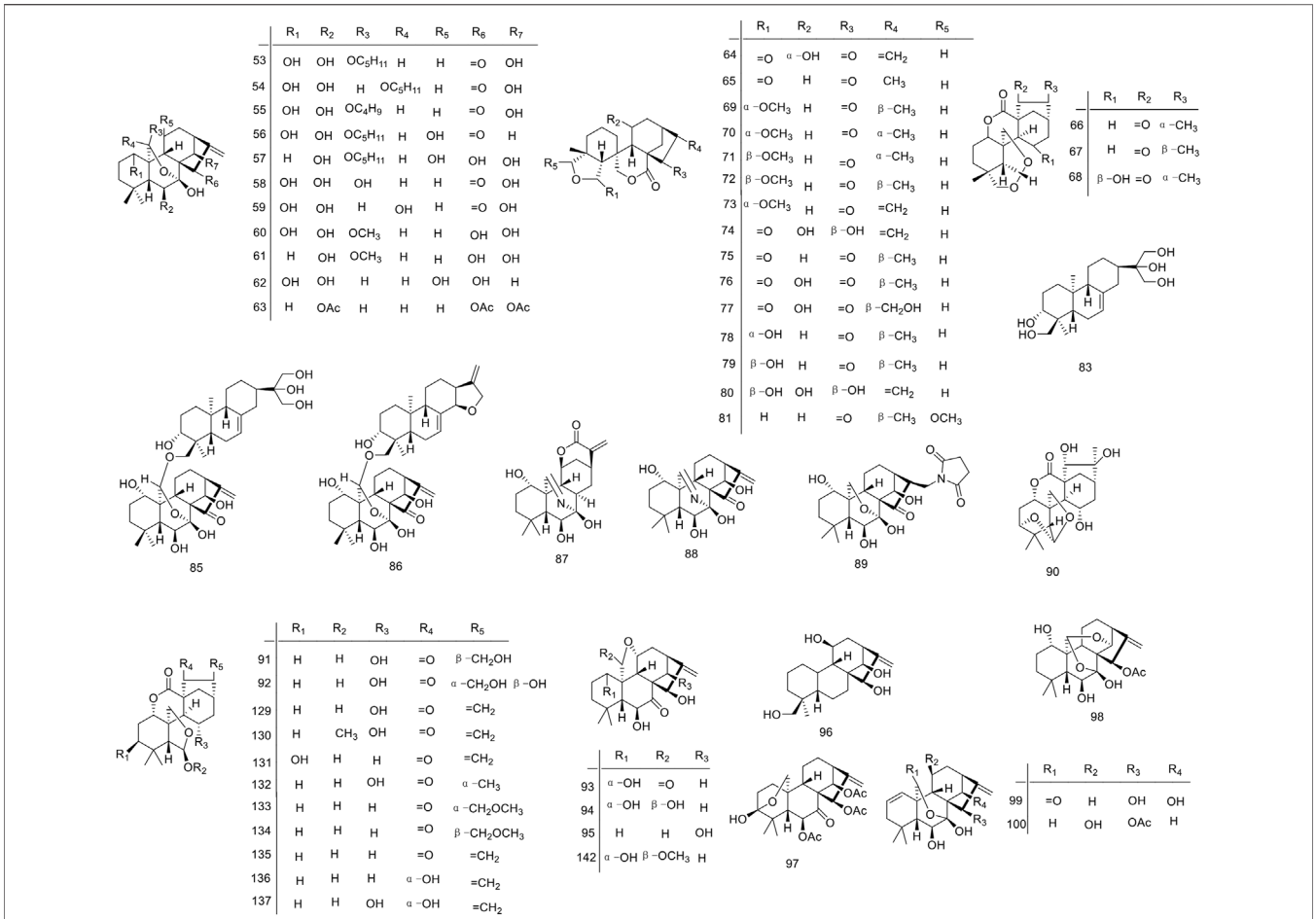

FIGURE 3 | (Continued).

in *I. rubescens* is oridonin (**1**), whose pharmacological activity has been proven to have significant cytotoxicity against various cancers such as liver, larynx, colon, pancreatic, breast, leukemia, lung, stomach, ovarian and bladder cancers (Ding et al., 2016; Jiang et al., 2017). The compound 14-O-acetyl-oridonin (**247**) showed a significant influence on the viability of the human cancer cell lines (HepG2, COLO 205, MCF-7, and HL-60), with IC_{50} values of 30.96, 14.59, 56.18, and 11.95 μM, respectively. Rosthorin (**203**) exhibited a better activity than 14-O-acetyl-oridonin under the same conditions, with IC_{50} values of 27.85, 6.63, 51.52, and 10.86 μM, respectively (Bai N. S. et al., 2010). Lushanrubescensin H (**46**) has significant anti-proliferative activity against tumor cell lines (K562, Bcap37, BGC823, and CA) at the concentrations of 100, 10, 1, 0.1, and 0.01 mg/ml after incubation for 48 or 72 h, and the corresponding IC_{50} values were 3.56, 13.42, 8.91, and 8.25 μM, respectively (Feng et al., 2008). Lushanrubescensin J (**48**) is a novel asymmetric ent-kauranoid dimer, which exhibited potent inhibitory activity against K562 cells with IC_{50} is 0.93 μg/ml (Han et al., 2005). In 2012, Liu et al. conducted a large number of phytochemical studies on *I. rubescens* and isolated 47 new diterpenoids. Pharmacological studies have shown that rabdosin A (**130**), isodocarpin (**135**), shikokianin (**153**), and lasiodin (**154**) showed *in vitro* cytotoxic activity against five species HL-60, SMMC-7721, A-549, MCF-7, and SW-480, which was equal to or stronger than that of the positive drug cisplatin. The structure-activity relationship confirms that unsaturated cyclopentanone is the active center responsible for the cytotoxic activity of enantio-kauri diterpene. The structure of kaurine A (**87**) is identical to that of oridonin (**1**) exhibiting unsaturated cyclopentanone fragments, but the nitrogen of kaurinea is replaced with oxygen in oridonin, which results in a greatly different activity. We speculate that the acid pK_a value of the imine conjugate is around 9, which leads to cell culture conditions around pH 7, where only about one percent of the unprotonated molecules can cross the membrane and enter the interior of the cell, such as other enantiotopic kauri diterpenes, which do not contain nitrogen (Liu, 2012). The drug resistance caused by chemotherapy during the treatment of malignant tumors has an important effect on the efficacy and prognosis of tumor patients. Jaridon 6 (**200**) is a novel diterpenoid isolated from *I. rubescens*, which can promote the early apoptosis of MGC803/5-FU cells. At the same time, it inhibited the proliferation of MGC-803 cells in a dose and time-dependent manner by blocking the G0/G1

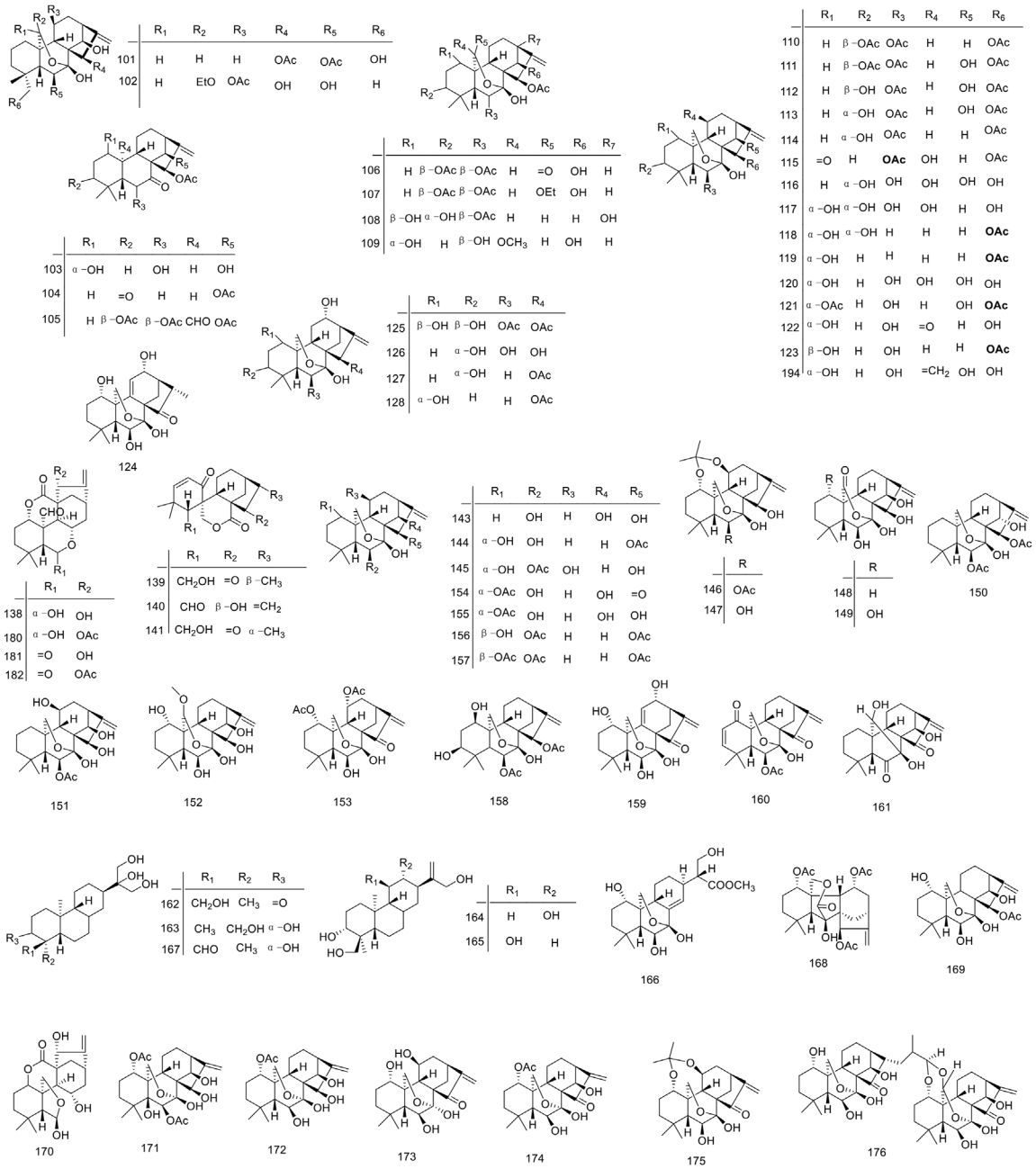

FIGURE 3 | (Continued).

phase. It decreased the protein expression levels of p-PI3K, p-AKT and p-GSK-3β in MGC803/5-Fu cells, increased the expression of cleaved caspase-9, cleaved caspase-3, and cleaved caspase-7 cleaved PARP-1 protein activated the intracellular caspase pathway and promoted apoptosis (Han, 2018). Jaridonin (**246**) exhibited strong anti-proliferative and pro-apoptotic effects in human EC cell lines by the activation of the mitochondria mediated apoptotic pathway, induction of G2/M arrest, as well as increased expression of p53 and p21 (Ma et al., 2013). Similarly, isojiangrubesin B (**226**), isojiangrubesin E (**229**), effusanin A (**251**), and 7, 14-O-(1-methylethylidene) oridonin (**254**) exhibited a significant inhibitory ability against all cell lines (HL-60, A-549, SMMC-7721, MCF-7, and SW-480), with IC_{50} values ranging from 0.5 to 6.5 μM. Their cytotoxic activity was better than that of cisplatin, but worse than that of paclitaxel (Zhang L. et al., 2017). These reported antitumor activities are consistent with the traditional usage such as the treatment of liver cancer, esophageal cancer, cardia cancer, lung cancer, prostate cancer, bladder cancer, colon cancer, breast cancer, cervical cancer, and gastric cancer. The

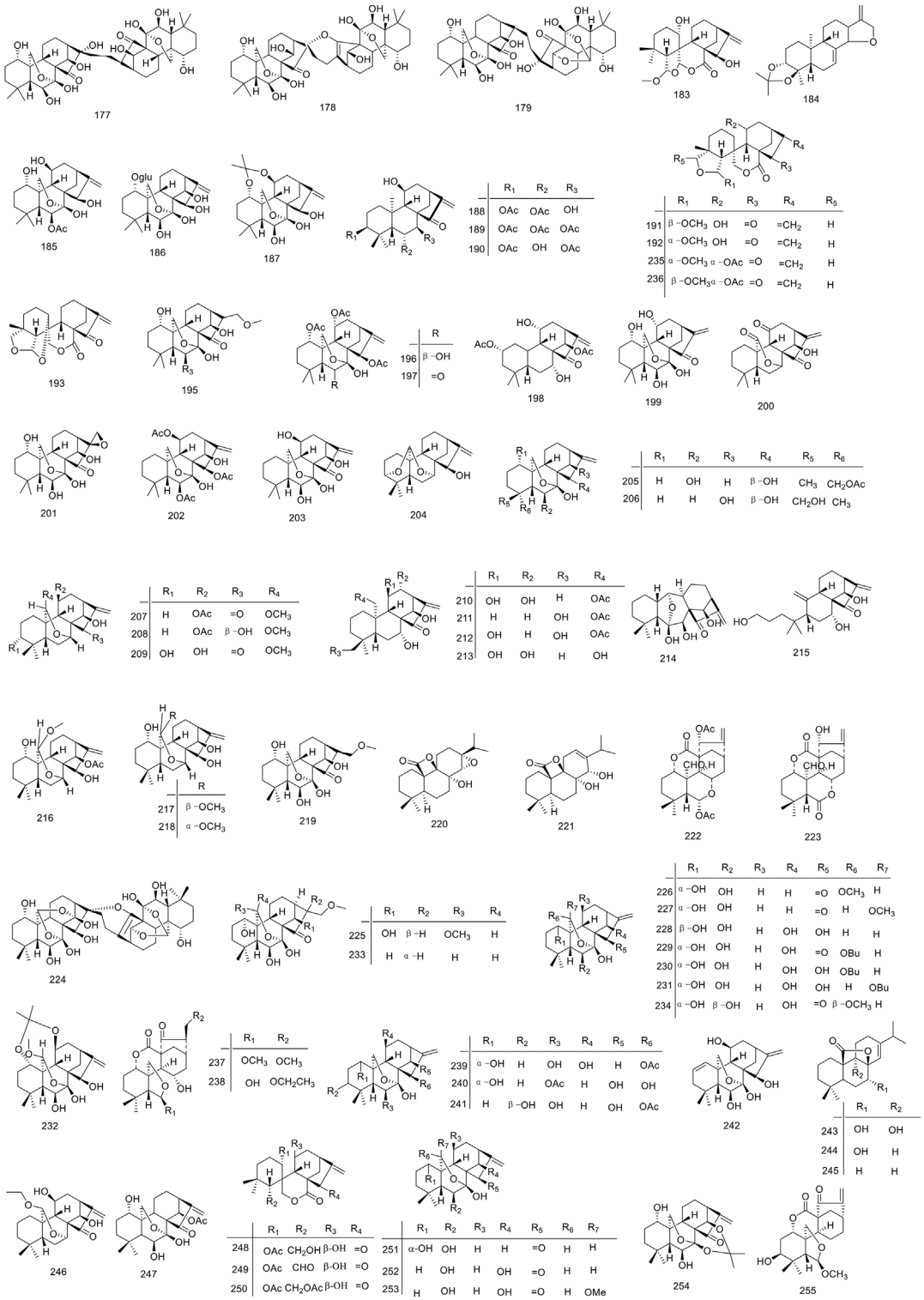

FIGURE 3 | (Continued).

pharmacological studies of the inhibition of tumor cells of esophageal cancer and oral cancer by *I. rubescens* also confirmed the traditional application of *I. rubescens* in the treatment of sore throat, tonsillitis, pharyngitis and stomatitis. Therefore, *I. rubescens* tea can be consumed as a daily health drink by patients with pharyngitis.

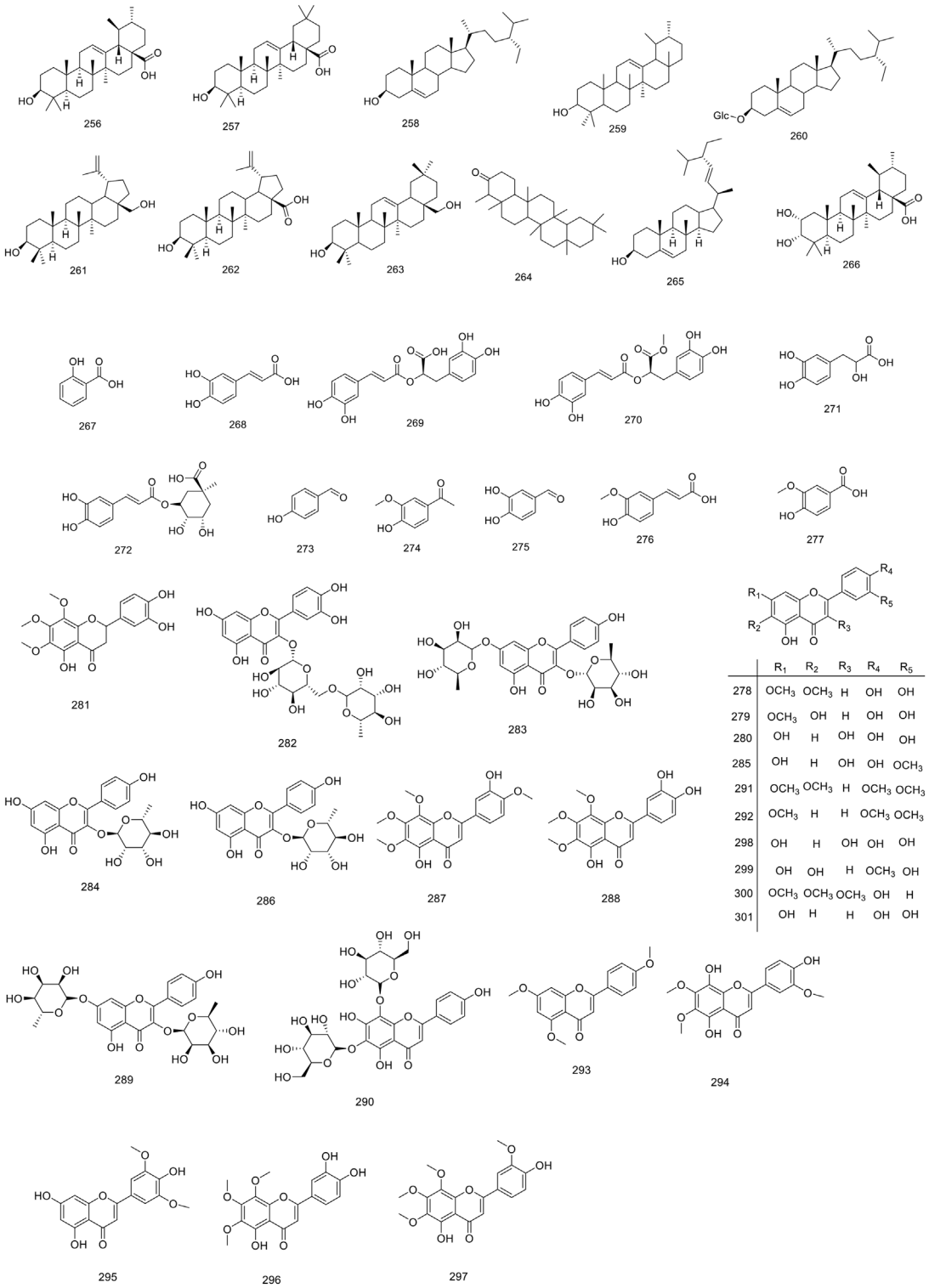

	R_1	R_2	R_3	R_4	R_5
278	OCH_3	OCH_3	H	OH	OH
279	OCH_3	OH	H	OH	OH
280	OH	H	OH	OH	OH
285	OH	H	OH	OH	OCH_3
291	OCH_3	OCH_3	H	OCH_3	OCH_3
292	OCH_3	H	H	OCH_3	OCH_3
298	OH	H	OH	OH	OH
299	OH	OH	H	OCH_3	OH
300	OCH_3	OCH_3	OCH_3	OH	H
301	OH	H	H	OH	OH

FIGURE 3 | (Continued).

In short, *I. rubescens* has significant antitumor activity and good health and medical effects on humans. However, it is worth noting that most of the research on its antitumor activity is still in its infancy, and the use of *in vitro* methods, further *in-vivo* and mechanism of action investigations and clinical research should therefore be encouraged and strengthened. Among the

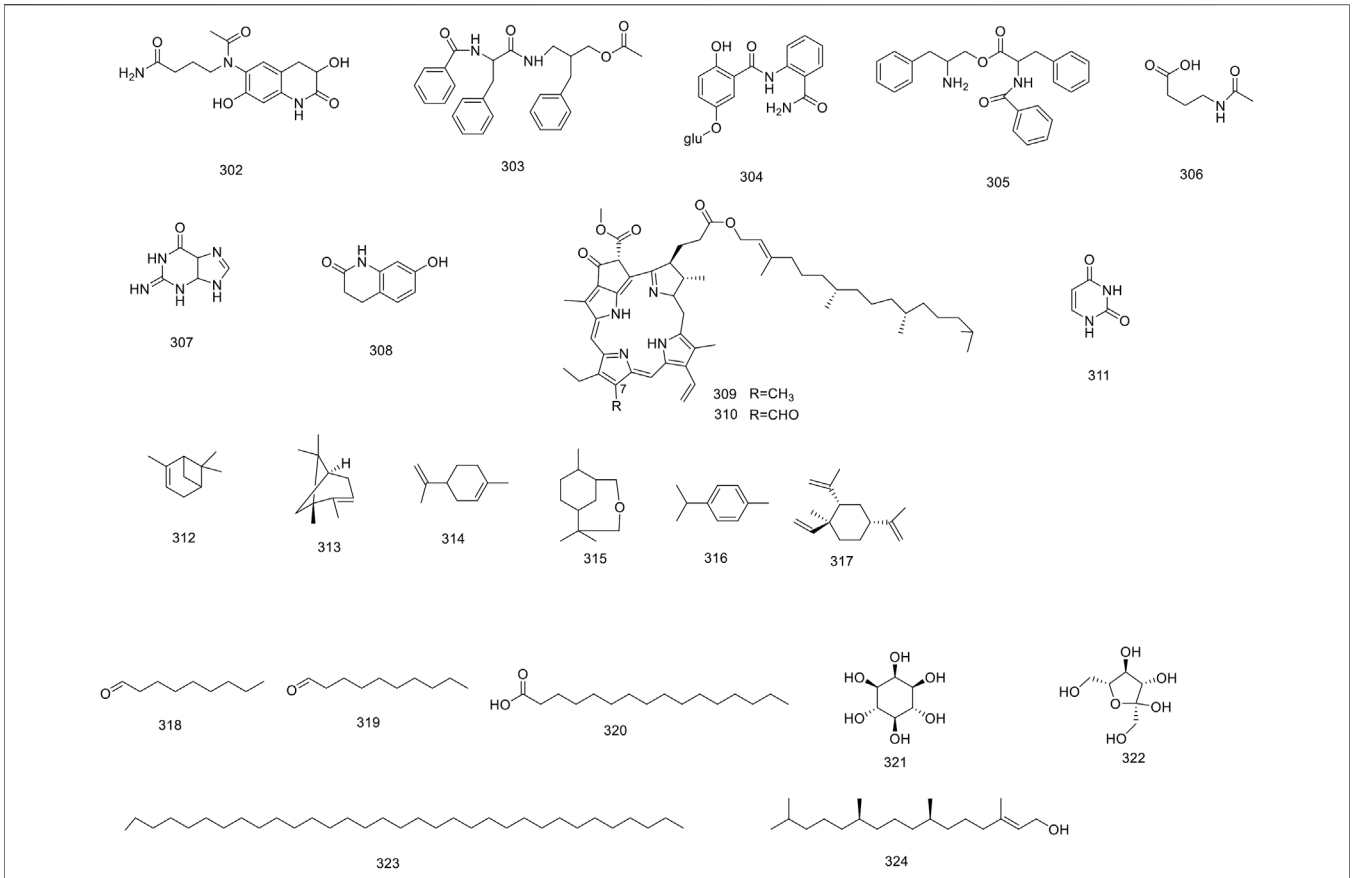

FIGURE 3 | (Continued).

compounds isolated from *I. rubescens*, diterpenoids showed excellent antitumor activity *in vitro*, but the specific mechanism of action is not well understood yet, and further studies on the mechanism of action are needed in the later stage. The antitumor activity of other compounds, such as flavonoids and triterpenoids, needed to be urgently enhanced.

Antibacterial Activity

Ethanol extract of *I. rubescens* has an obvious antibacterial effect on *Staphylococcus aureus* and *Streptococcus* A *hemolyticus*. The minimum effective concentration was in the range of 1:128–1: 256. The effect of the ethanol extract of *I. rubescens* on *Escherichia coli* was very weak, and the inhibitory effect of the water extract of *I. rubescens* on *Staphylococcus aureus* and *Escherichia coli* indicated that the effective antimicrobial component of *I. rubescens* was soluble in alcohol. Total diterpenes of *I. rubescens* also showed a strong inhibitory activity against *Staphylococcus aureus* and *Staphylococcus albicans*, and 80% acetone and ethanol extracts of *I. rubescens* had relatively higher antibacterial activities against Gram-positive strains with the lowest minimum inhibitory concentration and minimum bactericidal concentrations of 5 and 10 mg/ml, respectively (Feng and Xu, 2014). *In vitro* experiments showed that the extracts of *I. rubescens* had a certain inhibitory effect on *Verticillium* groundnut, and its n-butanol site had the best inhibitory activity with an inhibition rate of 94.61% and an EC_{50} value of 0.67 mg/ml which is the focus of antibacterial activity tracking. Extracts of *I. rubescens* had the best inhibitory activity against *Zygomycetes* of maize, wheat, tobacco, apple with EC_{50} values of 0.261, 0.689, 0.487, and 0.419 mg/ml, respectively. The efficacy of *I. rubescens* against *Rhizoctonia verticillioides* was studied, showing that the n-butanol part had the best control effect with an efficacy of 75.52%, and the ethyl acetate part had a better effect on powdery mildew of goldenrod with a long effect time. The possible mechanism is the inhibition of the bacterial growth by the *I. rubescens* extract by disrupting cell membrane permeability while disrupting the cellular metabolism (Li, 2020). The K-B method was used to screen the antibacterial active ingredients of *I. rubescens*, and the ethyl acetate part with the highest activity was separated by chromatography.

Several studies have demonstrated a significant inhibitory activity of the isolated compound of *I. rubescens* against a variety of bacterial strains. Of particular importance is the application of oridonin (**1**) to prevent methicillin resistance of *Staphylococcus aureus* (SA), Methcillin-resistant *Staphylococcus aureus* (MRSA), and β-lactamase-positive *Staphylococcus aureus* (ESBLs-SA), showing a certain antibacterial activity (MIC is 3.125, 6.25, 6.25 μg/disc) which is strong but still weaker than

TABLE 3 | Biological activities of bioactive compounds and extracts of *I. rubescens*.

Biological activities	Compounds/extracts	Types	Testing subjects	Doses/Duration	Mechanisms/Effects	References
Anticancer activity						
	oridonin (1)	*In vitro*	Human cancer cell lines (Hep G2, COLO 205, MCF-7, and HL-60)	5–100 μM for 24 h	IC_{50} values against 4 tumor cells were 26.90, 5.92, 50.32, and 6.42 μM, respectively	Bai N S. et al. (2010)
	14- O-acetyl-oridonin (247)	*In vitro*	Human cancer cell lines (Hep G2, COLO 205, MCF-7, and HL-60)	5–100 μM for 24 h	IC_{50} values against 4 tumor cells were 30.96, 14.59, 56.18, 11 and 11.95 μM, respectively	Bai N S. et al. (2010)
	rosthorin (203)	*In vitro*	Human cancer cell lines (Hep G2, COLO 205, MCF-7, and HL-60)	5–100 μM for 24 h	IC_{50} values against 4 tumor cells were 27.85, 6.63, 51.52, and 10.86 μM, respectively	Bai N S. et al. (2010)
	rubescensin B (2)	*In vitro*	Human cancer cell lines (Hep G2, COLO 205, MCF-7, and HL-60)	5–100 μM for 24 h	IC_{50} values against 4 tumor cells were 32.41, 6.47, 70.79, and 9.36 μM, respectively	Bai N S. et al. (2010)
	lushanrubescens-in H (46)	*In vitro*	Human cancer cell lines (K562 Bcap37, BGC823, and CA)	100, 10, 1, 0.1, 0.01 mg/ml for 48 h or 72 h	IC_{50} values against 4 tumor cells were 3.56, 13.42, 8.91, and 8.25 μM, respectively	Han et al. (2003d)
	lasiodonin (173)	*In vitro*	Human cancer cell lines (K562 and Bcap37)	100, 10, 1, 0.1, 0.01 mg/ml for 48 h or 72 h	IC_{50} values against 2 tumor cells were 5.35 and 112.53 μM, respectively	Han et al. (2003d)
	oridonin (1)	*In vitro*	Human cancer cell lines (K562 Bcap37, BIU87, CA, CNE, and Hela)	100, 10, 1, 0.1, 0.01 mg/ml for 48 h or 72 h	IC_{50} values against 5 tumor cells were 4.37, 8.32, 55.91, 0.06, 16.50, and 28.67 μM, respectively	Han et al. (2003d)
	ponicidin (2)	*In vitro*	Human cancer cell lines (K562 Bcap37, BGC823, BIU87, CA, CNE, and Hela)	100, 10, 1, 0.1, 0.01 mg/ml for 48 h or 72 h	IC_{50} values against 7 tumor cells were 2.26, 6.76, 55.17, 13.26, 0.06, 13.26, and 11.31 μM, respectively	Han et al. (2003d)
	isodonoiol (248)	*In vitro*	Human cancer cell lines (K562 and Bcap37)	100, 10, 1, 0.1, 0.01 mg/ml for 48 h or 72 h	IC_{50} values against 2 tumor cells were 10.15 and 101.32 μM, respectively	Han et al. (2003d)
	isodonal (249)	*In vitro*	Human cancer cell lines (K562 Bcap37, BGC823, and CA)	100, 10, 1, 0.1, 0.01 mg/ml for 48 h or 72 h	IC_{50} values against 4 tumor cells were 2.29, 28.64, 79.87, and 9.04 μM, respectively	Han et al. (2003d)
	rabdosin B (250)	*In vitro*	Human cancer cell lines (K562 Bcap37, and BGC823)	100, 10, 1, 0.1, 0.01 mg/ml for 48 h or 72 h	IC_{50} values against 3 tumor cells were 4.61, 15.84, and 10.93 μM, respectively	Han et al. (2003d)
	lushanrubescen-sin J (48)	*In vitro*	Human cancer cell lines K562	NM	IC_{50} values against K562 tumor cells were 0.93 μg/ml, respectively	Han et al. (2005)
	rabdosin A (130)	*In vitro*	Human cancer cell lines (HL-60, SMMC-7721, A-549, MCF-7, and SW-480)	NM	IC_{50} values against 5 tumor cells were 2.11, 2.15, 3.53, 2.82, and 2.85 μM, respectively	Liu, (2012)
	isodocarpin (135)	*In vitro*	Human cancer cell lines (HL-60, SMMC-7721, A-549, MCF-7, and SW-480)	NM	IC_{50} values against 5 tumor cells were 3.02, 2.57, 3.76, 3.07, and 3.05 μM, respectively	Liu, (2012)
	shikokianin (153)	*In vitro*	Human cancer cell lines (HL-60, SMMC-7721, A-549, MCF-7, and SW-480)	NM	IC_{50} values against 5 tumor cells were 3.98, 2.43, 5.22, 4.64, and 4.40 μM, respectively	Liu, (2012)
	lasiodin (154)	*In vitro*	Human cancer cell lines (HL-60, SMMC-7721, A-549, MCF-7, and SW-480)	NM	IC_{50} values against 5 tumor cells were 2.72, 2.81, 2.51, 3.58, and 3.14 μM, respectively	Liu, (2012)
	Parvifoline AA (161)	*In vitro*	Human cancer cell lines (HL-60, SMMC-7721, A-549, MCF-7, and SW-480)	NM	IC_{50} values against 5 tumor cells were 10.20, 10.20, 17.31, 17.61, and 24.11 μM, respectively	Liu et al. (2012)
	jaridon 6 (200)	*In vitro*	Drug resistant gastric cancer cells MGC803/5-Fu	0, 8, 16, 32 μM for 24 h	Induced apoptosis and increased the apoptosis rate by up- regulating the caspase-9, caspase-3, and caspase-7, down- regulating the p-PI3K, p-Akt, and p-GSK-3β	Han, (2018)
	jaridonin (246)	*In vitro*	Huma esophageal cancer cell lines (EC9706, EC109, EC1)	10, 20, 40 μM for 24 h	Induced apoptosis and increased the apoptosis rate by up- regulating the p21 and Bax	Ma et al. (2013)
	IsojiangrubesinB (226)	*In vitro*	Human cancer cell lines (HL-60, A-549, SMMC-7721, MCF-7, and SW-480)	0.064, 0.32, 1.6, 8, and 40 μM for 48 h	IC_{50} values against 5 tumor cells were 1.2, 5.3, 3.0, 2.9, and 0.8 μM, respectively	Zhang L et al. (2017)
	Isojiangrubesin C (227)	*In vitro*				

(Continued on following page)

TABLE 3 | (*Continued*) Biological activities of bioactive compounds and extracts of *I. rubescens*.

Biological activities	Compounds/extracts	Types	Testing subjects	Doses/Duration	Mechanisms/Effects	References
			Human cancer cell lines (HL-60, SMMC-7721, MCF-7, and SW-480)	0.064, 0.32, 1.6, 8, and 40 μM for 48 h	IC_{50} values against 4 tumor cells were 3.4, 8.6, 4.1, and 2.1 μM, respectively	Zhang Y et al. (2017)
	IsojiangrubesinE (229)	*In vitro*	Human cancer cell lines (HL-60, A-549, SMMC-7721, MCF-7, and SW-480)	0.064, 0.32, 1.6, 8, and 40 μM for 48 h	IC_{50} values against 5 tumor cells were 1.0, 5.8, 3.2, 3.4, and 1.9 μM, respectively	Zhang L et al. (2017)
	effusanin A (251)	*In vitro*	Human cancer cell lines (HL-60, A-549, SMMC-7721, MCF-7, and SW-480)	0.064, 0.32, 1.6, 8, and 40 μM for 48 h	IC_{50} values against 5 tumor cells were 1.8, 6.5, 3.2, 3.4, and 0.6 μM, respectively	Zhang Y et al. (2017)
	longikaurin A (252)	*In vitro*	Human cancer cell lines (HL-60, A-549, SMMC-7721, MCF-7, and SW-480)	0.064, 0.32, 1.6, 8, and 40 μM for 48 h	IC_{50} values against 5 tumor cells were 0.7, 2.9, 1.2, 2.7, and 0.5 μM, respectively	Zhang L et al. (2017)
	xerophinoid B (253)	*In vitro*	Human cancer cell lines (HL-60, MCF-7, and SW-480)	0.064, 0.32, 1.6, 8, and 40 μM for 48 h	IC_{50} values against 3 tumor cells were 3.6, 4.5, and 2.3 μM, respectively	Zhang Y et al. (2017)
	rabdoternin F (152)	*In vitro*	Human cancer cell lines (HL-60, and SW-480)	0.064, 0.32, 1.6, 8, and 40 μM for 48 h	IC_{50} values against 2 tumor cells were 3.2 and 2.3 μM, respectively	Zhang L et al. (2017)
	rabdoternin E (234)	*In vitro*	Human cancer cell lines (HL-60, and SW-480)	0.064, 0.32, 1.6, 8, and 40 μM for 48 h	IC_{50} values against 2 tumor cells were 2.7, and 3.0 μM, respectively	Zhang Y et al. (2017)
	Lasiodonin- acetonide (175)	*In vitro*	Human cancer cell lines (HL-60, SMMC-7721, MCF-7, and SW-480)	0.064, 0.32, 1.6, 8, and 40 μM for 48 h	IC_{50} values against 4 tumor cells were 0.9, 3.8, 2.9, and 0.9 μM, respectively	Zhang L et al. (2017)
	7,14-O-(1-met-hylethylidene) oridonin (254)	*In vitro*	Human cancer cell lines (HL-60, A-549, SMMC-7721, MCF-7, and SW-480)	0.064, 0.32, 1.6, 8, and 40 μM for 48 h	IC_{50} values against 5 tumor cells were 2.4, 3.8, 3.0, 3.9, and 1.1 μM, respectively	Zhang Y et al. (2017)
	6-epi-11-O-acetylangustifoli-n (235)	*In vitro*	Human lung cancer cell lines A549 and leukemia cell lines K562	NM	IC_{50} values against 2 tumor cells were 15.81 and 1.93 μM, respectively	Luo et al. (2017)
	11-O-acetylan-gustifolin (236)	*In vitro*	Human lung cancer cell lines A549 and leukemia cell lines K562	NM	IC_{50} values against 2 tumor cells were 9.89 and 0.59 μM, respectively	Luo et al. (2017)
Antibacterial activity						
	oridonin (1)	*In vitro*	Methicillin-resistant *Staphylococcus aureus* (MRSA) strain USA300	0, 8, 16, 32, 64, and 128 μg/ml	The MIC was 64 μg/ml, and the MBC value was 512 μg/ml	Yuan et al. (2019)
	oridonin (1)	*In vitro*	*C.albicans* strains (CA2489, CA3208, CA10, and CA136)	0, 8, 16, and 32 μg/ml	Promote the sensitization to azoles for azoles-resistant *C. albicans* by affect the expression level of efflux-related genes, inhibits drug efflux, and induces apoptosis of *C. albicans* after entering cells	Chen et al. (2020)
Anti-inflammatory activity						
	3β-hydroxy-6β-methoxy-6,7-seco-6,20-epoxy-1α,7-olide-ent-kaur-16-en-15-one (255)	*In vitro*	LPS-induced RAW 264.7 cells	NW	Inhibited NO production with IC_{50} values of 3.97 μM	Wen et al. (2019)
	enmein (131)	*In vitro*	LPS-induced RAW 264.7 cells	NW	Displayed NO production inhibitory effects with IC_{50} values of 17.43 μM	Wen et al. (2019)
	rabdosin A (130)	*In vitro*	LPS-induced RAW 264.7 cells	NW	Exhibited NO production inhibitory effects with IC_{50} values of 2.25 μM	Wen et al. (2019)
	epinodosin (129)	*In vitro*	LPS-induced RAW 264.7 cells	NW	Displayed NO production inhibitory effects with IC_{50} values of 18.25 μM	Wen et al. (2019)
	oridonin (1)	*In vitro*	LPS-induced RAW 264.7 cells	NW	Inhibited NO production with IC_{50} values of 6.51 μM	Wen et al. (2019)
	hubeirubesin I (111)	*In vitro*	LPS-induced RAW 264.7 cells	NW	Inhibited NO production with IC_{50} values of 1.48 μM	Wen et al. (2019)
	lasiokaurin (174)	*In vitro*	LPS-induced RAW 264.7 cells	NW	Inhibited NO production with IC_{50} values of 1.36 μM	Wen et al. (2019)
	pedalitin (270)	*In vitro*	LPS-induced RAW 264.7 cells	20, 40, 60, 80, and 100 μg/ml	Modestly active for inhibiting NO production in macrophage	Bai N et al. (2010)
	oridonin (1)	*In vivo*	Insulin resistance by fed a high-fat diet in mice	10 mg/kg/d	Reduced the levels of TNF-α, IL-6, IL-1β and MCP-1	Li et al. (2017)
	AEIRL	*In vivo*	Xylene induced mouse	0.32 g/kg	Effectively inhibit the inflammation and the pain of the treated mice, respectively	Tang et al. (2011)

(Continued on following page)

TABLE 3 | (*Continued*) Biological activities of bioactive compounds and extracts of *I. rubescens*.

Biological activities	Compounds/extracts	Types	Testing subjects	Doses/Duration	Mechanisms/Effects	References
Antioxidant activity						
	oridonin (1)	*In vitro*	H_2O_2-mediated formation of ROS HaCaT cells	1–20 μM for 24 h	Protect keratinocytes against H_2O_2-induced apoptosis of 1–5 μM	Bae et al. (2014)
	AEAIR	*In vitro*	DPPH and ABTS radical	NW	Exhibited the scavenging activities against DPPH and ABTS radical, and the EC_{50} was 1.63 and 9.02 mg/ml, respectively	Feng and Xu, (2014)
	EPIRAPEE	*In vitro*	DPPH and hydroxyl radicals	800 μg/ml	The scavenging rates of DPPH free radicals and hydroxyl free radicals were 94.30% and 89.46% respectively	Jiu et al. (2018)
Anti-cardiovascular activity						
	oridonin (1)	*In vivo*	Myocardial ischemia reperfusion rats	10 mg/kg for 7 d	Significantly decreased infarct size and reversed the abnormal elevated myocardial zymogram in serum	Zhang J. H et al. (2019)
	TFAIR	*In vivo*	BIT model mice	75 mg/kg, 150 mg/kg, 300 mg/kg for 5 days	Decrease the mortality and NSE level, increase the content of NO and the activity of NOS, and improve the pathological damage of cortex and hippocampus of mice	Kang et al. (2017)
Diarrhea treatment activity						
	oridonin (1)	*In vitro*	ΔF508-CFTR cells	10–100 μM	IC_{50} = 46.8 μM	Luan et al. (2015)
Hypoglycemic activity						
	AEIR	*In vitro*	HUVECs treated with high glucose	0.06 g/L, 0.13 g/L, 0.25 g/L, 0.50 g/L, and 1.00 g/L	Significant differences with that of the model group. 0.13 g/L-1.00 g/L had higher cell viability (101.37%–114.18%) than that of the positive control (102.49%)	Jintao et al. (2020)
Inhibit liver fibrosis activity						
	EPIRWPEE	*In vivo*	CCl_4-induced injury of chronic liver injury model mice	0.08, 0.04, and 0.02 g/(10 g·d)	Reduced the content of ALT, AST, TP, ALB, MDA, and increased SOD activity	Yao et al. (2010)
	oridonin (1)	*In vivo*	CCl_4-induced injury of chronic liver injury model mice	5 mg/kg for 6 weeks	Down-regulated the levels of ALT and α-SMA	Liu et al. (2020)
Anti-Alzheimer's activity						
	oridonin (1)	*In vivo*	APP/PS1-21 mice	20 mg/kg for 10 days	Reduced the autophagosome formation and synaptic loss and improved cognitive dysfunction in MHE rats	Zhang et al. (2013)
	oridonin (1)	*In vivo*	$Aβ_{1-42}$-induced AD mice	10 mg/kg for 15 days	Significant neuroprotective effects associated with the activation of the BDNF/TrkB/CREB signaling pathway	Wang et al. (2016)
Immunomodulatory activity						
	RPPSIIa	*In vitro*	Con A-induced T lymphocyte	5, 10, 50, and 100 μg/m L	At a dose of 5 and 50 μg/ml, effectively enhance the lymphocyte proliferation response induced by Con A	Liu et al. (2011)
	oridonin (1)	*In vivo*	1 day-old male broiler chicken	50, 80, and 100 mg/kg	Reduced the release and the mRNA expression of IL-2, IL-4, IL-6, IL-10, and TNF-α in the spleen	Wu et al. (2018)
Antidepressant activity						
	oridonin (1)	*In vivo*	mice	2.5, 9, and 12.5 mg/kg/d	Increased PPAR-γ protein expression and subsequent GluA1 (Ser845) phosphorylation and GluA1 levels	Liu and Du. (2020)

Note: NM, not mentioned; AEIRL, aqueous extract of I. rubescens *leaves; AEAIR, acetone extract from the aerial part of* I. rubescens*; EPIRAPEE, Ethyl acetate part form the* I. rubescens *aerial part ethanol extract; TFAIR, Total flavonoid from the aerial part of* I. rubescens*; AEIR, aqueous extract of* I. rubescens*; EPIRWPEE, Ethyl acetate part form the* I. rubescens *whole plant ethanol extract; RPPSIIa, Rhamnose: Glucose = 7:93.*

that of the positive control berberine (MIC is 0.156 μg/disc). Ferulic acid (**276**) has a certain antibacterial activity against SA and MRSA (MIC is 50 and 50 μg/disc), while salicylic acid (**267**) has only antibacterial activity against SA (MIC is 50 μg/disc) (Li et al., 2014). The MIC and MBC values of oridonin (**1**) against the MRSA strain USA300 were 64 and 512 μg/ml, respectively, and the mechanism underlying the antibacterial activity was related to changes in the cell membrane and cell wall permeability,

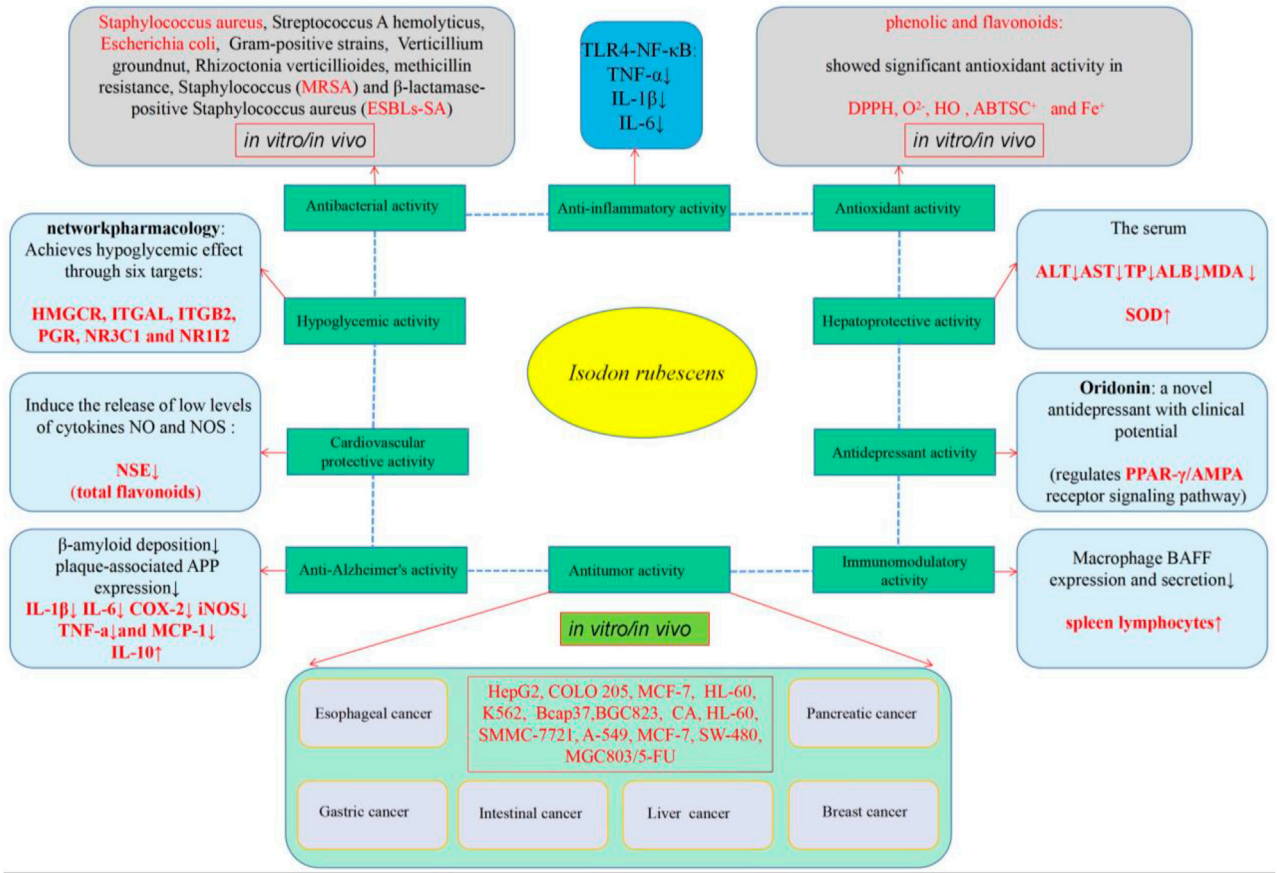

FIGURE 4 | Graphical summary of pharmacological properties of *I. rubescens*.

disturbance in the protein and DNA metabolism, and influence on the bacterial morphology (Yuan et al., 2019). In addition, the combination of oridonin (**1**) and azoles has a synergistic effect on drug-resistant *Candida albicans*. The mechanism of reversing FLC resistance comprises changes of the expression level of efflux-related genes, inhibition of drug efflux, and induction of apoptosis upon entry of *Candida albicans* into cells (Chen et al., 2020). The results suggest its potential to provide new leads for the development of highly antimicrobial drugs, which are a source of new lead compounds for the development of novel antimicrobial agents.

Cholera is an acute diarrheal infectious disease caused by the contamination of ingested food or water with *Vibrio cholerae*. Each year, there are an estimated 3–5 million cases of cholera. CFTR chloride channels are new molecular targets for the treatment of secretory diarrhea. It was shown that oridonin (**1**) significantly reduced the inward flow of iodine ions in wt-CFTR and F508-CFTR FRT epithelial cells in a dose-dependent manner, and also reduced cholera toxin-induced humoral secretion, making it a candidate compound for the treatment of cholera toxin-induced secretory diarrhea (Luan et al., 2015).

However, many antimicrobial studies have only provided preliminary information. The isolation of bioactivity-oriented antimicrobial compounds and their potential mechanisms of antimicrobial action need to be further investigated.

Anti-Inflammatory Activity

Studies have shown that *I. rubescens* shows better efficacy on some inflammatory diseases. In the xylene induced auricular edema mouse model, the aqueous extract of *I. rubescens* was administered orally at a dose of 0.32 g/kg, and the results showed that the anti-inflammatory activity of aspirin was significantly higher than that of the blank group, while the anti-inflammatory activity of the aqueous extract at this dose was significantly higher than that of aspirin at a dose of 30 mg/kg (Tang et al., 2011). The compounds, oridonin (**1**), hubeirubesin I (**111**), rabdosin A (**130**) and lasiokaurin (**174**) isolated from *I. rubescens* exhibited obvious NO production inhibitory effects with IC_{50} values of 6.51, 1.48, 2.25, and 1.36 μM, respectively. In the present study, 6, 7-seco-ent-kaurane diterpenoids, such as compounds **225** and **130** with an α, β-unsaturated ketone moiety, exhibited NO production inhibitory effects, indicating that the α, β-unsaturated ketone moiety is an essential pharmacophore (Wen et al., 2019). The therapeutic effect of the oral administration of oridonin (**1**) on acetic acid-induced ulcerative colitis in mice was reported in the literature related to the anti-inflammatory effect of oridonin. In

addition, the expression levels of TNF-α, IL-1β and IL-6 mRNA in RAW 264.7 cells were significantly reduced after administration of oridonin (10 μmol/L), and Western blot assay showed significantly reduced the expression levels of TNF-α, IL-1β and IL-6 mRNA in RAW 264.7 cells. These results suggest that oridonin can down-regulate the expression of LPS-induced pro-inflammatory factors in RAW 264.7 cells, and its anti-inflammatory immune mechanism is related to the activation of the TLR4-NF-κB signaling pathway. *In vivo* experimental results suggest that oridonin may target the p38-MAPK and NF-κB signaling pathways to inhibit the development of inflammation and significantly reduce the clinical symptoms of kidney injury in diabetic mice, including increased urine protein, creatinine and blood urea nitrogen levels, thus protecting from diabetic nephropathy (Kang and Liu, 2019). These findings suggest that *I. rubescens* diterpenoids are potent inhibitors of inflammation and may be useful in the development of anti-inflammatory drugs for the treatment of various inflammation-related diseases. However, studies on the crude extracts of *I. rubescens* and *in vivo* models are very limited, and more in-depth studies on the anti-inflammatory effects as well as possible mechanistic studies are urgently needed.

Antioxidant Activity

The crude extracts of *I. rubescens* have a certain scavenging activity for DPPH radicals, hydroxyl radicals and superoxide anion radicals. Studies showed that the scavenging rate of ethyl acetate extract was better than those of petroleum ether, chloroform and n-butanol extracts for DPPH radicals, hydroxyl radicals and superoxide anion radicals. At a mass concentration of 800 μg/ml, the ethyl acetate extraction site showed better scavenging of DPPH radicals, hydroxyl radicals and superoxide anion radicals of 94.30%, 89.46%, and 87.47% respectively. At the same mass concentration, the scavenging rates of DPPH radicals, hydroxyl radicals and superoxide anion radicals were 72.89%, 71.99%, and 50.60% for the n-butanol extraction site, but only 84.47%, 65.21%, and 20.37% for petroleum ether extraction site, respectively, while the scavenging rates of DPPH radical, hydroxyl radical and superoxide anion radical for the chloroform extraction site were only 62.47%, 63.03%, and 46.31%, respectively. The scavenging rates of DPPH radical, hydroxyl radical and superoxide anion radical by chloroform extraction site were only 62.47%, 63.03%, and 46.31%, respectively. The IC_{50} values of the ethyl acetate extraction site for DPPH radicals, hydroxyl radicals and superoxide anion radicals was significantly lower than those of the petroleum ether, chloroform and n-butanol extraction sites, but slightly higher than those of VC on DPPH radicals and hydroxyl radicals. The active ingredients of the ethyl acetate extract of *I. rubescens* were mostly identified by GC-MS as polyphenols, ketones and organic acids, among which the percentage of polyphenols reached 39.15%, which was consistent with the antioxidant activity (Jiu et al., 2018). In 2014, Feng et al. found that the 80% acetone extracts had the highest content of total polyphenols (equivalent to 8.09 mg GAE/g) and flavonoids (equivalent to 5.69 mg RE/g) and the strongest antioxidant activities, followed by those of 80% methanol and 80% ethanol, and finally hexane extracts (Feng and Xu, 2014). Determination of the total phenolic and flavonoid contents revealed that the ethanol extract of *I. rubescens* was equivalent to 8.40 mg GAE/g and 9.51 mg QE/g of dry weight, and the radical scavenging activities of the ethanol extracts were evaluated based on DPPHC and $ABTSC^{+}$ radicals. The free radical scavenging capacities of the ethanol extracts were 198.90 and 303.74 μM, respectively, equivalent to the amount of ascorbic acid. Phenolic and total flavonoid contents are important factors that determine the antioxidant activity of the extracts which lays the foundation for the development and utilization of antioxidant products of *I. rubescens* (Zhang Y. et al., 2017). In addition, oridonin isolated from *I. rubescens* has antioxidant properties and protects human keratin-forming cells from hydrogen peroxide-induced oxidative stress. Low doses of oridonin (1–5 μM) protected keratin-forming cells from hydrogen peroxide-induced apoptosis in a concentration and time-dependent manner and significantly reduced the production of H_2O_2-induced reactive oxygen species in cells (Bae et al., 2014).

Natural antioxidants have attracted much attention because of their high efficiency and low toxicity. It has become an inevitable trend in the development of modern medicine and health care industries to find new antioxidants from natural products that can remove free radicals in the body. Numerous antioxidant experiments have confirmed that *I. rubescens* has the potential to become a natural antioxidant. It can eliminate free radicals or inhibit the activity of free radicals, thereby helping the body maintain sufficient antioxidant status.

Hypoglycemic Activity

In 2020, Xue et al. found that ethanolic and aqueous extracts (0.06–1.00 g/L) of *I. rubescens* could increase the activity of DMEM-treated human umbilical vein endothelial cells (HUVECs). Treatment with the aqueous extract (0.13–1.00 g/L) resulted in a higher cell viability (101.37%–114.18%) than the positive control (102.49%), while the cell viability of the positive control was higher than that of cells treated with alcohol extracts (90.07%–103.44%). Furthermore, the ethanol extract did not reduce fasting blood glucose in diabetic rats. The results of cell and animal experiments showed that the main hypoglycemic components of *I. rubescens* are hydrophilic substances (polar components), while alcohol-soluble substances *I. rubescens* (non-polar components) have no significant hypoglycemic effect. Based on network pharmacology screening, 25 hypoglycemic components of *I. rubescens*, such as rabdoternin A (**148**), rabdoternin B (**149**), and epinodosinol (**137**), were identified. These components activate six hypoglycemic targets, including 3-hydroxy-3-methyl glutaraldehyde coenzyme A reductase (HMGCR), integrin α-L (ITGAL), integrin β-2 (ITGB2), progesterone receptor (PGR), glucocorticoid receptor (NR3C1) and nuclear receptor subfamily 1I member 2 (NR1I2). These targets are involved in 94 signaling pathways, such as Rap1, PI3K-Akt and HIF-1 signaling pathways (Jintao et al., 2020).

Hepatoprotective Activity

The Global Hepatitis Report 2017, published by the World Health Organization, shows that approximately 325 million people

worldwide were infected with chronic hepatitis B virus or hepatitis C virus in 2017. Moreover, 80% of liver cancers are caused by hepatitis B. Chronic hepatitis is the prevalent disease in China, usually caused by liver injury, which evolves into liver fibrosis and eventually leads to cirrhosis and liver cancer. Therefore, the prevention and treatment of liver injury and liver fibrosis receive much research attention. In 2010, Yao et al. found that *I. rubescens* extract had a protective effect against carbon tetrachloride-induced chronic liver injury and early hepatic fibrosis in mice. It significantly reduced the levels of serum alanine aminotransferase (ALT) and glutathione aminotransferase (AST), decreased the levels of total protein (TP), albumin (ALB), and malondialdehyde (MDA), increased the activity of superoxide dismutase (SOD), reduced the degree of liver tissue degeneration and necrosis, and alleviated the pathological changes of liver tissue (Yao et al., 2010). In 2019, Liu et al. discovered that oridonin (**1**) can reduce ALT levels in model mice and the expression of α-smooth muscle actin (α-SMA) in the liver of mice with fibrosis. It also reduced the expression of NLRP3, caspase-1, and IL-1β and the infiltration of inflammatory cells. Therefore, oridonin (**1**) is a potential drug for the treatment of liver fibrosis (Liu et al., 2020). Overall, the findings of these studies lay a research direction that points to prospective therapeutic efficacy of *I. rubescens* against hepatitis.

Cardiovascular Protective Activity

Cardiovascular disease is a common disease that seriously threatens human health and is characterized by a high prevalence, disability rate, and mortality rate. Cardiovascular diseases kill up to 15 million people worldwide each year, ranking first among all causes of death. In 2017, Kang et al. demonstrated that total flavonoids of *I. rubescens* can stimulate endogenous protective mechanisms and induce the release of low levels of the cytokines NO and NOS, thereby reducing the release of serum NSE, alleviating ischemia-reperfusion injury in brain tissue and further improving the protective effect of ischemic preconditioning on brain injury (Kang et al., 2017). Moreover, oridonin (**1**) ameliorated the abnormal elevation of ECG ST segment caused by myocardial ischemia-reperfusion injury. Furthermore, the myocardial infarct area was significantly reduced and serum CK-MB levels were decreased. Oridonin (**1**) exerted significant cardioprotective effects by regulating energy and amino acid metabolism. Research on the composition and mechanism of action of other components of *I. rubescens* for cardiovascular protection should be enhanced.

Anti-Alzheimer's and Antidepressant Activity

Alzheimer's disease (AD) is a neurodegenerative disorder characterized by β-amyloid aggregation, tau protein hyperphosphorylation, and neuroinflammation. In 2013, Zhang et al. found that oridonin significantly attenuated β-amyloid deposition, plaque-associated APP expression and microglial activation in the brain of transgenic mice, and additional *in vitro* studies indicated that oridonin effectively attenuated the inflammatory reaction of macrophages and microglial cell lines (Zhang et al., 2013). In 2014, Wang et al. found that oridonin could inhibit the mRNA levels of IL-1β, IL-6, COX-2, iNOS, TNF-a, and MCP-1 induced by Aβ, which also up-regulated the expression of IL-10 in $A\beta_{1\text{-}42}$-induced AD mice (Wang et al., 2014). Oridonin (**1**) was also found to rescue $A\beta_{1\text{-}42}$-induced synaptic loss, increase the expression of PSD-95 and synaptophysin in the synaptosomes of AD mice, and promote mitochondrial activity. In addition, oridonin also activated the BDNF/TrkB/CREB signaling pathway in the hippocampus of AD mice and improved the behavioral symptoms of AD mice (Wang et al., 2016). In summary, oridonin is a candidate compound with anti-Alzheimer's activity. Recently, oridonin was reported to regulate the PPAR-γ/AMPA receptor signaling pathway in the prefrontal cortex and identified as a novel antidepressant with clinical potential (Liu et al., 2020).

Immunomodulatory Activity

In 2011, Liu et al. isolated the polysaccharide fraction RPPSIIa from *I. rubescens*, analyzed its structural properties and explored its immunological activity. Structure analysis revealed that the polysaccharide RPPSIIa is a homogeneous compound composed of the monosaccharides rhamnose and glucose in the ratio of 7: 93. It can effectively stimulate the proliferation of mouse spleen lymphocytes in a concentration range of 5–100 μg/ml. Moreover, RPPSIIa at the concentrations of 5 and 50 μg/ml can effectively enhance lymphocyte proliferation induced by Con A (Liu et al., 2011). Moreover, oridonin also inhibits the transcriptional activation of the BAFF promoter in macrophages by significantly suppressing BAFF expression and secretion in macrophages. Lupus symptoms and tissue damage in MRL-lpr/lpr mice were effectively reduced by inhibiting BAFF (Zhou et al., 2013).

QUALITY CONTROL

In the past decades, different methods including TLC, HPLC, UPLC, and UV have been used to analyze the chemical constituents of and control the quality of derivatives isolated from *I. rubescens*. In 2007, Zou et al. established a reversed-phase high performance liquid chromatography (RP-HPLC) method to determine the content of ursolic acid and oleanolic acid in *I. rubescens* by using the chromatographic column NUCLEO-DURC18RP (250 × 4.6 mm, 5 μm), a methanol-water mobile phase (87: 13), a flow rate of 0.8 ml/min, and a photodiode array detector (detection wavelength: 210 nm; column temperature: 25°C). The sample recovery rates of ursolic acid and oleanolic acid were 96.2% and 98.7%, and the RSD were 1.9% and 0.9%, respectively (Zou and Chen, 2007). In the 2020 edition of the Chinese Pharmacopoeia, only oridonin was used as the standard for the evaluation of the *I. rubescens* quality in the pharmaceutical market. According to this source, chromatography was performed using octadecylsilane bonded silica gel as filler and methanol-water (55: 45) as the mobile phase, and the detection wavelength was 239 nm. HPLC analysis of oridonin in the dried aboveground parts of *I. rubescens* revealed a content of more than 0.25% (Chinese Pharmacopoeia, 2020). In fact, diterpenoids

especially oridonin (**1**) and ponicidin (**2**), are considered to be the main active ingredients of *I. rubescens*. Therefore, ponicidin (**2**) should be also used as quality control marker for *I. rubescens* and its medicinal extracts.

Due to different cultivation areas and climatic conditions, significant differences in the chemical compositions of Chinese herbal medicines may be found, and the interactions of multiple chemical compounds may contribute to the therapeutic effects of Chinese medicine. Therefore, a simple quantitative analysis of one or two active ingredients in herbal medicines cannot represent their overall quality, and the simultaneous quantitative analysis of active ingredients has become the most direct and important method for the quality of drugs control of TCM. Thus, it is necessary to establish standards for controlling the quality because of the need for its clinical application. In 2011, Zhang et al. established an ultra-high performance liquid chromatography (UPLC) method for the simultaneous determination of the contents of the five main active ingredients in *I. rubescens* by using a Waters UPLC chromatographic system, an ACQUITY BEH Shield PR18 column (2.1 × 100 mm, 1.7 μm), a mobile phase of 0.1% formic acid methanol solution (A)-0.1% formic acid aqueous solution (B) with a flow rate of 0.2 ml/min (detection wavelengths: 250 and 210 nm; column temperature: 23°C). The chromatographic analysis of the five components of oridonin, ponicidin, rosmarinic acid, oleanolic acid and ursolic acid could be completed within 22 min, the chromatographic peak of each component had a good resolution, and all calibration curves showed good linearity ($r^2 > 0.9991$) in the test ranges (Zhang et al., 2011). In 2013, Yuan et al. established an HPLC method for the simultaneous determination of rosmarinic acid, oridonin and chrysoplenetin in *I. rubescens*. With this method, phenolic acids, diterpenes and flavonoids can be simultaneously determined to obtain more comprehensive information about the intrinsic quality of *I. rubescens* (Yuan et al., 2013).

I. rubescens has complex components, some of which are low in content, and most diterpenes have weak or no UV absorption. It is particularly difficult to use conventional quality control methods for TCM such as HPLC, UPLC, UV, and TLC for the simultaneous determination of to determine more active ingredients. HPLC-MS/MS provides a good alternative for routine analysis due to its rapidness, sensitivity and specificity, and can be used as a reliable method for the quality evaluation of *I. rubescens*. In 2010, Du et al. established a new HPLC-MS/MS method for the qualitative identification and quantitative determination of 19 diterpenoids, 6 phenolic acids, and 3 flavonoids in *I. rubescens* (Du et al., 2010). The separation was carried out on a C_{18} column with a linear gradient of 0.1% formic acid/methanol containing 0.1% formic acid at a flow rate of 0.7 ml/min. This method has been successfully applied to the qualitative and quantitative analysis of 28 chemical components in natural and planted *I. rubescens* samples from different sources, providing strong support for the quality control of *I. rubescens*. Although the commonly used method for the determination of the content of *I. rubescens* is HPLC, considering the multiple components and efficacy of TCM, new determination methods should be studied and developed.

TOXICITY

Information on the side effects and safety evaluations of *I. rubescens* and its active ingredients is limited, and no major side effects have yet been discovered. The 2020 edition of the Chinese Pharmacopoeia recommends an exact dose of 30–60 g per day of *I. rubescens* (China Pharmacopoeia, 2020). In 2000, the chronic toxicity of *I. rubescens* tablets was measured by the intragastric administration of SD mice with a dose of 20 or 40 g/kg/day for 21 days, the results showed that the long-term administration of *I. rubescens* tablets had no toxic side effects on the organism (Hu et al., 2000). In 2011, Hu et al. observed the acute toxicity of the active parts of *I. rubescens*, and the mass fraction of oronidin in *I. rubescens* extract determined by HPLC was 62.4%. The maximum tolerated dose (MTD) of the effective parts of *I. rubescens* was 20 g/kg/d, which is 480 times the dose commonly used in human clinical administration, suggesting that the effective parts of *I. rubescens* had no toxicity in mice (Hu et al., 2011). In another safety evaluation experiment, the results of the acute oral toxicity test showed that the MTD of a concentrated solution of *I. rubescens* was greater than 20.3 g/kg/bw in Kunming mice of both sexes. The genetic toxic effects of different *I. rubescens* concentrations were verified in the three genetic toxicity tests of micronucleus test, sperm malformation test and Ames test of the cells, *in vivo* and *in vitro* in three aspects, revealing negative results. The 90 days feeding test showed that *I. rubescens* powder had no obvious toxic and side effects on the observed indexes of rats, and the maximum dose of *I. rubescens* powder was 5.0 g/kg/bw (Ma, 2010). In conclusion, the toxicity study of *I. rubescens* and its active components and traditional Chinese medicine preparations showed no toxicity, allowing for the development of *I. rubescens* related drugs and health food.

CONCLUSION AND FUTURE PERSPECTIVES

TCM is an important part of ancient medicine because of its wide range of uses, numerous types of chemical components, extensive pharmacological activity and reliable clinical effects. Moreover, it is an important source of lead compounds from numerous types of chemical components for modern drug development. In this review, we summarize the research progress in botany, ethnobotanical uses, phytochemistry, pharmacology, quality control and toxicity of *I. rubescens*. In ancient and modern China, *I. rubescens* was widely used to treat various diseases. Traditionally and ethnobotanically, *I. rubescens* was used for the treatment of esophageal, cardiac, liver, breast, rectal and other cancers, as well as sore throat, cold and headache, tracheitis, chronic hepatitis and snake and insect bites. To date, 324 compounds have been isolated and identified from this plant. A variety of biological activities have been reported for these components, especially their excellent and broad antitumor activity. Among these components, diterpenoids are the major bioactive component, but a large number of studies have focused on the pharmacology of enantio-kaurane type diterpenoids, such

as oridonin (**1**) and ponicidin (**2**), and oridonin was touted as the second best bioactive component after paclitaxel. A variety of Chinese medicinal preparations including *I. rubescens* tablets and dropping pills, have been marketed, and clinical studies on the effective ingredient oridonin have also been carried out. It can be expected that further studies may reveal more enantio-kaurane type diterpenes. Based on the described pharmacological activities of *I. rubescens*, many studies have been conducted using different *in vivo* and *in vitro* experimental biological techniques that support most of its traditional medicinal uses. However, scientific research on *I. rubescens* still exhibits gaps. Therefore, we summarize several topics herein that should be prioritized for future detailed investigation.

Firstly, diterpenoids have always been considered to be the most important active compounds in *I. rubescens*, because of their wide variety and extensive pharmacological studies. However, research on new saponins, alkaloids and flavonoids isolated from *I. rubescens* is still neglected, which seriously limits the diversity of *I. rubescens* research and application. Secondly, current research mainly focuses on antitumor pharmacological activities, and research on other traditional applications of *I. rubescens* in the treatment of bronchitis, rheumatic joint pain, snake and insect bites, etc. needs to be strengthened. Thirdly, the metabolism and serum pharmacology of *I. rubescens* and its active components should be further studied by *in vivo* and *in vitro* methods. Fourth, the diterpenoids in *I. rubescens* generally have antitumor activity. Research on structure-activity relationships should be increased to find the core chemical structure of antitumor drugs, and provide effective molecules for the creation of new drugs of *I. rubescens*. Last but not least, similar pharmacological activities of these different components that contribute to the pharmacological activity of crude *I. rubescens* have been reported, but the relationship between these components including synergistic or antagonistic effects should be clarified in future studies.

In conclusion, *I. rubescens* is a valuable medicinal resource. However, more comprehensive studies on the pharmacodynamics, metabolism, pharmacokinetics, toxicity and side effects as well as clinical trials are required to demonstrate the efficacy and safety of extracts of active compounds of *I. rubescens*. We also expect to find new skeletons and new active molecules of *I. rubescens*.

AUTHOR CONTRIBUTIONS

XD and YL obtained the literatures. XC wrote the manuscript. XH and GG gave ideas and edited the manuscript. All authors approved the paper for publication.

FUNDING

This work was supported by the Program for the Science and technology projects of Guizhou Province (Qian Kehe foundation-ZK (2021) General-550; Qian Kehe Platform Talents (2018)5772–074; Qian Kehe Platform Talents (2019)-017), and the Science and Technology Project of Zunyi (Grant No. ZSKH-HZ-(2020)-78). Logistics Support Department of the Military Commission, (Grant No. CCD16J001; Grant No. CLB19J051).

REFERENCES

Bae, S., Lee, E. J., Lee, J. H., Park, I. C., Lee, S. J., Hahn, H. J., et al. (2014). Oridonin Protects Hacat Keratinocytes against Hydrogen Peroxide-Induced Oxidative Stress by Altering Microrna Expression. *Int. J. Mol. Med.* 33 (1), 185–193. doi:10.3892/ijmm.2013.1561

Bai, N., He, K., Zhou, Z., and Lai, C.-S. (2010). Flavonoids from *Rabdosia Rubescens* Exert Anti-inflammatory and Growth Inhibitory Effect against Human Leukemia HL-60 Cells. *Food Chem.* 122 (3), 831–835. doi:10.1016/j.foodchem.2010.03.071

Bai, N. S., He, K., Zhu, Z., Tsai, M. L., Zhang, L., Quan, Z., et al. (2010). Ent-Kaurane Diterpenoids from *Rabdosia Rubescens* and Their Cytotoxic Effects on Human Cancer Cell Lines. *Planta Med.* 76 (02), 140–145. doi:10.1055/s-0029-1186002

Cai, M. L. (2009). *Study on the Constituents from* Rabdosia Rubescens *Hemsl.* [Master dissertations]. Xi′an: Shaanxi University of Chinese Medicine.

Cai, M. L., Gao, H. Y., Huang, J., Sun, B. H., Song, X. M., and Wu, L. J. (2008). Chemical Constituents from the Aerial Part of Dongling. *J. Shenyang Pharm. Univ.* 25 (11), 856–874. doi:10.14066j.cnki.cn21-1349/r.2008.11.003

Chen, H., Li, H., Duan, C., Song, C., Peng, Z., Li, H., et al. (2021). Reversal of Azole Resistance in Candida Albicans by Oridonin. *J. Glob. Antimicrob. Resist.* 24 (24), 296–302. doi:10.1016/J.JGAR.2020.10.025

Chinese Pharmacopoeia (2020). *Editorial Committee of Chinese Pharmacopoeia, 2020*. Beijing: China Medical Science and Technology Press.

Dai, Y., Song, Z. R., and Li, J. (2015). Extraction Characteristics of Polysaccharides, Total Flavonoids and Oridonin from *Rabdosia Rubescens*. *J. Jinggangshan Univ. (Natural Science).* 36 (03), 93–98. doi:10.3969/j.issn.1674-8085.2015.03.019

Deng, X. X., and Lv, X. (2017). Comparison of the Efficacy of Donglingcao Dripping Pills and Compound Donglingcao Buccal Tablets in the Treatment of Recurrent Oral Ulcer. *He'nan traditional Chin. Med.* 37 (04), 733–735. doi:10.16367/j.issn.1003-5028.2017.04.0261

Ding, Y., Ding, C. Y., Ye, N., Liu, Z. Q., Wold,Chen, E. A. H. Y., et al. (2016). Discovery and Development of Natural Product Oridonin-Inspired Anticancer Agents. *Eur. J. Med. Chem.* 2016, 122. doi:10.1016/j.ejmech.2016.06.015

Du, Y. F. (2008). *Quality Control of* Rabdosia Rubescens *and Pharmacokinetics of Two Mushroom Components*. [Doctor dissertations]. Hebei: Hebei Medical University.

Du, Y. F., Liu, P. W., Yuan, Z. F., Jin, Y. R., Zhang, X. W., Sheng, X. N., et al. (2010). Simultaneous Qualitative and Quantitative Analysis of 28 Components in Isodon Rubescens by HPLC-ESI-MS/MS. *J. Separation Sci.* 33 (4–5), 545–557. doi:10.1002/jssc.200900704

Feng, S. S., and Xu, J. G. (2014). Profile of Antioxidant and Antibacterial Activities of Different Solvent Extracts from. *Rabdosia Rubescens. Int. J. Food Sci. Tech.* 49 (11), 2506–2513. doi:10.1111/ijfs.12576

Feng, W. S., Li, H. W., Zheng, X. K., and Wang, Y. Z. (2008). Progress in Studies of Chemical Compositions from. *Isodon Rubescens. Chin. J. New Drugs.* 17 (23), 2003–2007.

Gao, S. Y., and Wang, L. (2014). Chemical and Pharmacological Effects of *Rabdosia Rubescens*. *J. Harbin Univ. Commerce (Natural Sci. Edition).* 30 (01), 1–6. doi:10.19492/j.cnki.1672-0946.2014.01.001

Guo, P., Li, Y. S., and Guo, Y. Q. (2010). Research Progress on Chemical Constituents and Pharmacological Activities of. *Rabdosia Rubescens. Drug Evaluation Research.* 33 (2), 144–147. doi:10.7501/j.issn.0253-6376

Han, B. K. (2018). *The Antitumor Mechanism of a Novel Diterpene Jaridon 6 from* Isodon Rubescens *on Gastric Cancer Resistant Cell MGC803/5-Fu*. Master, Zhengzhou University, Zhengzhou.

Han, Q. B., Mei, S. X., Jiang, B., Zhao, A. H., and Sun, H. D. (2003a). Kaurane Diterpenoids from. *Rabdosia Rubescens. Chin. J. Org. Chem.* 23 (3), 270–273.

Han, Q. B., Zhao, Q. S., Li, S. H., Peng, L. Y., and Sun, H. D. (2003b). Enantiokaurane Diterpenoids from. *Rabdosia Rubescens. Huaxue Xuebao*. 04 (07), 1077–1082. doi:10.3321/j.issn:0567-7351.2003.07.021

Han, Q. B., Zhao, A. H., Zhang, J. X., Lu, Y., Zheng, L. L., Zhang, Q. T., et al. (2003c). Cytotoxic Constituents of *Isodon Rubescens* Var. Lushiensis. *J. Nat. Prod.* 66 (10), 1391–1394. doi:10.1021/np030165w

Han, Q. B., Li, M. L., Li, S. R., Mou, Y. K., Lin, Z. W., and Sun, H. D. (2003d). Ent-kaurane Diterpenoids from *Isodon Rubescens* Var. Lushanensis. *Chem. Pharm. Bull.* 51 (07), 790–793. doi:10.1248/cpb.51.790

Han, Q., Lu, Y., Wu, L., He, Z. D., Qiao, C. F., Xu, H. X., et al. (2005). An Asymmetric Ent-Kauranoid Dimer from *Isodon Rubescens* Var. Lushanensis. *Tetrahedron Lett.* 46 (32), 5373–5375. doi:10.1016/j.tetlet.2005.06.004

Hu, Y. J., Zhang, J. C., Wang, L., and Cheng, L. (2011). Acute Toxicity Test of Active Parts of Rabdosia Rubescens. *Guangming J. Chin. Med.* 26 (11), 2216–2217. doi:10.3969/j.issn.1003-8914.2011.011.025

Hu, Y. X., Wang, D. P., and Yang, H. (2000). Chronic Toxicity Test of Donglingcao Buccal Tablets. *J. Med. Forum* 8 (12), 39–40.

Huang, S. X., Zhou, Y., Pu, J. X., Li, R. T., Li, X., Xiao, W. L., et al. (2006). Cytotoxic Ent-Kauranoid Derivatives from. *Isodon Rubescens. Tetrahedron* 62 (20), 4941–4947. doi:10.1016/j.tet.2006.02.079

Huang, S. X., Pu, J. X., Xiao, W. L., Li, L. M., Weng, Z. Y, Zhou, Y., et al. (2007). Ent-Abietane Diterpenoids from *Isodon Rubescens* Var. Rubescens. *Phytochemistry.* 68 (5), 616–622. doi:10.1016/j.phytochem.2006.11.007

Jiang, P., Jin, H., Jiang, J. H., Yang, F., Cai, H. H., Yang, P. H., et al. (2017). Single Molecule Force Spectroscopy for *In-Situ* Probing Oridonin Inhibited ROS-Mediated EGF-EGFR Interactions in Living KYSE-150 Cells. *Pharmacol. Res.* 119, 479–489. doi:10.1016/j.phrs.2016.11.036

Jintao, X., Shasha, Y., Jincai, W., Chunyan, L., Mengya, Y., and Yongli, S. (2020). Network Pharmacological Screening of the Active Ingredients and Hypoglycemic Effect of Isodon Rubescens in the Treatment of Diabetes. *Planta Med.* 86 (08), 556–564. doi:10.1055/a-1147-9196

Jiu, M., Liu, G. C., Zhao, Y. M., Yuan, J. F., and Wang, L. J. (2018). Antioxidant Activity and Component Analysis of. *Rabdosia Rubescens. Food Sci. Technbrazil.* 43 (05), 239–244. doi:10.13684/j.cnki.spkj.2018.05.042

Kang, J. J., and Liu, X. N. (2019). The New Progress of Oridonin's Anti-inflammatory Effect in the Treatment of many Diseases. Wild Plant Resources of China,. *Chin. Wild Plant Resour.* 38 (02), 47–51. doi:10.3969/j.issn

Kang, L., Miao, M. S., Bai, M., and Tian, S. (2017). Effect of Total Flavonoid in *Rabdosia Rubescens* on Tolerant Mice Models under Cerebral Anoxia - Sciencedirect. *Saudi J. Biol. Sci.* 24 (8), 1798–1802. doi:10.1016/j.sjbs.2017.11.015

Li, B. L., Shi, Z. X., and Pan, Y. J. (2002). A New Diterpenoid, Taibairubescensin C, from. *Isodon Rubescens. Pol. J. Chem.* 76 (5), 721–724. doi:10.1002/chin.200235171

Li, G. S., Zhang, W., Peng, T., and Guo, M. Z. (2014). Antibacterial Activity of Compounds from Rabdosia Rubescens. *World Sci. Technology-Modernization Traditional Chin. Med.* 3, 610–613. doi:10.11842/wst.2014.03.031

Li, J. S., Bao, L. P., Zha, D. Q., Zhang, L., Gao, P., Zhang, J., et al. (2017). Oridonin Protects against the Inflammatory Response in Diabetic Nephropathy by Inhibiting the TLR4/p38-MAPK and TLR4/NF-Kb Signaling Pathways. *Int. Immunopharmacol* 55, 9–19. doi:10.1016/j.intimp.2017.11.040

Li, M. R., Lu, Y. H., Zhou, M., and Ding, Z. J. (2001). Determination of Oridonin in Donglingcao Syrup by RP-HPLC. *Chin. J. Chin. Materia Med.* 26 (11), 64–65.

Li, Q. F., Feng, B. K., Li, W. M., and Xiao, F. (2011). Study on Dissolution Determination of *Rabdosia Rubescens* Dispersible Tablets. *Chin. Traditional Patent Med.* 33 (03), 442–445. doi:10.3969/j.issn.1001-1528.2011.03.021

Li, S., Zhang, Q., Li, X., Xu, J., and Guo, Y. Q. (2019). Studies on the Chemical Constituents of Rabdosia Rubescens. *J. Pharm. Res.* 38 (4), 194–197. doi:10.13506/j.cnki.jpr.2019.04.002

Li W, W., Wang, J. J., and Ma, D. W. (2019). Synthesis of Enantiokaurane Diterpenes. *Prog. Chem.* 031 (011), 1460–1471. doi:10.7536/PC190809

Li, X. X. (2020). *Preliminary Study on Anti-fungal and Insecticidal Activities and Anti-fungal Mechanism of* Isodon Rubescens *Extract*. Master, Zhengzhou University, Zhengzhou.

Liu, D., Qin, H. L., Yang, B. X., Du, B., and Yun, X. L. (2020). Oridonin Ameliorates Carbon Tetrachloride-Induced Liver Fibrosis in Mice through Inhibition of the NLRP3 Inflammasome. *Drug Dev. Res.* 81 (04), 526–533. doi:10.1002/ddr.21649

Liu, F., Liu, G. Y., Zhou, J., Che, X. P., and Han, R. F. (2011). Purification and Characterization of *Rabdosia Rubescens* Polysaccharide Rppsiia. *Zhongcaoyao Zazhi.* 42 (02), 241–243.

Liu, J., Liang, J. Y., and Xie, T. (2004a). Development of *Rabdosia Rubescens* (Hemsl.) Hara. *Strait Pharm. J.* 04 (02), 1–7.

Liu, J., Xie, T., Wei, X. L., Yang, H., Yang, C. H., and Liang, J. Y. (2004b). Studies on Chemical Constituents of. *Rabdosia Rubescens. Chin. J. Nat. Med.* 02 (05), 276–279.

Liu, P., and Du, J. (2020). Oridonin Is an Antidepressant Molecule Working through the PPAR-γ/AMPA Receptor Signaling Pathway. *Biochem. Pharmacol.* 180 (23), 114136. doi:10.1016/j.bcp.2020.114136

Liu, X. (2012). *Studies on Chemical Constituents and Bioactivity of* Isodort Rubescens *and I. Flexicaulis*. [Master dissertations]. Wuhan: Huazhong University of Science and technology.

Liu, X., Xue, Y. B., Dong, K., Li, X. N., Li, Y., Pu, J. X., et al. (2012). Three New Ent-Kaurane Diterpenoids from *Isodon Rubescens* and Their Cytotoxicities. *Chin. J. Nat. Med.* 10 (6), 464–470. doi:10.1016/S1875-5364(12)60088-0

Lu, F., and Xu, X. J. (2008). Chemical Constituents of *Rabdosia Rubescens*. *Zhongyaocai Zazhi* 09, 1340–1343. doi:10.13863/j.issn1001-4454.2008.09.021

Lu, H. Y., and Liang, J. Y. (2012). A New Asymmetric Ent-Kauranoid Dimer from. *Rabdosia Rubescens. Zhongcaoyao Zazhi* 4.01 (2012), 4–7. doi:10.3969/j.issn.1674-6384.2012.01.002

Lu, H. Y., Liang, J. Y., and Chen, R. (2007). Studies on the Chemical Constituents of. *Rabdosia Rubescens. Chin. J. Nat. Med.* 04 (04), 269–271.

Lu, H. Y., Liang, J. Y., Chen, R., and Yu, J. (2008). Chemical Constituents of. *Rabdosia Rubescens. Chem. Industry For. Prod.* 04 (03), 7–12.

Lu, H. Y., Wang, M. H., Zhang, X. Q., Wu, F. H., and Liang, J. Y. (2013). Studies on the Chemical Constituents of. *Rabdosia Rubescens. Strait Pharm. J.* 25 (12), 193–196.

Luan, J., Zhang, Y. F., Yang, S., Wang, X., Yu, B., and Yang, H. (2015). Oridonin: A Small Molecule Inhibitor of Cystic Fibrosis Transmembrane Conductance Regulator (CFTR) Isolated from Traditional Chinese Medicine. *Fitoterapia.* 100, 88–94. doi:10.1016/j.fitote.2014.11.001

Luo, G. Y., Deng, R., Zhang, J. J., Ye, J. H., and Pan, L. T. (2017). Two Cytotoxic 6,7-seco-spiro-lacton-ent-kauranoids from Isodon Rubescens. *J. Asian Nat. Prod. Res.* 20 (3), 1. doi:10.1080/10286020.2017.1317754

Luo, X., Pu, J. X., Xiao, W. L., Zhao, Y., Gao, X. M., Li, X. N., et al. (2010). Cytotoxic Ent-Kaurane Diterpenoids from *Isodon Rubescens* Var. Lushiensis. *J. Nat. Prod.* 73 (6), 1112–1116. doi:10.1021/np100110u

Ma, Y. C., Ke, Y., Zi, X. L., Zhao, W., Shi, X. J., and Liu, H. M. (2013). Jaridonin, a Novel Ent-Kaurene Diterpenoid from *Isodon Rubescens*, Inducing Apoptosis via Production of Reactive Oxygen Species in Esophageal Cancer Cells. *Curr. Cancer Drug Targets* 13 (06), 611–624. doi:10.2174/15680096113139990030

Ma, Z. (2010). *Study on Immune Regulation of* Rabdosia Rubescens *and its Safety Assessment*. [Master dissertations]. Changsha: Central South University.

Pi, J., Jin, H., Jiang, J. H., Yang, F., Cai, H. H., Yang, P. H., et al. (2017). Single Molecule Force Spectroscopy for *In-Situ* Probing Oridonin Inhibited ROS-Mediated EGF-EGFR Interactions in Living KYSE-150 Cells. *Pharmacol. Res.* 119, 479–489. doi:10.1016/j.phrs.2016.11.036

Ren, W., Zhu, S. R., Tao, X. J., Chen, W. M., Ma, J. Z., and Zhu, G. X. (2009). Clinical Study of Donglingcao Dropping Pills in the Treatment of Recurrent Aphthous Ulcer. *J. Clin. Stomatol.* 25 (12), 40–41.

Shi, J. F. (1984). Fifty Cases of Chronic Tracheitis Treated with Frost Eggplant Seedling. *J. GuiZhou Univ. Traditional Chin. Med.* 04 (02), 44–45.

Shu, J. W., Yuan, F., Wen, C. M., and Yang, G. Z. (2017). Studies on Diterpenoids from Rabdosia Rubescens. *J. Green Sci. Technology.* 04 (18), 216–218.

Si, X. W., Li, S. Y., Chen, S. H., and Tan, G. H. (1993). Clinical Report of Yantejia Buccal Tablets in Treating 120 Cases of Diseases in Department of Facial Features. *J. GuiZhou Univ. Traditional Chin. Med.* 06 (02), 31–32. doi:10.16588/j.cnki.issn1002-1108.1993.04.017

Song, F. J., Gao, J., Yang, G. Z., and Wang, S. T. (2011). Chemical Constituents of. *Rabdosia Rubescens. Lishizhen Med. Materia Med. Res.* 22 (05), 1069–1070. doi:10.3969/j.issn.1008-0805.2011.05.013

Sun, H. D., Lin, Z. W., Fu, J., Zheng, X. R., and Gao, Z. Y. (1985). Studies on the Structures of Oridonin and Oridonin B from Xinyang. *Acta Chim. Sinica* 04 (04), 353–359.

Tang, J. C., Zhao, M., Wang, Y. J., Kang, G. F., Wu, J. H., Zheng, M. Q., et al. (2011). One Single HPLC-PDA/(-)ESI-MS/MS Analysis to Simultaneously Determine

30 Components of the Aqueous Extract of Rabdosia Rubescens. *J. Chromatogr. B Analyt Technol. Biomed. Life Sci.* 879 (26), 2783–2793. doi:10.1016/j.jchromb.2011.07.046

The Plant List (2013). Version 1.1. Published on the Internet. Available at: http://www.theplantlist.org/(Accessed January 1.

Wang, D. H., Ji, Z. Q., Wei, S. P., Guo, Z. Y., and Wu, W. (2010). JStudy on Antibacterial Constituents of. *Rabdosia Rubescens. Agrochemicals.* 49 (06), 410–412. doi:10.16820/j.cnki.1006-0413.2010.06.005

Wang, S. L., Yang, H., Yu, L. J., Jin, J. L., Qian, L., Zhao, H., et al. (2014). Oridonin Attenuates Aβ1–42-Induced Neuroinflammation and Inhibits NF-kB Pathway. *PLoS One* 9 (8), e104745. doi:10.1371/journal.pone.0104745

Wang, S. L., Yu, L. J., Yang, H., Li, C. S., Hui, Z., Xu, Y., et al. (2016). Oridonin Attenuates Synaptic Loss and Cognitive Deficits in an Aβ1–42-Induced Mouse Model of Alzheimer′s Disease. *Plos One* 11, e0151397. doi:10.1371/journal.pone.0151397

Wei, J. J. (2012). *Primary Study on the Formation Mechanism of Chemotype in* Isodon Rubescens *(Hemsl.) H. Hara*. [Master dissertations]. Zhengzhou: Zhengzhou University.

Wen, C., Chen, S., Yuan, F., Liu, X. M., Song, F. J., Mei, Z. N., et al. (2019). Diterpenoids from *Isodon Rubescens* and Their Nitric Oxide Production Inhibitory Activity. *RSC Adv.* 9 (69), 40628–40635. doi:10.1039/C9RA08831H

Wu, Q. J., Zheng, X. C., Wang, T., and Zhang, T. Y. (2018). Effects of Oridonin on Immune Cells, Th1/Th2 Balance and the Expression of BLys in the Spleens of Broiler Chickens Challenged with Salmonella Pullorum. *Res. Vet. ence.* 119, 262–267. doi:10.1016/j.rvsc.2018.07.008

Xie, R. J. (2012). *Studies on the Chemical Constituents and Bioactivities of* Isodon Rubescens *and* Isodon Serra. [Master dissertations]. Xinxiang: Xinxiang Medical University.

Xie, R. J., Yan, F. L., Hai, G. F., Hou, R. J., Ding, M. M., and Bai, Y. X. (2011). Two New Diterpenoids and Other Constituents from *Isodon Rubescens*. *Fitoterapia* 82, 726–730. doi:10.1016/j.fitote.2011.03.003

Xiong, H. (2014). Study on Modern Pharmacological and Chemical Components and Clinical Medication of *Isodon Rubescens*. *Inner Mongolia traditional Chin. Med.* 33 (22), 2. doi:10.3969/j.issn.1006-0979.2014.22.081

Xue, J., Song, J., and Shen, C. X. (2007). Study on Antitumor Effect of. *Isodon Rubescens. Lishizhen Med. Materia Med. Res.* 2007 (9), 2277–2278. doi:10.3969/j.issn.1008-0805.2007.09.138

Yan, X. B., Lei, M., Ke, Y., Qu, H. L., Yin, P., and Liu, H. M. (2006). Chemical Constituents of Rabdosia Rubescens. *J. Chem. Res.* 17 (03), 80–82.

Yang, H. T., and Shen, C. L. (1997). Development of *Rabdosia Rubescens* Medicated Toothpaste. *Oral Care Industry* 04 (04), 16–18.

Yang, J., Ren, X. Y., Zhang, L. P., Li, Y. Y., Cheng, B., and Xia, J. (2018). Oridonin Inhibits Oral Cancer Growth and PI3K/Akt Signaling Pathway. *Biomed. Pharmacother.* 100, 226–232. doi:10.1016/j.biopha.2018.02.011

Yao, H. Z., Li, J. X., and Zheng, H. N. (2010). Protective Effect of Rabdosia Rubescens Extract on CCl_4 Induced Chronic Liver Injury in Mice. *Lishizhen Med. Materia Med. Res.* 03, 575–577. doi:10.3969/j.issn.1008-0805.2010.03.032

Yuan, X. L., Yan, L. H., Zhang, Q. W., and Wang, Z. M. (2013). HPLC Determination of Rosmarinic Acid, Oridonin and Cat's Eye Flavin in Rubescens Vulgaris. *Chin. J. Chin. Materia Med.* 14, 2343–2347. doi:10.4268/cjcmm20131426

Yuan, Z. W., Ping, O. Y., Gu, K. X., Rehman, T., Zhang, T. Y., Yin, Z. Q., et al. (2019). The Antibacterial Mechanism of Oridonin against Methicillin-Resistant staphylococcus Aureus (Mrsa). *Pharm. Biol.* 57 (1), 710–716. doi:10.1080/13880209.2019.1674342

Zhang, D., Zhou, Q., Huang, D. D., He, L., Zhang, H., Hu, B., et al. (2019). ROS/JNK/c-Jun axis Is Involved in Oridonin-Induced Caspase Dependent Apoptosis in Human Colorectal Cancer Cells. *Biochem. Biophys. Res. Commun.* doi:10.1016/j.bbrc.2019.04.011

Zhang, J. H, Zhou, Y. Y., Sun, Y. X., Yan, H., Han, W. C., Wang, X. Y., et al. (2019). Beneficial Effects of Oridonin on Myocardial Ischemia/reperfusion Injury: Insight Gained by Metabolomic Approaches. *Eur. J. Pharmacol.* 861, 172587. doi:10.1016/j.ejphar.2019.172587

Zhang, H., Du, X., Pu, J. X., Wang, Y. Y., He, F., and Zhao, Y. (2010a). Two Novel Diterpenoids from *Isodon Rubescens* Var. Lushanensis. *Tetrahedron Lett.* 51, 4225–4228. doi:10.1016/j.tetlet.2010.06.015

Zhang, H., Pu, J. X., Wang, Y. Y., He, F., Zhao, Y., Li, X. N., et al. (2010b). Four New Ent-Kauranoids from *Isodon Rubescens* Var. Lushanensis and Data Reassignment of Dayecrystal B. *Chem. Pharm. Bull. (Tokyo).* 41 (26), 56. doi:10.1248/cpb.58.56

Zhang, J. Q., Li, L., and Li, S. J. (2008). Clinical Observation on 160 Cases of Acute Pharyngitis Treated with Donglingcao Tablet. *Chin. Med. Mod. Distance Education China* 002, 119. doi:10.3969/j.issn.1672-2779.2008.02.016

Zhang, J., Yuan, K., Jin, Y. C., and Liu, Y. (2011). Simultaneous Determination of 5 Active Ingredients in Rubescens by UPLC Method. *Chin. J. Pharm. Anal.* 04, 641–644. doi:10.1142/s1793604711002202

Zhang, L., Khoo, C. S., Koyyalamudi, S. R., Pedro, N. D., and Reddy, N. (2017). Antioxidant, Anti-inflammatory and Anticancer Activities of Ethanol Soluble Organics from Water Extracts of Selected Medicinal Herbs and Their Relation with Flavonoid and Phenolic Contents. *Pharmacologia* 8, 59–72. doi:10.5567/pharmacologia

Zhang, Y., Jiang, H. Y., Liu, M., Hu, K., Wang, W. G., Du, X., et al. (2017). Bioactive Ent-Kaurane Diterpenoids from. *Isodon Rubescens. Phytochemistry.* 143, 199–207. doi:10.1016/j.phytochem.2017.08.009

Zhang, X. H. (2019). Clinical Effect of Donglingcao Capsule Combined with Western Medicine in the Treatment of Chronic Pharyngitis. *Chin. J. Clin. Rational Drug Use.* 12 (20), 85–86. doi:10.15887/j.cnki.13-1389/r.2019.20.055

Zhang, Z. Y., Daniels, R., and Schluesener, H. J. (2013). Oridonin Ameliorates Neuropathological Changes and Behavioural Deficits in a Mouse Model of Cerebral Amyloidosis. *J. Cell. Mol. Med* 17 (12), 1566–1576. doi:10.1111/jcmm.12124

Zhou, L., Sun, L. J., Wu, H. K., Zhang, L. Z., Chen, M. C., Liu, J. W., et al. (2013). Oridonin Ameliorates Lupus-like Symptoms of MRLlpr/lpr Mice by Inhibition of B-Cell Activating Factor (BAFF). *Eur. J. Pharmacol.* 715 (1-3), 230–237. doi:10.1016/j.ejphar.2013.05.016

Zou, J., Pan, L. T., Li, Q. J., Pu, J. X., Yao, P., Zhu, M., et al. (2012). Rubesanolides C-E: The Abietane Diterpenoids Isolated from *Isodon Rubescens* and Evaluation of Their Anti-biofilm Activity. *Org. Biomol. Chem.* 10 (26), 5039–5044. doi:10.1039/c2ob25192b

Zou, J., Pan, L. T., Li, Q. J., Zhao, J. H., Pu, J. X., Yao, P., et al. (2011). *Rubesanolides A. B: Diterpenoids Isodon Rubescens. Org. Lett.* 13 (6), 1406–1409. doi:10.1021/ol200086k

Zou, S. Q., and Chen, W. (2007). Determination of Ursolic Acid and Oleanolic Acid in Rubescens by Reversed-phase High Performance Liquid Chromatography. *Lishizhen Traditional Chin. Med. Materia Med.* 07, 1577–1578. doi:10.3969/j.issn.1008-0805.2007.07.018

Conflict of Interest: The authors declare that the research was conducted in the absence of any commercial or financial relationships that could be construed as a potential conflict of interest.

Publisher's Note: All claims expressed in this article are solely those of the authors and do not necessarily represent those of their affiliated organizations, or those of the publisher, the editors and the reviewers. Any product that may be evaluated in this article, or claim that may be made by its manufacturer, is not guaranteed or endorsed by the publisher.

GLOSSARY

A549 Human alveolar basal epithelial cells
ALT Alanine aminotransferase
AST Aspartate aminotransferase
ABTS 2, 2′-azino-bis (3-ethylbenzthiazoline-6-sulfonic acid
Aβ amyloid
A.D Anno domini
AKT Proteinkinase B
Aβ1-42 Human amyloid beta peptide 1-42
BAFF B-cell-activating factor
Bcap37 Human breast cancer cells
BGC823 Human gastric cancer cell line
BDNF Brain-derived neurotrophic factor
COX-2 Cyclooxygenase-2
CREB Cyclic-AMP response binding protein
COLO 205 Colorectal cancer line 205
DPPH 2,2-diphenyl-1-picrylhydrazyl
DMEM Dulbecco's modified eagle medium
EC_{50} Concentration for 50% of maximal effect
ECG Electrocardiogram
GAE Gallic acid equivalents
GC-MS Gas chromatography-mass spectrometer
GSK-3β Glycogen synthese kinase-3β
HPLC High performance liquid chromatography
HPLC-MS High performance liquid chromatography-mass spectrometer
HL-60 Human promyelocytic leukemia cells
HaCaT Human immortalized keratinocytes
HepG2 Liver hepatocellular cells
HIF-1 Hypoxia inducible factor
HUVECs Human umbilical vein endothelial cells
IC_{50} Half maximal inhibitory concentration
IL-1β Interleukin-1β
IL-6 Interleukin-6
IL-10 Interleukin-10
iNOS Inducible nitric oxide synthase
K562 Human chronic myeloid leukemia cells
MCF-7 Human breast adenocarcinoma cell line
MDA Malondialdehyde
MIC Minimum inhibitory concentration
MAPK Mitogen-activated protein kinase
MCP-1 Human macrophage chemoattractant protein-1
NLRP3 NOD-like receptor protein 3
NF-κB Nuclear factor-kappa B
NO Nitric oxide
PI3K Phosphatidylinositol 3-kinase
PPAR-γ Peroxisome proliferators-activated receptors
PSD-95 Postsynaptic density protein 95
pKa Dissociation constant
QE Quercetin equivalents
RAW 264.7 Mouse leukaemic monocyte macrophage cell line
RSD Relative standard deviation
SMMC-7721 Human hepatocellular carcinoma cells
SOD Superoxide dismutase
SW480 Human colon cancer cell line
TNF-α Tumor necrosis factor alpha
TLR4 Toll-like receptor 4
TrkB Tyrosine kinase receptor B
TLC Thin layer chromatography
TCM Traditional chinese medicine
UV Ultraviolet-visible spectroscopy
UPLC Ultra-high-performance liquid chromatography.

frontiers | Frontiers in Pharmacology

ORIGINAL RESEARCH
published: 29 June 2022
doi: 10.3389/fphar.2022.807831

Traditional Uses of Animals in the Himalayan Region of Azad Jammu and Kashmir

Maryam Faiz[1], Muhammad Altaf[2], Muhammad Umair[3], Khalid S. Almarry[4], Yahya B. Elbadawi[4] and Arshad Mehmood Abbasi[5,6]**

[1]Department of Zoology, Women University of Azad Jammu and Kashmir, Bagh, Pakistan, [2]Department of Forestry, Range and Wildlife Management, The Islamia University of Bahawalpur-Pakistan, Bahawalpur, Pakistan, [3]College of Chemistry and Life Sciences, Zhejiang Normal University, Jinhua, China, [4]Department of Botany and Microbiology, College of Science, King Saud University, Riyadh, Saudi Arabia, [5]Department of Environment Sciences, COMSATS University Islamabad, Abbottabad, Pakistan, [6]University of Gastronomic Sciences, Pollenzo, Italy

OPEN ACCESS

Edited by:
Norberto Peporine Lopes, University of São Paulo, Bauru, Brazil

Reviewed by:
Irwin Rose Alencar De Menezes, Regional University of Cariri, Brazil
Irshad A. Nawchoo, University of Kashmir, India

***Correspondence:**
Muhammad Umair
umairm@zjnu.edu.cn
umair.bot@gmail.com
Arshad Mehmood Abbasi
amabbasi@cuiatd.edu.pk
arshad799@yahoo.com

Specialty section:
This article was submitted to Ethnopharmacology, a section of the journal Frontiers in Pharmacology

Received: *02 November 2021*
Accepted: *06 May 2022*
Published: *29 June 2022*

Citation:
Faiz M, Altaf M, Umair M, Almarry KS, Elbadawi YB and Abbasi AM (2022) Traditional Uses of Animals in the Himalayan Region of Azad Jammu and Kashmir. Front. Pharmacol. 13:807831. doi: 10.3389/fphar.2022.807831

Background: The use of animals and animal-derived products in ethnopharmacological applications is an ancient human practice that continues in many regions today. The local people of the Himalayan region harbor rich traditional knowledge used to treat a variety of human ailments. The present study was intended with the aim of examining animal-based traditional medicine utilized by the population of the Himalayan region of Azad Jammu and Kashmir.

Methods: Data were collected from 2017 to 2019 through individual and group interviews. Data on traditional uses of animal products were analyzed, utilizing following indices such as the frequency of citation, use value, relative importance, similarity index, principal component analysis, and cluster analysis to find the highly preferred species in the area.

Results: Ethnomedicinal uses of 62 species of vertebrates and invertebrates were documented. Flesh, fat, bone, whole body, milk, skin, egg, head, feathers, bile, blood, and honey were all used in these applications. The uses of 25 animals are reported here for the first time from the study area (mainly insects and birds, including iconic species like the kalij pheasant, *Lophura leucomelanos*; Himalayan monal, *L. impejanus*; and western tragopon, *Tragopan melanocephalus*). The diversity and range of animal-based medicines utilized in these communities are indications of their strong connections with local ecosystems.

Conclusion: Our results provide baseline data valuable for the conservation of vertebrate and invertebrate diversity in the region of Himalayan of Azad Jammu and Kashmir. It is possible that screening this fauna for medicinally active chemicals could contribute to the development of new animal-based drugs.

Keywords: medicinal animals, zootherapy, ethnobiology, Kashmir, Himalayas

INTRODUCTION

Zootherapy is described as the use of animals or animal-derived materials to treat human ailments (Costa-Neto, 2005; Holennavar, 2015; Ahmad et al., 2021). The use of animals with medicinal properties continues to be a common practice worldwide. Zootherapy techniques and materials are utilized in traditional and nanomedicine for the treatment of different diseases (Kassam, 2002; Lawal and Banjo, 2007; Prakash and Verma, 2021). It is documented that almost 13% of the drugs used by traditional Chinese medicine are derived from vertebrates and invertebrates (Still, 2003). In Ayurvedic medicine, 15–20% of drugs contain vertebrate and invertebrate products (Unnikrishnan, 1998). In Tibetan medicine, the products of vertebrates and invertebrates are utilized in more than 111 drugs (Singh, 2000).

Many societies are rapidly losing their ethnopharmacological knowledge; so, documenting this knowledge before it is lost is increasingly important (Alves and Rosa, 2007; Löki et al., 2021; Mandal and Rahaman, 2022). Likely because of the dominance of plants in traditional medicine systems, the use of animals and animal-derived products in traditional medicine has been under-documented. Pakistan has a rich faunal diversity, including 195 species of mammals (Roberts, 1997), 668 species of birds (Mirza and Wasiq, 2007), 195 species of reptiles (Khan, 2006), and 24 species of amphibian studied by Khan (2010). To date, a number of studies have documented the use of animal parts in traditional medicine in different parts of Pakistan (Muhammad et al., 2018; Adil and Tariq, 2020; Aslam and Faiz, 2020; Mughal et al., 2020; Noor and Haider, 2020; Altaf et al., 2021; Haidar and Bashir, 2021; Ijaz and Faiz, 2021; Ijaz and Iftikhar, 2021; Saleem et al., 2021); however, ethnomedicinal uses of animals in Azad Jammu and Kashmir have never been reported.

Animals and its derived products are important elements in many traditional treatments (Ferreira et al., 2010; Albuquerque et al., 2012; Altaf and Faiz, 2021), and they have presumably utilized since prehistoric times (Alves et al., 2010; Prakash and Prakash, 2021). Traditional information can lead scientists to promising natural sources of new medicines, making it a powerful ally in the discovery of new drugs (Saleem et al., 2021; Habib, 2022). A suitable model for replicating contact dermatitis is phenol-induced ear edema. When phenol comes into direct contact with the skin, "keratinocytes" release chemical mediators that are crucial in prime contact irritation reactions, including as pro-inflammatory cytokines (Lim et al., 2004). These pro-inflammatory cytokines are made in a different way than those synthesized by PKC (as occurring in inflammations induced by croton oil). The rupturing of the "keratinocyte plasma membranes", which leads to the liberation of pre-formed IL-1, as well as other inflammation mediators, is thought to be the cause of cutaneous irritations (Murray et al., 2007).

Zoonotic diseases are transferable diseases caused by infectious agents (such as viruses, bacteria, prions, or parasites) that can be transferred from a non-human animal to a human. Zoonotic diseases have caused a series of major global public health issues (malaria, yellow fever, avian flu, swine flu, West Nile virus, MERS, SARS, etc.), culminating in the current coronavirus health crisis (Altaf, 2016; Altaf, 2020). Different pathogens have different modes of transmission (Kruse et al., 2004; Van Vliet et al., 2017), so the risk of zoonotic diseases depends on the type of animals with which humans are in contact (as well as the duration and nature of contact) (Bilal et al., 2021). For example, the prevalence of diseases from fish to humans is very low (EHS, 2016b), while the risk of transmission from amphibians is higher due to human sensitivity to their porous skin (EHS, 2016a). The main aim of this study is to determine what animals local populations in Pakistan are in contact with in order to contribute to an understanding of the risk of zoonotic disease transmission due to ethnopharmacological uses of animals.

Human impacts on natural systems are complex. Many indigenous cultures have traditionally promoted ways of life that are relatively balanced in relation to the sustainability of their resource use. On the other hand, the forces of capitalism coupled with a conceptual nature–culture divide and propagated through the global spread of colonialism have resulted in extractive approaches to resource use that threaten the resilience of the majority of ecosystems. Ethnozoological research is critical to understanding the sustainability of biocultural systems (Fopa et al., 2020). Cultural uses of animal species (i.e., food, hunting, medicine, entertainment, religious practice, and trade) may promote beliefs and behaviors that help to conserve these animal species; however, if they are practiced unsustainably, or affected by commercialization or other political and economic factors, they may negatively affect or even endanger these animals. The use of animal species for traditional medicine and cultural purposes by local communities must also be considered in relation to other factors, such as changes in climate and habitat (Alves, 2012; Alves et al., 2018). There exists a global need to find new approaches to dealing with the present crisis of biodiversity loss (Boivin et al., 2016), and ethnozoology provides critical insights into the practices of local communities, allowing conservation efforts to effectively partner with resource stewards to promote the overall integrity of biocultural systems (Saunders, 2003; Dickman, 2010). This study on the medicinal uses of fauna by the rural and urban people of the Himalayan region of Azad Jammu and Kashmir is part of a broader research project to document the uses of animals by local communities throughout Pakistan (Muhammad et al., 2017a; Muhammad et al., 2017b; Muhammad et al., 2017c; Altaf et al., 2018; Altaf, 2020).

METHODS

Description of the Study Area

Individual and group interviews were conducted in six different sites of the Himalayan region in Azad Jammu and Kashmir during 2017–2019 (**Figure 1**). The study area is located between 33° and 35° North latitude and 73° and 75° East longitude, in the foothills of Himalayas on the North East side of Pakistan, with an average elevation of 6,325 m in the north and 360 m in the south (Khan et al., 2017). Azad Jammu and Kashmir (AJ&K) is a cultural and geographical land of narrow, long, strip and occupies an area of 13,297 km^2, with >4 million population. The main rivers of AJ&K are Jhelum, Poonch, and Neelum. The climate of this region is subtropical with an average rainfall of

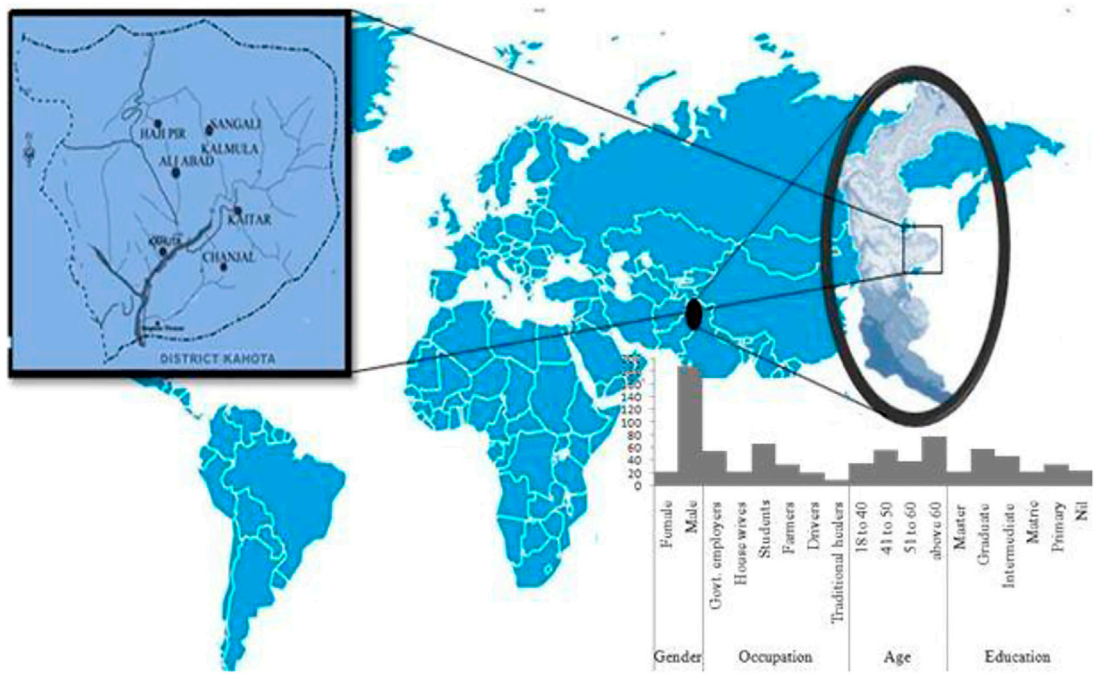

FIGURE 1 | Map and respondent profile of the study area of the district Haveli.

>150 cm. Spruce (*Abies pindrow*), Kail (*Pinus excelsa*), cheer (*Pinus willichiana*), deodar (*Cedrus deodara*), fur (*Pinus* spp.), and some other conifer species are dominant trees in AJ&K forests (PM, 2008; Ch et al., 2013; Khan et al., 2017; FWFD, 2021).

The study area is dominated by different tribal groups, such as Khawaja, Gujjar, and Rathor, which are the most common. Pahari, Kashmiri, and Gujjari are the major languages spoken, while Urdu is the official language, which is spoken as a second language by most people. The population of Haveli District was 112,000 in the census of 1998 and 157,000 in the census of 2015. The density was 262 people per sq. km in 2015. The average household size in the district is around 7, with most people living in joint family structures. The majority of the population lives in rural areas and is entirely Muslim. Most of the people (’70%) in the study area are educated (Khan et al., 2017).

Data Collection and Analysis

Before beginning fieldwork, consent was obtained from the “Department of Zoology, Women’s University of Azad Jammu and Kashmir, Bagh-Pakistan,” while questionnaires and interviews were arranged to record the ethnomedicinal uses of animals. Data were taken from respondents (n = 210) who included government employees, housewives, students, farmers, drivers, and customary wellbeing practitioners (**Supplementary Table S1**). Respondents were chosen based on their having basic awareness of folk medicines of wild animals. During the field survey, prior informed consent was obtained from each participant, and general standards/guidelines of the International Society of Ethnobiology (ISE) (http://www.ethnobiology.net/) and Consensus Statement on Ethnopharmacological Field Studies (ConSEFS) (https://www.journals.elsevier.com/journal-of-ethnopharmacology/) by Heinrich et al. (2018) were followed.

Field guides of mammals, birds, and herpetofauna *“Mammals of Pakistan”* (Roberts, 2005), *“Birds of Pakistan”* (Roberts, 1991, 1992), and *“Amphibian and Reptiles of Pakistan”* (Khan, 2006) were shown to informants to verify which species they described. Basic data on medicinal uses were then used to generate different indices including “frequency of citation,” “use value,” and “relative importance,” which were then analyzed using statistical methods including “similarity index,” “principal component analysis,” and “cluster analysis.”

Quantitative Analysis

The ethnozoological data were analyzed by various indices, which include “FC” (frequency of citation), RI (relative importance), and UV (used-value).

Frequency of Citation and Relative Importance

The frequency of citation is the number of respondents who described the medicinal uses of wild fauna species. The relative importance index was intended by the formula, as reported by Oliveira et al. (2010).

$$RI = PP + AC$$

where PP stands for pharmacological property quantity and AC is the maximum number of ailment categories treated by the most resourceful species divided by the number of ailment categories treated by a given species.

FIGURE 2 | Statistically significantly important pictures (**(A)** house sparrow; **(B)** Russet sparrow; **(C)** spotted dove; **(D)** oriental garden lizard; **(E)** honey bee; **(F)** common beak) from study areas.

Use Value and Similarity Index

The use value (UV) is the quantitative measure of the relative importance of specific animal species known locally. UV and the SI were calculated following the method reported previously (Trotter and Logan, 1986; Phillips and Gentry, 1993), using the formula:

$$UV = \sum U/n$$

The number of citations per species is n, and the number of informants is U.

$$SI = \frac{S_a}{T_a} \ (0 < SI < 1)$$

Note: S_a = Similar documented ailment in the previous and present studies, T_a = Total documented ailment in the present study.

Statistical Analysis

Data were analyzed in "Microsoft Excel 2010" (Microsoft, Redmond, WA, United States), whereas inferential statistical analysis was performed by using R software 3.6.3 and PAST 3.20 (Hammer et al., 2001). In addition, traditional uses of the body part(s) of animal species and their mode of application were represented in chord diagrams generated with the "circlize package (24)" in R software 3.6.1 (Gu et al., 2014).

RESULTS

Data were gathered from 188 males and 22 females in the Haveli District. Majority of the informants were males, because due to cultural restrictions, usually females avoid conversation with strangers. Most of the data were collected from the rural area as majority of the inhabitants (n = 127) live there. Informants were common people, government employees, teachers, students, farmers, and shopkeepers. Among these, ˃90% were literate and the rest were illiterate. Most of the informants (n = 78) were of age more than 60 years, while young respondents (18–40 years) were 36 in number (**Figure 1**). Cow, *Bos taurus;* hen, *Gallus gallusd omesticus;* buffalo, *Bubalus bubalis;* duck, *Anas platyrhynchos domesticus;* hill pigeon, *Columba rupestris;* common pigeon, *Columba livia*; russet sparrow, *Passer cinnamomeus*; house sparrow, *Passer domesticus*; common hoopoe, *Upupa epops*; spotted dove, *Spilopelia chinensis*; oriental turtle dove, *Streptopelia orientalis*; sheep, *Ovis aries*; Himalayan monal, *Lophophorus impejanus*; camel, *Camelus dromedaries*; honey bee, *Apis mellifera*; chukar partridge, *Alectoris chukar*; alpine musk deer, *Moschus chrysogaster* and goat, *Capra aegagrus hircus* were the commonly utilized species in the region of Himalayan, AJ&K (**Supplementary Table S1**; **Figure 2**).

Thirty-nine diseases were treated with different animal parts and products (**Figure 3**), such as flesh, bone, whole body, milk, skin, egg, head, feather, bile, blood, and honey. Flesh was the most consumed (n = 35) body part, followed by bone, whole body, milk, skin, egg, head, feather, bile, blood, and honey (**Figure 4**). Local inhabitants use the fat of different species such as little egret (*Egretta garzetta*) and cattle egret (*Bubulcus ibis*) to treat memory and epilepsy, golden eagle (*Aquila chrysaetos*) to treat wound healing, and regulate blood chemical, Alexandrine parakeet (*Psittacula eupatria*) to treat memory, great tit (*Parus major*) to treat male impotency and skin problem, duck (*Anas platyrhynchos domesticus*) to treat kidney problems, heart problems, BP, male impotency, piles, blindness,

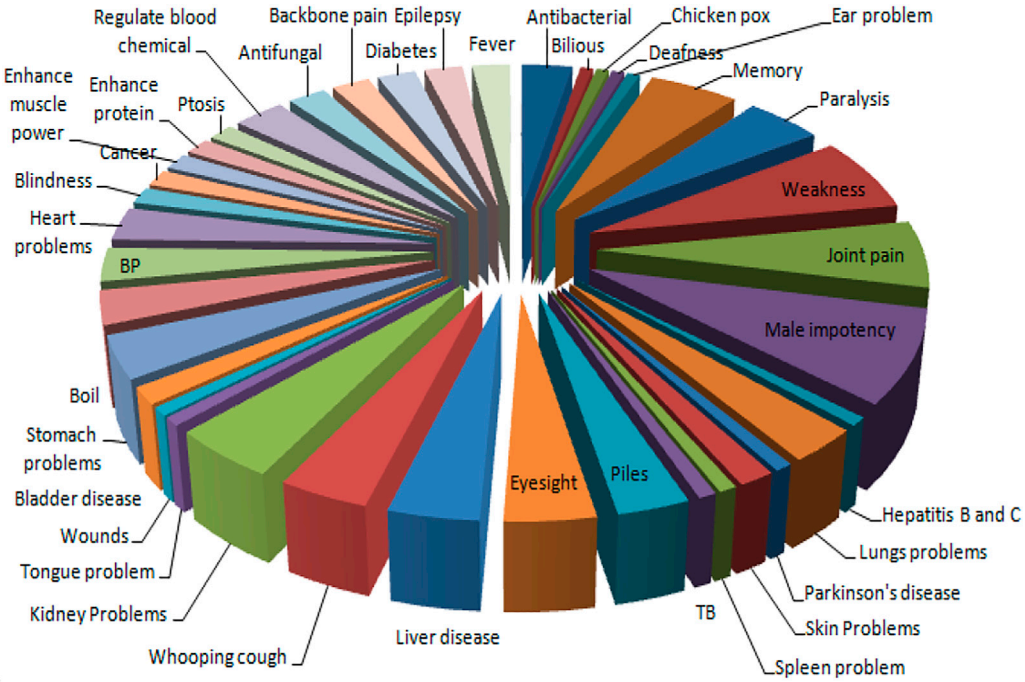

FIGURE 3 | Comparative analysis of species used to cure various ailments in the district Haveli, Azad Jammu and Kashmir.

and eyesight, Asiatic black bear (*Ursus thibetanus*) to treat joint pain and male impotency, Indian crested porcupine (*Hystrix indica*) to treat joint pain, Asiatic jackal (*Canis aureus*) to treat skin problems, Hazara gauk (*Duttaphrynus melanostictus*) to treat antibacterial and antifungal, agror agama (*Laudakia agrorensis*) to treat joint pain, backbone pain, and male impotency, brown cobra (*Naja oxiana*) to treat joint pain, piles, and eyesight, oriental garden lizard (*Calotes versicolor*) to treat joint pain, and leopard gecko (*Eublepharis macularius*) to treat cancer (**Figures 5**, **6**).

Likewise, the meat of snow partridge, *Lerwa lerwa,* was used to treat fever; western tragopan, *Tragopan melanocephalus,* was used to treat lung problems and weakness; common quail, *Coturnix coturnix,* was used to treat bilious, heart problems, TB, joint pain, backbone pain, and paralysis; rain quail, *Coturnix japonica,* was used to treat and regulate blood chemical; chukar partridge, *Alectoris Chukar,* was used to treat weakness; black francolin, *Francolinus francolinus,* was used to treat joint pain and lung problems; grey francolin, *Francolinus pondicerianus,* and Himalayan monal, *Lophophorus impejanus,* were used to treat weakness; kalij pheasant, *Lophura leucomelanos,* was used to treat weakness, fever, and memory; common pigeon, *Columba livia,* was used to treat Parkinson's disease, ptosis, and tongue problem; hill pigeon, *Columba rupestris,* was used to treat wound healing; spotted dove, *Spilopelia chinensis,* and oriental turtle dove, *Streptopelia orientalis,* were used to treat paralysis and enhance muscle power; Asian koel, *Eudynamys scolopaceus,* was used to treat spleen problem; oriental scopus owl, *Otus sunia,* was used to treat whooping cough; common hoopoe, *Upupa epops,* was used to treat stomach problems, liver disease, bladder disease, and eyesight; Asian house martin, *Delichon dasypus,* was used to treat male impotency; barn swallow, *Hirundo rustica,* was used to treat male impotency; streaked laughing thrush, *Trochalopteron lineatum,* was used to treat weakness; common myna, *Acridotheres tristis,* was used to treat whooping cough; russet sparrow, *Passer cinnamomeus,* was used to treat paralysis, male impotency, and liver; grey wagtail, *Motacilla cinerea,* white wagtail, *Motacilla alba,* and citrine wagtail, *Motacilla citreola,* were used to treat kidney problems; duck, *Anas platyrhynchos domesticus,* was used to treat kidney problems, heart problems, BP, male impotency, piles, blindness, and eyesight; hen, *Gallus gallus domesticus,* was used to treat kidney problems, heart problems, weakness, memory, eyesight, male impotency, diabetes, stomach problems, and BP; alpine musk deer, *Moschus chrysogaster,* was used to treat paralysis; Rhesus Macaque, *Macaca mulatta,* was used to treat wounds; red fox, *Vulpes vulpes,* was used to treat male impotency; giant red Himalayan squirrel, *Petaurista petaurista,* was used to treat diabetes; cow, *Bos taurus,* was used to treat and enhance protein, weakness, and boil; and *Bubalus bubalis* was used to treat fever and enhance protein (**Figures 5**, **6**).

Similarly, bones of *Coturnix japonica*, *Alectoris chukar, Neophron percnopterus, Columba rupestris, Otus sunia, Trochalopteron lineatum,* and *Psittacula eupatria* were used to treat and regulate blood chemicals, weakness, stomach problems, kidney problems, heart problems, wound healing, whooping cough, and memory. Similarly, bones of *Paraconophyma* spp., *Luciola substriata, Androctonus* spp., *Libythea lepita,* and *Pheretima hawayana* were used to treat lung problems, antibacterial, antifungal, deafness, ear problems, diabetes, stomach problems, and eyesight. Further, the head of *Meranoplus bicolor* and *Actias selene* was used to cure deafness and antibacterial. Milk, feather, bile, blood, and honey were used to treat piles, diabetes, stomach problems, eyesight, male impotency, paralysis,

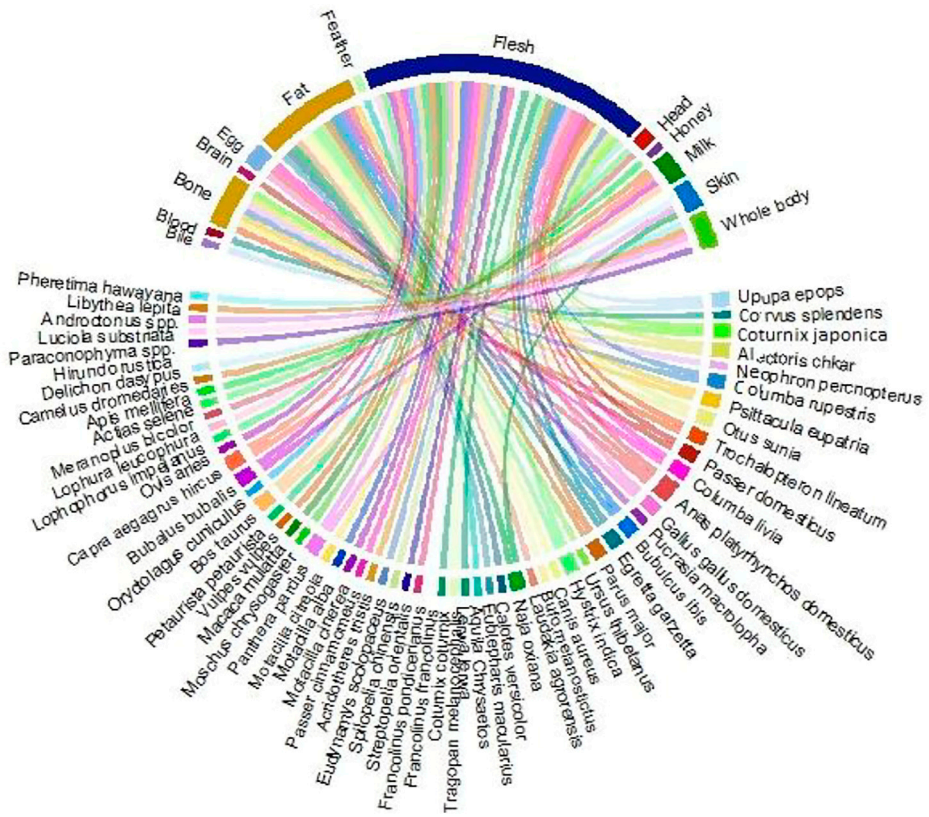

FIGURE 4 | Body parts of animal species used in different recipes.

measles, stomach problems, male impotency, and liver disease (**Figures 5**, **6**).

In the same way, eggs of *Columba livia*, *Anas platyrhynchos domesticus,* and *Gallus gallus domesticus* were used to treat Parkinson's disease, ptosis, kidney problems, stomach problems, heart problems, BP, male impotency, piles, blindness, eyesight, diabetes, wound healing, and memory (**Figures 5**, **6**).

Frequency of Citation

Species of vertebrates and invertebrates documented by the most respondents have high "frequency of citation" scores, which ranged from 1 to 29 (**Figure 7**). COEP and COPH were documented as the most often consumed, with FC = 29 in the region of Himalayan, AJ&K. WTA, CQHD, CQTB, RQIR, KPJP, CEMM, CEEL, LEMM, LEEL, WVHA, GEBP, AKSP, HCPL, AMMP, BSMP, HSCP, GWKS, WWKS, CWKS, DUES, RMW, RFMI, GLJP, and FFEP had the lowest frequencies of citation (n = 1) (codes are written in **Supplementary Table S1**).

Relative Importance

The "relative importance" values are presented in **Supplementary Table S1**. Most animals were documented to be highly versatile in their utilization (RI = 3.45) such as CQB, CQJP, CQBP, CQPL, CPPD, HPWH, HSMI, HSPL, RSPL, RSMI, DUKP, DUHP, HNKP, HNMI, PPCP, PPMI, COEP, and COPH (**Figure 7**), while the lowest value of RI (0.18) was recorded for DUES.

Use Value

Among the reported wild animal species, the highest "UVs" (maximum of 1.0) were for HSPL, RSPL, RSMI, DUKP, DUHP, HNKP, HNMI, PPCP, PPMI, COEP, COPH, CQB, CQJP, CQBP, CQPL, CPPD, HPWH, and HSMI (codes are presented in **Supplementary Table S1**). The lowest UVs of 0.05 were noted for DUES. The high "UVs" of these species showed their widespread use in the healing of ailments.

Similarity Index

Out of the total, 49 species have zero similarity index; this shows that the present study has a lot of novel data. The similarity index of *Gallus gallus domesticus* is 0.067 followed by *Capra aegagrus hircus* (SI = 0.056), *Camelus dromedaries* (0.17), *Passer domesticus* (0.2), *Laudakia agrorensis* (0.2), *Calotes versicolor* (0.2), *Passer cinnamomeus* (0.25), and *Naja oxiana* (0.34). *Columba rupestris, Eudynamys scolopaceus, Corvus splendens,* and *Acridotheres tristis,* which have a similarity index of 1 (**Supplementary Table S1**).

Principal Component Analysis and Cluster Analysis

Statistical analysis with the assistance of "PCA" showed that the first two axes of the "PCA" has 100% variation and "PC 1" and "PC 2" have 98.5 and 1.5% variations, respectively (**Figures 8**, **9**). Variables loaded onto the x-axis "PC 1" includes FC (r = 0.99454),

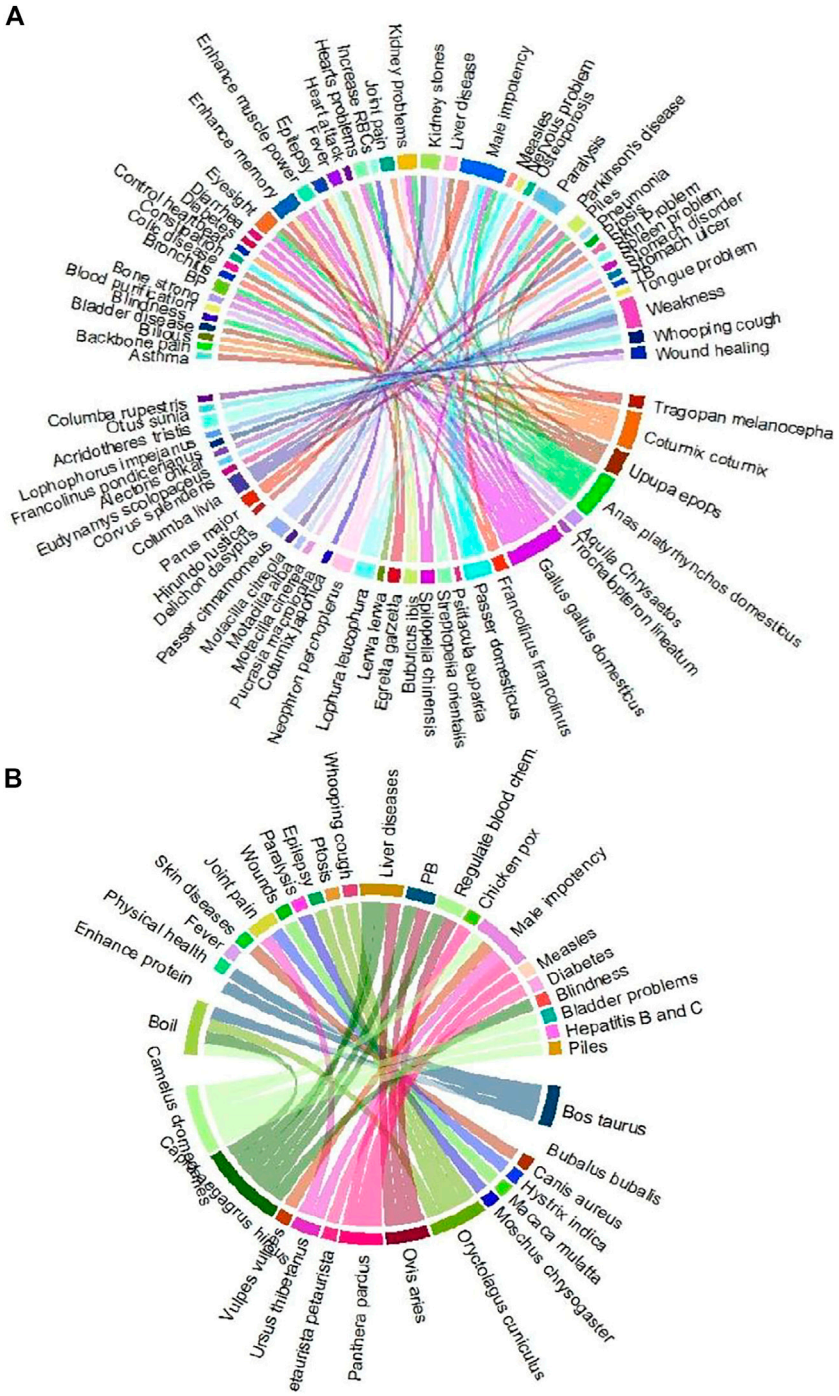

FIGURE 5 | Animal species distribution according to the treatment of various ailments in the Himalayan region of Azad Jammu and Kashmir. Animal species are classified into different groups such as **(A)** birds and **(B)** mammals.

UV (r = 0.029041), and RI (r = 0.10028), while "PC 2" included FC (r = -0.1044), UV (r = 0.27713), and RI (r = 0.95515). The "Cluster analysis" depicted various groups and sub-groups, which are distinguished on the basis of the source of the number of informants (**Figures 8**, **9**). The results of PC1 exhibit positive correlations between FC, UV, and RI, while that of PC2 indicate a negative correlation with FC and a positive correlation with UV, as well as RI variables.

The analysis demonstrated that two groups are noted in the "cluster analysis" in the Himalayan region, AJ&K, i.e., "group one" (G1) and "group two" (G2). "G1" and "G2" have a similarity of almost 0.8 points. G1 is further

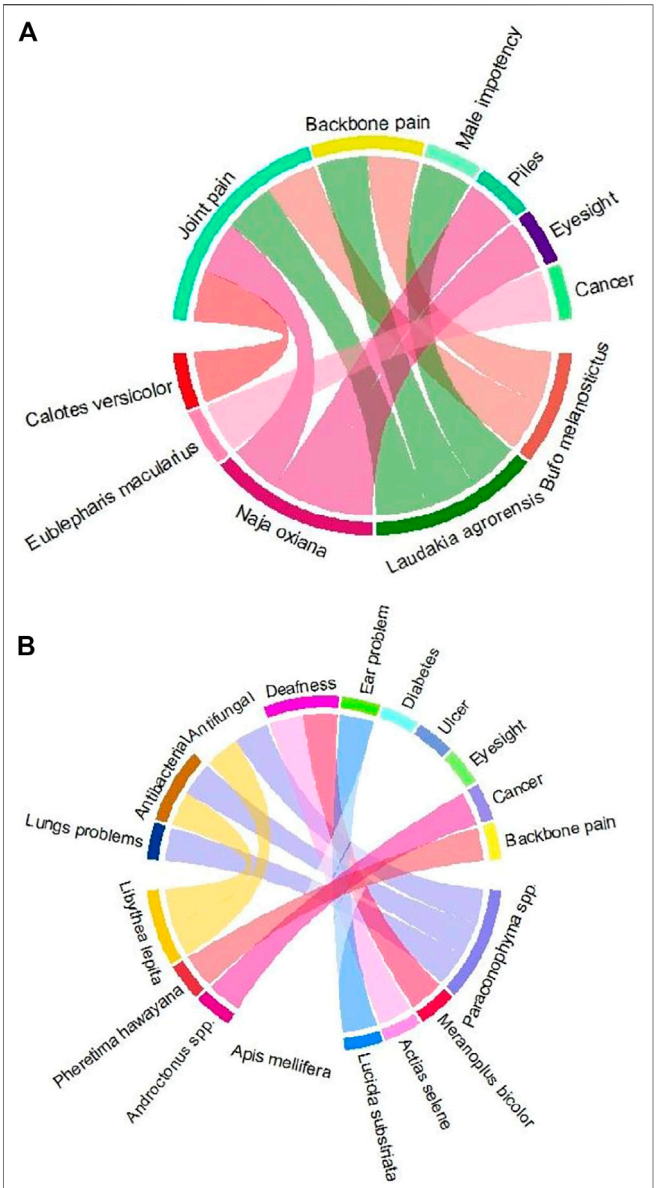

FIGURE 6 | Animal species distribution according to the treatment of various ailments in the Himalayan region of Azad Jammu and Kashmir. Animal species are classified into different groups such as **(A)** reptiles and **(B)** invertebrates.

divided into two groups known as SG1-I (subgroup 1-I) and SG1-II (subgroup 1-II), while both have a similarity of approximately 0.5 points. Likewise, G2 is further divided into two groups known as SG2-I (subgroup 2-I) and SG2-II (subgroup 2-II), while both have a similarity of about 0.6 points. SG1-II has the following species of animals with diseases coded as COEP, COPH, HNBP, HNMI, HNKP, HNEM, and HNSM; while SG1-II has the following BFFV, BFEP, DUHP, DUKP, HPWH, and CPPD (**Figure 10**).

DISCUSSION

In ethnozoological research, socio-demographic data on respondents (age, gender, occupation, ethnicity, and education) are incredibly useful, as this component plays a key role in interpreting and analyzing the feedback received (Easthope, 1995; Hanif et al., 2019). Male respondents made up 94% contribution, whereas female respondents were rare in the present study. This is because most of the females are housewives and do not meet with strangers, so more males are selected for interviews. Altaf et al. (2017) discovered similar results in a research of ethnomedicinal and cultural activities of mammalian and avian in the region of Punjab, Pakistan. In fact, males hunted animals for food as well as for medicine, which could explain our findings. Additionally, the informants in village areas had more knowledge and information regarding the use of species for human ailments when compared to the informants in urban regions. These results were alike to earlier information from the district of Negev, Israel (Friedman et al., 1986).

The inhabitants of the region of Himalayan in AJ&K reported the ethnomedicinal uses of 62 animal species to treat 39 different diseases including male impotency, weakness, joint pain, memory loss, paralysis, piles, eyesight, stomachache, whooping cough, liver, and kidney problems among others in the present study. Similarly, 32 animal species, invertebrates and vertebrates, for treating 37 types of ailments were reported in southern regions of KPK, Pakistan. The major treated ailments were night blindness, epilepsy, cancer, hepatitis, asthma, paralysis, whooping cough, and brain hemorrhage (Mussarat et al., 2021). They reported the use of *Gallus gallus domesticus* for joint pain, blood pressure, weakness, hepatitis, diabetes, *Capra hircus* for hepatitis C, night blindness and joint pain, *Passer domesticus* for abdominal pain, and *Ovis aries* for the regulation of blood level, which supports our findings.

Birds were the most regularly used animal group for therapeutic purposes in our study. Previous findings revealed that wild birds are used as a food source in many parts of the world, including Pakistan (Arshad et al., 2014; Altaf et al., 2017; Mughal et al., 2020), India (Jaroli et al., 2010; Chinlampianga et al., 2013), Brazil (Alves et al., 2013; Teixeira et al., 2014), and Philippines (Ploeg and Weerd, 2010). Bird species are commonly used to treat various human ailments such as body pain, arthritis, respiratory disorders, gastric ulcers, obesity, and piles in the present study. Previous reports also showed that bird species are utilized in different folk therapies e.g., infertility, asthma, abscess, anemia, body weakness, body strength, bronchitis, breathing trouble, enhanced memory, immune enhancer, fever, flue, epilepsy, menorrhagia, paralysis, puberty in young girls, skin diseases, sexual power, and wound healing (Arshad et al., 2014; Vijayakumar et al., 2015a; Bagde and Jain, 2015; Vijayakumar et al., 2015b; Aloufi and Eid, 2016; Chattha et al., 2017; Hakeem et al., 2017; Ali et al., 2018; Mughal et al., 2020; Haidar and Bashir, 2021). In fact, parts or products of bird species are highly nutritious food and composed of "calcium," "chlorine," "iron," "phosphorus," "potassium," "sodium," "glycogen," "lactic acid," "lipids," "magnesium," "nitrogenous compounds," "non-nitrogenous compounds," and "water" (Keeton and Eddy, 2004; Hui, 2012; Cheung and Mehta, 2015). Moreover, birds

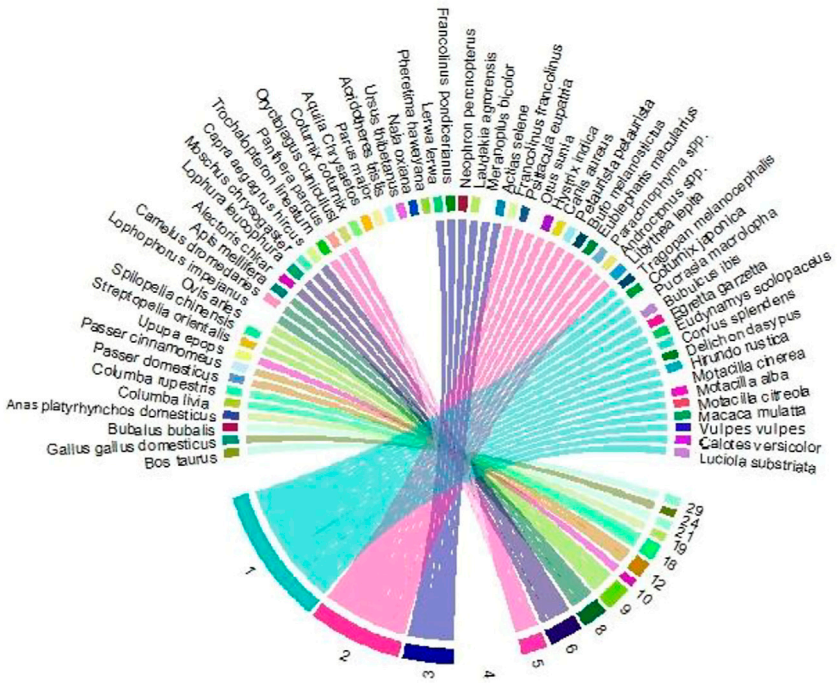

FIGURE 7 | The relationship between the FC and the number of species application in Haveli districts.

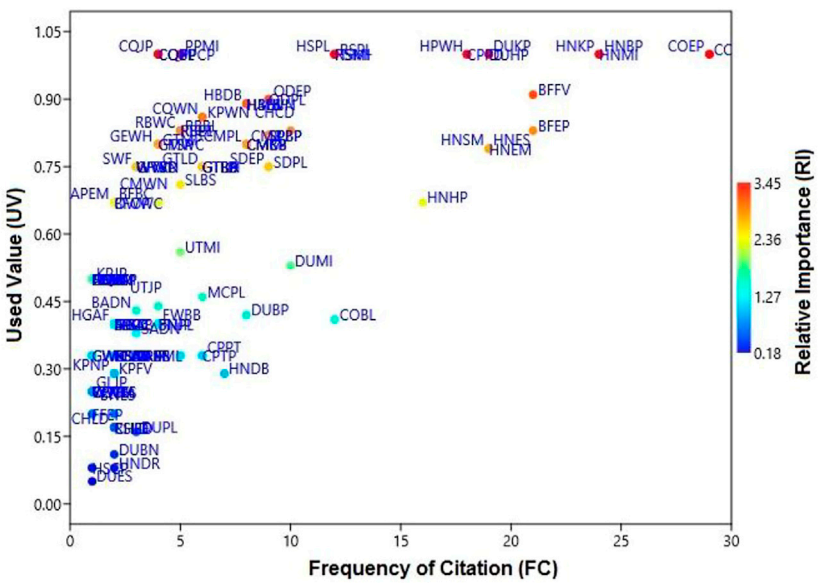

FIGURE 8 | Relationship between the frequency of citation (FC), use value (UV), and relative importance (RI) for a particular disease (UV). Codes represent the species names of birds that appear in **Supplementary Table S1**.

are also connected with superstitious beliefs, such as people of the local area who believe that ducks and gooses are the sign of prosperity. However, in some reports from Pakistan, mammals are most used animals in ethnomedicines (Altaf et al., 2018; Mussarat et al., 2021).

It has been documented that omega-3 fatty acid in vertebrates' fats decreases inflammation (Wilson, 2015; Ijaz and Faiz, 2021). Ethnobiologist documented that fats are used to treat a neurological disorder, atherosclerosis, thrombotic, and aging affects (Breteler, 2000; Haag, 2003).

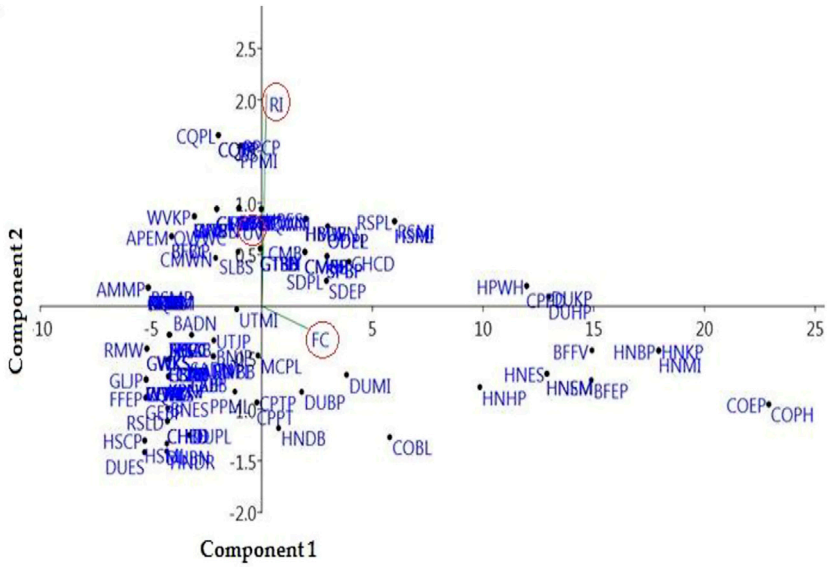

FIGURE 9 | Principal component analysis (PCA) (codes are present in **Supplementary Table S1**), showing the positions of the arrows relative to components 1 and 2, shows how strongly independent variables (UV, FC, and RI) are correlated with each other from the district Haveli.

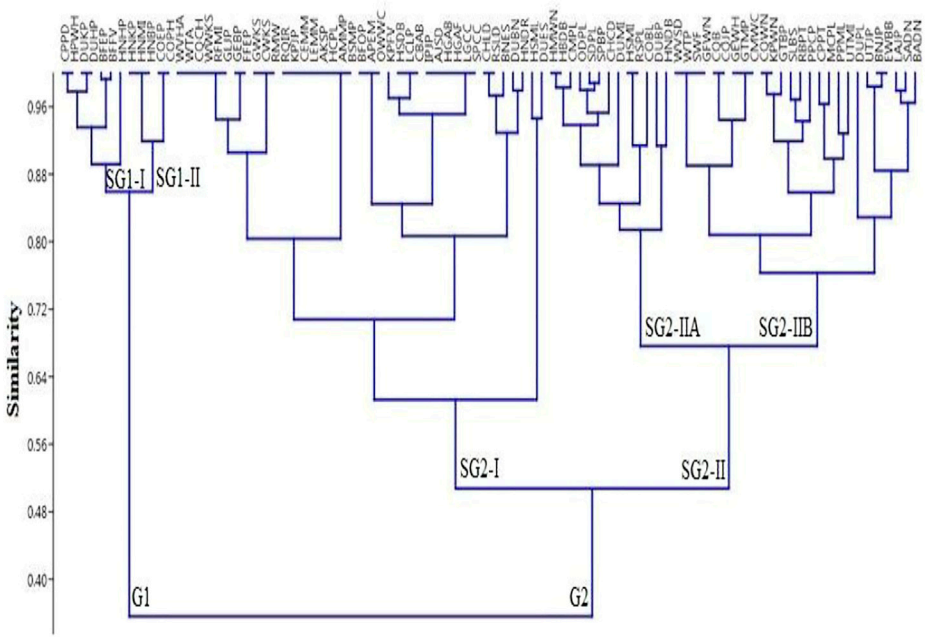

FIGURE 10 | Cluster analysis showing the similarities among species (codes are present in **Supplementary Table S1**) in different variables (UV, FC, and RI) of the district Haveli.

Meat is composed of water, nitrogenous compounds, lipids, non-nitrogenous compounds, glycogen, lactic acid, sodium, magnesium, calcium, chlorine, potassium, iron, and phosphorus (Keeton and Eddy, 2004; Hui, 2012). Meat composition is different due to the impacts of different environmental and internal factors like feeding, muscle, animal species, breed sex, etc. (Cheung and Mehta, 2015). Beef, poultry, lamb, fish, and pork are the most common meats consumed in the world. Camel meat, on the other hand, is renowned in a few nations, particularly in dry and semi-arid regions, as the principal source of animal protein that equals, if not surpasses, the economical value of other meats (Williams, 2007; Schönfeldt

and Gibson, 2008; Abrhaley and Leta, 2018; Haidar and Bashir, 2021).

It is documented that bones contain up to "95%" elastic protein, collagen fibers, as well as inorganic minerals such as calcium and phosphate. They improve bone fractures (Hall, 2011). Different species of animals, i.e., cinereous vulture, goat, alpine musk deer, crow, crab-eating macaque, common carp, fruit bat, deer, horse, and Indian gagata, were used for different ailments like improving wounds, digestion, heart strength, ear aches, lumbago, skin, chest pain, and urine problems (Ghosh et al., 2013; Vallejo and González, 2014; Vijayakumar et al., 2015a; Vijayakumar et al., 2015b; Yeshi et al., 2017; Altaf et al., 2018; Bullitta et al., 2018; Altaf, 2020; Abbasi, 2021; Ijaz and Iftikhar, 2021; Riaz and Altaf, 2021).

Eggs are an ideal source of protein and a balanced source of nutrients for humans of all ages, as well as also a supply of vitamins and other compounds and elements like "A," "B6," "B12," "folic acid," "phosphorus," "selenium," "amino acid," and "iron." Eggs are utilized to treat low blood pressure, fever, cold, weakness, breast cancer, weight loss, weak eye side, cold, bones, teeth, CNS, sprains, eye-each, BP, nourishing, bronchitis, asthma, burst furuncles, hemorrhoids, diabetes, jaundice, indigestion, to ease birth, diabetes, sinusitis, bronchitis, shortness of breath, rheumatism, stuffy nose, nervous problems, flu, weak bones, furuncle, burns, night blindness, weakness, sore throat, and otic infectivity (Padmanabhan and Sujana, 2008; Alves et al., 2010; Lohani, 2010; Oliveira et al., 2010; Alonso-Castro et al., 2011; Lohani, 2011b; Jacobo-Salcedoa et al., 2011; Alves et al., 2012; Barros et al., 2012; Haileselasie, 2012; Souto et al., 2012; Bagde and Jain, 2013; Betlu, 2013; Kim and Song, 2013; Martínez, 2013; Chellappandian et al., 2014; Bagde and Jain, 2015; Altaf et al., 2017; Dey et al., 2017; Altaf et al., 2018; Tariq, 2020). The egg is made up of structures that provide the optimum environment for the growth and development of an embryo. It is one of the biggest sources of essential nutrients for humans except the vitamin C. Eggs are surprisingly delicious and healthy foods used in different ways (Tariq, 2020).

Milk is one of the oldest foods (Wiley, 2015) and at the same time the most important one (Spreer, 1998). Milk of mammalian species consists of fats, proteins, lactose, ash, water, and solids (Guo et al., 2007; Hamad and Baiomy, 2010; Ballard and Morrow, 2013; Grădinaru et al., 2015; Merlin Junior et al., 2015; Getaneh et al., 2016; Kula and Tegegne, 2016; Abdullahi, 2019). Milk is utilized to cure a variety of sicknesses like hepatitis, measles, body pain, cancer, *tuberculosis*, diabetes, eye pain, whooping cough, cataract, sexual power, arthritis, and gastritis (Lev, 2003; WHO, 2005; Padmanabhan and Sujana, 2008; Alves et al., 2009; Benítez, 2011; Lohani, 2011b; Mishra et al., 2011; Yirga et al., 2011; Alves et al., 2012; Barros et al., 2012; Haileselasie, 2012; Martínez, 2013; Alonso-Castro, 2014; Betlloch Mas et al., 2014; Mootoosamy and Mahomoodally, 2014; Vijayakumar et al., 2015b; Borah and Prasad, 2017; Yeshi et al., 2017; Altaf et al., 2018; Aslam and Faiz, 2020).

Feathers are used because they are cheap and environmentally friendly for biomaterials. Feathers consist of α-helix and β-sheet. Bird feathers are utilized for decoration as well as for toys. Feathers of various species are used in traditional medicine, e.g., *Ceryle rudis, Nothura boraquira, Phalacrocorax brasilianus, Meleagris gallopayo, Coragyps atratus, Coryus splendens, Corythaeola cristata,* and *Columba livia,* which are utilized for the cure of cough, typhoid, headache, flu, asthma, alcoholism, love poison, and cough (Padmanabhan and Sujana, 2008; Alves et al., 2009; Lohani, 2011a; Jacobo-Salcedo et al., 2011; Haileselasie, 2012; Bezerra et al., 2013; Martínez, 2013; Alonso-Castro, 2014; Bobo et al., 2015; Vijayakumar et al., 2015b; Dos Santos Soares et al., 2018; Adil and Tariq, 2020). Feathers are utilized for various reasons, e.g., as a micro- and nanoparticle, bio-sorbent, enhance the viability of the cell, modify the antibacterial activity, and dressing of wounds, as well as in the cosmetic industries. Graphene oxide and derivatives are used as a biomaterial, films of thermoplastic, regenerated fibres, for ruminants as protein, feeding supplement, fire-resistant substance, handspun yarn, processing of leather, in the electrode material, formation of paper, textile fibers, bio-fertilizer, reformation of tissue, bio-composites, bio-plastic, and wound healing (Coward-Kelly et al., 2006; Karthikeyan et al., 2007; Reddy and Yang, 2007; Poole et al., 2009; Rouse and Van Dyke, 2010; Zhan and Wool, 2011; Gurav and Jadhav, 2013; Reddy et al., 2014a; Reddy et al., 2014b; Flores-Hernández et al., 2014; Manivasagan et al., 2014; Tsuda and Nomura, 2014; Xu et al., 2014; Amieva et al., 2015; Khajavi et al., 2016; Sharma et al., 2017a; Sharma et al., 2017b; Kumar et al., 2017; Tesfaye et al., 2017; Wang et al., 2017; Ramakrishnan et al., 2018; Nanthavanan et al., 2019; Adil and Tariq, 2020).

Honey is composed of "sugars" (Kamal and Klein, 2011), "disaccharides," "water," "proteins" (Moreira et al., 2007; Won et al., 2009; Sak-Bosnar and Sakač, 2012), "amino acids" (Hermosı´;n et al., 2003; Iglesias et al., 2006), "vitamins" (Bonté and Desmoulière, 2013), "minerals" (Alqarni et al., 2014), "organic acids," "phenolic compounds" (Andersen and Markham, 2005), and "solid particles" (Castro-Vázquez et al., 2007) as well as "volatile compounds" (Da Silva et al., 2016). Honey is used as a remedy in traditional medicine to cure gastritis, snake-bite, cold, myalgia, eye infection, teething in child, dark spots, skin, diarrhea, expectorant, migraine, allergy, burns, wounds in the stomach, spleen, toothache, mouth, influenza, hypertension, atherosclerosis, diabetes mellitus, Alzheimer's disease, cancer, urinary system, throat pain, asthma, acidity obesity, cough, and tonsils (Mahawar and Jaroli, 2006; Padmanabhan and Sujana, 2008; Dixit et al., 2010; Jaroli et al., 2010; Oliveira et al., 2010; Abbasi et al., 2011; Benítez, 2011; Deb and Haque, 2011; Lohani, 2011b; Yirga et al., 2011; Barros et al., 2012; Erejuwa et al., 2012; Haileselasie, 2012; Chinlampianga et al., 2013; Betlloch Mas et al., 2017; Mootoosamy and Mahomoodally, 2014; Sreekeesoon and Mahomoodally, 2014; Vallejo and González, 2014; Vijayakumar et al., 2015b; Waykar and Alqadhi, 2016; Yeshi et al., 2017; Altaf et al., 2018; Altaf and Umair, 2020). Honey is also utilized in nano-medicine to cure various ailments and acts as anti-apoptosis, anti-proliferative (Oršolić, 2009; Li et al., 2010; Mandal and Mandal, 2011; Vallianou et al., 2014), anti-diabetic, antioxidant (Omotayo et al., 2010; Erejuwa, 2014; Bobiș et al., 2018), antibiotic, anti-cataract, anti-inflammatory, antifungal and endophthalmitis (Rhone and Basu, 2008; Vit and Jacob, 2008;

Cernak et al., 2012; Salehi et al., 2014), blood pressure, heart problems (Al-Waili et al., 2013; Aluko et al., 2014), antibacterial, antioxidant (Francis et al., 2015; El-haskoury et al., 2018), and oxidative stress (Zhao et al., 2018).

COEP (flesh of *Bos taurus* enhances the amount of protein) and COPH (milk of *Bos taurus* is used to treat weakness) were documented as the most often consumed with FC = 29 in the Himalayan region of Azad Jammu and Kashmir. Most animals were versatile in the context of utilization (RI = 3.45), such as CQB (flesh of *Coturnix coturnix* is used to treat bilious), CQJP (flesh of *Coturnix coturnix* for joint pain), CQBP (i *Coturnix coturnix* is used to treat backbone pain), CQPL (flesh of *Coturnix Coturnix* is used against paralysis), and CPPD and HPWH (flesh of *Columba livia* and *C. rupestris* is used to treat Parkinson's disease). The maximum relative importance is an indication of high accessibility and affordability of a species (Umair et al., 2019). Animal species with high RI values could be focused to evaluate their pharmacological and therapeutic potential. Therefore, statistical analysis is of significant value in ethnobiological studies because it facilitates the researcher in the selection of appropriate species and their body parts for chemical profiling and pharmacological/clinical studies. The ethnopharmacological data were calculated through "PCA," which allocated for the ordination of designs in terms of three variables, i.e., FC, UV, and RI. Statistical analysis with the help of "PCA" showed that the first two axes have 100% difference and "PC 1" has 98.5% and "PC 2" has 1.5% variations. These findings were in agreement with other studies (Altaf, 2020).

Novelty of Data

The folklore is an animal-based-medicinal concept of populations of the region of Himalayas, AJ&K. It means that people have a strong association with the ecosystem. For the first time, medicinal uses of animals from Azad Jammu and Kashmir were investigated. Furthermore, applications of 49 animal species are used to cure different diseases in humans. Out of 35 avian species, 28 species (i.e., *Lerwa lerwa, Tragopan melanocephalus, Coturnix Coturnix*, *Coturnix japonica, Alectoris Chukar, Francolinus francolinus, Francolinu spondicerianus, Pucrasia macrolopha, Lophophorus impejanus*, *Lophura leucomelanos, Bubulcus ibis*, *Egretta garzetta*, *Neophron percnopterus, Aquila Chrysaetos, Columba livia*, *Streptopelia orientalis*, *Spilopelia chinensis*, *Psittacula eupatria*, *Otus sunia, Upupa epops*, *Delichon dasypus*, *Hirundo rustica, Trochalopteron lineatum, Motacilla cinerea*, *Motacilla alba*, *Motacilla citreola, and Anas platyrhynchos domesticus*) have a zero similarity index. Moreover, out of 14 mammalian species, 14 species, i.e., *Panthera pardus*, *Moschus chrysogaster*, *Ursus thibetanus, Hystrix indica, Macaca mulatta, Ovis aries*, *Canis aureus, Vulpes Vulpes, Petaurista petaurista, Bos Taurus, Oryctolagus cuniculus,* and *Bubalus bubalis,* have a zero similarity index. Additionally, out of five herpetofauna species, only two species, i.e., *Duttaphrynus melanostictus* and *Eublepharis macularius,* have a zero similarity index. Furthermore, it is noted that all species (i.e., *Paraconophyma* spp., *Meranoplus bicolor, Actias selene*, *Luciolasubstriata, Apis mellifera*, *Androctonus* spp., and *Libythea lepita*) of arthropods have a zero similarity index. Single species of earthworm also has a zero similarity index. Flesh, fat, bone, whole body, milk, skin, egg, head, feather, bile, blood, and honey were utilized as body parts. *Lerwa lerwa, Tragopan melanocephalus, Coturnix japonica*, *Alectoris chukar, Francolinus pondicerianus, Pucrasia macrolopha, Lophophorus impejanus*, *Lophura leucomelanos, Bubulcus ibis*, *Neophron percnopterus, Psittacula eupatria*, *Otussunia*, *Parus major*, *Delichon dasypus*, *Hirundo rustica, Motacilla cinerea, Motacilla alba*, *Motacilla citreola, Petaurista petaurista, Paraconophyma* spp., *Meranoplus bicolor, Actiasselene, Luciola substriata, Androctonus* spp., and *Libythea lepita* were noted for the first time from Himalayan region, AJ&K. This study gives information that could be useful in the conservation of animal biodiversity in Azad Jammu and Kashmir's Himalayan region. For wild animal-based new pharmaceuticals, the screening of medicinal-active compounds and either "*in vivo*" or "*in vitro*" examination of biological activities of fauna with maximal "FC," "UV," "RI," and "SI" could be relevant.

CONCLUSION

To the best of our knowledge, ethnomedicinal uses of the diverse fauna of the Himalayan regions of Azad Jammu and Kashmir have rarely been reported before. Our findings revealed that local inhabitants have strong associations with animal species in their surrounding environment and use them in their primary health-care system to treat various diseases. In addition, medicinal uses of more than 60% of the species were reported for the first time from this area. Animal species with high medicinal values should be further explored for bioactive compounds and *in vitro/in vivo* activates to introduce novel animal-based health-care products. *Bos taurus* was documented as the most often consumed with FC = 29, while *Coturnix Coturnix* and *Columba livia* were documented to be highly versatile in their utilization (RI = 3.45) in the Himalayan region of Azad Jammu and Kashmir.

DATA AVAILABILITY STATEMENT

The original contributions presented in the study are included in the article/**Supplementary Material**; further inquiries can be directed to the corresponding authors.

ETHICS STATEMENT

The present study focused on traditional uses of animal species by the local inhabitants of the Himalayan region of Azad Jammu and Kashmir. During the field survey, prior informed consent was obtained from each participant for the documentation and sharing of information. General standards/guidelines, ethical norms, and rules of the International Society of Ethnobiology (ISE) (http://www.ethnobiology.net/) and Consensus Statement on Ethnopharmacological Field Studies (ConSEFS) (https://www.journals.elsevier.com/journal-of-ethnopharmacology/) were followed.

AUTHOR CONTRIBUTIONS

MF performed field survey and formal analysis and wrote the original draft. MA and AA supervised the project, provided intellectual support and resources, was involved in the methodology and data analysis, and edited and revised the final article. MU helped in data analysis and reviewed the article. KA and YE provided financial assistance and was involved in the revision and editing.

FUNDING

This research project was funded by the "Researcher Support supporting Project" at "King Saud University" via Researcher Support Project no. RSP/2021/189.

ACKNOWLEDGMENTS

The authors extend their appreciation to the Researchers Supporting Project number (RSP-2021/189), King Saud University, Riyadh, Saudi Arabia. The authors are thankful to all the local people of the Himalayan region of Azad Jammu and Kashmir for sharing valuable information. The authors also highly appreciate Alex Green, Centre for Bio-cultural Diversity, and University of Kent, England, for the critical review of this article.

SUPPLEMENTARY MATERIAL

The Supplementary Material for this article can be found online at: https://www.frontiersin.org/articles/10.3389/fphar.2022.807831/full#supplementary-material

REFERENCES

Abbasi, A. M., Khan, M. A., Ahmad, M., and Zafar, M. (2011). *Medicinal Plant Biodiversity of Lesser Himalayas-Pakistan*. Springer Science & Business Media.

Abbasi, Z. (2021). Diversity and Folklore Medicinal Uses of Mammalian Species of Harighal, Azad Jammu and Kashmir, Pakistan. *J. Wildl. Ecol.* 5 (2), 60–65.

Abdullahi, A. (2019). Camel Milk-A Review. *J.Anim. Sci. Livest.* 3, 13–18.

Abrhaley, A., and Leta, S. (2018). Medicinal Value of Camel Milk and Meat. *J. Appl. Animal Res.* 46, 552–558. doi:10.1080/09712119.2017.1357562

Adil, S., and Tariq, S. (2020). Study of Traditional and Modern Applications of Feathers-A Review. *J. Wild. Ecol.* 4, 141–150.

Ahmad, S., Akram, M., Riaz, M., Munir, N., Mahmood Tahir, I., Anwar, H., et al. (2021). Zootherapy as Traditional Therapeutic Strategy in the Cholistan Desert of Bahawalpur,Pakistan. *Vet. Med. Sci.* 00, 1–8.

Ajagun, E. J., Anyaku, C. E., and Afolayan, M. P. (2017). A Survey of the Traditional Medical and Non-medical Uses of Animals Species and Parts of the Indigenous People of Ogbomoso, Oyo State. *Int. J. Herb. Med.* 5, 26–32.

Al-Waili, N., Salom, K., Al-Ghamdi, A., Ansari, M. J., Al-Waili, A., and Al-Waili, T. (2013). Honey and Cardiovascular Risk Factors, in Normal Individuals and in Patients with Diabetes Mellitus or Dyslipidemia. *J. Med. Food.* 16, 1063–1078. doi:10.1089/jmf.2012.0285

Albuquerque, U. P., Melo, J. G., Medeiros, M. F., Menezes, I. R., Moura, G. J., Asfora El-Deir, A. C., et al. (20122012). Natural Products from Ethnodirected Studies: Revisiting the Ethnobiology of the Zombie Poison. *Evid. based Complement. Altern.* doi:10.1155/2012/202508

Ali, A., Khan, M. S. H., and Altaf, M. (2018). Winter Survey of Birds at District of the Badin, Pakistan. *J. Wild. Ecol.* 2, 11–22.

Alonso-Castro, A. J., Carranza-Álvarez, C., Maldonado-Miranda, J. J., Del Rosario Jacobo-Salcedo, M., Quezada-Rivera, D. A., Lorenzo-Márquez, H., et al. (2011). Zootherapeutic Practices in Aquismón, San Luis Potosí, México. *J. Ethnopharmacol.* 138, 233–237. doi:10.1016/j.jep.2011.09.020

Alonso-Castro, A. J. (2014). Use of Medicinal Fauna in Mexican Traditional Medicine. *J. Ethnopharmacol.* 152, 53–70. doi:10.1016/j.jep.2014.01.005

Aloufi, A., and Eid, E. (2016). Zootherapy: A Study from the Northwestern Region of the Kingdom of Saudi Arabia and Hashemite Kingdom of Jordan. *Ind. J. Trad. Knowl.* 15, 561–569.

Alqarni, A. S., Owayss, A. A., Mahmoud, A. A., and Hannan, M. A. (2014). Mineral Content and Physical Properties of Local and Imported Honeys in Saudi Arabia. *J. Saudi Chem. Soc.* 18, 618–625. doi:10.1016/j.jscs.2012.11.009

Altaf, M., Javid, A., Umair, M., Iqbal, K. J., Rasheed, Z., and Abbasi, A. M. (2017). Ethnomedicinal and Cultural Practices of Mammals and Birds in the Vicinity of River Chenab, Punjab-Pakistan. *J. Ethnobiol. Ethnomed.* 13, 41. doi:10.1186/s13002-017-0168-5

Altaf, M., Umair, M., Abbasi, A. R., Muhammad, N., and Abbasi, A. M. (2018). Ethnomedicinal Applications of Animal Species by the Local Communities of Punjab, Pakistan. *J. Ethnobiol. Ethnomed.* 14, 55. doi:10.1186/s13002-018-0253-4

Altaf, M., Abbasi, A. M., Umair, M., Amjad, M. S., Muhammad, N., Iqbal, K. J., et al. (2021). The Usage of Freshwater Fishes in Cultural and Folklore Therapies Among the People along River Jhelum, Punjab, Pakistan. *J. Wildl. Ecol.* 5, 79–99.

Altaf, M. (2016). *Assessment of Avian and Mammalian Diversity at Selected Sites along River Chenab*. Lahore, Pakistan: PhD, University of Veterinary and Animal Sciences.

Altaf, M., and Faiz, M. (2021). Snake Venom-A Review. *J. Wildl. Ecol.* 5 (3), 146–158.

Altaf, M., and Umair, M. (2020). Diversity, Distribution and Medicinal Importance of Honeybees in the World-A Review. *J. Wildl. Ecol.* 4, 130–141.

Altaf, M. (2020). Wild Animals as Source of Zoonotic Diseases-A Review. *J. Wild. Ecol.* 4, 71–84.

Aluko, E. O., Olubobokun, T. H., Atang, D. E., and Nna, V. U. (2014). Honey's Ability to Reduce Blood Pressure and Heart Rate in Healthy Male Subjects. *Front. Sci.* 4, 8–11.

Alves, R. R., Leite, R. C., Souto, W. M., Bezerra, D. M., and Loures-Ribeiro, A. (2013). Ethno-ornithology and Conservation of Wild Birds in the Semi-arid Caatinga of Northeastern Brazil. *J. Ethnobiol. Ethnomed.* 9, 14. doi:10.1186/1746-4269-9-14

Alves, R. R., Léo Neto, N. A., Brooks, S. E., and Albuquerque, U. P. (2009). Commercialization of Animal-Derived Remedies as Complementary Medicine in the Semi-arid Region of Northeastern Brazil. *J. Ethnopharmacol.* 124, 600–608. doi:10.1016/j.jep.2009.04.049

Alves, R. R., Neta, R. O., Trovão, D. M., Barbosa, J. E., Barros, A. T., and Dias, T. L. (2012). Traditional Uses of Medicinal Animals in the Semi-arid Region of Northeastern Brazil. *J. Ethnobiol. Ethnomed.* 8, 41–4268. doi:10.1186/1746-4269-8-41

Alves, R. R., and Rosa, I. L. (2007). Zootherapy Goes to Town: The Use of Animal-Based Remedies in Urban Areas of NE and N Brazil. *J. Ethnopharmacol.* 113, 541–555. doi:10.1016/j.jep.2007.07.015

Alves, R. R. N., Oliveira, M. G. G., Barboza, R. R. D., Lopez, L. C. S., and Oliveira, M. G. G. (2010). An Ethnozoological Survey of Medicinal Animals Commercialized in the Markets of Campina Grande, NE Brazil. *Hum. Ecol. Rev.* 17, 11–17.

Alves, R. R. N., Rosa, I. L., and Santana, G. G. (2007). The Role of Animal-Derived Remedies as Complementary Medicine in Brazil. *Bioscience* 57, 949–955. doi:10.1641/b571107

Alves, R. R. N., Silva, J. S., Chaves, L. d. S., and Albuquerque, U. P. (2018). "Ethnozoology and Animal Conservation ∗," in *Ethnozoology* (Elsevier), 481–496. doi:10.1016/b978-0-12-809913-1.00025-9

Alves, R. R. (2012). Relationships between Fauna and People and the Role of Ethnozoology in Animal Conservation. *Ethnobiol. Conserv.* 1, 1–69. doi:10.15451/ec2012-8-1.2-1-69

Andersen, O. M., and Markham, K. R. (2005). *Flavonoids: Chemistry, Biochemistry and Applications*. Boca Raton, Florida, United States: CRC Press.

Arshad, M., Ahmad, M., Ahmed, E., Saboor, A., Abbas, A., and Sadiq, S. (2014). An Ethnobiological Study in Kala Chitta Hills of Pothwar Region, Pakistan: Multinomial Logit Specification. *J. Ethnobiol. Ethnomed.* 10, 13. doi:10.1186/1746-4269-10-13

Aslam, H., and Faiz, M. (2020). Ethnopharmacological and Modern Applications of Milk of Various Mammalian Species-A Review. *J. Wildl. Ecol.* 4, 211–226.

Bagde, N., and Jain, S. (2013). An Ethnozoological Studies and Medicinal Values of Vertebrate Origin in the Adjoining Areas of Pench National Park of Chhindwara District of Madhya Pradesh, India. *Ind. Int. J. Life Sci.* 1, 278–283.

Bagde, N., and Jain, S. (2015). Study of Traditional Man-Animal Relationship in Chhindwara District of Madhya Pradesh, India. *J. Glob.Biosci.* 4, 1456–1463.

Ballard, O., and Morrow, A. L. (2013). Human Milk Composition: Nutrients and Bioactive Factors. *Pediatr. Clin. North Am.* 60, 49–74. doi:10.1016/j.pcl.2012.10.002

Barros, F. B., Varela, S. A., Pereira, H. M., and Vicente, L. (2012). Medicinal Use of Fauna by a Traditional Community in the Brazilian Amazonia. *J. Ethnobiol. Ethnomed.* 8, 37–20. doi:10.1186/1746-4269-8-37

Benarjee, G., Srikanth, K., Ramu, G., and Ramulua, K. (2010). Ethnozoological Study in a Tropical Wildlife Sanctuary of Eturunagaram in the Warangal District, Andhra Pradesh. *Ind. J. Trad. Knowl.* 9, 701–704.

Benítez, G. (2011). Animals Used for Medicinal and Magico-Religious Purposes in Western Granada Province, Andalusia (Spain). *J. Ethnopharmacol.* 137, 1113–1123.

Betlloch Mas, I., Chiner, E., Chiner Betlloch, J., Llorca, F. X., and Martín Pascual, L. (2017). *The use of animals in medicine of Latin tradition: study of the Tresor de Beutat, a medieval treatise devoted to female cosmetics*. Photon.).

Bezerra, D. M., De Araujo, H. F., Alves, A. G., and Alves, R. R. (2013). Birds and People in Semiarid Northeastern Brazil: Symbolic and Medicinal Relationships. *J. Ethnobiol. Ethnomed.* 9, 3. doi:10.1186/1746-4269-9-3

Bilal, A., Ullah, M. K., Khan, M. S., Fatima, A., Iqbal, K., Abbasi, S. S., et al. (2021). Impacts of Covid-19 Pandemic on Wildlife-Mini Review. *J.Wildl. Ecol.* 5 (3), 135–138.

Bobiş, O., Dezmirean, D. S., and Moise, A. R. (20182018). Honey and Diabetes: The Importance of Natural Simple Sugars in Diet for Preventing and Treating Different Type of Diabetes. *Oxid. Med. Cell. Longev*.

Bobo, K. S., Aghomo, F. F., and Ntumwel, B. C. (2015). Wildlife Use and the Role of Taboos in the Conservation of Wildlife Around the Nkwende Hills Forest Reserve; South-West Cameroon. *J. Ethnobiol. Ethnomed.* 11, 2. doi:10.1186/1746-4269-11-2

Boivin, N. L., Zeder, M. A., Fuller, D. Q., Crowther, A., Larson, G., Erlandson, J. M., et al. (2016). Ecological Consequences of Human Niche Construction: Examining Long-Term Anthropogenic Shaping of Global Species Distributions. *Proc. Natl. Acad. Sci. U. S. A.* 113, 6388–6396. doi:10.1073/pnas.1525200113

Bonté, F., and Desmoulière, A. (2013). Le miel: origine et composition. *Actual. Pharm.* 52, 18–21.

Borah, M. P., and Prasad, S. B. (2017). Ethnozoological Study of Animals Based Medicine Used by Traditional Healers and Indigenous Inhabitants in the Adjoining Areas of Gibbon Wildlife Sanctuary, Assam, India. *J. Ethnobiol. Ethnomed.* 13, 39–13. doi:10.1186/s13002-017-0167-6

Breteler, M. M. (2000). Vascular Risk Factors for Alzheimer's Disease: an Epidemiologic Perspective. *Neurobiol. Aging* 21, 153–160. doi:10.1016/s0197-4580(99)00110-4

Bullitta, S., Re, G. A., Manunta, M. D. I., and Piluzza, G. (2018). Traditional Knowledge about Plant, Animal, and Mineral-Based Remedies to Treat Cattle, Pigs, Horses, and Other Domestic Animals in the Mediterranean Island of Sardinia. *J. Ethnobiol. Ethnomed.* 14, 50–26. doi:10.1186/s13002-018-0250-7

Castro-Vázquez, L., Díaz-Maroto, M. C., and Pérez-Coello, M. S. (2007). Aroma Composition and New Chemical Markers of Spanish Citrus Honeys. *Food Chem.* 103, 601–606.

Cernak, M., Majtanova, N., Cernak, A., and Majtan, J. (2012). Honey Prophylaxis Reduces the Risk of Endophthalmitis during Perioperative Period of Eye Surgery. *Phytother. Res.* 26, 613–616. doi:10.1002/ptr.3606

Ch, M. I., Ahmed, F., Maqbool, M., and Hussain, T. (2013). *Ethnomedicinal Inventory of Flora of Maradori Valley, District Forward Khahuta*. Pakistan: Azad Kashmir.

Chakravorty, J., Meyer-Rochow, V. B., and Ghosh, S. (2011). Vertebrates Used for Medicinal Purposes by Members of the Nyishi and Galo Tribes in Arunachal Pradesh (North-East India). *J. Ethnobiol. Ethnomed.* 7, 13–14. doi:10.1186/1746-4269-7-13

Chattha, S. A., Malik, M. F., Altaf, M., Mahmood, S., Khan, J., Ali, A., et al. (2017). Human Pursuits Cause of Road Killing of Wild and Domestic Animals by Accident on National Highway of Punjab, Pakistan. *J. Wildl. Ecol*. 1, 8–16.

Chellappandian, M., Pandikumar, P., Mutheeswaran, S., Gabriel Paulraj, M., Prabakaran, S., Duraipandiyan, V., et al. (2014). Documentation and Quantitative Analysis of Local Ethnozoological Knowledge Among Traditional Healers of Theni District, Tamil Nadu, India. *J. Ethnopharmacol.* 154, 116–130. doi:10.1016/j.jep.2014.03.028

Cheung, P. C. K., and Mehta, B. M. (2015). *Handbook of Food Chemistry*. Springer Berlin Heidelberg.

Chinlampianga, M., Singh, R. K., and Shukla, A. C. (2013). Ethnozoological Diversity of Northeast India: Empirical Learning with Traditional Knowledge Holders of Mizoram and Arunachal Pradesh. *Indian J. Tradit. Knowl.* 12, 18–30.

Costa-Neto, E. M. (2005). Entomotherapy, or the Medicinal Use of Insects. *J. Ethnobiol.* 25, 93–114. doi:10.2993/0278-0771(2005)25[93:eotmuo]2.0.co;2

Coward-Kelly, G., Chang, V. S., Agbogbo, F. K., and Holtzapple, M. T. (2006). Lime Treatment of Keratinous Materials for the Generation of Highly Digestible Animal Feed: 1. Chicken Feathers. *Bioresour. Technol.* 97, 1337–1343. doi:10.1016/j.biortech.2005.05.021

Da Silva, P. M., Gauche, C., Gonzaga, L. V., Costa, A. C., and Fett, R. (2016). Honey: Chemical Composition, Stability and Authenticity. *Food Chem.* 196, 309–323. doi:10.1016/j.foodchem.2015.09.051

de Melo, R. S., da Silva, O. C., Souto, A., Alves, R. R. N., and Schiel, N. (2014). The Role of Mammals in Local Communities Living in Conservation Areas in the Northeast of Brazil: an Ethnozoological Approach. *Trop. Conservation Sci.* 7, 423–439. doi:10.1177/194008291400700305

Deb, A. K., and Emdad Haque, C. (2011). 'Every Mother Is a Mini-Doctor': Ethnomedicinal Uses of Fish, Shellfish and Some Other Aquatic Animals in Bangladesh. *J. Ethnopharmacol.* 134, 259–267. doi:10.1016/j.jep.2010.12.001

Dey, A., Gorai, P., Mukherjee, A., Dhan, R., and Modak, B. K. (2017). Ethnobiological Treatments of Neurological Conditions in the Chota Nagpur Plateau, India. *J. Ethnopharmacol.* 198, 33–44. doi:10.1016/j.jep.2016.12.040

Dickman, A. J. (2010). Complexities of Conflict: the Importance of Considering Social Factors for Effectively Resolving Human-Wildlife Conflict. *Anim. Conserv.* 13, 458–466. doi:10.1111/j.1469-1795.2010.00368.x

Dixit, A., Kadavul, K., Rajalakshmi, S., and Shekhawat, M. (2010). Ethno-medico-biological Studies of South India. *Ind. J. Trad. Knowl.* 9, 116–118.

Dos Santos Soares, V. M., De Lucena Soares, H. K., Da Silva Santos, S., and De Lucena, R. F. P. (2018). Local Knowledge, Use, and Conservation of Wild Birds in the Semi-arid Region of Paraíba State, Northeastern Brazil. *J. Ethnobiol. Ethnomed.* 14, 77. doi:10.1186/s13002-018-0276-x

Easthope, G. (1995). "Ethnicity and Health," in *Sociology of Health and Illness: Australian Readings*. Editors N. J. Macmillan, and G. Lupton (Sydney, Australia), 143–161.

EHS (2016a). *Zoonotic Diseases – Amphibians*. Toronto, Ontario, Canada: EHS Occupational Health Clinic.

EHS (2016b). "Zoonotic Diseases – Fish," in *Environmental Health and Safety | Occupational Health* (Toronto, Ontario, Canada: EHS Occupational Health Clinic).

El-Haskoury, R., Al-Waili, N., Kamoun, Z., Makni, M., Al-Waili, H., and Lyoussi, B. (2018). Antioxidant Activity and Protective Effect of Carob Honey in CCl4-Induced Kidney and Liver Injury. *Arch. Med. Res.* 49, 306–313. doi:10.1016/j.arcmed.2018.09.011

Erejuwa, O. O. (2014). Effect of Honey in Diabetes Mellitus: Matters Arising. *J. Diabetes Metab. Disord.* 13, 23. doi:10.1186/2251-6581-13-23

Erejuwa, O. O., Omotayo, E. O., Gurtu, S., Sulaiman, S. A., Ab Wahab, M. S., Sirajudeen, K. N., et al. (2010). Hypoglycemic and Antioxidant Effects of Honey Supplementation in Streptozotocin-Induced Diabetic Rats. *Int. J. Vitam. Nutr. Res.* 80, 74–82. doi:10.1024/0300-9831/a000008

Erejuwa, O. O., Sulaiman, S. A., and Wahab, M. S. (2012). Honey--a Novel Antidiabetic Agent. *Int. J. Biol. Sci.* 8, 913–934. doi:10.7150/ijbs.3697

Ferreira, F. S., Brito, S. V., Saraiva, R. A., Araruna, M. K., Menezes, I. R., Costa, J. G., et al. (2010). Topical Anti-inflammatory Activity of Body Fat from the Lizard Tupinambis Merianae. *J. Ethnopharmacol.* 130 (3), 514–520. doi:10.1016/j.jep.2010.05.041

Flores-Hernández, C. G., Colín-Cruz, A., Velasco-Santos, C., Castaño, V. M., Rivera-Armenta, J. L., Almendarez-Camarillo, A., et al. (2014). All Green Composites from Fully Renewable Biopolymers: Chitosan-Starch Reinforced with Keratin from Feathers. *Polymers* 6, 686–705.

Fopa, G. D., Simo, F., Kekeunou, S., Ichu, I. G., Ingram, D. J., and Olson, D. (2020). Understanding Local Ecological Knowledge, Ethnozoology, and Public Opinion to Improve Pangolin Conservation in the Center and East Regions of Cameroon. *J. Ethnobiol.* 40 (2), 234–251. doi:10.2993/0278-0771-40.2.234

Francis, A., Cho, Y., and Johnson, D. W. (2015). Honey in the Prevention and Treatment of Infection in the CKD Population: a Narrative Review. *Evid. Based Complement. Altern. Med.* 2015, 261425–261428. doi:10.1155/2015/261425

Friedman, J., Yaniv, Z., Dafni, A., and Palewitch, D. (1986). A Preliminary Classification of the Healing Potential of Medicinal Plants, Based on a Rational Analysis of an Ethnopharmacological Field Survey Among Bedouins in the Negev Desert, Israel. *J. Ethnopharmacol.* 16, 275–287. doi:10.1016/0378-8741(86)90094-2

Fwfd (2021). *Montane Temperate Forest*. AJK, Pakistan: Forestry, Wildlife & Fisheries Department.

G, G., A, M., A, W., and H, K. (2016). Review on Goat Milk Composition and its Nutritive Value. *J. Nutr. Health Sci.* 3, 401–409. doi:10.15744/2393-9060.3.401

Galave, P., Jain, A., and Katewa, S. (2013). Traditional Veterinary Medicines Used by Liestock Owner of Rajhastan, India. *Ind. J. Trad. Knowl.* 12, 47–55.

Ghosh, T., Singhamahapatra, R., and Mandal, F. (2013). Traditional Use of Animals Among Santhals of Bankura District. *Int. J. Sci. Res. Sci. Technol.* 2, 95–96.

Grădinaru, A. C., Creangă, Ș., and Solcan, G. (2015). Milk–a Review on its Synthesis, Composition, and Quality Assurance in Dairy Industry. *Hum. Vet. Med.* 7, 173–177.

Gu, Z., Gu, L., Eils, R., Schlesner, M., and Brors, B. (2014). Circlize Implements and Enhances Circular Visualization in R. *Bioinformatics* 30, 2811–2812. doi:10.1093/bioinformatics/btu393

Guo, H. Y., Pang, K., Zhang, X. Y., Zhao, L., Chen, S. W., Dong, M. L., et al. (2007). Composition, Physiochemical Properties, Nitrogen Fraction Distribution, and Amino Acid Profile of Donkey Milk. *J. Dairy Sci.* 90, 1635–1643. doi:10.3168/jds.2006-600

Gurav, R. G., and Jadhav, J. P. (2013). A Novel Source of Biofertilizer from Feather Biomass for Banana Cultivation. *Environ. Sci. Pollut. Res. Int.* 20, 4532–4539. doi:10.1007/s11356-012-1405-z

Haag, M. (2003). Essential Fatty Acids and the Brain. *Can. J. Psychiatry* 48, 195–203. doi:10.1177/070674370304800308

Habib, S. (2022). Antibacterial Activity of Biogenic Synthesized Silver Nanoparticles Using Skin of Kashmir Nadi Frog *Paa Barmoachensis*. *J.Wildl. Ecol.* 6 (1), 07–12.

Haidar, R., and Bashir, S. M. (2021). Chemical Composition, Traditional and Modern Uses of Meat of Animals-A Review. *J. Wildl. Ecol.* 5, 47–55.

Haileselasie, T. H. (2012). Traditional Zootherapeutic Studies in Degu'a Tembien, Northern Ethiopia. *Curr. Res. J. Biol. Sci.* 4, 563–569. doi:10.5897/ijbc11.274

Hakeem, F., Altaf, M., Manzoor, S., Rauf, K., Mumtaz, B., Bashir, M., et al. (2017). Assessment of Behavioral Study, Human Activities Impacts and Interaction with Streak Laughingthrush (*Trochalopteron Lineatum*) in District Bagh, Azad Jammu and Kashmir-Pakistan. *J. Wildl. Ecol.* 1, 1–7.

Hall, J. (2011). *Textbook of Medical Physiology*. Philadelphia: Elsevier.

Hamad, M., and Baiomy, A. (2010). Physical Properties and Chemical Composition of Cow's and Buffalo's Milk in Qena Governorate. *J. Food Dairy Sci.* 1, 397–403. doi:10.21608/jfds.2010.82466

Hammer, Ø., Harper, D., and Ryan, P. (2001). Paleontological Statistics Software: Package for Education and Data Analysis. *Palaeontol. Electron.* 1, 9.

Hanif, M., Iqbal, K. J., Javid, A., Khan, N., et al. (2019). Socio Economic Status of Fishermen Community, South Punjab, Pakistan. *Punjab Univ. J. Zoology* 34 (2), 115–118. doi:10.17582/journal.pujz/2019.34.1.115.118

Heinrich, M., Lardos, A., Leonti, M., Weckerle, C., Willcox, M., Applequist, W., et al. (2018). Best Practice in Research: Consensus Statement on Ethnopharmacological Field Studies - ConSEFS. *J. Ethnopharmacol.* 211, 329–339. doi:10.1016/j.jep.2017.08.015

HermosíN, I., Chicon, R. M., and Cabezudo, M. D. (2003). Free Amino Acid Composition and Botanical Origin of Honey. *Food Chem.* 83, 263–268.

Holennavar, P. (2015). Use of Animal and Animal Derived Products as Medicines by the Inhabitants of Villages in Athani Taluka of Belagavi District, Karnataka. *Int. J.Appl.Res.* 1, 437–440.

Hui, Y. H. (2012). *Handbook of Meat and Meat Processing*. Boca Raton, Florida, United States: CRC Press.

Iglesias, M. T., Martín-Alvarez, P. J., Polo, M. C., De Lorenzo, C., Gonzalez, M., and Pueyo, E. (2006). Changes in the Free Amino Acid Contents of Honeys during Storage at Ambient Temperature. *J. Agric. Food Chem.* 54, 9099–9104. doi:10.1021/jf061712x

Ijaz, S., and Faiz, M. (2021). Chemical Composition, Folk and Modern Uses of Fats and Oil-A Review. *J. Wildl. Ecol.* 5, 104–110.

Ijaz, S., and Iftikhar, A. (2021). Chemical Composition, Ethnomedicinal and Industrial Uses of Bones-A Review. *J. Wildl. Ecol.* 5, 56–59.

Jacobo-Salcedo, M. R., Alonso-Castro, A. J., and Zarate-Martinez, A. (2011). Folk Medicinal Use of Fauna in Mapimi, Durango, México. *J. Ethnopharmacol.* 133, 902–906. doi:10.1016/j.jep.2010.10.005

Jaroli, D. P., Mahawar, M. M., and Vyas, N. (2010). An Ethnozoological Study in the Adjoining Areas of Mount Abu Wildlife Sanctuary, India. *J. Ethnobiol. Ethnomed.* 6, 6. doi:10.1186/1746-4269-6-6

Jimenez-Cervantes Amieva, E., Fuentes-Ramirez, R., Martinez-Hernandez, A. L., Millan-Chiu, B., Lopez-Marin, L. M., Castaño, V. M., et al. (2015). Graphene Oxide and Reduced Graphene Oxide Modification with Polypeptide Chains from Chicken Feather Keratin. *J. Alloys Compd.* 643, S137–S143. doi:10.1016/j.jallcom.2014.12.062

Kamal, M. A., and Klein, P. (2011). Determination of Sugars in Honey by Liquid Chromatography. *Saudi. J. Biol. Sci.* 18, 17–21. doi:10.1016/j.sjbs.2010.09.003

Karthikeyan, R., Balaji, S., and Sehgal, P. (2007). *Industrial Applications of Keratins–A Review*.

Kassam, A. (2002). World Resources 2000–2001: People and Ecosystems: The Fraying Web of Life. *Exp. Agric.* 38, 389111–389113. doi:10.1017/s0014479702210194

Keeton, J. T., and Eddy, S. (2004). "Chemical Composition," in *Enyclopedia of Meat Sciences*. Editors W. Jensen, C. Devine, and M. Dikeman (Enc. Elsevier Academic Press, Oxford). doi:10.1016/b0-12-464970-x/00118-5

Khajavi, R., Rahimi, M. K., Abbasipour, M., and Brendjchi, A. H. (2016). Antibacterial Nanofibrous Scaffolds with Lowered Cytotoxicity Using Keratin Extracted from Quail Feathers. *J. Bioact. Compatible Polym.* 31, 60–71. doi:10.1177/0883911515598793

Khan, M. S. (2006). *Amphibians and Reptiles of Pakistan*. Malabar, Florida, USA: Krieger Publishing Company.

Khan, M. S. (2010). Checklist of Amphibians of Pakistan. *Paki. J.Wildl.* 1.

Khan, S. M. N., Masud, A., Ahmed, W., Ayub, M. I., Khan, R., and Khan, A. T. (2017). *Haveli District Disaster Risk Management Plan ". (Azad Jammu and Kashmir, Pakistan: Disaster & Climate Resilience Improvement Project*. Planning & Development Department, Azad Govt. of State of Jammu & Kashmir.

Kim, H., and Song, M. J. (2013). Ethnozoological Study of Medicinal Animals on Jeju Island, Korea. *J. Ethnopharmacol.* 146, 75–82. doi:10.1016/j.jep.2012.11.011

Kruse, H., Kirkemo, A. M., and Handeland, K. (2004). Wildlife as Source of Zoonotic Infections. *Emerg. Infect. Dis.* 10, 2067–2072. doi:10.3201/eid1012.040707

Kula, J. T., and Tegegne, D. (2016). Chemical Composition and Medicinal Values of Camel Milk. *Int. J. Res. Stud. Biosci.* 4, 13–25.

Kumar, S. L., Anandhavelu, S., Sivaraman, J., and Swathy, M. (2017). Modified Extraction and Characterization of Keratin from Indian Goat Hoof: A Biocompatible Biomaterial for Tissue Regenerative Applications. *Integr. Ferroelectr.* 184, 41–49. doi:10.1080/10584587.2017.1368642

Lalmuanpuii, J., Rosangkima, G., and Lamin, H. (2013). Ethno-medicinal Practices Among the Mizo Ethnic Group in Lunglei District, Mizoram. *Sci. Vis.* 13, 24–34.

Lawal, O. A., and Banjo, A. D. (2007). Survey for the Usage of Arthropods in Traditional Medicine in Southwestern Nigeria. *J. Entomology* 4, 104–112. doi:10.3923/je.2007.104.112

Li, X., Huang, Q., Ong, C. N., Yang, X. F., and Shen, H. M. (2010). Chrysin Sensitizes Tumor Necrosis Factor-Alpha-Induced Apoptosis in Human Tumor

Cells via Suppression of Nuclear Factor-kappaB. *Cancer Lett.* 293, 109–116. doi:10.1016/j.canlet.2010.01.002

Lim, H., Park, H., and Kim, H. P. (2004). Inhibition of Contact Dermatitis in Animal Models and Suppression of Proinflammatory Gene Expression by Topically Applied Flavonoid, Wogonin. *Arch. Pharm. Res.* 27 (4), 442–448. doi:10.1007/BF02980087

Lohani, U. (2010). Man-animal Relationships in Central Nepal. *J. Ethnobiol. Ethnomed.* 6, 31–11. doi:10.1186/1746-4269-6-31

Lohani, U. (2011a). Eroding Ethnozoological Knowledge Among Magars in Central Nepal. *Ind. J. Trad. Knowl.* 10, 466–473.

Lohani, U. (2011b). Traditional Uses of Animals Among Jirels of Central Nepal. *Stud. Ethno-Medicine* 5, 115–124. doi:10.1080/09735070.2011.11886398

Löki, V., Nagy, J., Nagy, A., Babai, D., Molnár, Z., and Lukács, B. A. (2021). Known but Not Called by Name: Recreational Fishers' Ecological Knowledge of Freshwater Plants in Hungary. *J. Ethnobiol. Ethnomed.* 17 (1), 63–16. doi:10.1186/s13002-021-00489-2

Mahawar, M. M., and Jaroli, D. P. (2006). Animals and Their Products Utilized as Medicines by the Inhabitants Surrounding the Ranthambhore National Park, India. *J. Ethnobiol. Ethnomed.* 2, 46. doi:10.1186/1746-4269-2-46

Mandal, M. D., and Mandal, S. (2011). Honey: its Medicinal Property and Antibacterial Activity. *Asian pac. J. Trop. Biomed.* 1, 154–160. doi:10.1016/S2221-1691(11)60016-6

Mandal, S. K., and Rahaman, C. H. (2022). Perception and Application of Zootherapy for the Management of Cattle Diseases Occurred in Northern Laterite Region of West Bengal, India. *Asian J. Ethnobiol.* 5 (1).

Manivasagan, P., Sivakumar, K., Gnanam, S., Venkatesan, J., and Kim, S.-K. (2014). Production, Biochemical Characterization and Detergents Application of Keratinase from the Marine Actinobacterium Actinoalloteichus Sp. MA-32. *J. Surfact Deterg.* 17, 669–682. doi:10.1007/s11743-013-1519-4

Martínez, G. J. (2013). Use of Fauna in the Traditional Medicine of Native Toba (Qom) from the Argentine Gran Chaco Region: an Ethnozoological and Conservationist Approach. *Ethnobiol. Conserv.* 2, 1–43.

Merlin Junior, I. A., Santos, J. S., Costa, L. G., Costa, R. G., Ludovico, A., Rego, F. C., et al. (2015). Sheep Milk: Physical-Chemical Characteristics and Microbiological Quality. *Arch. Latinoam. Nutr.* 65, 193–198.

Mirza, Z. B., and Wasiq, H. (2007). A Field Guide to Birds of Pakistan *Bookland*. Lahore.

Mishra, N., Rout, S., and Panda, T. (2011). Ethno-zoological Studies and Medicinal Values of Similipal Biosphere Reserve, Orissa, India. *Afr. J. Pharm. Pharmacol.* 5, 6–11.

Mootoosamy, A., and Mahomoodally, M. F. (2014). A Quantitative Ethnozoological Assessment of Traditionally Used Animal-Based Therapies in the Tropical Island of Mauritius. *J. Ethnopharmacol.* 154, 847–857. doi:10.1016/j.jep.2014.05.001

Moreira, R. F. A., De Maria, C. A. B., Pietroluongo, M., and Trugo, L. C. (2007). Chemical Changes in the Non-volatile Fraction of Brazilian Honeys during Storage under Tropical Conditions. *Food Chem.* 104, 1236–1241. doi:10.1016/j.foodchem.2007.01.055

Mughal, S., Pervaz, M., Bashir, S. M., and Shamashad, S. S. (2020). Assessment of Diversity and Ethnopharmacological Uses of Birds in Chakar, Hattian Bala District, Azad Jammu and Kashmir -Pakistan. *J. Wildl. Ecol.* 4, 35–44.

Muhammad, N., Khan, A. M., Iqbal, K. J., Haider, M. S., Ashraf, S., Ansari, Z. S., et al. (2017a). Assessment of Distribution and Ethnocultural Uses of the Baringo tilapia (*Oreochromis niloticus*) in Punjab, Pakistan. *J. Wildl. Ecol.* 1, 7–13.

Muhammad, N., Khan, A. M., Umair, M., Qazi, A., Yaqoob, A,M., Ashraf, S., et al. (2017b). Assessment of Distribution and Ethnocultural Uses of the Sol (*Channa Marulius*) in Punjab, Pakistan. *J. Wildl. Ecol.* 1, 35–41.

Muhammad, N., Umair, M., Khan, A. M., Abbasi, A. R., Khan, Q., Khan, A., et al. (2017c). Assessment of the Diversity and Ethno-Medicinal Uses of the Carps in Punjab, Pakistan. *J. Wildl. Ecol.* 1, 52–60.

Muhammad, N., Umair, M., Khan, A. M., Yaqoob, M., Haider, M. S., Khan, Q., et al. (2018). Assessment of Cultural Uses of Mrigal Carp (*Cirrhinus Mrigala*) in Gujranwala Division, Pakistan. *J. Wildl. Ecol.* 2, 1–9.

Murray, A. R., Kisin, E., Castranova, V., Kommineni, C., Gunther, M. R., and Shvedova, A. A. (2007). Phenol-induced *In Vivo* Oxidative Stress in Skin: Evidence for Enhanced Free Radical Generation, Thiol Oxidation, and Antioxidant Depletion. *Chem. Res. Toxicol.* 20 (12), 1769–1777. doi:10.1021/tx700201z

Mussarat, S., Ali, R., Ali, S., Mothana, R. A., Ullah, R., and Adnan, M. (2021). Medicinal Animals and Plants as Alternative and Complementary Medicines in Southern Regions of Khyber Pakhtunkhwa, Pakistan. *Front. Pharmacol.* 1764.

Nanthavanan P, P., Kandasamy Arungandhi, K., Sunmathi D, D., and Niranjana J, J. (2019). Biological Synthesis of Keratin Nanoparticles from Dove Feather (*Columba livia*) and its Applications. *Asian J. Pharm. Clin. Res.* 12, 142–146. doi:10.22159/ajpcr.2019.v12i10.34572

Nijman, V., and Shepherd, C. R. (2017). Ethnozoological Assessment of Animals Used by Mon Traditional Medicine Vendors at Kyaiktiyo, Myanmar. *J. Ethnopharmacol.* 206, 101–106. doi:10.1016/j.jep.2017.05.010

Noor, U., and Haider, R. (2020). Assessment of Herpetofauna Diversity and Human-Herpetofauna-Interaction in District Sudhnoti, Azad Jammu and Kashmir, Pakistan. *J. Wildl. Ecol.* 4, 156–163.

Oliveira, E. S., Torres, D. F., Brooks, S. E., and Alves, R. R. (2010). The Medicinal Animal Markets in the Metropolitan Region of Natal City, Northeastern Brazil. *J. Ethnopharmacol.* 130, 54–60. doi:10.1016/j.jep.2010.04.010

Oršolić, N. (2009). Bee Honey and Cancer. *J. Apiproduct apimedical Sci.* 1, 93–103.

Padmanabhan, P., and Sujana, K. (2008). Animal Products in Traditional Medicine from Attappady Hills of Western Ghats. *Ind. J. Trad. Knowl.* 7, 326–329.

Paudyal, R., and Singh, N. B. (2014). Ethno-medicinal Uses of Animals and Plants Among the Migratory Tangbetons of Pokhara, Nepal. *J.Instit. Sci. Technol.* 19, 145–149.

Phillips, O., and Gentry, A. H. (1993). The Useful Plants of Tambopata, Peru: I. Statistical Hypotheses Tests with a New Quantitative Technique. *Econ. Bot.* 47, 15–32. doi:10.1007/bf02862203

Ploeg, J. V. D., and Weerd, M. V. (2010). Agta Bird Names : an Ethno-Ornithological Survey in the Northern Sierra Madre Natural Park, Philippines. *Forktail* 26, 127–131.

PM (2008). AJ & K Government. Available: www.pm.ajk.gov.

Poole, A. J., Church, J. S., and Huson, M. G. (2009). Environmentally Sustainable Fibers from Regenerated Protein. *Biomacromolecules* 10, 1–8. doi:10.1021/bm8010648

Prakash, S., and Prakash, S. (2021). Ethnomedicinal Use of Fishes by Tribal Communities in India: A Review. *Pharma Innov.* 10 (5), 1315–1321. doi:10.22271/tpi.2021.v10.i5q.6395

Prakash, S., and Verma, A. (2021). Relevance of Ethnomedicines of Invertebrate Origin Used by Tribals at Indo-Nepal Border. *Int. J. Biol. Sci.* 10 (1).

Ramakrishnan, N., Sharma, S., Gupta, A., and Alashwal, B. Y. (2018). Keratin Based Bioplastic Film from Chicken Feathers and its Characterization. *Int. J. Biol. Macromol.* 111, 352–358. doi:10.1016/j.ijbiomac.2018.01.037

Rauf, K., Altaf, M., Mumtaz, B., Altaf, M., Haider, R., Safeer, B., et al. (2017). Assessment of Behavior, Distribution, Ecology and Interaction Study of Cinnamon Tree Sparrow (*Passer Rutilans*) in District Bagh-Pakistan. *J. Wildl. Ecol.* 1, 43–49.

Reddy, N., Shi, Z., Temme, L., Xu, H., Xu, L., Hou, X., et al. (2014b). Development and Characterization of Thermoplastic Films from Sorghum Distillers Dried Grains Grafted with Various Methacrylates. *J. Agric. Food Chem.* 62, 2406–2411. doi:10.1021/jf405499t

Reddy, N., Chen, L., Zhang, Y., and Yang, Y. (2014a). Reducing Environmental Pollution of the Textile Industry Using Keratin as Alternative Sizing Agent to Poly(vinyl Alcohol). *J. Clean. Prod.* 65, 561–567. doi:10.1016/j.jclepro.2013.09.046

Reddy, N., and Yang, Y. (2007). Structure and Properties of Chicken Feather Barbs as Natural Protein Fibers. *J. Polym. Environ.* 15, 81–87. doi:10.1007/s10924-007-0054-7

Rhone, M., and Basu, A. (2008). Phytochemicals and Age-Related Eye Diseases. *Nutr. Rev.* 66, 465–472. doi:10.1111/j.1753-4887.2008.00078.x

Riaz, T., and Altaf, M. (2021). Diversity and Cultural Uses of Mammals in Dhirkot, Azad Jammu and Kashmir, Pakistan. *J. Wildl. Ecol.* 5 (3), 159–167.

Roberts, T. J. (1991). *The Birds of Pakistan*, Vol. I. Karachi: Oxford University Press.

Roberts, T. J. (1992). *The Birds of Pakistan*, Vol. II. Karachi: Oxford University Press.

Roberts, T. J. (2005). *Field Guide to the Large and Medium-Sized Mammals of Pakistan*. Oxford University Press.

Roberts, T. J. (1997). *The Mammals of Pakistan*. New Yark: Oxford University Press.

Rouse, J. G., and Van Dyke, M. E. (2010). A Review of Keratin-Based Biomaterials for Biomedical Applications. *Materials* 3, 999–1014. doi:10.3390/ma3020999

Sajem Betlu, A. L. (2013). Indigenous Knowledge of Zootherapeutic Use Among the Biate Tribe of Dima Hasao District, Assam, Northeastern India. *J. Ethnobiol. Ethnomed.* 9, 56–16. doi:10.1186/1746-4269-9-56

Sak-Bosnar, M., and Sakač, N. (2012). Direct Potentiometric Determination of Diastase Activity in Honey. *Food Chem.* 135, 827–831. doi:10.1016/j.foodchem.2012.05.006

Saleem, R., Altaf, M., Umair, M., Amjad, M. S., and Abbasi, A. M. (2021). Ethnopharmacological Applications of the Amphibians and Reptiles Among the People in the Vicinity of Margalla Hill National Park, Islamabad, Pakistan. *J. Wildl. Ecol.* 5, 13–25.

Salehi, A., Jabarzare, S., Neurmohamadi, M., Kheiri, S., and Rafieian-Kopaei, M. (2014). A Double Blind Clinical Trial on the Efficacy of Honey Drop in Vernal Keratoconjunctivitis. *Evid. -based Complement. Altern.* 2014. doi:10.1155/2014/287540

Saunders, C. D. (2003). The Emerging Field of Conservation Psychology. *Hum. Ecol. Rev.*, 137–149.

Schönfeldt, H. C., and Gibson, N. (2008). Changes in the Nutrient Quality of Meat in an Obesity Context. *Meat Sci.* 80, 20–27.

Sharma, S., Gupta, A., Chik, S. M. S. T., Kee, C. G., Mistry, B. M., Kim, D. H., et al. (2017a). Characterization of Keratin Microparticles from Feather Biomass with Potent Antioxidant and Anticancer Activities. *Int. J. Biol. Macromol.* 104, 189–196. doi:10.1016/j.ijbiomac.2017.06.015

Sharma, S., Gupta, A., Bin Tuan Chik, S. M. S., Gek Kee, C. Y., and Poddar, P. K. (2017b). "Dissolution and Characterization of Biofunctional Keratin Particles Extracted from Chicken Feathers, *IOP Conf. Ser. Mat. Sci. Eng.*, 191," in IOP conference series: materials science and engineering (Bristol, United Kingdom: IOP Publishing), 012013. doi:10.1088/1757-899X/191/1/012013

Singh, V. (2000). *A Note on the Use of Wild Animal Organs in Tibetan Medicine*. Traffic IndiaLodhi Estate, New Delhi: World Wide Fund for Nature.

Souto, W. M. S., Barboza, R. R. D., Da Silva Mourão, J., and Alves, R. R. N. (2012). Traditional Knowledge of Sertanejos about Zootherapeutic Practices Used in Ethnoveterinary Medicine of NE Brazil. *Ind. J. Trad. Knowl.* 11, 259–265.

Spreer, E. (1998). *Milk and Dairy Product Technology*. Boca Raton, Florida, United States: CRC Press.

Sreekeesoon, D. P., and Mahomoodally, M. F. (2014). Ethnopharmacological Analysis of Medicinal Plants and Animals Used in the Treatment and Management of Pain in Mauritius. *J. Ethnopharmacol.* 157, 181–200. doi:10.1016/j.jep.2014.09.030

Still, J. (2003). Use of Animal Products in Traditional Chinese Medicine: Environmental Impact and Health Hazards. *Complement. Ther. Med.* 11, 118–122. doi:10.1016/s0965-2299(03)00055-4

Tariq, M., Ahmed, M., Iqbal, P., Fatima, Z., and Ahmad, S. (2020). Crop Phenotyping. *J. Wild. Ecol.* 4, 45–60. doi:10.1007/978-981-15-4728-7_2

Teixeira, P. H., Thel, Tdo. N., Ferreira, J. M., De Azevedo, S. M., Junior, W. R., and Lyra-Neves, R. M. (2014). Local Knowledge and Exploitation of the Avian Fauna by a Rural Community in the Semi-arid Zone of Northeastern Brazil. *J. Ethnobiol. Ethnomed.* 10, 81. doi:10.1186/1746-4269-10-81

Tesfaye, T., Sithole, B., Ramjugernath, D., and Chunilall, V. (2017). Valorisation of Chicken Feathers: Application in Paper Production. *J. Clean. Prod.* 164, 1324–1331. doi:10.1016/j.jclepro.2017.07.034

Trotter, R. T., and Logan, M. H. (1986). "Informant Consensus: a New Approach for Identifying Potentially Effective Medicinal Plants," in *Plants in Indigenous Medicine and Diet, Biobehavioural Approaches*. Editor N. L. E. Etkin (Bedford Hills, NY: Redgrave Publishers).

Tsuda, Y., and Nomura, Y. (2014). Properties of Alkaline-Hydrolyzed Waterfowl Feather Keratin. *Anim. Sci. J.* 85, 180–185. doi:10.1111/asj.12093

Umair, M., Altaf, M., Bussmann, R. W., and Abbasi, A. M. (2019). Ethnomedicinal Uses of the Local Flora in Chenab Riverine Area, Punjab Province Pakistan. *J. Ethnobiol. Ethnomed.* 15, 7. doi:10.1186/s13002-019-0285-4

Umair, M., and Yaqoob, M. (2018). Traditional Medicinal Uses of Honey in the District Gujranwala, Punjab, Pakistan. *J. Wildl. Ecol.* 2, 11–19.

Unnikrishnan, P. M. (1998). Animals in Ayurveda. *Amruth* 1–15.

Vallejo, J. R., and González, J. A. (2014). Fish-based Remedies in Spanish Ethnomedicine: a Review from a Historical Perspective. *J. Ethnobiol. Ethnomed.* 10, 37. doi:10.1186/1746-4269-10-37

Vallianou, N. G., Evangelopoulos, A., Skourtis, A., and Kazazis, C. (2014). HONEY AND CANCER--A REVIEW. *Curr. Top. Nutraceutical Res.* 12.

Van Vliet, N., Moreno Calderón, J. L., Gomez, J., Zhou, W., Fa, J. E., Golden, C., et al. (2017). Bushmeat and Human Health: Assessing the Evidence in Tropical and Sub-tropical Forests. *J. Ethnobiol.Conser.* 6, 1–45. doi:10.15451/ec2017-04-6.3-1-45

Vats, R., and Thomas, S. (2015). A Study on Use of Animals as Traditional Medicine by Sukuma Tribe of Busega District in North-western Tanzania. *J. Ethnobiol. Ethnomed.* 11, 38–11. doi:10.1186/s13002-015-0001-y

Vijayakumar, S., Yabesh, J. E., Prabhu, S., Ayyanar, M., and Damodaran, R. (2015b). Ethnozoological Study of Animals Used by Traditional Healers in Silent Valley of Kerala, India. *J. Ethnopharmacol.* 162, 296–305. doi:10.1016/j.jep.2014.12.055

Vijayakumar, S., Prabhu, S., Yabesh, J. M., and Prakashraj, R. (2015a). A Quantitative Ethnozoological Study of Traditionally Used Animals in Pachamalai Hills of Tamil Nadu, India. *J. Ethnopharmacol.* doi:10.1016/j.jep.2015.05.023

Vit, P., and Jacob, T. J. (2008). Putative Anticataract Properties of Honey Studied by the Action of Flavonoids on a Lens Culture Model. *J. Health Sci.* 54, 196–202. doi:10.1248/jhs.54.196

Wang, J., Hao, S., Luo, T., Cheng, Z., Li, W., Gao, F., et al. (2017). Feather Keratin Hydrogel for Wound Repair: Preparation, Healing Effect and Biocompatibility Evaluation. *Colloids Surf. B. Biointerfaces.* 149, 341–350. doi:10.1016/j.colsurfb.2016.10.038

Waykar, B., and Alqadhi, Y. A. (2016). Beekeeping and Bee Products; Boon for Human Health and Wealth. *Ijpbr* 4, 20–27. doi:10.30750/ijpbr.4.3.4

WHO (2005). *Technical Updates of the Guidelines on Integrated Management of Childhood Illness (IMCI). Evidence and Recommendations for Further Adaptations*. Geneva: World Health Organization.

Wiley, A. S. (2015). *Re-imagining Milk: Cultural and Biological Perspectives*. England, United Kingdom: Routledge.

Williams, P. (2007). Nutritional Composition of Red Meat. *Nutr. Dietetics* 64, S113.

Wilson, L. (2015). *Fats and Oils for Optimum Health*. Prescott, United States: The Center for Development.

Won, S.-R., Li, C.-Y., Kim, J.-W., and Rhee, H.-I. (2009). Immunological Characterization of Honey Major Protein and its Application. *Food Chem.* 113, 1334–1338. doi:10.1016/j.foodchem.2008.08.082

Xu, . (2014). Water-stable Three-Dimensional Ultrafine Fibrous Scaffolds from Keratin for Cartilage Tissue Engineering. *Langmuir* 30, 8461–8470. doi:10.1021/la500768b

Yeshi, K., Morisco, P., and Wangchuk, P. (2017). Animal-derived Natural Products of Sowa Rigpa Medicine: Their Pharmacopoeial Description, Current Utilization and Zoological Identification. *J. Ethnopharmacol.* 207, 192–202. doi:10.1016/j.jep.2017.06.009

Yirga, G., Teferi, M., and Gebreslassea, Y. (2011). Ethnozoological Study of Traditional Medicinal Animals Used by the People of Kafta-Humera District, Northern Ethiopia. *Int. J. Res. Med. Sci.* 3, 316–320.

Zhan, M., and Wool, R. P. (2011). Mechanical Properties of Chicken Feather Fibers. *Polym. Compos.* 32, 937–944. doi:10.1002/pc.21112

Zhao, H., Cheng, N., He, L., Peng, G., Liu, Q., Ma, T., et al. (2018). Hepatoprotective Effects of the Honey of *Apis cerana* Fabricius on Bromobenzene-Induced Liver Damage in Mice. *J. Food Sci.* 83, 509–516. doi:10.1111/1750-3841.14021

Conflict of Interest: The authors declare that the research was conducted in the absence of any commercial or financial relationships that could be construed as a potential conflict of interest.

Publisher's Note: All claims expressed in this article are solely those of the authors and do not necessarily represent those of their affiliated organizations, or those of the publisher, the editors, and the reviewers. Any product that may be evaluated in this article, or claim that may be made by its manufacturer, is not guaranteed or endorsed by the publisher.

frontiers | Frontiers in Pharmacology

TYPE Original Research
PUBLISHED 26 July 2022
DOI 10.3389/fphar.2022.893561

OPEN ACCESS

EDITED BY
X. Y. Zhang,
University of Guelph, Canada

REVIEWED BY
Jianye Dai,
Lanzhou University, China
Milton Prabu,
Annamalai University, India

*CORRESPONDENCE
Puyang Gong,
gongpuyang1990@163.com

SPECIALTY SECTION
This article was submitted to Ethnopharmacology, a section of the journal Frontiers in Pharmacology

RECEIVED 10 March 2022
ACCEPTED 29 June 2022
PUBLISHED 26 July 2022

CITATION
Luo X, Zhang B, Pan Y, Gu J, Tan R and Gong P (2022), Phyllanthus emblica aqueous extract retards hepatic steatosis and fibrosis in NAFLD mice in association with the reshaping of intestinal microecology.
Front. Pharmacol. 13:893561.
doi: 10.3389/fphar.2022.893561

Phyllanthus emblica aqueous extract retards hepatic steatosis and fibrosis in NAFLD mice in association with the reshaping of intestinal microecology

Xiaomin Luo[1], Boyu Zhang[1], Yehua Pan[1], Jian Gu[1], Rui Tan[2] and Puyang Gong[1]*

[1]College of Pharmacy, Southwest Minzu University, Chengdu, China, [2]College of Life Science and Engineering, Southwest Jiaotong University, Chengdu, China

Accumulating evidence suggests that dysregulation of the intestinal flora potentially contributes to the occurrence and development of nonalcoholic fatty liver disease (NAFLD). *Phyllanthus emblica* (PE), an edible and medicinal natural resource, exerts excellent effects on ameliorating NAFLD, but the potential mechanism remains unclear. In the present study, a mouse NAFLD model was established by administering a choline-deficient, L-amino acid-defined, high-fat diet (CDAHFD). The protective effects of the aqueous extract of PE (AEPE) on the gut microbiota and fecal metabolites in NAFLD mice were detected by performing 16S rRNA gene sequencing and untargeted metabolomics. The administration of middle- and high-dose AEPE decreased the levels of ALT, AST, LDL-C, TG, and Hyp and increased HDL-C levels in CDAHFD-fed mice. Hematoxylin–eosin (H&E), Oil Red O, and Masson's trichrome staining indicated that AEPE treatment attenuated hepatic steatosis and fibrotic lesions. Moreover, the disordered intestinal microflora was remodeled by AEPE, including decreases in the abundance of *Peptostreptococcaceae*, *Faecalibaculum*, and *Romboutsia*. The untargeted metabolomics analysis showed that AEPE restored the disturbed glutathione metabolism, tryptophan metabolism, taurine and hypotaurine metabolism, and primary bile acid biosynthesis of the gut bacterial community in NAFLD mice, which strongly correlated with hepatic steatosis and fibrosis. Collectively, AEPE potentially ameliorates NAFLD induced by a CDAHFD through a mechanism associated with its modulatory effects on the gut microbiota and microbial metabolism.

KEYWORDS

nonalcoholic fatty liver disease, *Phyllanthus emblica*, gut microbiota, fecal metabolites, hepatic fibrosis

1 Introduction

Nonalcoholic fatty liver disease (NAFLD) is characterized by the excessive accumulation of lipids in hepatocytes of individuals without alcohol abuse or other specific liver damage factors (Ren et al., 2021). The global incidence of NAFLD is approximately 25%, and NAFLD has become the most frequent cause of chronic liver disease worldwide with the increasing prevalence of obesity and metabolic syndrome (Vernon et al., 2011; Wong and Chan, 2021). NAFLD, which is characterized by a spectrum of hepatic pathology, ranges from simple hepatic steatosis to nonalcoholic steatohepatitis (NASH), which further progresses to fibrosis, cirrhosis, and eventually liver carcinoma (Song et al., 2020). At the NASH stage, hepatic steatosis coexists with inflammation, causing progressive fibrosis to develop into long-term complications (Li et al., 2022a). However, currently, approved therapeutic agents to restrain and reverse the progression of NAFLD are still unavailable (Schwabe et al., 2020; Parlati et al., 2021).

Based on accumulating evidence, the gut microbiome–liver axis plays an important role in NAFLD, especially in progression toward a more advanced disease stage (Tilg et al., 2021). Alterations in the structure and abundance of the gut microbiota might influence the metabolism of lipids, carbohydrates, and amino acids, which contribute to the development of NAFLD (Chen et al., 2021; Ren et al., 2021). The changes of the intestinal microbiota could promote the incidence and progression of NAFLD (Diehl and Day, 2017; Fang et al., 2018; Kolodziejczyk et al., 2019; Tilg et al., 2020). A study on microbial transplantation showed that sterile mice receiving gut microbiota from high-fat diet (HFD)-induced NAFLD mice increased liver fat accumulation and reduced short-chain fatty acid production, and the changes were more pronounced than in simple diet-induced NAFLD (Porras et al., 2019). Likewise, germ-free mice colonized with cecum contents from HFD-induced NAFLD mice exhibited hepatic steatosis and increased NAFLD susceptibility (Le Roy et al., 2013). Furthermore, extensive studies have demonstrated that disruption of metabolites mediated by intestinal flora, such as bile acids, tryptophan, and branched-chain amino acids, can induce the development or worsening of NAFLD (Ni et al., 2020). These studies highlight that modulation of gut microecology may be a new strategy to prevent or treat NAFLD.

Phyllanthus emblica L. (PE) is an edible and medicinal homologous plant belonging to the family *Euphorbiaceae*, which is widely distributed in subtropical and tropical areas of China and India (Variya et al., 2016). It possesses the properties of cooling blood, eliminating food, and suppressing cough and is used to treat heat in blood, indigestion, and hepatobiliary disease (Saini et al., 2022). Extensive pharmacodynamic studies have reported that PE extracts exert remarkable effects on ameliorating liver diseases, such as viral hepatitis, alcoholic hepatitis, NAFLD, and hepatocellular carcinoma (Yin et al., 2022). Among these extracts, the aqueous extract of PE (AEPE) has been shown to ameliorate hepatic steatosis and inflammation in a mouse model of NAFLD induced by a methionine–choline-deficient (MCD) high-fat diet (Huang et al., 2017; Tung et al., 2018). Meanwhile, our previous study showed that AEPE attenuates liver fibrosis caused by carbon tetrachloride *in vivo* (Yin et al., 2021). However, researchers have not clearly determined whether AEPE ameliorates fibrosis in subjects with NAFLD, and the mechanism by which it treats NAFLD must be further investigated.

In the current study, we first confirmed the protective effects of varying doses of AEPE on mice with CDAHFD-induced NAFLD by measuring biochemical markers and performing a histopathological examination. Then, 16S rRNA gene sequencing was performed to detect changes in the structural composition of the gut microbiota caused by AEPE treatment, and ultra-performance liquid chromatography with mass spectrometry (UPLC-MS) was applied to characterize metabolites in feces. Additionally, a correlation analysis was conducted to reveal the relationship between the altered microbiome and microbial metabolites induced by AEPE. The present study provides a novel mechanistic perspective of the role of PE in preventing the deterioration of NAFLD and facilitating the development of medicinal and healthcare applications of PE.

2 Materials and methods

2.1 Materials

Silymarin was purchased from Madaus (Cologne, Germany). The chemical reference standards, gallic acid, corilagin, and ellagic acid were purchased from Sichuan Weikeqi Biological Technology Co., Ltd. (Chengdu, China). Commercial diagnostic kits of alanine aminotransferase (ALT), aspartate aminotransferase (AST), triglyceride (TG), high-density lipoprotein cholesterol (HDL-C), low-density lipoprotein cholesterol (LDL-C), and hydroxyproline (Hyp) were obtained from Jiancheng Bioengineering Institute (Nanjing, China). Magnetic Soil and Stool DNA Kit (DP712) was obtained from Tiangen Biotech Co., Ltd. (Beijing, China). Phusion® High-Fidelity PCR Master Mix was purchased from New England Biolabs LTD. (Beijing, China). GeneJET Gel Extraction Kit and Qubit® 2.0 Fluorometer were purchased from Thermo Fisher Scientific. TruSeq DNA PCR-Free Library Preparation Kit was purchased from Illumina Co., Ltd.

Methanol, formic acid, and ammonium acetate were purchased from Sigma-Aldrich Chemical Co. (St. Louis, MO, United States). LC–MS grade water was purchased from Merck KGaA (Darmstadt, Germany). The dried *Phyllanthus emblica* L. (PE) fruits were obtained from the Lotus Pond herbal medicine market (Chengdu, China) and were authenticated by Prof. Jian Gu from the College of Pharmacy, Southwest Minzu University.

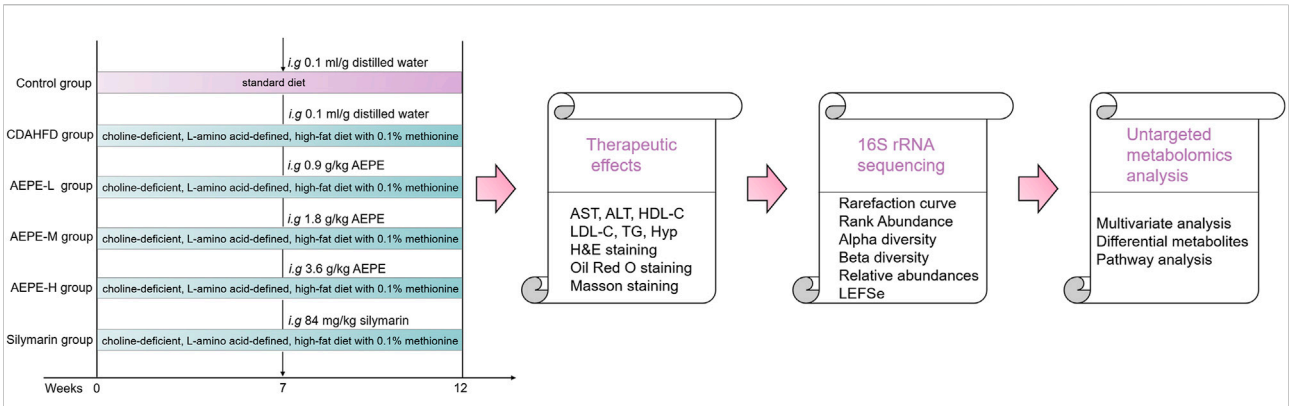

FIGURE 1
Overview of the experimental design for all groups.

The voucher specimen (No. 20201212) has been deposited at the herbarium of the College of Pharmacy, Southwest Minzu University.

2.2 Preparation and analysis of the chemical profile of AEPE

AEPE was prepared as described in our previous study (Yin et al., 2021). Briefly, 200 g of dried PE power was added to 2,000 ml of distilled water and extracted on a rotary shaker (150 rpm) at 37°C for 24 h. The extract solutions were filtrated and concentrated to 200 ml. The HPLC analysis was performed using an Agilent 1260 HPLC system equipped with a Kromasil 100-5-C18 column (4.6 × 250 mm, 5 μm). The mobile phase consisted of water (A) and acetonitrile containing 0.1% formic acid (B) as follows: 3% B (0–6 min), 3%–4% B (6–15 min), 4%–14% B (15–20 min), 14% B (20–50 min), and 14%–40% B (50–80 min). The UV detection wavelength was set at 254 nm. The flow rate was 0.6 ml/min, and the injection volume was 5 μl. The column temperature was maintained at 37°C. The constituents were quantified using external standards based on the analytical curves of gallic acid ($y = 13006x + 97.108$, $r^2 = 0.9996$, 0.25–4 mg ml^{-1}), corilagin ($y = 12259x - 721.79$, $r^2 = 0.9995$, 0.16–3.5 mg ml^{-1}), and ellagic acid ($y = 13488x - 161.95$, $r^2 = 0.9995$, 0.16–4 mg ml^{-1}).

2.3 Experimental animals and treatment

Five-week-old male C57BL/6J mice (18–22 g, specific pathogen free) were purchased from GemPharmatech Co., Ltd. (Jiangsu, China) and maintained at a controlled temperature (22.0 ± 2°C) and relative humidity (50%–60%) on a 12-h light/12-h dark cycle with free access to food and drink. All animal procedures were approved by the Animal Ethics Committee of Southwest Minzu University.

After acclimation and feeding for 1 week, the mice were randomly assigned to two groups: the control group (control), which received a standard diet (11% kcal fat, TP36225MCS, Trophic Animal Feed High-tech Co., Ltd., Jiangsu, China, n = 10), and the CDAHFD groups, which were fed a choline-deficient, L-amino acid-defined, high-fat diet with 0.1% methionine (65% kcal fat, TP36225MCD, Trophic Animal Feed High-tech Co., Ltd, Jiangsu, China, n = 50). After 6 weeks, mice in CDAHFD groups were randomly divided into the following five groups (n = 10 mice per group) according to the treatment and fed for a period of 6 weeks. The groups included the CDAHFD group, AEPE low-dose (0.9 g of crude drug/kg) treatment group (AEPE-L), AEPE middle-dose (1.8 g of crude drug/kg) treatment group (AEPE-M), AEPE high-dose (3.6 g of crude drug/kg) treatment group (AEPE-H), and 84 mg/kg silymarin treatment group (Silymarin) (Figure 1).

2.4 Sample collection

Mouse feces were collected daily at the same time in the twelfth week, and fecal samples from each mouse were immediately collected in 2.0-ml cryogenic vials, immersed in liquid nitrogen, and stored at −80°C until further analysis. After the last feeding, all mice were fasted for 12 h, weighed, and then completely anesthetized with 1.5% isoflurane. Blood samples were obtained from the retro-orbital plexus. The samples were incubated at 25°C for 1 h and then centrifuged at 862 *g* for 15 min to separate the serum, which was stored at −20°C. A small piece of fresh liver was removed and immersed in a tissue fixative solution (4% paraformaldehyde solution) for subsequent staining and assessment. The remainder of the liver tissue was stored at −80°C until further analysis.

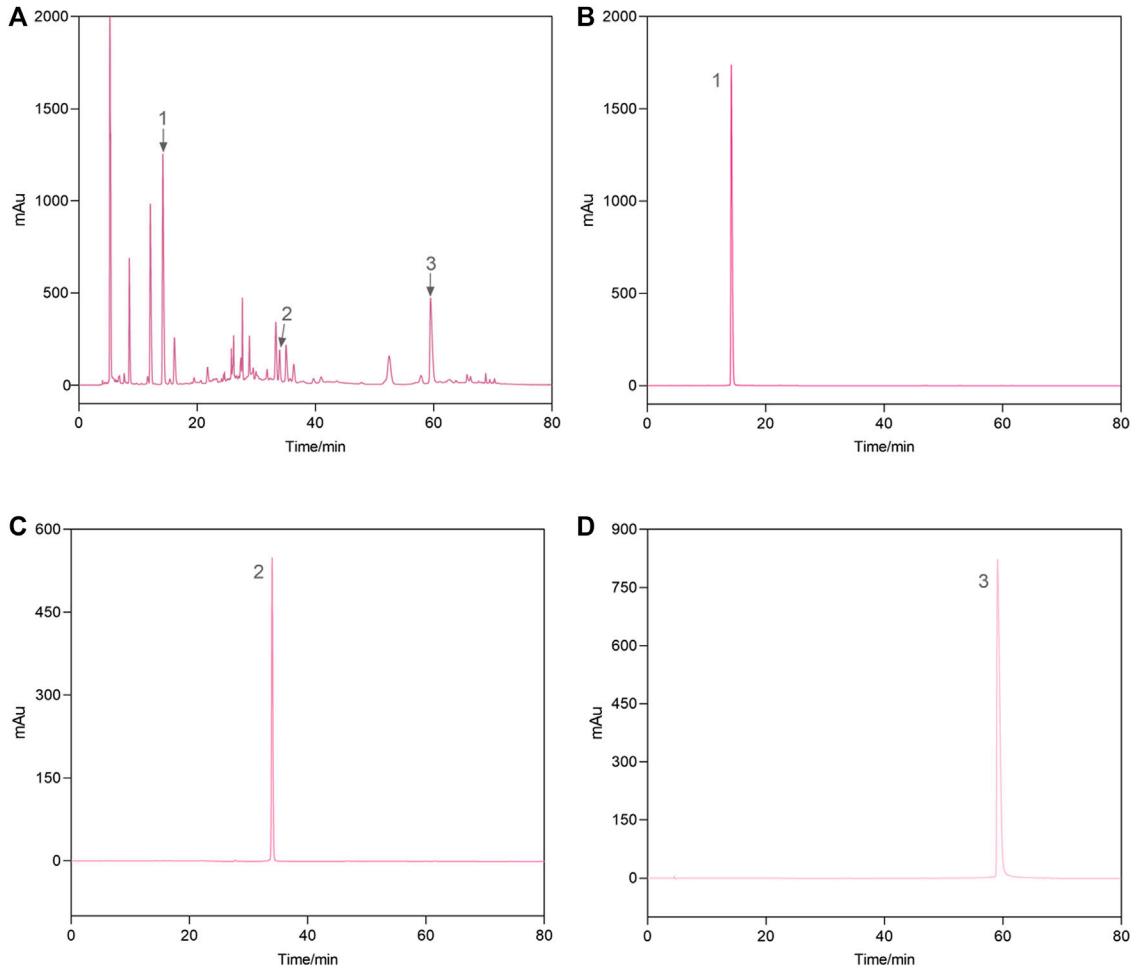

FIGURE 2
Representative high-performance liquid chromatograms of the AEPE sample **(A)** and standard compounds **(B–D)**. 1, gallic acid; 2, corilagin; 3, ellagic acid.

2.5 Analysis of serum and liver biochemical parameters

Serum AST and ALT levels were determined with appropriate kits according to the manufacturer's instructions. The contents of TG, HDL-C, LDL-C, and Hyp in the liver tissue homogenates were measured using commercially available kits.

2.6 Histological analysis

The liver tissue samples were fixed with 4% paraformaldehyde, processed, and embedded in paraffin for hematoxylin and eosin (H&E) staining. Slices were stained with Masson's trichrome to observe the progression of hepatic fibrosis. Frozen sections of the liver were stained with Oil Red O to visualize lipid accumulation within the hepatocytes. Images of pathological sections were captured using an Olympus BX53 microscope.

2.7 Gut microbiota analysis

2.7.1 Extraction of fecal genomic DNA for 16S rRNA sequencing

The total genomic DNA was extracted from fecal samples in the control, CDAHFD, and AEPE-M groups (six samples per group) using a Magnetic Soil and Stool DNA Kit according to the manufacturer's instructions. The V3-V4 hypervariable region of the bacterial 16S rRNA gene was amplified with the primers 341F (5′-CCTAYGGGRBGCASCAG-3′) and 806R (5′-GGACTACNNGGGTATCTAAT-3′). The polymerase chain reaction (PCR) was performed with 30 and 15 μl of Phusion®

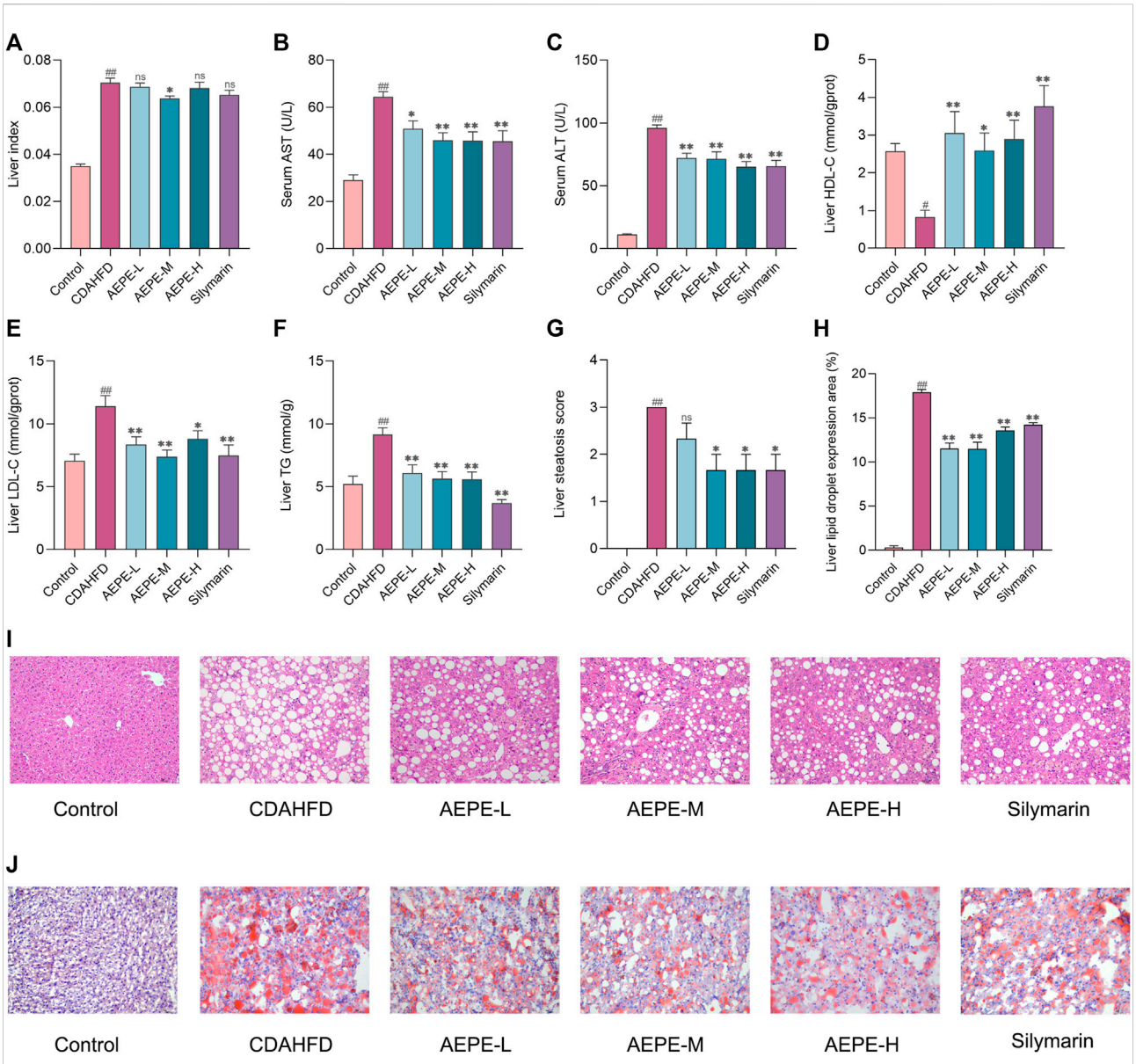

FIGURE 3
AEPE treatment attenuated hepatic steatosis in CDAHFD-fed mice. **(A)** AEPE-M treatment decreased the liver index in CDAHFD mice. **(B)** AEPE treatment decreased the level of AST in CDAHFD mice. **(C)** AEPE treatment decreased the level of ALT in CDAHFD mice. **(D)** AEPE treatment increased the level of HDL-C in CDAHFD mice. **(E)** AEPE treatment decreased the level of LDL-C in CDAHFD mice. **(F)** AEPE treatment decreased the level of TG in CDAHFD mice. **(G,I)** H&E staining showed that AEPE treatment significantly improved the pathological changes in the liver (×200). **(H,J)** Oil Red O staining showed that AEPE treatment significantly improved the accumulation of red lipid droplets in the liver (×200). Control, CDAHFD, AEPE-L, AEPE-M, AEPE-H, and silymarin (n = 10 per group) groups. Data were presented as the mean ± SEM. $^{\#}p < 0.05$, $^{\#\#}p < 0.01$ as compared to the control group; $^{*}p < 0.05$, $^{**}p < 0.01$ as compared to the CDAHFD group.

High Fidelity PCR Master Mix; 0.2 μM forward and reverse primers; and approximately 10 ng of template DNA. The thermal cycle involved an initial denaturation at 98°C for 1 min, denaturation at 98°C for 10 s, annealing at 50°C for 30 s, extension at 72°C for 30 s, and a final extension at 72°C for 5 min. An equal volume of loading buffer was mixed with the PCR product and detected after electrophoresis on a 2% agarose gel. A sample with a clear main band of 400–450 bp was selected for a subsequent experiment. PCR products were blended in a ratio of equal densities. The hybrid PCR products were then purified using the GeneJET Gel Extraction Kit.

2.7.2 Bioinformatics analysis

A sequencing library was generated, and an index code was added using the Illumina TruSeq DNA PCR-Free Library

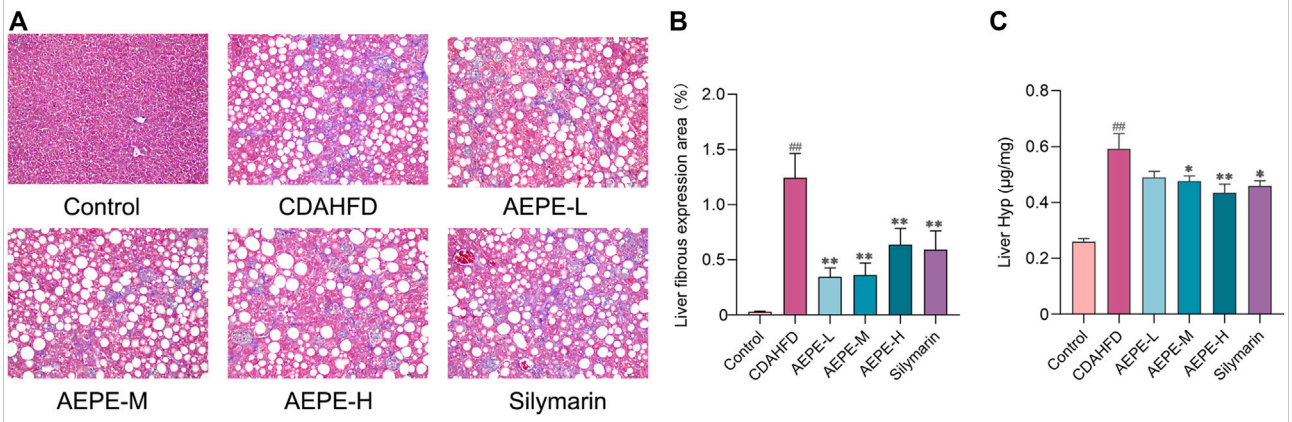

FIGURE 4
AEPE treatment attenuated hepatic fibrosis in CDAHFD-fed mice. **(A,B)** Masson's staining showed that AEPE treatment significantly decreased blue collagen fibers in the liver (×200). **(C)** AEPE treatment decreased the level of Hyp in CDAHFD mice. Control, CDAHFD, AEPE-L, AEPE-M, AEPE-H, and silymarin (n = 10 per group) groups. Data are presented as the mean ± SEM. $^{\#\#}p < 0.01$ as compared to the control group; $^{*}p < 0.05$, $^{**}p < 0.01$ as compared to the CDAHFD group.

Preparation Kit according to the manufacturer's instructions. Library quality was assessed using a Qubit® 2.0 fluorometer and an Agilent Bioanalyzer 2100 system. Ultimately, the library was sequenced with the Illumina NovaSeq platform to generate a 250-bp paired read sequence. Quality filtering of the paired-end raw reads was performed under specific filtering conditions, and paired-end clean reads were merged. 16S rRNA gene sequences were analyzed using the Quantitative Insights Into Microbial Ecology (QIIME) software (version 1.9.1). The operational taxonomic unit (OTU) cluster sequence analysis was performed using pick_de_novo_otus.py; sequences with greater than or equal to 97% similarity were assigned to the equivalent OTUs. Then, species annotation was performed on the OTU sequence and SILVA_138 database. The alpha diversity and beta diversity indices of the samples were calculated immediately afterward using the QIIME software and displayed using the R software (version 2.15.3).

2.8 UHPLC-MS/MS analysis of fecal metabolites

2.8.1 Fecal sample preparation

Fecal samples (0.1 g) were ground in liquid nitrogen, and the homogenate was resuspended by vortexing in precooled 80% methanol. The specimens were placed on ice, incubated for 5 min, and centrifuged at 15,000 ×g for 20 min at 4°C. After centrifugation, a portion of the supernatant was diluted with LC-MS grade water to a final concentration containing 53% methanol. The specimens were then transferred to a new microcentrifuge tube and centrifuged at 15,000 ×g for 20 min at 4°C. Afterward, the supernatant was placed in an autosampler vial for further analysis.

2.8.2 UHPLC-MS/MS analysis

The UHPLC-MS/MS analysis was performed using a Vanquish ultra-high-performance liquid chromatograph (UHPLC) in combination with an Orbitrap Q Exactive™ HF-X mass spectrometer. The supernatant was separated on a Hypersil GOLD column (100 × 2.1 mm, 1.9 μm) with a 17-min linear gradient and a flow rate of 0.2 ml per min. The eluents for the positive polarity mode were eluent A (0.1% formic acid in water) and eluent B (methanol). The eluates for the negatively polarized mode were eluate A (5 mm ammonium acetate, hydrogen potential of 9.0) and eluate B (methanol). The procedure for gradient elution with the solvent was as follows: 2% B, 0–1.5 min; 2%–85% B, 1.5–3 min; 100% B, 3–10 min; 100%–2% B, 10–10.1 min; and 2% B, 10.1–12 min. A Q Exactive™ HF-X spectrometer was operated in positive and negative ion mode with a voltage of 3.5 kV, the capillary temperature of 320°C, a sheath gas flow rate of 35 psi, an aux gas flow rate of 10 L per min, a S-lens RF class level of 60, and an auxiliary gas heater temperature of 350°C. The full-scan range was m/z 100–1500.

2.8.3 Data processing and analysis of metabolites

The original UHPLC-MS/MS data files were manipulated using Compound Discoverer 3.1 (CD 3.1) software (Thermo Fisher) for peak alignment, peak picking, and quantification of the individual metabolites. Then, the peak intensity was normalized to the total spectral intensity. The molecular formula based on additive ions, molecular ion peaks, and fragment ions was predicted from the normalized data. Then, the mzCloud (https://www.mzcloud.org/), mzVault, and MassList databases were used to obtain accurate qualitative

and relative quantitative results. Normalized data were imported into the SIMCA-P software (version 14.1; SIMCA-P). Principal component analysis (PCA), partial least squares discriminant analysis (PLS-DA), and orthogonal partial least squares discriminant analysis (OPLS-DA) were conducted to obtain clustering information and salient variables. The Kyoto Encyclopedia of Genes and Genomes (KEGG) database (https://www.genome.jp/kegg/pathway.html), Human Metabolome Database (HMDB) (https://hmdb.ca/metabolities), and LIPID MAPS database (http://www.lipidmaps.org/) were used to annotate these metabolites. MetaboAnalyst (https://www.metaboanalyst.ca/) (version 5.0) was used to identify metabolic pathways.

2.9 Statistical analysis

All data are presented as the means ± S.E.M. Graphical representations of the results were performed using GraphPad Prism 8.3.0 software. The significance level of differences between two groups was analyzed using Student's unpaired t-test, while the data from multiple groups were statistically analyzed using one-way analysis of variance (ANOVA) followed by Dunnett's multiple comparisons post hoc test. A p-value < 0.05 was regarded as statistically significant.

3 Results

3.1 Quantitative analysis of representative components of AEPE

As shown in Figure 2, the HPLC chromatogram indicated that AEPE contained gallic acid, corilagin, and ellagic acid, with retention time peaks at 14.203, 33.938, and 59.462 min, respectively. The gallic acid, corilagin, and ellagic acid contents in PE were 14.6, 2.8, and 9.5 mg/g, respectively.

3.2 AEPE alleviated hepatic steatosis in mice treated with CDAHFD

As illustrated in Figure 3A, a medium dose of AEPE (1.8 g of crude drug/kg) significantly reduced the elevated liver index of NAFLD mice ($p < 0.05$). Additionally, compared with the control diet, the CDAHFD triggered not only significantly abnormal serum AST and ALT levels but also abnormal LDL-C, TG, and HDL-C concentrations in liver tissue. However, AEPE (0.9, 1.8, and 3.6 g of crude drug/kg) and silymarin (84 mg/kg) treatments reversed these changes (Figures 3B–F). The results obtained here are similar to those obtained by Huang et al. (2017), who found that the water extract of PE significantly decreased the levels of ALT, AST and LDL-C in rats with HFD-induced NAFLD. Hence, the results further confirmed that AEPE improved liver function and lipid metabolism in NAFLD mice.

H&E staining and Oil Red O staining were performed to further verify the degree of hepatic steatosis. As shown in Figures 3G,I, the liver histology of mice in the CDAHFD group revealed apparent hepatocyte swelling and necrosis, balloon-like changes, and slight inflammatory cell infiltration. Compared with the CDAHFD group, the AEPE groups displayed substantial amelioration of these changes. Oil Red O staining (Figures 3H,J) showed the accumulation of numerous red lipid droplets in the CDAHFD group, which was significantly improved by AEPE and silymarin treatments. Hence, AEPE prevented NAFLD development in CDAHFD-fed mice, especially the medium dose of AEPE.

3.3 AEPE attenuates hepatic fibrosis progression in NAFLD mice

Liver fibrosis is an important pathological marker for the deterioration of NAFLD; hence, the protective effects of AEPE were further evaluated using Masson's trichrome staining and measurements of Hyp levels. As shown in Figures 4A,B, no obvious change in collagen expression was observed in the control group, but a large amount of collagen was expressed and deposited in the liver tissue of CDAHFD mice. The AEPE intervention noticeably decreased the number of collagen fibers. Moreover, the Hyp content in the CDAHFD group increased significantly ($p < 0.01$, Figure 4C) compared to that in the control group and was significantly reduced ($p < 0.05$) following the consumption of medium and high doses of AEPE and silymarin. Taken together, these results showed that the AEPE-M treatment better prevented the progression of NAFLD.

3.4 AEPE-M regulates the composition of the gut microbiota that is altered by CDAHFD

A rarefaction curve has been used to determine whether the current sequencing depth of each sample adequately reflects the microbial diversity of the sample. As shown in Figure 5A, the rarefaction curve flattened out, and we considered that the sequencing depth basically covered all the species in the sample. The rank abundance showed that the libraries were sufficiently large to cover most of the bacterial diversity in each sample (Figure 5B). Based on the richness and alpha diversity analyses, Simpson's and Shannon's indices were significantly higher in the CDAHFD group than in the control group ($p < 0.01$; Figures 5D,E), whereas this change was moderated by the AEPE-M treatment. We performed a similarity analysis to test whether the between-group

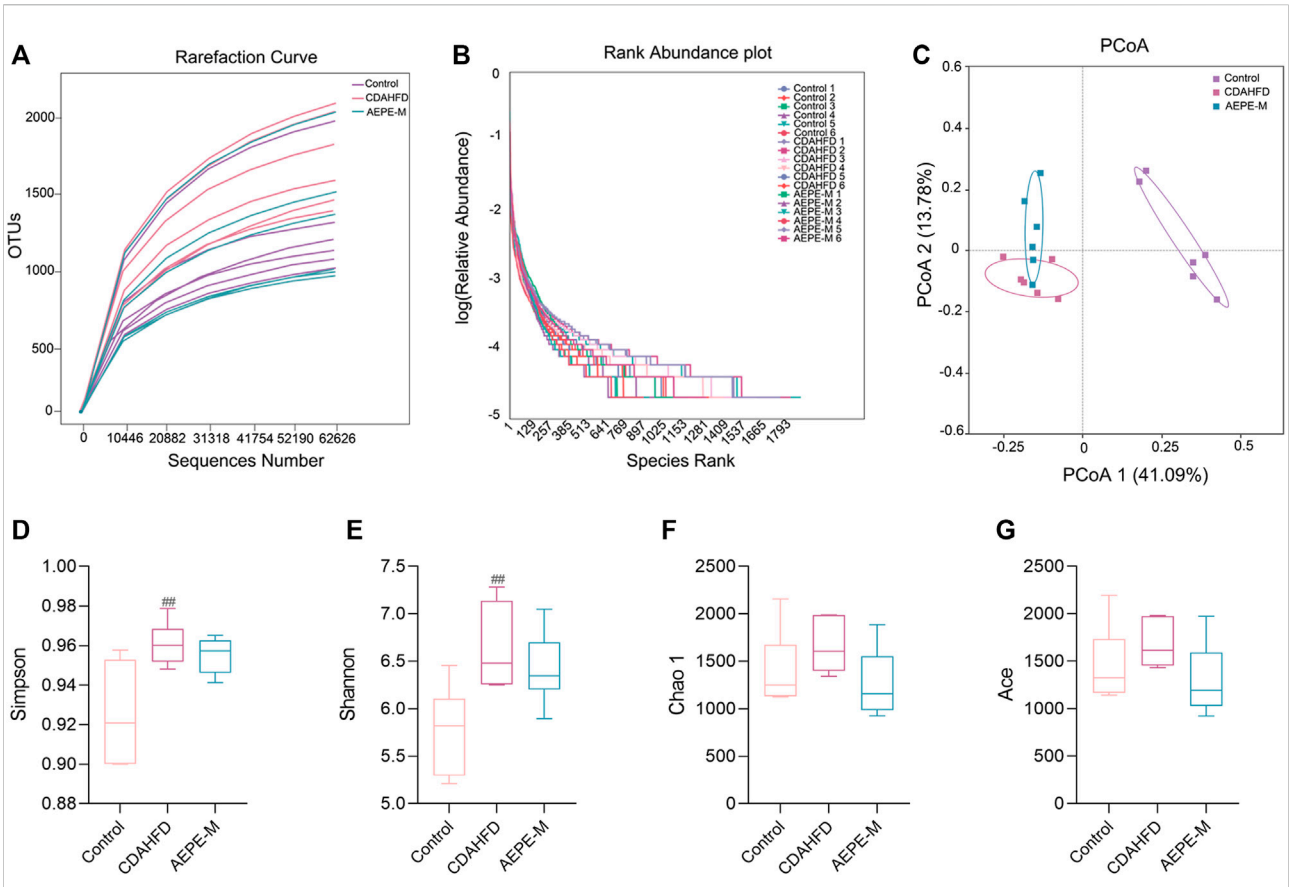

FIGURE 5
AEPE treatment affected the diversity in CDAHFD mice. **(A)** Rarefaction curve flattened out indicated that the sequencing depth has basically covered all the species in the sample. **(B)** Rank abundance indicated that the libraries were large enough to cover most of the bacterial diversity in each sample. **(C)** PCoA indicated more similar beta diversity between the AEPE-M and control groups than that between the CDAHFD and control groups. **(D,E)** Simpson's and Shannon's indexes were higher in the CDAHFD group than in the control group. **(F,G)** There were no significant differences in the Chao 1 index and the Ace index in each group. Control, CDAHFD, and AEPE-M (n = 6 per group) groups. Data are presented as the mean ± SEM. $^{\#\#}p < 0.01$ as compared to the control group.

TABLE 1 Analysis of differences between ANOSIM groups.

Group	*R*-value	*P*-value
Control vs. AEPE-M	0.9556	0.002
CDAHFD vs. AEPE-M	0.6389	0.004
CDAHFD vs. control	0.9889	0.004

The R-value was found to be between −1 and 1, when $R > 0$, indicating that the between-group differences were significant, and $R < 0$ indicated that the within-group differences were greater than between-group differences. The reliability of the statistical analysis was expressed as p-value, and $p < 0.05$ indicated that the difference was statistically significant.

differences were greater than the within-group differences and to show that the groups were meaningful. According to the current experimental results (Table 1), by observing the R-value and p-value between the groups, the difference between the groups was greater than the difference within the group.

Principal coordinates analysis (PCoA) was used to evaluate the differences and similarities in the gut microbiota components of mice in the control group, CDAHFD group, and AEPE-M group (Figure 5C). As shown in the results of PCoA, the samples of the control group were significantly separated from those of the other two groups. As expected, the samples obtained after the AEPE-M intervention tended to be close to the control group. Therefore, AEPE-M and CDAHFD altered the overall composition of the gut microbiota.

We assessed the bacteria with the top 10 relative abundance at the phylum (Figure 6A), family (Figure 6B), and genus (Figure 6C) levels to clarify which bacteria accounted for the differences in the intestinal microbiota structure among the different groups. At the phylum level, the relative abundance of *Firmicutes* and *Bacteroidetes* accounted for a greater proportion of the total. The ratio of *Firmicutes* to *Bacteroidetes* (F/B) in mice fed the CDAHFD was obviously higher than that in the control mice. After AEPE-M treatment, this change was reversed and reduced to

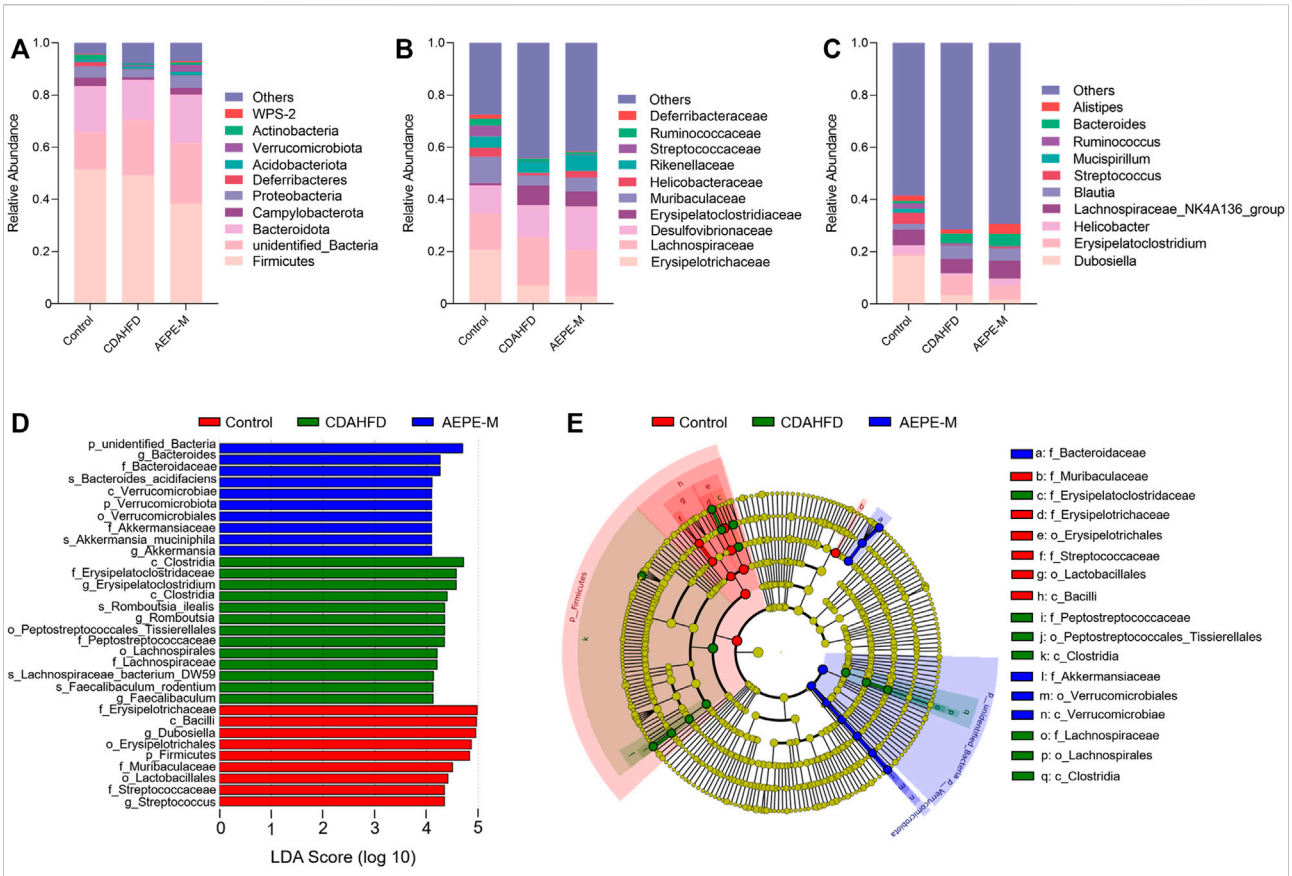

FIGURE 6
AEPE treatment affected the abundance of gut microbiota in CDAHFD mice. **(A)** At the phylum level, the top 10 relative abundances in each group. **(B)** At the family level, the top 10 relative abundances in each group. **(C)** At the genus level, the top 10 relative abundances in each group. **(D,E)** LEFSe showed significant differences in gut microbiota among groups. Control, CDAHFD, and AEPE-M (n = 6 per group) groups.

levels close to the ratio in control mice. We used linear discriminant analysis effect size (LEFSe) to further identify the flora that plays an important role in the gut microbiota and showed significant differences between groups. The statistical results of the LEFSe include two parts, the linear discriminant analysis (LDA) value distribution histogram (Figure 6D) and an evolutionary branching diagram (Figure 6E). As shown in the figure, nine strains of bacteria were significantly enriched in the control group, including *Erysipelotrichaceae*, *Bacilli*, *Dubosiella*, *Erysipelotrichales*, *Firmicutes*, *Muribaculaceae*, *Lactobacillales*, *Streptococcaceae*, and *Streptococcus*. Thirteen strains of bacteria were significantly enriched in the CDAHFD group, and the relative abundance of *Clostridia*, *Erysipelatoclostridiaceae*, *Romboutsia_ilealis*, *Peptostreptococcales_Tissierellales*, and *Peptostreptococcaceae* was relatively high. A previous study reported that *Peptostreptococcaceae* was significantly elevated in NAFLD mice induced by HFD (Soares et al., 2021), which is consistent with our findings. Ten strains of bacteria that were significantly enriched in the AEPE-M group were as follows: *unidentified_Bacteria*, *Bacteroides*, *Bacteroidaceae*, *Bacteroides_acidifaciens*, *Verrucomicrobiae*, *Verrucomicrobiota*, *Verrucomicrobiales*, *Akkermansiaceae*, *Akkermansia_muciniphila*, and *Akkermansia*. Collectively, these findings suggest that AEPE-M supplementation regulated the composition of the intestinal flora in CDAHFD-fed mice.

Specifically, as presented in Figure 7, at the phylum level, the relative abundance of *Actinobacteria* in the control and AEPE-M groups was 1.839 ± 0.3898% and 0.8804 ± 0.2726%, respectively, which were higher than that in the CDAHFD group (0.5991 ± 0.1401%). The relative abundance of *Desulfobacterota* in the control and AEPE-M groups was 0.2626 ± 0.03626% and 0.1200 ± 0.01966%, respectively, which were slightly lower than that in the CDAHFD group (0.3068 ± 0.05706%). At the family level, the relative abundance of *Peptostreptococcaceae* in the control group was 0.6545 ± 0.09701%, which was significantly lower than that in the CDAHFD group (4.772 ± 0.5602%) ($p < 0.01$), and this change was significantly reversed by AEPE-M (2.573 ± 0.2426%) ($p < 0.01$). In addition, the relative abundance of *Muribaculaceae* and *Streptococcaceae* in the control group was 10.20 ± 1.554% and 4.280 ± 1.359%, respectively, which was

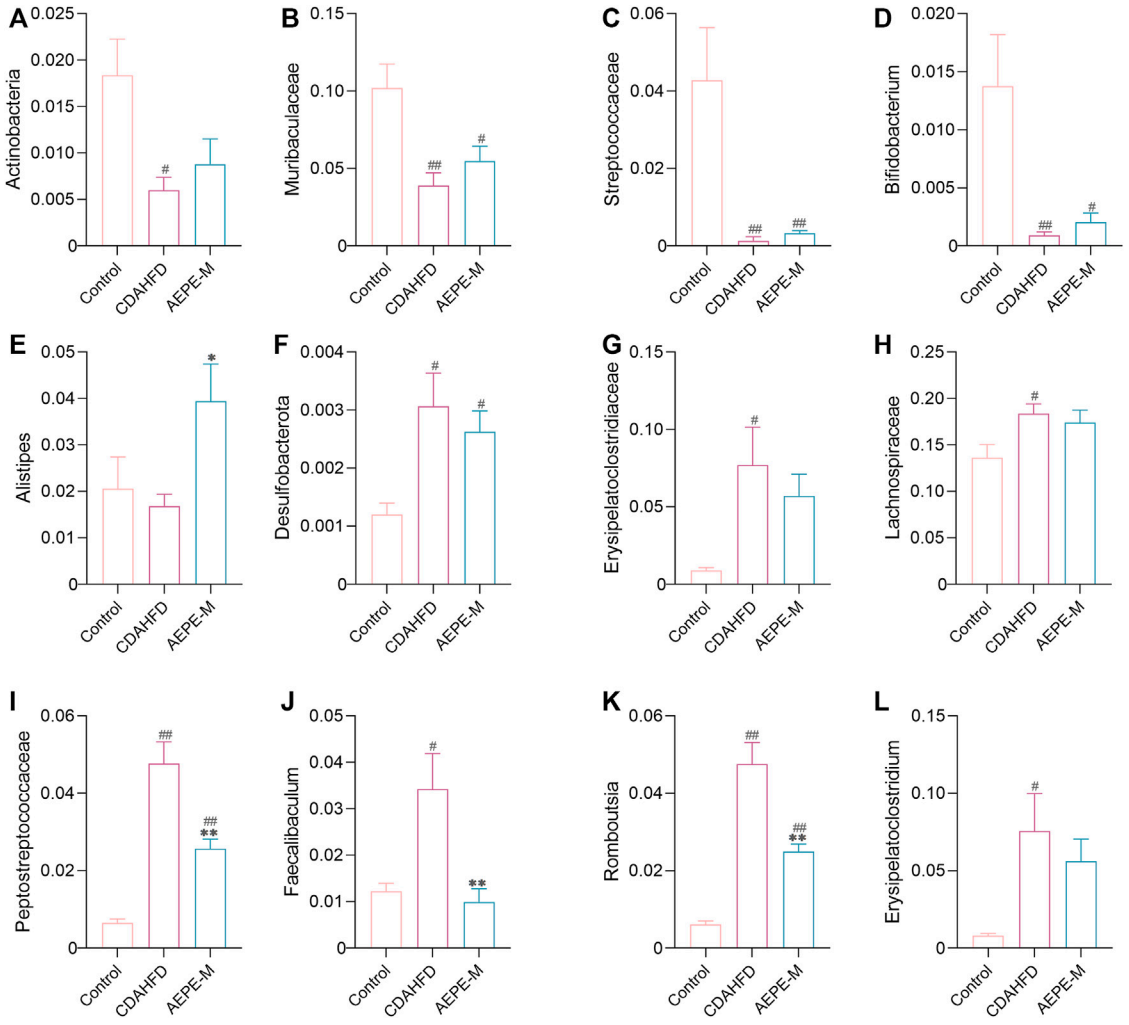

FIGURE 7
Relative abundance of mice at phylum, family, and genus levels. Compared with the control group, the relative abundance of *Actinobacteria* **(A)**, *Muribaculaceae* **(B)**, *Streptococcaceae* **(C)**, *Bifidobacterium* **(D)**, and *Alistipes* **(E)** obviously decreased in the CDAHFD group; *Desulfobacterota* **(F)**, *Erysipelatoclostridiaceae* **(G)**, *Lachnospiraceae* **(H)**, *Peptostreptococcaceae* **(I)**, *Faecalibaculum* **(J)**, *Romboutsia* **(K)**, and *Erysipelatoclostridium* **(L)** obviously increased in the CDAHFD group. AEPE treatment could effectively improve this change. Control, CDAHFD, and AEPE-M (n = 6 per group) groups. Data are presented as the mean ± SEM. $^{\#}p < 0.05$, $^{\#\#}p < 0.01$ as compared to the control group; $^{*}p < 0.05$, $^{**}p < 0.01$ as compared to the CDAHFD group.

significantly higher than that in the CDAHFD group (3.890 ± 0.8296% and 0.1316 ± 0.1075%, respectively) ($p < 0.01$) and AEPE-M group (5.486 ± 0.9541% and 0.3287 ± 0.06166%, respectively) ($p < 0.05$ and $p < 0.01$, respectively). At the genus level, the CDAHFD group presented significantly increased levels of *Faecalibaculum* and *Romboutsia* (3.426 ± 0.7685% and 4.757 ± 0.5592, respectively) ($p < 0.05$ and $p < 0.01$, respectively) compared with the control group (1.222 ± 0.1721% and 0.6125 ± 0.08919%, respectively), and the levels were significantly decreased when animals were treated with AEPE-M (0.9926 ± 0.2854% and 2.490 ± 0.2024%, respectively) ($p < 0.01$).

3.5 AEPE-M repaired metabolic disorders induced by CDAHFD

UPLC–MS/MS was used to analyze the metabolites in fecal samples and systematically confirm that AEPE-M retards the progression of NAFLD by reshaping the intestinal microecology. As metabolite groups are susceptible to external factors and change rapidly, data quality control (QC) is necessary to obtain stable and accurate results for different metabolites. The total ion current (TIC) of QC samples analyzed using mass spectrometry in positive (Figure 8A) and negative (Figure 8B) ion modes showed a high overlap between the

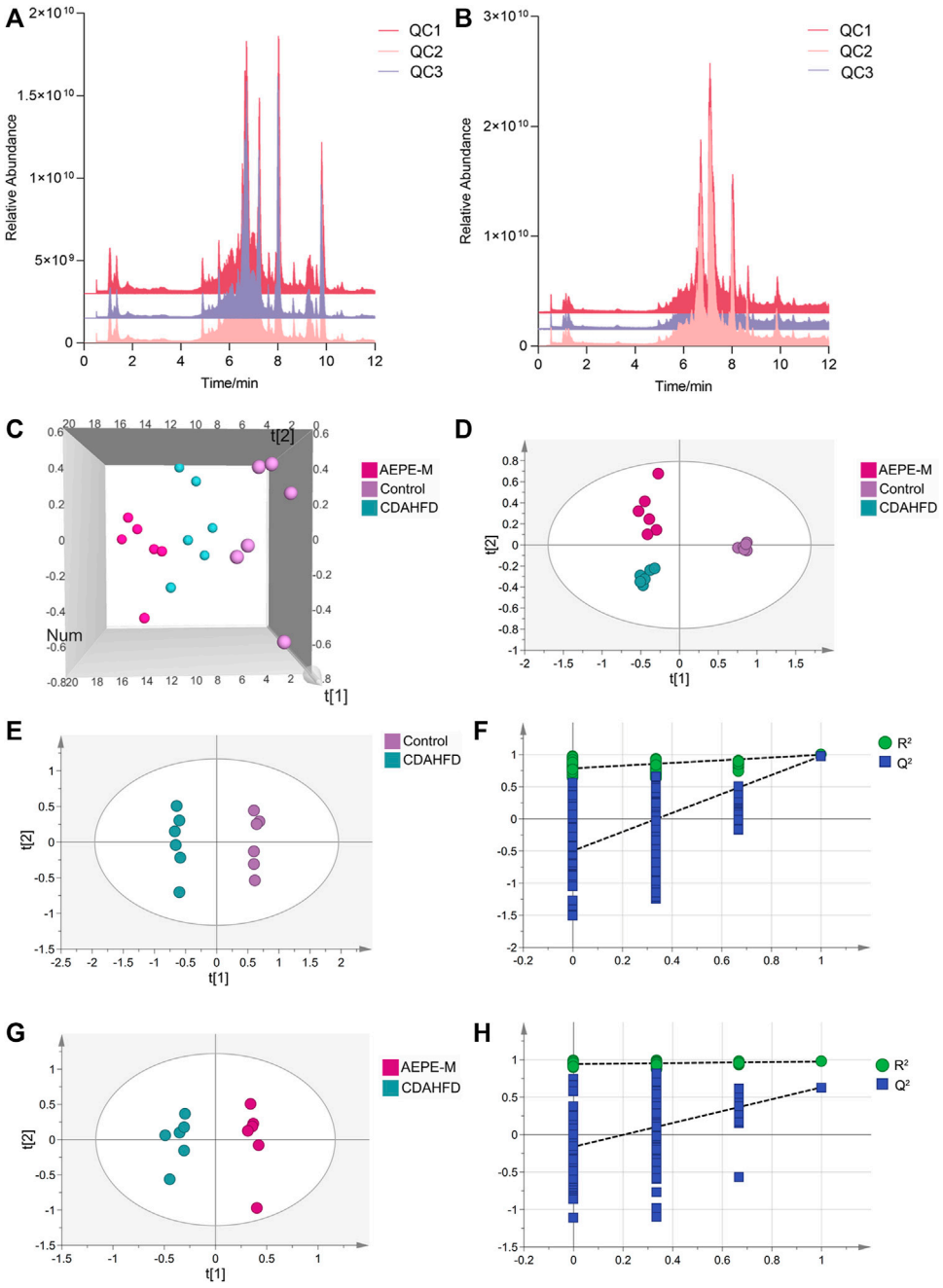

FIGURE 8
AEPE treatment modulated the fecal metabolites in CDAHFD mice. Positive **(A)** and negative **(B)** ions showed a high overlap between the TIC of different QC samples. **(C)** Score plots of 3D PCA between the control, CDAHFD, and AEPE-M groups. **(D)** Score plots of PLS-DA between the control, CDAHFD, and AEPE-M groups. **(E,F)** Score plots of OPLS-DA between the control and the CDAHFD groups and the corresponding coefficient of loading plots. **(G,H)** Score plots of OPLS-DA between the AEPE-M and CDAHFD groups and the corresponding coefficient of loading plots. Control, CDAHFD, and AEPE-M (n = 6 per group) groups.

TIC of different QC samples, indicating that the mass spectrometer had better signal stability for the same sample at different times. The metabolites obtained in positive and negative ion modes were combined for further principal component analysis (PCA). As shown in the PCA 3D diagram (Figure 8C), there was a clear separation between the three groups. In addition, partial least squares discriminant analysis (PLS-DA) was performed to distinguish the differences in

TABLE 2 Differential metabolites in fecal after AEPE-M treatment.

No.	Rt (min)	m/z	Formula	Metabolite	MS/MS	VIP		FC		Trend	
						C vs. M	A vs. M	C vs. M	A vs. M	C vs. M	A vs. M
1	1.11	133.0972	$C_5H_{12}N_2O_2$	L-Ornithine	132.99745, 119.01838, 114.98771, 101.00803, 87.99341, 86.99271, 70.06506, 69.98296, 69.15391, and 68.98217	1.13	1.68	0.29	0.44	↓##	↓*
2	1.22	124.0075	$C_2H_7NO_3S$	Taurine	127.03908, 126.09113, 126.06609, 126.05488, 109.02833, 96.04423, 84.0444, 81.03347, 80.04948, and 69.03353	1.50	1.68	0.80	0.21	↓##	↓*
3	1.29	261.0372	$C_6H_{13}O_9P$	Glucose 1-phosphate	262.25247, 212.50664, 145.04935, 127.03897, 122.79235, 98.98416, 97.02851, 89.64538, 85.02845, and 72.50112	1.07	1.67	5.48	4.42	↑##	↑*
4	1.43	226.0839	$C_9H_{13}N_3O_4$	Deoxycytidine	229.00197, 228.17061, 228.08607, 210.07626, 166.0502, 157.09702, 112.05047, 84.08077, 72.0809, and 70.06501	1.14	1.40	0.52	0.66	↓#	↓*
5	2.56	117.0196	$C_4H_6O_4$	Methylmalonic acid	117.92876, 117.01919, 116.92859, 100.9259, 99.92582, 99.00894, 80.46878, 73.0295, and 66.29874	1.21	1.80	0.40	0.49	↓##	↓*
6	4.71	119.0705	$C_5H_{10}O_3$	3-Hydroxy-3-methylbutanoic acid	129.1019, 104.96317, 102.94769, 100.51136, 91.05414, 86.99245, 86.95286, 72.93713, 68.98221, and 56.94242	1.45	2.03	0.11	0.37	↓##	↓*
7	4.80	177.1023	$C_{10}H_{12}N_2O$	5-Hydroxytryptamine	-	1.01	2.23	0.23	0.42	↓##	↓*
8	4.97	238.1076	$C_{12}H_{15}NO_4$	N-Lactoyl-phenylalanine	238.14291, 238.1068, 238.07872, 224.06406, 124.03922, 106.02879, 96.04425, 78.03376, 73.04677, and 69.06993	1.60	1.41	3.43	1.71	↑##	↑*
9	5.67	182.1180	$C_{10}H_{15}NO_2$	2-(3,4-Dimethoxyphenyl) ethanamine	182.10657, 182.08101, 165.07375, 164.07042, 137.0786, 136.07561, 122.0599, 108.08056, 93.06973, and 91.05442	1.24	1.74	0.50	0.63	↓##	↓*
10	5.70	164.0359	$C_8H_7NO_3$	Indoleacrylic acid	167.07295, 167.05589, 166.07224, 149.04567, 138.0547, 135.02998, 124.05039, 121.02822, 120.08071, and 74.02355	1.24	1.86	0.54	0.64	↓##	↓*
11	6.40	188.0707	$C_{11}H_9NO_2$	3-Indoleacrylic acid	188.07043, 170.05988, 146.05989, 144.08067, 143.07275, 142.06517, 118.06502, 117.06979, 115.05425, and 86.09643	1.17	2.39	1.81	2.14	↑##	↑*
12	6.99	498.2893	$C_{26}H_{45}NO_6S$	Taurochenodeoxycholic acid	501.23895, 500.37692, 500.31119, 500.24118, 454.30618, 377.17145, 156.0768, 110.07115, 95.0603, and 83.06045	1.28	1.68	0.26	0.36	↓#	↓*
13	7.37	333.2074	$C_{20}H_{32}O_5$	Prostaglandin H2	353.24774, 335.23715, 252.18697, 211.14816, 183.1169, 157.10127, 155.0856, 143.08546, 129.06982, and 95.08549	1.46	1.56	0.37	0.59	↓##	↓*
14	7.55	657.1525	$C_{20}H_{32}N_6O_{12}S_2$	Glutathione disulfide	—	1.62	1.44	3.58	1.71	↑##	↑**

Control, CDAHFD, AEPE-M ($n = 6$ per group) groups. $^{\#}p < 0.05$, $^{\#\#}p < 0.01$ as compared to the control group; $^{*}p < 0.05$, $^{**}p < 0.01$ as compared to the AEPE-M group; ↑, content increased; ↓, content decreased; vs., versus; C, control group; M, CDAHFD group; A, AEPE-M group.

metabolites between the control group, CDAHFD group, and AEPE-M group, and the plot of PLS-DA scores indicated that these three groups were obviously distinguished (Figure 8D).

Subsequently, we used orthogonal partial least squares discriminant analysis (OPLS-DA) to further observe the metabolic changes between the control and CDAHFD groups,

and between the CDAHFD and AEPE-M groups. The OPLS-DA models showed significant differences in metabolomic data between the control group and the CDAHFD group (Figure 8E), as well as between the CDAHFD group and the AEPE-M group (Figure 8G). After randomization to 200 replacement tests, the OPLS-DA model had R^2 and Q^2 values of 0.786 and −0.497 for the comparison of the control and CDAHFD groups, respectively (Figure 8F). The OPLS-DA model had R^2 and Q^2 values of 0.941 and −0.162 for the comparison of the CDAHFD and AEPE-M groups, respectively (Figure 8H). These results revealed that the OPLS-DA models were reliable and robust.

Metabolites with a VIP > 1, $p < 0.05$, FC > 1.2, or FC < 0.833 between the control and CDAHFD groups and the CDAHFD and AEPE-M groups were selected as differential metabolites. In positive ion mode, 407 differential metabolites were identified between the control and CDAHFD groups, 76 between the CDAHFD and AEPE-M groups, and 32 metabolites in common. In negative ion mode, 231 differential metabolites were identified between the control and CDAHFD groups, 70 between the CDAHFD and AEPE-M groups, and 16 metabolites in common. Then, these 48 differential metabolites were identified by searching a database. After removing the metabolites of nonhuman origin and drugs, 14 common differential metabolites were finally identified. Detailed information on the metabolites is shown in Table 2. The contents of glucose 1-phosphate, N-lactoyl-phenylalanine, 3-indoleacrylic acid, and glutathione disulfide decreased significantly after mice were fed the CDAHFD and increased significantly after AEPE-M treatment. The contents of the metabolites 5-hydroxytryptamine, L-ornithine, prostaglandin H2, methylmalonic acid, indoleacrylic acid, taurine, deoxycytidine, taurochenodeoxycholic acid, 3-hydroxy-3-methylbutanoic acid, and 2-(3,4-dimethoxyphenyl) ethanamine increased significantly after mice were fed the CDAHFD and decreased significantly after AEPE-M treatment.

3.6 Analysis of metabolic pathways of differential metabolites

According to the position of metabolites in related pathways, topology and pathway enrichment analyses were conducted to evaluate the roles of differential metabolites in biological reactions and determine the involved metabolomic pathways. All differential metabolites were imported into MetaboAnalyst for the metabolic pathway analysis. The analysis results are presented in visual form, as shown in Figures 9A,B. The results of metabolic pathway enrichment and topological analysis indicated that the treatment of CDAHFD-induced NAFLD mice was mainly related to the metabolic pathways of glutathione metabolism, tryptophan metabolism, taurine and hypotaurine metabolism, primary bile acid biosynthesis, arginine biosynthesis, starch and sucrose metabolism, pentose and glucuronate interconversions, glycolysis/gluconeogenesis, galactose metabolism, arachidonic acid metabolism, amino sugar and nucleotide sugar metabolism, arginine and proline metabolism, pyrimidine metabolism, and valine, leucine, and isoleucine degradation.

3.7 Correlation analysis of physiological data, fecal differential metabolites, and differential microorganisms

As shown in Figure 10, *Faecalibaculum*, *Erysipelatoclostridium*, *Erysipelatoclostridiaceae*, *Desulfobacterota*, *Peptostreptococcaceae*, and *Romboutsia* showed significant positive correlations with changes in AST, ALT, LDL-C, TG, and Hyp levels in NAFLD mouse models. *Faecalibaculum*, *Peptostreptococcaceae,* and *Romboutsia* showed significant negative correlations with changes in HDL-C levels in NAFLD mouse models. *Muribaculaceae*, *Streptococcaceae*, *Bifidobacterium,* and *Actinobacteria* exhibited significant negative correlations with changes in AST, ALT, and Hyp levels in NAFLD mouse models.

Pearson's correlation analysis was performed to determine the correlation between the three groups with differences in the gut microbiota and their metabolites. The result was presented in a clustered heatmap that illustrated the relative increasing (purple) or decreasing (blue) trends, as shown in Figure 11. *Actinobacteria*, *Bifidobacterium*, *Streptococcaceae*, and *Muribaculaceae*, which were present at higher levels in the control and AEPE-M groups than in the CDAHFD group, were negatively correlated with prostaglandin H2, deoxycytidine, methylmalonic acid, indoleacrylic acid, L-ornithine, 5-hydroxytryptamine, 3-hydroxy-3-methylbutanoic acid, taurine, 2-(3,4-dimethoxyphenyl) ethanamine, and taurochenodeoxycholic acid. *Romboutsia*, *Peptostreptococcaceae*, *Desulfobacterota*, *Erysipelatoclostridiaceae*, *Erysipelatoclostridium*, *Faecalibaculum*, and *Lachnospiraceae*, which were present at higher levels in the CDAHFD group than in the control and CDAHFD groups, were negatively correlated with glutathione disulfide, N-lactoyl-phenylalanine, 3-indoleacrylic acid, and glucose 1-phosphate.

4 Discussion

A multitude of animal models are currently used to study NAFLD, including genetic leptin-deficient (ob/ob) or leptin-resistant (db/db) mouse and dietary MCD mouse models (Matsumoto et al., 2013). MCD model mice exhibit numerous pathological changes associated with NAFLD. It also leads to rapid weight loss and liver atrophy, which is inconsistent with the phenotype of human patients with NAFLD. In contrast, the CDAHFD model has been shown

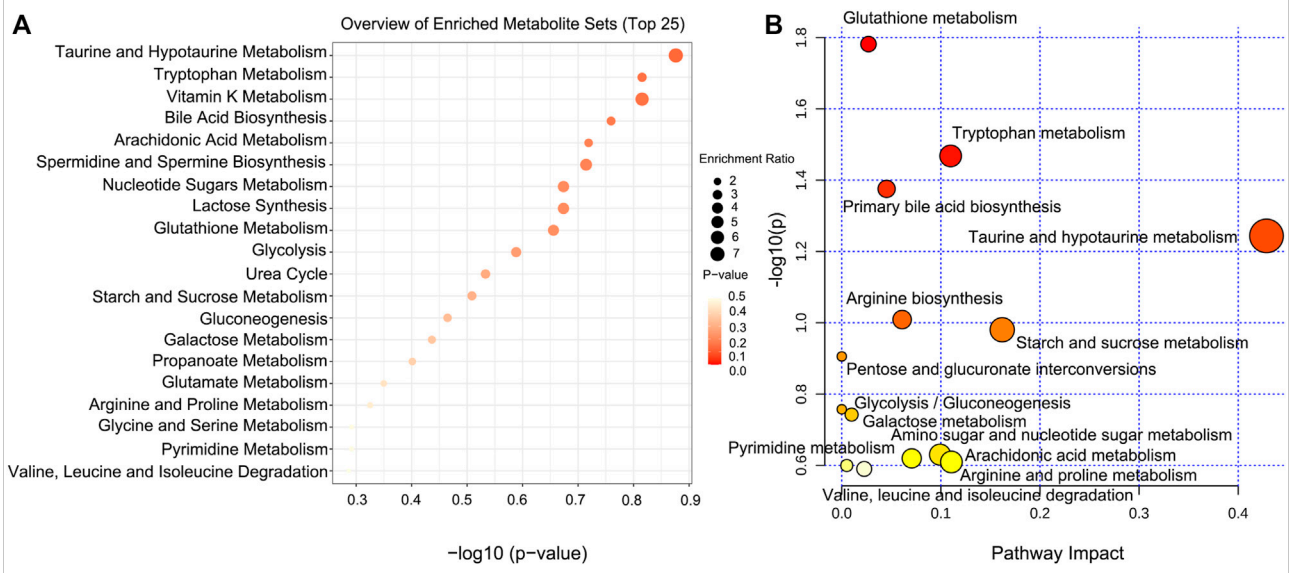

FIGURE 9
Pathway analysis of significantly altered metabolites for NAFLD. **(A)** Visual analysis of enrichment pathway of altered metabolites. **(B)** Pathway analysis of typical metabolites in response to NAFLD. Each dot represents a metabolic pathway.

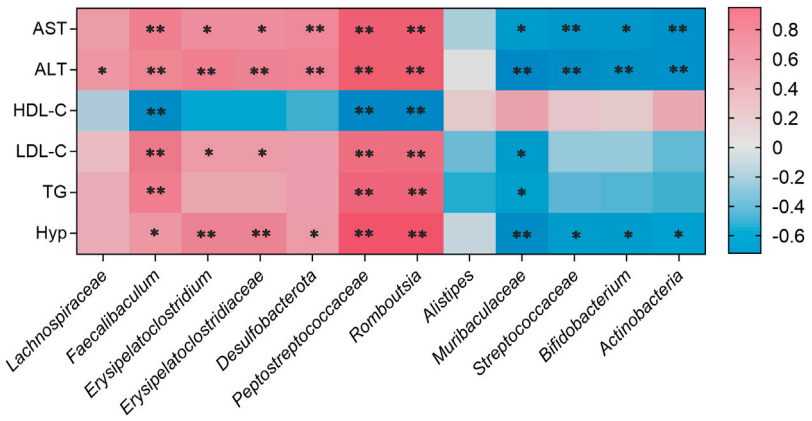

FIGURE 10
Correlations between physiological data and gut microbiota were analyzed using Spearman's analysis (heatmap). The x-axis represents the gut microbiota with differential abundance. The y-axis represents the physiological data. The colors of grids represent the value of Spearman's correlation analysis. Grids in red indicate positive correlations (correlation analysis value greater than 0.1), while grids in blue indicate negative correlations (correlation analysis value less than −0.1). Color coding scale indicates the correlation analysis value from heatmap; the deeper red or blue indicates higher correlation values. $^{**}p < 0.01$ between physiological data and gut microbiota. $^{*}p < 0.05$ between physiological data and gut microbiota.

to simulate human NAFLD characteristics while overcoming the problems that arise when using the MCD model (Matsumoto et al., 2013). Therefore, CDAHFD can be used to establish a mouse model of rapid progressive liver fibrosis, which is more conducive to understanding the pathogenesis of NAFLD and facilitating the development of effective drugs or dietary supplements. In the present study, model mice incurred remarkable disorders in the levels of AST, ALT, HDL-C, LDL-C, TG and Hyp after CDAHFD feeding. The results of H&E staining, Oil Red O staining, and Masson's trichrome staining showed that hepatocytes in the CDAHFD group displayed severe steatosis, obvious cell damage, and obvious deposition of collagen. AEPE treatment significantly improved liver steatosis and alleviated fibrosis.

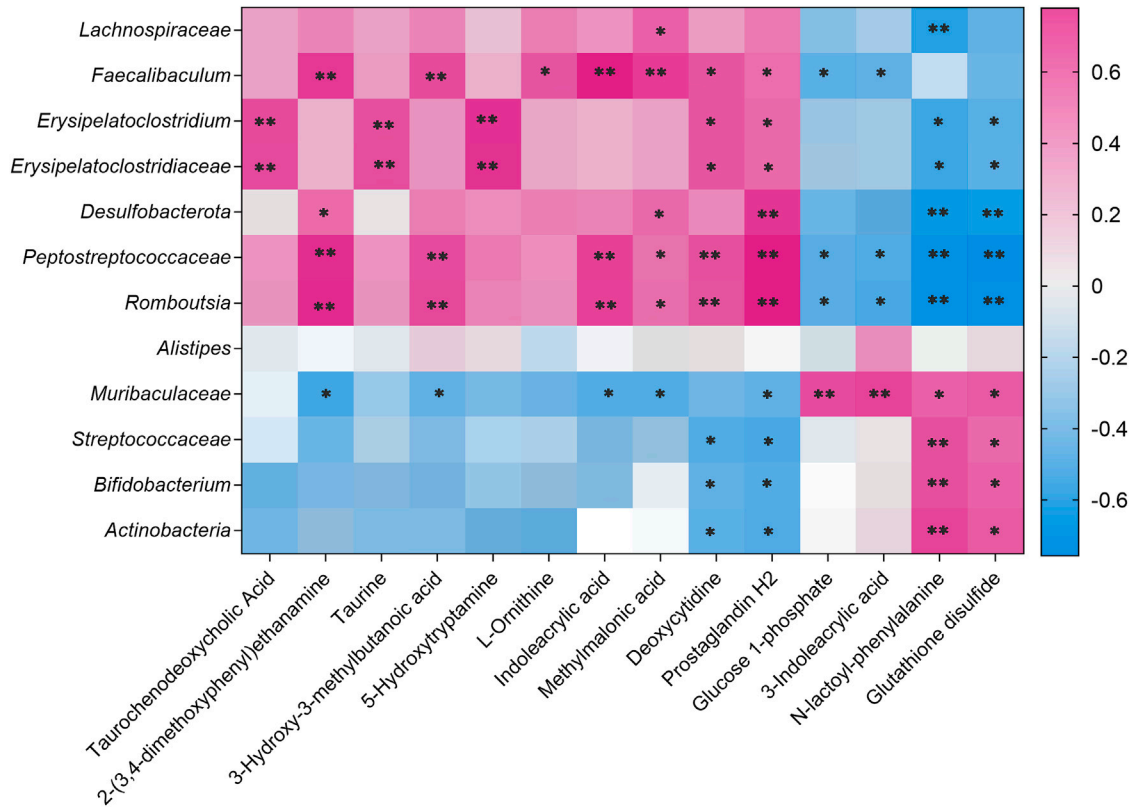

FIGURE 11
Correlation analysis of untargeted metabolomics and 16S rRNA sequencing. Correlations between untargeted metabolomics and gut microbiota were analyzed using Spearman's analysis (heatmap). The x-axis represents the differential metabolites in the fecal. The y-axis represents the gut microbiota with differential abundance. The colors of grids represent the correlation analysis value of Spearman's correlation analysis. Grids in purple indicate positive correlations (correlation analysis value greater than 0.1), while grids in blue indicate negative correlations (correlation analysis value less than −0.1). Color coding scale indicates the correlation analysis value from heatmap; the deeper purple or blue indicates higher correlation values. $^{**}p < 0.01$ between fecal metabolites and gut microbiota. $^{*}p < 0.05$ between fecal metabolites and gut microbiota.

The fecal microbiota transplantation (FMT) experiment confirmed that obesity and metabolic syndrome were improved by regulating the intestinal microbiota, and thus, it could be considered a new organ involved in the pathophysiology of NAFLD (Aron-Wisnewsky et al., 2020). Based on accumulating evidence, regulating intestinal flora using probiotics or prebiotics is a practical and effective method to prevent or treat gut microbiota-related diseases (Xue et al., 2017; Suk and Kim, 2019). As the intermediate phenotype between host and bacteria, changes in intestinal microbial metabolites play an essential role in understanding the effects of intestinal flora on diseases (Shi et al., 2022). Hence, treatments designed to regulate the intestinal microflora composed of intestinal microorganisms and microbial metabolites have become a research hot spot to prevent the development and deterioration of NAFLD.

In this study, we investigated the effect of the AEPE intervention on the intestinal flora of NAFLD mice. During the development of progressive hepatic fibrosis in NAFLD mice, AEPE reversed the changes in the diversity of the intestinal flora and adjusted the levels of components of the intestinal flora to restore them to normal levels. A clinical study showed that the intestinal microflora of patients with NAFLD is dominated by *Firmicutes* and *Bacteroidetes*, followed by *Proteobacteria* and *Actinobacteria*; however, *Proteobacteria* markedly increased in abundance, while the abundance of *Firmicutes* decreased as the disease progressed to advanced fibrosis (Loomba et al., 2017). Meanwhile, another report showed that the proportion of F/B in patients with NAFLD is increased (Li et al., 2021a). In this experiment, AEPE reversed the increase in the F/B ratio caused by CDAHFD. *Bifidobacterium* is a beneficial bacterium in the phylum *Actinobacteria*. Increased growth of *Bifidobacterium* contributes to the production of butyrate and other short-chain fatty acids (SCFAs) (Fang et al., 2021), which inhibit the production of proinflammatory factors and have the potential to contribute to the maintenance of host body weight and intestinal homeostasis, as well as improve the glucose and lipid metabolism (Bashiardes et al., 2016). *Bifidobacterium bifidum* and *Bifidobacterium adolescentis* inhibit hepatic inflammation and ameliorate NAFLD caused by a high-fat diet (HFD) by regulating intestinal microflora and increasing

the content of propionic acid (Zhang et al., 2022). Meanwhile, transplantation with different strains of *Bifidobacterium* alleviates liver injury induced by various factors (He et al., 2022a; Zha et al., 2022). Ellagic acid, an active compound in PE, increases the relative abundance of *Bifidobacterium* in an alcoholic liver injury model (Zhao et al., 2021a). Compared with the control group, the levels of *Actinobacteria* and *Bifidobacterium* decreased significantly in the CDAHFD group but increased obviously after AEPE treatment. Moreover, a preliminary study has evaluated the effect of the PE extract on the intestinal flora in ob/ob mice (Brochot et al., 2019). In the experiment, the relative abundance of *Eubacterium* in the genus level of mice treated with PE extract was significantly increased, but other altered gut microbes were unidentified. In the present study, there was no significant difference in the relative abundance of *Eubacterium* among groups, and we speculate that this may be related to the difference in the induction factors of the model animals.

Additionally, the observation of clinical samples showed that the abundance of *Alistipes* in patients with NAFLD presenting liver fibrosis was lower than that in healthy patients (Rau et al., 2018). It was found in the HFD model and high-fat and high-fructose diet model mice that the relative abundance of *Alistipes* was significantly reduced compared with that in the control group (Wang et al., 2022; Yan et al., 2022). In addition, studies of mice with liver cancer have shown that *Alistipes* assists in inhibiting Th17 cells in the intestine and ultimately reduces Th17 cell recruitment to the liver, thereby reducing liver inflammation and improving liver fibrosis (Parker et al., 2020). At the same time, *Alistipes* also produces acetate and SCFAs with anti-inflammatory effects (Li et al., 2021b). Upon AEPE-M treatment, the relative abundance of *Alistipes* significantly increased compared with the CDAHFD-fed mice. Hence, we speculate that *Alistipes* may alleviate NAFLD by reducing intestinal inflammation and maintaining intestinal balance.

In addition, intervention with AEPE-M reversed the changes in other bacteria in CDAHFD mice. *Muribaculaceae*, a probiotic that produces SCFAs and o-glycans, maintains the dynamic balance of the intestinal mucosal barrier and assists in microbial colonization (Liang et al., 2021). In our experiment, compared with NAFLD mice, the relative abundance of *Muribaculaceae* in AEPE-M mice was obviously increased. Zhao et al. found that ellagic acid increases the relative abundance of *Muribaculaceae* in a mouse alcoholic liver injury model (Zhao et al., 2021a). Notably, gallic acid is an important marker component in AEPE. After FMT with feces from mice orally administered gallic acid, the relative abundance of *Muribaculaceae* in the gallic acid–FMT group was increased (He et al., 2022b). A clinical study showed that the abundance of the *Lachnospiraceae* family was significantly increased in fecal samples from patients with NAFLD compared with that in fecal samples from healthy subjects (Shen et al., 2017). In the present study, the highest relative abundance of *Lachnospiraceae* was observed in the CDAHFD group, consistent with that in a clinical report. Nevertheless, in our experiment, the relative abundance of *Faecalibaculum* in mice fed with CDAHFD was significantly increased compared with that in the control mice, and the trend was reversed in mice fed with AEPE-M. However, a study showed that in animals with NAFLD induced by an HFD, the relative abundance of *Faecalibaculum* in HFD-fed mice was significantly reduced compared with that in the control group (Hu et al., 2021). We assume that the explanation for this phenomenon is the induction of NAFLD by different factors. Members of the *Erysipelotrichaceae* family are closely related to clinical indicators of impaired glucose and lipid metabolism and are important targets of metabolic diseases (Zhao et al., 2021b). The reduction in *Erysipelotrichaceae* may be beneficial for lipid metabolism. Taken together, AEPE-M can be used to reduce the degree of steatosis and fibrosis in NAFLD mice by modulating bacteria at multiple levels.

Changes in intestinal flora must be accompanied by alterations in different metabolites, such as bile acids, amino acids, and SCFAs. The metabolites of the intestinal flora have become an important factor regulating the pathological process of NAFLD. Therefore, this study examined the effect of AEPE on fecal metabolites. Fourteen differential metabolites were identified, including 5-hydroxytryptamine, glucose 1-phosphate, and L-ornithine. Based on the result of the correlation analysis, the levels of the aforementioned metabolites, namely, glutathione disulfide and N-lactoyl-phenylalanine, were positively correlated with the abundance of *Actinobacteria*, *Bifidobacterium*, *Streptococcaceae*, and *Muribaculaceae*.

A study reported the dysregulation of bile acid metabolism in patients with NAFLD, including elevated levels of primary conjugated bile acids (BAs), decreased levels of specific secondary Bas, and alteration of excreted BAs (Masoodi et al., 2021). Primary BAs are conjugated to glycine or taurine before being secreted into the bile for storage. The conjugated primary BAs are then released into the small intestine to facilitate lipid absorption and conversion to secondary bile acids by intestinal microorganisms. Secondary BAs are reabsorbed into the liver via the liver–gut circulation to inhibit bile acid synthesis. The continuous intrahepatic circulation of BAs ensures the steady state of BAs and the physiological function of the hepatic–intestinal axis (Li et al., 2020). Based on the results from this experiment, we found significantly higher contents of taurine and taurochenodeoxycholic acid in the feces of mice fed the CDAHFD than in those of mice fed the control diet, while these changes were reversed after AEPE consumption. We suggested that AEPE modifies the metabolic disorders caused by CDAHFD by regulating primary bile acid biosynthesis and taurine and hypotaurine metabolism.

Tryptophan metabolism is associated with a variety of diseases, including NAFLD, metabolic syndrome, obesity, and irritable bowel syndrome (Pyun et al., 2021). In the present study, several differential metabolites were related to the tryptophan metabolism pathway, such as 5-hydroxytryptamine (5-HT), indoleacrylic acid, and 3-indoleacrylic acid. Over 90% of peripheral 5-HT is produced in the gut (Agus et al., 2018). Actually, the enteric microorganism has been proved to be a primary contributor to the production of 5-HT in the gut (Ni

et al., 2020). According to previous studies, a 5-HT antagonist effectively improves fatty and fibrotic changes in a mouse NAFLD model induced by CDAHFD (Ko et al., 2021). Interestingly, our findings manifested that AEPE significantly reduced the increase in the fecal 5-HT content observed in CDAHFD mice, suggesting that AEPE may ameliorate hepatic steatosis and fibrosis by reducing 5-HT production in the gut. Indoleacrylic acid is a compound from a group of molecules known as indoles. Intestinal microorganisms catabolize tryptophan to produce indole derivatives, which are then absorbed and converted into indoleacrylic acid. Indole and its derivatives are beneficial in the treatment of liver diseases; for example, oral indole administration inhibits the NF-κB pathway and reduces LPS-induced inflammation in the liver (Beaumont et al., 2018). Yu et al. suggested significant differences in indoleacrylic acid levels between rats with hepatic fibrosis and normal rats, although its biological role in liver pathology remains unclear (Yu et al., 2019). 3-Indoleacrylic acid, a tryptophan metabolite (Roager and Licht, 2018), activates the aryl hydrocarbon receptor (AHR) and thus maintains the integrity of the intestinal barrier (Li et al., 2021c). Increased intestinal permeability exacerbates the development of NAFLD (Portincasa et al., 2022); therefore, AEPE may improve NAFLD by regulating the balance of intestinal microecology and decreasing intestinal permeability. The correlation analysis revealed that 3-indoleacrylic acid levels were positively correlated with the abundance of *Muribaculaceae* and negatively correlated with the abundance of *Romboutsia*, *Peptostreptococcaceae*, and *Faecalibaculum*. Consequently, we presumed that the effect of AEPE on tryptophan metabolism may be related to its regulation of the abundance of *Muribaculaceae*, *Romboutsia*, *Peptostreptococcaceae*, and *Faecalibaculum*.

Glucose-1-phosphate (G-1-P) is the product of the reaction in which glycogen phosphorylase cleaves molecules of glucose from the larger glycogen structure. Our results showed that decreased G-1-P levels in NAFLD mice were inversely regulated following AEPE treatment, which may be mediated by *Muribaculaceae*, *Romboutsia*, *Peptostreptococcaceae,* and *Faecalibaculum*. In the present study, G-1-P is a common key metabolite involved in multiple metabolic pathways, including starch and sucrose metabolism, amino sugar and nucleotide sugar metabolism, and galactose metabolism. Among them, the dysfunction of amino sugar and nucleotide sugar metabolism has been reported in individuals with various metabolic diseases, such as dyslipidemia, type 2 diabetes, and NAFLD (Huang et al., 2020; Li et al., 2022b). However, evidence to clarify the relationship between the metabolic pathway and NAFLD in previous studies is insufficient. The potential mechanism by which AEPE ameliorates NAFLD by regulating multiple metabolic pathways mediated by GP is worthy of in-depth investigation. Methylmalonic acid (MMA), a malonic acid derivative, is a crucial intermediate in lipid and protein metabolism. Abnormal accumulation of MMA disrupts normal glucose and glutamic acid metabolism in the rat liver (Toyoshima et al., 1996). Another study proposed MMA as a biomarker reflecting the degree of hepatic mitochondrial fatty acid oxidation in rats (Bjune et al., 2021). AEPE treatment significantly decreased the MMA content in the feces of NAFLD mice. Therefore, our results also provide clues to further explore the role of MMA in the pathogenesis of NAFLD.

Moreover, L-ornithine is involved in glutathione metabolism, arginine biosynthesis, and arginine and proline metabolism. Dysfunctional glutathione metabolism may lead to excessive reactive oxygen species production, aggravate lipid peroxidation and oxidative stress, and exacerbate liver injury. In addition, glutathione metabolism has been proven to be one of the main mechanisms affecting hyperlipidemia (Xiao-Rong et al., 2021). Thus, we hypothesized that AEPE may ameliorate NAFLD by modulating L-ornithine-mediated glutathione metabolism, reducing the accumulation of lipids in the liver, and increasing the antioxidant capacity of the body.

In summary, our studies have identified various effects of AEPE on ameliorating NAFLD, including reducing hepatic steatosis, improving dyslipidemia, and reducing fibrosis. The mechanism of AEPE in the treatment of NAFLD is associated with reshaping the intestinal microecology.

Data availability statement

The datasets presented in this study can be found in online repositories. The names of the repository/repositories and accession number(s) can be found at: NCBI BioProject—PRJNA821399.

Ethics statement

The animal study was reviewed and approved by the Animal Ethics Committee of Southwest Minzu University.

Author contributions

PG conceived the research and designed all of the experiments. XL, BZ, and PG carried out the experiments. XL and YP performed the statistical analysis. XL and PG wrote the manuscript. JG and RT guided the experiments. All the authors checked and approved the submitted version of the manuscript.

Funding

The present work was supported by the National Natural Science Foundation of China (No. 82004069), the Natural Science Foundation of Sichuan Province (No. 2022NSFSC1524), the Fundamental Research Funds for the Central Universities of Southwest Minzu University (No. 2021121), and the College Students' Innovation and

Entrepreneurship Training Program of Southwest Minzu University (No. S202110656138).

Conflict of interest

The authors declare that the research was conducted in the absence of any commercial or financial relationships that could be construed as a potential conflict of interest.

Publisher's note

All claims expressed in this article are solely those of the authors and do not necessarily represent those of their affiliated organizations, or those of the publisher, the editors, and the reviewers. Any product that may be evaluated in this article, or claim that may be made by its manufacturer, is not guaranteed or endorsed by the publisher.

References

Agus, A., Planchais, J., and Sokol, H. (2018). Gut microbiota regulation of tryptophan metabolism in health and disease. *Cell Host Microbe* 23, 716–724. doi:10.1016/j.chom.2018.05.003

Aron-Wisnewsky, J., Warmbrunn, M. V., Nieuwdorp, M., and Clément, K. (2020). Nonalcoholic fatty liver disease: modulating gut microbiota to improve severity? *Gastroenterology* 158, 1881–1898. doi:10.1053/j.gastro.2020.01.049

Bashiardes, S., Shapiro, H., Rozin, S., Shibolet, O., and Elinav, E. (2016). Non-alcoholic fatty liver and the gut microbiota. *Mol. Metab.* 5, 782–794. doi:10.1016/j.molmet.2016.06.003

Beaumont, M., Neyrinck, A. M., Olivares, M., Rodriguez, J., De Rocca Serra, A., Roumain, M., et al. (2018). The gut microbiota metabolite indole alleviates liver inflammation in mice. *FASEB J.* 32, 6681–6693. doi:10.1096/fj.201800544

Bjune, M. S., Lindquist, C., Hallvardsdotter Stafsnes, M., Bjørndal, B., Bruheim, P., Aloysius, T. A., et al. (2021). Plasma 3-hydroxyisobutyrate (3-HIB) and methylmalonic acid (MMA) are markers of hepatic mitochondrial fatty acid oxidation in male Wistar rats. *Biochim. Biophys. Acta. Mol. Cell Biol. Lipids* 1866, 158887. doi:10.1016/j.bbalip.2021.158887

Brochot, A., Azalbert, V., Landrier, J. F., Tourniaire, F., and Serino, M. (2019). A two-week treatment with plant extracts changes gut microbiota, caecum metabolome, and markers of lipid metabolism in ob/ob mice. *Mol. Nutr. Food Res.* 63, 1–12. doi:10.1002/mnfr.201900403

Chen, L., Kan, J., Zheng, N., Li, B., Hong, Y., Yan, J., et al. (2021). A botanical dietary supplement from white peony and licorice attenuates nonalcoholic fatty liver disease by modulating gut microbiota and reducing inflammation. *Phytomedicine.* 91, 153693. doi:10.1016/j.phymed.2021.153693

Diehl, A. M., and Day, C. (2017). Cause, pathogenesis, and treatment of nonalcoholic steatohepatitis. *N. Engl. J. Med.* 377, 2063–2072. doi:10.1056/nejmra1503519

Fang, Y. L., Chen, H., Wang, C. L., and Liang, L. (2018). Pathogenesis of non-alcoholic fatty liver disease in children and adolescence: from "two hit theory" to "multiple hit model. *World J. Gastroenterol.* 24, 2974–2983. doi:10.3748/wjg.v24.i27.2974

Fang, Z., Li, L., Lu, W., Zhao, J., Zhang, H., Lee, Y. K., et al. (2021). Bifidobacterium affected the correlation between gut microbial composition, SCFA metabolism, and immunity in mice with DNFB-induced atopic dermatitis. *Food Biosci.* 41, 100648. doi:10.1016/j.fbio.2020.100648

He, Q., Yang, C., Kang, X., Chen, Y., Zhang, T., Zhang, H., et al. (2022a). Intake of Bifidobacterium lactis Probio-M8 fermented milk protects against alcoholic liver disease. *J. Dairy Sci.* 105, 2908–2921. doi:10.3168/jds.2021-21265

He, Z., Ma, Y., Chen, X., Liu, S., Xiao, J., Wang, Y., et al. (2022b). Protective effects of intestinal gallic acid in neonatal dairy calves against extended-spectrum β-lactamase producing enteroaggregative *Escherichia coli* infection: modulating intestinal homeostasis and colitis. *Front. Nutr.* 9, 864080. doi:10.3389/fnut.2022.864080

Hu, M., Zhang, L., Ruan, Z., Han, P., and Yu, Y. (2021). The regulatory effects of citrus peel powder on liver metabolites and gut flora in mice with non-alcoholic fatty. *Foods* 10, 3022. doi:10.3390/foods10123022

Huang, C. Z., Tung, Y. T., Hsia, S. M., Wu, C. H., and Yen, G. C. (2017). The hepatoprotective effect of Phyllanthus emblica L. fruit on high fat diet-induced non-alcoholic fatty liver disease (NAFLD) in SD rats. *Food Funct.* 8, 842–850. doi:10.1039/c6fo01585a

Huang, Z. R., Chen, M., Guo, W. L., Li, T. T., Liu, B., Bai, W. D., et al. (2020). Monascus purpureus-fermented common buckwheat protects against dyslipidemia and non-alcoholic fatty liver disease through the regulation of liver metabolome and intestinal microbiome. *Food Res. Int.* 136, 109511. doi:10.1016/j.foodres.2020.109511

Ko, M., Kamimura, K., Owaki, T., Nagoya, T., Sakai, N., Nagayama, I., et al. (2021). Modulation of serotonin in the gut-liver neural axis ameliorates the fatty and fibrotic changes in non-alcoholic fatty liver. *Dis. Model. Mech.* 14, dmm048922. doi:10.1242/dmm.048922

Kolodziejczyk, A. A., Zheng, D., Shibolet, O., and Elinav, E. (2019). The role of the microbiome in NAFLD and NASH. *EMBO Mol. Med.* 11, e9302. doi:10.15252/emmm.201809302

Le Roy, T., Llopis, M., Lepage, P., Bruneau, A., Rabot, S., Bevilacqua, C., et al. (2013). Intestinal microbiota determines development of non-alcoholic fatty liver disease in mice. *Gut* 62, 1787–1794. doi:10.1136/gutjnl-2012-303816

Li, Q., Li, M., Li, F., Zhou, W., Dang, Y., Zhang, L., et al. (2020). Qiang-Gan formula extract improves non-alcoholic steatohepatitis via regulating bile acid metabolism and gut microbiota in mice. *J. Ethnopharmacol.* 258, 112896. doi:10.1016/j.jep.2020.112896

Li, C., Zhou, W., Li, M., Shu, X., Zhang, L., Ji, G., et al. (2021a). Salvia-Nelumbinis naturalis extract protects mice against MCD diet-induced steatohepatitis via activation of colonic FXR-FGF15 pathway. *Biomed. Pharmacother.* 139, 111587. doi:10.1016/j.biopha.2021.111587

Li, H., Wang, Q., Chen, P., Zhou, C., Zhang, X., Chen, L., et al. (2021b). Ursodeoxycholic acid treatment restores gut microbiota and alleviates liver inflammation in non-alcoholic steatohepatitic mouse model. *Front. Pharmacol.* 12, 788558. doi:10.3389/fphar.2021.788558

Li, X., Zhang, B., Hu, Y., and Zhao, Y. (2021c). New Insights into gut-bacteria-derived indole and its derivatives in intestinal and liver diseases. *Front. Pharmacol.* 12, 769501. doi:10.3389/fphar.2021.769501

Li, S., Li, X., Chen, F., Liu, M., Ning, L., Yan, Y., et al. (2022a). Nobiletin mitigates hepatocytes death, liver inflammation, and fibrosis in a murine model of NASH through modulating hepatic oxidative stress and mitochondrial dysfunction. *J. Nutr. Biochem.* 100, 108888. doi:10.1016/j.jnutbio.2021.108888

Li, Z., Nie, L., Li, Y., Yang, L., Jin, L., Du, B., et al. (2022b). Traditional Tibetan medicine twenty-five wei'er tea pills ameliorate rheumatoid arthritis based on chemical crosstalk between gut microbiota and the host. *Front. Pharmacol.* 13, 828920. doi:10.3389/fphar.2022.828920

Liang, W., Zhou, K., Jian, P., Chang, Z., Zhang, Q., Liu, Y., et al. (2021). Ginsenosides improve nonalcoholic fatty liver disease via integrated regulation of gut microbiota, inflammation and energy homeostasis. *Front. Pharmacol.* 12, 622841. doi:10.3389/fphar.2021.622841

Loomba, R., Seguritan, V., Li, W., Long, T., Klitgord, N., Bhatt, A., et al. (2017). Gut microbiome-based metagenomic signature for non-invasive detection of advanced fibrosis in human nonalcoholic fatty liver disease. *Cell Metab.* 25, 1054–1062.e5. doi:10.1016/j.cmet.2017.04.001

Masoodi, M., Gastaldelli, A., Hyötyläinen, T., Arretxe, E., Alonso, C., Gaggini, M., et al. (2021). Metabolomics and lipidomics in NAFLD: biomarkers and non-invasive diagnostic tests. *Nat. Rev. Gastroenterol. Hepatol.* 18, 835–856. doi:10.1038/s41575-021-00502-9

Matsumoto, M., Hada, N., Sakamaki, Y., Uno, A., Shiga, T., Tanaka, C., et al. (2013). An improved mouse model that rapidly develops fibrosis in non-alcoholic steatohepatitis. *Int. J. Exp. Pathol.* 94, 93–103. doi:10.1111/iep.12008

Ni, Y., Ni, L., Zhuge, F., and Fu, Z. (2020). The gut microbiota and its metabolites, novel targets for treating and preventing non-alcoholic fatty liver disease. *Mol. Nutr. Food Res.* 64, e2000375. doi:10.1002/mnfr.202000375

Parker, B. J., Wearsch, P. A., Veloo, A. C. M., and Rodriguez-Palacios, A. (2020). The genus Alistipes: gut bacteria with emerging implications to inflammation, cancer, and mental health. *Front. Immunol.* 11, 906. doi:10.3389/fimmu.2020.00906

Parlati, L., Régnier, M., Guillou, H., and Postic, C. (2021). New targets for NAFLD. *JHEP Rep.* 3, 100346. doi:10.1016/j.jhepr.2021.100346

Porras, D., Nistal, E., Martínez-Flórez, S., Olcoz, J. L., Jover, R., Jorquera, F., et al. (2019). Functional interactions between gut microbiota transplantation, quercetin, and high-fat diet determine non-alcoholic fatty liver disease development in germ-free mice. *Mol. Nutr. Food Res.* 63, e1800930. doi:10.1002/mnfr.201800930

Portincasa, P., Bonfrate, L., Khalil, M., De Angelis, M., Calabrese, F. M., D'amato, M., et al. (2022). Intestinal barrier and permeability in health, obesity and NAFLD. *Biomedicines* 10, 83. doi:10.3390/biomedicines10010083

Pyun, D. H., Kim, T. J., Kim, M. J., Hong, S. A., Abd El-Aty, A. M., Jeong, J. H., et al. (2021). Endogenous metabolite, kynurenic acid, attenuates nonalcoholic fatty liver disease via AMPK/autophagy- and AMPK/ORP150-mediated signaling. *J. Cell. Physiol.* 236, 4902–4912. doi:10.1002/jcp.30199

Rau, M., Rehman, A., Dittrich, M., Groen, A. K., Hermanns, H. M., Seyfried, F., et al. (2018). Fecal SCFAs and SCFA-producing bacteria in gut microbiome of human NAFLD as a putative link to systemic T-cell activation and advanced disease. *United Eur. Gastroenterol. J.* 6, 1496–1507. doi:10.1177/2050640618804444

Ren, S. M., Zhang, Q. Z., Chen, M. L., Jiang, M., Zhou, Y., Xu, X. J., et al. (2021). Anti-NAFLD effect of defatted walnut powder extract in high fat diet-induced C57BL/6 mice by modulating the gut microbiota. *J. Ethnopharmacol.* 270, 113814. doi:10.1016/j.jep.2021.113814

Roager, H. M., and Licht, T. R. (2018). Microbial tryptophan catabolites in health and disease. *Nat. Commun.* 9, 3294. doi:10.1038/s41467-018-05470-4

Saini, R., Sharma, N., Oladeji, O. S., Sourirajan, A., Dev, K., Zengin, G., et al. (2022). Traditional uses, bioactive composition, pharmacology, and toxicology of Phyllanthus emblica fruits: a comprehensive review. *J. Ethnopharmacol.* 282, 114570. doi:10.1016/j.jep.2021.114570

Schwabe, R. F., Tabas, I., and Pajvani, U. B. (2020). Mechanisms of fibrosis development in nonalcoholic steatohepatitis. *Gastroenterology* 158, 1913–1928. doi:10.1053/j.gastro.2019.11.311

Shen, F., Zheng, R. D., Sun, X. Q., Ding, W. J., Wang, X. Y., Fan, J. G., et al. (2017). Gut microbiota dysbiosis in patients with non-alcoholic fatty liver disease. *Hepatobiliary Pancreat. Dis. Int.* 16, 375–381. doi:10.1016/S1499-3872(17)60019-5

Shi, W., Ye, H., Deng, Y., Chen, S., Xiao, W., Wang, Z., et al. (2022). Yaobitong capsules reshape and rebalance the gut microbiota and metabolites of arthritic rats: an integrated study of microbiome and fecal metabolomics analysis. *J. Chromatogr. B Anal. Technol. Biomed. Life Sci.* 1190, 123096. doi:10.1016/j.jchromb.2021.123096

Soares, E., Soares, A. C., Trindade, P. L., Monteiro, E. B., Martins, F. F., Forgie, A. J., et al. (2021). Jaboticaba (Myrciaria jaboticaba) powder consumption improves the metabolic profile and regulates gut microbiome composition in high-fat diet-fed mice. *Biomed. Pharmacother.* 144, 112314. doi:10.1016/j.biopha.2021.112314

Song, L., Li, Y., Qu, D., Ouyang, P., Ding, X., Wu, P., et al. (2020). The regulatory effects of phytosterol esters (PSEs) on gut flora and faecal metabolites in rats with NAFLD. *Food Funct.* 11, 977–991. doi:10.1039/c9fo01570a

Suk, K. T., and Kim, D. J. (2019). Gut microbiota: novel therapeutic target for nonalcoholic fatty liver disease. *Expert Rev. Gastroenterol. Hepatol.* 13, 193–204. doi:10.1080/17474124.2019.1569513

Tilg, H., Zmora, N., Adolph, T. E., and Elinav, E. (2020). The intestinal microbiota fuelling metabolic inflammation. *Nat. Rev. Immunol.* 20, 40–54. doi:10.1038/s41577-019-0198-4

Tilg, H., Adolph, T. E., Dudek, M., and Knolle, P. (2021). Non-alcoholic fatty liver disease: the interplay between metabolism, microbes and immunity. *Nat. Metab.* 3, 1596–1607. doi:10.1038/s42255-021-00501-9

Toyoshima, S., Watanabe, F., Saido, H., Pezacka, E. H., Jacobsens, D. W., Miyatake, K., et al. (1996). Accumulation of methylmalonic acid caused by vitamin B 12 -deficiency disrupts normal cellular metabolism in rat liver. *Br. J. Nutr.* 75, 929–938. doi:10.1079/bjn19960198

Tung, Y. T., Huang, C. Z., Lin, J. H., and Yen, G. C. (2018). Effect of Phyllanthus emblica L. fruit on methionine and choline-deficiency diet-induced nonalcoholic steatohepatitis. *J. Food Drug Anal.* 26, 1245–1252. doi:10.1016/j.jfda.2017.12.005

Variya, B. C., Bakrania, A. K., and Patel, S. S. (2016). Emblica officinalis (amla): a review for its phytochemistry, ethnomedicinal uses and medicinal potentials with respect to molecular mechanisms. *Pharmacol. Res.* 111, 180–200. doi:10.1016/j.phrs.2016.06.013

Vernon, G., Baranova, A., and Younossi, Z. M. (2011). Systematic review: the epidemiology and natural history of non-alcoholic fatty liver disease and non-alcoholic steatohepatitis in adults. *Aliment. Pharmacol. Ther.* 34, 274–285. doi:10.1111/j.1365-2036.2011.04724.x

Wang, T., Ye, Y., Ji, J., Zhang, S., Yang, X., Xu, J., et al. (2022). Astilbin from Smilax glabra Roxb. alleviates high-fat diet-induced metabolic dysfunction. *Food Funct.* 13, 5023–5036. doi:10.1039/d2fo00060a

Wong, W. K., and Chan, W. K. (2021). Nonalcoholic fatty liver disease: a global perspective. *Clin. Ther.* 43, 473–499. doi:10.1016/j.clinthera.2021.01.007

Xiao-Rong, L., Ning, M., Xi-Wang, L., Shi-Hong, L., Zhe, Q., Li-Xia, B., et al. (2021). Untargeted and targeted metabolomics reveal the underlying mechanism of aspirin eugenol ester ameliorating rat hyperlipidemia via inhibiting FXR to induce CYP7A1. *Front. Pharmacol.* 12, 733789. doi:10.3389/fphar.2021.733789

Xue, L., He, J., Gao, N., Lu, X., Li, M., Wu, X., et al. (2017). Probiotics may delay the progression of nonalcoholic fatty liver disease by restoring the gut microbiota structure and improving intestinal endotoxemia. *Sci. Rep.* 7, 45176. doi:10.1038/srep45176

Yan, J., Nie, Y., Liu, Y., Li, J., Wu, L., Chen, Z., et al. (2022). Yiqi-bushen-tiaozhi recipe attenuated high-fat and high-fructose diet induced nonalcoholic steatohepatitis in mice via gut microbiota. *Front. Cell. Infect. Microbiol.* 12, 824597. doi:10.3389/fcimb.2022.824597

Yin, K., Li, X., Luo, X., Sha, Y., Gong, P., Gu, J., et al. (2021). Hepatoprotective effect and potential mechanism of aqueous extract from Phyllanthus emblica on carbon-tetrachloride-induced liver fibrosis in rats. *Evid. Based. Complement. Altern. Med.* 2021, 5345821. doi:10.1155/2021/5345821

Yin, K. H., Luo, X. M., Ding, Y., Que, H. Y., Tan, R., Li, D. P., et al. (2022). Research progress on hepatoprotective effect and mechanism of Phyllanthus emblica and its active components. *Chin. Tradit. Herb. Drugs* 53, 295–307. doi:10.7501/j.issn.0253-2670.2022.01.034

Yu, J., He, J. Q., Chen, D. Y., Pan, Q. L., Yang, J. F., Cao, H. C., et al. (2019). Dynamic changes of key metabolites during liver fibrosis in rats. *World J. Gastroenterol.* 25, 941–954. doi:10.3748/wjg.v25.i8.941

Zha, H., Li, Q., Chang, K., Xia, J., Li, S., and Tang, R. (2022). Characterising the intestinal bacterial and fungal microbiome associated with different cytokine profiles in two bifidobacterium strains pre-treated rats with D-galactosamine-induced liver injury. *Front. Immunol.* 13, 791152. doi:10.3389/fimmu.2022.791152

Zhang, H., Zhao, J., and Chen, W. (2022). Bifidobacterium bifidum shows more diversified ways of relieving non-alcoholic fatty liver compared with bifidobacterium adolescentis. *Biomedicines* 84, 10. doi:10.3390/biomedicines10010084

Zhao, L., Mehmood, A., Soliman, M. M., Iftikhar, A., Iftikhar, M., Aboelenin, S. M., et al. (2021a). Protective effects of ellagic acid against alcoholic liver disease in mice. *Front. Nutr.* 8, 744520. doi:10.3389/fnut.2021.744520

Zhao, T., Zhan, L., Zhou, W., Chen, W., Luo, J., Zhang, L., et al. (2021b). The effects of erchen decoction on gut microbiota and lipid metabolism disorders in zucker diabetic fatty rats. *Front. Pharmacol.* 12, 647529. doi:10.3389/fphar.2021.647529

Frontiers in Pharmacology

Explores the interactions between chemicals and living beings

The most cited journal in its field, which advances access to pharmacological discoveries to prevent and treat human disease.

Discover the latest Research Topics

See more →

Frontiers

Avenue du Tribunal-Fédéral 34
1005 Lausanne, Switzerland
frontiersin.org

Contact us

+41 (0)21 510 17 00
frontiersin.org/about/contact